INEEL/EXT-01-01403

Environmental Systems Research Candidates Final Report FY 2000-2001

D. L. Miller, Program Manager
S. J. Piet, Deputy Program Manager

March 2001

Idaho National Engineering and Environmental Laboratory
Bechtel BWXT Idaho, LLC

INEEL/EXT-01-01403

Environmental Systems Research Candidates Final Report FY 2000–2001

D. L. Miller, Program Manager
S. J. Piet, Deputy Program Manager

March 2001

Idaho National Engineering and Environmental Laboratory
Idaho Falls, Idaho 83415

Prepared for the
U.S. Department of Energy
Office of Environmental Management
Under DOE Idaho Operations Office
Contract DE-AC07-99ID13727

ABSTRACT

The Environmental Systems Research Candidates (ESRC) Program ran from April 2000 through September 2001 as part of the Environmental Systems Research and Analysis (ESRA) Program at the Idaho National Engineering and Environmental Laboratory (INEEL). ESRA provides key science and technology to meet the cleanup mission of the U.S. Department of Energy Office of Environmental Management (EM), and performs research and development that will help solve current legacy problems and enhance the INEEL's scientific and technical capability for solving longer-term challenges. This report documents the accomplishments of the ESRC Program. The ESRC Program consisted of 25 tasks subdivided within four research areas:

A. **Environmental Characterization Science and Technology.** This research explored new data acquisition, processing, and interpretation methods that support cleanup and long-term stewardship decisions.

B. **Subsurface Understanding.** This research expanded understanding of the biology, chemistry, physics, hydrology, and geology needed to improve models of contamination problems in the earth's subsurface.

C. **Environmental Computational Modeling.** This research developed INEEL computing capability for modeling subsurface contaminants and contaminated facilities.

D. **Environmental Systems Science and Technology.** This research explored novel processes to treat waste and decontaminate facilities.

Our accomplishments include the following:

- Demonstrated improvements in ion mobility spectrometry for in situ, field-deployable, environmental monitoring of benzene, toluene, acetone, chlorinated hydrocarbons, as well as organic and inorganic cations and anions.

- Advanced nuclear nondestructive assay detection capability for nuclear and non-nuclear materials in soils and waste containers, e.g., using accelerator-based x-ray fluorescence to detect uranium and heavy metals representative of the soils at the INEEL Radioactive Waste Management Complex at concentrations below 100 ppm.

- Determined, through analysis of samples taken in and around the INEEL site, that mercury emissions from 36 years of environmental mangement high-level waste treatment operations have not raised regional off-INEEL mercury contamination levels above normal background.

- Improved conceptual models for contaminant transport in the vadose zone by demonstrating that traditional deterministic models overlook critical aspects of dynamic behavior.

- Began the integration of geophysical tomography with hydrological state variable data to better describe flow and transport parameters in the earth's subsurface, which in turn leads to better understanding of the functional relationship between specific geophysical

and hydrogeophysical parameters, ultimately contributing to more accurate modeling of contaminant transport in the subsurface.

- Increased the total environmental data transfer rate in/out of the INEEL by a factor of 30, and improved the maximum onsite processing rate for environmental calculations by a factor of 10.

- Developed the Advanced Decontamination and Decommissioning System by (a) completing the key elements (such as radiation field visualization) of the Decontamination, Decommissioning, and Remediation Optimal Planning System for modeling a facility for preplanning and waste minimization, (b) completing an initial Robotic Waste Packaging System for material handling, optimal waste packaging, and sorting/recycling during decommissioning, and (c) completing initial system testing of the Waste Characterization and Sorting System.

CONTENTS

INTRODUCTION

Welcome to the final program report of the Idaho National Engineering and Environmental Laboratory's (INEEL's) Environmental Systems Research Candidates (ESRC) Program. The ESRC Program started in April 2000 and ended in September 2001. The research and development performed by the ESRC Program provided key science and technology to (a) meet the clean-up mission of the U.S. Department of Energy (DOE) Office of Environmental Management (EM), (b) help DOE clean up the cold-war legacy both at the INEEL and across the DOE Complex, and (c) enhance the INEEL's ability to solve longer-term challenges, like DOE's environmental stewardship of former defense sites.

Background

In March 2000, Congress approved DOE's request to use $10.7M of EM program funds at the INEEL to develop: "…a suite of research areas comprising a new program of critical importance to the EM mission both at the INEEL and across the DOE complex. These environmentally applicable new research activities will address an agenda responsive to long-term stewardship with a special emphasis on subsurface science." In April 2000, the ESRC Program was established at the INEEL to meet this challenge and to develop novel processes or materials to treat, decontaminate, or store hazardous or radioactive waste.

Scope

The ESRC Program's science and engineering research was targeted at four major research areas critical to EM:

- Environmental Characterization Science and Technology
- Subsurface Understanding
- Environmental Computational Modeling
- Environmental Systems Science and Technology.

The relevance of each of these research areas to EM's mission is illustrated in Figure 1. The ESRC Program's technical staff developed 25 tasks within these four research areas, consistent with commitments to DOE and to Congress. The INEEL's approach was to focus the research on addressing important EM needs while enhancing key "technical capabilities" in areas important to EM. Enhancing key technical capabilities includes building additional scientific and technical proficiency, strengthening the research staff, and enhancing the INEEL's relevant EM research infrastructure. The research tasks were started in April and May 2000. The four research areas are described below.

Environmental Characterization Science and Technology

This set of research tasks explored the potential offered by novel or improved ways to measure or gather information that is important to assessing environmental issues. These research tasks should help obtain the quality and type of data needed to make DOE's environmental decisions more scientifically defensible. The research should improve the efficiency of data acquisition, processing, interpretation, and use of environmental data. Most of the research tools developed as part of this technical area should help us gather both more of and the right type of information required to understand the subsurface environment, which consists of the root zone, unsaturated (vadose) zone, and saturated groundwater (the aquifer).

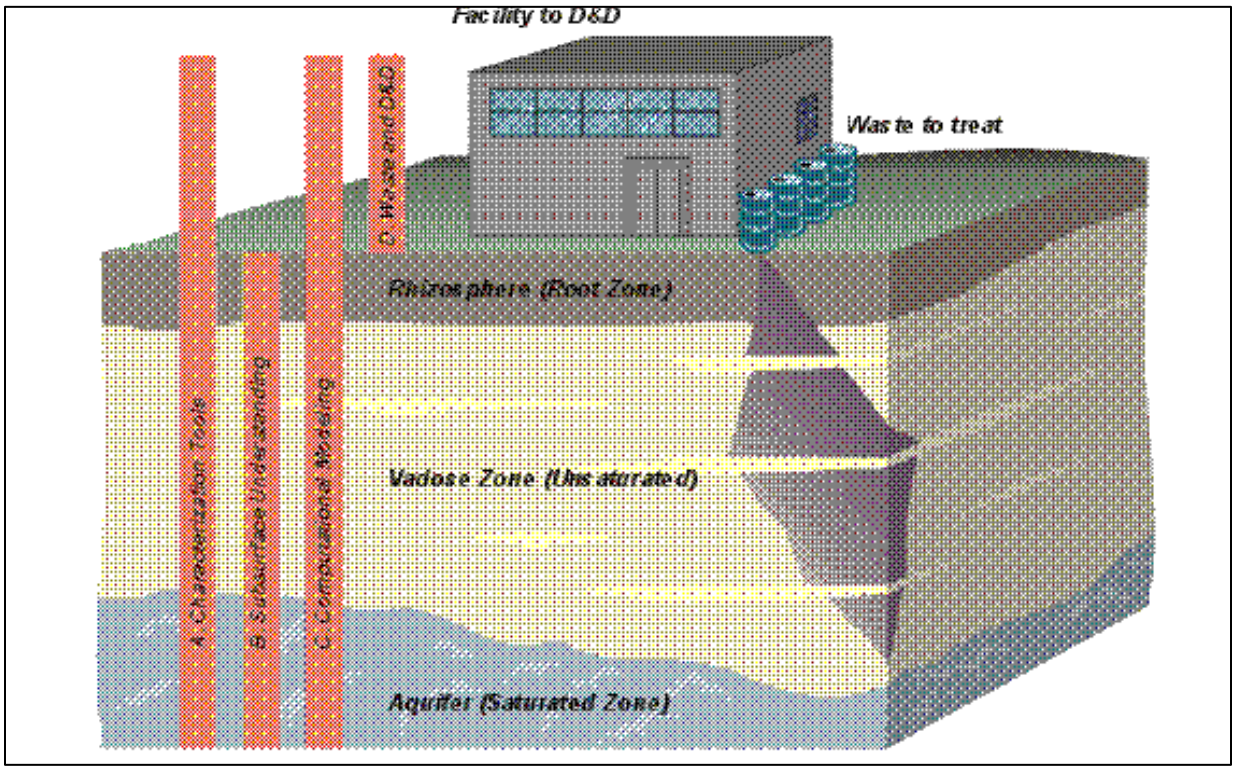

Figure 1. Relevance of research areas to EM's mission.

Some research tools developed will apply to assessing contamination above ground, either on the surface or in contaminated facilities. All of the research is relevant to broader issues of site characterization and monitoring for long-term stewardship of DOE facilities.

Subsurface Understanding

This research improved understanding of the complex subsurface environment and should advance the science to enable EM to model and manage waste and contamination problems more effectively. The research should enhance understanding of the biology, chemistry, physics, hydrology, and geology of types of waste and contaminants in the earth's subsurface.

This research enhanced our understanding of the complex interactions between contaminants and the environment at the range of physical scales (kilometers to microns) relevant to EM cleanup. Understanding how all aspects of the subsurface environment function and interact is critical to making good long-term remediation and disposition decisions.

Environmental Computational Modeling

This research developed computational science, modeling capabilities, and computing resources with an emphasis on current and future applications to EM. For example, technical tasks will be focused on modeling the behavior of chemical contaminants in the subsurface and modeling of contaminated facilities before decommissioning and decontamination. The goal of this research was to develop the computing framework that can use the knowledge gained in research (such as that developed under the first two research areas) to more accurately model and predict what will happen to contaminants in the environment. This will allow DOE to make better and more informed decisions for clean up.

Environmental Systems Science and Technology

This research explored novel processes or materials to treat, decontaminate, or store hazardous or radioactive waste.

Selection Process

Research performed as part of the ESRC Program was been selected from two principal sources:

- *Research tasks with prior foundations in the INEEL's discretionary research programs*. These were primarily research tasks that have a basis in prior discretionary research at the INEEL. These tasks had already passed a rigorous technical peer review and were positively evaluated by the DOE Idaho Operations Office (DOE-ID) and by the INEEL EM Program staff who are cognizant of INEEL and DOE needs.

- *Invited new research tasks*. The INEEL's laboratory management solicited a small number of research proposals on critical additional subjects consistent with the four research areas; these were new research tasks relevant to subsurface science, environmental computational modeling, and long-term stewardship. INEEL experts familiar with EM needs and with INEEL research capabilities worked with the Lab's management to identify what technical areas should be targeted for invited research.

Review Process

All research proposed for this program passed the following four independent rigorous reviews to be started, and a fifth review to ensure that the work was on track after it started:

1. *EM relevance review to ensure significance to the DOE EM mission*. The INEEL staff, who work in INEEL EM programs and who understand the science and engineering needs of EM, evaluated each task for its potential to solve critical EM problems. The results of these reviews categorized most research tasks as both contributing to the understanding of the subsurface environment and important to long-term stewardship of DOE's contaminated sites—over $7M of the $10.7M was categorized as contributing to subsurface science and over $8M of the $10.7M was categorized as contributing to long-term stewardship. The rest of the research tasks advance knowledge in other environmental areas, such as waste management and decontamination of facilities.

2. *Technical review to ensure high technical quality*. The technical review ensured that only research of high technical potential was funded. The technical review provided constructive feedback to help principal investigators implement the research tasks that were ultimately funded.

3. *Management review to ensure adherence of each task to ESRC scope and purpose*. INEEL management reviewed all research tasks to make sure that the work was consistent with the ESRC objectives agreed upon with DOE and with the direction and intent of the Congressional reprogramming approval.

4. *DOE reviews.* In consultation with DOE-EM Science and Technology, DOE-ID reviewed the proposed research tasks and work packages and then approved the content prior to initiating work.

5. *Annual external peer and progress review*. All research performed in the Environmental Systems Research (ESR) Program, including these tasks in the ESRC Program, was reviewed in July 2000 by an external scientific and technical peer review committee. The peer review ensured that the

work is meeting required scientific and technical standards and is progressing according to the research outline for the particular task. Twenty-one of 24 tasks were graded as meeting or exceeding expectations (a 25th task started later.) The primary issue with the other three tasks was slow startup, given the history of the program; they were helped and guided accordingly. The review also ensured that the work was appropriately targeted to solving real scientific and technical needs.

Program Highlights

Twenty-five research tasks were selected and approved. The research has produced 34 reviewed papers and 75 presentations (see Appendix A). The program collaborated with 20 other institutions and supported numerous students. As of this report, two-thirds of the tasks have been successful in aquiring additional funding. We expect this fraction to reach four-fifths over the coming year.

A significant effort was expended to disseminate the information gained from the ESRC projects to the INEEL environmental management community. Twenty seminars were conducted, encompassing 23 of the 25 ESRC tasks. Attendance averaged 21 people per seminar, which we feel is a good response. Also, almost half of the seminars resulted in followup meetings between the principle investigator and potential users to explore the research further and to identify ways that the research may be of benefit to the user community. We believe we accomplished our goal to improve communication between R&D and EM Operations.

Through the coordinated efforts of the ESRC Program and research and development (R&D) integration, we established a systematic approach to ensure that EM research tasks are relevant to operational needs. This successful effort provided a methodology to facilitate and expedite the development and transition of science and technology to Site Operations. The real improvements in communications and potential beneficial impact on operational programs provide opportunities to significantly enhance EM performance, reduce costs, and efficiently manage our R&D effort.

As described in Appendix B, all ESRC tasks were mapped to EM needs as listed in the INEEL Site Technology Coordinating Group (STCG) lists of needs and opportunities. INEEL Integration personnel analyzed the ESRC portfolio to determine the extent to which it aligns with and is relevant to INEEL environmental management needs. Each ESRC project was found to be focused on at least one identified STCG need with the aggregate 25 ESRC projects providing information relevant to 14 science needs and 60 EM program needs. The bulk of the needs addressed (61%) were in the High Level Waste and D&D programs. The rest were relatively evenly split among the Spent Nuclear Fuel (SNF), Waste Management, and Environmental Restoration. This analysis confirms that the ESRC program was properly focused on addressing environmental management needs.

We have categorized the ESRC research portfolio from the standpoint of the seven EM stages or “gates” of technology maturity:

1. Basic Research
2. Applied Research
3. Exploratory Development
4. Advanced Development
5. Engineering Development

6. Demonstration

7. Deployment.

As shown in Figure 2, two-thirds of the funded work is applied research; this is appropriate given ESRC objectives. Also consistent with the objectives and nature of ESRC, none of the tasks were categorized at Stages 5 through 7.

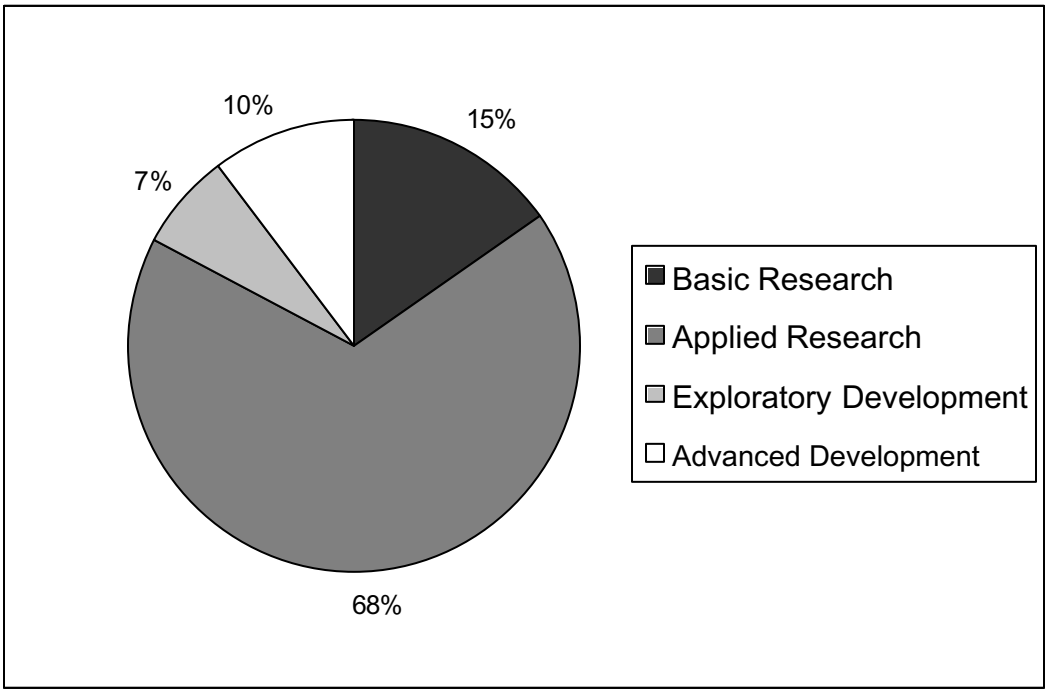

Figure 2. ESRC portfolio by technology maturity.

We have also categorized the ESRC portfolio from the perspective of the ESRC objective to enhance the INEEL's science and technology capabilities for longer-term challenges, such as environmental stewardship. Appendix C provides additional explanation. Two-thirds of the nine INEEL R&D capability areas will be improved by ESRC research. The following disciplines are primarily supported:

- Applied Engineering
- Biotechnology
- Chemistry and Chemical Engineering
- Earth Science
- Information Management Technologies.

We find that two-thirds of the 49 INEEL R&D capabilities will be improved by ESRC research. Consistent with ESRC objectives, the following capabilities are primarily supported:

- Environmental monitoring
- Groundwater hydrology and hydrochemistry
- Vadose zone hydrology and soil physics
- Modeling, simulation, and information visualization
- Environmental engineering
- Engineered systems.

Highlights of Individual Research Tasks

The following items provide a sample of the research highlights of individual ESRC tasks:

- The task, "Ion Mobility Spectrometry (IMS) for Environmental Monitoring and In Situ Measurement of Hazardous Organics" successfully demonstrated how some of the issues of using IMS for environmental analysis in the field can be overcome. One subtask developed a novel IMS system for deployment into the subsurface to provide quality analytical measurements for a number of chemicals of environmental concern, such as benzene, toluene, acetone, and chlorinated hydrocarbons. A deployment of the miniature sensor into a soil column demonstrated that the technique can measure the transport of organics through the subsurface. A second subtask provided a high speed, field deployable method for analyzing ground and surface waters for environmentally significant organic and inorganic cations and anions. This subtask provided a real-time monitor for water samples, which can also be set up for unattended operation to monitor levels of specific contaminants. This system is rugged and easy to use, and has advantages in time and cost over traditional water analyses. Part per billion (ppb) sensitivity with real time analysis and no sample preparation was demonstrated. A third subtask established a pathway to use IMS in the field for monitoring chlorinated hydrocarbon compounds. Although IMS is an attractive instrument for monitoring volatile organic species in a number of media, its use has been hindered by the difficulties in speciating various chlorinated hydrocarbons. Nevertheless, this subtask provided a mechanism by which IMS can successfully identify chlorinated organics in real time without the use of gas chromotagraphy. It also suggests a potential path where IMS can be used for other problematic analytes through the study of the ionization mechanisms and manipulation of the chemistry involved in producing desired product ions.

- The task, "Nondestructive Assay (NDA) Science and Technology Proof-of-Concept Testing for Environmental Characterization and Stewardship", advanced NDA detection capability for both nuclear and non-nuclear materials in soils and waste containers. Tests with AXRF techniques detected uranium and heavy metals representative of the Radioactive Waste Management Complex (RWMC) Subsurface Disposal Area (SDA) in soil columns at concentrations below 100 ppm. Three-dimensional images were formed of the rotating soil column to determine spatial resolution using the XRF technique, and it was found that the linear resolution was less than 3 mm. Proof-of-concept was demonstrated for using the Advanced Data Validation and Verification System (ADVVS) software to monitor the operation of accelerator-based systems in subsurface science research and applications, in conjunction with the Idaho Accelerator Center (IAC) at the Idaho State University (ISU). The ADVVS software, a multivariate analysis software package, was updated for the subsurface science research. Finally, extensions to the NDA Data Review Expert System (NDA-DRXS) were implemented and, when deployed, the complete system will improve

the throughput of waste containers at the INEEL's Stored Waste Examination Pilot Plant (SWEPP) and the consistency and quality of the data review process. Debris rule requirements were specified and the debris rules were manually produced, thus extending the applicability of the NDA-DRXS with respect to the types of waste streams encountered at the SWEPP facility.

- In the task, "Assessment of Mercury Environmental Fate and Transport from INEEL Waste Processing Facilities for Long-term Stewardship Concerns and Development of Improved Modeling Methods," analysis of samples in and around the INEEL site show that mercury emissions from the INEEL calciner (and other EM high level waste treatment operations) over the past 36 years have not raised regional off-INEEL mercury contamination levels above normal background.

- The task, "Complex Systems Theory Applied to Subsurface Transport", improved conceptual models for contaminant transport in the vadose zone by demonstrating that traditional deterministic models overlook critical aspects of dynamic behavior. When comparing several vadose zone transport models, the data suggest a common emergent property for vadose zone transport—small volumes of relatively high concentrations (compared to center-of-mass calculations) of contaminants travel faster routes. A series of small-scale (1-meter) infiltration pond tests conducted over a fractured basalt ledge in the Hell's Half Acre (HHA) lava field during 1998 and 1999 (and analyzed under ESRC) show highly variable flow rates, unrelated to the water head in the infiltration pond. Evaluation of the data set for the existence of chaos did not determine whether the system was chaotic because of problems associated with an integrate-and-fire data set. The task developed and evaluated a promising numerical tool for screening time series data sets for nonlinear behavior. The task also developed an approach for building a theoretical model of the HHA experiment that will capture the dynamical behavior of the system without the inherent problems of short, noisy data sets. The team performed the first two steps for determining whether the governing equations of vadose zone flow and transport*, which relate in nonlinear fashion,* will act to generate chaotic, nonlinear dynamics. This line of research continues under the ESRA program in FY2002.

- The task, "Unified Hydrogeophysical Parameter Estimation Approach to Subsurface Contaminant Transport, " began the integration of geophysical tomography with hydrological state variable data to better describe flow and transport parameters in the earth's subsurface. This will lead to a better understanding of the functional relationship between specific geophysical and hydrogeophysical parameters, and ultimately contribute to more accurate modeling of contaminant transport in the subsurface. A 3-D level set inversion algorithm was developed through collaboration with the NSF Center for Subsurface Imaging Systems (CenSSIS) at Northeastern University, and was partially evaluated through imaging a controlled laboratory experiment. This inversion technique will be useful in defining boundaries of electrically contrasting subsurface media. Such a technique will be valuable for defining geologic boundaries in the subsurface, plume shapes, and buried waste pit extents. Capabilities at the INEEL have been enhanced through the purchase of Electrical Resistivity Tomography (ERT) data collection equipment, acquiring a state-of-the-art ERT Occam inversion code, and establishment of procedures to accurately obtain and process the ERT data. This line of research continues under the ESRA program in FY2002.

- The task, "Computing Framework for Environmental Cleanup, Restoration, and Long-Term Stewardship" increased the total environment data transfer rate in/out of the INEEL by a factor of 30 and improved the maximum onsite processing rate for environmental calculations by a factor of 10. The task purchased and installed a new Silicon Graphics Incorporated (SGI) 64 processor Origen 3800 computer with associated disk and tape storage systems. It also implemented a DS-3 line (45 MB/s) to Idaho State University (ISU) and from there to the Internet2 Abilene network. In

cooperation with INEEL Information Resource Management, this task also coordinated the installation of a new 45 MB/s DS-3 line to DOE's energy sciences network (ESNet), through which INEEL researchers are now able to transmit large data files, access high-end computing resources, and collaborate with researchers at other DOE national laboratories. These activities have led to significant improvements of the EM-focused computing infrastructure at the INEEL. The base of regular users of high-performance computing at INEEL has increased by a factor of three as a result.

¢# The Advanced Decontamination and Decommissioning System tasks start with the Decontamination, Decommissioning, and Remediation Optimal Planning System (DDROPS), a computer planning system previously developed at the INEEL that allows an operator to model a facility for remediation preplanning and waste minimization. The work completed included: (a) completion of optimal tank cutting optimization; (b) modeling of the evaporator pit at the INEEL TAN-616 facility, which is slated for decommissioning soon; (c) development of a method to calculate and visualize (in three dimensions [3-D]) radiation fields and worker paths through radiation fields, thereby helping to minimize exposure; and (d) initiation of integration of portions of DDROPS (radiation visualization, optimization, 3-D modeling, radiation calculations, etc.) into one coherent package. The Robotic Waste Packaging System (RWPS) performs the material handling, optimal waste packaging, and sorting/recycling steps of the D&D process. Several subtasks were completed: (a) The design of the material handling station and a vision system was completed—the vision system software uses depth, color, and edge detection to discriminate overlapping/adjacent objects specified by an operator; (b) Collaboration with the University of Utah (USU) established basic 3-D packing algorithms—the 3-D packing algorithm could pack a 3-D bin at 85–95% efficiency depending on the size of the boxes being packed; (c) Designed, built and tested a low-profile z-mast that would be appropriate for deployment in a semi-trailer—this is the only z-mast that would allow deployment of an xyz robotic arm system in a trailer while leaving enough room for the waste containers. This low-profile z-mast design is also being used by the HANDS-55 project. The Waste Characterization and Sorting System (WCSS) supports material identification and characterization, sorting and recycling during the disassembly process, and accurate documentation of waste containers. The work completed included hardware assembly and software development. The gamma spectroscopy unit was mounted in a box on the scanning bed and is integrated into one cable from the various instruments. A laser scanner was included at the start of the conveyer belt and a camera attached to take pictures of the waste item as it is transported on the belt. The software development was completed to allow automated calibration, computerized self-testing and data storage for producing accurate waste manifests. Initial system testing was completed, and the system is ready for system operability testing for a particular application.

Research Description

The rest of this document describes the individual research tasks. These descriptions are grouped under the four research areas described above. Figure 3 shows the areas on the INEEL where research tasks are being conducted.

ANL-W	Argonne National Laboratory - West
CFA	Central Facilities Area
INTEC	Idaho Nuclear Technology and Engineering Center
NRF	Naval Reactors Facility
PBF	Power Burst Facilities
RWMC	Radioactive Waste Management Complex
TAN	Test Area North
TRA	Test Reactor Area
WROC	Waste Reduction Operations Complex

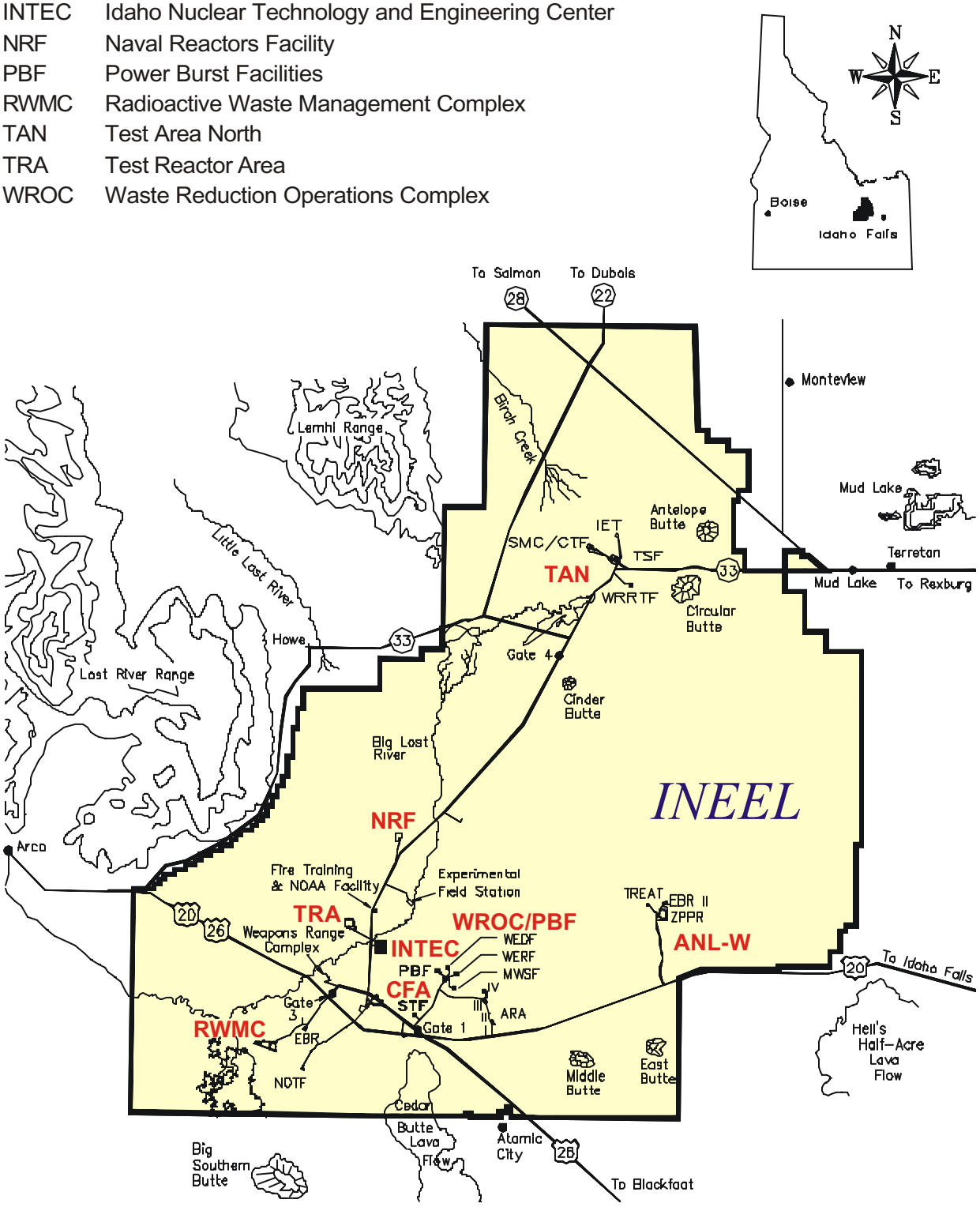

Figure 3. Map of the INEEL showing major facilities.

Science and Technology for Environmental Characterization

DOE needs sound scientific data so it can make sound decisions about our environment. This requires reliable chemical and biological data from air, water, and land. The research tasks in this section were chosen because they will provide the best possible science and technology available to characterize the environment. The research methods used in these tasks include mechanical, electrical, chemical, and mocrobiological techniques, and the use of robotics, modeling, enzymes, and other innovations.

Of special concern is the need to locate, identify, and quantify hazardous materials (certain organics, heavy metals, and radioactive isotopes) that have the potential to poison transient environments, such as the atmosphere or groundwater. A special emphasis in this work is the study of the subsurface, which has been inherently difficult to characterize. In all aspects of this work, the goal is to improve the acquisition, processing, interpretation, and use of environmental data.

The following tasks are reported in this section:

- Ion Mobility Spectroscopy for Environmental Monitoring and In Situ Measurement of Hazardous Organics
- Nondestructive Assay Science and Technology Proof-of-Concept Testing for Environmental Characterization and Stewardship
- Isobaric Groundwater Well for Precise Water Level Measurement Relevant to Long-Term Surveillance and Stewardship
- Assessment of Mercury Environmental Fate and Transport from INEEL Waste Processing Facilities for Long-Term Stewardship Concerns and Development of Improved Modeling Methods
- Advanced Robotic Technologies for Remote Environmental Surveillance and Stewardship
- Secondary Ion Mass Spectromety Characterization of Environmental Microbial Processes
- Biologically Based Catalysts as Sensors to Detect Contaminants in Harsh Service Environments
- Molecular Engineering and Genomics for Development of Environmental Biosensors Using Robust Biocatalysts
- Determining Soil Moisture Over Wide Areas for DOE Site Stewardship Hydrology
- Using Environmental Records in Mid-Latitude Glacier Ice to Better Define Environmental Management Contaminant Inputs to the Subsurface

Ion Mobility Spectrometry for Environmental Monitoring and In Situ Measurement of Hazardous Organics

Enhancing Environmental Chemical Data Gathering and Analysis In the Field

David A. Atkinson, Robert G. Ewing, and Keith A. Daum (INEEL); Herbert H. Hill (Washington State University); Gary Eiceman (New Mexico State University)

SUMMARY

Environmental monitoring scenarios often require considerable chemical analyses to monitor contaminant levels and define transport and exposure potential. Long-term stewardship of federal lands entails extensive chemical monitoring and characterization. The costs and operational complications involved in this process can be staggering. Advanced chemical analysis technologies are needed to reduce the burden of characterization and monitoring. Ion mobility spectrometry (IMS) is a field proven, sensitive, rugged, portable detection device able to detect a wide variety of trace organics. IMS characterizes chemicals by their behavior in an electric field. Many difficult environmental monitoring challenges involve getting high quality analytical field data with high sample throughput. IMS is well suited to this, and can provide high speed, high quality data while deployed at the problem site. The flexibility of the IMS inlet can be exploited with a variety of analytical sample types, including ambient air samples, soil gas samples, groundwater samples, and organic waste samples. This task further develops IMS technology such that it will become a tool of choice for onsite analysis.

This research project focused on developing IMS for onsite/in situ environmental detection in soil and water and for more efficient detection of chlorinated organic compounds—contaminants of significant interest at the INEEL and across the DOE complex. Exploiting the capability of IMS should create a powerful tool for environmental management (EM) that is faster, less expensive, and more accurate than existing detection and analysis methods.

TASK DESCRIPTION

This project consisted of three major subtasks focused on using IMS as an environmental monitor with emphasis on onsite or in situ monitoring.

Monitoring Volatile Organic Transport Using a Miniature Field Asymmetric Waveform IMS Sensor

The objective of this subtask was to develop a miniature field asymmetric waveform IMS (FAIMS) sensor for monitoring the transport of volatile organic vapors through soil. FAIMS, a relatively new technique, is a variation of traditional IMS. FAIMS operates with a high-voltage, high-frequency asymmetric waveform between parallel plates. A stable ion trajectory between these two plates is established with a compensating direct current (dc) voltage. Ions with varying mobility under these conditions require different compensating voltages to obtain a stable trajectory and reach the detector. Thus, a spectrum is obtained by scanning this compensation voltage and monitoring ion current. The advantages of this sensor over those of conventional IMS are sensitivity gains achieved due to the absence of an ion shutter, and anticipated reduced instrument size, since the actual sensor is approximately 25 mm

in diameter. Current size limitations are due to supporting electronics. With the sensitivity and size of this sensor, it is envisioned as an ideal tool for monitoring specific volatile organic compounds downhole. This monitoring could allow for mapping of the underground transport of organic vapors and provide data to support transport modeling efforts. For this subtask, the INEEL collaborated with New Mexico State University to develop the proof-of-concept sensor for soil monitoring.

The use of ion mobility spectrometry as a modern analytical method for environmental sensing has historically been limited to widespread in-lab applications because of the high cost of instruments, particularly drift tubes, where ion formation and separation occurs. Where cost has not been as important, such as in chemical agent detection and explosives screening, traditional drift tubes have served well and demonstrated the intrinsic advantages of IMS principles. Today, however, the advent of micromachined, mass produced, low cost, nearly disposable drift tubes have altered this condition, making it possible to exploit the intrinsic advantages of IMS. In this task, a microscale drift tube has been characterized for response toward halocarbons, including those found as waste solvents in DOE facilities. Further, laboratory trials using columns of soil have been completed with the development of a membrane inlet that prevents fouling of the drift tube with particulate matter found in soils and drilling operations.

Until recently, miniaturization of IMS drift tubes had been considered unpromising because conventional ion injection schemes lead to losses in resolution with small drift tubes, and because unacceptably high noise is created through microphonics in the aperture grid detector. This noise obscures the extra low signal levels found in drift tubes of reduced dimensions. In spite of these barriers, a few small drift tubes have been successfully demonstrated on the miniature scale by several teams (U.S. Army at Edgewood Research Development and Engineering Center[1] and Oak Ridge National Laboratory[2]). The concept of a microscale drift tube was proposed by a team in Germany,[3] and New Mexico State University researchers described a micromachined drift tube based on the Radio Frequency (RF)-IMS method in 1999.[4] In this microanalyzer, the drift region had rectangular dimensions of 30 Δ 10 Δ 20 mm. In the FAIMS design, the ion shutters, voltage dividers, and aperture grids are eliminated from the drift tube, which greatly simplifies the complexity of drift tube fabrication. Ions are carried through the drift region using a flow of gas and ion trajectories between parallel plates, which are proscribed by ion interactions with a high voltage, oscillating, electric field. Mobility becomes field dependent under the RF field in contrast to the low field regimes used in conventional IMS drift tubes. A second electric field (a weak dc voltage) is superimposed on the high voltage RF waveform. The dc field may be between 0 and 400 V/cm and the peak amplitude of the RF field is ~25,000 V/cm with a frequency of 1.2 MHz. The fields are said to be asymmetric since the portion of the RF waveform at high voltage is shorter than that at low voltage. These fields are applied perpendicular to the carrier gas flow direction in the drift region, and only certain ion species will reach the detector at the end of the drift tube, as governed by the dc field for a given RF field. Previous studies on the role of the high fields on ion behavior[5–10] have illustrated that the RF method is a plausible tool to characterize organic ions of all sizes.

In a FAIMS drift tube, ions are transported through a drift region by a carrier gas flow while an RF electric field is applied to plates in the drift region that are spaced by 10 mm. This field is 90 degrees to the gas flow and causes the ions to oscillate in a direction transverse to the carrier gas flow. The amplitude of the RF waveform under high field conditions is >10,000 V/cm and the ion is moved rapidly toward the top plate (or electrode). In contrast, the ion under the low field portion of the RF waveform (~100 V/cm) moves toward the bottom plate at a comparatively slow velocity, which draws the ion toward one plate by a net amount ÷h for each RF period. The average value of ÷h for an ion species is determined by the duty cycle of the RF field and the field dependence of the mobility K(E). Thus, the total displacement of the ion in space is n÷h as governed by the number of RF periods, wherein ion separation occurs, which can also be understood as a differential mobility analysis ($K(E) - K_o$). The resultant motion in the drift region appears to be specific to each ion species, though this requires further investigation.

Only ions with a total transverse displacement less than the drift region width will reach the detector; all other ions will collide with drift tube wall (or plates). These ions are neutralized or annihilated and removed from the drift region in the gas flow. Ions of a given kind can be kept from striking the plates (allowing a stable passage to the detector) by applying a low voltage dc field to the ion plates in opposition to the net RF-induced transverse motion of the ion. A sweep of compensation voltage will provide a measure of all the ions in the analyzer and results in a RF high field mobility spectrum. In traditional low field IMS, ion mobility are reasonably well described through the Mason-Schamp equation[13] and reduced mobility constants (Ko) are related to reduced mass and cross section areas for ion molecule collisions where ion mobility are independent of electric field. In contrast (part of the time for ion drift), the ion experiences high fields and mobility that are field dependent. The RF field interacts with ions in ways that allow ion separations based on ion molecular interactions, which are not available for use in low field (or time-of-flight) mobility spectrometers. Thus, some intractable challenges for ion separation in time-of-flight IMS analyzers are easily resolved in the FAIMS drift tube.

The setup and testing of the system for this subtask was done by Professor Gary Eiceman's laboratory at New Mexico State University, under subcontract to the INEEL. The FAIMS sensor cell is illustrated in Figure 1. The initial studies looked at the environmentally important hydrocarbons benzene, xylenes, and toluene, as well as a suite of chlorinated hydrocarbons. Figure 2 illustrates toluene response at sub-ppm levels for a number of different concentrations. Photoionization is used, since hydrocarbons such as toluene do not respond well with traditional beta decay driven ionization processes. The use of photoionization can provide a response to many analyte groups that respond poorly in traditional IMS. Figure 3 illustrates the area and height response curves to the various toluene concentrations. The response is strongly linear over the concentration range studied. Figure 4 demonstrates the separation power of the prototype FAIMS system. Mixtures of benzene/acetone as well as toluene/acetone were evaluated. Baseline resolution between all components was achieved. This is a difficult separation in conventional time-of-flight IMS, but easily resolved using the FAIMS technique. IMS is traditionally considered a fairly low resolution technique (especially in comparison to other analytical techniques such as gas chromatography (GC) and mass spectrometry), however, the FAIMS device offers much promise in this area. Figure 5 further illustrates the separation power of the FAIMS. An analysis of a mixture of the three xylene isomers is shown for both conventional time-of-flight IMS and the FAIMS. The rightmost peaks in the conventional IMS system correspond to the xylene isomers; it can be seen that no separation is achieved. The peaks to the left in the conventional IMS spectrum correspond to the reactant ions, which are developed from the ionization of the air bath gas. In the FAIMS spectra, the m-xylene isomer is well resolved from the ortho- and para-isomers. There is no separation between the ortho- and para-isomers. Given that IMS separates based on the charge, size, and shape of molecules through collision processes, it is no surprise that these isomers are difficult to separate.

To insure response to authentic compounds and preclude the interference from impurities, first studies were based on a gas chromatograph IMS drift tube instrument where the heart cut of the GC elution profile allows best reliability for documenting response. A GC inlet also allows convenient handling of samples quantitatively and collection of response for several compounds in a single experiment. Results for halocarbons are shown in Figure 6 for a GC/IMS experiment with the chromatogram shown in the right frame. The frames labeled cation and anion are the topographic plots of the FAIMS scans for positive and negative ions respectively. The findings demonstrate that the halocarbons exhibited positive and negative product ions and that these ions were distinctive of each chemical. The solvent peak at 50-seconds elution time was methylene chloride.

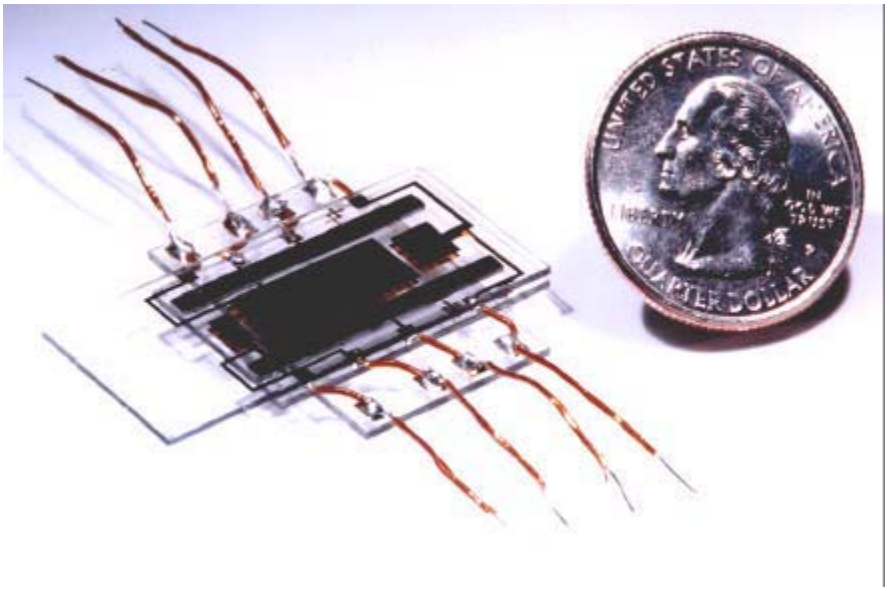

Figure 1. Photograph of FAIMS sensor cell typical of that used for the project.

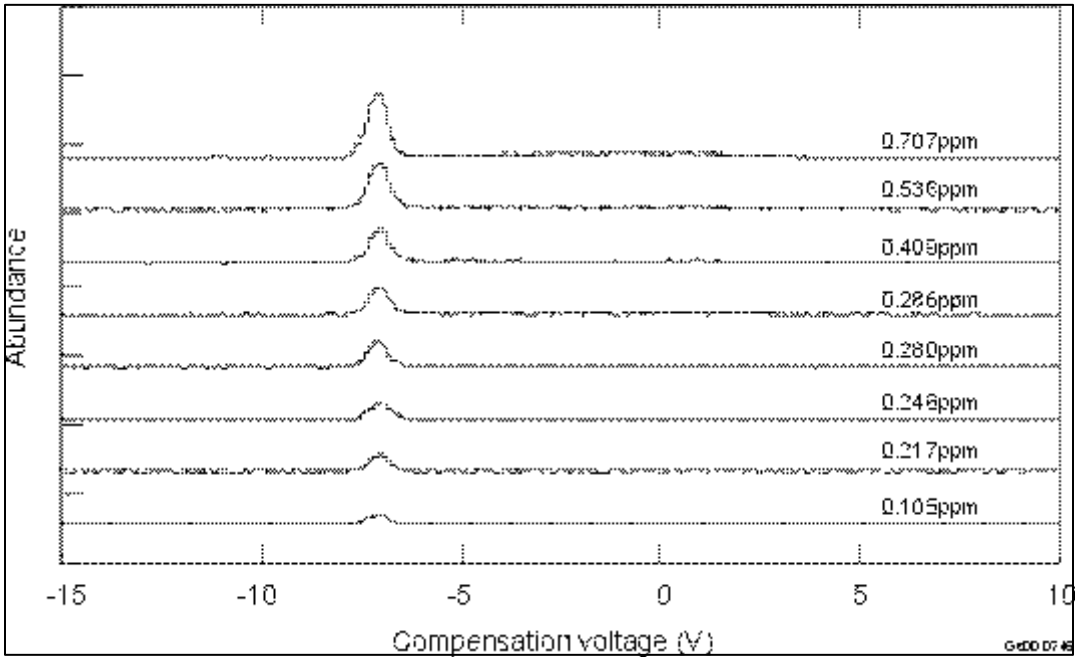

Figure 2. FAIMS spectra for toluene at varying concentrations.

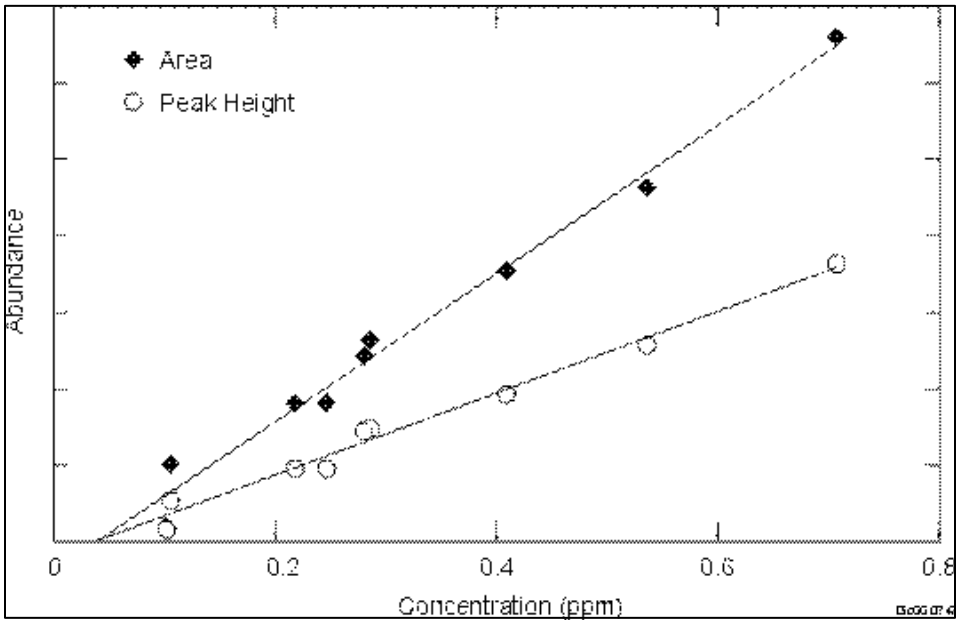

Figure 3. Toluene response curves.

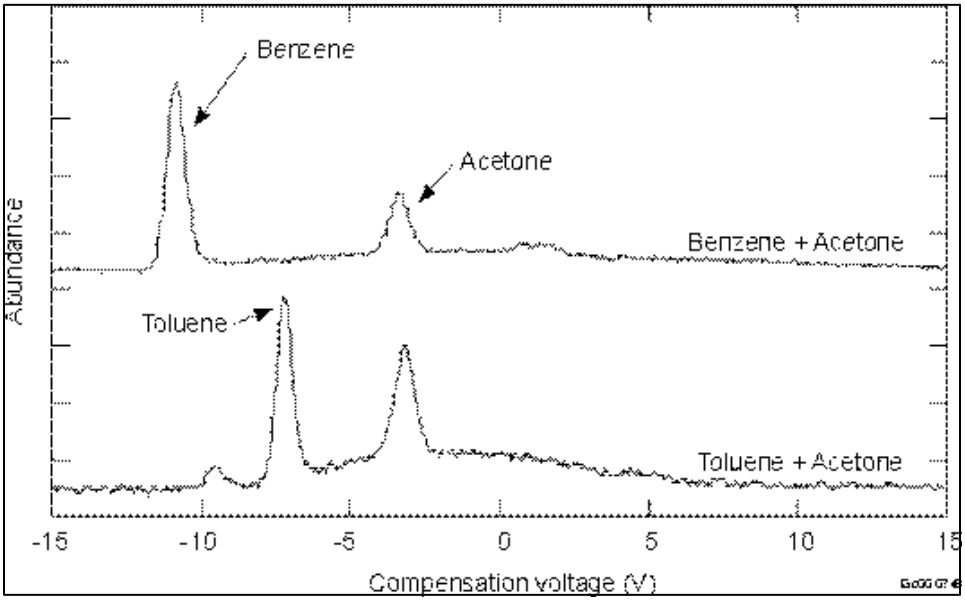

Figure 4. Separation of benzene/acetone and toluene/acetone mixtures.

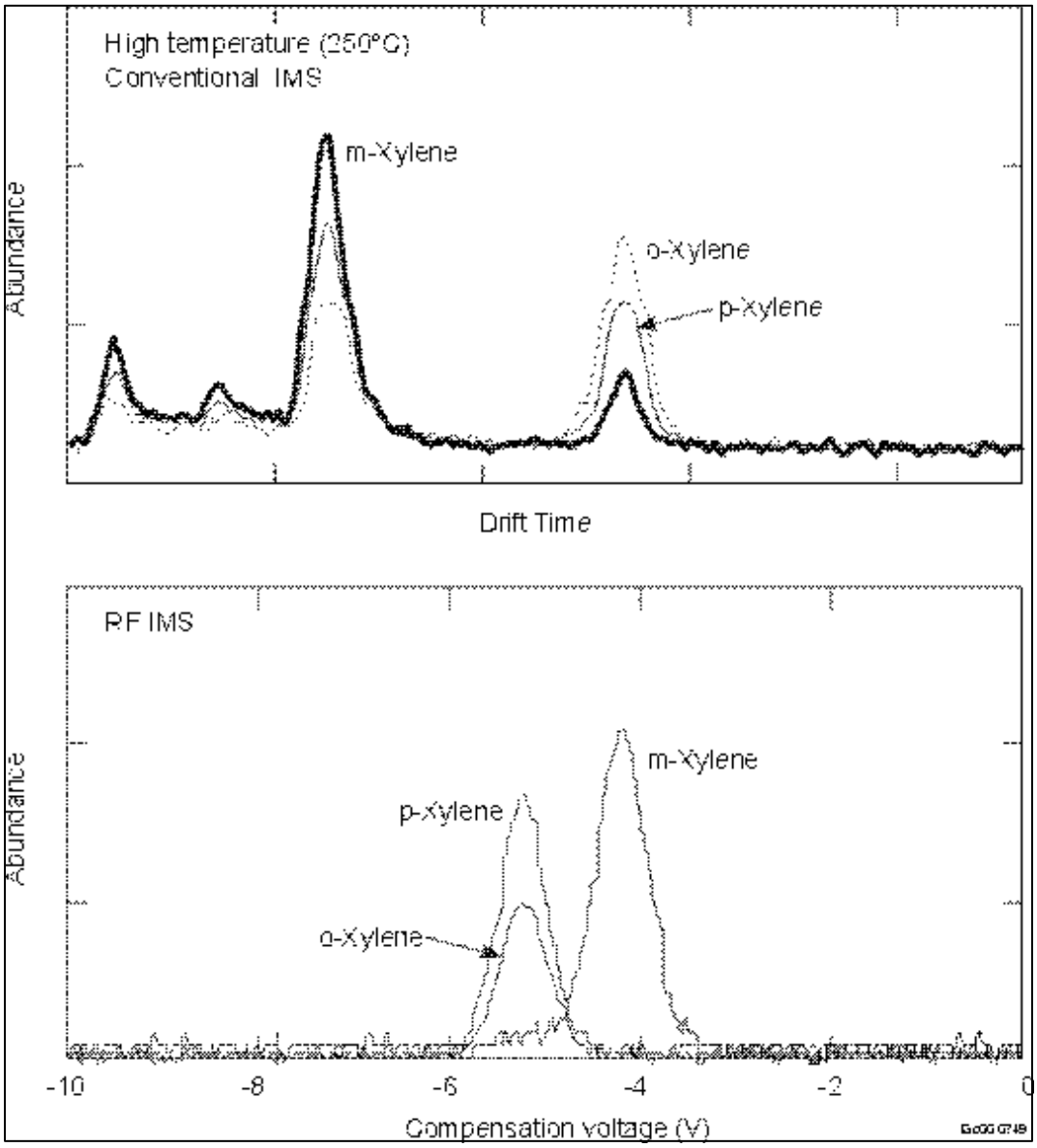

Figure 5. Comparison of xylene isomer separation in different IMS systems.

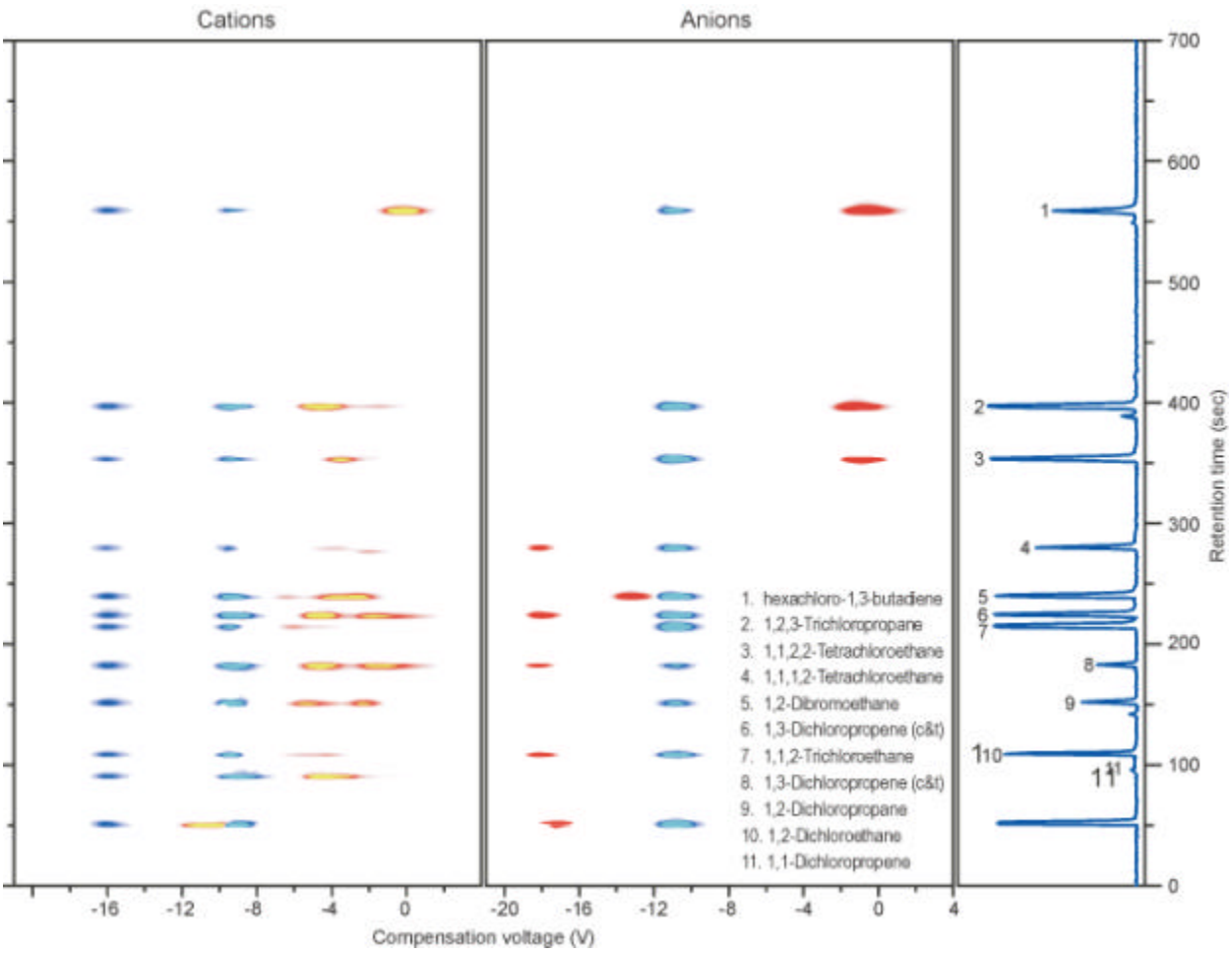

Figure 6. GC/FAIMS data from 11 chlorinated hydrocarbons.

The FAIMS scans for these compounds are shown in Figure 7. These scans clearly show the distinctive profiles as positive ions. Consequently, a single IMS sensor should be sufficient to distinguish chemicals without a chromatographic inlet in instances of uncomplicated waste mixtures. Complex mixtures will provide the spectra of nonlinear composites of all chemicals, or a total halocarbon response. Results from these spectra are shown in Table 1. The ions in negative polarity showed principally the dissociated product Cl^4 though large halocarbons also exhibited a clustered product ions (see hexachloro-1,3,-butadiene). Since positive and negative ion information are obtained simultaneously, both polarities are available for use in analytical measurements.

Quantitative response for halocarbons was made using negative polarity with the Cl^4 ion as shown in Figure 8. The limits of detection were commonly in the 10 to 20 pg without sample preconcentration in a flow of 2 L/min. Improved limits of detection can be envisioned with optimized flow rates or even mild preconcentration. Linear ranges at present are narrow, but are well known for beta sources operated in the null to saturation ranges. The range of response is widely distributed without a particular pattern evident with the number of halogens as might be expected from electron capture detectors.

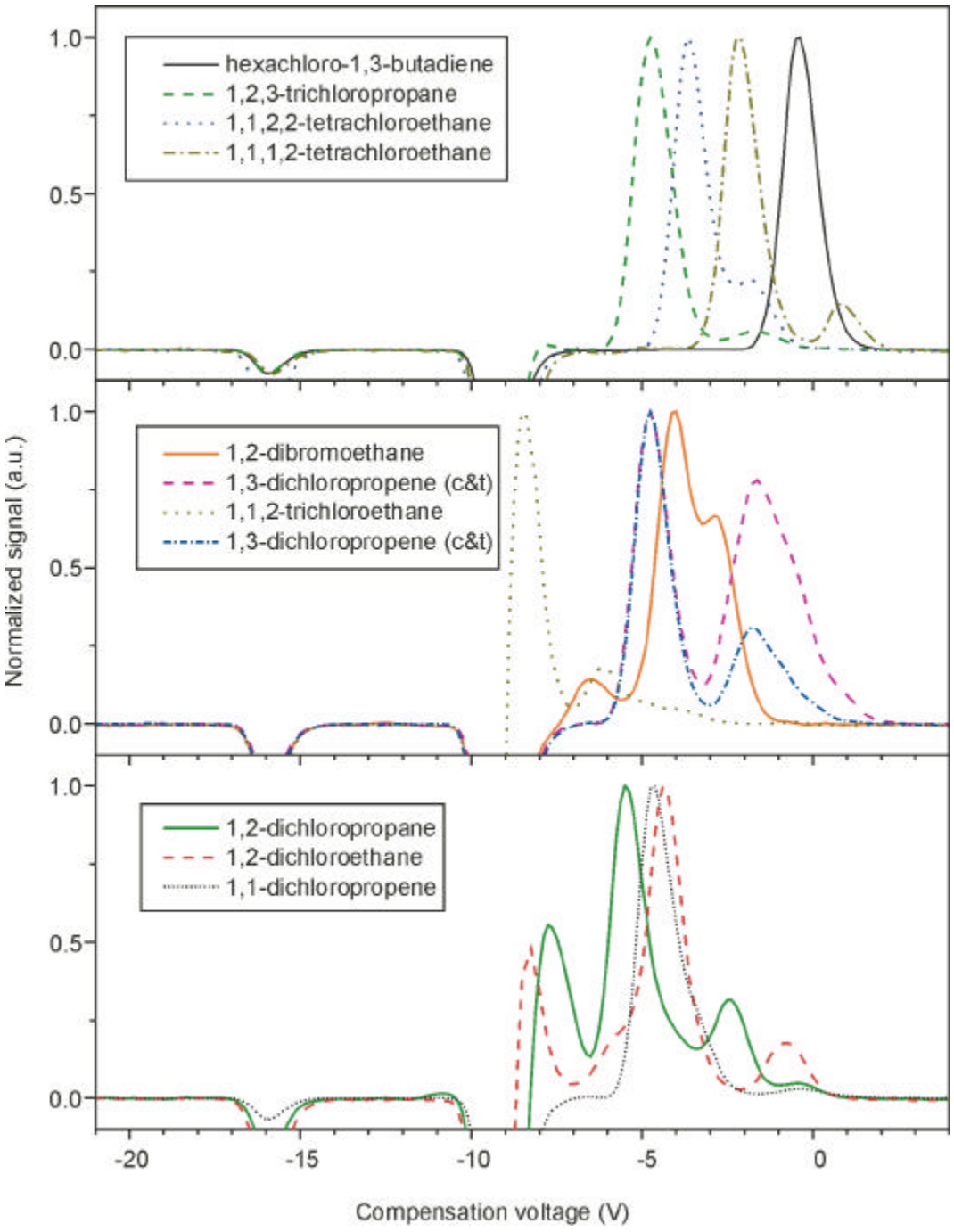

Figure 7. FAIMS positive ion spectra for chlorinated hydrocarbons.

Table 1. Results from separation of halocarbons using GC with miniature RF-IMS analyzer.

Compound	Retention Time, s	H mm	Peak Maximum from RF-Mobility Scan V_{dc}	LOD, pg (S/N=2)	Linear Range, ng	Asymmetry Factor ν
1,1-Dichloropropene	172	0.59	44.66; 40.3	100	—	2
1,2-Dichloroethane	190	0.48	44.34; 40.76	90	0.09–4	2
1,2-Dichloropropane	233	0.32	45.5; 42.4	200	0.2–7.2	2
1,3-Dichloropropene (trans)	264	0.17	44.78; 41.8	1,000	1–8	1
1,1,2-Trichloroethane	296	0.46	48.4; 46.17	34	0.03–1.2	3
1,3-Dichloropropene (cis)	305	0.19	44.78; 41.8	33	0.03–1.9	2
1,2-Dibromoethane	321	0.4	46.52; 44.0; 42.8	26	0.02–7	3
1,1,1,2-Tetrachloroethane	361	0.13	42.16; 40.88	130	0.13–4.9	2
1,1,2,2-Tetrachloroethane	435	0.22	43.62; 41.66	10	0.1–1.3	3
1,2,3-Trichloropropane	478	0.09	44.74; 41.6	14	0.1–5.2	1
hexachloro-1,3-butadiene	640	0.1	40.44;	40	0.4–5.5	1.5

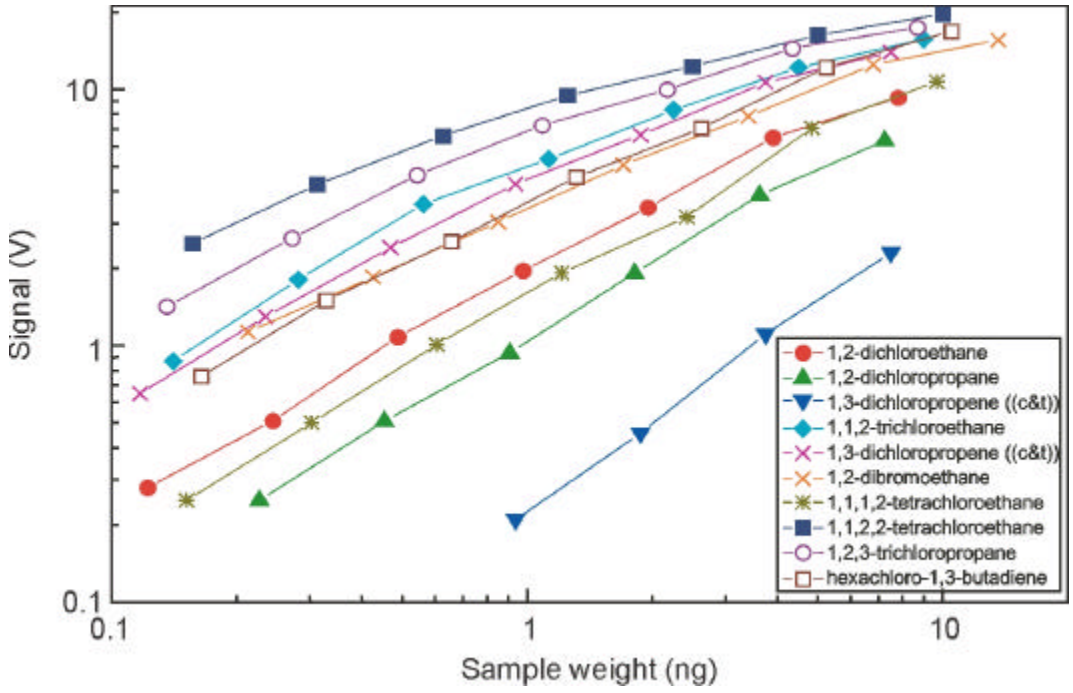

Figure 8. Response curves using micro FAIMS for halocarbons.

We tested the FAIMS system for subsurface monitoring by injecting halocarbon samples through a syringe in the amounts of 0.2–0.5 mL to avoid signal saturation. A short column (i.d. = 3 mm) filled with bentonite mineral was used as a test bed to simulate contaminant transport. The column was kept at 55∀C to reduce the experiment time and purged with dry air at a rate of 50 ml/min. The output air from the column was directly introduced to a membrane interface inlet for transport monitoring measurements.

The membrane interface to the FAIMS sensor consisted of a 10-cm-long silicone tube (Dow Corning). The unit was kept at 50∀C to facilitate samples diffusion through the membrane. The FAIMS ion source was heated to 50∀C to shift equilibrium from clusters toward Cl^{4} anions, so that all halocarbons resulted in a single signal of Cl^{4} anion. Transfer time through the membrane depended on the chemical studied and varies from approximately 10 sec for methylene chloride to 1–2 min for 1,1,2,2-tetrachloro-ethane. Figure 9 illustrates the breakthrough curves from the column for three halocarbons.

In this project, the FAIMS microdrift tube exhibited response properties suitable for environmental field monitoring for a broad range of halocarbons. The combined properties of simultaneous detection of positive and negative ions offers good detection limits (negative polarity) and specificity of response (positive ions). Alternatively, the sum of all negative response could be a total halocarbon monitor. The device, successfully deployed in a simulated contaminant transport scenario, provided exciting results.

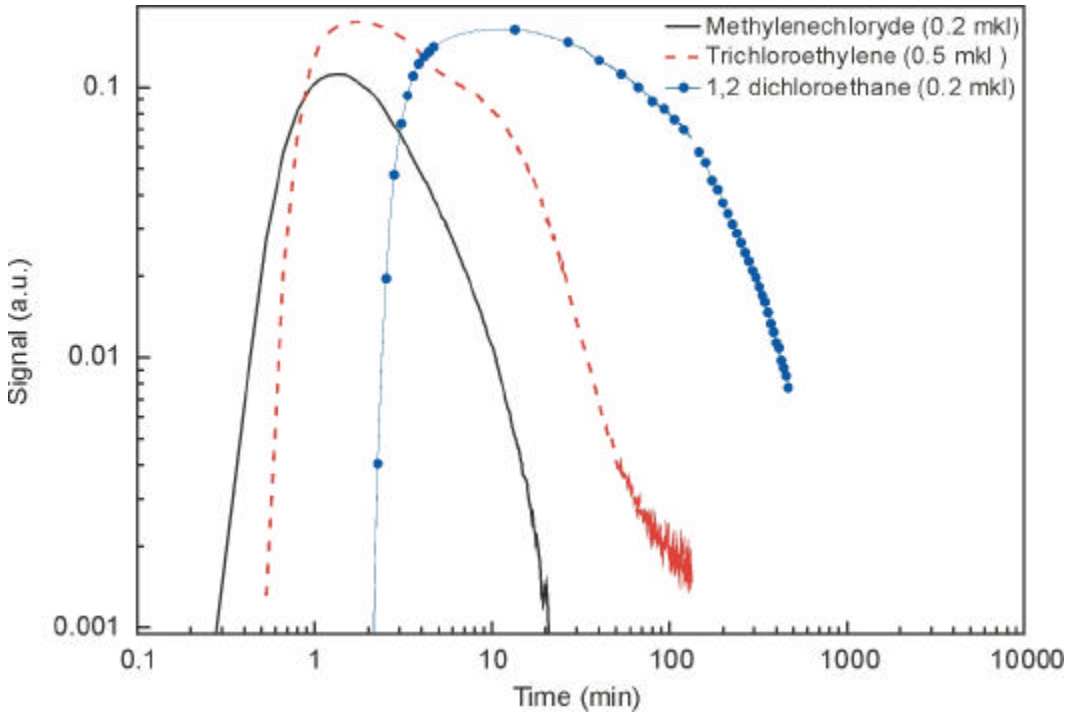

Figure 9. Soil column breakthrough curves for three halocarbons measured using FAIMS.

Electrospray Ionization/IMS for Surface and Groundwater Monitoring

This subtask involved the development of an electrospray ionization (ESI) front-end to ion mobility spectrometry for a high speed detection system for organic and inorganic pollutants in environmental water samples. The ESI source can directly inject environmental water samples into an ion mobility spectrometer system for analysis. This combination provides a sensitive, rugged, and high throughput direct water analysis system that requires essentially no sample preparation. This device can be packaged

into a portable format, for deployment in the field. The INEEL and Washington State University (WSU) collaborated on the assembly of a prototype instrument from existing WSU equipment. Figure 10 shows the schematic diagram of the ESI/IMS system that was used.

Elevated nitrogen species present in groundwater due to fertilization practices cause concentration in water to reach unhealthy levels, which can cause a variety of health problems including one type of cancer,[12] and alter the ecology of soils and plant systems.[13] In addition, the conversion of nitrate to nitrites imposes elevated health risks due to the increased toxicity of nitrite.[13] For these reasons, a rapid and sensitive method of determining nitrate and nitrite concentrations in aqueous samples is desired.

Analytical methods that can measure low levels of nitrate and nitrite directly from aqueous samples would aid in identifying the contaminated water areas. In this research, ESI coupled with IMS was employed for direct water analysis of nitrate/nitrite. IMS offers several advantages for water analysis including portability and good sensitivity. Employing ESI as an ionization sources enables the direct analysis of aqueous samples. Previous studies from this lab showed that water samples obtained from several natural water reservoirs were easily analyzed without any sample preparation. In this way, ESI/IMS offers a technique that can be used to rapidly (under 1 second) separate the species of interest, which we expect will greatly improve the sample throughput over current techniques.

The lack of field-based methods for detecting polar and ionic compounds has resulted in a poor understanding of these compounds in soil and aqueous environments. The information that is available for these compounds has been obtained at considerable expense. The reasons that rapid, field-based methods for polar and ionic compounds do not exist are complex, but are primarily due to the water solubility of these compounds. Because of the polar and ionic nature of these compounds, they are difficult to extract from aqueous samples. Gas chromatography has been developed for field analysis, but is best suited for nonpolar, volatile compounds. Samples dissolved in water are difficult to inject efficiently onto a gas chromatographic column. One approach for the determination of polar and ionic compounds is to derivatize the analyte by blocking the polar moiety—decreasing the solubility of the compound in water and increasing its volatility for GC analysis. The most common approach for the determination of polar and ionic compounds is by liquid chromatography. Liquid chromatographic methods are slow, cumbersome, and not sufficiently sensitive for many field applications.

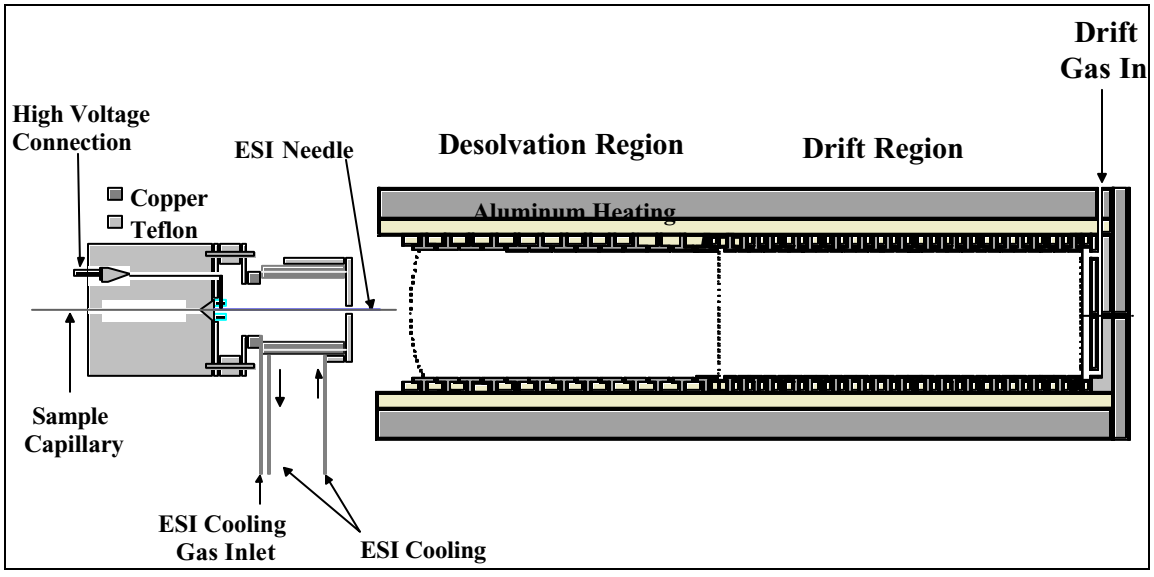

Figure 10. ESI/IMS schematic diagram.

In this work, initial IMS studies of ions in aqueous based standards focussed on cations, due to the stability and ease of development in the positive mode. Negative mode electrospray has proven to be more difficult, and less stable. Thus, it was more expedient to develop the initial methodology in the positive mode for cations before moving over to explore anions. After the initial setup of the electrospray IMS system, the instrument parameters were adjusted to provide optimal response to the cations being studied. Figure 11 illustrates the electrospray IMS response to lanthanum and strontium chloride. The bottom spectrum in the figure is a mixture of the two salts. The product ion peaks in the mixture match the individual peaks from the standards, demonstrating the utility of the technique in separating cations within a very short analysis time. A similar separation using a standard method, such as ion chromatography, would take 5 to 10 minutes. This separation using IMS takes place in milliseconds. Separation of the cation species is fairly easy to achieve directly from a water sample with minimal sample preparation.

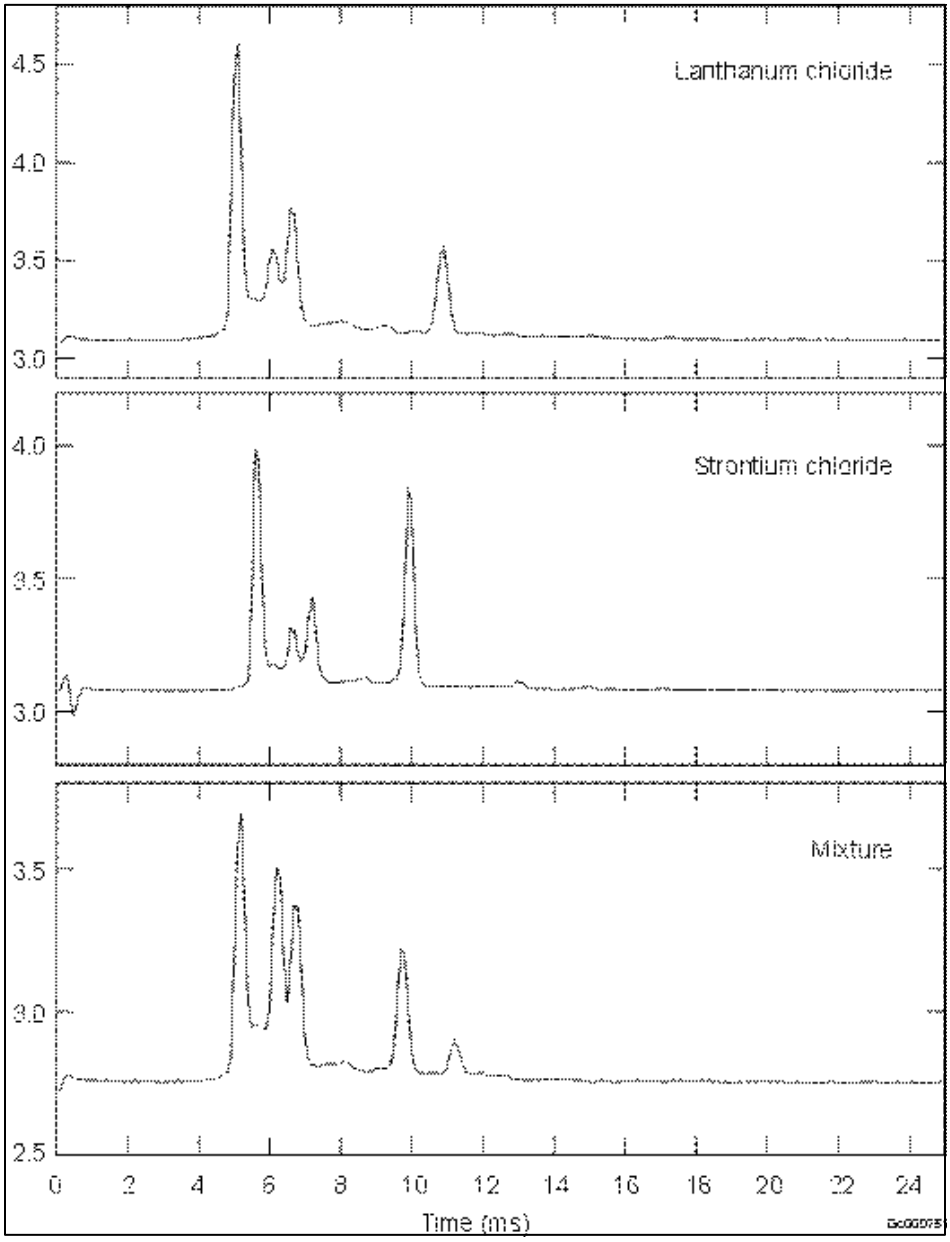

Figure 11. Lanthanum/strontium electrospray IMS spectra.

Figure 12 shows the electrospray IMS spectra for uranyl acetate and uranyl nitrate from aqueous solution. There is a difference in the product ion peak position, suggesting that the cation is different, even though both samples are uranyl species. This suggests that the counter ion has an effect on the product ion identity, most likely through effects on clustering. This phenomenon will need to be studied in more detail, including IMS/mass spectrometry data. However, the fact that an ion signal from a large cation such as uranyl ion shows the immense promise of electrospray IMS as a technique for measuring specific cations directly from water solutions. Figure 13 demonstrates a separation of phosphonic acid compounds in water solution. The product ions are most likely water clustered cations from acid species.

Negative mode electrospray IMS is more difficult due to signal instabilities and the electrical arcing that takes place. Figure 14 illustrates a spectrum containing a mixture of explosive compounds done via negative mode electrospray IMS. There is excellent separation among the five compounds (nitrobenzene; 2,4-dinitrotoluene; 2-amino-4,6-dinitrotoluene; 2,4,6-trinitrotoluene; and 1,3,5-trinitro-benzene). Again, IMS provides a high speed (millisecond) separation that would take up to 20 minutes via a standard method such as EPA 8330 or a high performance, liquid-chromatography-based method.

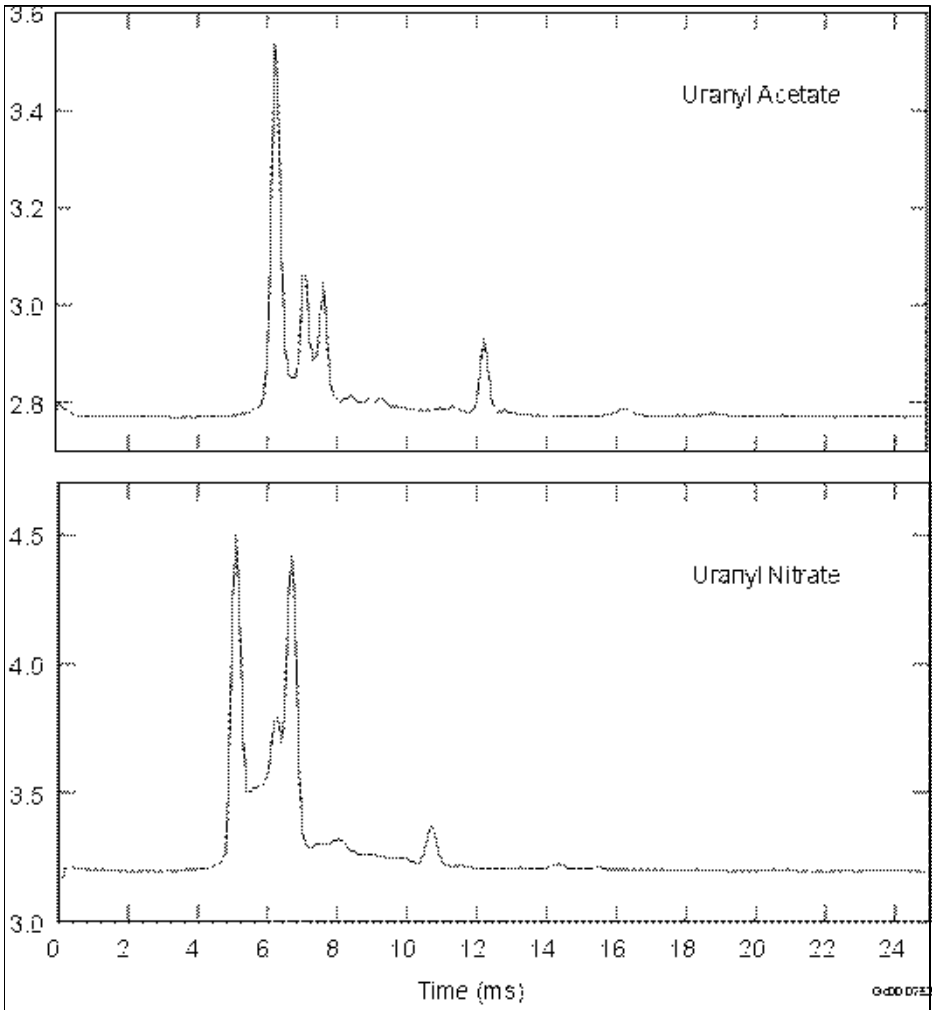

Figure 12. Electrospray IMS spectra of uranyl compounds.

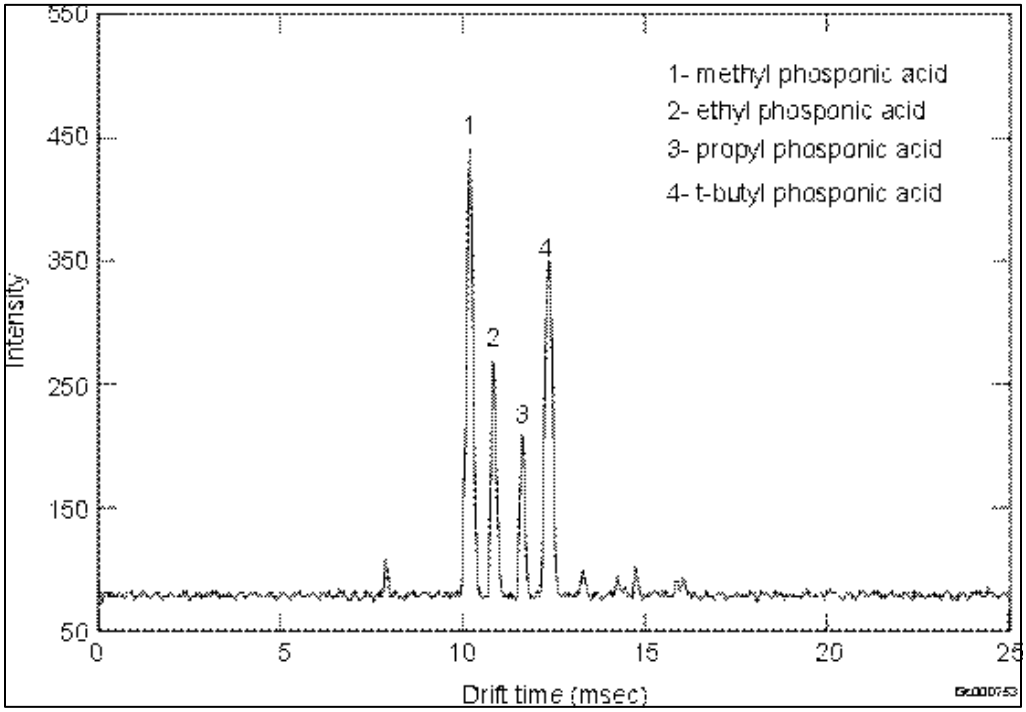

Figure 13. Electrospray IMS spectra of phosphonic acids.

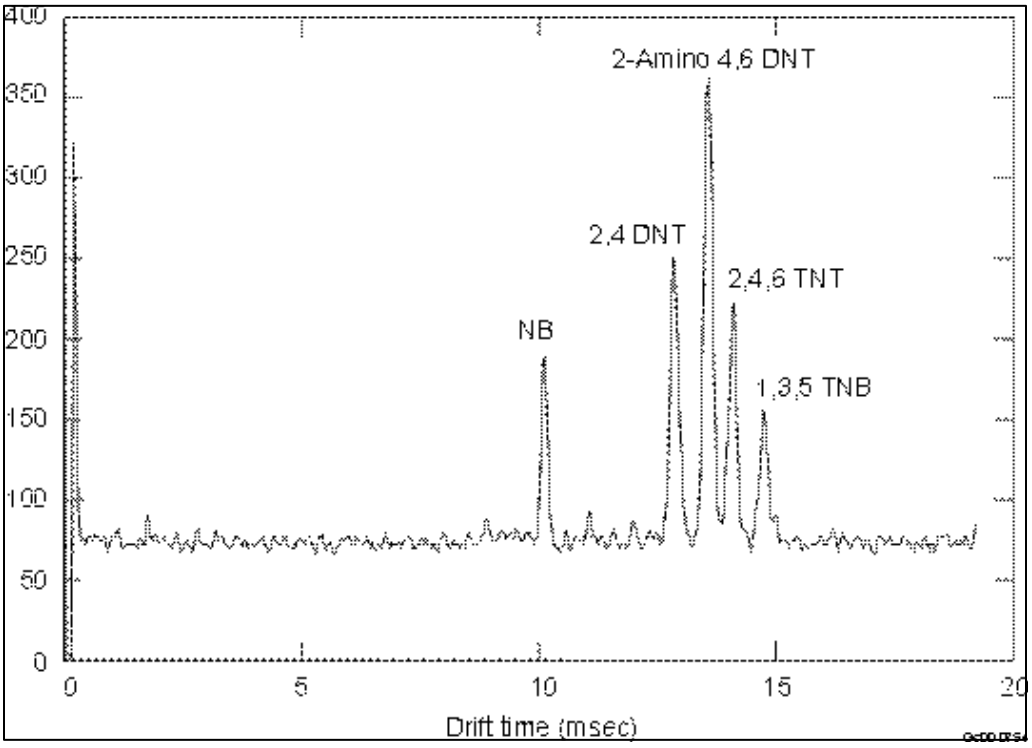

Figure 14. Negative mode electrospray IMS of explosive compounds in water.

The ESI/IMS system was adjusted and stabilized for the detection of nitrate and nitrate. Nitrate and nitrite salt standards were analyzed and found to provide excellent sensitivities for each (minimum detection limits ~50 ppb for nitrate). A linear dynamic range of 3 orders of magnitude was obtained for nitrate. The identity of the nitrite and nitrate mobility peaks were verified by comparison of reduced mobility values that were calculated from mass identified mobility peaks. Comparison of several nitrate and nitrite salt standards were also employed to ensure the mobility identity. Different drift gases and solvent modifiers were evaluated to attain optimal sampling conditions.

Initial experiments were performed with the ESI/IMS to verify that solvent ions similar to those previously mass-identified were obtained. We knew from the previous study that high aqueous percentages for the ESI solvent composition caused corona discharge to occur. Therefore, the ESI solvent composition was maintained at 90% methanol and 10% water. Figure 15 shows a comparison of the mass identified mobility peaks[14] and the solvent spectra obtained with the current ESI/IMS. the spectra in both figures are very similar in appearance (relative intensity and number of peaks). The identity of the five peaks was confirmed by comparing the K_o values obtained from the previous study with the current study; these values are listed in Table 2. Also, they were cross-referenced with K_o values obtained by other researchers. The numbers assigned to each peak in Figure 15 and Table 2 are maintained in all figures.

We prepared standards of two nitrate (Figure 16) and nitrite (Figure 17) salts to confirm that the measured nitrate and nitrite mobility peaks would be sensitive to changes in aqueous concentrations. We also needed to determine if the presence of different counter ions would alter the identity or sensitivity of the ion. These factors are important when trying to directly measure trace level concentrations in complex backgrounds where a wide range of counter-ions would be present. In Figure 16, the nitrate concentrations were similar and only the counter-ion was varied, sodium (top) and calcium (bottom). In both cases, the mobility intensity for nitrate increased considerably and the presence decreased the other solvent ions intensities considerably. The reduced mobility values obtained for the primary peaks in Figure 16 were consistent with the mobility peak that was identified in the solvent spectra. Similar results were seen for nitrite as well (see graphs in Figure 17 where the top graph is sodium nitrite and the bottom graph is potassium nitrite).

Once the nitrate/nitrite peak intensities were influenced by the solution composition, the next goal was to determine whether the nitrate peak intensity would be sensitive to changes in concentration. In Figure 18, ion mobility spectra are shown for three solutions containing varied concentrations of nitrate (sodium nitrate salt) as labeled on the graph. Comparison of the three graphs and intensities for Peak 4 (nitrate) shows that the peak intensity increased with increasing concentration; the greatest peak intensity was approximately 2.5 nA (30 ppm) and the lowest was 1.5 nA (5 ppm).

A complete calibration curve for nitrate was generated in Figure 19 with a range of 0.3 to 30 ppm. From the curve fitting applied to the calibration, the relationship between nitrate concentration was found to be linear within the concentration range studied. The concentration ranges studied here are indicative of trace level concentrations found in real world samples. The detection limits were estimated to be approximately 50 ppb for nitrate.

ESI/IMS is shown to be a viable tool for the detection and measurement of nitrate and nitrite in water samples. The technique also shows much promise for inorganic cations, as well as organic species found as contamination in water. More study is needed to elucidate matrix effects, but this early research has proven to be extremely promising. ESI/IMS should be studied in more detail as a potential field deployable analytical tool for a variety of environmentally significant analytes.

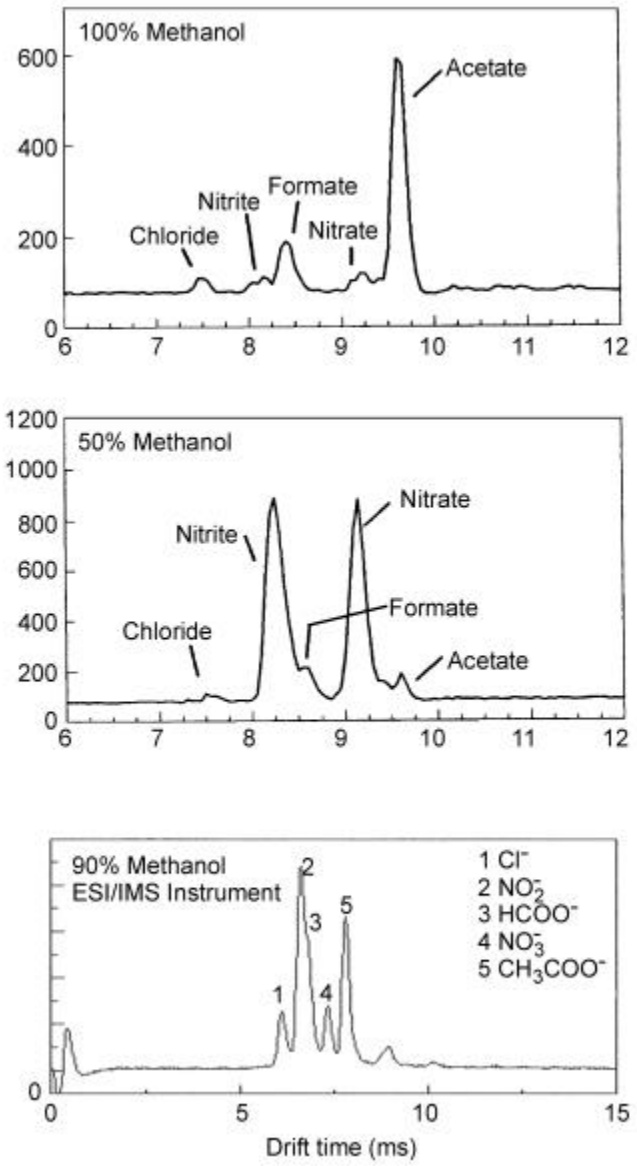

Figure 15. ESI/IMS/MS (top two plots) and ESI/IMS spectra of anions of interest (bottom plot).

Table 2. Mobility data for anions.

Anions	Peak No.	K_o value (ref.14)	K_o value from other ref.	Experimental K_o value (N_2), 5.0 kV	Experimental K_o value (N_2), 5.26 kV
Chloride	1	2.81	2.94, 3.01, 3.14,	3.12	3.07
Nitrite	2	2.55	2.70, 2.76.	2.94	2.82
Formate	3	2.47		2.85	2.75
Nitrate	4	2.29	2.46, 2.48, 2.57	2.64	2.55
Acetate	5	2.19		2.46	2.40

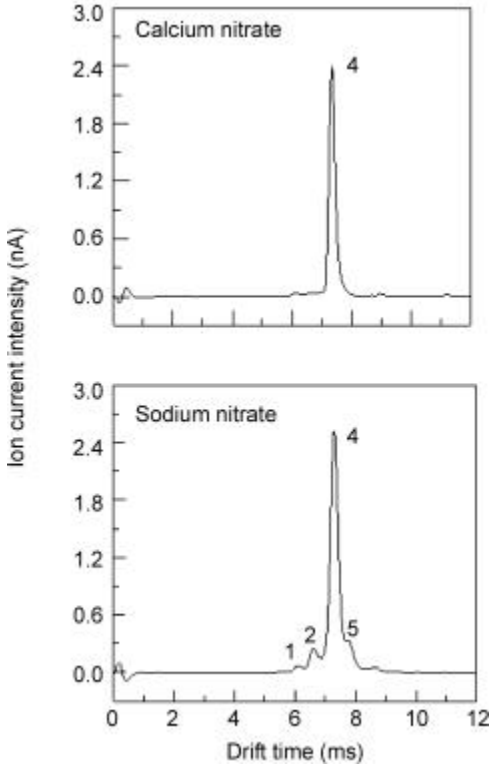

Figure 16. Nitrate anions by ESI/IMS with different counter-ions.

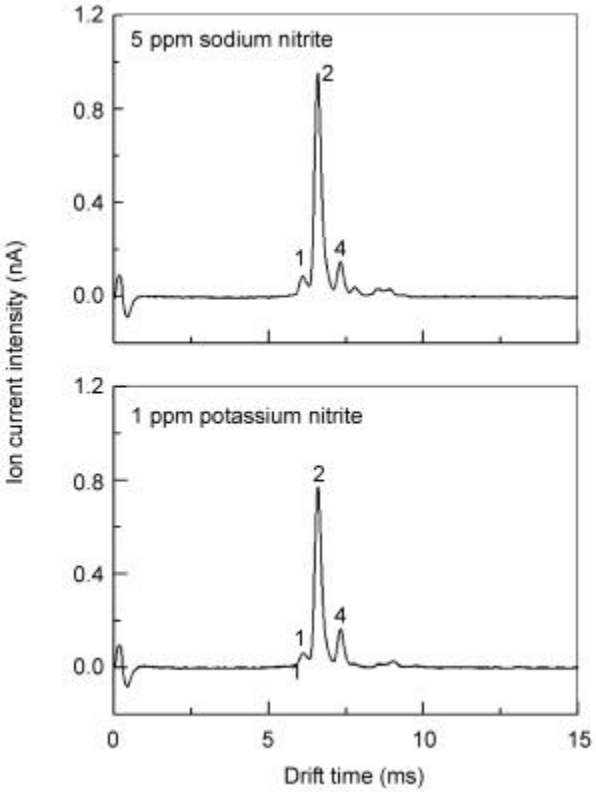

Figure 17. Nitrite anions by ESI/IMS with different counter-ions.

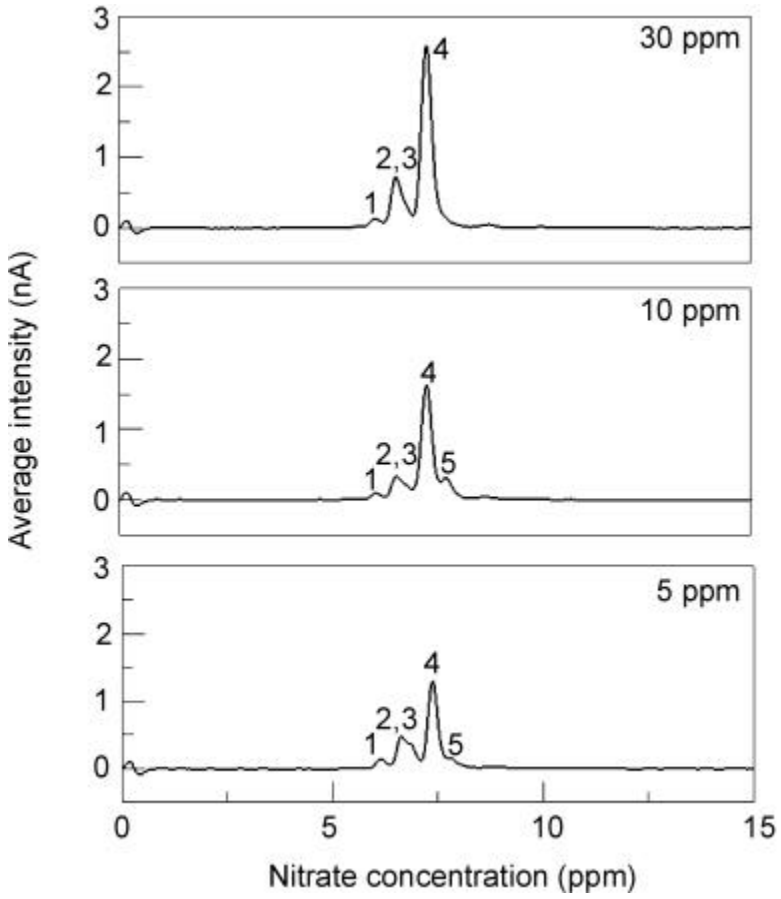

Figure 18. ESI/IMS spectra at varied nitrate concentrations.

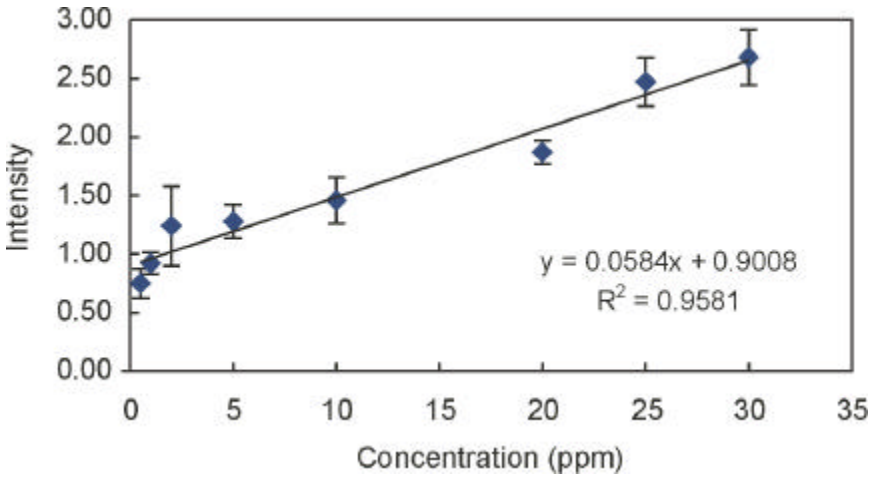

Figure 19. Nitrate calibration curve for ESI/IMS.

Speciation of Chlorinated Hydrocarbons in IMS by Gas Phase Ion Chemistry Manipulation

This subtask involved the speciation of chlorinated hydrocarbons in IMS by gas phase ion chemistry manipulation. Trichloroethene (TCE), 1,1,1-trichloroethane, and chloroform are all contaminants of great interest at the INEEL site and across the DOE complex. They are found in groundwater, the vadose zone, surface water, and above ground waste sites. Ion mobility spectrometry offers an extremely promising potential field method for the detection of these compounds with large advantages over current methods. The use of IMS for direct, in-the-field analysis eliminates sample collection and storage and provides real-time data, allowing IMS to be faster, cheaper, and probably more accurate than existing methods. The main drawback to using IMS in this application is that these compounds tend to provide only a chloride response through dissociative electron capture. Therefore, speciation among the various chlorinated hydrocarbons is difficult to impossible to achieve under standard IMS operating conditions. The key to IMS identification and quantification of these compounds is the formation of a unique molecular ion species from the contaminant of interest. Recent work with explosives at the INEEL shows that molecular ion species not seen under standard conditions can be formed through the manipulation of the gas phase ion-molecule reaction chemistry. This subtask demonstrates the ability to form a molecular ion for chlorinated hydrocarbons, allowing the use of hand-held IMS units for rapid screening and characterization of chlorinated hydrocarbon contamination in a variety of monitoring scenarios.

Figure 20 illustrates the use of a charge transfer agent to provide molecular ion species for 1,1,1-tetrachloroethane (1,1,1-TCA) and 1,1,2-tetrachloroethane (1,1,2-TCA). The top trace illustrates 1,1,1-TCA using standard air based ionization chemistry in the IMS. The bottom two traces illustrate the compounds using an altered chemistry with a charge transfer agent added. Note the peak in each of the bottom two traces to the right of 12 ms. This product ion peak is most likely due to a molecular species of the chlorinated hydrocarbons or a cluster. In either case, there is a unique product ion present that can be used to identify the species.

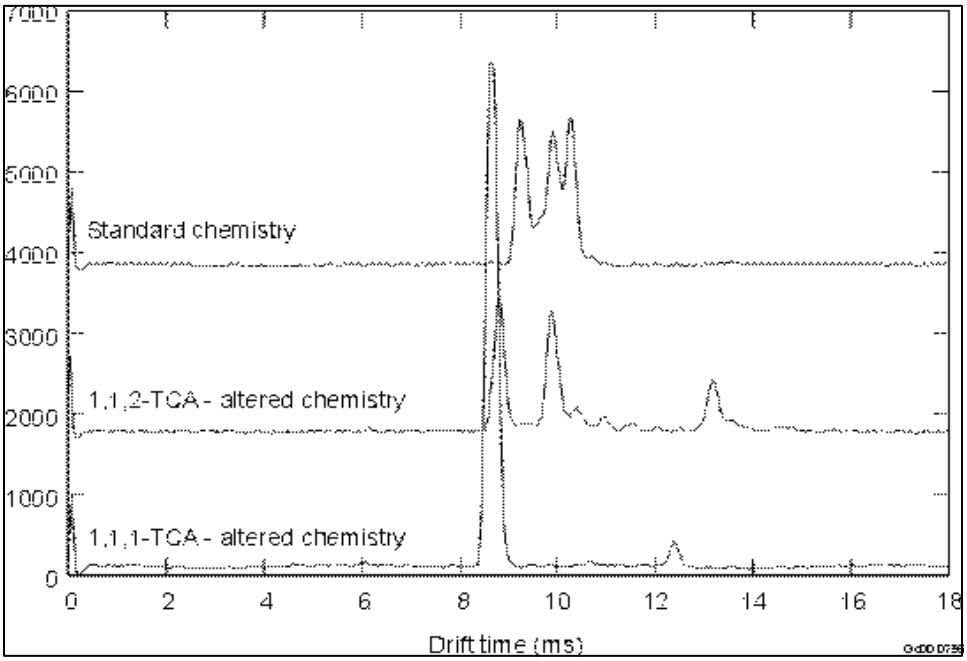

Figure 20. Tetrachlorinated ethanes via differing ionization chemistries.

A second method of providing a molecular species is to take advantage of both the dissociative chment and the adduct formation capabilities of the chlorinated hydrocarbons. Chlorinated hydrocarbons with enough polarity can form a chloride adduct species, with the chlorine ion being produced from the molecule of interest.

As shown in Table 3, atmospheric pressure chemical ionization of chlorinated ethanes can produce such ions as the chloride ion, the hydrated chloride ion and molecular adducts with the chloride ions. These ions were mass identified and several peaks were present corresponding to the variety of abundances from both the ^{35}Cl and the ^{37}Cl isotopes. For the compounds exhibiting a Cl^4 (M) ion, another ion was observed in the IMS spectrum with a drift time longer than the reactant ion, pentachloroethane being the exception. The lack of appearance of a pseudomolecular ion for pentachloroethane in a Graseby LCDABBII IMS system could have resulted from instrument conditions. A pseudomolecular ion was observed at 80∀C in a Barringer Sabre 2000 IMS, from vapors of pentachloroethane.

As indicated in Table 3, the only chemicals that did not exhibit a molecular chloride adduct were 1,1,1-trichloroethane and hexachloroethane. The common feature between these two is the absence of a hydrogen and a chlorine on the same carbon atom. The electron withdrawing characteristics of the chlorine atoms should make the partial charge on any hydrogen, located on the same carbon, more positive. This increased positive charge should increase the binding energy of a chloride ion with this hydrogen. Spectra comparing 1,1,1- and 1,1,2-trichloroethane are shown in Figure 21. Figures 21A and 21C contain the APCI mass spectra and Figures 21B and 21D are the IMS spectra for these compounds. A clear indication of the chloride ion is apparent in the mass spectra with ions at 35 and 37 amu, while the chloride ion appears at about 4.3 ms in the IMS spectra. The molecular chloride adduct is apparent in the mass spectra at 167, 169, 171, 173, and 175 amu for the 1,1,2-trichloroethane and it is presumed that this same ion appears at about 5.9 ms in the IMS spectra. The only difference between these two chemicals is the location of the hydrogen and chlorine atoms around the carbons, yet it makes a significant difference on the adduct stability. An attempt was made to model some of these compounds and compare the charge distributions on the atoms of the neutral molecules. Further modeling was applied in an attempt to calculate the binding energies of chloride ions to the same molecules. These results are listed in Table 4. The modeling shows a definite trend in the partial charge on the hydrogen atoms related to the location of the chlorine atoms. The hydrogen on the pentachloroethane had the largest partial charge of 0.311 while the hydrogen on the 1,1,1-trichloroethane had the lowest partial charge of 0.251. There is also a reasonable correlation between the magnitude of this charge and the calculated binding energy with a chloride ion.

Table 3. Summary of responses for IMS- and APCI-MS to chlorinated ethanes.

Chlorinated ethane	Ion other than Cl^4 in IMS	APCI/MS ions amu (^{35}Cl)	Ion Species
1,1 dichloro-	yes	35, 133	Cl^4, $M(Cl^4)$
1,2-dichloro-	yes	35, 53, 133	Cl^4, $H_2O(Cl^4)$, $M(Cl^4)$
1,1,2-trichloro	yes	35, 167	Cl^4, $M(Cl^4)$
1,1,1-trichloro-	no	35, 53	Cl^4, $H_2O(Cl^4)$
1,1,2,2-tetrachloro	yes	35, 201, 367	Cl^4, $M(Cl^4)$, $M_2(Cl^4)$
1,1,1,2-tetrachloro-	no	35,53,213	Cl^4, $H_2O(Cl^4)$, ?
Pentachloro-	?	35, 53, 235	Cl^4, $H_2O(Cl^4)$, $M(Cl^4)$
Hexachloro-	no	35, 53, 70	Cl^4, $H_2O(Cl^4)$, $Cl_2{}^4$

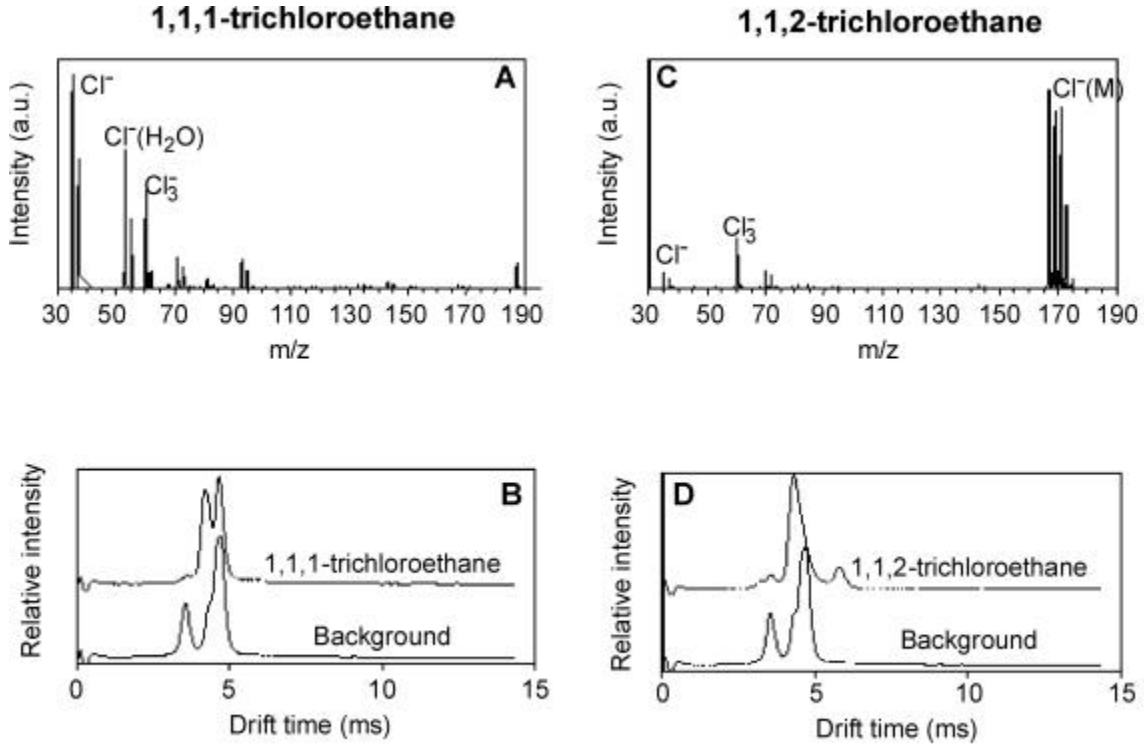

Figure 21. IMS- and APCI-MS spectra of 1,1,1-trichloroethane and 1,1,2-trichloroethane.

Table 4. Results for molecular modeling of chlorinated ethanes.

Chlorinated ethane	Mulliken Atomic Charge (on most positive hydrogen)	÷H∀of association Cl^{4}(M) kcal/mol
1,1-dichloro-	0.271	415.30
1,2-dichloro-	0.261	412.32
1,1,1-trichloro	0.251	412.7
1,1,2-trichloro	0.290	416.2
1,1,1,2-tetrachloro-	0.285	416.2
Pentachloro-	0.311	419.15

It appears that with the chlorinated ethanes, most of the chemicals produce a pseudomolecular ion, and thus could be distinguished in the field using IMS. Since the ion is an adduct between the molecule and a chloride ion, it is assumed that sensitivity could be increased by providing a source of chloride reactant ions. Further, since adduct stability is known to be temperature dependant,[15] specific adducts could be selected by altering the temperature, leading not only to enhanced sensitivity, but also a potentially huge increase in selectivity.

ACCOMPLISHMENTS

This task has successfully applied new technology ideas to long running environmental issues. As the paradigm shift in analytical chemistry takes the traditional laboratory analysis and moves it to real-time portable instrumentation used in the field, IMS will be a major player. IMS is a highly sensitive, yet versatile and rugged instrument that will be a focus for environmental monitoring measurements in the field. There are some issues in applying IMS immediately to environmental analysis, such as subsurface deployment and measurement, aqueous sample analysis, and chlorinated solvent contamination response, but these issues have been directly addressed and solved by this task.

This task successfully demonstrated how some of the issues of moving IMS into environmental analysis can be overcome. One subtask developed a novel IMS system (FAIMS) for deployment into the subsurface to provide chemical measurements. The system provided quality analytical measurements in the laboratory for a number of chemicals of environmental concern, such as benzene, toluene, acetone, and chlorinated hydrocarbons. A deployment of the miniature sensor into a soil column demonstrated that the technique can be deployed to measure the transport of organics through the subsurface.

A second subtask developed a high speed, field deployable method for analyzing ground and surface waters for various analytes, including organic and inorganic cations and anions. Monitoring water can be challenging due to transport and movement. Contaminant pulses can be difficult to track using the traditional sample/laboratory analysis approach. This subtask developed a real-time monitor for water samples that can also be set up for unattended operation to monitor levels of specific contaminants. It also demonstrated a rugged, easy to use system that has advantages in time and cost over traditional water analyses. A focus of the subtask was to monitor water samples for nitrate and nitrite, which was successfully performed, with part-per-billion range sensitivity in a real-time analysis with no sample preparation.

A third subtask demonstrated a pathway to use IMS in the field for monitoring chlorinated hydrocarbon compounds. Although IMS is an attractive instrument for monitoring volatile organic species in a number of media, its use has been hindered by the difficulties in speciating chlorinated hydrocarbons. Nevertheless, this subtask provided a mechanism by which IMS can successfully measure chlorinated organics in real-time without the use of GC. It also suggests a potential path where IMS can be used for other problematic analytes through the study of the ionization mechanisms and manipulation of the chemistry involved in producing desired product ions.

This task provides real value to DOE and the INEEL by enhancing analytical capabilities required for environmental monitoring and long-term stewardship. The goal of better, faster, and less costly characterization can be realized through the deployment of new technologies suited to the need, and this research offers new solutions to realize this goal.

REFERENCES

1. R. Bradshaw, "Engineering Approaches and Compromises in the Design of Small IMS Spectrometers," *3rd International Workshop on Ion Mobility Spectrometry, Galveston, TX, October 16–19, 1994*; also, C. S. Harden, "Relative Performance Characteristics of Handheld Ion Mobility Spectrometers—The Chemical Agent Monitor and a New Miniaturized Instrument," *5th International Workshop on Ion Mobility Spectrometry, Cambridge, UK, August 1995.*

2. J. Xu, W. B. Whitten, and J. M. Ramsey, "Miniature Ion Mobility Spectrometry," *8th International Workshop on Ion Mobility Spectrometry, Buxton, UK, August 8–12, 1999.*

3. J. I. Baumbach, D. Berger, J. W. Leonhardt, and D. Klockow, "Ion Mobility Sensor in Environmental Analytical Chemistry-Concept and First Result," *Intl. J. Environ. Analy. Chem.* Vol. 52, 1993, p. 189.

4. R. A. Miller, G. A. Eiceman, E. G. Nazarov, "A Micromachined High-Field Asymmetric Waveform-Ion Mobility Spectrometer (FA-IMS)," *Sensor and Actuators B. Chemical*, 2000, in press.

5. A. Buryakov, E. V. Krylov, A. L. Makas, E. G. Nazarov, V. V. Pervukhin, and U. Kh. Rasulev, *Sov. Tech. Phys. Lett 17(6),* June 1991.

6. I. A. Buryakov, E. V. Krylov, E. G. Nazarov, and U. Kh. Rasulev, *Int. J. Mass Spectrometry and Ion Processes*, Vol. 128, 1993, pp. 143–148.

7. B. Carnahan, S. Day, V. Kouznetsov, and A. Tarassov, "Development and Applications of a Transverse Field Compensation Ion Mobility Spectrometer," *5th International Workshop on Ion Mobility Spectrometry, Cambridge, UK, August 6–9, 1995*.

8. B. Carnahan, S. Day, V. Kouznetsov, M. Matyjaszczyk, A. Tarassov, "Field Ion Spectrometry—A New Analytical Technology For Trace Gas Analysis," *Proceedings of the 1996 International Conference on Advances in Instrumentation and Control, ISA 1996*.

9. R. W. Purves, R. Guevremont, S. Day, C. W. Pipich, and M. S. Matyjaszczyk, *Review of Scientific Instruments*, Vol. 69, 1998, pp. 4094–4105.

10. R. Guevremont and R. W. Purves, *Review of Scientific Instruments*, Vol. 70, 1999, p. 1370.

11. G. A. Eiceman, S. Sowa, S. Lin, and S. E. Bell, "Ion Mobility Spectrometry for Continuous On-Site Monitoring of Nicotine Vapors in Air During the Manufacture of Transdermal Systems," *Journal of Hazardous Materials*, Vol. 43, 1995, pp.13–30.

12. E. Wasik, J. Bohdziewicz, M. Blaszczyk, "Removal of Nitrates from Ground Water by a Hybrid Process of Biological Denitrification and Microfiltration Membrane," *Process Biochemistry*, Vol. 37, 2001, pp. 57–64.

13. D. Connolly and B. Paull, "Rapid Determination of Nitrate and Nitrite in Drinking Water Samples Using Ion-interaction Liquid Chromatography," *Anal. Chim. Acta*, Vol. 441, 2001, pp. 53–62.

14. G. R. Asbury, H. H. Hill, Jr., "Negative Ion Electrospray Ionization Ion Mobility Spectrometry," *Int. J. of Ion Mobility Spec*, Vol. 2, 1999, pp. 1–8.

15. R. G. Ewing, G. A. Eiceman, J. A. Stone, *Int. J. Mass Spectrom.*, Vol. 193, 1999, pp. 57–68.

Nondestructive Assay Science and Technology Proof-of-Concept Testing for Environmental Characterization and Stewardship

Looking at Environmental Samples with Nondestructive Techniques

Michael J. Connolly, Gail A. Cordes, James L. Jones, John C. Determan, Greg K. Becker

SUMMARY

A critical part of environmental management programs, which include waste treatment, storage, and disposal, is a scientifically based assessment of site hazards, and the risks involved with the cleanup activities. There is a constant need to be able to quantitatively characterize materials without disturbing or degrading them. This is especially true of waste and radioactive materials such as waste containers, but also true of subsurface samples or in-field measurements.

This task collectively supported environmental management and long-term monitoring by (a) providing intelligent information processing techniques for the interpretation and review of nondestructive assay (NDA) measurement data, (b) demonstrating proof-of-concept for using a novel accelerator based NDA techniques that support subsurface science predictive model development, and (c) validating and verifying NDA system operation.

Nuclear-based nondestructive techniques enable materials assay without disturbing or degrading the materials, and typically prove to be faster, more environmentally benign, and cheaper than destructive analysis methods. Intelligent information processing techniques contribute to the speed and accuracy of data acquisition. Such techniques can provide rapid to real-time data validation, verification, analysis, and interpretation of the measurement data as well as the NDA system operation. This task involved three specific subtasks:

1. Evaluating intelligent information processing methods for application to NDA techniques, including accelerator-based methods. In the first approach, neural networks were studied for use on measurement data sets from two neutron waste assay measurement systems. In the second approach, the Advanced Data Validation and Verification System, a multivariate analysis software package, was modified to monitor operation of the accelerator-based NDA system in Subtask 2, the software was trained with a subset of the accelerator operational data, and the system was successfully demonstrated.

2. Assembly and demonstration of an accelerator-based NDA system on a laboratory simulation of subsurface isotope movement. The NDA system, which is located at the Idaho Accelerator Center (IAC) at Idaho State University (ISU), uses Accelerator-based X-ray Fluorescence (AXRF) to detect uranium and transuranics in soil samples representative of the Radioactive Waste Management Complex (RWMC) Subsurface Disposal Area (SDA). Tests successfully demonstrated AXRF techniques to detect uranium and heavy metal concentrations of less than 100 ppm, and image sources with a resolution of less than 3 mm.

3. Expanding an existing expert system to allow easy modification of existing rules sets for application to different waste forms, and demonstrating this new capability by adapting existing rule sets for application to debris type waste forms. The measurement data are passive/active neutron data and gamma-ray spectroscopy data, from waste drum assay systems at the INEEL's

Stored Waste Examination Pilot Plant (SWEPP). The data are reviewed with the expert system to verify that measurements are self-consistent and reasonable, and that there are no biases in the data that are unaccounted for. The debris rule requirements were specified and the new rule editor system was designed.

TASK DESCRIPTION

This task collectively supported environmental management and long-term monitoring by (a) providing intelligent information processing techniques for validating and verifying NDA system operation, (b) demonstrating proof-of-concept for use of a novel accelerator-based nondestructive assay (NDA) technique that supports subsurface science predictive model development, and (c) interpreting and reviewing NDA measurement data.

This task involved three specific subtasks:

1. Evaluating intelligent information processing methods for application to NDA techniques, including accelerator-based methods.

2. Assembling and demonstrating an accelerator-based NDA system on a laboratory simulation of subsurface isotope movement.

3. Expanding an existing expert system to allow easy modification of existing rules sets for application to different waste forms, and demonstrating this new capability by adapting existing rule sets for application to debris type waste forms.

Intelligent Information Processing Techniques

This subtask applied pattern recognition techniques to nondestructive assay (NDA) processes to assist and improve NDA system design; provide measurement data acquisition strategies, data reduction methods, and data interpretation; and provide hardware operation status and data validation.

Pattern Recognition for NDA Measurement Data Sets

This subtask studied state-of-the-art NDA measurement processes to exploit acquired data sets for information not noted or used in conventional data analysis techniques. Neural network approaches were studied for use in identifying and extracting unknown data features and relationships not used due to constraints inherent in conventional approaches. Features and relationships of interest are those that can be used to improve NDA system design, data acquisition strategies, data reduction methods, and data interpretation. Conventional approaches to these NDA process categories are generally based on first principle techniques that, for the most part, are time and resource intensive, and in many cases subject to unknown error components. Often conventional techniques are incapable of recognizing the presence of a bias source, and therefore, it is not corrected for in the NDA assay quantification.

This task addressed certain NDA measurement deficiencies. The neural network pattern recognition techniques were studied with the intent of demonstrating benefit through either reduction in required resources or gain of information in the overall NDA process. These techniques have a potential to yield benefit in quantifying the following three known biases in NDA systems: radioactive material spatial dependent bias; radioactive material physical form dependent bias; and matrix elemental composition, density, and spatial distribution.

These known deficiencies are to be processed relative to the ability of neural network techniques to properly identify presence or absence in complex NDA data patterns.

The NDA measurement system data sets selected for use in this task were recorded from the Los Alamos National Laboratory (LANL) Crated Waste Assay Monitor (CWAM) and NIS-6 Combined Thermal Epithermal Neutron (CTEN) assay systems. Both of these systems are neutron measurement systems. The data sets are comprised of many different measurement sample configurations, each with known source/matrix configurations. Each measurement consists of hundreds of data fields.

The various data sets were formatted and cataloged as to inherent characteristics that will be useful in later intelligent processing manipulations. Appropriate neural network pattern recognition techniques and hybrids were investigated. Follow-on work will be required to:

- Evaluate at least three existing neural network pattern recognition techniques for suitability and subsequent application to the NDA data sets.

- Identify instrument response data patterns attributable to specified bias sources (listed above) contained in the selected data sets.

- Define capabilities and limits of selected neural network pattern recognition techniques to detect the presence of selected bias sources through data features and relationships, and other information related to the measurement.

- Evaluate the useful features identified in the previous step (3) per their physical meaning, and in what manner they can be used in NDA measurement improvement.

Pattern Recognition for NDA System Operability Data Sets

The purpose of this task was to provide a proof-of-principle for the use of pattern recognition intelligent information processing methods to improve the speed and quality of NDA techniques. Pattern recognition techniques provide real-time capability to monitor the performance of NDA hardware systems and interpret the resulting performance data by acting across the time-stamped vector of system parameters. One of the pattern recognition techniques available at the INEEL, the Advanced Data Validation and Verification System (ADVVS), was selected for this task. The software was demonstrated on the Varitron accelerator in the hardware system built at the IAC at ISU for Subtask 2. The ADVVS algorithms are proprietary to Dr. Jack Mott of Triant Technologies, Corp., in Idaho Falls. The INEEL and Dr. Mott entered into a nondisclosure agreement, and the INEEL used his expertise and our existing software license in this task under a services subcontract.

The ADVVS is a pattern recognition technique using multivariate analysis of incoming data. The real-time data values are compared with data estimates calculated from functional relationships that model known modes of system operation or system data outputs. Any statistically significant deviation from these calculated patterns is flagged. Depending on the specific application, the system operation may be modified or terminated. The data deviations may be analyzed offline and new data included in the functional relationships if it is adopted and classified as normal but unanticipated. In summary, the entire variable vector is considered a pattern and is analyzed in real time to recognize pattern changes that can be interpreted as data characteristics or operating system anomalies.

The ADVVS was installed on a Windows NT machine at the INEEL and re-run to ensure it would run and provide the proper results in a DOS window in the Windows NT environment. A LabView-ADVVS interface was developed, and ADVVS was updated for the subsurface science research.

Eleven data signals from the Varitron were logged and the data files were analyzed using ADVVS. The results showed that sensors initially thought to be unnecessary actually could contain important information that would contribute to accurate analysis of the accelerator operation. It was also shown that the ADVVS could identify when sensors were malfunctioning and require calibration; that some data spikes represented anomalous system noise that could be filtered prior to analysis; and that the source of periodicity in the beam current data was the accelerator waveguide cooling system that is automatically controlled (i.e., chilled water is injected into a cooling jacket around the waveguide cavity when the temperature reaches a predetermined set point, roughly every two or three minutes depending on selected operation conditions). Subsequent accelerator operations showed that increased data stability is obtained by using facility cooling rather than separate chiller units. This enabled more "stable" data acquisitions. The LabView, ADVVS, and Varitron-operator interfaces were programmed, tested, installed on the IAC Varitron accelerator control computer, and field-tested. The capability to handle additional signals was included in the programming.

To allow a better analysis of the operational data, a test matrix provided the necessary reference data to estimate a beam current and energy for any setup that is within the established operating range. The expanded set of operational data was logged using a test matrix of electron beam energies between 4.5 and 13.5 MeV, and the ADVVS was trained against the expanded set of data. The software was run real-time with the Varitron on a stand-alone basis and was readied for application with the integrated system assembled for the subsurface science research work of Subtask 2.

In conclusion, the proof-of-concept was demonstrated for using the ADVVS software for monitoring the operability of accelerator-based systems in subsurface science research and applications. In addition, the accelerator team recognized that the performance of the Varitron operation was improved considerably by monitoring the various accelerator parameters applicable to the ADVVS multivariate analysis program. Related follow-on work is being funded by other sources to investigate extensions of the ADVVS software to feedback control and unfolding of gamma-ray spectra.

Accelerator Based NDA Technique in Support of Subsurface Science Predictive Model Development

This subtask demonstrated the proof-of-concept of applying an electron accelerator-based system to the detection of uranium, transuranics, and heavy metals in soil samples representative of the RWMC SDA. This subtask leveraged heavily on the "unconventional" XRF (or AXRF, Accelerator-based XRF) and nuclear resonance fluorescence (NRF) scattering research being developed and tested at the IAC and supported by the INEEL/ISU Accelerator Alliance Initiative. However, initial experimentations for this application quickly showed the dominance of the AXRF process when compared to the NRF process and, hence, AXRF was selected for this study. AXRF results at the IAC, before this subtask began, allowed thorium characterization through about 1 cm of lead shielding.

In this interrogation process, electrons are accelerated up to several MeVs in kinetic energy. These electrons interact with a high-Z (atomic number) material to produce high-energy bremsstrahlung (photons) radiation having a maximum photon energy corresponding to the maximum electron energy. Based on the selected electron beam energy, these photons are highly penetrating. These penetrating photons will excite atomic energy levels (up to 120 keV) in the AXRF process during the accelerator pulse. The "unconventional" nature of the AXRF process comes from the use of these high-energy, highly penetrating bremsstrahlung photons, the high-intensity level of XRF stimulation, and the specialized, "in-beam" detection systems.

Specifically, the proof-of-concept demonstration involved identifying and characterizing inhomogeneous uranium, americium, and neptunium materials in several applicable soil samples. Initially, the research setup used a fixed energy, 6-MeV electron accelerator as the primary investigating probe and up to three detectors: a thin window (~1%) high-purity germanium, a larger volume (~10%) high-purity germanium, and a large 5 Δ 5 sodium iodide (NaI). The variable energy Varitron electron accelerator was also included in this research. For each soil sample, the detection limit of each nuclear material was defined as a function of soil thickness and nuclear material quantity.

To begin the research, the experimental test stand was designed and constructed and initial tests were run with the 6-MeV accelerator. The testing configuration consisted of an electron accelerator in one room and the soil sample stand in an adjacent room. The accelerator is a 6-MeV, S-band-type, electron accelerator oriented to direct energetic (up to 6 MeV) bremsstrahlung photons into a collimator assembly consisting of a 20.3-cm hole in a 2-m-thick concrete facility wall. Each end of the hole was supplied with custom-built, stainless-steel end plugs containing a 1-cm-diameter hole. The soil sample stand consisted of a vertically oriented, 1-m-tall, up to 25-cm-inside-diameter, Plexiglas tube atop a rotating stand assembly. Initial tests used a 60% high-purity germanium and two beryllium-windowed, low-energy-sensitive germanium detectors to measure the induced annihilation and XRF radiation emissions. The soil sample surrogate was "standard clean" sand with uniform density and good compaction properties.

A photo of the experimental test stand is shown in Figure 1. Its associated process schematic is shown in Figure 2. Figure 3 is a photo of the 6-MeV accelerator positioned in the room adjoining the experimental test stand. The tests with the 6-MeV accelerator showed that it is possible to detect uranium and heavy metals (down to ~30 Z) in the soil column at concentrations below 100 ppm. Lower concentration levels can be detected for higher Z materials. Crude 3-D images were formed of the rotating soil column to determine spatial resolution of the XRF technique, and it was found that the linear resolution was less than 3 mm.

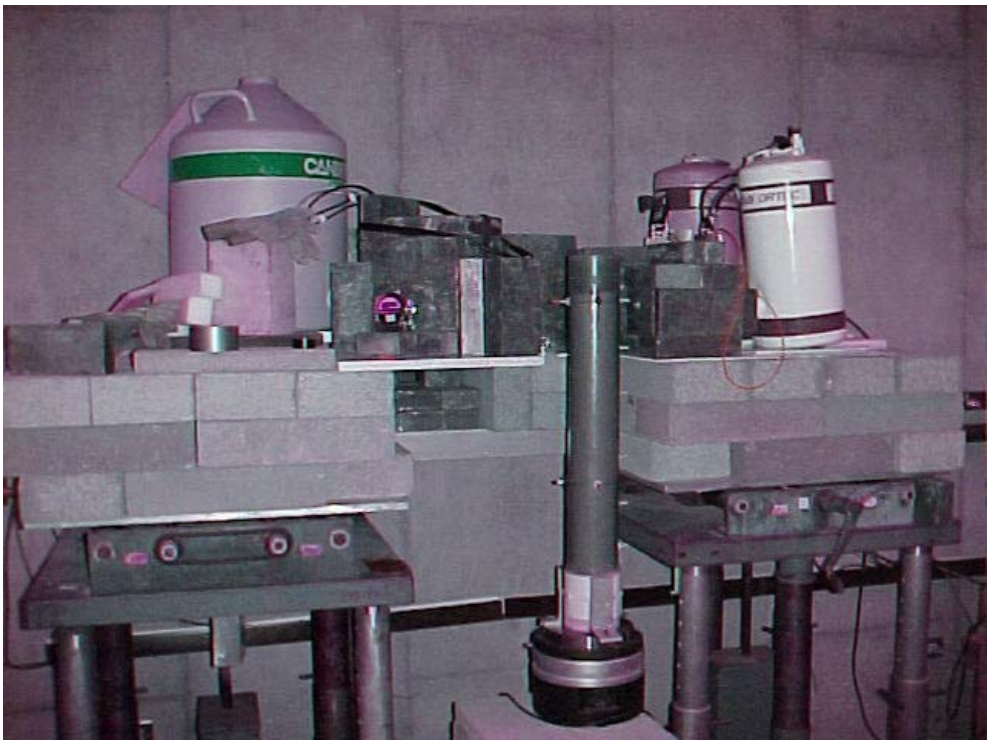

Figure 1. Subsurface science research test configuration showing vertical soil column and detectors.

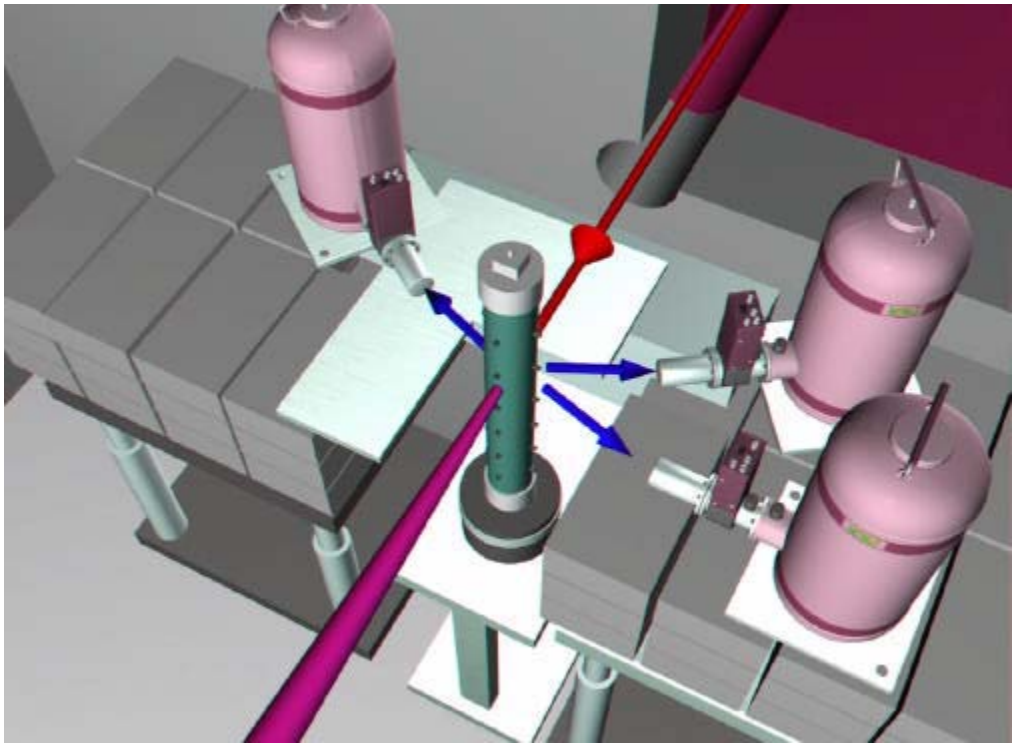

Figure 2. Test configuration schematic.

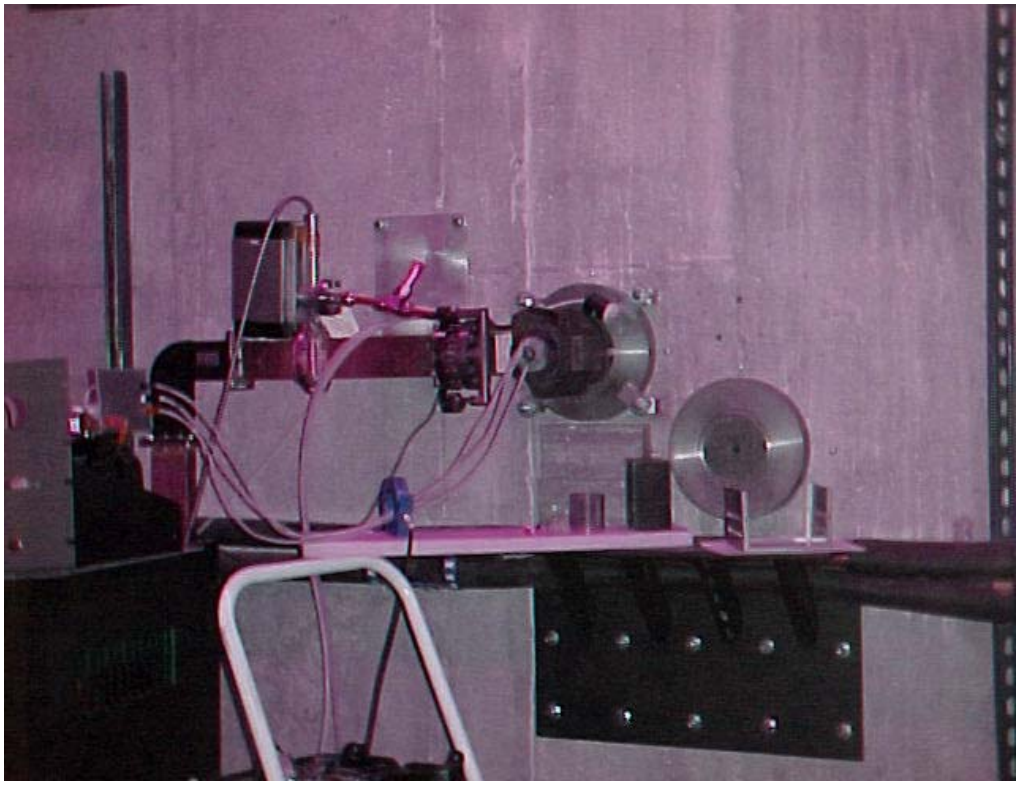

Figure 3. The 6-MeV accelerator positioned in room adjoining the test configuration.

In another test series, the INEEL Varitron, a selectable energy electron accelerator located at the IAC, replaced the 6 MeV electron accelerator. The instrumented Varitron allowed multivariate analysis of the operation during each XRF acquisition and the assessment of different operational responses.

The performance of the Varitron operation has been improved considerably via the monitoring of the various accelerator parameters applicable to the ADVVS multivariate analysis program. Two multi-parameter data collections were performed. Each collection of multiparameter operational data resulted in a better characterization and operation of the Varitron.

For the final demonstration tests, the Varitron was positioned 1 m from a 2-m-thick concrete wall. Although various electron beam energies and test configurations were assessed to enable a normal 6-MeV operation of the accelerator and maximize AXRF emission detection from the soil samples, it was a 3-MeV operation that resulted in the most successful tests, primarily due to the "in-beam" nature of the required data collection. Additional testing and computer modeling are needed in follow-on work to optimize testing configuration and the data acquisition method. These final tests included a bare tungsten/gold foil case and two cases involving the composite foils located within 2 and 4 inches of the "standard" soil samples.

In conclusion, the results of demonstration tests provided proof-of-concept for using this detection capability for characterizing materials in various different soil environments (homogenous dispersal, wetness factor, soil grain surface effects, microorganism effects, mineral content, etc). This type of detection capability can be used very effectively in the future in helping benchmark numerous subsurface science predictive models for many materials of interest.

The Inland Northwest Research Alliance has funded a 3-year follow-on NDA research project for using accelerator-based XRF for subsurface science. The research team comes from ISU, BSU, and the INEEL. W ork began at the IAC during FY 2001.

Modify and Demonstrate INEEL CLIPS Based NDA Expert System for Application to Transuranic Debris Waste Forms

This subtask modified the NDA Data Review Expert System (NDA-DRXS), an INEEL CLIPS-based NDA expert system for transuranic sludge waste, and provided proof-of-concept for using the modified system for other waste forms by demonstrating the modified system on transuranic debris waste forms. The expert system is being developed to review transuranic waste nondestructive assay data. The measurement data are passive/active neutron data and gamma ray spectroscopy data, both off of waste drums at the SWEPP. The review is performed to verify that measurements are self-consistent and reasonable, and that there are no biases present that have not been accounted for.

The current design of NDA-DRXS allows easy adaptation of the generic framework to different waste assay configurations through an innovative combination of rule-based and object-oriented programming techniques. The initial set of validation rules dealt explicitly wit h sludge waste forms. But many of these rules can be modified to be applicable to other waste forms. The ability to make the system easily adaptable to different waste forms, such as debris waste forms, had not been developed prior to FY 2000, but is of importance to both our internal and external customers. Improving system adaptability also addresses the important issue of expert system maintenance. Customers need to know that the capabilities of the expert system will be able to progress as their domain experience grows. Rule update and maintenance should not require a software specialist, but be performable by knowledgeable users of the expert system.

The key issue here is to address the form of knowledge representation in a systematic manner; therefore, this work included the following steps:

1. Discover the structure, or "grammar" of data validation rules. At the start of the project, rules were available for two different organizations, already specified in the CLIPS expert system language. These rules provided the raw material for determining the structure, or common form and necessary elements, of validation rules.

2. Design a validation rule representation that is consistent with the analysis in Step 1.

3. Specify one of the sets of validation rules in the new format.

4. Design a user interface based on this format for performing validation rule updates, modification, and maintenance. The interface would require specific inputs from the user and would update the validation rules; therefore, specific knowledge of the CLIPS expert system language would not be required to modify and update validation rules.

5. Use the interface to adapt the sludge validation rules to be appropriate for other waste forms, such as debris, as a demonstration of the capability.

During this subtask, the debris rule requirements were specified and the debris rules were manually produced, which greatly extending the applicability of the NDA-DRXS with respect to the types of waste streams encountered at the SWEPP facility. The rule editor system was designed with three components: a database to store the data needed to form CLIPS code, a program to form CLIPS code from the database, and a program to allow editing of the database entries. The database was designed to store not only data needed to build CLIPS code, but enough information to build the C++ code used to initialize key CLIPS structures from the waste measurement database. A CLIPS code building program was produced. A rule editor to operate on the rule structure database was designed (an object model). The rule editing tool makes the expert system more flexible, and also speeds the process of specifying new expert system rule modules.

When deployed, the completed system will improve the throughput of waste containers at SWEPP and the consistency and quality of the data review process. Follow-on work was already generated through work on this subtask. We are currently extending the concepts developed in this project into a fully practical system to be used by Los Alamos National Laboratory.

ACCOMPLISHMENTS

Most of the files of waste assay data sets were cataloged for the neural network research.

The proof-of-concept for the first subtask was demonstrated for using the ADVVS software to monitor the operability of accelerator-based systems in subsurface science research and applications. In addition, the accelerator team recognized that the performance of the Varitron operation was improved considerably by monitoring the various accelerator parameters applicable to the ADVVS multivariate analysis program. The ADVVS software was updated for the subsurface science research. The LabView, ADVVS, and Varitron-operator interfaces were programmed, tested, installed on the IAC Varitron accelerator control computer, and field-tested with 11 Varitron data signals. The tests showed that the ADVVS can be used to monitor the operation of an accelerator like the Varitron and reveal important operational information. In addition, the accelerator team recognized that the performance of the Varitron operation was improved considerably by monitoring the various accelerator parameters applicable to the ADVVS multivariate analysis program.

The demonstration tests conducted during the second subtask provided proof-of-concept for using this detection capability for characterizing both nuclear and non-nuclear materials in various different soil environments. The tests used AXRF techniques and showed that it is possible to detect uranium and heavy metals (down to Z ~30) in the soil column at concentrations below 100 ppm. Lower concentration levels can be detected for materials with higher Z. Three-dimensional images were formed of the rotating soil column to determine spatial resolution using the XRF technique, and it was found that the linear resolution was less than 3 mm.

The extensions to the NDA-DRXS were successfully implemented in the third subtask, and when deployed, the complete system will improve the throughput of waste containers at SWEPP and the consistency and quality of the data review process. The debris rule requirements were specified and the debris rules were manually produced, thus greatly extending the applicability of the NDA-DRXS with respect to the types of waste streams encountered at the SWEPP facility. The rule editor system was designed with three components: a database to store the data needed to form CLIPS code, a program to form CLIPS code from the database, and a program to allow editing of the database entries. The database was designed to store not only data needed to build CLIPS code, but enough information to build the C++ code used to initialize key CLIPS structures from the waste measurement database. An initial design for the CLIPS code building program was produced as an object model. A rule editor to operate on the rule structure database was partially designed (an object model). The rule editing tool when complete will make the expert system more flexible, and also speed the process of specifying new expert system rule modules. In follow-on work, the concepts developed in this project are being further extended into a fully practical system to be used by Los Alamos National Laboratory.

REFERENCES

None

Isobaric Groundwater Well for Precise Water Level Measurement Relevant to Long-Term Surveillance and Stewardship

Measuring Groundwater Aquifer Water Levels More Accurately

Joel M. Hubbell

SUMMARY

DOE depends on accurate data of groundwater elevations to characterize sites, develop site-specific conceptual models of groundwater flow and transport at sites, provide data for predictions of contaminant transport and model calibration, and monitor migration phenomena for long-term stewardship of existing disposal sites and new facilities. Barometric pressure fluctuations influence measured water levels in wells where deep vadose zones or slowly permeable materials overlie unconfined aquifers. These barometric influences are due to the artificial disturbance of installing a well that pneumatically bypasses the vadose zone. Barometric water fluctuations may be severe enough to mask water level trends or pumping test measurements. These barometric pressure fluctuations have been observed in water level measurements obtained from many of the national laboratories including the INEEL, Los Alamos National Laboratory, Savanna River Site, and Hanford (tank farms) as well as numerous commercial facilities. The purpose of this research and development task is to research, design, build, and test isobaric groundwater wells for obtaining accurate aquifer water levels in unconfined aquifers. These water levels may be used in determining water level trends, groundwater flow rates, groundwater direction, and aquifer hydraulic properties. This isobaric well completion technique seals the interior of the well from atmospheric pressure, and references the water level transducer to the gas phase pressure above the water table (screened across the water table). Water levels were obtained from wells drilled into the Eastern Snake River Plain aquifer to depths of 60 and 180 m below land surface to test the effectiveness of the isobaric technique. Alternating water level data from a standard and isobaric well were collected. Daily water level fluctuations were reduced by over an order of magnitude from the standard well configuration of ±5.0 cm/d, compared to about ±0.1 cm/d using the isobaric technique. The improved precision in the water table data will allow a better understanding of aquifer properties and movement of contaminants in the subsurface for ongoing risk assessment activities, planning and performing remediation actions, and long-term stewardship of the environment at DOE facilities.

TASK DESCRIPTION

Background

DOE facilities require an accurate understanding of aquifer hydraulic properties as determined from the groundwater elevation and from the response of aquifer stress (pumping) tests. Water level elevations can be affected by changes in barometric pressure that are difficult to eliminate by conventional techniques. Current state-of-the-art methods cannot accurately account for fluctuations in the water table caused by these pressure changes, which can cause variations of up to 0.3 meters (m). This is most pronounced at sites with deep vadose zones or low hydraulic gradients, such as the INEEL. This task will research, design, build, and test an isobaric groundwater well for obtaining accurate aquifer water levels in unconfined aquifers. These water levels may be used in determining water level trends, groundwater flow rates, groundwater direction, and aquifer hydraulic properties. The isobaric technique can be used to measure more precise water levels for long term monitoring and stewardship activities.

The measurement of hydraulic gradients requires a minimum of three wells completed to obtain precise water levels at the same time. If the gas pressure above the aquifer is the same in all of these wells, the calculations can be easily performed without additional data. If the gas pressures are significantly different in the wells and they impact the gradient calculations, then the gas pressure in each well must be measured and included in the calculation of total head.

Successful installation and application of the isobaric groundwater well technique can provide an enhanced determination of local hydraulic gradient and aquifer properties at field sites as well as identify and quantify the effects of sources of recharge to aquifers. This task will develop these techniques to provide more accurate data about aquifers to improve risk assessment modeling of the time to exposure and location of exposure from current contaminant sources. This technique can provide more accurate aquifer hydraulic property results while using fewer wells, pumping less water, and spending less money compared to current practices.

To prove the practicability of the isobaric groundwater well technique, this task will design, manufacture, install, and test the devices on multiple wells in varying geologic media. The objective is to reduce the water level fluctuation to about 0.003 m by removing the barometric pressure influence with an innovative technique. Current practices require water level measurements, barometric pressure measurements, and complex, expensive, computer convolution techniques to generate an estimate of the water level. The isobaric groundwater well design automatically removes the effects of barometric pressure fluctuations without requiring further data manipulation. Figure 1 presents data from a well where standard water level measurements were obtained for about a month, after which the well was modified to collect data using the isobaric technique. The data shows a significant improvement in the water level measurements.

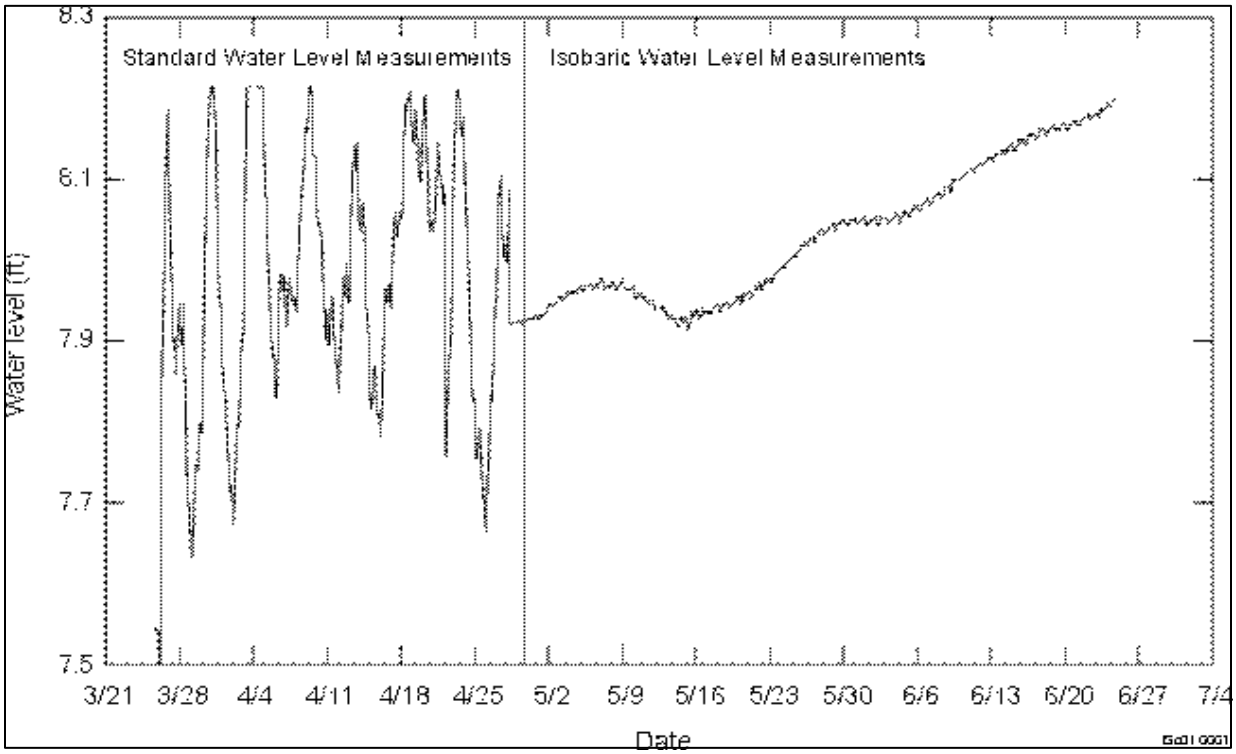

Figure 1. Comparison of water level in a standard and isobaric well.

The isobaric well technique can be used on both groundwater wells and perched water wells in the vadose zone. Following demonstration of this technique, the we expect to transfer this technology to the Environmental Restorations Department and United States Geological Survey at the INEEL, other DOE sites, and the private sector by publishing journal articles and making presentations at conferences.

Task Scope

The overall scope of this task is to (a) determine the theoretical basis and limiting physical factors for use of the isobaric technique for new and existing wells, (b) evaluate the literature to determine locations where this technique can be applied, (c) produce sets of design requirements to build isobaric wells, (d) write procedures for conducting measurements and tests in the field, (e) build new or modify existing wells for testing the isobaric technique, (f) test and demonstrate under variable field conditions, (g) generate a data set of temporal and spatial fluctuations of groundwater hydraulic gradient and flow directions, (h) conduct an aquifer stress (pumping) test using the isobaric technique, (i) submit a paper to a peer-reviewed journal, and (j) conduct tech transfer activities that will include submitting new invention disclosures, preparing patents, and making presentations.

Theoretical basis

The underlying theory for the isobaric well indicates that when electronic pressure sensors are used to monitor ground water levels over time, the observed pressures are the result of several forces as depicted in Figure 2. The hypothetical case where no fluids are flowing into or out of the well bore is presented as illustration A in Figure 2. For this case:

$$P_{obs} = P_w + P_{sg} - P_{ref} \quad (1)$$

where:

P_{obs} = value indicated at the data logger

P_w = height of water above the transducer

P_{sg} = gas phase pressure above phreatic surface

P_{ref} = gas phase pressure at the transducer reference port.

The reference pressure port is generally open to the barometric pressure. The gas phase pressure above the water table (P_{sg}) may be equivalent to the barometric pressure (P_{ref}), but where the vadose zone is thick or slowly permeable, P_{sg} can differ significantly from P_{ref}.[1] A well bore sealed from the atmosphere is presented as illustration B in Figure 2. When the P_{sg} is used to reference the transducer so that $P_{sg} = P_{ref}$, then this equation becomes:

$$P_{obs} = P_w \quad (2)$$

The effect of referencing the transducer to P_{sg} is to remove barometric fluctuations from P_{obs} so that water levels obtained using the isobaric technique (the well is sealed from the atmosphere and the pressure sensor is referenced to the gas pressure above the aquifer) will provide the true water level, thus eliminating the need for further data manipulation. This technique provides a direct measurement of the water level, unaffected by barometric fluctuations.

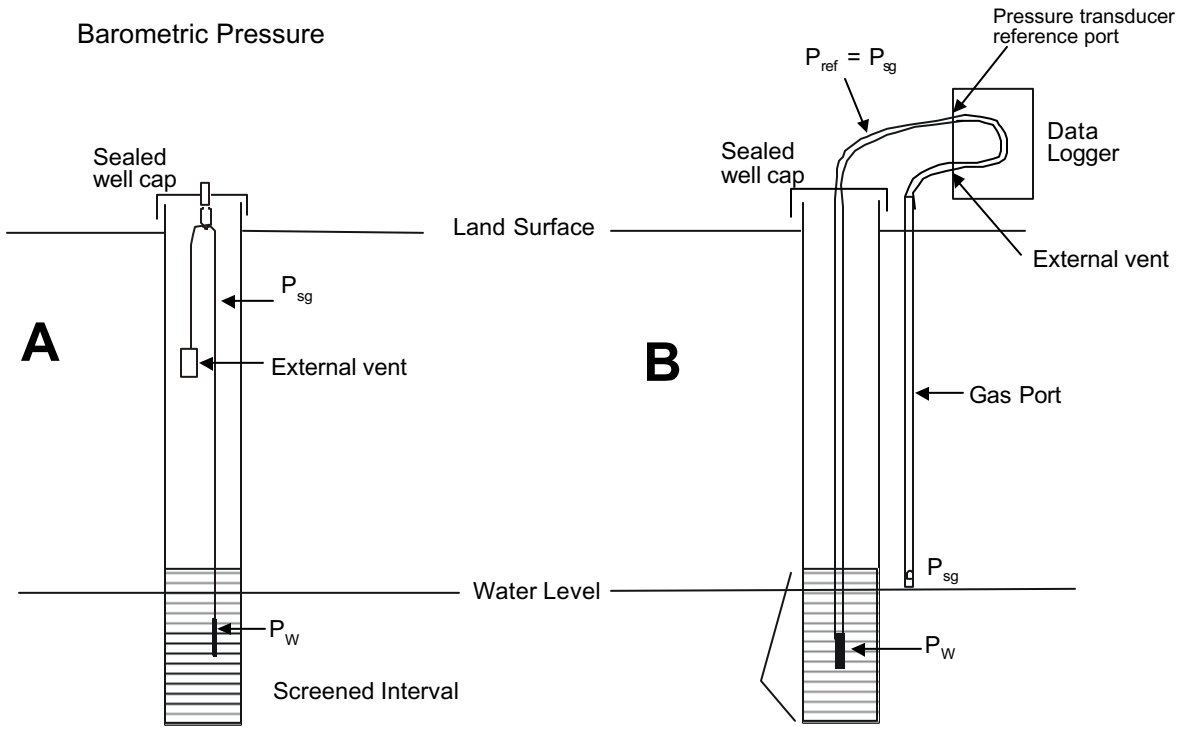

Figure 2. Pressure distribution and isobaric well configuration.

Should there be reason to believe that P_{sg} varies over the water table (phreatic) surface then P_{sg} should be monitored to estimate total head, thus referencing to a standard pressure instead of the barometric pressure. Should there be reason to believe that P_{sg} varies over the water table (phreatic) surface, then P_{sg} should be monitored to estimate total head. Precise water level trends obtained in this manner reflect the true water level in the aquifer, without the influence of the well. Wells that are screened or opened across the water table, so that air moves in and out of the vadose zone, will change the water level in the area surrounding the well, acting like a pumping or injection well.

Applicable Sites

The interaction of water level with external forces of barometric pressure and earth tides was researched to determine if there is new literature pertaining to this topic. The problem of barometric pressure changes affecting the measured water level is fairly common and has been noted as a problem at many of the DOE sites, including the INEEL, Los Alamos National Laboratory, the Savannah River Site, and the Hanford site. This problem is most pronounced at sites with deep vadose zones, sites with low permeability materials in the vadose zone, and fractured rock sites. The problem becomes more acute where the ground water has low hydraulic gradients or where hydraulic gradient calculations are being calculated from closely spaced wells. The isobaric technique has widespread application at both DOE and commercial sites where precise water levels are required. The technique can be applied at nearly any site with an unconfined or semiconfined aquifer.

Design Requirements, Procedure Development, and Well Construction

Our objective for this subtask was to prove that many existing wells, with standard configurations, could be modified and used for precise water level measurements. Most existing well configurations can be used for that purpose, but determining hydraulic gradients using isobaric wells is more complex due to the different reference pressures measured in wells with different designs. Wells used to calculate hydraulic gradients must have configurations that allow the same reference pressures and may require measurement of both water level elevation and gas pressure. These wells must have sealed joints on the casing and sound annular seal so that air does not move down the annular space to change air pressure at the water table.

Our design emphasized isobaric monitoring systems that did not interfere with the use of the well (sampling or collection of water level measurements) or increase the complexity of well construction. We used standard data logger systems for taking precise water level measurements, and restricted our modifications to simply replacing the original well caps with new sealable well caps.

We prepared procedures for conducting precise water level measurements and for evaluating data.

We then constructing several different wells and evaluated the water level data. The wells we tested were located at Test Area North (TAN) and the Radioactive Waste Management Complex (RWMC) on the INEEL. These wells had depths to ground water of about 60 and 178 m, and had different completion configurations representing the most common designs of existing wells at the INEEL.

Both sites showed significant improvement in determining precise water level measurements.

Field Testing of the Isobaric Technique: Water Level

We modified four wells at the RWMC to use for our research. One of these wells operated continuously for 14 days while collecting precise water level data (Figure 1 is an excerpt of this water level data). The precision of these water level measurements appears to be primarily limited by the precision of the transducers. These ground water level measurements can be correlated to water recharging the aquifer from the spreading areas and Big Lost River. One of these wells, located about 1,400 miles southeast of this surface water recharge site, responded about 4 months from the date that surface water was introduced to this site. We were unable to seal several of the RWMC wells at land surface because the initial well-cap design did not fit the pump, riser pipes, and electrical wiring. Consequently, a replacement well-cap was designed and submitted as an invention disclosure, and tested on one of the wells monitored at TAN. Subsequent testing of RWMC wells suggests that some of the newer wells, which have threaded stainless-steel casing, were not properly sealed during installation, making them unsuitable for conversion to isobaric wells.

We also tested several wells at TAN to measure precise water levels. The geologic setting at TAN is slightly different than at the RWMC—the water table is closer to land surface and surficial sediments are thicker. These wells showed a similar improvement in water level measurements as observed in wells at the RWMC. Several wells at TAN were converted to isobaric wells and water level data collected while pumping TAN-2, located about 300 m from these wells. Data analysis indicated that the pressure waves from the pumping well could be clearly observed in the isobaric wells for both pumping and recovery portions of the test, while the response in the standard-unsealed wells was not as clear. Being able to observe the pressure response in the standard-unsealed observation wells depended on the barometric pressure fluctuations observed during the tests. Even normal barometric fluctuations tended to obscure the water level trends in the standard observation wells.

We chose the TAN site to run the hydraulic gradient portion of the isobaric well tests.

Field Testing of the Isobaric Technique: Hydraulic Gradients

Wells at TAN at the INEEL were evaluated to conduct a hydraulic gradient test using the isobaric wells. Several wells were field pressure tested to determine their suitability for conversion to isobaric wells and four were chosen based on accessibility, construction, location, and hydraulic properties. These wells were sealed and their water levels measured using the isobaric technique. These tests were conducted assuming that the gas pressure immediately above the aquifer is equal at each of these wells. Because we used existing wells, each had a different well construction and well seal configuration. One of these wells could not be sealed, presumably due to a poor seal in the casing, so the data set from this well was corrected using the deconvolution techniques for subsequent analysis.

Precise water level measurements were collected for several weeks and the wells opened to the atmosphere to collect standard water level measurements, for comparative analysis. Data analysis indicates that using the isobaric technique allows precise water level determination for calculation of hydraulic gradients. There were small changes in head in some of the wells that changed the direction of flow that would not be able to be detected using standard well designs. These tests also indicated that the sensitivity of the water level measurements may exceeded the accuracy of the surveyed well elevations and the well deviation. Thus, wells may need to be resurveyed to a standard baseline and well deviations (using gyroscopic tools) determined to use with the precise water level elevations.

Tests at TAN indicated that several different techniques can be used to add an isobaric surface seal to an existing well without interfering with existing uses of the well. One of these techniques is proposed as the standard for future wells designed at the INEEL. These well caps could be installed during routine work, and a transducer/data logger then installed later. Sealing a well from the atmosphere adds an enhanced level of physical protection for the vadose zone, thus reducing the potential for cross contamination, chemical transfers from air borne contaminants such as tritium or volatile organic compounds, and airborne particles. It also prevents air movement into and out of a well, which may affect the water levels immediately around the well.

Our research and development of precise water level measurements has opened the path for future work. Networks of isobaric wells could be used to measure long-term water levels in both ground water and perched water. The data obtained could be used to better estimate the hydraulic properties in aquifers. The technique could also be used to determine the continuity of perched water bodies, by pumping from one well and monitoring water levels in adjacent wells. This analysis could also look at the response of the water levels for locating boundaries using the techniques described by Lohman.[2] An analysis of precise water levels from multiple wells at the INEEL would improve our understanding of water flow in fractured rock. Comparison of water level deconvolution techniques versus isobaric measurements should be evaluated. The isobaric water level measurement technique allows direct measurement of the true water level, which could be compared to results from analytical techniques (such as the deconvolution technique). The effect of airflow into and out of unsealed wells may induce ground water flow at sites like the INEEL with very low gradients. Also the presence of gas pressure gradients above the ground water should be evaluated. Series of isobaric wells should be used around TAN, INTEC, and the RWMC to map the temporal aspects of hydraulic gradients (for direction of ground water flow).

The isobaric technique will allow DOE and commercial sites to measure precise water levels at their sites and determine long-term water levels and hydraulic gradients using direct measurements. These precise water levels will provide a better understanding of flow and transport in ground water for characterization, remediation, and long-term stewardship activities.

ACCOMPLISHMENTS

We determined the theoretical basis and physical limiting factors for measuring precise water level elevations using isobaric wells at the INEEL, for both new and existing wells.

We produced design requirements and procedures for measuring precise water levels using existing well configurations and for constructing new wells.

We modified several new and existing wells at the RWMC and TAN sites on the INEEL to collect precise water level measurements for time periods up to 14 months. The precision of the water level measurement was controlled by the precision of the transducer used for the measurements.

We conducted aquifer stress tests at TAN while monitoring water levels in isobaric wells. The improved water level measurements provided a better data set for analysis than water level data from conventional wells.

We used the isobaric technique as the basis for developing a design for a tensiometer that can obtain improved soil water potential measurements from the vadose zone. This design was submitted as an invention disclosure. A patent application was prepared and submitted for consideration to the U.S. Patent and Trademark Office.

We submitted an invention disclosure for a well cap design and sealing technique that can be used to construct an isobaric well and on either new or existing wells. This simplified well cap design seals the well, but has minimal impact on groundwater sampling and manual water level measurements.

We were granted U.S. Patent number 5,969,242 for the Isobaric Groundwater Well by the U.S. Patent and Trademark Office.

Discussions with representatives of the INEEL Environmental Restorations Department indicate that they hope to install a network of new wells specifically for the purpose of monitoring water levels using the isobaric technique, but there were no set dates for this work to begin.

REFERENCES

1. E. P. Weeks, "Barometric Fluctuations in Wells Tapping Deep Unconfined Aquifers," *Water Resources*, Vol. 15 (5), 1979, pp. 1167–1176.

2. S. W. Lohman, "Ground-Water Hydraulics," *United States Geological Professional Paper* 708, 1979, pp. 57–60.

Assessment of Mercury Environmental Fate and Transport from INEEL Waste Processing Facilities for Long-Term Stewardship Concerns and Development of Improved Modeling Methods

Understanding the Movement of Mercury in the Environment Surrounding the INEEL

Michael L. Abbott

SUMMARY

Environmental fate and transport of the toxic air pollutant mercury (Hg) is currently a high-priority regional concern for the INEEL, and national and global concern for the U.S. Environmental Protection Agency (EPA). At the INEEL's Idaho Nuclear Technology and Engineering Center (INTEC), significant quantities (est. 40 kg/year) of Hg may have been released over 37 years of Environmental Management's (EM's) high-level waste (HLW) calcination operations. The EPA is very concerned about the continued global buildup of Hg in the atmosphere and aquatic ecosystems, and has recently invested heavily in Hg research to better understand its complex environmental cycling.[1,2] This task is a joint INEEL and U.S. Geological Survey field research effort to better understand the fate of Hg emissions (operational component) from the INEEL's calciner (New Waste Calcining Facility [NWCF]) and contribute at a national level to the scientific understanding of local, regional, and global Hg fate and transport (research component). This task consists largely of Hg fallout sampling in precipitation and soils in two geographic areas: the INEEL and surrounding airshed, which includes the Eastern Snake River Plain and adjacent elevated areas; and two high-elevation, mid-latitude glaciers—the Upper Fremont Glacier (UFG) in Wyoming and the Inilchek Glacier in Central Asia. Glacial snowpack provides a preserved annual record of both regional and global Hg fallout that can be used to answer questions about long-range INEEL transport and help to fill existing data gaps on the relative importance of local versus global source contributions to fallout.

Samples of snow (n = 130), rain (n = 6), soil (n = 103), and air (n = 5) were successfully collected on the INEEL and at 11 regional background sites from January through March 2002. Analytical results for snow before startup of the calciner indicated relatively low Hg concentrations within the range of the western regional background (3 ng/L) and unexpectedly high concentrations (10 to 20 ng/L) near INTEC, which may be due to Hg evasion from the soil followed by entrapment in the overlying snowpack. Because startup of the NWCF was delayed until March 15, 2000, and no appreciable snow fell after this date, snow sampling to determine NWCF fallout rates on the INEEL was not possible. Snow samples were successfully obtained from the UFG in May (n = 20) and the Inilchek in July (n = 50). The UFG data indicated very low (0.3 to 0.9 ng/L) concentrations relative to regional background, and the Inilchek samples have not yet been analyzed. Surface soil sampling around INTEC showed (a) very low Hg concentrations overall compared to background levels in similar soils across the U.S., (b) a 4% per cm reduction in Hg concentration with depth, and (c) significantly higher Hg concentrations in soils under shrubs (likely due to fixation by organic matter) and in depressions (likely due to Hg runoff). Using these data, mass balance calculations were able to account for approximately 40–300 kg of calciner Hg in the soil, which is only 3–20% of the estimated total Hg emitted over the 37-year calciner operating history. These results provide evidence that much of the Hg deposited from calciner operations may have been reduced in the soil and reemitted as Hg(0) to the global atmospheric pool.

TASK DESCRIPTION

Summary of Sampling Activities

Table 1 summarizes the multimedia sampling activities during FY 2000. All samples were analyzed for total mercury (THg), and a small fraction were analyzed for methylmercury (MHg). Total Hg includes all chemical forms of Hg, including (a) divalent Hg(II), which readily deposits and is the predominant form of Hg emitted by the calciner; (b) elemental Hg(0), which comprises the bulk of the global atmospheric pool, but does not readily deposit (until some of it is oxidized by downwind atmospheric chemistry); and (c) methyl mercury, which is of concern because it is a more toxic species and bioaccumulates in aquatic organisms (up to 10^7 times the water concentration). Snow and rain were sampled because these are the dominant scavenging mechanisms that transport Hg from the atmosphere to the ground, where it is of primary concern (Reference 1). Also, precipitation concentrations can be linked with precipitation time intervals to calculate Hg deposition rates, which can then be used to validate deposition models. Snow was the primary sampling medium because it is the dominant form of precipitation in this region and because it usually remains on the ground, allowing sampling at a later date. However, because startup of the NWCF was delayed until March 15, 2000, and very little snow fell on the INEEL after this date, only five snow samples on the INEEL were obtained during NWCF operations. Because of the lack of the INEEL NWCF data, proposed source apportionment methods (principal component analysis and isotopic ratios) were not implemented. Limited rain sampling was done after this time because of the continuing dry conditions this spring and the difficulty of coordinating rain sampler deployment during the few short-term rainfall events that occurred. Soil sampling was

Table 1. Summary of mercury sampling activities for FY 2000.

Location	Month/00	No. Samples	Analyzed?	Purpose
		Snow		
INTEC 5-km Grid	Jan 4–6	50	Yes	Pre-NWCF startup baseline
(Figure 1)	Mar 17	8	Yes	Post-NWCF impacts
Background sites (10)	Dec 20	15	Yes	Regional background surrounding
(Figure 2)	Jan 17–19	24	Yes	INEEL
	Mar 25–26	34	Yes	
W. Slope Teton Range (5 sites from 6,000 to 10,000 ft)	Jan 17–18	20	Yes	1) High precipitation/fallout rates 2) Sensitive "downwind" ecosystem
Upper Fremont Glacier, WY (13,200 ft)	May 1–8	20	Yes	1) Long-range INEEL transport 2) preserved annual fallout record in snowpack
Inilchek Glacier, Asia (16,000 ft)	July	50	No	Global fate/transport data gaps
		Rain		
INTEC Grid – NE1, NE2, NW1	May	6	Yes	1) Rain sampling method 2) NWCF fallout
		Air		
INTEC Grid—1–4 km downwind of NWCF plume; rest area	Mar	5	Yes	1) Air sampling method, 2) regional background
		Soil		
Experiment 1	Jul	24	Yes	Sampling methods-depth
Experiment 2	Jul	20	Yes	Sampling methods-vegetation
INTEC Grid	Aug	59	No	Residual cumulative deposition

successfully accomplished in late summer to determine the Hg variability in soil (Experiments 1 and 2) and to estimate the cumulative residual Hg load in the soil around INTEC after 36 years of calcining operations.

Most of the sampling on the INEEL was conducted on the INTEC 5-km grid—an array of 64 sampling locations located on 22.5-degree radials at distances of 1, 2, 3, and 5 km (Figure 1). This grid was designed, based on previous air modeling studies of the INTEC 250-ft main stack,[3] to provide an adequate assessment of the fallout pattern around the facility with a reasonable number of samples. The 10 background sites (Figure 2) were selected based on their location surrounding the INEEL, their likelihood of snowfall accumulation, and winter access. Snow was also sampled in January on an elevation gradient extending from the Teton Valley outside Driggs, Idaho (6,000 ft) to the summit of Grand Targhee Ski Area (10,000 ft). This area was selected because it (a) receives very high snowfall (maximizes air pollutant scavenging) and snow accumulation (allows sampling of a long-term fallout period), (b) is an optimum location to investigate changes in Hg fallout with elevation (current high interest to EPA), and (c) is located between the INEEL and concerned public interest groups in Jackson, Wyoming (stakeholder considerations). Snow sampling was conducted at the Upper Fremont Glacier (UFG) and Inilchek Glacier sites because of (a) the comprehensive annual fallout record preserved in their winter snowpack, (b) their mid-latitude locations and elevations, and (c) ongoing research activities at these locations by the U.S. Geological Survey, which allowed sharing of field trip expenses. The UFG site was also investigated to determine if long-range transport of Hg from the INEEL could be detected.

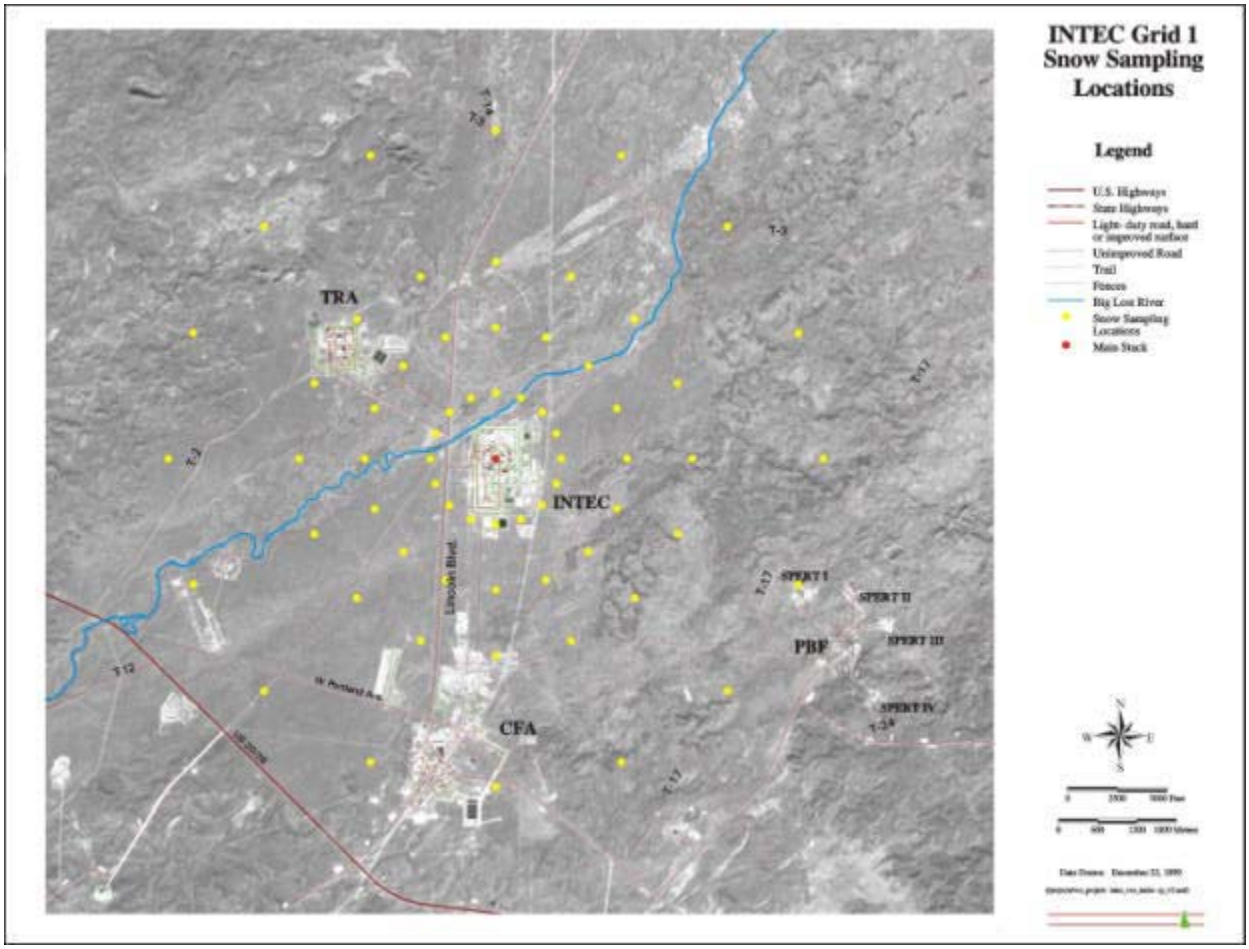

Figure 1. INTEC 5-km sampling grid–64 locations on 22.5º radials at distances of 1, 2, 3, and 5 km.

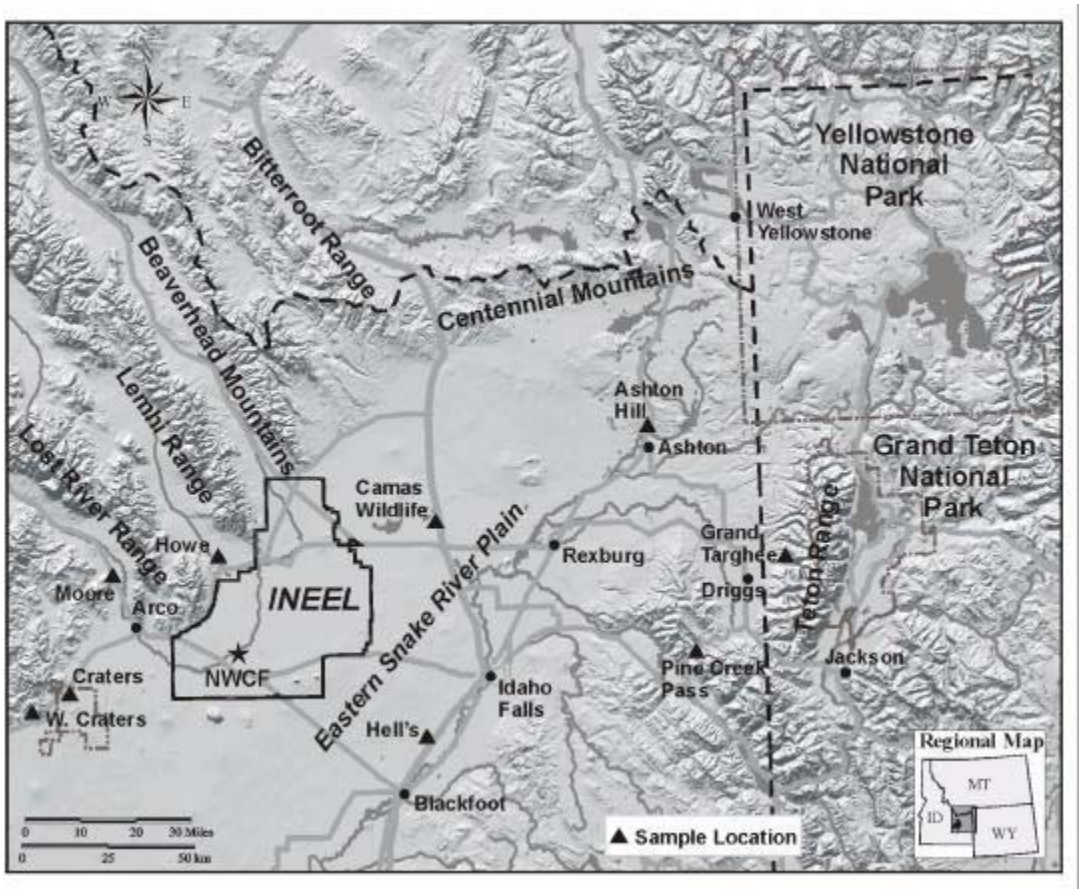

Figure 2. Regional background snow sampling locations (Pebble Creek site is 10 km south of map).

Sampling and Analytical Methods

Laboratory analysis and sample bottles were provided by the U.S. Geological Survey Wisconsin District Mercury Laboratory (WDML) in Madison, Wisconsin. The WDML is one of two full-service environmental mercury laboratories in the U.S. All sampling is done using laboratory cleaned, Hg-free sampling bottles (30 mL, 250 mL, 500 mL, and 2 L) and shoulder-length gloves; the sample bottles are kept upwind during sampling.

For snow samples, the snowpack was excavated to the ground and the snow face was cleaned using a clean lexan shovel (Hg sticks to metal). At the INEEL, composite samples of the entire snowpack thickness (typically about 20 cm) were collected using special precleaned 500 mL and 2 L teflon bottles. At background and glacier sites with significant (>50 cm) snowpack, a snow pit was dug, and 10-cm interval samples were collected in addition to a composite. Snow density measurements were made which are later multiplied by the snow depth to determine the snow water equivalent (SWE) at each location (SWE is equivalent to the mass [kg] or depth of water [mm] per unit area). After sampling, the bottles were double-bagged, placed into a cooler, and shipped frozen to the WDML.

Rain samples were collected in portable collectors consisting of custom-made 20 L teflon bag liners inside 55-cm-wide Δ 37-cm-long Δ 15-cm-high plastic storage containers (Sterilite® Clearview). The collectors were deployed at model-predicted maximum impact downwind locations on the INTEC

Grid. After the rainfall event (typically overnight), the sample (if any) was poured into a 500 mL teflon bottle. Soil samples were collected in 30 mL teflon vials after suface litter and pebbles were removed.

In the laboratory, samples were melted, acidified (to keep the mercury oxidized and in solution), and analyzed for total mercury (THg) and methylmercury (MHg).[4] THg includes all chemical forms of Hg, including divalent Hg(II), elemental Hg(0), and methyl mercury. THg analysis was performed using EPA Method 1631, "Mercury in Water by Oxidation, Purge and Trap, and Cold Vapor Atomic Fluorescence Spectrometry (CVAFS)," with modifications. MHg analyses were preformed using EPA Method 1630, "Methyl Mercury in Water by Distillation, Aqueous Ethylation, Purge and Trap, and CVAFS," with minor modifications. For some samples, a filtered/unfiltered (FTHg/UTHg) split was analyzed, which can provide information on whether the Hg was associated with particulate or existed as a gas in the atmosphere (which provides evidence of the fallout source). Soil samples are analyzed in a similar way, except that a subsample was first taken and then digested in a mixture of nitric and sulfuric acid. The laboratory uses a rigorous QA/QC procedure, which includes duplicate analyses on every sample, spike recovery analyses at least once every 10 samples, quality control check samples, and bubbler blanks to check for background contamination (see Reference 1).

Sampling Results—Snow

A summary of the Hg snow sampling results (in ng/L) for the INEEL and background sites is provided in Table 2. For comparison, the EPA maximum contaminant level (MCL) for Hg in drinking water is 2,000 ng/L. Most of the snow samples were taken before the NWCF was started on March 15, 2000. A few background sites with late winter snowpacks (Pebble Creek, Pine Creek Pass, and Ashton Hill) were sampled after the startup date, but very limited snow sampling was possible on the INTEC grid because of the late calciner start date.

The INTEC grid sampling results conducted before calciner startup showed statistically higher Hg concentrations compared to the background sites, which was very surprising given the NWCF had not operated through the winter (see Figure 3). The following are possible reasons for these unusual results:

- Another unknown Hg source at INTEC operating during the period of snowfall (primarily in late December 1999) before the sampling (Jan 4–6, 2000)—investigated but none found. The previous calciner campaign (NWCF4) was completed in May 1999, and the High-Level Liquid Waste Evaporator was last run in July 1998.

- Soil cross-contamination during sampling—not likely because (a) the increase in concentration around INTEC was relatively uniform, which would require consistent cross-contamination with soil, and (b) the "ultraclean" sampling techniques specifically avoid contact of any sampling material with the soil surface; these methods have been previously used numerous times without any indication of cross-contamination.

- Reemission of deposited Hg in the soils around INTEC followed by absorption or hold-up in the snowpack prior to release to the atmosphere. This is a likely explanation because (a) the filtered versus unfiltered fraction (FTHg/UTHg) for the January grid samples (0.42) were higher than what has been previously measured suggesting a gaseous Hg source, (b) a mass balance calculation on the soil sampling results (see below) indicates significant reemission loss of deposited Hg from soils, and (c) soil reduction of the deposited Hg(II) and reemission as Hg(0) has been well documented, especially in high pH, low organic content soils characteristic of the INEEL. Snow and soil flux experiments are planned for FY 2001 to confirm and quantify these reemission rates.

Table 2. Summary of Hg concentrations in snow (F/U = filtered/unfiltered; M/THg = methyl/total).

Sampling Location	No. samples	THg Concentration in Snow (ng/L)			Fraction F/U THg	Fraction M/T Hg
		High	Low	Avg.		
INTEC Grid (1/4–1/6/00, prior to calciner start):						
1 km radius	8	22	8.9	15	0.41	0.017
2 km radius	16	15	5.5	9.3	0.45	0.019
3 km radius	13	14	5.6	8.9	—	—
4 km radius	12	11	4.7	7.7	0.38	0.013
			Average =	***10***	***0.42***	***0.02***
INTEC Grid (3/17/00, after calciner start):						
1 km radius	5	141	6.4	55	—	—
Background Sites [(A) = after calciner startup]:						
Pebble Creek	2	4.5	3.6	4.0	0.25	0.03
Pebble Creek (A)	3	2.7	1.1	2.1	.35	0.02
Hell's Half Acre	2	8.5	5.2	6.9	0.19	0.01
Pine Creek Pass	13	6.8	1.5	2.2	0.33	0.03
Pine Creek Pass (A)	6	5.9	1.7	2.2	0.26	0.01
Ashton Hill (top)	18	12	1.8	3.3	0.42	0.02
Ashton Hill (A)	5	5.0	2.3	3.8	0.21	0.04
Camas Wildlife Refuge	5	3.4	1.6	2.3	0.30	0.01
Howe area	3	6.2	1.2	3.8	0.38	0.01
Moore area	8	7.3	0.9	3.0	0.29	0.01
Craters of the Moon	7	3.7	1.9	2.6	0.37	0.01
West Craters	3	4.6	2.7	3.3	0.27	0.01
			Average =	***3.3***	***0.30***	***0.02***
W. Slope Teton Range:						
Tetons – 10,000 ft	6	7.8	2.56	3.5	0.31	0.004
Tetons – 8,000 ft	4	9.3	3.6	4.0	0.28	0.04
Tetons – 7,000 ft	3	3.1	1.7	1.7	0.33	0.01
Tetons – 6,600 ft	4	2.6	2.0	2.6	0.19	0.01
Teton Valley	3	6.9	2.5	4.6	0.26	0.02
			Average =	***3.3***	***0.28***	***0.02***

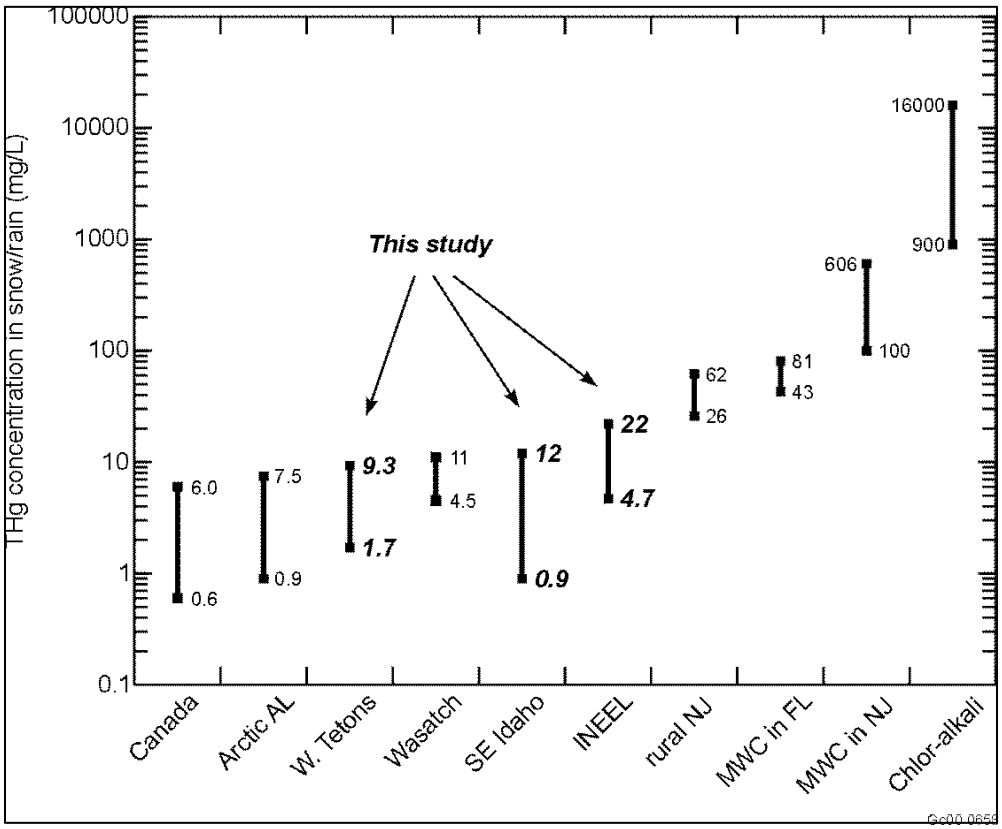

Figure 3. Comparison of snow THg concentrations found in this study (INEEL, SE Idaho, and W. slope Teton Range) with published values for precipitation (snow and rain) in other U.S. and Canadian areas.

The INTEC grid snow sampling conducted after calciner startup indicated much higher concentrations at two locations (134 ng/L at 1 km northeast of INTEC and 141 ng/L at 1 km east-northeast). However, only a limited number of samples could be taken because of the poor snow conditions at this late date, and these samples may have been cross-contaminated with soil because of the difficulty of sampling the shallow (<2 cm) snow depth.

At background sites and the west slope of the Teton Range, snow concentrations were low (3.3 ng/L), similar to those measured in other remote low-impact locations, including arctic Alaska (0.9 to 7.5 ng/L),[5] Ontario, Canada (0.6 to 6.0 ng/L),[6] and in Utah's Wasatch Range (4.5 to 11 ng/L)[7] (see Figure 4). Concentrations in precipitation in eastern industrialized areas have been measured at much higher levels, i.e., 26 to 62 ng/L in a rural New Jersey area,[8] 606 ng/L near a municipal waste combustor (MWC) in New Jersey, and 16,000 ng/L near a chlor-alkali plant in an urban residential area.[9]

Snow sampling on the Upper Fremont Glacier, Wind River Range, Wyoming was successfully completed May 1–8, 2000. Twenty 500-mL snow samples were collected from the full winter snowpack (two replicate pits 2.3 m deep) on the glacier at 13,200-ft elevation. The analytical results indicated very low mercury concentrations (0.3 to 0.9 ng/L) relative to the expected background concentration in precipitation in this region (1 to 3 ng/L). The laboratory analytical QA procedures were verified, and the results were found to be valid. These low results are currently being investigated but may be due to excessive Hg volatilization in the snowpack driven by the unusually dry winter (and therefore relatively old age of the snow sampled) and the high solar radiation conditions that existed during the months prior to sampling (a reemission driver).

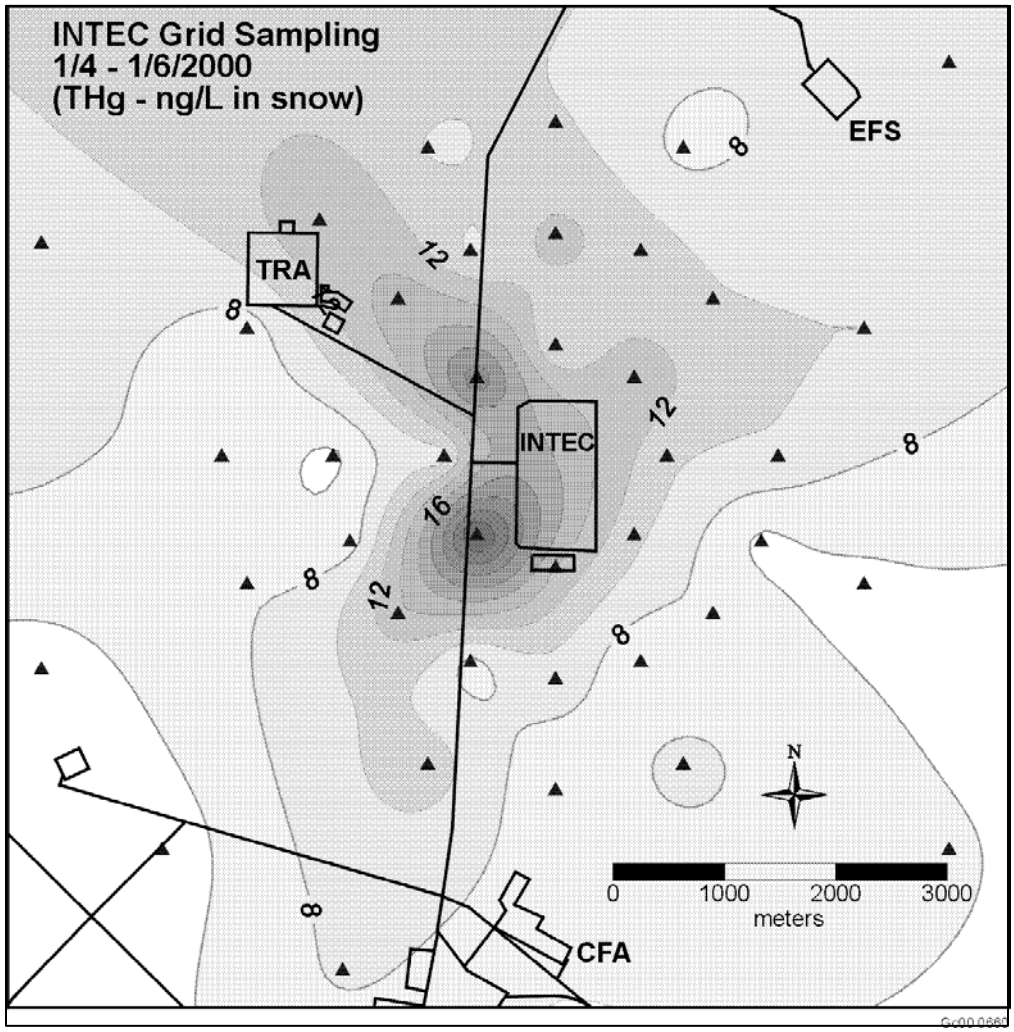

Figure 4. THg concentrations in snow (ng/L) sampled on the INTEC 5-km grid prior to startup of the calciner (3/15/00).

Sampling Results—Rain

Snow sampling on the Inilchek Glacier in Central Asia was successfully accomplished during the first two weeks of July 2000 in collaboration with a USGS glacier ice-coring expedition. Fifty snow samples from three 3-m-deep snow pits (two to three seasons of snow) were obtained and are currently being analyzed. These samples will help fill important data-gaps on global cycling of Hg in remote locations. The EPA Office of International Activities expressed interest in this work during a May 25, 2000 conference call.

Only three significant rain events occurred before shutdown of the calciner at the end of May 2000. Six rain samples were successfully obtained at three locations on the INTEC grid during one of these events (May 17, 2000). Two of these locations were chosen to be directly in the plume path (northeast at 1 and 2 km) and one was taken in the cross-wind direction (northwest at 1 km). Concentrations ranged from 14 to 20 ng/L in the plume path to 11 ng/L in the cross-wind direction. The demonstration of a successful collector design that is inexpensive and easily deployed is considered the most important result from these sampling activities.

Sampling Results—Air

Some limited air sampling was performed on the INTEC 5-km grid while the calciner was operating using a Bios AirPro portable air sampler (1 L/min) and goldtraps (gold-coated silica sand in a glass tube). The results (n = 3, u = 2.23 ng/m^3) were within the global background range (1 to 3 ng/m^3) expected for this region. These results are not unexpected since goldtraps only trap elemental Hg(0), and emissions from the calciner are believed to be primarily in the divalent Hg(II) state.

Passive integrated mercury samplers (PIMs), still in a developmental stage, were obtained without cost through collaboration with the USGS Columbia Environmental Research Center (CERC) in Columbia, Missouri. Three of these units were deployed for 25 days on the INTEC sampling grid during calciner operations. Analytical results showed a blank contamination problem (from the stainless steel shipping cans), and the results were not considered valid. The CERC has fixed the problem and may provide more PIMs (in different Hg-free shipping containers) for INEEL deployment in the future.

Sampling Results—Soil

Before comprehensive INTEC grid soil sampling, two experiments were conducted in July 2000 to determine Hg distribution in the soil around INTEC. The first experiment examined Hg concentration as a function of soil depth at a high-fallout location 1 km northeast of INTEC. Twenty-four soil samples were taken at 1-in.-depth intervals down to 4 in. using a custom-made soil horizon sampler (borrowed from the State of Idaho INEEL Oversight Program). Results showed that Hg soil concentrations decrease about 10%/in. of soil depth (see Figure 5) and that overall soil concentrations near INTEC are low relative to background levels published for similar soils in other regions in the U.S. (50 to 60 ng/g).

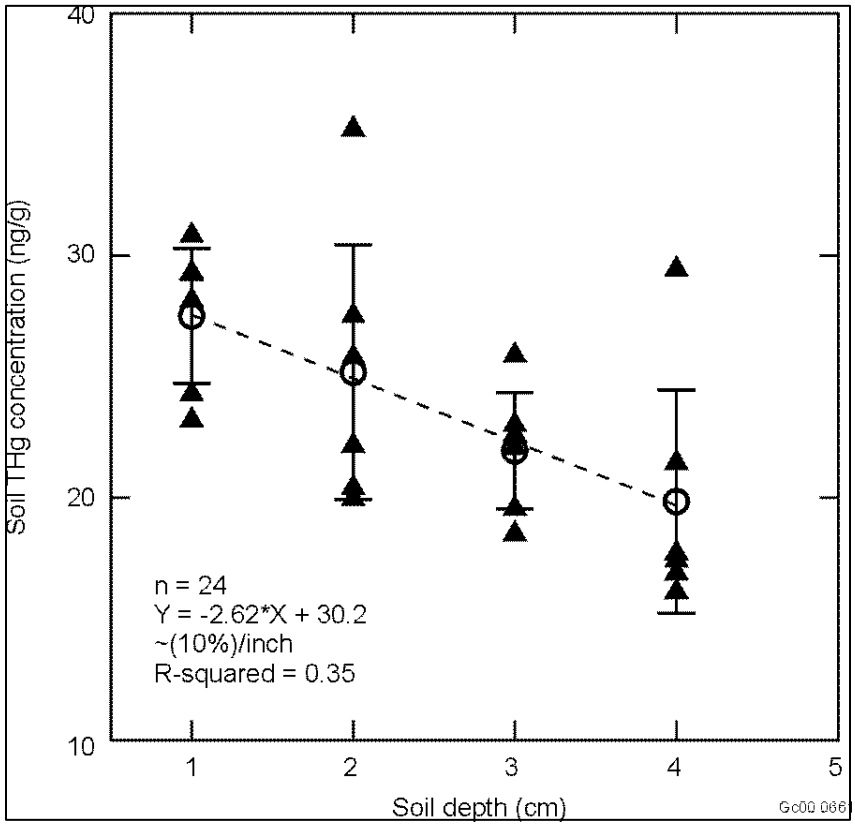

Figure 5. THg concentrations in soil near INTEC decreased approximately 10%/in. with depth.

The second experiment examined the variability of surface soil Hg concentrations as a function of vegetation type/cover and soil runoff features (rise vs. depression). These results (see Figure 6) show (a) Hg soil concentrations under shrub (sagebrush and rabbitbrush) canopies are a factor of 2 higher ($p < 0.05$) than soil concentrations in grassy or bare areas, likely due to fixation by the higher organic matter content of soils there, and (b) Hg soil concentrations in depressions are a factor of 2 higher than in adjacent elevated areas, likely due to runoff.

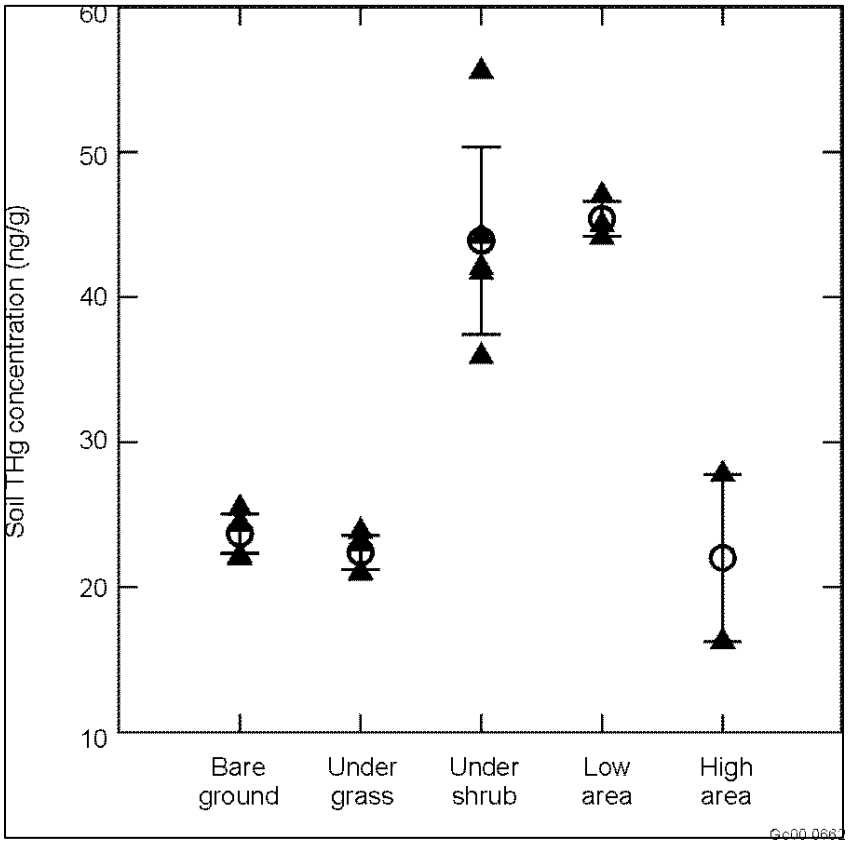

Figure 6. THg concentrations in soil under shrubs and in depressions were found to be a factor of 2 higher ($p < 0.01$) than concentrations in soil under grass, with no vegetation, or in elevated areas.

Comprehensive soil sampling results on the INTEC grid (see Figure 7) showed very low Hg concentrations overall compared to similar soils across the U.S. and a slight increase ($p < 0.05$) in concentrations within 5 km of INTEC (the "halo" in Figure 7). An estimate of the total calciner Hg load in the soil around INTEC and a mass balance of calciner Hg emissions over its 37-year operating history was made by (a) integrating surface soil concentrations across the 5-km grid (where most of the fallout was observed) and out to a conservative range of 20 km using Surfer® 7[a] kriging and volume tools and a conservatively-low background level of 7 ng/g; (b) repeating this process at 1-cm depth layers, reduced in concentration by 4% per cm (from the soil depth experiment), down to "0" integrated concentration; and (c) summing the calculated Hg mass in the 1-cm layers. The results show a total surface soil load near the facility of 37–300 kg which is a small fraction (3–20%) of the estimated cumulative 37-year emissions from the calciner (1,500 kg).

---

a. Golden Software, Inc., Golden, Colorado 80401; www.goldensoftware.com

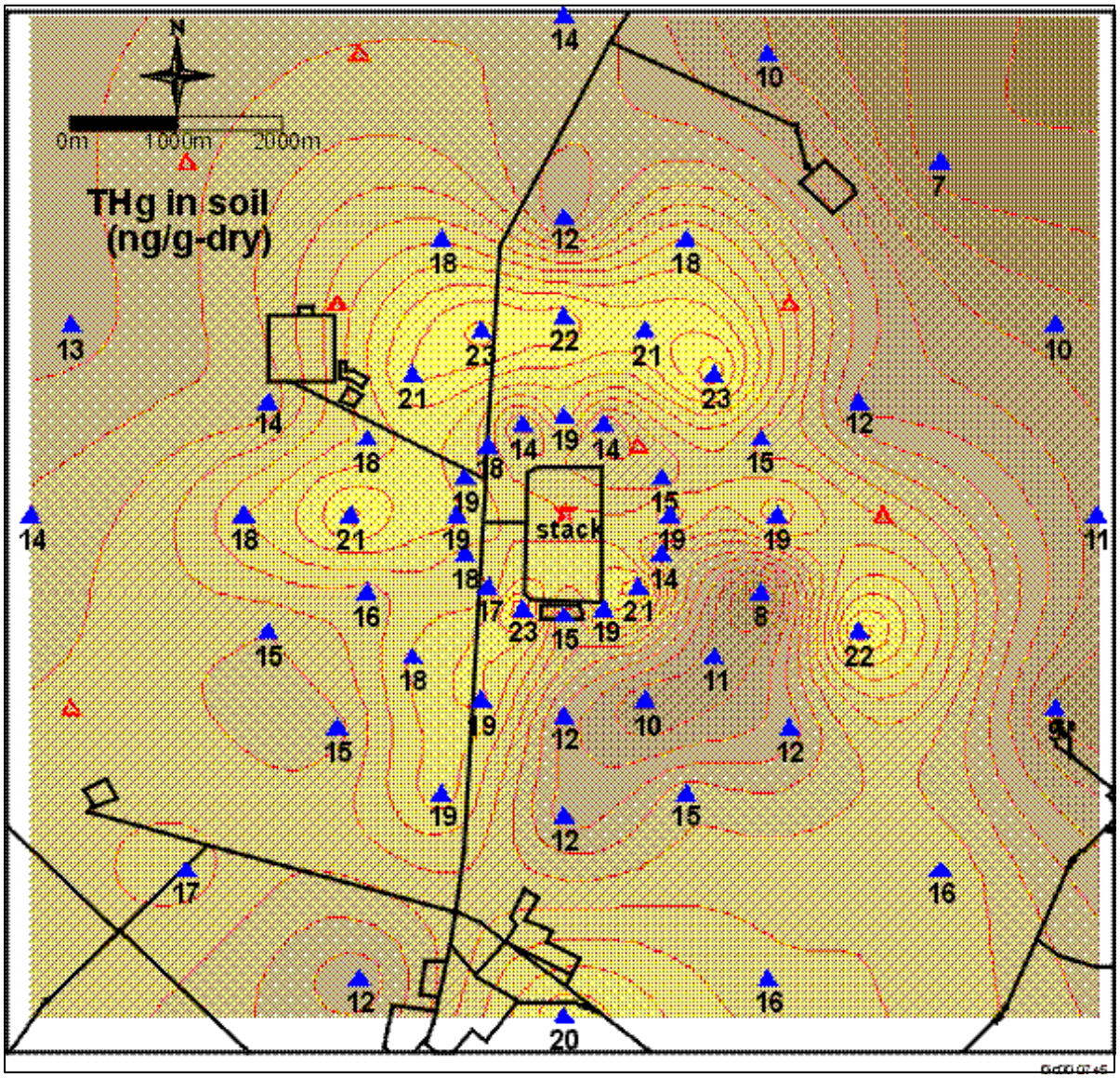

Figure 7. Hg concentrations (ng/g) in surface soil within 5-m of the INTEC main stack.

These soil sampling results, the mass balance calculations, and the high grid snow sampling results before calciner startup provide good evidence that most of the Hg initially deposited on the INEEL from calciner emissions were likely reduced in the soil from the emitted divalent Hg(II) species (known to be the primary form in the stack gas and readily deposit close to the source) to elemental Hg(0) where it was subsequently reemitted to the atmosphere. Once reemitted, the Hg(0) would become part of the global Hg pool which does not readily deposit locally (see Reference 1). However, this reemitted Hg does contribute to the increasing global atmospheric Hg pool, a fraction of which eventually is oxidized to Hg(II) and then subsequently deposited elsewhere. Confirmation and quantification of snow and soil Hg reemission losses will be pursued using flux chamber measurements in FY 2001.

ACCOMPLISHMENTS

Samples of snow (n = 130), rain (n = 6), soil (n = 103), and air (n = 5) were successfully collected on the INEEL and at 11 regional background sites from January through March 2000. Snow samples were successfully obtained from the Upper Fremont Glacier, Wyoming, in May (n = 20) and the Inilchek Glacier, Central Asia, in July (n = 50). This sampling required development and successful implementation of ultraclean sampling techniques necessary for consistent preservation of ambient Hg at parts-per-trillion levels, and successful and safe field operations in harsh winter conditions, even at some high-altitude locations. All samples except one passed rigorous laboratory QA/QC procedures, which included duplicate analyses on every sample (<10% variation), spike recoveries and quality control check samples every 10 samples (±10%), and bubbler blanks for background correction.

The major conclusions from this field research are as follows:

- Mercury concentrations in precipitation fallout are very low both on the INEEL and regionally. The highest concentration found on the INEEL during calciner operations was 141 ng/L, less than one-tenth the EPA's MCL for Hg in drinking water (2 ppb or 2,000 ng/L). Most concentrations on the INEEL were significantly lower. Concentrations at regional background sites were much lower and similar to the background fallout rate (3 ng/L) expected for this region. This background fallout rate is as low or lower than anywhere else in the U.S.

- Most of the Hg in the calciner emissions, which is almost 100% Hg(II), is deposited within 10 km of the stack, based on reconnaissance field sampling and model validation work done in 1999.[10]

- Mercury concentrations in surface soil near INTEC (15 to 20 ng/g) increase slightly at distances closer than 5 km, indicating a contribution from the calciner. However, the concentrations measured at all locations near INTEC are very low compared background Hg concentrations in similar soils around the U.S. (50 to 70 ng/g).

- A mass balance of the soil sampling data near INTEC indicate 40 to 300 kg of Hg from calciner emissions remain in the surface soil. This is estimated to be 3 to 20% of the cumulative 37 years of Hg deposition from the calciner (est. 1,500 kg).

- It is likely that most of the Hg fallout from calciner operations was initially deposited as Hg(II) close to INTEC, subsequently reduced in the soil to Hg(0), and then reemitted to the atmosphere where it would have become part of the global atmospheric Hg pool. Elemental Hg(0) does not readily deposit to the ground, and may be transported long distances in the atmosphere before a small fraction of it is oxidized and subsequently deposited on the ground. Confirmation and quantification of snow and soil Hg reemission losses on the INEEL will be pursued using flux chamber measurements in FY 2001.

Future Work

Future work includes continued precipitation and soil sampling on the INEEL and regionally, and new efforts on reemission flux measurements and aquatic ecosystem sediment sampling.

To better understand Hg cycling on a global scale, additional parameters affecting Hg speciation and transport between various environmental compartments (air, soil, sediment, and biota) may need to be investigated. One area currently thought to be important, but of which very little is known, is the effect of soil microorganisms and biochemistry.

REFERENCES

1. Environmental Protection Agency, *Mercury Study Report to Congress (Vols. I-VIII)*, http://www.epa.gov/oar/mercury.html, EPA-452/R-003 through 010, December 1997.

2. Environmental Protection Agency, "Mercury Research Strategy," *NCEA-I-0710 Workshop Review Draft*, November 1999.

3. M. L. Abbott, K. N. Keck, R. E. Schindler, R. L. VanHorn, N. L. Hampton, and M. B. Heiser, *Screening Level Risk Assessment for the New Waste Calcining Facility*, INEEL/EXT-97-00686 Rev. 5a, May 1999.

4. M. L. Olson and J. F. DeWild, "Techniques for the Collection and Species Specific Analysis of Low Levels of Mercury in Water, Sediment and Biota," D. W. Morganwalp and H. T. Buxton (eds.), *U.S. Geological Survey Toxic Substances Hydrology Program—Proceedings of the Technical Meeting*, Charleston, SC, USA, March 8–12, 1999, Volume 2 of 3—*Contamination of Hydrologic Systems and Related Ecosystems: U.S. Geological Survey Water-Resources Investigations Report,* 99-4018A, 1999, pp. 191–201.

5. E. Snyder-Conn, J. R. Garbarino, G. L. Hoffman, and A. Oelkers, "Soluble Trace Elements and Total Mercury in Arctic Alaskan Snow," Arctic, 50, 1997, pp. 201–215.

6. V. L. St. Louis, J. W. Rudd, C. A. Kelly, and L. A. Barrie,"Wet Deposition of Methylmercury in Northwestern Ontario Compared to Other Geographic Locations," *Water, Air, and Soil Pollution*, 80, 1995, pp. 405–414.

7. D. D. Susong, M. L. Abbott, and D. P. Krabbenhoft, "Reconnaissance of Mercury Concentrations in Snow from the Teton and Wasatch Ranges to Assess the Atmospheric Deposition of Mercury from an Urban Area," Abstract H12b-06, Eos, *Transactions of the American Geophysical Union*, 80, 1999, p. 46.

8. A. Greenberg, I. Wojtenko, H. Chen, S. Krivanek, J. Butler, J. Held, P. Weis, and N. Reiss, "Mercury in Air and Rainwater in the Vicinity of a Municipal Resource Recovery Facility in Western New Jersey," *The International Symposium on Measurement of Toxic and Related Pollutants, Durham, North Carolina, May 8, 1992*.

9. P. J. Temple, and S. N. Linzon, "Contamination of Vegetation, Soil, Snow, and Garden Crops by Atmospheric Deposition of Mercury from a Chlor-Alkali Plant," in D.D. Hemphill (ed.), *Trace Substance in Environmental Health – XI*, University of Missouri, Columbia, Missouri, 1977, pp. 389–398.

10. M. L. Abbott, D. D. Susong, and D. Krabbenhoft, "Comparison of Mercury Measurements in Snow with ISCST3 Model-Predicted Deposition Near an Industrial Emission Source in Southeastern Idaho." *Air & Waste Management Association International Conference on Measurement of Toxic and Related Air Pollutants, Research Triangle Park, North Carolina, September 13, 2000.*

Advanced Robotic Technologies for Remote Environmental Surveillance and Stewardship

Robots to Measure Hazardous Materials and Contaminated Sites

Mark D. McKay, Ron A. Lujan, and Derek C. Wadsworth

SUMMARY

Advanced technologies for unmanned autonomous systems are important for future characterization, mapping, navigation, and communication in EM hazardous environments. Remote monitoring techniques may be more cost effective and safer than sending people out to inspect property, particularly when certain areas of a site are inaccessible. They crosscut needs in multiple EM focus areas and programs in which site characterization and monitoring are required, such as decontamination and decommissioning, and they have application in improved navigation of autonomously guided subsurface sensors and improved systems for long-term stewardship of DOE assets. The Cleanup to Stewardship document states that: "…of 109 sites currently expected to require stewardship, 103 are expected to require active stewardship. Active stewardship includes detection monitoring on a continuous or periodically recurring basis…. Sites expected to require active stewardship vary in size and complexity." These sites range from the size of a football field to the size of the state of Rhode Island. The complexity and unstructured environment of the sites require higher levels of intelligence and mobility for future surveillance and monitoring than currently available. The following areas of our investigation are meeting these needs:

- Sensor deployment using multiple agents and improved navigation sensors
- Improved wireless data transfer
- Improved perception of remote environments through charge-coupled device (CCD) sensors.

TASK DESCRIPTION

Sensor Deployment Using Multiple Agents and Improved Navigation Sensors

Safety considerations and increased regulatory requirements for EM programs require sophisticated sensors to detect hazardous materials. These sensors often require precision deployment to guarantee the most accurate detection. Additionally, hazards inherent in the remediation tasks, such as confined spaces, chemical remediation, radiological contamination, and high radiation fields, add health and safety risks to operators, making remote and automatic deployment of the sensors highly desirable. Because of the unique nature of each activity, a flexible platform that can be reconfigured for each deployment, sensor equipment, and operating condition is needed. To meet these need, we (a) developed a mobile sensor interface design and various mobility platforms (ground and aerial) to test sensor, robot, and human interface; (b) investigated distributed robotics for deploying heterogeneous sensors; and (c) modified, developed, and optimizerd sensors for field-ready deployment and improved navigation of mobile platforms.

Improved Wireless Data Transfer

Operating remotely controlled equipment in hazardous areas requires a constant transmission of data to communicate control signals, video, etc. This often requires breaching the containment boundary with cables that eventually become contaminated, creating additional waste. One solution to this problem is to develop a wireless communication system capable of penetrating physical structures without requiring line-of-sight contact between operator and manipulator. To meet this need, we developed a non-line-of-sight wireless communication link capable of transmitting control signals, video, and data over long distances and inside buildings.

Improved Perception of Remote Environments through CCD Sensors

Current handling of radiological materials requires operators to perform work in hot cells. Decommissioning and dismantling hazardous environments and remediating radiation or performing work in other hazardous environments require remote operations. Currently, remote viewing of hazardous environments is with video cameras, which have limited resolution and available field of view. Our research is developing technologies that offer a wide field-of-view (similar to human perception) video system for remote operations. It will enhance operator performance, reduce exposure to hazards, and result in lower operational costs.

It is well documented that high radiation fields generate a visual effect on modern CCD cameras by over energizing individual pixels, causing them to display as bright white points (white-out). If enough pixels white-out, we get the sparkling or snow effect commonly encountered when commercial grade cameras are deployed in radiation fields. It is both intuitive and sufficiently supported by experience to say that the higher the radiation fields, the greater the snow effect. The intent of our research was to explore this relationship by exposing a CCD camera to known levels of radiation at various distances from a controlled source and in various orientations to the source. We used the data gathered to develop a means to quantify the number of pixels over energized in any given frame of video. This quantified information could in turn be used to estimate the radiation fields to which any given CCD camera is exposed. Successfully quantifying the snow effect on CCDs offers a method whereby the camera (often much smaller than conventional radiation detectors) can become a radiation detector.

ACCOMPLISHMENTS

Sensor Deployment Using Multiple Agents and Improved Navigation Sensors

Sensor Deployment

We identified two Russian sensor technologies, a gamma locating detector and an isotopic identification instrument, to be demonstrated at the INEEL by the Large Scale Demonstration and Deployment Program; collaboration is necessary to accomplish the demonstration. We supported the integration and testing the Russian technologies on the iRobot ATRV-Jr robotic platform. This collaboration allowed us to use one of our robotic vehicles to develop the sensor interface for a needed stewardship application. The integrated Russian technologies and robotic platform was deployed at the Test Area North (TAN) TAN-616 and Power Burst Facility (PBF) Cubicle 13 at the INEEL. Figure 1 shows the robotic platform with the gamma locating detector mounted on top of the robot. For deployment the entire system was wrapped in a protective covering (not shown).

Figure 1. ATRV-Jr with a gamma locating detector.

We successfully deployed a small unmanned aerial vehicle (SUAV) using a small global positioning system (GPS) navigation package. This low cost (less than $500) navigation package, including the GPS unit and servo controller, which weighs approximately 7 oz. During the deployment, a SUAV was air lifted to a starting altitude and position, and the autonomous control system was activated. The SUAV successfully flew the preprogrammed course autonomously while maintaining the desired altitude and relaying real-time sensor data (video and GPS coordinates). Figure 2 shows scenes from this deployment. The significant activity was the development of a small low cost controller/interface board. The board, shown in the bottom right corner of Figure 2 with its processor, is capable of controlling 6 pwm axes and interface to 4 RS232 serial ports as well as, several digital and analog I/O lines. The controller board allows for complete autonomous flight of a SUAV as well as manual override. The board is designed with a safety watchdog that monitors both the processor and the communication/control signal. If any fail, the system automatically switches to a "recovery" position. The new board adds the capability to do autonomous takeoff and landing. Beyond the SUAV application, the controller board has applications in small or large ground based robotics systems. The cost of the interface board, including parts and labor (with the exception of the processor), was approximately $500 for 3 boards. This work has led to follow on funding within the Environmental Monitoring Group at the INEEL to use the small low-cost aerial platforms to retrieve real-time samples of air during wildfires.

Improved Navigation

Sensor deployment is a major component of mobile robot systems. Sensors are typically grouped into two categories, navigation and surveillance. Navigation sensors are those associated with the autonomous guidance of the vehicle. Surveillance sensors are mission specific, and the most difficult to integrate into the robot because of the large variety of interfaces. We designed and tested a generic

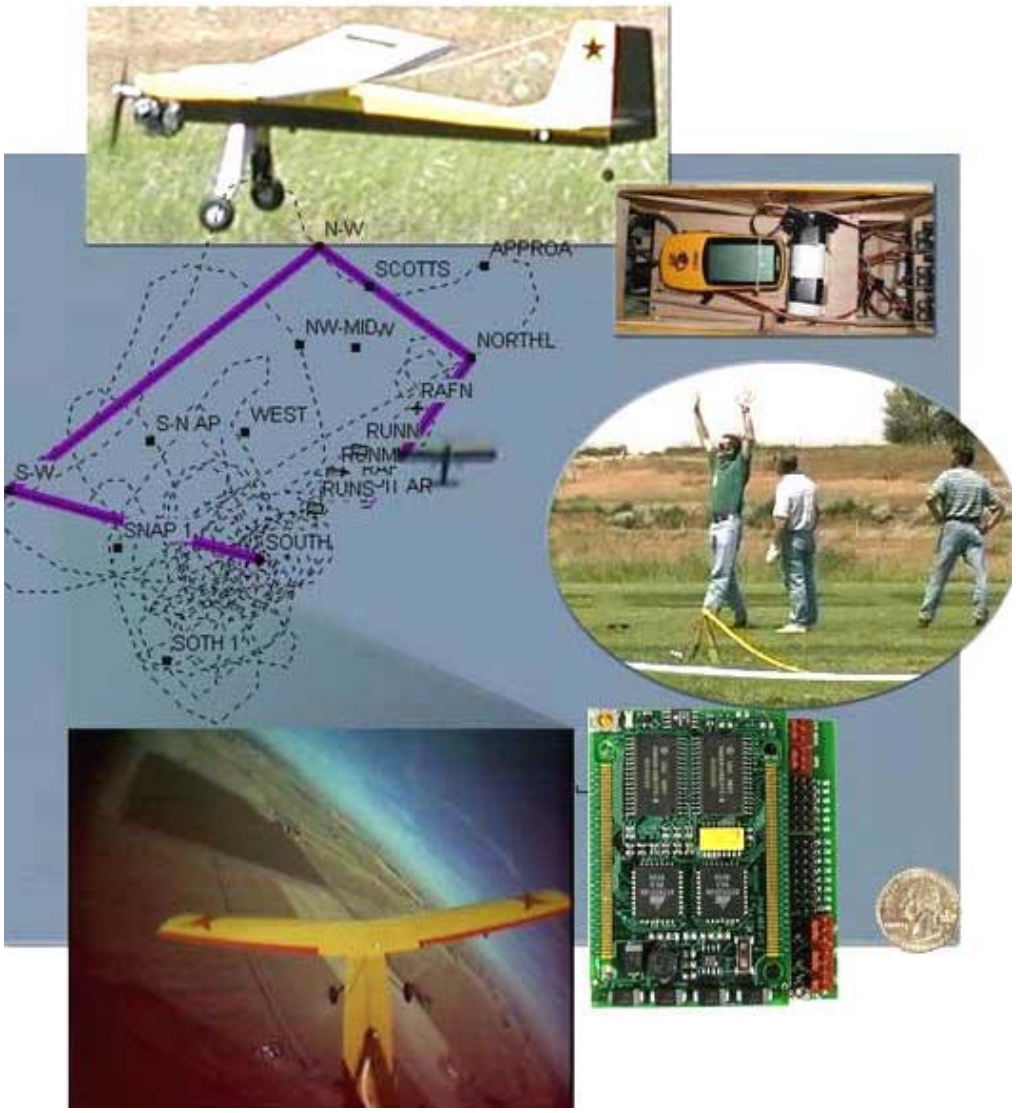

Figure 2. SUAV testing data and images.

wireless sensor interface to investigate the idea of deploying a system that could be a stand-alone sensor. The design allows for deployment of a small wireless communications package (cellular, radio frequency, Bluetooth, etc.) and interfaces with a serial or TCP port for the sensor. For sensors without serial output capability, it has an analogue-to-digital converter with a serial or TCP/IP output.

We identified an inertial mass unit (IMU), called the Precision Strike Navigator (PSN), from China Lake as a potential low-cost design for improving navigation, and we arranged an agreement to obtain a test prototype. We also investigated development of our own low cost precision navigation system. We purchased and tested a small (3/16 × 3/16 × 1/16-inch), low cost, low power tilt sensor/accelerometer. Initial results were very promising. The device will measure the angle of inclination in two axes with a maximum sensitivity of about 0.45 degrees. We conducted tests to determine the accuracy of the sensor on the ATRV-Jr robot. The sensor is self powered and operated for more than three days. Initial results from the tests show that the sensor is capable of measuring angles from 0 to 90 degrees at 0.5-degree increments. Figure 3 shows the INEEL sensor mounted on a basic stamp development system. The system outputs RS232 data that can be read by any standard serial device.

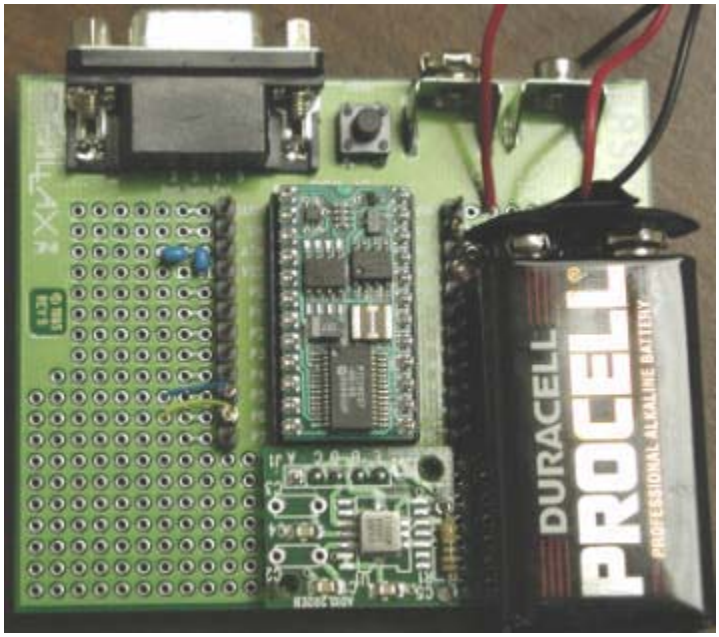

Figure 3. INEEL inclination and accelerometer sensor.

Multiagent

In many situations, multiple robots are an advantage. For example, two robots can be deployed in a cluttered environment and use the sensors from both robots to enhance their capability. We deployed two ATRV-Jr robots in a cluttered environment to demonstrate the benefits of multirobot cooperation. Each robot was equipped with wireless video and sonar sensors (Figure 4). The robots successfully navigated through a laboratory cluttered with obstacles by relying on the data from the sensors of both robots.

Figure 4. Multirobot cooperation experiment.

Improved Wireless Data Transfer

The goal of this research was to investigate development of non-line-of-sight wireless communications capable of transmitting control signals, video, and data over long distances, and inside building structures. Technologies investigated to achieve these capabilities were analog cellular, high radio frequency (RF) local area network, and high RF video.

Cellular Communication

For non-line-of-sight applications requiring outdoor and indoor capability, ubiquitous cellular technology holds the greatest promise for success. In our investigation in this area, we used the commercially available analog cellular phone network covering the entire United States. We designed and prototyped a test system consisting of an analog handheld cellular phone, a handset-to-phone-tone converter, and a PCMCIA cellular modem to test what data rates were most reliable when moving the system from indoors to outdoors. We determined that 1200 baud was the most reliable and robust data rate. Further testing on two INEEL robots followed to determine reliability of robot control using this data link. We successfully operated the robots from indoors to outdoors without vehicle failure or communication dropout. These tests investigated only the control commands of the vehicle, not sensor feedback. Figure 5 shows one of the INEEL robots with the analog cellular prototype used for these tests.

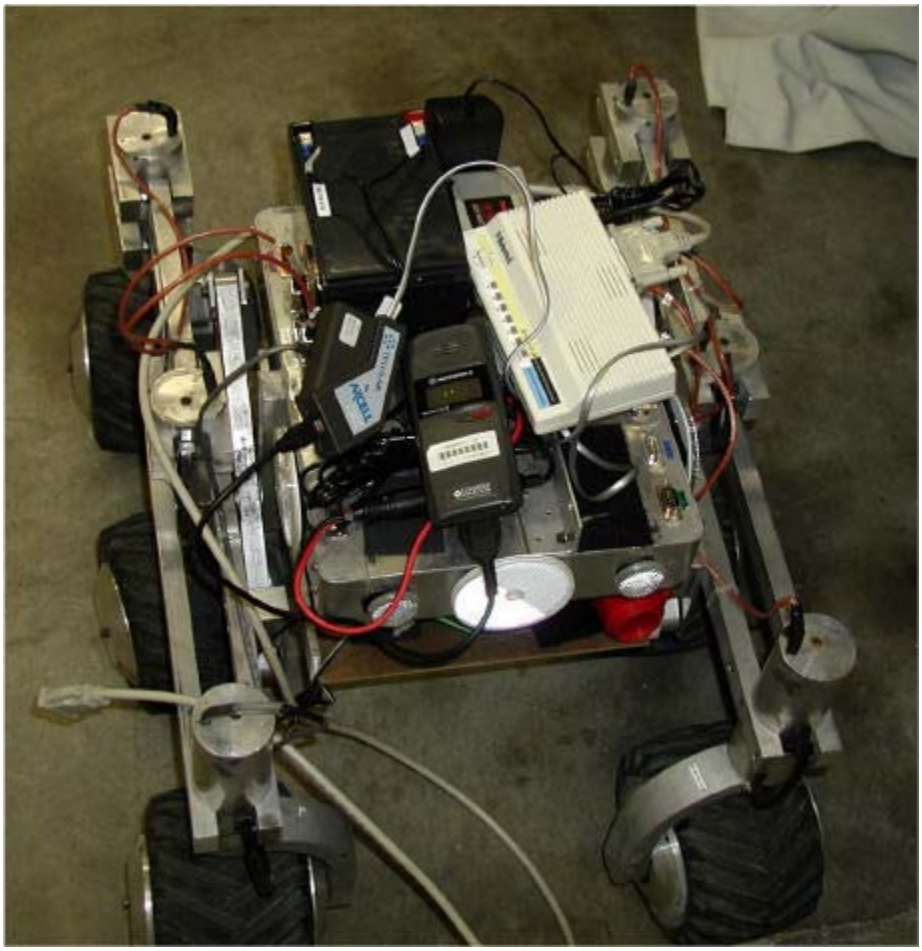

Figure 5. Wireless interface using the cellular communications link on ARC III.

High RF Local Area Network

Streaming real-time video (~15 frames/second) at an image size of 160 × 128 pixels requires a minimum data rate of 58K baud. We investigated the maximum number of data that could be relayed using the low-bandwidth of the analog cellular 1200 baud data link. We used a high RF local area network and the ATRV-Jr robot to determine the minimum number of video data (picture size) required for teleoperated robot control. From these tests, we determined that an image size of no less than 50 × 50 pixels at 1/4 Hz is adequate when driving the vehicles approximately two vehicle lengths per image. A commercially available technology is capable of streaming 80 Δ 64 images at 1/10 Hz over a wireless CDPD (digital) cellular data link.

High RF Video

We conducted a final investigation on transmitting video by high radio frequency. During the past few years, the INEEL purchased and used state-of-the-art wireless video systems that, nonetheless, are susceptible to dropout and interference and require very directional antennas. During the investigation, we discovered a new technology, available from DTC Communications, Inc., called quality video detect (QVD). It consists of simultaneously sampling multiple receivers at the horizontal line rate of ~15,725 times/sec. The technology promises to optimize signal reception, thus eliminating signal dropout and interference. The QVD receiver was able to pickup the one-fourth watt transmitter signal from a range of about 2 to 3 miles line of sight from a fast moving platform (SUAV). Figure 2 above shows a picture captured from the live video stream taken during one of the missions. The QVD system has since been used to demonstrate two wireless video concepts for other programs within the INEEL: (a) a helmet mounted camera for firefighters and swat teams, and (b) a hazmat suit camera. Both applications require reliable non-line-of-site real-time video.

Improved Perception of Remote Environments through CCD Sensors

Wide Field-of-View CCD Sensor

The purpose of this research was to investigate how to best apply current common video camera technology (also known as charge-coupled devices or CCDs) to remote perception. The primary application investigated was real-time observation of a remote area and use of that visual information for a constructive purpose. To gain experience with current CCD technology, we experimented using video camera/television pairs in ground vehicle operation, which were selected for several reasons:

- Most of the equipment was on hand (vehicle, cameras, televisions), saving significant cost
- Driving is a task most people are intimately familiar with and do every day
- A successful system will apply to remote perception applications such as navigation of a robotic vehicle in hazardous environments.

The information gained directed our selection of currently available components for further investigation.

To that end, we installed five camera/TV pairs on an available all-terrain vehicle (ATV). The cameras were arranged in a semicircular fan and adjusted so their fields of view were continuous. This provided approximately 240 degrees of horizontal view and 90 degrees of vertical. The televisions were arranged in a pattern corresponding to the cameras' positions and were located in a secondary driver's seat in the rear of the vehicle. This seat was covered to force the rear operator to exclusively use the video

information to drive the vehicle. Another person rode along in the primary driver's seat during the experiments to observe and ensure safety. It quickly became apparent that a rear view was essential to comfortable operation, prompting installation of a sixth camera, providing a revised total view angle of about 300 degrees. Figure 6 shows various views of this ATV-based system.

We collected experimental data on two pavement courses and several runs in rough terrain (dirt, brush, weeds, and small hills) under a variety of conditions. Results indicate that the video system was useable for most operators, and that performance and confidence increased with both experience and familiarity with the test area. We also observed video quality issues. Small object recognition and distance estimation in the absence of visual clues was difficult for all operators. Of particular interest were identical trials taken with various cameras deactivated. We found that vehicle operation was still reasonably comfortable with the horizontal view reduced to about 150 degrees (three cameras), but reducing it to 80 degrees (front camera only) was not practical.

Based on our conclusion that a wider, lesser quality field of view was better than having a restricted, high quality one, we decided to invest in a new panoramic camera technology for the next phase of this task. After a vendor search, we ordered cameras manufactured by Remote Reality. We selected these units because each uses a single video signal channel (versus six for our initial test system),

Figure 6. ATV test vehicle.

which facilitates their use over a wireless link, have a wide field of view (180 and 360 degrees available), and are compact. This facilitates their use in a wide range of applications. The cameras were received in October and tested. The results of one of the tests are pictured below in Figure 7. The top image is a capture of the raw picture taken from the camera; notic e the camera misses the four corners and the very center of the image. The max resolution of the camera is 320 Δ 280, making it difficult to resolve any image detail. Although the observer (in image) is only 2 feet away from the cameras it is difficult to see any definition in the image. The bottom image is the same data, except "unraped." The image clearly slows that there are issues with image distortion in the unraped images. Our tests indicate that there remains a good deal of work in this area.

Figure 7. Distorted view from panoramic camera.

Radiation CCD Sensor

Our primary object for this research was to gather quantifiable data of the well know sparkle effect that results on video produced from CCD chips exposed to significant radiation fields. The data were obtained at DOE's Laboratory Accreditation Program facility. The facility has two Cs-137 test sources, one 20 curie and one 1,000 curies, which we used to expose a typical commercial grade camera at various distances from the sources. The distances were predetermined to target desired radiation field levels as determined by the inverse square law[1] and a data point measured at 2 m from the sources. Table 1 presents the exposures in the order in which they were performed, which give the true or measured dose-rate actually encountered by the camera, as given by a RO7 Radiation Detector mounted in tandem with the camera.

The intent of the exposures was to gradually step up the dose rate, recording the video image produced at each exposure for approximately 1 minute. Each 1 minute of video produced approximately 1,800 still frames from which we drew random samples to build our visual database. The immediate results of these tests indicate three items of importance.

Table 1. Actual dose rate encountered by the camera at predetermined radiation field levels.

Exposure	Special Configuration	Curies from Source (Ce-137)	Radiation Level
1	None	20	580 mR/hr
2	None	20	800 mR/hr
3	None	20	5.2 R/hr
4	None	20	10.5 R/hr
5	None	20	50.2 R/hr
6	None	1,000	12.8 R/hr
7	None	1,000	52.7 R/hr
8	None	1,000	105.6 R/hr
9	None	1,000	500.0 R/hr
10	None	1,000	1,000.0 R/hr
11	None	1,000	3,200.0 R/hr
12	Lens removed to maximize approach.	1,000	4,000.0 R/hr
13	Lens removed to maximize approach.	1,000	1,000.0 R/hr
14	Lens replaced, camera perpendicular to source.	1,000	140.3 R/hr
15	Lens replaced, camera perpendicular to source.	1,000	113.0 R/hr
16	Camera perpendicular to source, CCD shielded (independent measurement indicated 85 R/hr at CCD).	1,000	4,000.0 R/hr
17	Camera perpendicular to source, CCD not shielded.	1,000	4,000.0 R/hr
18	Camera facing source, low level sensitivity check	1,000	12.9 R/hr

First, the visual radiation effect on the recorded video was not effected by orientation of the camera to the source. This verified that the interaction of the high-energy photon field with the atoms constituting the CCD did not depend on whether the CCD was normal or perpendicular to the rays of the field, but rather, derived from the probability of encountering an atom based on the volume in space the CCD chip occupied.

Second, the visual effect was completely generated by exposure on the CCD, not on the electronics contained in other parts of the camera housing. We verified this by shielding the CCD chip while exposing the electronics package of the camera to a very high field (approximately 4,000 R/Hr). The visual effect was comparable to that seen at previous exposures taken at radiation fields in the range of 100 R. We then placed a standard radiation detector behind the shielding with the CCD. Its measurement indicates that the CCD was indeed only seeing an 85-R/hr field.

Third, by gradually increasing the exposure levels on the CCD into the 1,000s of R/Hr and then reversing the process by stepping the exposure back down, we determined that little or no sensitization of the CCD occurred once exposed to high radiation fields. That is, the lower exposure levels produced visual results directly comparable to those taken at the same exposure levels earlier in the experiment.

We next processed the collection of video frame still images in a digital video editing station. A series of bitmap images showing the exposure effect at various known radiation levels were reproduced on a series of CD-ROM disks and distributed to Remote Video Inspection personnel for visual comparison during future inspections. This visual reference database can begin providing immediate estimations of radiation fields encountered during the course of further remote video inspections. Note that in order to make the best possible comparisons, the iris on the inspecting cameras must be shut down for a short time to allow the visual *sparkle* effect to display against a completely black background, thereby duplicating the video captured during our tests.

The final accomplishment of this task was to create a Microsoft Windows-based program that can analyze a bit-mapped image from the video still frames and rapidly count all the over-charged pixels displayed, quantifying the result of the exposure level. The program also offers a means whereby neighboring pixels *smeared* with residual energy from the high-energy impact can be eliminated by setting the appropriate brightness threshold. The images shown in Figures 8 through 10 were captured from video recorded during the experiment; the field strength is the gamma radiation field strength in R. The counts are the number of over-energized pixels on the CCD above a background threshold of 80%.

With further development, we could provide near real-time analysis of live video, coupled with a look-up database whereby the number of over-energized pixels are first counted, then compared to results from known radiation levels. The estimated radiation level based on this comparison could then be realized as an on-screen display and recorded with the inspection video.

REFERENCE

1. Glenn F. Knoll, *Radiation Detection and Measurement,* Third Edition, John Wiley & Sons, 2000, pp. 497–501.

Figure 8. In a 105-R field, the algorithm counted 113 over-energized pixels.

Figure 9. In a 500-R field, the algorithm counted 532 over-energized pixels.

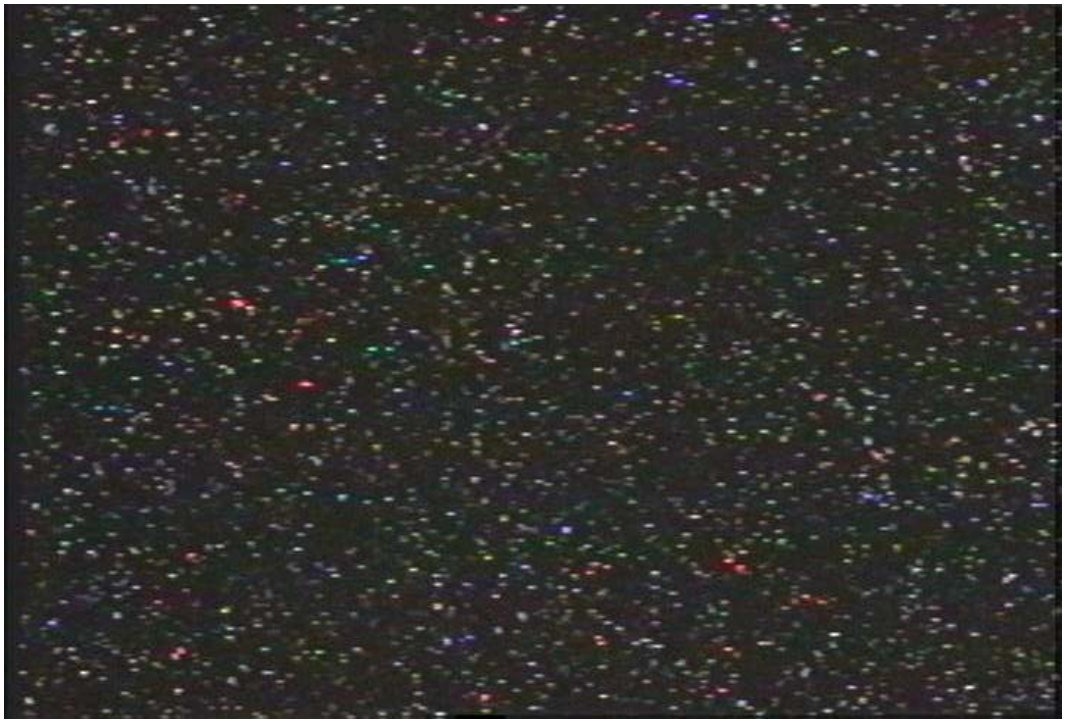

Figure 10. In a 1,000-R field, the algorithm counted 973 over-energized pixels.

Secondary Ion Mass Spectrometry Characterization of Environmental Microbial Processes

Identifying Microbe Chemical Signatures More Easily and Quickly for Remediation

Jani C. Ingram, R. Michael Lehman, William F. Bauer, F. S. (Rick) Colwell, A. D. Shaw

SUMMARY

In situ bioremediation—the ability to use naturally occurring microbes to remediate the effects of man-made contamination—is an important research thrust in EM's mission. Its potential for reducing overall cleanup costs is significant. Researchers need improved, direct methods for detecting and characterizing microorganisms in situ, and to understand which microbes already exist in target sites so they can take optimal advantage of those microbes for cleanup activities.

Current microbial characterization methods require researchers to extract microbes from the surface of samples and culture them in the laboratory. This research task explored the possible use of secondary ion mass spectrometry (SIMS)—a surface chemistry detection technique—to identify microbes in situ by examining their outer cell membranes. This technique is already being used on the minerals and plants that the microbes live on. Enhancing SIMS for this purpose could significantly advance microbial ecology studies because it will not separate microbial cells from the mineral surface and can be coupled with mineralogical analyses. This new tool should promote better understanding of bioremediation processes through in situ characterization. Our approach uses static SIMS to probe the top layers (membrane) of intact microbial cells using two SIMS instruments built in-house: a triple quadruple, and an ion trap mass analyzer. These instruments are unique, being built on several SIMS research and development (R&D) projects at the INEEL over the past 15 years.

Our objectives were to (a) generate MS^n approaches and protocols for ionic fragmentation of the diagnostic ions, (b) make software modifications to the ion trap SIMS operating systems to allow for longer ionization and trapping times, and (c) begin testing SIMS as a tool for characterizing microbial species of interest to bioremediation efforts.

TASK DESCRIPTION

Introduction

The surface structures of microbial cells are important because they are in direct contact with the external environment and are highly dynamic in order to withstand environmental changes. These alterations in the surface chemistry of the cells provide a means for gaining insights into microbiological processes occurring in the environment. Owing to its importance, characterization of the microbial cell surface chemistry is an expanding field in microbiology. A widely used approach in the study of the surface chemistry of microbial cells is to use staining techniques coupled with various microscopy approaches for probing specific components of the microbial cells. For example, negative staining techniques coupled with electron microscopy have been extremely useful in studying the ultrastructure of flagella, fimbriae, F-pili, fibrils, and S-layers.[1] By using these visual techniques, much can be learned about the physiology of the cells, with the various stains providing insight into specific components of the microbial cells. These reaction chemistries are not always specific, however, and can be hampered by unwanted side reactions occurring between the stain and other components within the cells.

Another widely used approach to characterize the surface chemistry of microbial cells is to extract the components of the cell membrane, then to perform chemical analyses on the extract. With the maturity of analytical techniques to provide specific identification of highly complex, biochemical compounds, much has been learned concerning the constituents of the microbial membrane. A wide variety of mass spectrometry techniques have been developed[2] capable of determining species as small as the electrolytes within the cells[3] to as large as proteins and polypeptides.[4,5] The major limitation of this approach is that components of interest must be extracted from the cells and isolated from the cell matrix before analysis, which precludes the possibility of investigating the microorganisms under near in situ conditions.

Clearly, direct analysis of microbial cell surface chemistry is desired. A variety of surface analysis techniques exist; however, many of those techniques, such as energy (or wavelength) dispersive x-ray spectroscopy and Auger electron spectroscopy, provide only elemental information, which has limited application for characterizing biochemical systems. In contrast, x-ray photoelectron spectroscopy (XPS) can give more than just elemental composition and has been used to investigate the chemical composition of the microbial cell surface.[6,7] XPS is capable of interrogating the surface of intact cells, but is limited in that it provides chemical state or oxidation information that is reflected by small shifts (less than 1 eV) in the binding energies of the core electrons. These small shifts are difficult to resolve instrumentally. Thus, interpretation of the spectra of organic compounds is limited to identifying classes of organic compounds by this technique.[8] Determination by XPS of specific molecular information about the cell surface chemistry is problematical.

Some surface analysis techniques, however, have the capability to more specifically characterize the surface chemistry of intact microbial cells. Infrared spectroscopy (IR) is a vibrational spectroscopy that interrogates molecular bonding. Because the energies of molecular bonds in biochemical systems are very sensitive to changes in chemical structure, IR is very useful for identifying specific molecular species, and to potentially provide molecular compositional information from intact microorganisms has been demonstrated. Using synchrotron radiation (SR) as the excitation source is particularly promising, as the SR source provides improvement in the signal-to-noise ratio over that of FTIR spectra recorded from a conventional blackbody source.[9]

Our approach was to use static SIMS equipped with a molecular primary beam. In static SIMS, the surface is interrogated by bombardment with particles (a primary beam of molecular ions) that dislodge molecular species from the solid, ejecting (or sputtering) them into the gas phase where the ionized molecules and their fragments can be mass analyzed. These ionized pieces of the surface reflect a detailed picture of the surface chemistry of the solid.[10] An advantage of SIMS relative to other surface analysis techniques is that it is extremely sensitive; SIMS has the capability of detecting molecular species at 0.001 monolayer levels.[11] Although mainly used by the semiconductor and polymer industries, some initial effort has applied SIMS to the study of biological samples. Winograd's group has demonstrated that SIMS can interrogate the exposed head groups and tail groups of phospholipid membrane molecules in freeze-fractured red blood cells.[12] These results demonstrate the utility of SIMS for not only chemical analysis but also for determining the molecular orientation of cell surface molecules. Todd and coworkers used SIMS to map phosphocholine in rodent brain tissue.[13]

We use a molecular primary beam for bombarding the sample.[14,15] We use ReO^-_4 in place of the conventional Cs^+ or Ga^+ atomic beams typical of commercial SIMS instruments. Our previous studies with molecular primary beams[16–18] show an increase in sensitivity by a factor of 10 to 30. This becomes increasingly important as the surface concentration of the analyte decreases, and, on environmental samples, we anticipate the need to detect submonolayer concentrations. Schamberger and coworkers report using SIMS with a Cs^+ primary ion beam to study microbial cell surfaces.[19] Limitations relating to the cationic molecular fragments produced by the Cs^+ beam made it difficult to observe quantifiable

differences in the SIMS spectra of various microbial species. Our work indicates that the ReO^-_4 primary beam can overcome these limitations.

Experimental Section

Microbiology

We analyzed 38 bacterial strains by both SIMS and the Sherlock Microbial Identification System (MIS; MIDI, Inc., Newark, DE, USA). The purpose of the MIS analyses was to determine the fatty acid methyl ester (FAME) profiles of each bacterium. The bacteria were obtained either from an established culture collection and initially cultured on the recommended solid media, or isolated from environmental samples on R2A solid media, as noted in Table 1. With one exception, all organisms were then grown aerobically on trypticase soy broth-agar (TSBA) and harvested for FAME analysis as recommended by the MIS operating manual. We determined taxonomic affiliations using the MIS library for the *aerobe method*. Similar cultures grown on TSBA were harvested for SIMS analyses. The one exception was the obligate anaerobe, *Methanoculleus marisnigri.* This organism was obtained from the Oregon Collection of Methanogens and cultured in the recommended anaerobic liquid media. *Methanoculleus marisnigri* was then prepared for analysis by pelleting by centrifugation and washing with phosphate buffer. We used the pellet for both SIMS and FAME analysis.

Table 1. Information on microorganisms.

Isolate	Organism	Identification	Source	Cell Wall
1	*Paenibacillus macerans*	American Type Culture Collection (ATCC) 49035	culture collection	gram positive
2	R2A Bug	*Bacillus filicolonicus* (0.259)	media contaminant	gram positive
3	USGS103-Y	*Arthrobacter ramosus* (0.706)	groundwater	gram positive
4	USGS103-Z	*Bacillus atrophaeus* (0.605)	groundwater	gram positive
5	TAN33 Matt-F	No database match	basalt core	unknown
6	TAN33 Matt-H	No database match	basalt core	unknown
7	TAN33 Matt-K	No database match	basalt core	unknown
8	*Staphylococcus aureus*	*Staphylococcus aureus* (0.797)	lab contaminant	gram positive
9	TAN33 MLS-49	No database match	groundwater	unknown
10	TAN33 MLS-52	No database match	groundwater	unknown
11	TAN33 MLS-73	No database match	groundwater	unknown
12	TAN33 MLS-88	No database match	groundwater	unknown
13	*Methanoculleus marisnigri*	Oregon Collection of Methanogens	culture collection	Archaea
14	TAN37 38-1	*Pseudomonas syringae* (0.515)	basalt core	gram negative
15	TAN37 43A-9	*Arthrobacter globiformis* (0.422)	basalt core	gram positive
16	TAN37 43B-1	*Rhodococcus sp.* (0.042)	basalt core	gram positive
17	TAN37 43B-2	*Rhodococcus sp.* (0.010)	basalt core	gram positive
18	TAN37 43B-3	*Rhodococcus luteus* (0.715)	basalt core	gram positive
19	TAN37 43BW-1	*Pseudomonas putida* (0.257)	groundwater	gram negative

Table 1. Continued.

Isolate	Organism	Identification	Source	Cell Wall
20	TAN37 43BW-6	*Pseudomonas fluorescens* (0.487)	groundwater	gram negative
21	TAN37 43BW-11	*Pseudomonas alcaligenes* (0.147)	groundwater	gram negative
22	*Stenotrophomonas maltophilia*	ATCC 13637	culture collection	gram negative
23	*Pseudomonas stutzeri*	ATCC 17588	culture collection	gram negative
24	*Rhodococcus globerulus*	ATCC 19370	culture collection	gram positive
25	*Alcaligenes xylosoxydans*	ATCC 15173	culture collection	gram negative
26	*Agrobacterium tumefaciens*	ATCC 15955	culture collection	gram negative
27	*Hydrogenophaga pseudoflava*	ATCC 33668	culture collection	gram negative
28	TAN37 18BW-2	*Hydrogenophaga pseudoflava* (0.935)	groundwater	gram negative
29	TAN37 18-3	*Acinetobacter genospecies 9* (0.486)	basalt core	gram negative
30	TAN37 18-7	*Sphingobacterium spiritivorum* (0.218)	basalt core	gram negative; sphingolipids
31	TAN37 18-9	*Rhodococcus equi* (0.013)	basalt core	gram positive
32	TAN33 Matt-A	*Rhodococcus sp.* (0.227)	basalt core	gram positive
33	TAN33 Matt-B	*Brevundimonas vesicularis* (99.3%)2	basalt core	gram negative
34	TAN33 Matt-C	*Sphingomonas macrogoltabidus* (97.8%)3	basalt core	gram negative; sphingolipids
35	TAN37 Matt-U	*Rhodococcus erythropolis* (0.239)	basalt core	gram positive
36	*Agrobacterium tumefaciens*	ATCC 15955	culture collection	gram negative
37	*Arthrobacter globiformis*	ATCC 8010	culture collection	gram positive
38	*Sphingomonas capsulata*	ATCC 14666	culture collection	gram negative; sphingolipids

SIMS Instrumentation

The SIMS instrument used in these studies is described in detail by Appelhans et al.[20]; a brief description is provided here. The instrument uses ReO^-_4 at 5.25 keV as the primary bombarding particle, which is produced by heating an $Eu_2O_3/Ba(ReO_4)_2$ ceramic in vacuum (see Reference 15). We synthesized the ceramic in our laboratories and processed it in a form that could be used as an ion source. The ion gun was typically operated at 250 pA. Acquisitions required less than 100 s, and a typical sample had an area of about 0.06 cm^2; thus, primary ion doses were less than $2.6 \Delta 10^{12}$ ions/cm^2, which is below the commonly accepted static SIMS limit.[21]

We have developed patented methods to overcome surface charging in which the extraction of positive and negative charge is balanced so that the sample, on average, gains no net charge.[20,22] This technique, when used with the ReO^-_4 primary ion gun, mitigates charge buildup on the surface of the sample and thus permits facile analysis of electrically insulating samples such as minerals and leaves. We used two different mass spectrometers in this work. We used a triple quadruple system (2 to 600 amu) manufactured by Extrel (Pittsburgh, Pennsylvania) and modified in our laboratory. The base pressure in the instrument was typically $3 \Delta 10^{-7}$ torr. The quadruple was tuned for unit mass resolution and optimum sensitivity for m/z 81^- and 198^+ in the SIMS spectrum of tetrahexyl ammonium bromide. We also used a modified Varian Saturn 2000 ion trap mass spectrometer (Walnut Creek, California) adapted for secondary ion mass spectrometry. The Varian-based IT-SIMS has not been described previously in the literature, but is very similar in design and operation to the Finnigan-based IT-SIMS instrument described in detail by Groenewold et al.[23] Briefly, the instrument is equipped with a ReO^-_4 primary ion gun and an offset venetian dynode/multichannel plate detector system housed in a custom-fabricated vacuum chamber.

Statistical Analysis

Multivariate analysis methods[24] commonly used to determine analyte concentrations in overlapped spectra include classical least squares,[25] partial least squares,[26] principal component regression,[27] and occasionally, neural networks.[28] Multivariate analyses have been successfully used for interpretation of mass spectra of microorganism-related chemistry.[29,30]

After the initial attempts at principal components analysis (PCA), using grams/32 with the PLS/IQ package, we focused on finding the optimum mass ranges and optimum methodologies to design a methodology that for proof-of-principal could be used to classify bacteria based on their SIMS spectra. One problem has been that because the number of spectra is relatively limited for the calibration set (224) and the number of microbial types is large, there is currently no really good set of spectra to use as a verification set. For development, our initial primary focus was on the gram negative and gram positive character of the microbes. We generally used the correlation coefficient of a principal components analysis/regression (PCA/R) or a partial least squares (PLS) calibration for gram positive bacteria as an indicator. For the initial calibrations, we selected factors using the F-statistic at $p = 0.05$ applied to the Eigen values. This worked quite well for the PCA/R calibrations; however, this was not as useful for the PLS and the PLS factors we usually picked by the minimum calculated F-statistic. In the final stages, we only performed the more rigorous selection of factors based on a cross-correlation analysis—using the calibration set as the verification set by recursively performing the calibration with n-1 spectra and using the ith spectrum as the unknown—because the calculation time was excessively long. We performed calculations in MatLab using the PCA/R and PLS routines available in the chemometric toolbox for MatLab by Richard Kramer. The routines in the toolbox allow one to select either the nonlinear iterative partial least squares or decomposition algorithms.

We made several attempts to determine which masses were best for determining the gram negative/positive nature of the microbes from the SIMS spectra. The major downfall of this type of analysis is how to normalize the spectrum. We achieved some limited success by using a moving window of 3, 5, 10, 20, etc., points (m/z's). Each window was normalized to the maximum value and a PLS performed using the entire data set or a subset in which potential outliers were removed. The net result of this was that the best correlation to the gram +/4 was in the positive ion spectrum in the m/z range of ~70–110. We noted that with the smaller windows, correlation centers around the common fatty acid ions in both the positive and negative ion spectra. Close examination of the spectra revealed that in the negative ion mode, the spectra of Paenbacillis and R4A consisted primarily of noise, so subsequently we considered the spectra for these bacteria as possible outliers.

Detection Limit Study

A detection limit was performed using *Arthrobacter globiformis* (ATCC #8010) which was initially cultured on R2A solid media. These organisms were then grown aerobically on trypticase soy broth-agar (TSBA). SIMS analyses were performed on these bacteria taken directly from the agar. The Bio-Rad DC Protein Assay (Lowry method) using a visible absorption measurement to quantify NaOH-extracted proteins from whole cells was used to determine the number of cells analyzed by SIMS. The lower limit of detection by this method for *A.globiformis* is ca.7 $\Delta 10^7$ cells.

Results

This section describes project results in terms of the objectives set at the start of the program to: (a) generate MS^n approaches and protocols for ionic fragmentation of the diagnostic ions, (b) modify software of the ion trap SIMS operating systems to allow for longer ionization and trapping times, and (c) begin testing SIMS as a tool for characterizing microbial species of interest to bioremediation.

Generation of MS^n Approaches

An objective of this task was to develop MS/MS methods for identifying diagnostic ions present in the microbial cell membrane. The purpose for developing MS^n methods is to enable specific identification of chemical species, which is important in chemical characterization of microorganisms. In our initial work, we observed cations at even masses in the SIMS data of intact microorganisms. These even mass cations are typically associated with organic amines, which suggests that fragment ions associated with proteins may be present in the SIMS cation spectra. An example of this is the comparison of SIMS spectra of two strains of *Shewanella alga* (BrY and adhesion-deficient RAD20), which differ mainly in their ability to bind to ferric oxides. Biochemical evidence showed that the BrY strain contained proteins on the cell surface that enabled adhesion to occur, whereas those proteins were absent in the adhesion-deficient RAD20 strain. The SIMS cation spectra of these strains shows marked differences in the even mass ions, which suggests that the differences in protein composition of these two strains is reflected in the SIMS data.

Based on these observations, we collected SIMS data on 20 amino acids as a start for detecting protein development. Overall, we observed good spectral signatures of the amino acids in the single MS of the SIMS data. A second stage of MS was performed (MS/MS) on the molecular ions ($[M+H]^+$) of the amino acids. We observed (see Figure 1) that $[M+H]^+$ could be fragmented by a loss of formic acid, which could be used as a diagnostic for identifying the amino acids present.

Our next step is to analyze peptides by SIMS to determine its capability for identifying the amino acids present in the various peptide compounds. We collected SIMS data for a variety of commercially available peptides. For example, the peptide pro-leu-gly amide forms an abundance $[M+H]^+$ at m/z 285 (see Figure 2). It fragments at the leucine carboxyl linkage to form an ion at m/z 183. Additionally, a very abundant fragment ion associated with proline is observed at m/z 70 as well as a fragment ion originating from leucine (m/z 86). These ions produce a spectroscopic signature for the peptide, and are readily fragmented in MS/MS analyses. However, SIMS is not capable of determining the amino acid sequence or how many of each amino acid is present in the peptide. Thus, SIMS could be useful for tracking specific proteins in a microorganism if the spectroscopic signature of the protein could be determined from reference materials.

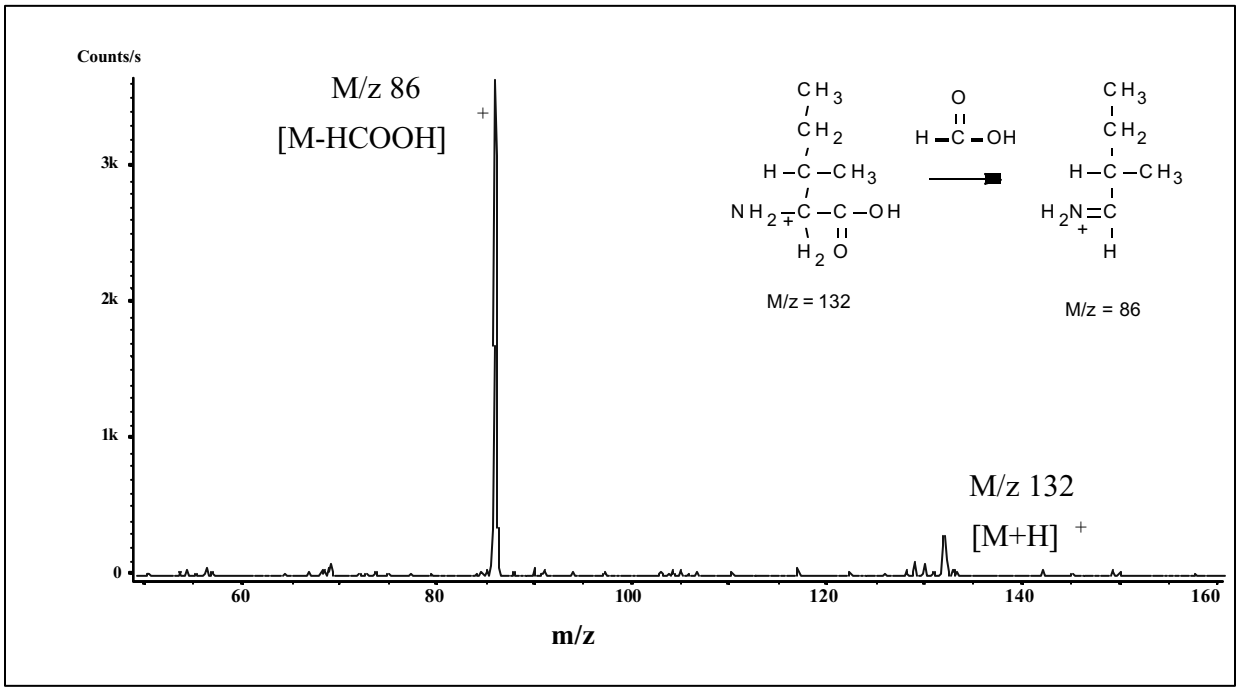

Figure 1. MS/MS of isoleucine by ion trap SIMS.

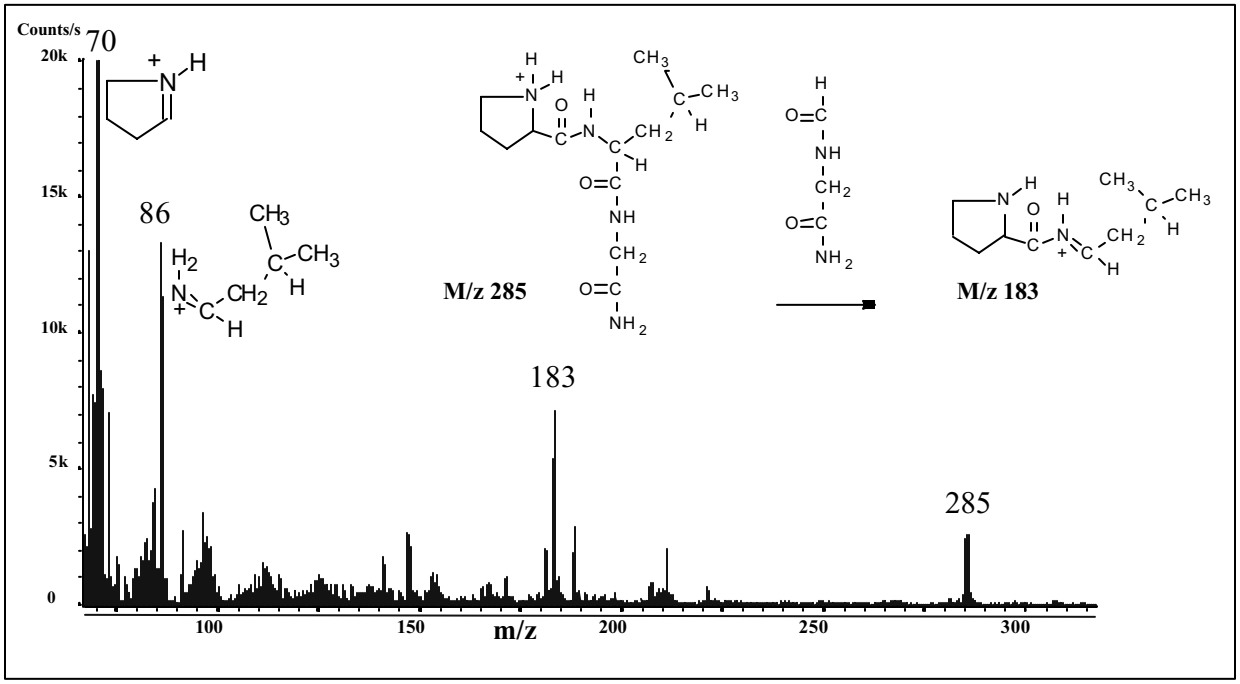

Figure 2. Cation SIMS spectrum of pro-leu-gly amide isoleucine.

Software Modifications

The objective to modify software for the ion trap SIMS data systems to achieve longer ionization times (necessary for some of the ion trap SIMS analyses) was accomplished by John Olson, who has been working on instrument development of the IT-SIMS system for the past few years. Using information gained through a nondisclosure agreement with Varian, the total time that can be used for scan functions, which includes the ionization time, has been extended from ~2 to ~130 s. This allows for virtually any ionization time needed for IT-SIMS. This capability also allows for longer collision-induced dissociation (CID) times. Longer CID times allow the use of lower dissociation energy to fragment the ions, which is an advantage when investigating less stable ions in a MS/MS analysis.

Testing SIMS for Microorganism Analysis

The object of the first set of experiments was to determine if SIMS was capable of providing a spectral signature for different intact microorganisms. In this study, we compared the SIMS data of 38 microorganisms to fatty-acid profiles determined by MIS. The results indicate that surface bombardment using a ReO^-_4 Primary beam cleaves the ether linkage characteristic of Archea at the glycerophosphate backbone of the phospholipid components of the cell membrane. Similar cleavage at the ester linkage in eubacteria was also observed. This cleavage enables direct detection of the fatty acid conjugate base by static SIMS. An example of SIMS' detecting fatty acids by SIMS is shown in Figure 3, which compares the anion SIMS spectrum of *Methanoculeus marisnigri* to the fatty acid profile generated by MIS. The labeled anions in the SIMS spectrum correspond to the fatty acids described in the fatty acid table. The results indicate that the fatty acids present at mid to high mole% (as determined by MIS) are also observed in the SIMS anion spectrum. SIMS does not detect those fatty acids present in trace amounts (less than 1 mole%).

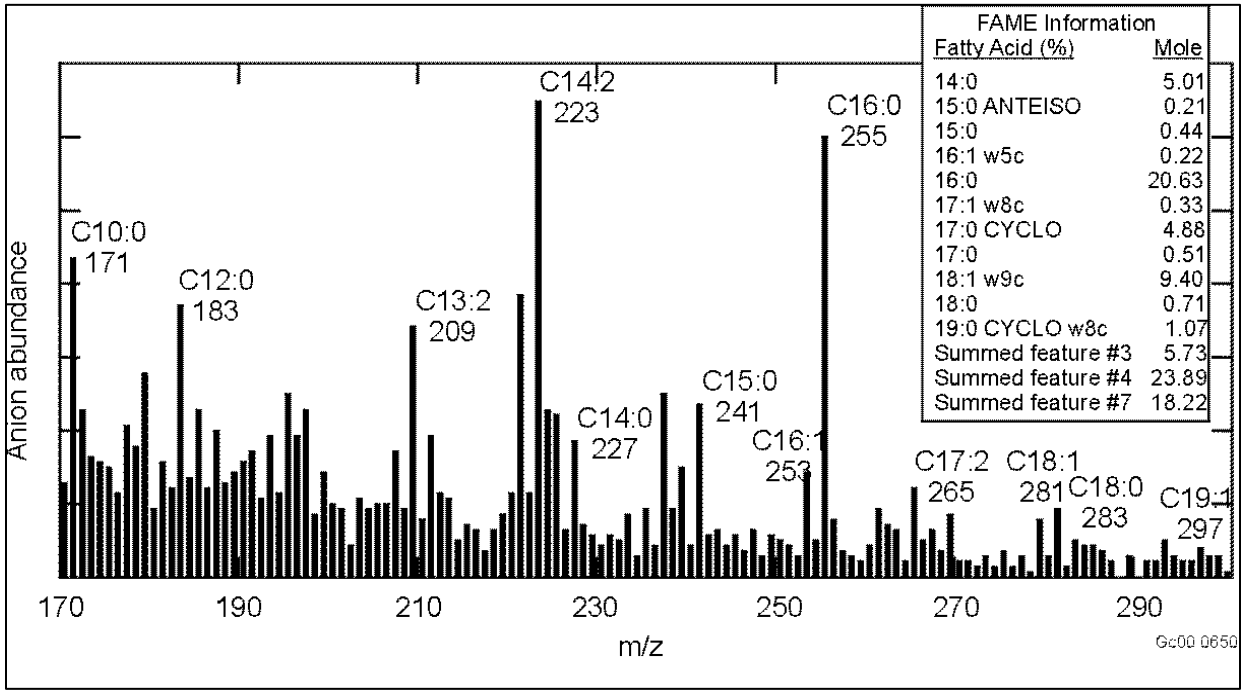

Figure 3. Under: anion SIMS spectrum of *Methanoculeus marisnigri*; Over: Fatty acid methyl ester profile of *Methanoculeus marisnigri*.

In addition to detecting fatty acid, we performed partial least squares analyses of the SIMS data to determine if SIMS were capable of differentiating gram positive and gram negative bacteria. We hypothesized that since the differences in gram positive and negative bacteria is due to differences in their cell wall chemistries, SIMS would be capable of interrogating this outer region of intact bacteria. Partial least squares (PLS) regression analysis (R2 = 0.988) for gram positive/negative character of the 38 different bacteria using the SIMS anion spectra resulted in a clear grouping of the gram-positive and gram-negative species (see Figure 4). The first PLS factor has many of the ions expected from membrane fatty acids that would be more prevalent in the spectra from gram negative bacteria (see Figure 5).

In addition to qualitative information, it was important to establish detection limits of the measurement to assess the usefulness of SIMS in analyzing environmental samples. Since we were developing SIMS to analyze intact microorganisms directly on environmental surfaces, we had to know how many microbial cells had to be present on the sample for detection by SIMS. For these experiments we selected *Arthrobacter globiformis*, a well-characterized soil bacteria. Anions originating from phospholipid fatty acids were used as detection markers and identified using MIS. In this work, 19 samples taken from two different cultures were analyzed. Two blank samples (stainless steel sample holder only) were analyzed, and 1 sample of the growth media was analyzed. The samples were allowed to dry 10 to 20 minutes in the lab air, then analyzed by SIMS. Immediately after analysis, the sample and sample holder were submerged in a 1 N NaOH solution to prepare the sample for the protein assay.

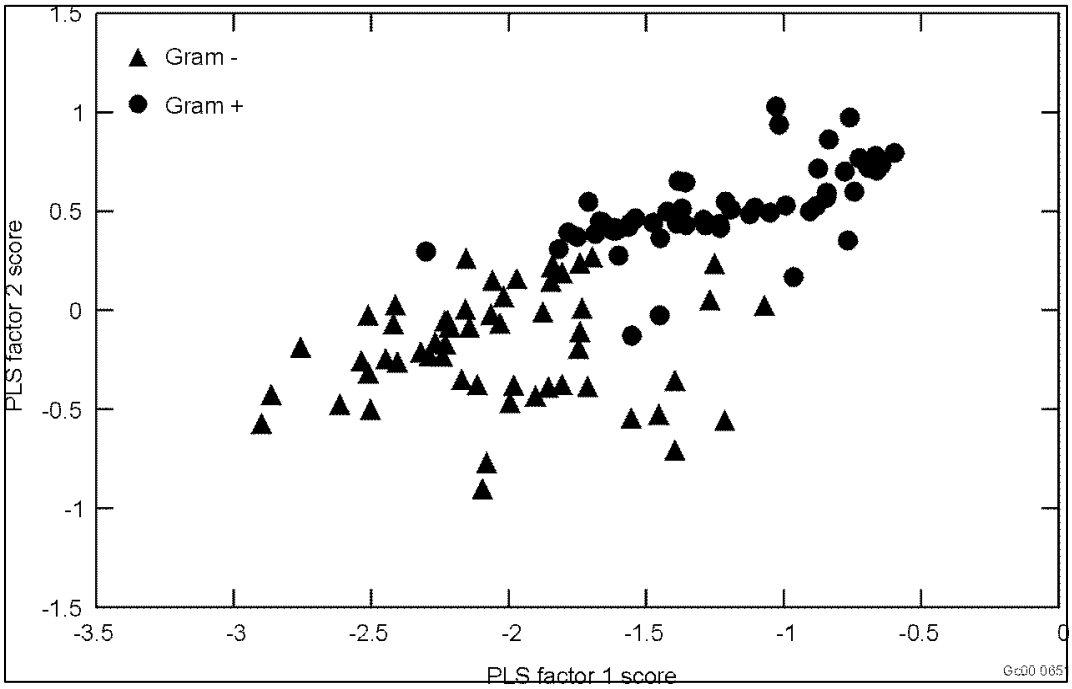

Figure 4. Partial least squares analysis of SIMS data demonstrating statistical grouping of Gram positive and negative bacteria.

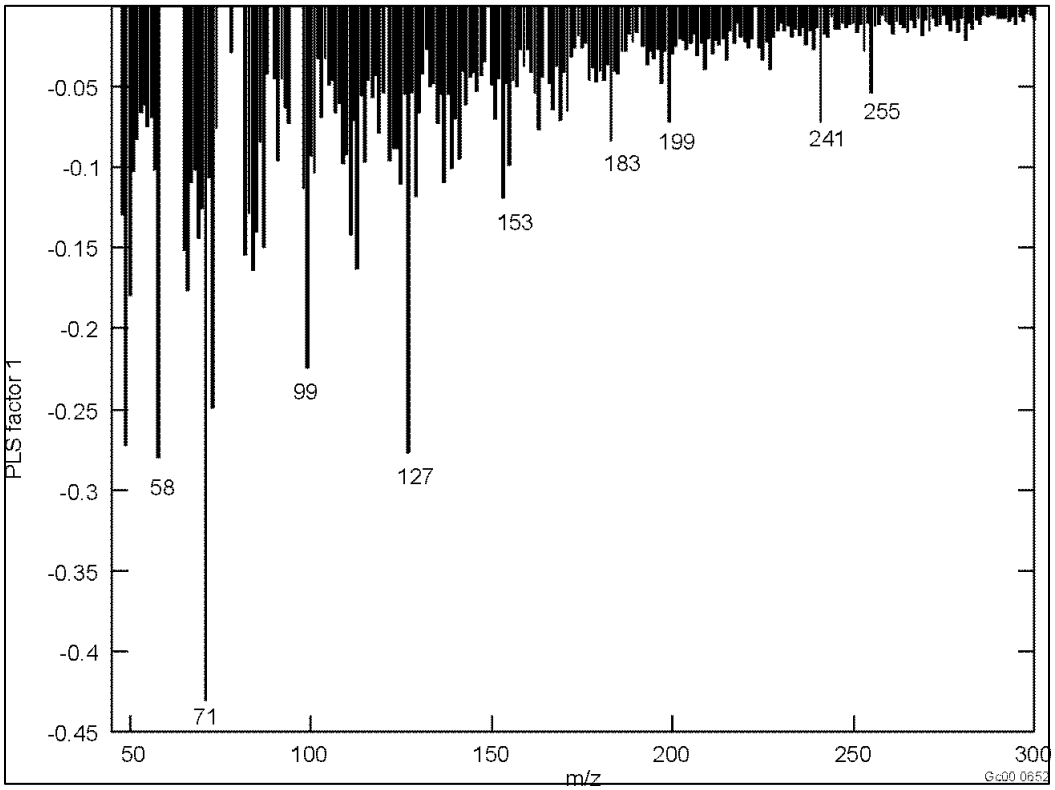

Figure 5. The first PLS factor for the Gram negative bacteria plotted versus m/z which contains a number of fatty acid-related ions.

Detection of *A. globiformis* by SIMS was determined by measuring the anion abundance of the m/z 241, which is the $[M-H]^-$ from $C_{15}H_{30}O_2$ fatty acid. The results show that SIMS is capable of detecting $<7 \Delta 10^7$ cells of *A. globiformis* present on a stainless steel sample holder (See Figure 6). The protein assay technique used to quantitate the number of cells analyzed by SIMS was less than the SIMS measurement; thus a more sensitive technique is needed to quantitate the minimum number of cells detected. Since *A. globiformis* has a dominant fatty acid ($C_{15}H_{30}O_2$) component, the detection limits of other microorganisms must be determined to better assess the sensitivity of SIMS for detecting microbes. These results are encouraging for future utilization of SIMS to directly investigate microorganisms present on environmental sample as common cell concentrations in the soils are 10^9 cells per gram, which are approximately 10^5 cells per cm^2. The work presented here suggests that the SIMS approach may be capable of detecting cells at this level. Continued work is needed to identify an analytical technique that will provide us with a quantitative measure of the number of cells analyzed when analyzing by SIMS. We are hoping that since the number of cells is low, an imaging approach such as scanning electron microscopy will work. Additionally, the dependence of the detection limit on the specific microorganism analyzed and the underlying substrate material needs to be determined.

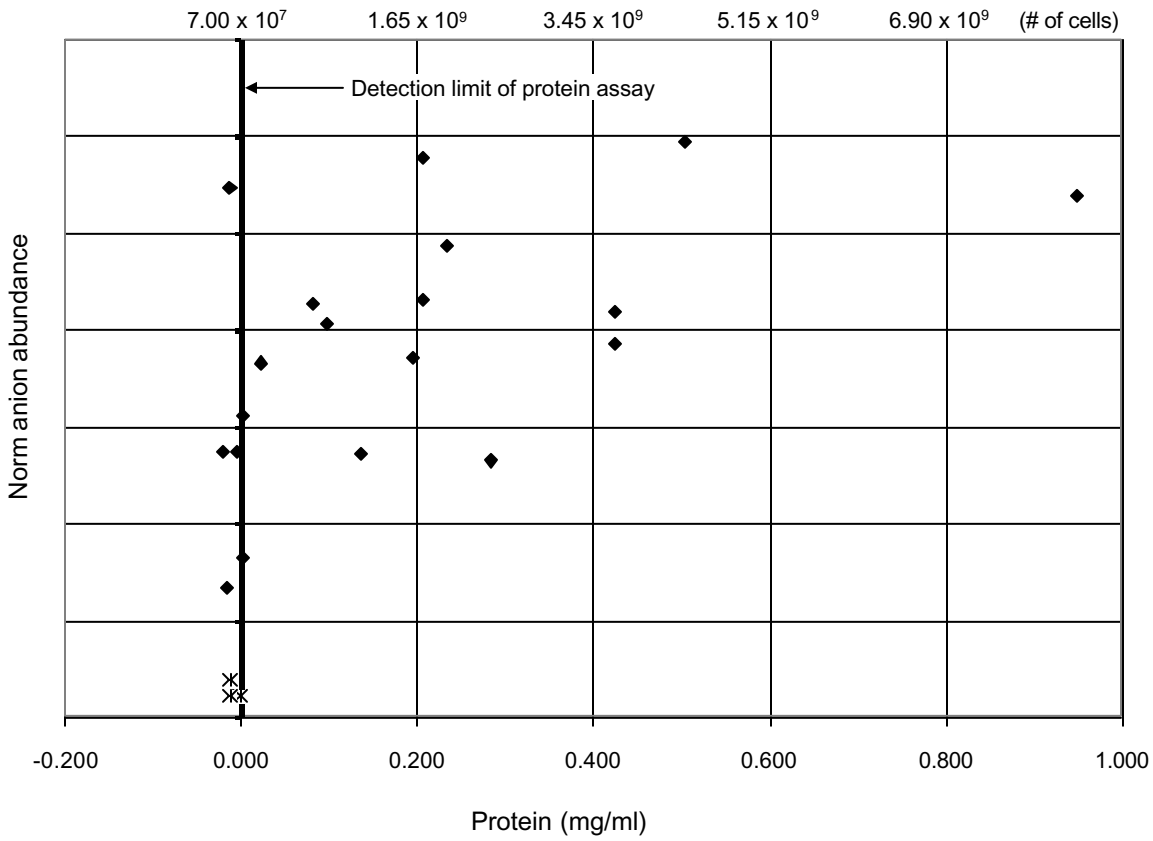

Figure 6. Detection of A. globiformis represented by the normalized anion abundance of the m/z 241 [M-H]– (from C15H30O2 fatty acid) plotted against the cell number (measured by the protein assay). ↓ = A. globiformis, ? = blanks.

ACCOMPLISHMENTS

The INEEL advanced toward having the unique capability to detect and identify microorganisms using SIMS. Results of this task demonstrate that SIMS can provide fatty acid chemical information about the cell membrane of microorganisms comparable to the information obtained from the microorganism identification system (standard technology used by microbiologists), which is a much more labor-intensive approach. Further, the amino acid and peptides work suggests that SIMS has some capability for detecting and identifying proteins present in the cell membrane, which can be very useful chemical signatures for use as biomarkers. The detection limit results are promising as they indicate that SIMS is capable of detecting cell concentrations near those that exist on environmental samples. The recommendations for future work is to have parallel efforts of continued development of this capability along with the application of this technique to assistance in microbiological research. This combined approach is necessary because the application of SIMS in microbiological research provides much needed insights into how best to improve SIMS for use as a tool for microbial studies.

REFERENCES

1. P. S. Handley, "Negative Staining," in N. Mozes, P. S. Handley, H. J. Busscher, P. G. Rouxhet, (Eds.), *Microbial Cell Surface Analysis Structural and Physicochemical Methods*, VCH Publishers, New York, 1991, p. 65.

2. C. Fenselau, (Ed.), "Mass Spectrometry for the Characterization of Microorganisms," *ACS Symposium Series 541, ACS, Washington D.C., 1994*, see chapters within.

3. M. L. Pacholski, D. M. Cannon, Jr., A. G. Ewing, and N. Winograd, "Molecule Specific Imaging of Human Red Blood Xells Using TOF-SIMS," In: G. Gillen, R. Lareau, J. Bennett, F. Stevie, (Eds.), *Secondary Ion Mass Spectrometry (SIMS XI)*. John Wiley and Sons, New York, 1998, p. 93.

4. C. Fenselau, "MALDI MS and Strategies for Protein Analysis," *Anal. Chem*, Vol. 69, 1997, pp. 661A–665A.

5. E. R. Williams, "Tandem FTMS of Large Biomolecules," *Anal. Chem.*, Vol. 70, 1998, pp. 179A–185A.

6. P. G. Rouxhet, M. J. Genet, "Chemical Composition of the Microbial Cell Surface by X-ray Photoelectron Spectroscopy," in: Mozes, N., Handley, P. S., Busscher, H. J., Rouxhet, P. G. (Eds.), *Microbial Cell Surface Analysis Structural and Physicochemical Methods*, VCH Publishers, New York, 1991, p. 175.

7. F. Caccavo, Jr., P. C. Schamberger, K. Keiding, P. H. Nielsen, "Role of Hydrophobicity In Adhesion of the Dissimilatory Fe(III)-reducing Bacterium *Shewanella Alga* to Amorphous Fe(III) Oxide," *Appl. Environ. Microbiol.,* Vol. 63, 1997, pp. 3837–3843.

8. D. Briggs, M. P. Seah, "Practical Surface Analysis, Volume 1–Auger and X-ray Photoelectron Spectroscopy," *J. Wiley*, 1990, Chichester, England, p. 437.

9. H. Y. N. Holman, D. L. Perry, J. C. Hunter-Cevera, "Surface-Enhanced Infrared Absorption-Reflectance (SEIRA) Microspectroscopy for Bacteria Localization on Geologic Material Surfaces," *J. Microbiol. Methods*, Vol. 34, 1998, pp. 59–71.

10. J. C. Vickerman, "The SIMS phenomenon—the experimental parameters," In: Vickerman, J. C., Brown, A., Reed, N. M. (Eds.), *Secondary Ion Mass Spectrometry Principles and Applications,* Oxford Science Publications, New York, 1989, p. 31.

11. G. S. Groenewold, A. D. Appelhans, G. L. Gresham, J. E. Olson, M. Jeffery, J. B. Wright, "Analysis of VX On Soil Particles Using ion Trap Secondary Ion Mass Spectrometry," *Anal. Chem.,* Vol. 71, 1999, pp. 2318–2323.

12. M. L. Pacholski, D. M. Cannon, Jr., A. G. Ewing, N. Winograd, "Imaging of Exposed Headgroups and Tailgroups of Phospholipid Membranes by Mass Spectrometry," *J. Am. Chem. Soc.*, Vol. 121, 1999, pp. 4716–4717.

13. J. M. McMahon, R. T. Short, C. A. McCandlish, J. T. Brenna, P. J. Todd, "Identification and Mapping of Phosphocholine in Animal Tissue by Static Secondary Ion Mass Spectrometry and Tandem Mass Spectrometry," *Rapid Commun. Mass Spectrom.,* Vol. 10, 1996, pp. 335–340.

14. J. E. Delmore, A. D. Appelhans, E. S. Peterson, "Tube Ion Source for the Study of Chemical Effects In Surface Ionization," *Int. J. Mass Spectrom. Ion Proc.,* Vol. 108, 1991, pp. 179–87.

15. J. E. Delmore, A. D. Appelhans, E. S. Peterson, "A Rare Earth Oxide Matrix for Emitting Perrhenate Anions," *Int. J. Mass Spectrom. Ion Proc.,* Vol. 146/147, 1995, pp. 15–20.

16. G. S. Groenewold, J. E. Delmore, J. E. Olson, A. D. Appelhans, J. C. Ingram, D. A. Dahl, "Secondary Ion Mass Spectrometry of Sodium Nitrate: Comparison of ReO^-_4 and Cs^+ Primary Ions," Int. *J. Mass Spectrom Ion Proc.,* Vol. 163, 1997, pp. 185–95.

17. K. Poels, L. Van Vaeck, R. Gijbels, "Microprobe Speciation Analysis of Inorganic Solids by Fourier Transform Laser Mass Spectrometry," *Anal. Chem.,* Vol. 70, 1998, pp. 504–512.

18. A. D. Appelhans, J. E. Delmore, "A Comparison of Polyatomic and Atomic Primary Beams for Secondary Ion Mass Spectrometry of Organics," *Anal. Chem.,* Vol. 61, 1989, pp. 1087–93.

19. P. C. Schamberger, F. Caccavo, Jr., F. V. O. Kloeke, G. G. Geesey, "Microbial Cell Fingerprinting – Development of TOF-SIMS for the Study of Microbial Cell Surfaces," *Abstract for Surfaces in Biomaterials Conference, Phoenix, AZ, 1996.*

20. A. D. Appelhans, D. A. Dahl, J. E. Delmore, "Neutralization of Sample Charging in Secondary Ion Mass Spectrometry Via a Pulsed Extraction Field," *Anal. Chem.,* Vol. 62, 1990, pp. 1679–1686.

21. J. C. Vickerman, "Introducing Secondary Ion Mass Spectrometry" In: *Vickerman, J. C., Brown, A., Reed, N. M. (Eds.), Secondary Ion Mass Spectrometry Principles and Applications,* Oxford Science Publications, New York, 1989, p.1.

22. D. A. Dahl and A. D. Appelhans, "Sample Charge Compensation Via Self-Charge-Stabilizing Ion Optics," *Int. J. Mass Spectrom. Ion Proc. 178*, 1998, pp. 187–204.

23. G. S. Groenewold, A. D. Appelhans, J. C. Ingram, "Characterization of Bis(alkylamine)mercury Cations from Mercury Nitrate Surfaces By Using an Ion Trap Secondary Ion Mass Spectrometer," *J. Am. Soc. Mass Spectrom. 9*, 1998, pp. 35–41.

24. S. D. Brown, "Chemical Systems Under Indirect Observation: Latent Properties and Chemometrics," *Appl. Spectrosc.*, Vol. 49, 1995, pp. 14A–31A.

25. D. M. Haaland, R. G. Easterling, D. A. Vopicka, "Multivariate Least-Squares Methods Applied to Quantitative Spectral Analysis of Multicomponent Samples," *Appl. Spectrosc,* Vol. 39, 1985, pp. 73–84.

26. D. M. Haaland, E. V. Thomas, "Partial Least-Squares Methods for Spectral Analysis. 1. Relation to Other Quantitative Calibration Methods and Extraction of Qualitative Information," *Anal. Chem.,* Vol. 60, 1988, pp. 1193–1201.

27. T. Naes, H. Martens, "Principal Component Regression In NIR analysis: Viewpoints, Background Details and Selection of Components," *J. Chemom.,* Vol. 2, 1988, pp. 155–67.

28. L. Dolmatova, C. Ruckebusch, N. Dupuy, J. P. Huvenne, P. Legrand, "Quantitative Analysis of Paper Coatings Using Artificial Neural Networks," *Chemom. Intel. Lab. Syst.,* Vol. 36, 1997, pp. 125–40.

29. F. Basile, M. B. Beverly, C. Abbas-Hawks, C. D. Mowry, K. J. Voorhees, T. L. Hadfield, "Direct Mass Spectrometric Analysis of in situ Thermally Hydrolyzed and Methylated Lipids From Whole Bacterial Cells," *Anal. Chem.,* Vol. 70, 1998, pp. 1555–1562.

30. S. A. Barshick, D. A. Wolf, and A. A. Vass, "Differentiation of Microorganisms Based on Pyroloysis-ion Trap Mass Spectrometry Using Chemical Ionization," *Anal. Chem.*, vol. 71, 1999, pp. 633–641.

Biologically Based Catalysts as Sensors to Detect Contaminants in Harsh Service Environments

Harnessing Microbial Enzymes to Detect Hazardous Metals for Cleanup and Stewardship

William Apel and Vicki Thompson

SUMMARY

Harnessing and controlling the effects of microbial activity is of significant interest to DOE in their mission of environmental cleanup and long-term stewardship. Microbes called extremophiles thrive in even the harshest of environments, and their enzymes offer promise for being developed into biologically-based sensors for the detection of hazardous metals and radionuclides.

This research task focused on developing enzymes as catalysts—substances that lower the activation energy of chemical reactions—for potential use in sensors to detect hazardous substances under the relatively harsh service conditions associated with many environmental applications. Our effort concentrated on developing enzymes from extremophiles, since these microorganisms literally live at life's physical extremes, such as very high or low temperatures, or high radiation fields. Extremophilic enzymes (extremozymes derived from these microorganisms) often share their adaptation to extreme conditions and maintain their specific catalytic activity and stability under the same extreme conditions.

We have analyzed extremophilic enzymes for various properties to learn how to optimally use the enzymes in sensors. In the future, we plan to use these results to develop and test heavy metal detecting sensors for stability under varying temperature and pH conditions.

TASK DESCRIPTION

Background

Heavy metal contamination is a pervasive problem throughout the DOE complex and the United States. A recent report shows lead, chromium, arsenic, zinc, copper, cadmium, nickel, and mercury contamination in soils and groundwater at 16 DOE sites.[1] Similar metals have been found at approximately 75% of the Superfund sites across the United States.[2]

Current methods to assess and monitor sites for heavy metal contamination include atomic absorption and inductively coupled plasma emission spectrometry. These methods, while sensitive and reliable, are not readily adaptable to field use. Samples must be sent to a remote laboratory for analysis, and results are often delayed for weeks, making these methods unsuitable for continuous monitoring of contaminated sites. Additionally, analysis using these methods is expensive, and thorough characterization of contaminated sites is often economically unfeasible. Owing to these drawbacks, new methods are required for inexpensive, continuous, high sensitivity, and high reliability monitoring of contaminated sites. Biological sensors offer a solution. Biological sensors consist of two parts: a biological part, such as antibodies, enzymes or whole cells; and a transducer, such as optical fiber, a field effect transistor, or an amperometric sensor.[3] The compound to be measured reacts with or binds to the biological part of the sensor and generates a signal based on the strength of this interaction. Signals that can be generated include production of fluorescent or luminescent compounds, generation or consumption of electrons, and generation of heat. The transducer picks up the signal and generates an output, such as a

current or voltage. Because biological reactions are highly specific for their target compound, sensors can be produced with sensitivity in the part-per-billion or part-per-trillion range. This specificity also gives biosensors an advantage in measuring complex mixtures, and reduces or eliminates the necessity of removing interfering compounds in samples prior to measurement. Finally, biological reactions are rapid. Typically, measurement with biological sensors can be performed in a few minutes. Despite these advantages, biological sensors have one serious drawback—fragility of the biological component to extreme conditions. Most biological systems (mesophiles) are active within only a narrow range of conditions, typically 20 to 40°C, near neutral pH, and low salt concentrations. Outside this range, the activity and stability of biological systems fall off rapidly, which limits their use in biosensors to the same narrow range of conditions. Our solution to this problem is to use biological components derived from extremophilic microorganisms. These organisms thrive under extremes of temperature (up to 110°C and below 20°C), pH (below 4 and above 9), salt concentration (up to 5M), and/or pressure (up to 500 atm).[4] Biological components such as enzymes derived from these organisms typically share their tolerance for extreme conditions. Using these types of enzymes would produce a biological sensor that could be measured under extreme conditions and be more stable than enzymes derived from mesophilic organisms.

A number of biosensors have been developed for detecting heavy metals. These sensors rely on the inhibition of many enzymatic reactions in the presence of heavy metals. Classes of enzymes that have shown this behavior include ureases, peroxidases, phosphatases, cholinesterases, dehydrogenases, reductases, and oxidases.[5] As an example, a metal ion biosensor was developed using the enzyme lactate dehydrogenase that had a limit of detection of 0.4 ppb for mercury. The sensor could also detect other metals, including silver, lead, copper, and zinc.[6]

This research task followed two approaches to examine enzymes sensitive to heavy metals. First, we isolated and purified an extremophilic enzyme: one derived from a thermophilic organism (catalase). Second, we undertook studies to examine the heavy metal sensitivity of a nitrate reductase enzyme derived from fungi. This portion of the study occured in collaboration with Washington State University. Additional funding was pursued to characterize the thermostable catalase enzyme kinetics, stability, tolerance to extreme conditions, and inhibition by heavy metals; and to isolate and purify an extreme nitrate reductase from a halophilic microorganism. After characterization, we used the enzymes to develop heavy metal biosensors that were characterized for sensitivity and selectivity and field tested at contaminated sites.

Task Summary: Catalase

The enzyme catalase catalyzes the dismutation reaction of hydrogen peroxide to form water and oxygen, as $2H_2O_2 \Downarrow 2H_2O + O_2$.

The enzyme is found in most aerobic organisms and protects cells against oxidative damage caused by hydrogen peroxide. The average molecular weight of catalases is 240,000. Catalases typically consist of four to six identical subunits that all have catalytic activity. Catalases are usually heme enzymes, though Mn catalases have also been reported. Reports from the literature indicate that catalases are sensitive to several heavy metals, including Cu, Fe, Pb, Zn, and Ni.[7]

Thermophilic microorganisms (49 strains) isolated previously from Yellowstone National Park hot springs and from Amalgamated Sugar (Twin Falls, Idaho) process streams were tested for catalase activity; 28 of those strains tested positive. We selected the strain with the strongest catalase reaction for isolation of the catalase enzyme. This strain was identified by 16S RNA analysis as *Thermus brockianus.*

This isolate was grown aerobically at 70°C in 4-liter cultures to obtain sufficient biomass to isolate the enzyme. We examined several methods for cell lysis, including chemical treatment, sonication, and

the French press. The best results were obtained using the French press. After the cells had been lysed, we removed cell debris by centrifugation and kept the supernatant for further purification. After examining the catalase literature, we developed a purification strategy that included precipitation, ion exchange chromatography, hydrophobic interaction chromatography, and gel filtration chromatography.

We first examined precipitation of the enzymes through the salting-out effect. Sequential additions of ammonium sulfate were added to the crude cell extract to precipitate proteins. After each addition, we centrifuged the solution to remove precipitated protein, but kept the pellet for further analysis. Ammonium sulfate concentrations of 20, 40, 60, and 80% of saturation were used in this study. Each pellet was resolubilized in buffer and tested for catalase activity. The catalase activity was distributed fairly evenly through all the ammonium sulfate cuts, and no one cut represented the bulk of the enzyme activity. Since this step did not result in appreciable purification, we did not pursue it further.

Next, we investigated ion exchange chromatography as the first purification step. This technique separates proteins based on their net charge. We selected a diethylaminoethyl (DEAE) anion exchange column for this application. Crude cell extract was loaded onto a DEAE column and washed with buffer. Proteins were eluted off the column with increasing amounts of salt (0 to 1.0 M KCl) in a stepwise fashion. Figure 1 shows the results from a typical run. A large amount of protein did not bind to the column and passed through during the wash step, but had very little catalase activity. As we increased the salt concentration to 0.25 M, we saw a second peak with high catalase activity. The last peak came off at 0.5 M KCl, and, again, there was very little catalase activity present. Further increases in salt concentration did not release any more protein. We optimized ionic strength and pH by examining column performance at pH ranging from 4 to 9 and buffers from 10 to 100 m*M*. Optimum conditions were found at 20-m*M* buffer strength and pH of 8.0.

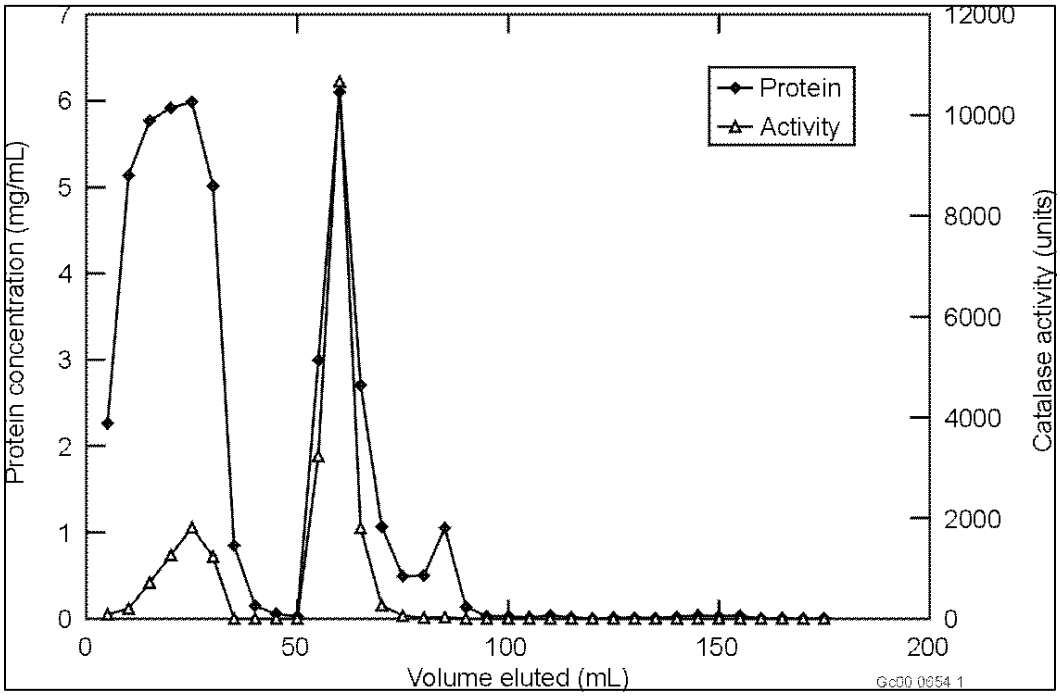

Figure 1. Results of DEAE ion exchange chromatography.

The high catalase activity fractions obtained from the DEAE column were pooled, brought up to 1.0-M ammonium sulfate, and applied to a hydrophobic interaction column that separated the proteins based on their hydrophobicity. Reducing the salt concentration in a stepwise fashion caused the proteins to become less hydrophobic, and they were eluted from the column (Figure 2). Each decrease in salt concentration resulted in a protein peak from the column. The bulk of the catalase activity came off in the first peak. We examined five different types of hydrophobic interaction columns and found that the phenyl active group gave best results.

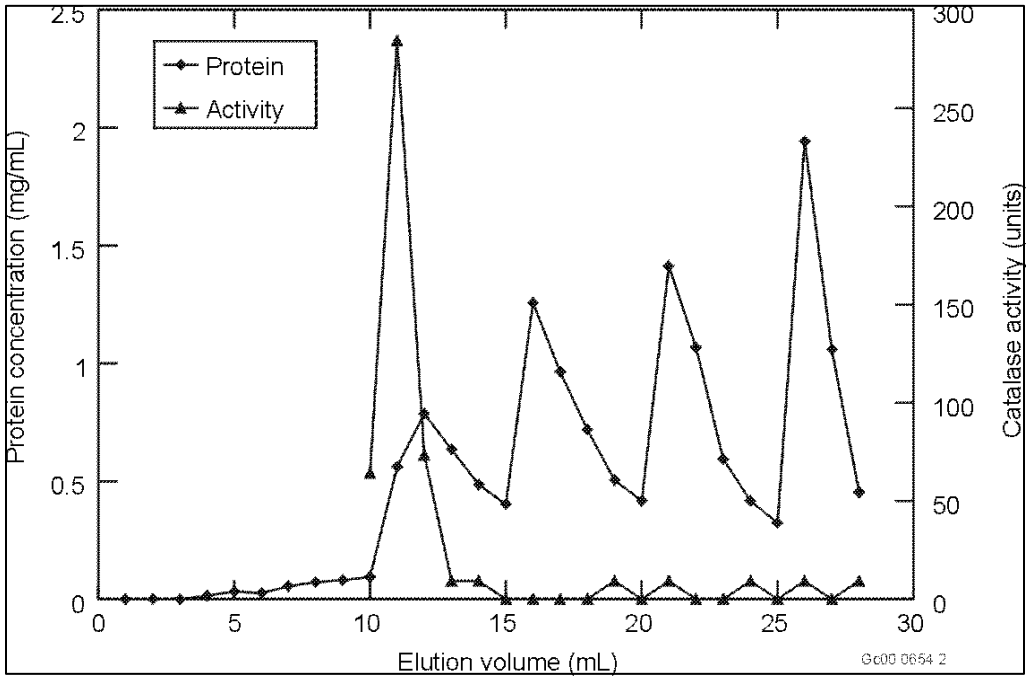

Figure 2. Results from hydrophobic interaction chromatography (HIC).

Table 1 summarizes the purification obtained from each step. The ion exchange chromatography step resulted in a small amount of purification, as evidenced by the increase in specific activity (units of activity divided by total protein present); however, the hydrophobic interaction chromatography resulted in the most purification. The 30% yield is typical of protein purification protocols seen in the literature. We also subjected the proteins to gel electrophoresis to see how much contaminating protein was present after each step (see Figure 3). After each chromatography step, the number of bands present decreased, indicating that contaminating proteins had been removed. At least one more purification step will be necessary to remove all the contaminating protein. We will examine gel filtration as the next step.

Table 1. Summary of protein purification.

	Total Units (U)	Specific Activity (U/mg)	Purification (fold)	Yield (%)
Cell extract	1420	87	1	100
DEAE step	1100	118	1.3	77
HIC step	420	5390	62	30

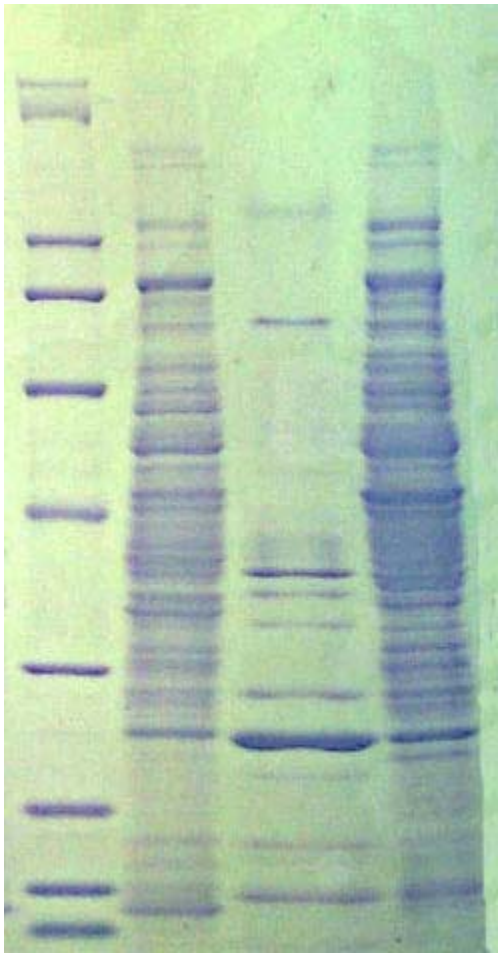

Figure 3. Gel electrophoresis of each stage of purification. Lane 1—molecular weight standards, Lane 2—DEAE fraction, Lane 3—HIC fraction, and Lane 4—cell extract.

We examined the ionic strength buffers from 20 to 100 m*M* and pH from 6–9 and found identical optimum conditions to those obtained for the ion exchange column, a 20 m*M* buffer and a pH of 8.0.

Next, gel filtration was examined for further purification. In this type of chromatography, a column is packed with a gel that contains a range of pore sizes. Smaller proteins are readily able to diffuse into the pore, while larger proteins cannot. This results in a retardation of smaller proteins as they progress down the column, enabling the separation of proteins based on their size. High catalase activity fractions from the hydrophobic interaction chromatography step were loaded onto a gel filtration column and the fractions collected. These fractions were tested for protein concentration and catalase activity. Somewhat surprisingly, none of the fractions collected contained either protein or catalase activity. Further investigation revealed that the amount of protein loaded onto the column was too small and the fractions collected from the column were diluted below the detection limit for protein and catalase activity.

Due to the above finding, we elected to scale up the purification process so that larger amounts of protein could be produced for the gel filtration step. To this end, we collaborated with the Utah State University Biotechnology Center to grow up a 100 L batch of *T. brockianus.* This resulted in about 270 g of wet cell paste as compared to the 10 g usually obtained from growing up 4-L cultures. This allowed us

to start with much larger quantities of cell extract for purific ation. We started with the ion exchange step by moving from a 5 mL column to a 20 mL column. The amount of protein loaded was scaled up in a linear fashion. We also used a linear salt gradient to elute protein from the column rather than the step gradient used previously. Linear gradients produce sharper peaks and result in better purification than step gradients. All other conditions from the previous purification were kept the same. Results from the larger scale ion exchange purification are shown in Figure 4. The top graph in Figure 4 shows the protein concentration in peaks collected from the column. The results are very similar to those obtained with the small scale ion exchange. A large amount of protein comes off the column initially that was not able to bind to the column. As the linear salt gradient commences a large peak of protein was collected from the column. The bottom graph in Figure 4 shows the catalase activity of each fraction and most of the activity came off the column in three fractions. Again, this is similar to results obtained previously.

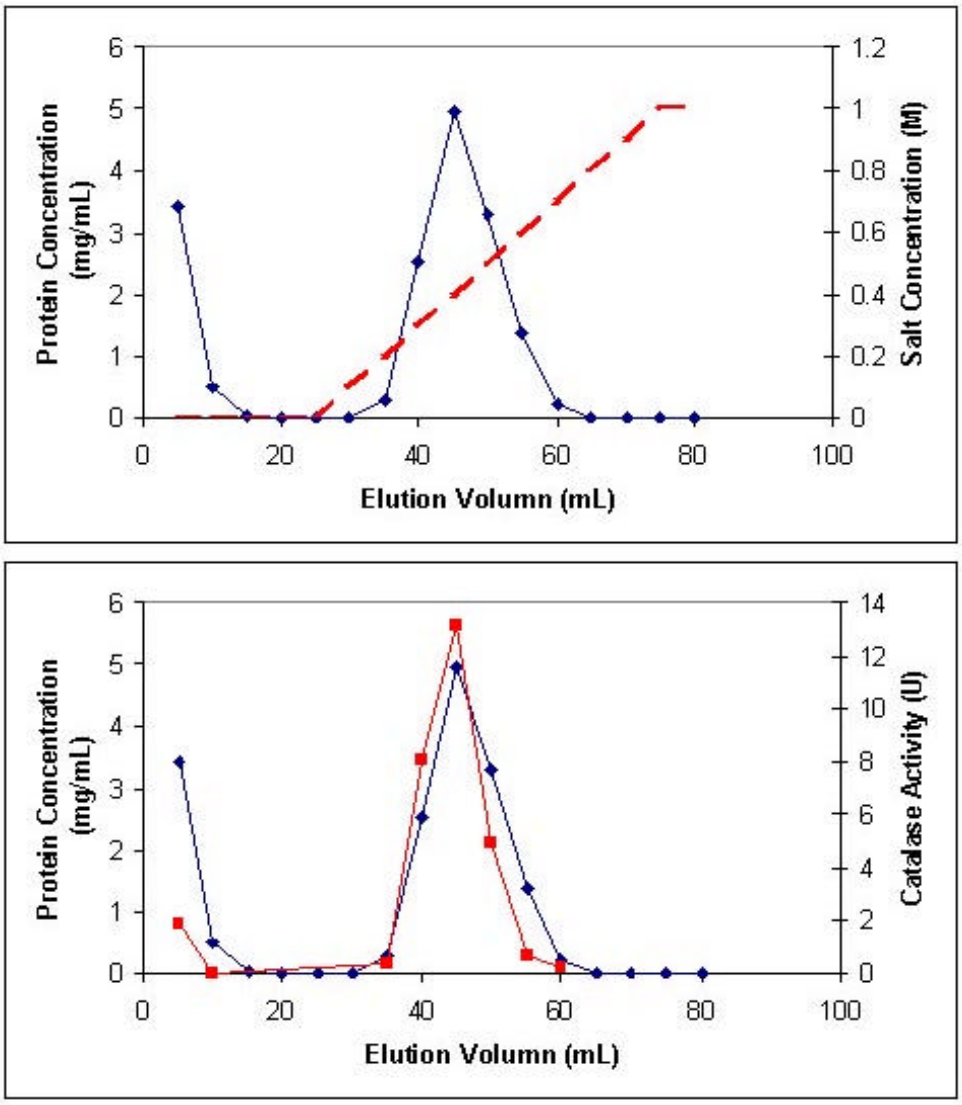

Figure 4. Results of large scale ion exchange chromatography purification of catalase enzyme. Protein concentration (mg/mL) as a function of elution volume (top); Catalase activity (U) recovered from the column as a function of elution volume (bottom).

High activity catalase fractions were pooled from the ion exchange column, brought up to 1 *M* salt concentration and loaded onto a 20 mL hydrophobic interaction column. We also used a linearly decreasing salt gradient to elute protein from this column instead of a step gradient. Again, all other conditions were kept the same. Results from this are shown in Figure 5. The upper graph in Figure 5 shows protein elution from the hydrophobic column. No protein eluted off the column at 1 *M* salt concentration indicating that all protein was able to bind to the column. As the salt concentration started to decrease, two distinct peaks eluted from the column. The lower graph in Figure 5 shows that most of the catalase activity came off the column in the first peak in three fractions. The results using a linear salt gradient were different than those obtained using the step gradient (see Figure 2). Four distinct peaks were observed to elute with each step change in salt concentration while only two peaks came off using the linear gradient. It is not clear why there is a difference between the two methods. Again, however, the high activity catalase fractions eluted early in the gradient and were concentrated in three fractions, which is comparable to the results shown in Figure 2.

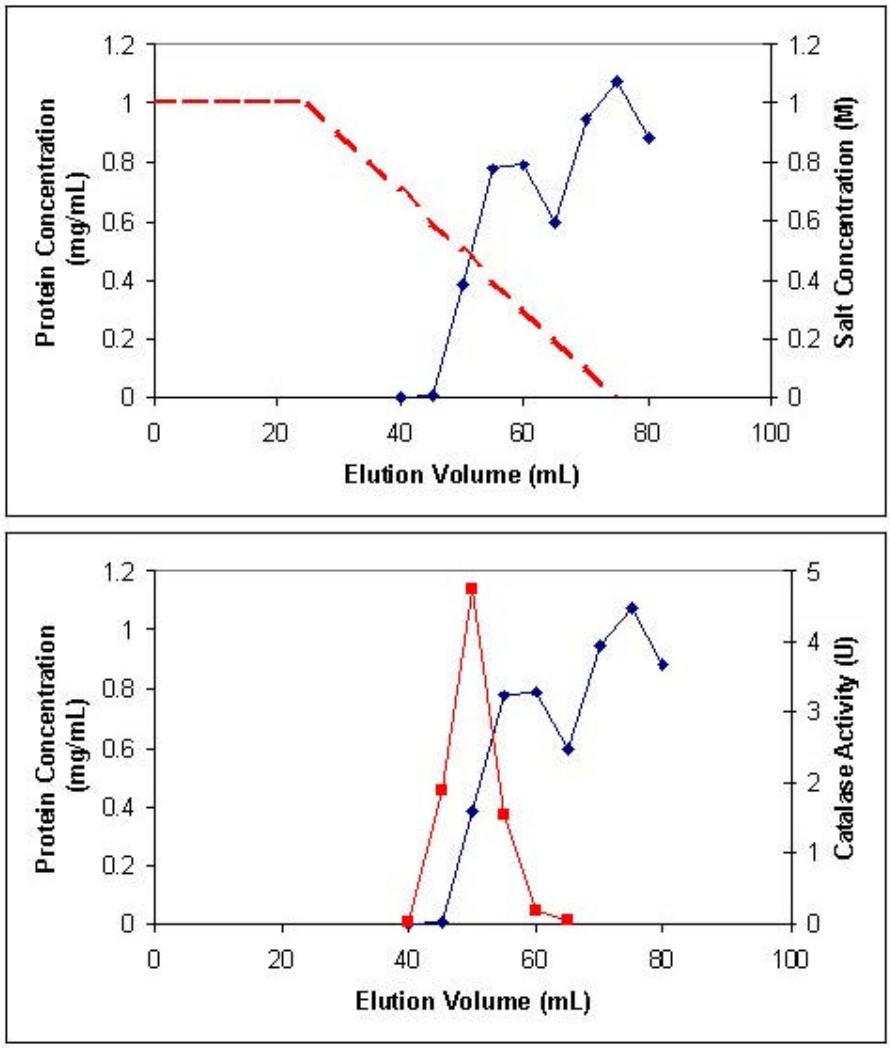

Figure 5. Results of large scale hydrophobic interaction chromatography purification of catalase enzyme. Protein concentration (mg/mL) as a function of elution volume (top); Catalase activity (U) recovered from the column as a function of elution volume (bottom).

The three high activity catalase fractions from the hydrophobic column were pooled, desalted, and concentrated down to about 1 mL. This represented approximately 6 mg of protein. This was loaded onto the gel filtration column and fractions were collected. Results from this experiment are shown in Figure 6. Two small peaks and a large peak eluted off this column with the majority of the catalase eluting off the column in two fractions of the large peak.

To determine how well our purification scheme worked, we used gel electrophoresis as described above (Figure 7). After the ion exchange step, there were numerous bands representing contaminating proteins remaining in the gel. After the hydrophobic interaction step, there were approximately 8 to 10 proteins remaining in the sample. Finally, after the gel filtration step, there were 3 to 4 proteins remaining. While this is not a completely pure catalase, we do have a relatively pure catalase sample that could be further tested for kinetics, stability, and metal sensitivity. Table 2 shows the amount of purification attributed to each step in the purification protocol. The amount of catalase activity at each step was much higher than reported (see Table 1) for the small scale purification. This is indicative of the much larger amounts of protein that could be loaded onto the larger-scale columns. There was a loss of total catalase activity with each subsequent purification step that is typical of any purification. The specific activity increased markedly for each step indicating that contaminating proteins were being removed. The scaled up protocol used here resulted in greater purification for the ion exchange method (specific activity of 340 U/mg for large scale versus 118 U/mg for the small scale). However, the hydrophobic interaction method resulted in somewhat less purification at the larger scale (2,400 U/mg for large scale versus 5,390 U/mg for the small scale) This may be the result of the linear gradient used with this method and may also be related to the column size. Ultimately, our protocol resulted in an increase in specific activity from 24 U/mg to 4,700 U/mg and a purification factor of almost 200. A total of 3 mg of essentially pure catalase was produced as a result of this procedure. This catalase is planned to be used in future work (not part of the ESRC task) that will center on characterizing enzyme properties and its inhibition by metal ions, and developing and testing a catalase metal ion biosensor.

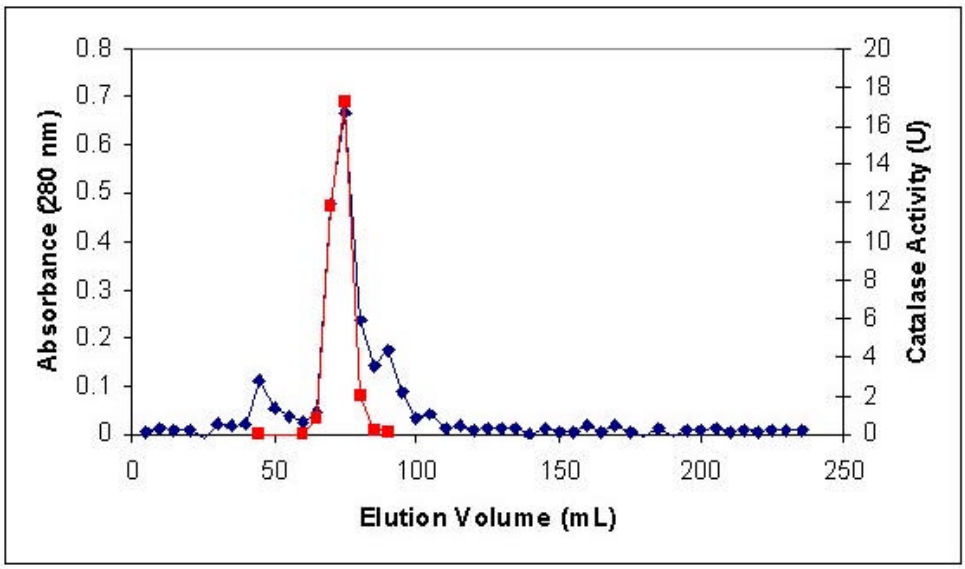

Figure 6. Results of the gel filtration chromatography—catalase activity recovered from the column as a function of elution volume.

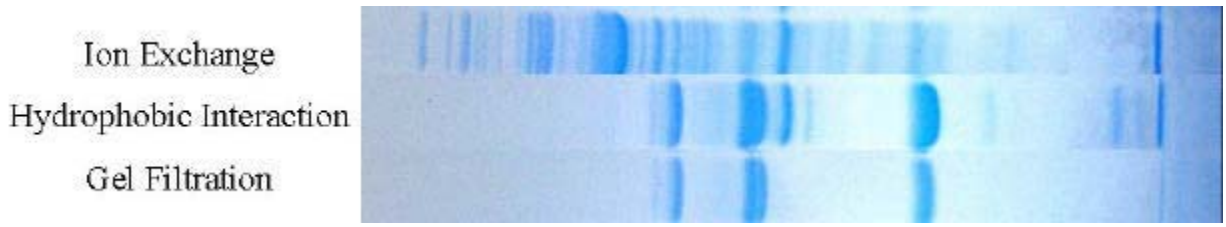

Figure 7. Gel electrophoresis results for each purification step.

Table 2. Summary of large scale protein purification steps.

Sample	Total Catalase Activity (U)	Specific Activity (U/mg)	Purification (fold)
Cell Extract	38,500	24	1
Ion Exchange	36,200	340	14
Hydrophobic Interaction	33,700	2,400	101
Gel Filtration	14,500	4,700	196

Task Summary: Nitrate Reductase

Nitrate reductase catalyzes the reduction of nitrate to nitrite. This enzyme is typically about 230,000 molecular weight and consists of three subunits. In contrast to catalase, each subunit is a different size and serves a different function. Previous work showed that nitrate reductase is sensitive to chromium, lead, nickel (see Figure 8), copper, zinc, and cadmium.[8]

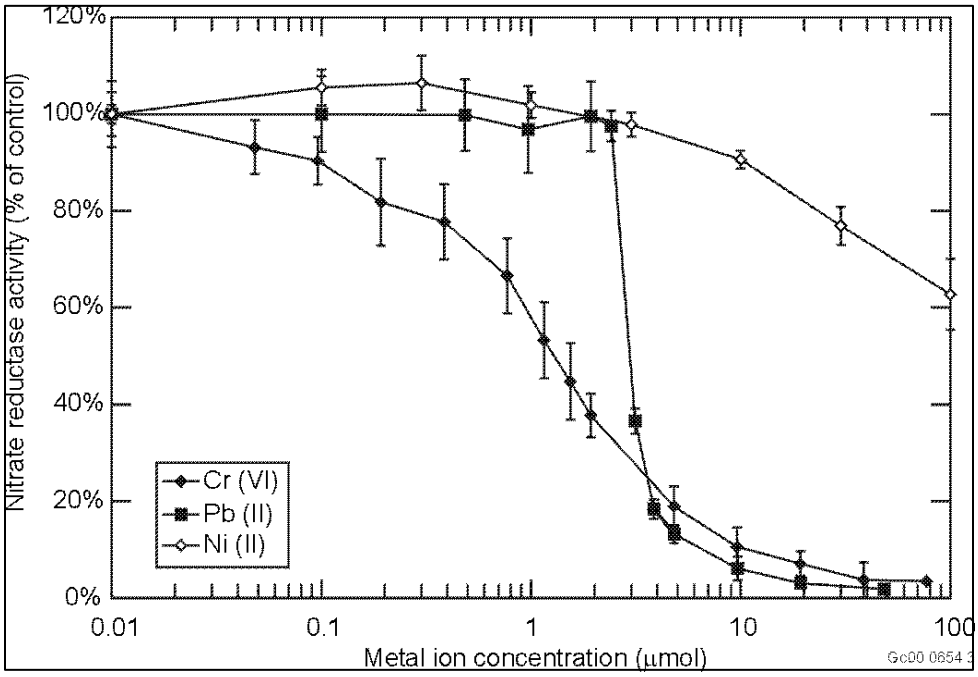

Figure 8. Inhibition of nitrate reductase by various heavy metal ions.

This task, conducted at Washington State University by a graduate student (Abbie Aiken) pursuing a Ph.D. in Chemical Engineering under the guidance of Drs. James Peterson and Brent Peyton, focuses on purifying nitrate reductase from a halophilic microorganism, *Halomonas campisalis.*[9] Further research was conducted characterizing the inhibition of nitrate reductase by metals in the presence of chelators.

The growth curve for *Halomonas campisalis* was determined in batch cultures (see Figure 9). After a short lag phase, this organism had a 12-hour log growth phase followed by entry into a stationary phase at 16 hours of growth. We also conducted a study to determine the amount of nitrate reductase produced during each phase of growth and find the optimal time to harvest the culture. The relative amount of nitrate reductase increased with increased biomass and leveled off as the stationary phase was reached. These results indicate that the optimal time to harvest cells is during the late log or early stationary phase.

We searched the literature to examine purification strategies for nitrate reductase and developed the following strategy for purifying nitrate reductase from *Halomonas campisalis*.[10] We will lyse cells with a French press and centrifuge to remove cell debris. Since nitrate reductase is a membrane bound enzyme, we will subject the supernatant to ultracentrifugation (70,000 g) to separate cell membranes from the soluble protein fraction. The pellet will be resolubilized, nitrate reductase will be separated from the membranes with a detergent, and the solution centrifuged again at 70,000 g. We will then subject the supernatant to ion exchange chromatography, hydrophobic interaction chromatography, and gel filtration chromatography. Buffer concentrations, pH, and ionic strengths will be optimized for each chromatography step.

Finally, we examined the inhibition of nitrate reductase caused by various metals in the presence of a metal ion chelator, EDTA (ethylenediaminetetraacetic acid) (see Figure 10). Zinc was completely non-inhibitory to nitrate reductase in the presence of even low levels of EDTA, indicating that the EDTA completely chelated the zinc. Chromium (VI), on the other hand, still inhibited nitrate reductase with up to 100 m*M* EDTA present. These results showed it is possible to completely remove the inhibition of a given metal by adding metal ion chelators. This is an important result for future metal ion biosensor development, since it will be possible to make a biosensor that is specific for a given metal, simply by adding different metal ion chelators.

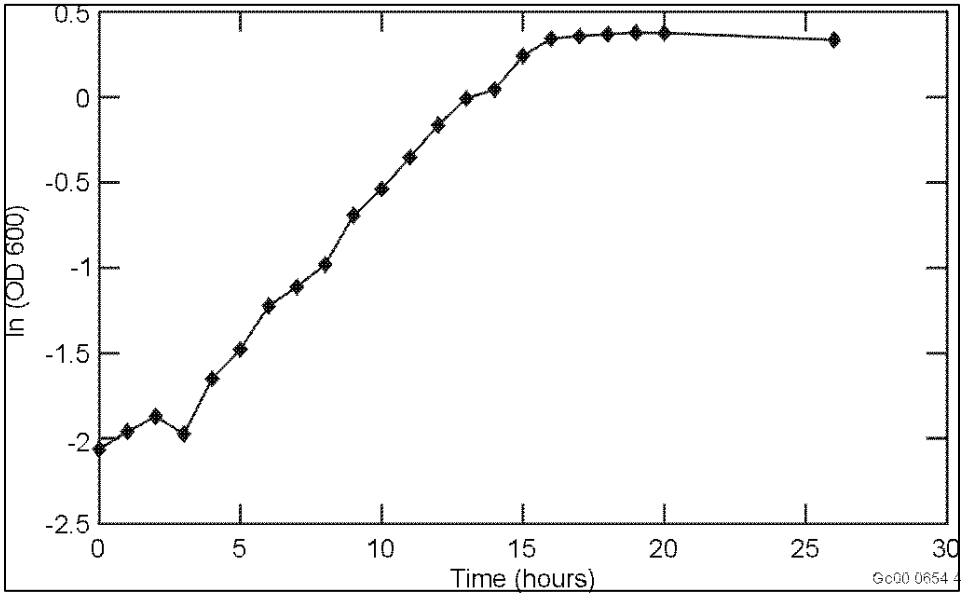

Figure 9. Growth curve for *Halomonas campisalis.*

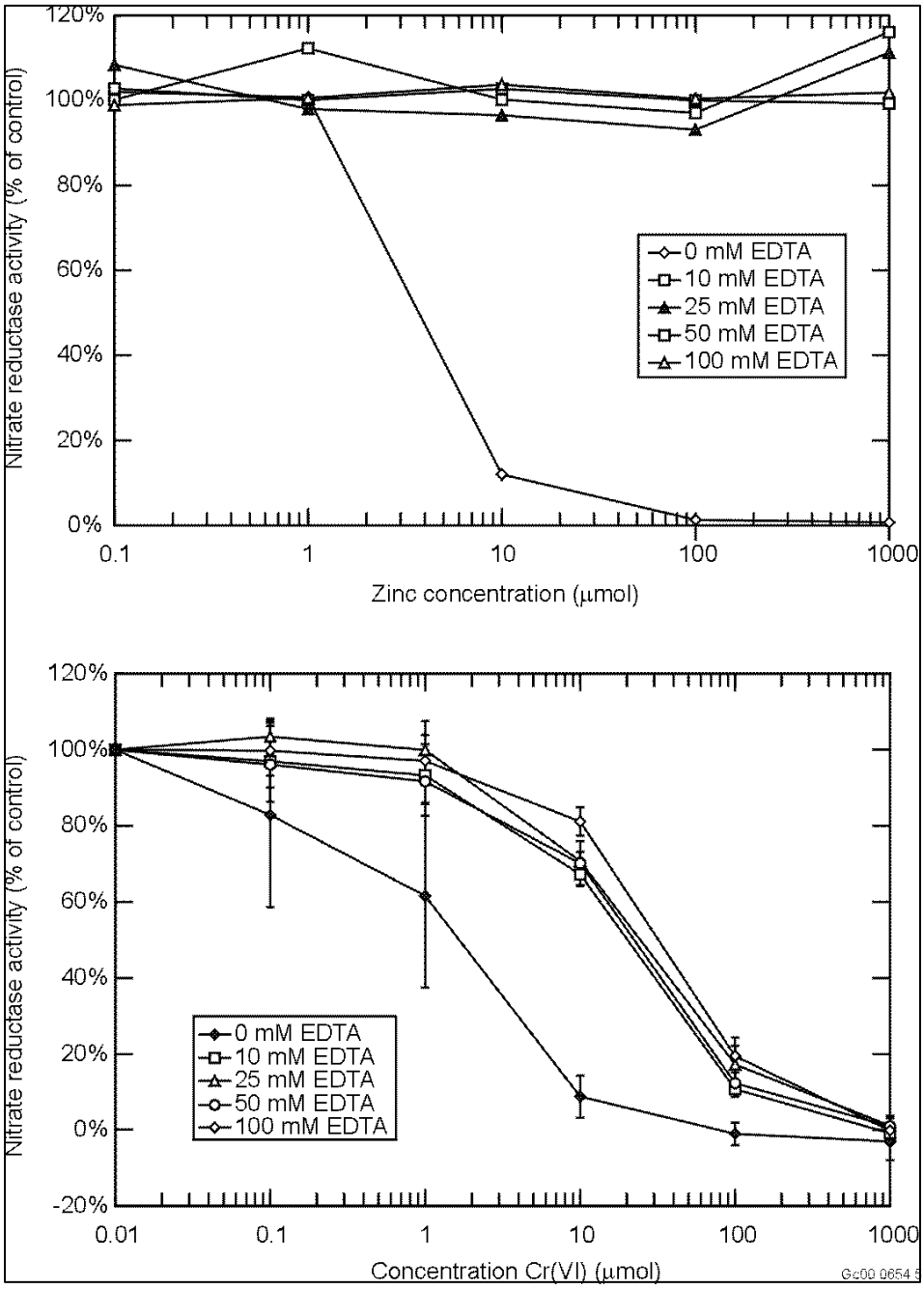

Figure 10. Metal inhibition of nitrate reductase in the presence of metal ion chelator, EDTA. (A) Zn; (B) Cr(VI).

Future work, not part of the ESRC task, will entail characterizing the nitrate reductase enzyme, developing a metal ion assay with the enzyme, and purifying a salt tolerant nitrate reductase from *Halomonas campisalis*.

ACCOMPLISHMENTS

During our FY 2000 research activities we:

- Discovered a thermophilic organism with catalase activity
- Identified that thermophilic organism through 16s RNA analysis as Thermus brockianus
- Developed a purification strategy for catalase
- Optimized ion exchange chromatography
- Initially developed a hydrophobic interaction chromatography step
- Achieved 60-fold purification of catalase through two purification steps
- Characterized the *Halomonas campisalis* strain, to be used for purifying nitrate reductase
- Assessed metal inhibition characteristics of nitrate reductase
- Developed a purification strategy for nitrate reductase through studying the literature
- Started optimization of ion exchange chromatography step for nitrate reductase.

During our FY 2001 research activities we:

- Optimized hydrophobic interaction chromatography step
- Developed and optimized a larger scale catalase purification procedure
- Optimized a gel filtration procedure
- Achieved a 200-fold purification of catalase
- Produced approximately 3 mg of essentially pure catalase.

REFERENCES

1. R. G. Riley, and J. M. Zachara , *DOE/ER-0547T,* 1992.
2. C. R. Evanko, and D. A. Dzombak, "Technology Evaluation Report TE-97-01," Pittsburgh, PA: GWRTAC, 1997.
3. M. A. Arnold, and M. E. Meyerhoff, "Recent advances in the development and applications of biosensing probes," *CRC Critical Reviews Anal. Chem.*, Vol. 20, No. 3, 1988, pp. 149–196.
4. M. W. W. Adams, and R. M. Kelly, "Enzymes from microorganisms in extreme environments," *Chemical & Eng. News*, Dec. 18, 1995.

5. T. K. Krawczyk, "Analytical applications of inhibition of enzymatic reactions," *Chem. Anal. (Warsaw)*, Vol. 43, 1998, pp. 135–157.

6. S. Fennouh, V. Casimiri, A. Geloso-Meyer, and C. Burstein, "Kinetic study of heavy metal salt effects on the activity of L-lactate dehydrogenase in solution or immobilized on an oxygen electrode," *Biosensors & Bioelectronics*, Vol. 13, 1998, pp. 903–909.

7. M. P. Popova, and C. H. S. Popov, "Effect of heavy metal salts on the activity of rat liver and kidney catalase and lysosomal hydrolases," *J. Vet. Med. A*, Vol. 45, 1998, pp. 343–351.

8. A. Aiken, B. Peyton, J. Peterson, and W. Apel, "Metal-induced inhibition of nitrate reductase," *Second Internat. Biometals. Symp, Tubingen, Germany, 2000*.

9. M. R. Mormile, M. F. Romine, M. T. Garcia, A. Ventosa, T. J. Bailey, and B. M. Peyton, "*Halomonas campisalis* sp. nov., a denitrifying, moderately haloalkaliphilic bacterium," *Sys. Appl. Microbiol.*, Vol. 22, 1999, pp. 551–558.

10. K. Yoshimatsu, Sakurai, and T. Fujiwara, *FEBS Letters*, Vol. 470, 2000, pp. 216–220.

Molecular Engineering and Genomics for Development of Environmental Biosensors using Robust Biocatalysts

Exploring the Genetic Potential of Microbes to Detect Hazardous Metals for Cleanup and Stewardship

Frank Roberto, Ph.D.

SUMMARY

Biologically based sensors (biosensors) offer the potential for improved, more cost effective detection, monitoring, and surveillance of hazardous metals and radionuclide contaminants in both the environment and large scale processes. However, we need more stable enzymes to use this science in harsh environments (radioactive, highly alkaline, high temperature, or nonaqueous environments). Consequently, we are studying the organisms that live in these "extreme" environments (extremophiles), rather than those that live in ambient conditions. High-throughput genomic sequencing was directed at microorganisms that will likely be useful in solving DOE environmental problems associated with alkaline radioactive wastes. By determining the complete DNA sequence of a halophilic (salt-loving) bacterium (*Halomonas campisalis*) bioinformatics permits the assessment of the metabolic potential, and thus, the biochemical functions of this organism that could be applied to DOE wastes. We can use the microorganism's genetic blueprint to identify strategies that can utilize specific functions of the bacterium and approaches for using the intact microbe in harsh environments. For example, tank wastes at a variety of DOE facilities contain not only radioactive materials, but also hazardous organics and heavy metals. Identifying genes for organic compound degradation (benzene, toluene, or xylene) could lead to a biodegradation process with *Halomonas campisalis* to treat tank contents to eliminate the mixed waste designation.

PROJECT DESCRIPTION

Our task objective was to support the development of biocatalysts capable of surviving the harsh physical conditions associated with many environmental processes. These catalysts will have the reaction specificity associated with "conventional" enzymes, but without the inherent instability and related inactivation problems often displayed by enzymes obtained from mesophilic (15–37°C, circumneutral environmental conditions) organisms. Genomic and molecular biology are crucial to the success of this overall effort, since the DNA sequence of an individual enzyme gene, or of a whole extremophilic microorganism, provide access to the genetic blueprint of the individual function, or overall metabolic capability. Recently acquired high-throughput sequencing capability in the INEEL Biotechnology Department has focused on addressing specific functions, and also on the genomic sequencing of a selected halophilic eubacterium, *Halomonas campisalis*.

Our technical approach used the following general strategy for genome sequencing:

1. Genomic DNA isolated from each candidate were physically sheared to generate fragments in the 2–10 kilobase (kb) range; these fragments were enriched by density gradient centrifugation or size fractionation on agarose gels.

2. Fragment size (2–3 kb and 6–10 kb) cuts were cloned into the vector pUC18 and the resulting libraries stored as glycerol stocks at 470°C.

3. Libraries were plated and individual colonies picked to deep-well microtiter plates for plasmid isolation and purification. Robotics were implemented to reduce labor costs associated with this task.

4. Plasmids were screened on 1% agarose gels as a quality check prior to sequencing using Applied Biosystem's BigDye terminator chemistry. We also automated sequencing reaction chemistry in FY 2001.

5. Sequences were determined on an Applied Biosystems Model 3700 DNA analyzer. After quality assessment and editing the resulting data was assembled into contiguous segments.

6. Gene analysis was initiated by BLAST analysis via the National Center for Biotechnology Information (NCBI) servers. In order to streamline this process, network upgrades were performed at the INEEL Research Center to provide 100 Mb/s bandwidth for data obtained in the laboratory. Workstation upgrades were made to improve throughput of raw sequence information through automated sequence editors and alignment algorithms. The INEEL Numerical Simulation Lab also provided technical support and accounts on Sun Enterprise servers to accelerate the bioinformatics activities of this project. The entire GenBank database, and BLAST web server software were installed on INEEL systems to permit more rapid analysis, as the NCBI servers are often unavailable due to the large number of worldwide queries. The bioinformatics infrastructure being established at the INEEL will be made available to collaborators to promote the capabilities of the Lab in microbial genomics and provide tools to enhance collaboration.

Halomonas campisalis

Halomonas campisalis is a member of the Family *Halomonadaceae* and is part of the gamma subdivision of the Proteobacteria.[1] Based on 16S rRNA sequence analysis, the organism was placed in this family because of a distinctive cytosine residue at Position 486, which is found in all members of the *Halomonadaceae*, including *Deleya*, *Volcaniella*, and *Chromohalobacter*.[2] *Halomonas campisalis* was isolated from Alkali Lake in Washington and characterized as a new species because of DNA to DNA hybridization experiments and phenotypic and phylogenetic studies with other members of the *Halomonas* genus.[3] Although it can tolerate a wide range of salt, pH and temperature, it grows optimally in 1.5 M NaCl, having a pH of 9.5 at 30ºC.[4] This organism is of interest to this project because of the similarities between its natural environment and the hostile environments found in DOE waste streams, such as the Hanford high-level waste tanks.

1.1.1.1 Library Construction and Sequencing. Isolation of genomic DNA was found to be efficient using conventional techniques. Purified DNA was sheared by sonication to produce fragments ranging in size from 1–4 kb, and cloned into plasmid vector pUC18. Resulting clones were purified using 96-well plasmid isolation kits (PerfectPrep-96Vac, Eppendorf, Boulder, CO). Purified plasmid DNA was quantified by UV absorbance measurement at 260 nm, or by comparison with known quantities of DNA after agarose gel electrophoresis. Sequencing reactions were performed using fluorescent dideoxynucleotide analogs (BigDye Terminator ver. 2.0, Applied Biosystems, Foster City, CA) and sequences determined on a Model 3700 DNA analyzer (Applied Biosystems, Foster City, CA). Over 1,000 sequences have been generated.

1.1.1.2 Bioinformatics. With the assistance of the Numerical Simulation Lab and Network Support, significant new capabilities in bioinformatics have been established at the INEEL. One of two

outdated Unix systems has been upgraded to a Sun Ultra 60, and a 1 Gb/sec ethernet switch was placed proximal to the sequencing lab. This permits substantially higher bandwidth communication via optical fiber with NSL servers which now host the BLAST software, the entire GenBank database, phred/phrap/consed quality and assembly software (Univ. of Washington), and Artemis, a web-based genome annotation package. We continue to refine the integration of these packages with a goal of automating much of the preliminary analyses, and ultimately having the ability to collaborate with other researchers in genome annotation via the Internet.

Results of BLAST analysis (showing only the highest similarities with sequences in Genbank) are shown in Table 1. Numerous hits with the Gram positive eubacterium *Bacillus halodurans* give us confidence that our sequences are yielding reasonable information. A surprise has been the number of similarities identified with *Deinococcus radiodurans*, the most highly radiotolerant bacterium known. At this time we do not know the relative radiotolerance of *Halomonas campisalis*, but the sequencing results suggest it could in fact be radio tolerant. DOE supported the sequencing of the genome of *D. radiodurans* several years ago,[5] with precisely the same justification we have used for *Halomonas campisalis:* that understanding the genome will assist us in understanding the basis for unique microbial physiologies, and in using these novel microbes to deal with DOE environmental problems.

Table 1. Halomonas campisalis BLAST search results.

Description	Length	Score	E Value
Putative aromatic efflux pump membrane protein *Sphingomonas aromaticivorans*	352	41	0.013
Phage-related protein *Bacillus halodurans*	334	39.5	0.029
Flagellar biosynthesis (flhS-related protein) *Bacillus halodurans*	381	35.6	0.44
Phosphate acetyltransferase *Deinococcus radiodurans*	319	70.2	3.00E-11
Phosphoenolpyruvate carboxylase *Deinococcus radiodurans*	320	67.5	2.00E-10
E coli probable copper-transporting ATPase	99	40.2	0.021
Cation transport ATPase E1-E2 family *Vibrio cholerae*	1073	156	2.00E-37
Cation transport ATPase *Synechococcus sp.*	823	72.2	4.00E-12
Copper-transporting ATPase *Bacillus halodurans*	1065	69.5	3.00E-11
Serine hydroxymethyltransferase (*Acinetobacter radioresistans*)	1036	64	1.00E-09
Organic solvent tolerance protein *OstA* precursor PA0595 (imported)	704	121	5.00E-37
Hypothetical protein – *Deinococcus radiodurans* (strain R1)	722	127	8.00E-37
Oligopeptide transport permease protein appb PAB1194— *Pyrococcus abyssi* (strain Orsay)	714	125	1.00E-36
Hydrolase-related protein – *Deinococcus radiodurans* (strain R1)	329	68.7	2.00E-11
Mercuric reductase – *Synechocystis sp.* (strain PCC 6803)	829	62.5	3.00E-09
Carboxynorspermidine decarboxylase (*Bacillus halodurans*)	426	60.9	2.00E-08
Molybdopterin oxidoreductase, iron-sulfur binding subunit (*Archaeoglobus fulgidus*)	448	54.7	1.00E-06
Conserved hypothetical protein H1434 – *Halobacterium sp*. (strain NRC-1) plasmid pNRC100	625	81.1	4.00E-15
Extracellular nuclease, putative (*Deinococcus radiodurans*)	437	115	8.00E-25

ACCOMPLISHMENTS

We upgraded the laboratory network and computational infrastructure for bioinformatics.

We generated and analyzed over 1,000 genomic sequences from *Halomonas campisalis.*

We trained six undergraduate (University of Idaho, Idaho State University, and Skidmore College) and High School (Skyline and Idaho Falls) students in state-of-the-art genomic sequencing techniques.

We supported sequencing activities through collaboration with researchers at Washington State University (*H. campisalis* genome), Montana State University (thermophilic viruses), and the University of Wales, Bangor (thermophilic bacteria).

REFERENCES

1. A. Balows, H. G. Truper, M. Dworkin, W. Harder, and K. Schleifer, -H. (ed.), *The Prokaryotes*, 2nd *ed.*, Volume IV, 1992, Springer-Verlag, New York.

2. E. Mellado, E. R. B. Moore, J. J. Nieto, and A. Ventosa, "Phylogenetic Inferences and Taxonomic Consequences of 16S Ribosomal DNA Sequence Comparison of *Chromohalobacter marismortui*, *Volcaniella eurihalina*, and *Deleya salina* and reclassification of *V. eurihalina* as *Halomonas eurihalina* Comb," *Int. J. System. Bacteriol*, Vol. 45, November 1995, pp. 712–716.

3. M. R. Mormile, M. F. Romine, M. T. Garcia, A. Ventosa, T. J. Bailey, and B. M. Peyton, *Halomonas campisalis* sp., a Denitrifying, Moderately Haloalkaliphilic Bacterium, *System, Appl. Microbiology*, 22, November 1999, pp. 551–558.

4. F. Ausubel, R. Brent, R. E. Kingston, D. D. Moore, J. G. Seidman, J. A. Smith, and K. Struhl (ed.), *Short Protocols in Microbiology*, 4th Edition, John Wiley and Sons, New York., 1999.

5. O. White, J. A. Eisen, J. F. Heidelberg, E. K. Hickey, D. Peterson , R. J. Dodson, D. H. Haft, M. L. Gwinn, W. C. Nelson, D. L. Richardson, K. S. Moffat, H. Qin, L. Jiang, W. Pamphile, M. Crosby, M. Shen, J. J. Vamathevan, P. Lam, L. McDonald, T. Utterback, C. Zalewski, K. S. Makarova, L. Aravind, M. J. Daly, C. M. Fraser, et al., "Genome Sequence of the Radioresistant Bacterium *Deinococcus radiodurans* R1," *Science 286* (5444), 1999, pp. 1571–1577.

Determining Soil Moisture Over Wide Areas for DOE Site Stewardship Hydrology

Wide-Area Moisture Sensing and Mapping

John (Jack) M. Slater, John M. Svoboda, and James Lee

SUMMARY

The goal of this research was to develop a new sensing technology for detecting subsurface moisture in soil over wide areas. Thus far, we have developed a platform for sensors that can be embedded in soil (or elsewhere) and that communicate by novel short-range telemetry. The technology will facilitate low-cost acquisition of data for hydrological studies and for long-term monitoring relating to environmental stewardship. The key characteristic of the technology is that the buried sensors are passive, that is, they have no internal power; they communicate with a reader via short range inductive magnetic coupling. The sensor will have a long lifetime and require no maintenance. Nearly all our efforts have gone into developing the platform rather than any specific sensor. Our initial demonstration was to sense moisture.

The passive telemetry architecture has general utility when sensing is required without physical connection between the probe and reader, and when the probe must operate over extended periods of time. This sensing technology can be used to sense chemical species within a sealed container, moisture below a moisture cap in a landfill, and chemical process parameters such as acidity, with a probe traveling in a process stream (which could be within a living organism).

The key component of the technology is a long-lived, passive probe that can be embedded in any nonconductive media at desired measurement points. The probe carries passive telemetry for communication with a data logger. Electrical power for the telemetry is derived from magnetic induction between the probe and a small inductive loop within the reader. The probe contains a sensor (moisture or other) that is also driven from this power. We estimate that the physical separation between the probe and reader is viable to at least two meters, using the approach described herein. If the probe carries a moisture sensor based on measuring the soil dielectric constant, the outer surface of the probe can be fully inert (e.g., plastic), so life expectancy is long. Accelerated aging tests for integrated circuits often predict failure rates that exceed 100 years, even for continuous operation at 55∀C ambient temperature.[1] Failure rates at low temperatures can be substantially lower.

We call this sensor platform architecture the passively telemetered probe (PTP), which contains the sensor (or sensors), the telemetry unit, and the remote reader. This architecture was designed with long-term monitoring of landfill caps in mind, but the concept is widely applicable.

Monitoring the performance of landfill barriers can determine when a barrier is operating within previously determined limits, or to calculate performance parameters such as water flux through the landfill cap. Little research has been conducted to establish viable strategies for long-term monitoring. Often, life cycle monitoring costs at closed waste sites are estimated to 30 years without consideration of additional monitoring. At present, a water moisture monitoring strategy might involve multiple embedded sensors, each wired to a data logger or telemetry unit. The wires present obstacles to heavy equipment at the time of cap construction and subsequent cap maintenance, and the use of wired sensors also implies cap penetrations. Any maintenance of sensors means additional penetrations. Our goal is to offer a penetration-free, maintenance-free monitoring system.

The general configuration as it relates to a landfill cap can be understood from Figure 1. The basic approach is that one or more probes, in this case probes containing moisture sensors and passive telemetry, are mounted at points of interest that will allow determining the integrity of the landfill cap.

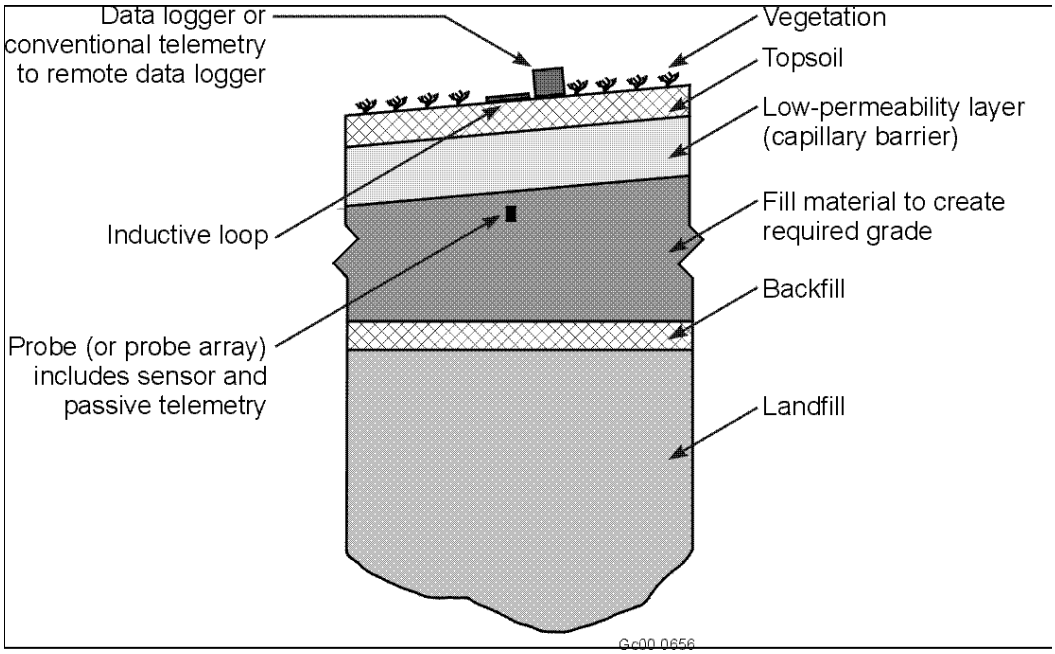

Figure 1. Cross section showing a landfill barrier.

Recognizing that the cap must retard the downward flow of moisture, e.g., by an actual barrier or by evapotranspiration from vegetation. At least one probe would be mounted below the cap's moisture barrier, while the inductive loop of the reader, which requires power, resides on top of the barrier. The moisture barrier within a landfill cap generally does not exceed two meters in depth, even for complex designs.[2] The data logger can be located at any convenient spot, and linked by conventional radio frequency telemetry to the reader. Use of multiple probes with a single reader is possible, allowing measurement of vertical moisture profiles and area monitoring. Moisture infiltration maps can be generated from such data.

This sensor architecture has several desirable attributes: (a) there are no wires to impede barrier construction activity; (b) there is no penetration of the barrier; (c) the probe can be robust and small, and thereby useful as an insertion-mounted retrofit to existing caps; (d) data acquisition can be remote and automated, as long as it is consistent with the approximate two meter limitation between probe and reader; (e) the probe is low-cost and deployable in large numbers; (f) multiple sensors can be incorporated into a single probe; and (g) multiple probes can be interrogated by a single reader.

The overall status of the research is that we have performed an end-to-end system demonstration of the PTP using an existing time domain reflectometry (TDR) moisture sensor. All work was at the breadboard level and over only a short range between the probe and reader, about 60 cm. We expect that that range will be increased substantially as the system is optimized. The anticipated range after development is about two meters. Our work constitutes proof-of-principle demonstration.

TASK DESCRIPTION

The telemetry concept is for low frequency magnetic fields, approximately 125 kHz, to carry both energy and information. Low frequency has acceptable penetration in moist soil. Key parameters relating to penetration depth are the soil electrical conductivity and the frequency of the penetrating field. The magnetic field is attenuated roughly at the same rate an electromagnetic field would be, the latter being governed by the well know skin depth equation. Conductivities in arid soils have been measured at the INEEL[3] with typical maximum (saturated soil) direct current values of order 0.1 siemen/meter. Using this value, we expect that attenuation is not important if we stay with low frequencies and distances of about two meters or less. For reference, the electromagnetic skin depth at 100 kHz and the above conductivity value is 5 m. Von Hippel[4] has measured conductivity values at 100 kHz, but for lower moisture levels, which is consistent with this 5-m estimate.

The system is designed around a microcontroller produced by Microchip Technology.[b] It is essentially a single-chip computer programmable in a C-like language. It contains onboard nonvolatile memory, multiple analogue-to-digital (A/D) channels, and digital communication ports. The microcontroller can handle all the logic needed for power management, operation of a sensor, and communication with the reader.

For the reader to acquire a reading from the probe, the following basic sequence occurs. The reader sends out energy in the form of a pulsating magnetic field, which is captured and stored in a capacitor within the probe. The captured energy then powers the microcontroller, which instructs the sensor to perform a measurement, which value (e.g., moisture content) is then digitized. At that point, the microcontroller powers the probe transmitter and also controls frequency-shift keying to impress the digital reading on the transmitted waveform, with subsequent decoding by the reader. A variation would be that the reader supplies instructions to the probe, as well as energy. For example, the probe might be instructed to report the value of a particular onboard sensor or to adjust the operating range of a sensor.

Figure 2 shows a simplified block diagram of the probe. The antenna, actually a resonant circuit, is used both for capturing energy from the reader and transmitting data back to the reader. As energy builds in the storage capacitor, the microcontroller begins to operate and polls the energy detector circuit to determine if the capacitor is fully charged, in which case about 5 volts are available. When that condition is achieved, the RF detection circuit is polled to determine if the reader (not shown) is still transmitting the energizing pulse. If not, the reader has stopped to listen. If so, the microcontroller interrogates the sensor, which requires applying power to it and digitizing its analog output.

At this point, the measurement result is stored in the microcontroller's memory. Power is then applied to the transmitter, which in turn drives the antenna. Frequency-shift keying is accomplished by switching a small capacitance in and out of the resonant circuit of the antenna; the switching is controlled by the communications port on the microcontroller.

The receiving process is straightforward. An FM receiver is tuned such that its passband is centered on one of the frequency components of the modulated wave. This produces analogue output from the receiver, which is level-shifted to become a proper RS-232 signal. That signal is captured by the serial port of a computer, which serves as the data logger.

---

b. Programmable Interface Controller PIC16F876-04/SP produced by Microchip Technology, Inc. A low-power version of this chip is available (but not used in this program), PIC16LF876-04/SP. The differences are indicated in Table 1.

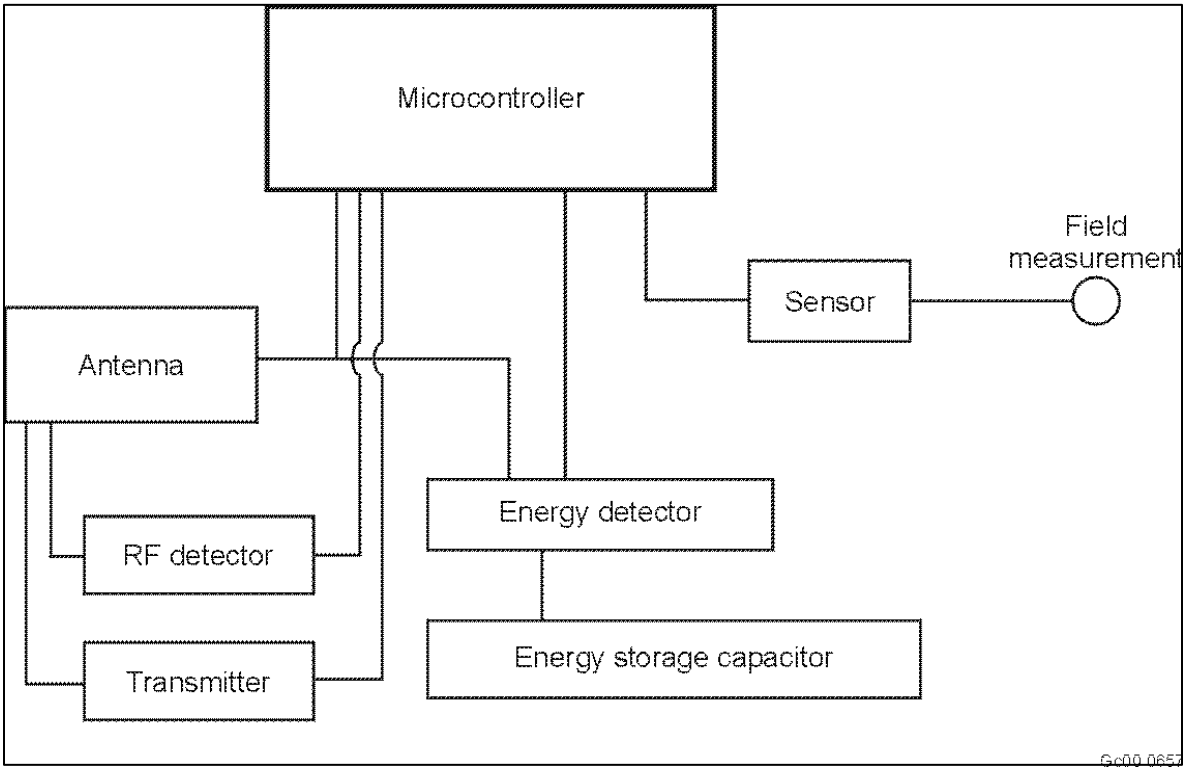

Figure 2. Simplified block diagram of the probe.

One of the most important elements of the whole system is the method of power management within the probe, since the probe must operate on the low power available from the induced currents. Table 1 presents the basic power management information. The charge rate refers to current delivered to the probe's energy storage capacitor. The given value corresponds to use of a charging loop at 60-cm separation used in our early testing. We used a different B-field driver for all later tests. The early driver was able to operate the microcontroller at maximum distances of 60 cm, but we did not document its charge rate. Improving this separation distance is a follow-on task. We anticipate achieving a 2 m or better separation, but have not yet made a defensible calculation of the expected maximum range.

The microcontroller has a low power *sleep* mode that is used during the charging period. During sleep, the chip periodically awakens at predetermined intervals to execute the instructions outlined above. The maximum separation of the probe from the reader is determined by the point at which the charging current is less than the sleep current. The values in the table were satisfactory for our proof-of-principle demonstration. However, as indicated in the table, a low-power version of the chip is available that substantially lessens the current draw in sleep mode and would lead to larger physical separation of the probe from the reader.

The important current usage comes from the bottom three entries of Table 1, which give the total charge used by the probe following charging. Their combined charge use is 0.53 millicoulombs, which can be conveniently supplied from a 400-microfarad capacitor. If charged at a 50-microamp rate, the charge time is 40 seconds. Note also that the charge usage for the TDR moisture sensor accounts for only about 3% of the total charge usage, even though its instantaneous current draw is comparatively high.

Table 1. Power Management Parameters. All current draw values are at approximately 5 volts.

Parameter	Current Draw (μamp)	Time (ms)	Condition
Charge rate	50	N/A	Example value attained in early tests at 60-cm separation from B-field driver. See text.
Microcontroller in sleep mode	20 1*	N/A	Charge rate must exceed this value for a viable system.
Microcontroller active, less all peripherals	50 20*	N/A	With microcontroller program running at 32 MHz clock speed.
Microcontroller active, with peripherals but no sensor or transmitter	440	550	Peripherals active: RF detect, voltage measurement on storage capacitor, reference voltage generated for A/D converter, sensor enable circuit, transmitter enable circuit.
Moisture Sensor	2,250	8	Time for sensor to generate analog output is 5 ms, additional time required for digitizing.
Microcontroller in transmit mode	840	320	Transmitting at 125 kHz with frequency shift keying. Signal received at a 2-m separation.

* Values indicate the manufacturer's specification for the low current version of this microcontroller, 5 which was not us.

Figure 3 shows the vertical breadboard (4 x 6 in.) attached to a horizontal interface board, with a TDR moisture probe in front, connected by a long flexible wire. In practice, the electronics and sensor could be collocated. The microcontroller chip is in the socket (the large dark rectangular shape) in the lower left corner of the breadboard. The horizontal dumbbell-shaped object on the top of the breadboard is the magnetic field induction loop on a ferrite core, used for both receiving and transmitting. This particular loop was adapted from a transponder manufactured by TIRIS.[c] The TIRIS hardware we worked with has the capability to relay a preprogrammed identification number from a *tag* to a reader by means of passive telemetry. Our work extends and generalizes that concept. Near the left hand of the circuit board, between the antenna and microcontroller, is the energy storage capacitor. Its value was 1,000 microfarads for these tests.

We were able to make all functions of the prototype work simultaneously and self-consistently. This included energy transfer from a loop energizer to the probe (at 60-cm distance) and full function of the probe under control of the microprocessor. All necessary actions were present: acquisition of analog data (moisture) and digitization, transmission of the data back to a receiver (at 120-cm distance, with separate loops for transmitting and receiving), and capture of that data on a data logger. Moisture sensing was quantitative only, as the emphasis has been on the probe system.

c. The TIRIS subsidiary of Texas Instruments is found at www.ti.com/tiris.

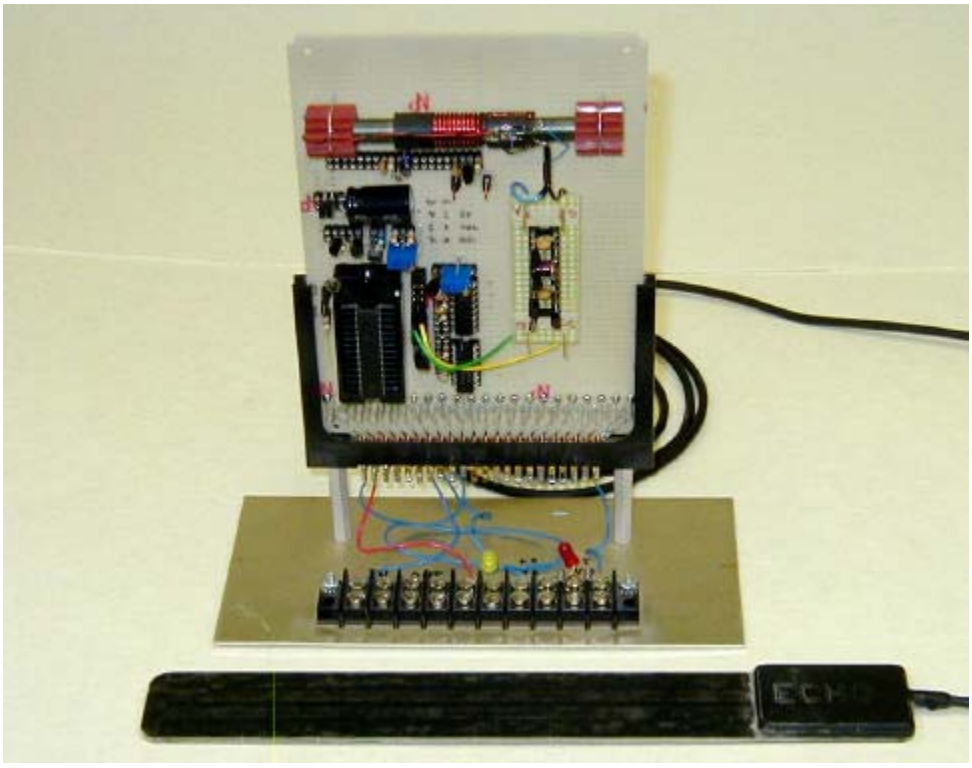

Figure 3. Photograph of the breadboard probe.

Figure 4 shows a real-time data stream plotted by a data logger, generated as follows. A hand-controlled potentiometer has been substituted for the moisture sensor and is a stand-in for a generic analog sensor. The resistance value is varied, and the scope trace so indicates. The inductive input power to the probe has been replaced with a constant 5-volt supply so that the system can trigger repeatedly (our B-field generator has not yet been set up for a pulsed mode that allows for repeated probe transmissions), and the receiver is 120 cm from the probe. The receiving and decoding of the frequency-shift-keyed signal from the probe is fully functional, as described above. The scope trace shows a real-time plot of the digital data being entered into the data logger as the potentiometer is varied by hand, simulating a varying parameter.

We still have work to complete in several areas to prepare a fieldable system. Electrical engineering refinements are required to improve the distance from reader to probe. First, the B-field driver can be improved both in the level of electrical current and the diameter of the coil. Neither of these parameters has been driven to any reasonable engineering limit. Second, a low current version of the microprocessor is available that draws substantially less current. This is especially important during the sleep period, since that current draw determines the maximum separation between probe and reader. As indicated in Table 1, an improvement factor of 20 is possible by using the low power version chip. Third, the circuit can be improved in terms of the current draw from the ancillary functions, such as reference voltages and RF detect. These circuit elements need to be powered only at specific times; the present arrangement has them powered at other times as well. We have not produced an engineering estimate of the maximum separation distance, but we anticipate distances of about two meters based on experience with the commercial devices used to communicate identification numbers. Packaging and hardening are also required for a field unit. Ideally, the system would be hardened to the level at which it can be inserted in earthen landfill caps by a simple penetrator rod, and left in place.

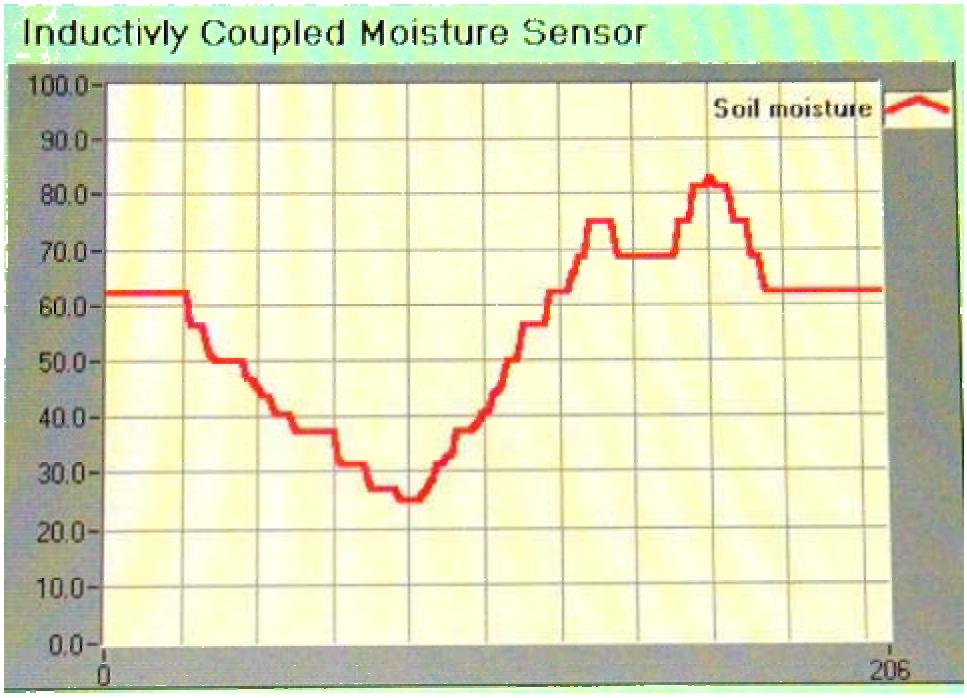

Figure 4. Illustration of a real-time data stream plotted by a data logger.

ACCOMPLISHMENTS

This research offers a proof-of-principle demonstration of the PTP concept as a sensor platform. Although the prototype is still being developed, all necessary functions have been generated in a self-consistent parameter set: energy capture and storage by the probe, use of a microcontroller for power management, acquisition of data, and communication to a receiver and database. The digital nature of the system allows numerous possibilities. These include use of multiple probes with one reader reading simultaneously, use of multiple sensors on one probe, instructions delivered to the probe, and data validation within the probe. The concept also has substantial application beyond landfill caps.

Further development of the PTP concept will proceed via a CFRD (Corporate Financed Research and Development) project to develop and test a field deployable moisture sensor module. The work will be performed in collaboration with researchers at Hanford and Nevada Test Site. Both locations have instrumented caps that will permit the PTP concept to be directly compared to current moisture measurement technologies.

REFERENCES

1. Microchip Technology, Inc. “Product Reliability Technical Publication DS11008K,” 1998.

2. G. W. Lee and A. L. Ward, “Still in Quest of the Prefect Cap,” conference proceedings of “Landfill Capping in the Semi-Arid West: Problems, Perspectives, and Solutions,” edited by T. D. Reynolds and R. C. Morris for the Environmental Science and Research Foundation, ESRF-019, Idaho Falls, ID, 1997.

3. W. M. Roggenthen and D. K. Parrish, *South Dakota School of Mines, "Factors Affecting Ground Probing Radar at the Radioactive Waste Management Complex Idaho National Engineering Laboratory*, prepared for EG&G Idaho, Contract No. C92-17099 (1994).

4. A. R. Von Hippel, editor, "Dielectric Materials and Applications," *The Technology Press of MIT*, John Wiley and Sons, New York.

Using Environmental Records in Midlatitude Glacier Ice to Better Define EM Contaminant Inputs to the Subsurface

Travis L. McLing

SUMMARY

The Department of Energy's Office of Environmental Management (DOE-EM) is charged with establishing radionuclide inputs to the environment from facilities within the DOE complex. In some instances, disposal of radionuclide-bearing waste has resulted in large diffuse groundwater contamination plumes. Responsible stewardship of the INEEL requires that scientist understand the fate and transport issues dealing with such plumes within the Snake River Plain (SRP) aquifer. Chlorine-36, a constituent in one such plume located at the Idaho Nuclear Technology and Engineering Center (INTEC) on the INEEL, has potential as an ideal tracer to define the extent of contamination spread from the point source. To use chlorine-36 as a tracer, all of its potential sources—weapons test, in situ production, disposal, and natural background—must be fully characterized. Long-term background and weapons test inputs are the most difficult parameters to define, because precipitation records are not available for the last 50 to 60 years. However, the isotopic record locked up in glacial ice provides a region-specific record of the weapons-tests inputs as well as background values for cosmogenic isotopes prior to the weapons test of the 1950s and 60s. Therefore, midlatitude glacial ice needs to be collected and analyzed to determine long-term background and weapons test input baselines. The research funded in this work package on midlatitude glaciers will significantly enhance our understanding of Pu, ^{14}C, ^{3}H and chlorine-36 inputs to the environment, and help delineate multiple sources worldwide, which will also allow us to better characterize contributions from DOE-EM operations.

This research has permitted the quantification of preanthropogenic background concentrations of several radioactive constituents such as chlorine-36, which is the primary focus of this study. Chlorine-36 is being used to better define aquifer characteristics such as flow velocity, dispersivity, and attenuation for use in flow and transport models at contaminated sites within the DOE complex. Chlorine-36 concentrations in midlatitude glacier ice cores has allowed us to further define the preweapons test and weapons test (non-INEEL source) inputs to the hydrosphere for this radionuclide. Increased precision in calibrating groundwater modeling in the SRP aquifer will also result in unprecedented resolution for flow and transport models at DOE sites.

PROJECT DESCRIPTION

Groundwater modeling is a key component of characterization and remediation activities throughout the DOE complex. However, models must be validated (compared against measurements) and calibrated (fit to measurements by refining input parameter values) to be valid and useful. Because we are using cosmogenic isotopes, multiple background sources must be subtracted from concentrations in the aquifer. This requires that nonsource inputs such as natural background be identified and subtracted at any given point in the aquifer. Subtracting background is especially difficult at the leading edge of a plume where source to background ratio is very low and modeling results are most critical. Currently these background numbers suffer from a high degree of error associated with the lack of accurate atmospheric inputs. Our previous research (Upper Freemont; Cecil et al. 1999) interrogated the only source of cosmogenic isotope data for the 1950s to 60s in North America. To support the data collected in 1998 we are studying several midlatitude glacial sites in central Asia. This new information will be used to test the new model for groundwater flow and transport in and near the INEEL.

We were particularly interested in chlorine-36 because it:

- is found in a contaminant plume originating from INTEC
- has a high electron affinity, which occurs in virtually all natural systems as an anion, resulting minimal chemical interaction
- is extremely hydrophilic, making it an especially good hydrologic tracer
- has a long half-life (3 Δ 105-y) eliminating decay concerns
- AMS detects it at extremely low levels.

There are difficulties with using chlorine-36 as a tracer. The following information is needed to fully utilize this methodology:

- the global preanthropogenic background must be well characterized
- atmospheric weapons test input (1950–1960s) must be well characterized
- regional transport/deposition properties for the Eastern SRP (ESRP) need to be better characterized
- inputs from sources other than the INTEC deep injection well must be characterized, and the resulting background concentration in the aquifer must be accurately determined
- Input concentration for injected water at INTEC needs to be known.

The isotope is produced naturally by neutron activation of ^{35}Cl in the upper atmosphere. The largest historical input of chlorine-36 to the hydrosphere is from atomic weapons testing in the 1950s and 60s. This record of events is now preserved in glacier ice. Because of midlatitude atmospheric global circulation patterns, it is highly desirable to obtain ice-core isotopic data from glaciers that are located at midlatitudes. There are a limited number of glaciers at these temperate latitudes that are at a high enough elevation to not experience melt water percolation which will "smear" the isotopic record through deeper ice-core layers making the concentration measurement meaningless. The Upper Fremont Glacier (UFG) in Wyoming and the Inilchek Glacier in Asia meet this specific criteria.

Chlorine-36 concentrations have been measured in an ice core from the UFG in the Wind River Range of Wyoming, 260 km east of the INEEL. Providing the only available data for determining regional chlorine-36 background input. The validity of using UFG data to represent the chlorine-36 background at the INEEL needs to be confirmed by data collected from another site. It is expected that data collected will support the data collected from midlatitude glaciers throughout the world and will provide an applicable data set for other midlatitude aquifers including the ESRP aquifer.

A small portion of the ESRC funding supported the completion of a snow survey that was conducted at the UFG to determine the fraction of chlorine-36 lost to ablation and melt-water. Having a knowledge of this "loss" is critical in determining the true atmospheric input of chlorine-36 to the ESRP. The final portion of these research dollars were used to remove all traces of our research from the UFG.

ACCOMPLISHMENTS

We visited three midlatitude sites: the UFG in Wyoming, the Inilchek Glacier in Kyrghyzstan, and the Yulong Glacier in southern People's Republic of China (PRC). The expedition to the PRC was at the invitation of the Chinese Academy of Sciences and the Lanzhou Glacial Institute to perform joint glacial studies with the U.S. Geological Survey (USGS) and Dr. Vladimir B. Aizen at the University of California Santa Barbara.

During the expedition to the Inilchek Glacier two deep ice cores were drilled to total depths of 162 m and 167 m, a 100 m of core was collected for radioisotope analysis, and snowpit samples spanning the entire elevation range of the glacier, as well as fresh snowfall events were collected. Analysis of ice collected is in process. In addition, a GPS survey of a network of stakes positioned on the glacier was conducted at the beginning and ending of the expedition to determine surface velocity of the glacier and to aid in modeling glacier flow. Temperature measurements of the first borehole showed that the temperature of the glacier was 411.3∀C at 160 m below the surface, indicating that the glacier is frozen to bedrock. A radio-echo sounding survey was completed with over 150 locations measured across the surface of the glacier. A borehole gamma spectrometer was used to log radioactivity in the upper 30 m of the first borehole. An automated weather station collected meteorological data during the 2-month expedition.

We made a reconnaissance trip to the Alti Mountains located in southern Siberia and revisited the UFG in Wyoming. The purpose of the reconnaissance expedition to the Alti Mountains was to establish another midlatitude glacial study site, which turned out to be a great success with researchers from Japan, Russia, and the U.S. taking part. Several shallow ice cores where collected and shipped intact to the U.S. During the expedition to the UFG in Wyoming we removed the meteorological and depth-sensor stations and collected more than 50 water and snow samples for future analysis by the USGS. The trip to the UFG concluded the INEEL's involvement with the ice-core investigations.

REFERENCES

None

Subsurface Understanding

This area of research deals with the subsurface environment. The characterization and control of this complex domain is vital to successful environmental management. The research here encompasses a broad range of activities involving the sciences of biology, chemistry, physics, hydrology, and geology. Furthermore, the physical scale of measurement is vast, extending from microns to kilometers. Our overall success in meeting our EM goals will depend in large part on our ability to understand and control contaminates within the earth's surface.

The following tasks are reported in this section:

- Complex Systems Theory Applied to Subsurface Transport
- Unified Hydrogeophysical Parameter Estimation Approach to Subsurface Contaminant Transport—Subsurface Imaging Collaboration with the Center for Subsurface Sensing and Imaging Systems
- Long-Term Biogeochemical Destruction and Control of Aquifer Contaminants Using Single-Well Push-Pull Tests
- Ecological Engineering of Rhizosphere Systems
- Investigation of Factors Influencing Cesium Mobility and Uptake In Plant/Soil Systems
- Innovative Approaches to Characterize Vadose Zone Hydraulic Properties.
- Geological, Geophysical, and Hydrological Environs of the INEEL Site
- Advanced Geophysical Characterization to Enhance Earth Science Capabilities at the INEEL to support Remediation and Stewardship.

Complex Systems Theory Applied to Subsurface Transport

Exploring the Complexity of How Contaminants Move Through the Ground

Thomas Wood, Daphne Stoner, Charles Tolle, Randall LaViolette, John James (INEEL); John Crepeau (ISU); Boris Faybishenko (LBNL); David Peak (USU)

SUMMARY

The capability to predict the transport of radionuclides, chlorinated hydrocarbons, and other pollutants in the subsurface has become one of the most important challenges facing DOE. Computer modeling of the vadose zone and contaminant monitoring strategies are paramount to long-term remedial actions required to meet DOE stewardship commitments and understand contaminant fate and transport for more immediate EM remediation activities. Many computer simulations rely on simplified flow and transport models. Unfortunately, the existing subsurface computer models are inaccurate because they do not adequately factor in the dynamics of complex systems. Examples can be cited wherein vadose zone fate and transport models require updating and recalibration (even within months of completion). This constant revising occurs despite the fact that the models purport to determine risk hundreds to thousands of years in the future.

Research into vadose zone flow and transport reveals that the vadose zone is a complex environment. Accurate computer models that incorporate the complex interactions of geological, hydrological, chemical, and biological parameters will not only reflect that complexity, but make significant improvements in transport predictions. Incorporating nonequilibrium transport processes into numerical predictions and monitoring strategies will improve models required to meet long-term DOE stewardship commitments. Our long-term goal is to develop new algorithms for predicting flow and transport based on chaos theory or on a solution from complex systems theory (cellular automata, artificial neural networks, etc.). By doing so, we will advance the understanding of fundamental multiscale processes.

Our research consisted of five major subtasks: (1) We analyzed monitoring data by comparing several vadose zone transport models, which suggest that a common emergent property for vadose zone transport may be that small volumes of relatively high concentrations (compared to center-of-mass calculations) of contaminants travel faster routes. (2) We conducted a series of small scale (1-meter) ponded infiltration tests over a fractured basalt ledge in the Hell's Half Acre lava field during 1998 and 1999. Results showed highly variable flow rates, unrelated to the water head in the infiltration pond. We evaluated the data set for the existence of chaos, but could not determine if the system was chaotic due to problems associated with an integrate-and-fire data set. (3) We evaluated a numerical tool for screening time-series data sets for nonlinear behavior. The results are promising for application to environmental problems. (4) We developed an approach for building a theoretical model of the Hell's Half Acre experiment that will capture the dynamical behavior of the system without the inherent problems of short, noisy data sets. (5) We performed the first two steps for determining whether the governing equations of vadose zone flow and transport, which relate in nonlinear fashion, will act to generate chaotic dynamics. Although work continues on this task under the ESRA program, we believe the final results will improve how conceptual models are created for vadose zone transport by demonstrating that deterministic models overlook critical aspects of dynamic behavior.

TASK DESCRIPTION

We can make predictive models more reliable by developing conceptual models that incorporate the complex interactions of geological, hydrological, chemical, and biological parameters arising from their nonlinear and nonadditive interactions. Incorporating nonequilibrium transport processes into monitoring strategies will improve the data interpretation and system performance required to meet long-term DOE stewardship commitments. Many existing deterministic [d] and stochastic [e] subsurface models appear unreliable because they do not include the dynamics of complex systems.[f] To make significant improvements in contaminant transport predictions, the onset and occurrence of chaotic [g] and or complex behavior must be incorporated into the models. The detection of a few low-concentration contaminants in groundwater outside of the predicted limits can likely be explained or accounted for by incorporating complex systems theory into predictive transport codes.

Developing scientifically sound, coupled experimental, theoretical, and mathematical arguments to describe the impacts of complex system behavior on contaminant fate and transport movement will help DOE alleviate stakeholder concern over the apparent mismatch of occasional detection of contaminants outside zones predicted with traditional center-of-mass transport models. The project supports several major initiatives for understanding and predicting contaminant fate and transport in complex subsurface environments, and for applying this understanding to long-term stewardship of DOE legacy waste.[1,2]

We identified two major objectives for this research:

1. Explore application of innovative approaches that are not limited to idealized and simplified situations but that reflects real-world complexity.

2. Demonstrate a proof of concept that alternative approaches may be more appropriate than traditional methods of data analysis for vadose zone transport. This will be demonstrated by testing the validity of a complex systems theories approach, in this case deterministic chaos, on an INEEL data set.

To address these two objectives, we established five major subtasks; one observational, two numerical, and two theoretical. These multidisciplinary subtasks are briefly summarized below.

Looking for Complexity in Real Vadose Zones

Our objective for this subtask was to compare predicted values for contaminant transport in vadose zone with contaminant levels determined by field monitoring activities so we could qualitatively assess whether emergent patterns generally exist in vadose zone transport. We considered DOE waste disposal sites at the INEEL, Hanford Reservation, Yucca Mountain, and Nevada Test Site. Transport through the vadose zone to the ground water at these sites has been shown not to follow predictive models. Our

---

d. Determinism is the philosophical belief that every event or action is the inevitable result of preceding events and actions. Thus, in principle at least, every event or action can be completely predicted in advance, or in retrospect if the starting points are exactly known.

e. Relating to, or governed by, probability. The behavior of a probabilistic system cannot be predicted exactly, but the probability of certain behaviors is known.

f. A complex system is a collection of many simple nonlinear units that operate in parallel and interact locally with each other so as to produce emergent behavior.

g. Chaos implies the ability to predict, at least for a few time steps, the system behavior based on previous system responses.

cursory review suggests that widespread problems indeed exist between volume-averaged predictive models and real vadose zone transport. Several observations are common:

- Reviewing publicly available information via publications and DOE web sites, we generated Figure 1, which in summary compares predicted and subsequently measured values. Our intent was not to discredit or compromise any modeling effort but to compare idealized predictions with actual data in order to look for common patterns. Our first observation was that none of the four predictions we considered accounted for all future contaminant concentrations. That is, it is common for a few concentration measurements to exist outside the envelope of the predictive model. Furthermore, these differences between predicted versus actual concentration can be much higher than the predicted first-arrival concentration.

- In the cases considered, predicted travel times were longer than actual values for at least a small percentage of monitoring points. Measured contaminant arrival was generally faster by a factor of about 500 than first arrival by volume-averaged predictive models.

This limited study suggests that an emergent property for vadose zone transport may be that small volumes of relatively high concentrations (compared to center-of-mass calculations) of contaminants find faster routes through vadose zones. Work continues on this subtask.

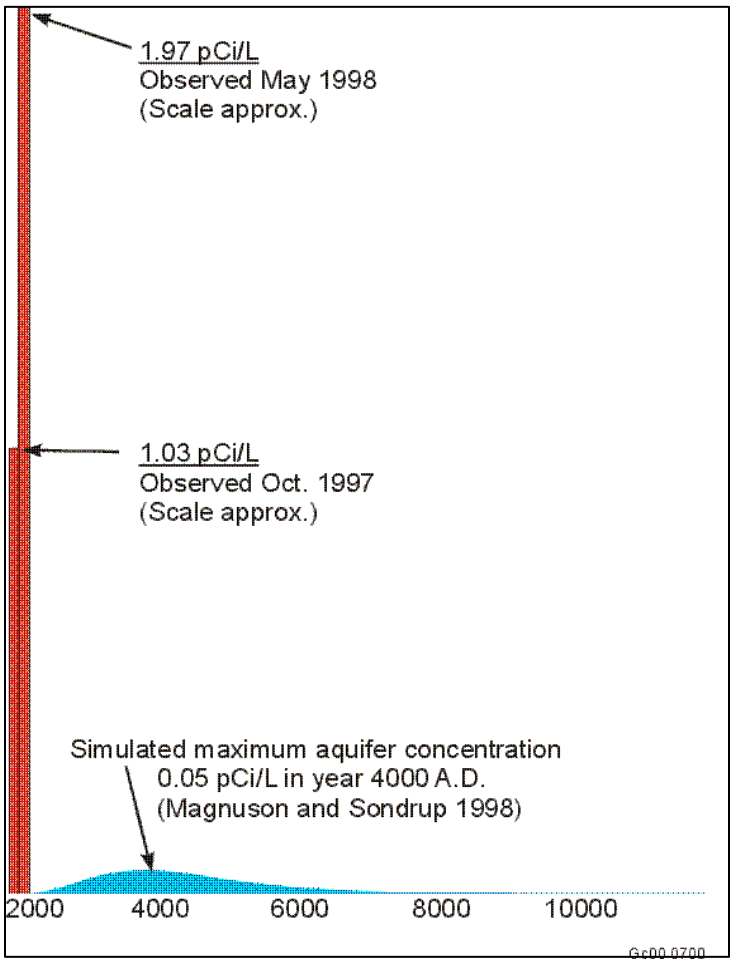

Figure 1. Comparison of actual to modeled aquifer concentrations of Am-241 for the Radioactive Waste Management Complex.

Chaotic Analysis of the Hell's Half Acre Data Set

Our objective for this numerical analysis was to apply traditional chaotic procedures to achieve a better understanding of the underlining dynamics of flow through a fractured basalt vadose zone. This subtask was designed to reconstruct the phase-space attractor dynamics of the system based on observed droplet events. Many of these techniques are rooted in Taken's Embedding Theorem, which main techniques include: mutual information, false nearest neighbors, forward and reverse Lyapunov exponents, and phase-space reconstruction (see Figure 2).

One of the difficulties encountered during this study was the size of the Hell's Half Acre time-series data set. While a large number of data points were collected, only small subsets (less than 5,000 sequential points) exhibited nonuniform dripping behavior. We used a clean, long, noise-free data set from an aluminum weld process to test the selected chaos techniques before assessing the Hell's Half Acre data set.

After validating the general analysis procedure, we evaluated the Hell's Half Acre data set. The measured dynamics (drip intervals) of the Hell's Half Acre data were integrate-and-fire dynamics instead of direct state measurements as in our original test system. Basically, integrate-and-fire means that instead of measuring a state variable directly, such as pressure or flow, the Hell's Half Acre data set was a measure of the culmination of these state variables in the form of a drip. Taken's Embedding Theorem does not directly apply to an integrate-and-fire data set. We began a detailed study of what type and amount of integrate-and-fire dynamics are needed to reproduce a Taken's style, embedded-phase space under Sauer's new integrate-and-fire embedding theorem.[3] In order to address this and further validate the desired test procedure, we returned to our welding test system, which also exhibited integrate-and-fire

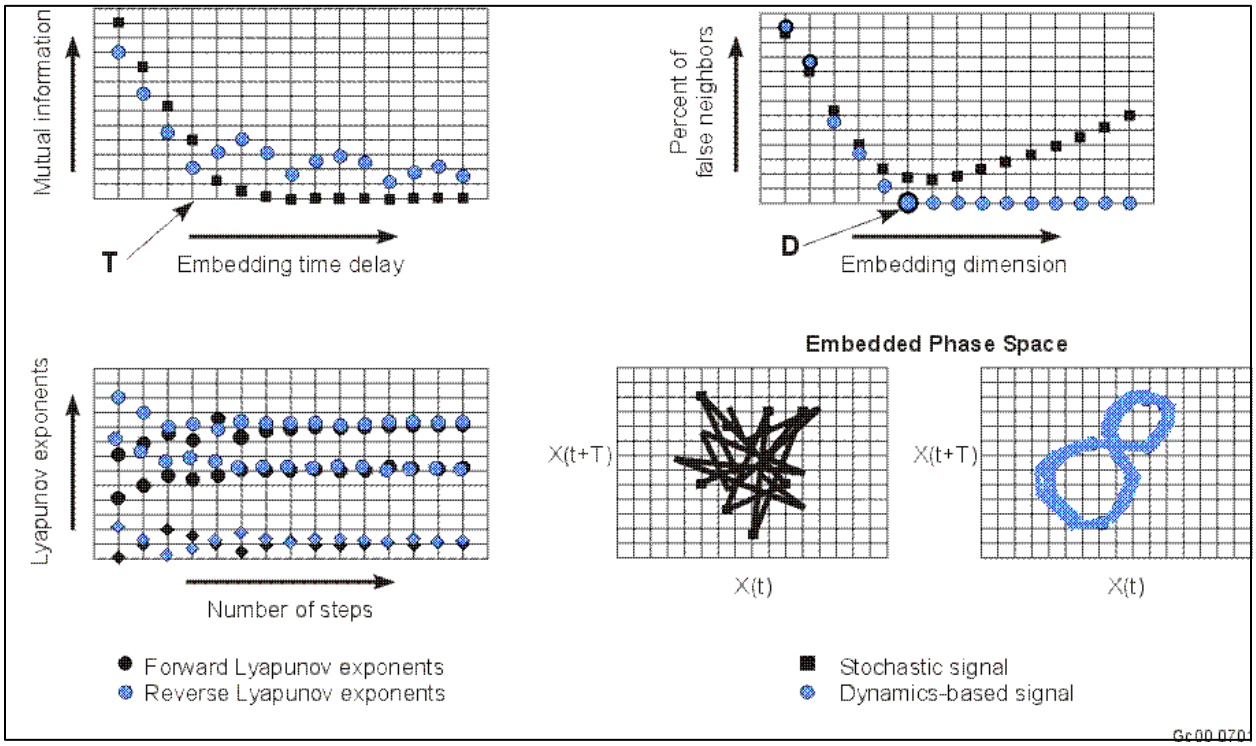

Figure 2. Example of chaotic tools used for inferring dynamics within sampled signals.

dynamics. Weld measurement data were in the form of droplet detachment events, just as the data in the Hell's Half Acre data set. For the traditional Lorenz and Rossler Systems, there is a basic requirement of at least 50,000 and 5,000 samples, respectively, for accurate estimates of the embedding dimension (see Figure 3). However, as with the Hell's Half Acre data set, our current welding data set did not contain enough useable integrate-and-fire dynamics to result in conclusive answers about the system.

We have been able to reconstruct the attractor dynamics based on the integrate-and-fire measurements for the Rossler and Lorenz systems. This was a test case to verify the process for the drip data reconstruction effort. To date, it appears that we do not have enough data to proceed with attractor reconstruction with the drip data. Traditional chaotic analysis of environmental data is problematic because of the extreme length of data sets required and the need to measure state variables directly.

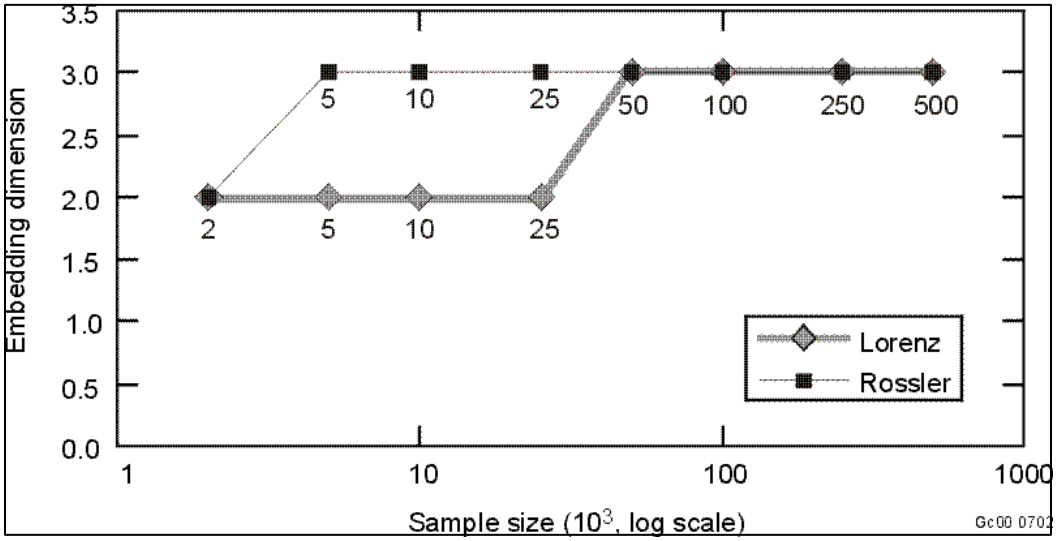

Figure 3. Plot showing the size of data sets required to estimate the correct embedding dimension for the Lorenz and Rossler chaotic systems in thousands of samples; 50,000 and 5,000 samples are required respectively.

A Numerical Technique to Screen Time Series Data for Nonlinear Behavior

Our objective for this subtask was to develop and implement methods that could quickly screen time series data for signs of significant nonlinear behavior. With such methods, large data sets could quickly be screened for nonlinear behavior and these parts of the data sets more carefully analyzed, as in the first subtask. Our approach was to compare empirical time series with surrogates generated under various hypotheses. The idea was to choose hypotheses that correspond to trivial or linear dynamics, so that the failure of the original data to agree with the surrogate is taken as an indication of nontrivial and, possibly, complex behavior. In order to define what "agree with" means, one needs to consider a statistic capable of discriminating between complex and trivial dynamics. A robust statistic employed to study time series for complexity is approximate entropy (ApEn), developed by Steve Pincus. ApEn can be viewed as the average of the log of the conditional probability that a particular pattern exhibited in a time series persists given that it occurred before. Therefore, ApEn is at a maximum when all patterns are available; ApEn is minimal when only one pattern is found. Therefore, ApEn is a measure of disorder in a series of symbols.

We tested the idea of ApEn as a discriminating statistic in a variety of contexts. We generated surrogate data according to the hypothesis that the dynamics are linear. Therefore, we generated surrogate data subject to the condition that they yield the same spectrum (and autocorrelation function) as the original data. Our tests included random systems, periodic systems, the logistic map, the Henon map, the Rossler system, the Lorenz system, and the Mackey-Glass system. The results show that the failure of the linear-dynamics hypothesis under ApEn is sufficient but not necessary to identify nonlinear dynamics. The linear dynamics surrogate data method requires that the original data be evenly spaced in time; this is not the case for many data of interest. For this reason, among many others, it is important to investigate the performance of ApEn and other statistics, as we are now doing, with alternative hypotheses under which surrogate data may be generated.

Evaluation of Theoretical Low-Dimensional Dynamics

Our objective for this subtask was to develop a theoretical model that would not harbor environmental noise nor be limited by short data sets. Preliminary analysis of the Hell's Half Acre droplet interval data suggests the possible existence of a low-dimensional attractor. It is likely, however, that the existing data set contains sufficient sources of ambiguity or noise that no conclusive outcomes will be achieved. Irrespective of what the analyses show, it is important to consider the possibility that vadose zone flow is a low-dimensional process. A theoretical model for the Hell's Half Acre experiment may show low-dimensional dynamics in autonomous form (no external driving), but may be an example of self-organized criticality in the presence of external perturbations. The latter is especially interesting in terms of the long range goals of subsurface science at the INEEL, because self-organized criticality behavior is scalable, which means that a series of laboratory experiments done on different mesoscales may allow correct inferences to be drawn about macroscale behavior. To begin, consider a system of substantial fame in the nonlinear dynamics literature—the dripping faucet. It has been known for many years that a slowly dripping faucet can exhibit complicated dynamics, purportedly ranging from simple periodic behavior to perhaps even low-dimensional chaos.[4] Of course, the claim for low-dimensionality in real (as opposed to simulated) data is obscured by ever-present instrumental uncertainties and environmental variability. The claim is also confounded by the fact that a flowing fluid is thought to be aptly modeled by the Navier-Stokes equations (a set of partial differential equations). Systems of partial differential equations typically produce infinite- (not low-) dimensional dynamics, though there are circumstances under which such systems can become episodically low-dimensional. How this reduction occurs in the dripping faucet is not yet clear.[5,6] Nonetheless, we will assume that in a clean, well controlled experiment the fluid dynamics of drop formation is low-dimensional, and that drop formation can somehow be adequately described by a small set of ordinary differential equations.

It is extremely unlikely that a single dripping faucet model will adequately capture the essence of the Hell's Half Acre data set. The Hell's Half Acre experiment was performed in complex soil, consisting of fractured and porous rock and loosely bound grains. The flow paths through this test bed vary in cross section and roughness. The flow is undoubtedly multiphasic with complicated wetting characteristics, and possibly evaporation.[7] Furthermore, the dripping into the cavity below the test bed occurs at multiple sites, not at a single orifice.

We put forth a model developed to approximate the spatial variability of the experimental conditions at Hell's Half Acre. The model is a modification of one that has been employed to study imbibition fronts of fluid climbing up vertical filter sheets.[8,9] In this model, the medium is represented by a square lattice of pipes oriented at 45 degrees, as shown in the Figure 4. The nodes in the lattice are at the intersection of four pipes (except at the surfaces, where they are at the intersection of two pipes) and are assumed to contain no volume. The network scheme can be combined with the dripping faucet model to obtain a better approximation to the Hell's Half Acre dripping experiment than provided by the latter alone. In this figure, each of the output nodes is a faucet, and each drips according to the scenario for a

single faucet. The driving parameter for each node is the total mass flow into that node from the two pipes connecting to it. Some nodes will have very low flow rates, while others will have larger rates. Drop detachment will be asynchronous over the entire set of output nodes. Depending on the network configuration and imposed pressure difference between the top of the test bed and the cavity, all output nodes may be dripping periodically, some periodically and some chaotically, or all chaotically. Such a system will have very rich dynamics indeed. The network model described here can be modified so that flow changes in one pipe affect flow in neighboring pipes. It would be very interesting to see if such a model has self-organized criticality characteristics. If it does, and if such a network aptly models the Hell's Half Acre experiment, then the impetus for constructing several mesoscale experiments that investigate forecasting and control would become much more compelling.

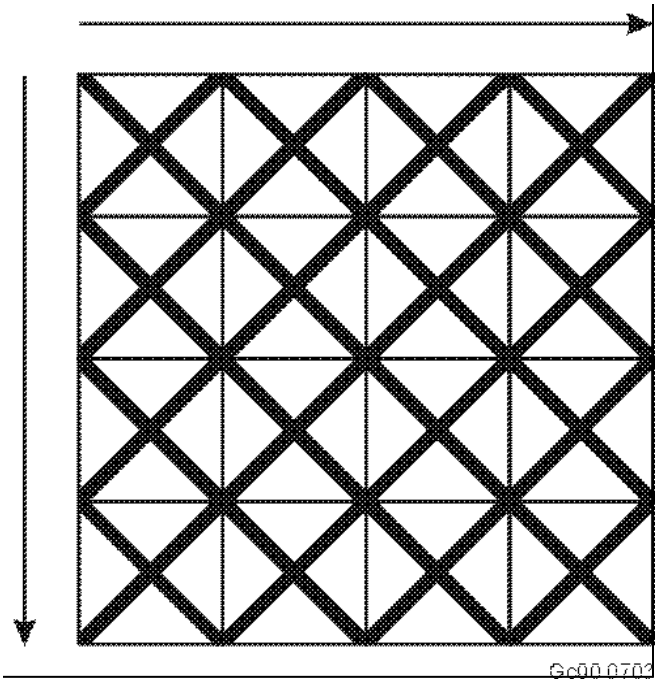

Figure 4. A square lattice of pipes oriented at 45 degrees.

A Theoretical Evaluation from First Principles for Complex Behavior

The purpose of this subtask was to determine whether the governing equations of vadose zone flow and transport, which are related in nonlinear fashion, will act to generate chaotic dynamics. This analysis was similar to the analysis performed by Lorenz on governing equations of convection cells in the atmosphere. We first performed a literature survey in scientific journals to identify previous work on employing methods of nonlinear dynamical systems theory to model flow in porous media. We found several articles where nonlinear dynamics had been applied to the results of experimental data, but none were found that attempted a first-principle analysis as we propose. This gave us encouragement to proceed to identify rational methods of reducing the governing nonlinear equations of flow in porous media. Key to performing a nonlinear analysis is to reduce large dimensional governing equations into a set of low-order ordinary differential equations. We investigated three techniques: the center manifold reduction, parabolized stability technique, and proper orthogonal decomposition. The center manifold method seems to be the most robust. The ultimate goal of this line of research is to generate noise-free data sets using surrogate values.

ACCOMPLISHMENTS

We observed that several examples of vadose zones across the DOE complex show characteristics of complex, nonlinear systems.

We used weld data to verify applicability of the chaos analysis toolbox to the characterization of vadose zone. Because of the limited number of data available for Hell's Half Acre, a rigorous evaluation of this data set for chaotic properties is not possible with the analysis tools we are validating.

The majority of time delay traces in the Hell's Half Acre data set exhibit evidence of periodic or discrete behavior, as indicated by a formal mathematical evaluation.

Several governing equations for flow in porous media could be transformed for flow in fractured media such as that observed at Hell's Half Acre.

On January 18, 2001, Mr. John James, a 2000 summer intern displayed a poster he had created in the first annual "Posters On the Hill," exhibit—a celebration of undergraduate research in the Utah State Capitol. The purpose of this event was to show the legislature the opportunities for hands-on research available to students at a research university.

REFERENCES

1. DOE, *From Cleanup to Stewardship, A Companion Report to Accelerating Cleanup: Paths to Closure and Background Information to Support the Scoping Process Required for the 1998 PEIS Settlement Study*, 1998.

2. U.S. Department of Energy, Environment Management Science Program, Board on Radioactive Waste Management Water Science, and National Research Council Technology Board, *Research Needs in Subsurface Science*, ISBN 0-0309-06646-8, 2000.

3. Timothy Sauer, "Reconstruction of Integrate-and-Fire Dynamics," George Mason University, Department of Mathematical Sciences, *http://math.gmu.edu/~tsauer/pre/index.html,* 2000.

4. R. S. Shaw, "The Dripping Faucet as a Model Chaotic System," *Santa Cruz: Ariel*, 1984.

5. S. D. R. Wilson, *Journal of Fluid Mechanics*, Vol. 190, 2000, p. 561.

6. N. Fuchikami, S. Ishioka, and K. Kiyono, *Journal of the Physical Society of Japan*, Vol. 68, No. 4, April 1999, pp. 1185–1196.

7. D. Or and T. A. Ghezzehei, *Water Resources Research*, Vol. 36, 2000, p. 381.

8. E. Aker and K. J. Måløy, *Physical Review E*, Vol. 58, 1998, p. 2217.

9. C. H. Lam and V. K. Horvath, *Physical Review Letters*, Vol. 85, 2000, p. 1238.

Unified Hydrogeophysical Parameter Estimation Approach to Subsurface Contaminant Transport—Subsurface Imaging Collaboration with the Center for Subsurface Sensing and Imaging Systems

Integrating Cross-Discipline Data to Image the Subsurface

Earl D. Mattson (INEEL); Eric Miller and Mohammed Khames (CenSSIS)

SUMMARY

A major barrier to incorporating geophysical characterization techniques to subsurface contaminant transport predictions is nonintegration of multiple disciplines. Too often, geophysical, hydrological, forward transport model, and geochemical data are collected and analyzed independently of one another, resulting in disjointed data interpretation and analysis. Our research suggests a unified approach to integrate geophysical tomography with hydrological state variable data to better describe flow and transport parameters in the subsurface. This research will focus on using quantitative optimization tools to integrate geophysical and hydrological data for imaging the subsurface. Results of these research efforts is leading to better understanding of the functional inter-relatedness between specific geophysical and hydrogeophysical parameters, and ultimately contribute to more accurate subsurface modeling.

This project has developed alternative geophysical inversion techniques as well as examined functional relationships between geophysical electrical resistivity signals and hydrogeophysical parameters. The results described in this report was a collaborative effort between the INEEL Geoscience Research Department and the National Science Foundation's (NSF's) Center for SubSurface Imaging Systems (CenSSIS) at Northeastern University. CenSSIS is a new NSF center, with expertise in quantitative optimization tools to invert geophysical signal data to geophysical parameters. The advantage of using subsurface geophysical signals to characterize the vadose zone is the ability to provide spatial measures between boreholes. The INEEL has expertise with vadose zone measurement techniques and field and laboratory experimental design. These soil physical measurement techniques allow continuous measurement of contaminant transport variables but lack the advantage of spatially continuous measurements. Combining the strengths of CenSSIS's geophysical inversion techniques and the INEEL's soil physics measurement expertise has integrated multidisciplines to better constrain the inverse method.

To begin the integration of geophysics with hydrological predictions, a number of tasks were accomplished in this research project. First, the ability to obtain high quality geophysical data is necessary. This project led the purchasing of electrical resistivity tomography (ERT) data collection equipment. Secondly, a new three-dimensional (3-D) level set inversion approach was developed through INEEL's collaboration with CenSSIS. Verification of the level set inversion approach was examined through inverting ERT data sets from an INEEL laboratory experiment. Results of this verification indicated that the level set approach was able to identify the basic boundary structure between a binomial system. Inversion results from the more typically used Occam's inversion was also able to identify the target but suffered from blurry distinction of the target boundary and inaccurate quantification of the electrical conductivity distribution. Real subsurface field testing of the inversion technique will be accomplished in FY 2002 through the ESRA program. Subsequently, this methodology will be incorporated into numerical models of contaminant transport through the vadose zone.

TASK DESCRIPTION

Mineral exploration has incorporated surface direct current (dc) resistivity methods since the 1880s in the search for mineral deposits. More recently, electrical methods have been adapted to obtain physical properties of groundwater and vadose zone materials. These properties include porosity, water saturation, temperature, pore water ionic concentration, and the presence of clay minerals.

Beginning in the 1980s, dc resistivity surveys were modified by placing electrodes into boreholes rather than solely on the surface. Collecting data through this multidimensional electrode layout and by analyzing the data with inversion algorithms, researchers could obtain detailed maps of the resistivity distribution between a set of boreholes. This innovation is called electrical resistance tomography (ERT). ERT was successfully used in several studies to monitor soil saturation,[1] temperature during infiltration experiments at air injection,[2] and thermal remediation sites.[3]

ERT data are collected by transmitting a constant current through a pair of electrodes while measuring the resultant voltage potentials between all possible receiving-electrode pairs. A second pair of electrodes is then selected to transmit the electrical current while measuring the voltage potential field. This process is repeated until every possible pair of electrodes is being used as transmitters and receivers (see Figure 1).

Typically, a tomographic or inverse scattering type of imaging approach is used to convert ERT data into a 3-D volumetric rendering of the subsurface, space-varying electrical resistance. However, this image formation problem is highly ill posed. Sensor noise and other unmodeled effects can cause the resulting renderings to possess nonphysical artifacts, making them practically useless.[4] A common method used in an effort to overcome this difficulty is to examine temporal differences of the electrical

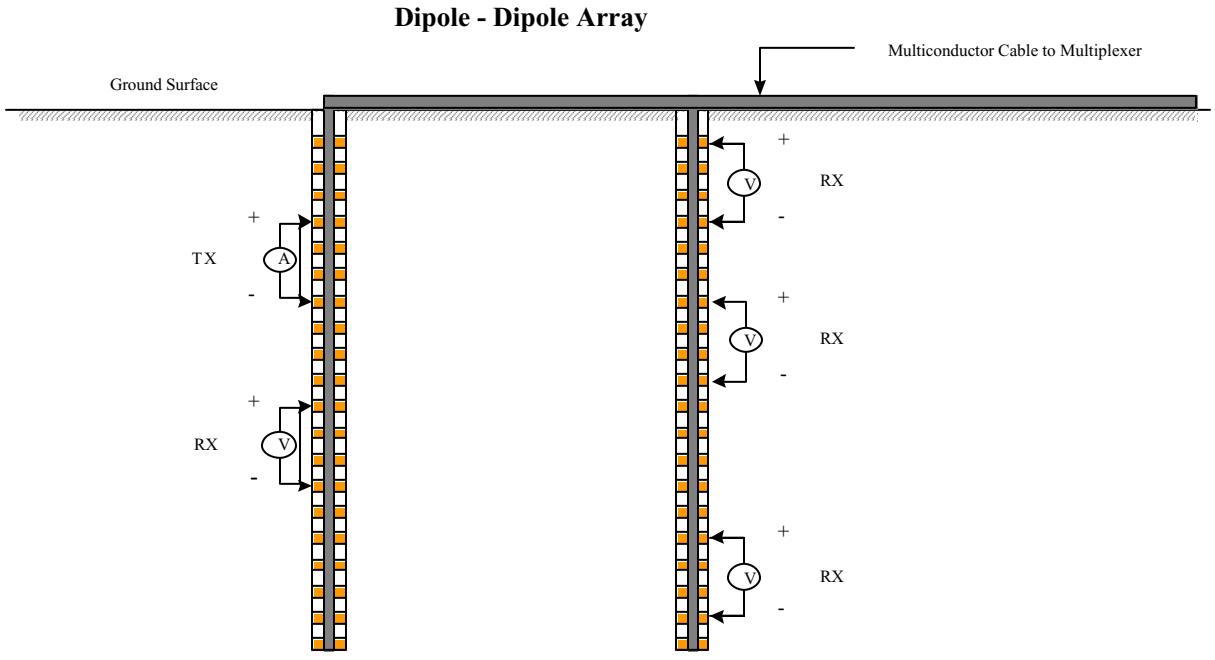

Figure 1. Hypothetical example of electrical resistivity tomography data acquisition between two boreholes in the subsurface.

tomographic images in an effort to detect anthropogenic electrical conductivity changes. Although this method should detect any changes in the tomographic image, the change cannot be quantitatively described. A method for overcoming such difficulties is to incorporate constraints into the processing scheme to quantify the real electrical conductivity. The method we propose draws on CenSSIS's previous work in this area (e.g., level set and other geometric imaging methods), in addition to incorporating constraints through the point measurements described above.

Our general approach is to explore using level set methods for anomaly characterization coupled with low-order models for describing the background structure. Level sets have proved very useful in the image processing community as a tool for automatically and robustly locating objects of unknown geometry in a scene. Moreover, there have been some very promising theoretical results in the past few years on the use and application of level-set methods for tomographic inverse problems like ERT, but at radar frequencies. One drawback of a level-set approach is that it typically requires rather detailed knowledge of the background in which the object is embedded. Moreover, it is typically assumed that the objects of interest have the same contrast against the background and that this contrast is known. Finally, level sets are most often implemented in two-dimensional (2-D) problems.

Theory of Level Sets

An ERT system functions by injecting dc electrical currents into the medium and measuring the resulting voltages at some specific locations. The distribution of the electrical potential depends on the injected currents and the conductivity distribution within the medium. This physical interaction can be described by the potential equation:

$$\subseteq\omega\ \left(\subseteq\Upsilon\Sigma\left(\begin{array}{c}\circledR\in\\ \circledS\\ \circledcirc\\ \text{TM}\end{array}\right.\in x\ \omega\frac{\in}{\in x}\ 2\ \frac{\in}{\in y}\omega\frac{\in}{\in y}\ 2\ \frac{\in}{\in z}\omega\frac{\in}{\in z}\left.\begin{array}{c}\urcorner\\ \\ \\ \urcorner\end{array}\right|\quad v\mid\ i \tag{1}$$

where ω, ν and i represent, respectively, the spatial distributions of the conductivity, electrical potential and electrical current sources and sinks in the medium.

Let $G(\omega)$ $\left(\begin{array}{c}\circledR\in\\ \circledS\\ \circledcirc\\ \text{TM}\end{array}\right.\in x\ \omega\frac{\in}{\in x}\ 2\ \frac{\in}{\in y}\omega\frac{\in}{\in y}\ 2\ \frac{\in}{\in z}\omega\frac{\in}{\in z}\left.\begin{array}{c}\urcorner\\ \\ \\ \urcorner\end{array}\right|$ then (1) can be written as:

$$G(\omega)\nu\mid\ i \tag{2}$$

Given different realizations of the distribution of current sources, $i_k, k = 1, 2,\ldots, M$, and corresponding observations of the electrical potential for each current source $\nu_{k,i}$ $i = 1, 2,\ldots P$, our aim is to reconstruct ω. The data $\nu_{k,i}$ may be mathematically represented as follows:

$$\nu_{k,i}\mid\ \left|dr\iota(r-r_i)\nu_k(r)\right. \tag{3}$$

where $\nu_k(r) = G^{-1}(\omega(r))i_k(r)$ is the solution to (1) for the k-th input current source, r_i is the location of the I-th sensor, and ι (r) is the 3-D Dirac delta function. Note that (3) implicitly represents a nonlinear mapping of the conductivity, ω, to the data, $\nu_{k;i}$. We denote by F(ω) the forward model, which takes ω into the length $M \Delta P$ vector of data comprised of all the $\nu_{k;i}$. It will also be convenient in the following to consider inverting, not for conductivity but rather its reciprocal, resistivity which is given as $\psi = 1/\omega$. With a slight abuse of notation, F(ψ) will represent the forward model mapping resistivity into data.

A key component of any inversion routine is the numerical method used to solve the forward problem, $G(\omega)v_k = i_k$, for $v_k(r)$. Indeed this solver affects both the efficiency and accuracy of the 3-D inversion algorithm. In this project, we use the network model described in Reference 5. The medium is discretized and seen as a lumped network with R_x, R_y, and R_z representing the network impedance in the x, y, and z directions, respectively. These vector quantities are functions of ˆ(x; y; z) and the grid spacing for each block. Using R_x, R_y, and R_z, a sparse matrix G can be constructed such that a discrete form of $G(\omega)v_k = i_k$ can be obtained as:

$$Gv_k \mid i_k \tag{4}$$

To determine v_k, Equation (4) is solved using the conjugate gradient method. The model is relatively faster and more reliable when compared to other forward modeling techniques (see Reference 5).

In geophysical applications, the inverse problem is nonunique due to insufficient observation data and the misfit of the forward model to the field data. As a result, the problem was approached from different perspectives. In Reference 6 the observed data is inverted with a regularization scheme, whereas in References 5 and 7 the inversion process is a fitting to the observation data under the constraint of prior information. The last approach is more reliable as it incorporates prior data. However, in some cases, such geophysical data is not available.

In our approach, we assume that the resistivity distribution of the subsurface is piecewise continuous. In such a case, knowing the resistivity values reduces the problem to shape identification of the different regions in the medium. Using level sets, the regions interfaces can be reliably tracked. However, such a technique has been applied for binary media only. Staring from an "evolution approach" of level sets,[8] we introduce an extension that can handle n-ary media with no increase in complexity. The idea consists in associating multiple evolving contours with the same level sets function.

Given M different distributions of the current sources i_k, $k = 1, 2,\ldots, M$, let v_k and $F_k(\psi)$ be, respectively, the corresponding observation vector and forward model data. We define the total mean square misfit error as:

$$C(\psi) \mid \frac{1}{2}\sum_{k=1}^{M} \| F_k(\psi) - v_k \|_2^2 \tag{5}$$

Since the problem is nonunique, it is difficult to minimize $\mathbf{C}(\psi)$ directly in terms of ψ. Instead, we assume that the medium is binary, with D being the shape of the inner region, then the problem can be formulated as:

$$\min_{D} \quad C(\psi) \tag{6}$$

$$where: \quad \psi(x,y,z) = \begin{cases} \psi_{int} & for\ (x,y,z) \in D \\ \psi_{ext} & otherwise \end{cases}$$

The resistivity values ψ_{int} and ψ_{ext} correspond to the inner region and the background, respectively. This formulation is not implementable because of the lack of a mathematical description for D. Note that the goal here is to reconstruct the full shape of the different regions, with constant resistivity, instead of making a pixel by pixel inversion.

Using level sets, a more convenient formulation becomes possible. Specifically, we define an auxiliary function λ (*x; y; z; t*) such that the boundary of *D*, denoted ∈*D* is implicitly defined by way of:

$$\in D: \quad \gamma(x, y, z, t) = \lambda(x, y, z) = 0 \in \tag{7}$$

then the zero level of λ at any time, *t*, completely identifies the interface of the region *D* with the background. The goal of a level set approach to inversion is to "evolve" over time in such as way that as *t* ⇓ ←, the zero level set of λ corresponds to the true boundary of *D*. With this as motivation, the inversion problem is:

$$\min_{\lambda} \quad C(\psi) \tag{8}$$

$$where: \quad \psi(x, y, z) = \begin{cases} \psi_{\text{int}} & \gamma(x, y, z) = \lambda = 0 \in \\ \psi_{ext} & \gamma(x, y, z) = \lambda = 0 \in \end{cases}$$

In Reference 8, an "evolution approach" to solve for λ, in the case of a 2-D deconvolution, is derived. Following the same derivations, the solution for the 3-D ERT inversion comes out to be the initial value problem:

$$\lambda(x, y, z, 0) = \lambda_0(x, y, z) \tag{9}$$

$$\lambda(x, y, z, t + \iota t) = \lambda(x, y, z, t) - \left(J(\psi)^T (F(\psi) - v) \right) \nabla \lambda \, \iota t \tag{10}$$

where J(ψ) is the Jacobian of F(ψ) with respect to ψ and ι t is the time step. In the case of multiple observations, the algorithm should be repeatedly iterated over $v_k, k = 1, 2, \ldots, m$. In order to force C(ψ) to be nonincreasing, i.e.:

$$\frac{\in}{\in t} C(\psi) \Omega 0,$$ the constraint $\psi_{int} > \psi_{ext}$ needs to be satisfied.

The main computational issue with Equation (10) is associated with the matrix J(ψ). This problem is addressed in References 5 and 6 where the adjoint method is proposed. The idea consists in computing the vector quantity $J(\psi)^T(F(\psi) - v)$. In Reference 5, the observed data is normalized by the current source's amplitudes so that the last vector quantity can be computed without increasing the number of forward problems per inversion iteration. The procedure is implemented in a code for 3-D ERT inversion using conjugate gradient method. We used this code and made the appropriate modifications required for the level sets approach.

In the rest of this section, we derive and simulate the ERT inversion for *n*-ary media. Consider a medium with *n* different regions D_i, $i = 1, 2, \ldots, n$. Define ∈*Di* and ψ*i*, respectively, as the outer contour and the resistivity of D_i. Assume that $\in D_i$ is inside $\in D_{i+1}$, for $i = 1, 2, \ldots, n-1$. This assumption makes the structure conforming with level sets, where contours are noncrossing and exocentric. Our mathematical modeling of the interfaces consists in associating each one with a level value, i.e., contour, in the level sets function λ:

$$\in D_i(t) = \gamma r : \lambda(r, t) = c_i \in \tag{11}$$

such that $c_1 < c_2 < \ldots < c_n - 1$. Such modeling is based on the fact that the evolution of the contours in λ is driven by the velocity function only; the latter is specified pointwise. Moreover, the usual choice of the zero level to track the interface of interest is quite arbitrary. Furthermore, the variations of the equations $\lambda(r; t) = c_i$ for $1 \Omega i < n$ provide the same result as for $\lambda(r; t) = 0$:

$$\iota \lambda 2 \subseteq \lambda \; \{ \iota r | \; 0 \tag{12}$$

Given the interface surfaces separating the different regions, we are interested in the partial change in the resistivity distribution due to small variations in ιD_i's. In Reference 8 this vector quantity, for a binary medium, was shown to be:

$$\iota \psi | \; / \psi_{\text{int}} \; 4 \; \psi_{ext} 0 \frac{\subseteq \lambda / p 0}{| \subseteq \lambda / p 0 |} \{ p | p \subset \in D \tag{13}$$

where p = (*x, y, z*) is any point of $\# D$. In our case, and because there are $n - 1$ different ιD_i's, $\iota \psi$ becomes:

$$\iota \psi | \sum_{i | 1}^{n 4 1} \psi_i \; 4 \; \psi_{i 2 1} 0 \frac{\subseteq \lambda / p_i 0}{| \subseteq \lambda / p_i 0 |} \{ p_i |_{p_i \subset \in D_i} \tag{14}$$

Assuming that contours move only in their normal direction, we can write

$$\iota r | \; \zeta / r, t 0 \frac{\subseteq \lambda}{| \subseteq \lambda |} \tag{15}$$

where $\zeta(p_i; t)$ represents the velocity function at the point p_i. Substituting (14) in (13), we get:

$$\iota \psi | \sum_{i | 1}^{n 4 1} \psi_i \; 4 \; \psi_{i 2 1} 0 \zeta / p_i, t 0_{p_i \subset \in D_i} \tag{16}$$

Knowing $\in \psi$, the change in the cost function $\mathbf{C}(\psi)$, as a result of the same variations in $\in D_i$'s, is defined as:

$$\iota C / \psi 0 \; \{ \; J / \psi 0^T / F / \psi 0 4 v 0 \in \psi \} \tag{17}$$

That is:

$$\iota C / \psi 0 \sum_{i | 1}^{n 4 1} \Psi \int_{\in D_i / t 0} \Psi / \psi 0^T / F / \psi 0 4 v 0 \beta \{ \psi_i \; 4 \; \psi_{i 2 1} 0 \zeta / \psi_i, t 0 \iota s / \psi_i \beta \tag{18}$$

In order to achieve convergence, the update in λ should result in decreasing the misfit error, that is $\iota \mathbf{C}(\psi) < 0$. Assuming that $\psi_i > \psi_{i+1}$ for any $i < n$, a sufficient condition would be:

$$\zeta / r, t 0 |_{r \subset \in e_i / t 0} | \; 4 \; J / \psi 0^T / F / \psi 0 4 v 0 \tag{19}$$

Extending the last equality for all **r**, we get a trivial choice for ζ (**r**; *t*). Using Equations (12), (15), and (19) we get the innovation in λ at each iteration:

$$\iota\lambda \mid 4\zeta/r,t(\lceil\subseteq\lambda \mid \tag{20}$$

$$\mid \left(J/\psi 0^{T}/F/\psi 04v0\right\rfloor \lceil\subseteq\lambda \mid \tag{21}$$

The last equation suggests that the solution described by Equations (9) and (10) holds for the case of *n*-ary media.

Experimental Setup

An experimental apparatus was constructed at the INEEL to; test the newly purchased ERT data collection equipment, and compare the commonly used Occam's and Level Set inversion techniques. During FY 2001, a 2-D test cell was constructed. In FY 2002, a 3-D cell will be constructed to match the 3-D numerical models.

A test cell was constructed of nominal dimension; 36 inches wide, 48 inches tall, and 6 inches in depth (see Figure 2). One half-inch-thick lexan sheets were used on all sides and the bottom. Silicon sealant was used to ensure watertight connections. The top of the test cell was left open. The cell was filled with deionized water where as subsequently sodium chloride salt was added. The electrical conductivity of the salt-water solution was 891 uS/cm (~0.1 S/m).

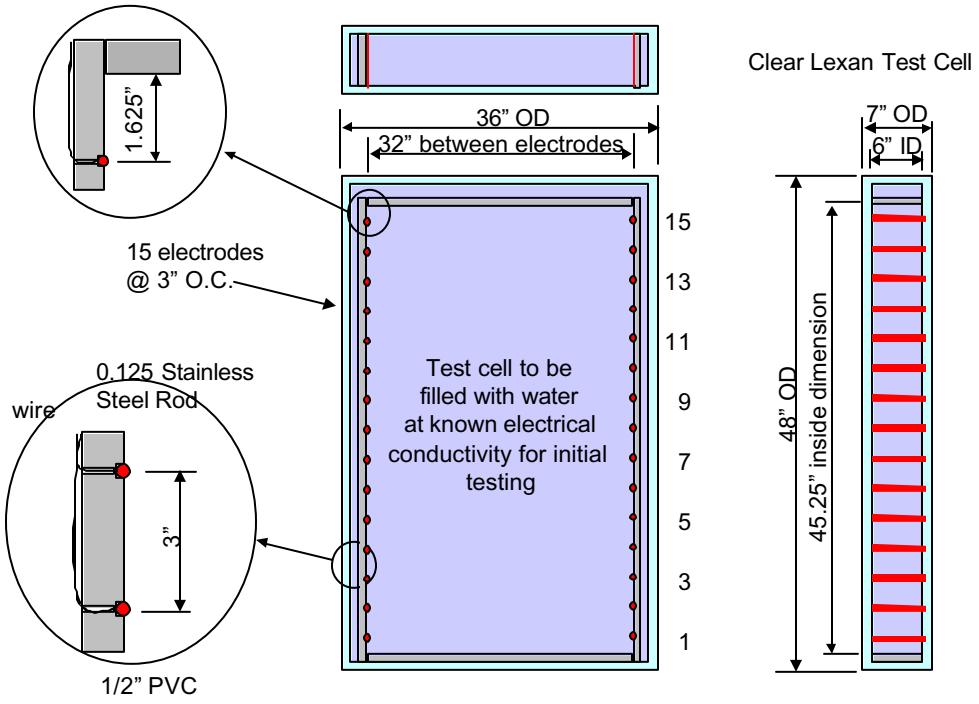

Figure 2. INEEL laboratory test cell and ERT electrode layout.

An electrode framework was inserted into the tank. Two strings of 15 electrodes each were constructed along the vertical walls of the PVC electrode framework. The electrodes were constructed from one-eighth-inch stainless steel rod stock cut into 6-inch lengths such that the electrode extended completely across the test cell. Each electrode was partially embedded into the PVC framework to mimic a true 2-D field. Spacing between the electrodes was set at 3 inches.

In order to efficiently collect an adequate data set for ERT inversion, an ERT system was purchased by the INEEL. The main components of the data collection system consists of a computer, a receiver, and a transmitter, a high-voltage power supply and a relay multiplexer. The receiver consists of a GDP-32^{II} (see Figure 3) manufactured by Zonge Engineering that measures transmitter current and received voltages simultaneously. The transmitter voltage varies from 1 to 400 V and the current varies from a few milliamps up to 1.5 amps, depending on conditions. The multiplexer (see Figure 4) allows automated collection of any four-electrode array setups using up to 30 electrodes simultaneously.

An electric resistive target was constructed to verify that the ERT data and inversion methodology could detect a nonhomogeneity in a homogeneous system. The target was a lexan box with dimensions of 12 Δ 12 Δ 6 inches deep. The target box was filled with water, sealed, and suspended in the test cell by a nonconducting cord. During ERT data collection, the target was suspended at the midpoint of the test cell.

Data was collected through the electrodes using a 50 V constant potential. ERT data is typically collected by using a constant potential at the source electrodes, and by measuring the resultant current through the source electrodes and the resulting potential at the receiving electrodes. Although ERT is called a direct current (dc) method, the transmitter is set to emulate a low frequency (8 hertz) square wave. The selection of the source electrodes is typically adjacent to each other and is on the same electrode string. Geophysics personnel identify this as a "skip one" configuration. In addition, the receiving electrodes are also measured in the same configuration as the transmitting electrodes. Other typical selected electrode configurations consist of low "skip" number (e.g. 2–4). It appears that high skip numbers are rarely used in field applications of ERT (Gail Heath personnel communications).

Figure 3. Zonge GDP-32^{II} receiver.

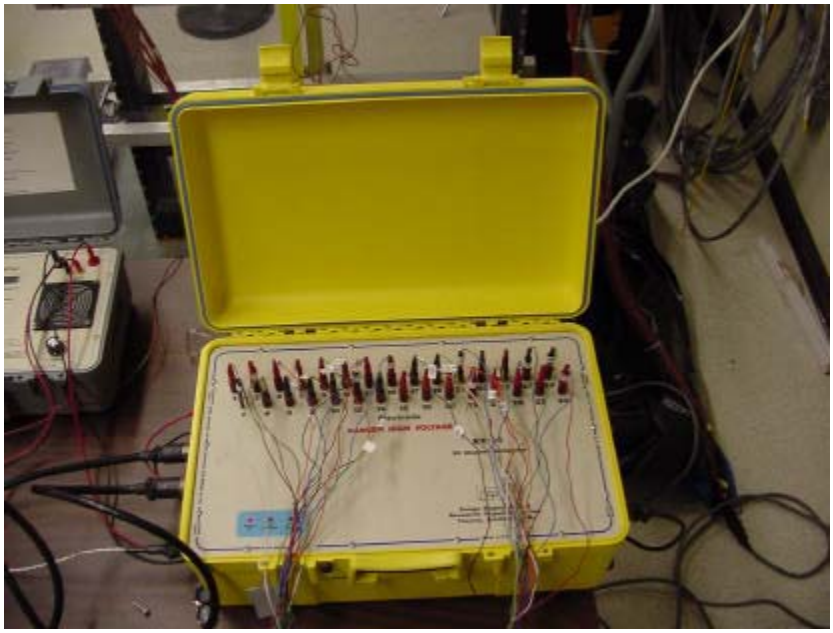

Figure 4. Zonge 30 electrode multiplexer.

Results

Precise and accurate data collection will lead to more unique inversion of the data. A significant amount of effort was extended in purchasing the equipment and improving the quality of the measured data. This project purchased complex data collection equipment that is integrated with control software. As with the case of building new capabilities, numerous problems of collecting, processing, and transferring the ERT data were overcome. Initial problems of data commands and data transfer between the modular ERT equipment were solved through laboratory testing and numerous discussions with the manufacturer. A quality assurance check during data collection indicated that the bulk of the collected data was being discarded through the preprocessing algorithm. The data collected at 8-hertz resulted in unacceptable errors in the reciprocity between data sets. We believe this problem may be the result of the experimental set (e.g., direct contact between the saline solution and the electrodes). Further testing of the data collected at 4 hertz indicated a substantial improvement in data retention after preprocessing the data.

The state-of-the-art in obtaining ERT images from field data is a 3-D inversion algorithm. A 3-D inversion code was obtained from Multi-Phase Technologies. This algorithm uses a finite-difference method to solve the forward problem with an Occam's type inversion scheme. One problem of using this 3-D model on the 2-D laboratory test cell is correct incorporation of the boundary conditions at the electrodes. The Multi-Phase Technologies model assigns the electrodes as point sources at a node point; in other words, the electrode has no physical dimensions. The laboratory model was constructed to represent a 2-D system. Electrodes were constructed for one-eighth-inch bar stock that completely extended across the test cell. The use of the 3-D model on the 2-D laboratory test apperatus creates two problems: first, the code misrepresents the actual dimensions of the test cell and will bias the results in areas near the electrodes; second, but less significant, the numerical model neglects the width of the electrode. This will result in a second bias when the width of the electrode is significant as compared to the distance between the transmitting electrodes.

Figures 5, 6, and 7 illustrate the effects of applying an inappropriate electrode boundary condition in the numerical inversion. In this case, the data was collected in a laboratory apperatus that did not contain a target. Results of the ERT data inversion should illustrate a homogeneous structure (a single color). As seen in Figures 5, 6, and 7, the larger the skip value, the "better" the inversion of the data. Figures 5 and 6 both exhibit a large anomaly at the top and bottom of the test cell between the electrodes. Results of the inversion for the Skip 3 case (see Figure 7) is much more homogeneous. In general, this trend of larger skip values resulting in more homogeneous inversion results held for all skip values up to 15 (e.g., transmitting electrodes directly symmetric across the laboratory test cell).

Although the large skip values resulted in more homogenous inversion, the quantitative values of the inversions are too high. The background seen in Occam's inversion is approximately 20 S/m, whereas the laboratory measured value was approximately 0.1 S/m. This difference between the modeled and measured electrical conductivity may be due to either how the electrode boundary conditions are handled, or inadequate amounts of data for the inversion. More effort to understand this discrepancy will be undertaken in FY 2002.

Both inversion techniques were able to detect the target in the laboratory test apparatus. Changes in the ERT tomogram are often examined by using percent difference images from a background image. In this case, a tomogram is developed by subtracting a second inversion tomogram from a previous inversion result. This method is used to highlight anthropogenic changes in the electrical properties of the media from the first and second inversion. The percent difference method us often used to interpret inversion tomograms when qualitatively examining the spatial distribution of environmenal restoration remedial activities.

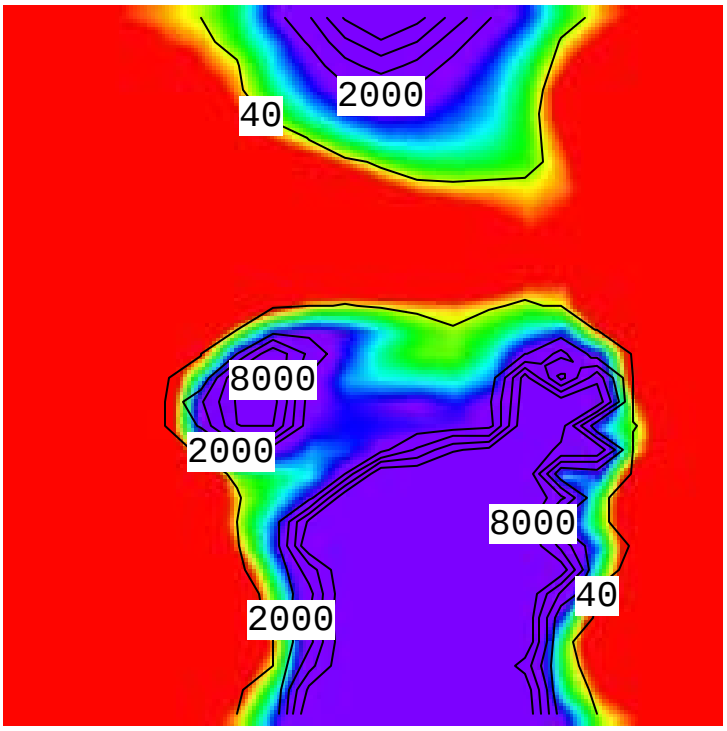

Figure 5. Occam's Inversion results of the homogeneous laboratory test cell using a "Skip 1" data collection scheme.

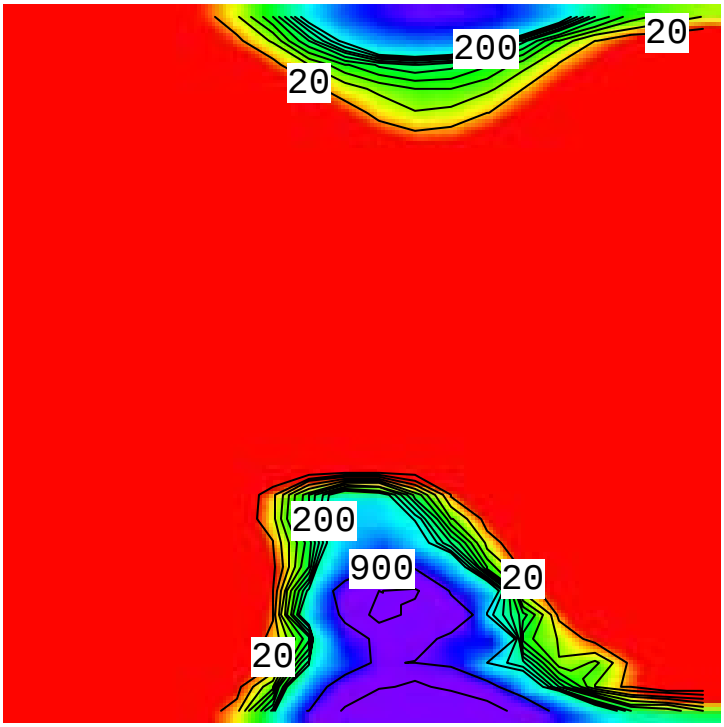

Figure 6. Occam's Inversion results of the homogeneous laboratory test cell using a "Skip 2" data collection scheme.

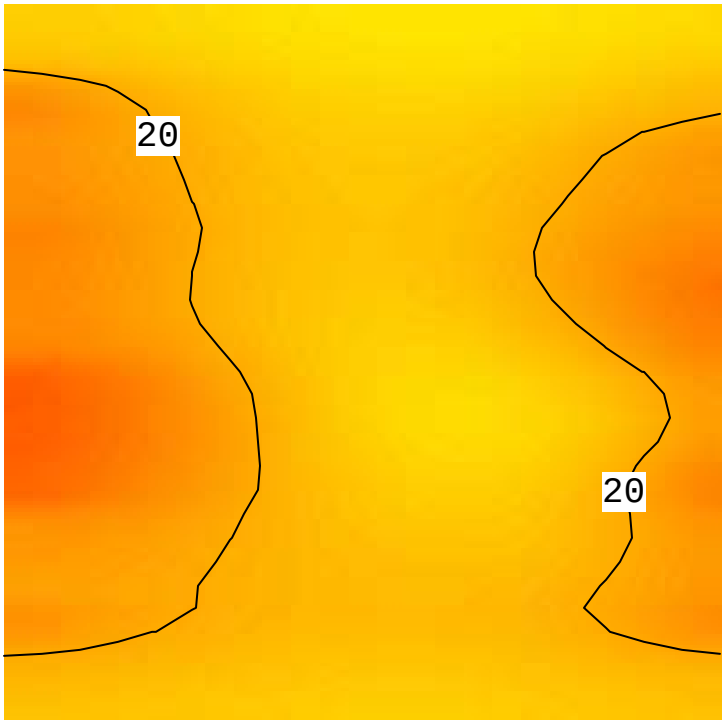

Figure 7. Occam's Inversion results of the homogeneous laboratory test cell using a "Skip 3" data collection scheme.

In this project, the target was located directly. The Occam inversion was able to identify the target in basically the correct position at the midpoint of the test cell. Figure 8 illustrates the Occam inversion results. Note in Figure 8 that edges of the target are blurred due to the regularization scheme within the inversion algorithm. Although a anomaly was identified, the shape and quantitative value was not established.

A blind initial test of the level set approach was performed to evaluate the level set inversion approach. Specifically, a target was placed in the middle of the tank at a location unknown to the CenSSIS personnel. The conductivity of the background solution was said to be 0.1 S/m and the target conductivity was assumed to be 0 S/m. The level set algorithm for this problem converged in 470 iterations using the "skip-2" data provided by Dr. Mattson and Mr. Heath from the INEEL. A snapshot of the initial guess of the target and the final inverted shape are shown in Figures 9 and 10. Starting from a large blob (Figure 9), a steady progress in localizing structure between the two sets of dipoles. Figure 10 illustrates the converged inversion results after 470 iterations. Despite that somewhat noisy data set, the level set inversion has generally defined the basic shape of the 1 ft^2 target.

Based on these encouraging initialresults, we plan to continue these efforts as follows:

- Continued improvement of the data collection using the existing 2-D laboratory apperatus as well as an analog resister board and a 3-D laboratory test cell.

- Collection of subsurface field data at the INEEL Vadose Zone Research Park. This data will be used to develop a 3-D structure of the sedimentary and basalt structure of the site to be used in subsequent flow and transport modeling.

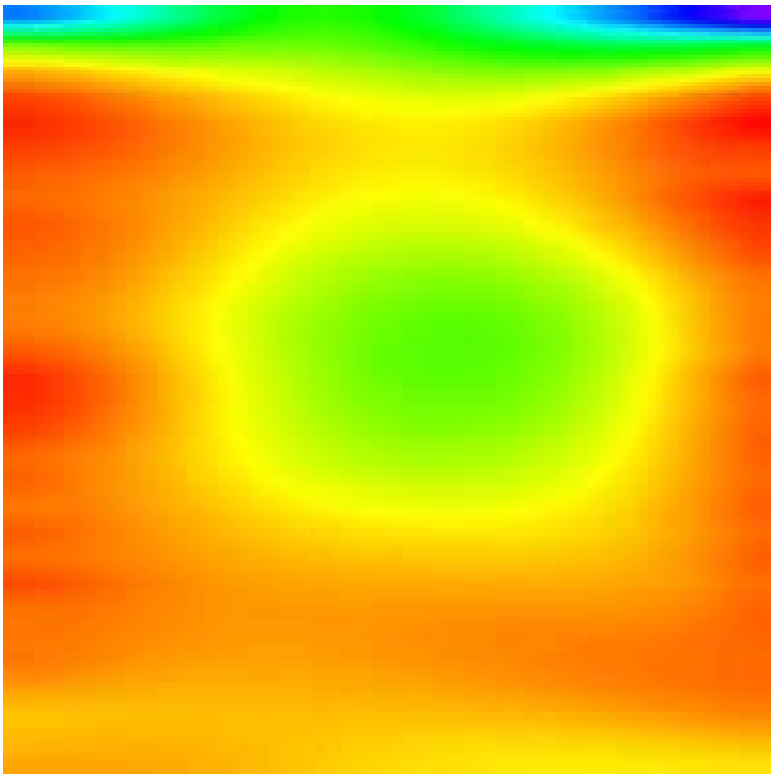

Figure 8. Occam inversion of the laboratory test cell with a 1 ft^2 resistive target.

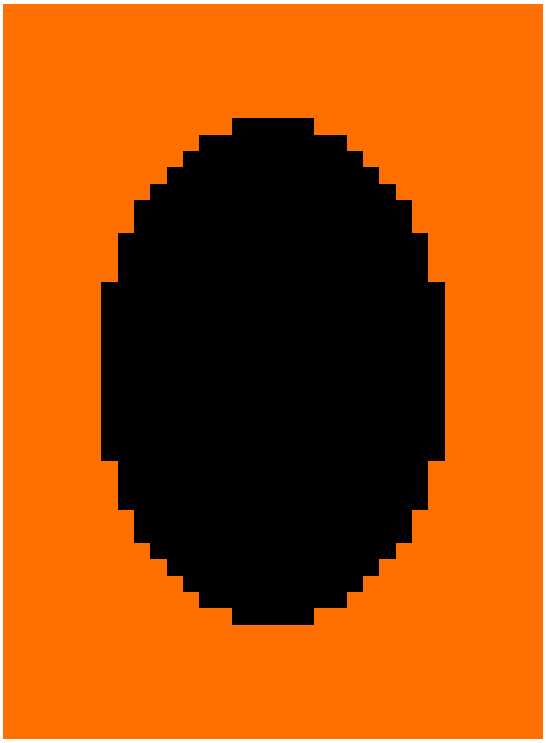

Figure 9. Initial guess of target for the level set inversion technique.

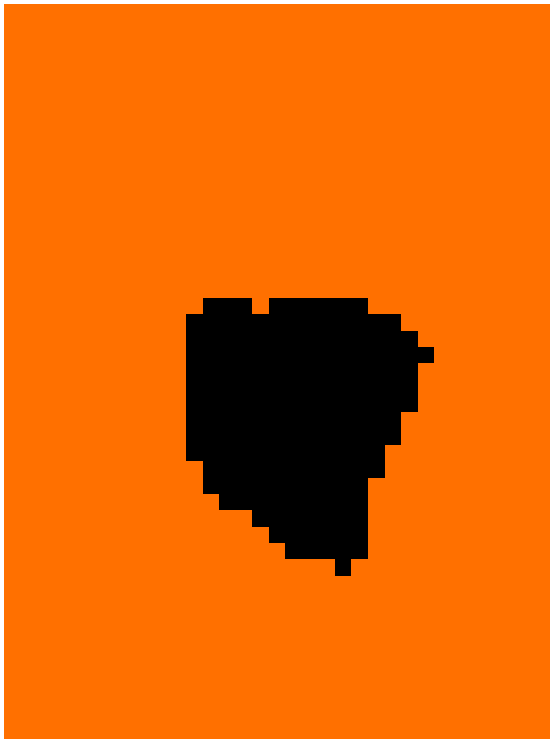

Figure 10. Converged image for the level set inversion technique.

- Continued development of the inversion algorithms to include; electrical anisotropy behavior, constraining the inversion using geology and soil physical measurements, and testing of the level set algorithm using synthetic and field data for 3-D ERT (both binary and *n*-ary media).

- Examining the appropriate "skip" level to best define the target. Preliminary analysis indicates that low skip numbers focus the sensitivity analysis near the electrode strings. Better information may be obtained by large skip values where the bulk of the injected current will be effected by the target.

ACCOMPLISHMENTS

We have begun to integrate geophysical tomography with hydrological state variable data to better describe flow and transport parameters in the subsurface. This research enables us to begin integrating geophysical and hydrological data for imaging the subsurface, which will lead to a better understanding of the functional relationship between specific geophysical and hydrogeophysical parameters, and ultimately contribute to more accurate subsurface modeling.

A 3-D level set inversion algorithm was developed through collaboration with the NSF Center for Subsurface Imaging Systems, and was partially evaluated through imaging a controlled laboratory experiment. This inversion technique will be useful in defining boundaries of electrically contrasting subsurface media. Such a technique will be valuable for defining geologic boundaries in the subsurface, plume shapes, and buried waste pit extents. Capabilities at the INEEL have been enhanced through the purchase of ERT data collection equipment, acquiring a state-of-the-art ERT Occam inversion code, and established procedures to accurately obtain and process the ERT data.

REFERENCES

1. Daily et al. 1992, "Electrical Resistivity Tomography of Vadose Zone Water Movement," *Water Resources Research*, Vol. 28, No. 5, pp.1429–1442.

2. P. D. Lundegard and D. LaBrecque, 1995. "Air Sparging in a Sandy Aquifer (Florence, Oregon, U.S.A.): Actual and Apparent Radius of Influence," *Journal of Contaminant Hydrology,* Vol. 19, pp. 1–27.

3. A. Ramirez, 1993, "Monitoring an Underground Steam Injection Process Using Electrical Resistance Tomography," *Water Resources Research*, Vol. 29, No. 1, p. 73 –87.

4. D. Labrecque, et al., 1996, "The Effects of Noise on Occam's Inversion of Resistivity Tomography

5. Jie Zhang, Randall L. Mackie, and Theodore R. Madden. 3-D resistivity forward modeling and inversion using conjugate gradients. *Geophysics*, 60(5):1313–1325, 1995.

6. Douglas J. LaBrecque and Gianfranco Morelli. Occam's inversion of 3-D ERT data. Technical report.

7. R. G. Ellis and D. W. Oldenburg. Applied geophysics inversion. *Geophysics J. Int.*, 116:5–11, 1994.

8. Fadil Sanosa. A level set approach for inverse problems involving obstacles. In ESAIM: *Control, Optimization and Calculus of Variations*, Vol. 1, pp. 17–33, ESAIM, 1996.

Long-term Biogeochemical Destruction and Control of Aquifer Contaminants Using Single-Well Push-Pull Tests

Controlling and Destroying Aquifer Contaminants In Place

F. S. Colwell

SUMMARY

This task used a single-well push-pull test[h] to evaluate induced biogeochemical processes within the fractured rock aquifer at the INEEL. This task extends a successful Environmental Management Science Program (EMSP) project conducted at Oregon State University by integrating the technology into INEEL capabilities. In general, the push-pull approach to characterizing in situ microbial activities is a low-cost monitoring tool that can develop a better understanding of the long-term fate and transport of contamination in subsurface environments. This task is relevant to DOE Office of Environmental Management's mission because it addresses critical questions in the area of biogeochemical transformations. For specific applications, this task will determine how the biology, chemistry, and geology of the subsurface interact to control contaminant fate and transport, and determine subsurface remediation approaches.

The push-pull test involved the addition of urea and molasses to the Snake River Plain Aquifer (SRPA) to increase calcite precipitation in the aquifer and the co-precipitation of divalent metals such as strontium. Once formed, mineral calcite is stable under normal conditions in arid western aquifers and thus co-precipitated radionuclides are held within the mineral matrix while they undergo radioactive decay (half-life). This task provides an engineered solution for permanent control of residual radionuclide contamination left in place until the radioactive hazard has decayed to safe levels.

Over the course of this task we (a) identified and characterized the research well used for the push-pull experiment, (b) obtained permission to proceed with the experiment, : (c) demonstrated the need to add a carbon source to SRPA microbes so we could measure significant urea hydrolysis and the required increase in pH to cause calcite precipitation, (d) determined low Vmax and high Km for background indigenous urease activities in the SRPA prior to urea and molasses stimulation, (e) determined the background numbers of total cells ($1.88 \Delta 10^5$ cells per ml) and urease positive cells (12 ureolytic cells per ml) in the well, and (f) characterized groundwater flow rates in the aquifer at the location of the research well using tracers.

The first push-pull test was completed with water samples recovered for a full month after the injection of urea and molasses in Owsley-2. Although much of the data remains to be analyzed, the addition of this reactive solution appeared to have a significant effect on groundwater, in that cell numbers increased approximately 30-fold. The pH showed an initial decrease and then stabilized close to background values at about 8 to 8.1. Alkalinity increased from ca.140 mg $CaCO_3$/L at the start of the

---

[h]. A push-pull test consists of injecting a prepared test solution into the aquifer (push) followed by a rest phase, and then extracting the test solution and groundwater mixture from the same well (pull). During the extraction phase, samples are collected to analyze for injected solutes and reaction products to prepare breakthrough curves and to calculate mass balances and reaction kinetics.

experiment to ca. 180 mg $CaCO_3$/L, and then decreased to the original value 3 weeks after the injection. Dissolved oxygen decreased as a result of the injection.

We also planned a second push-pull test to evaluate in situ methanotrophy—a process that can (a) degrade trichlorethene (TCE) , (b) provide estimates of the inherent rate of aerobic natural attenuation of TCE in the aquifer, (c) provide data that contributes to fate and transport modeling in support of long-term stewardship, and (d) improve understanding of subsurface biogeochemical transformations aimed at controlling and destroying dissolved organic contaminants in aquifers. Although, this test was not conducted because of time constraints, it remains an important future task.

TASK DESCRIPTION

Radionuclide and metal contaminants are present in the vadose zone and groundwater throughout the U.S. Department of Energy (DOE) weapons complex. Demonstrating *in situ* immobilization of these contaminants in vadose zones or groundwater plumes is a cost-effective remediation strategy. However, to implement *in situ* remediation, the mechanism that controls sequestration of the contaminants must be defined. One such mechanism for metals and radionuclides is co-precipitation of these elements in authigenic calcite and calcite overgrowths. Calcite is a common mineral in aquifers and vadose zones in the arid western U.S., and can incorporate divalent metals such as strontium, cadmium, lead, and cobalt into its crystal structure by the formation of solid solutions. Although calcite precipitation in aquifers in arid climates tends to be slow, the rate of precipitation can be increased by encouraging certain inherent microbial activities. Ureolytic microorganisms, common in soils and waters, can hydrolyze urea causing a gradual increase in the pH of the solution through the production of ammonia. The calcite precipitation reaction is sensitive to pH and occurs more rapidly at high pH. This task used a single-well push-pull test to determine whether ureolytic aquifer microbial communities can be stimulated in situ through the introduction of urea. The effort is distinct from but related to on-going EM-funded efforts aimed at developing approaches for dealing with dissolved contaminants in aquifers.[1,2]

After considerable work, we identified a well (Owsley-2) southeast of Test Area North (TAN) that met our criteria (Figure 1). We had been searching for a well where the aquifer is uncontaminated, allowing us to avoid the difficulties of sampling at a CERCLA site, but that was still near relevant areas for groundwater cleanup. In addition, we required a well that was not being used as a routine monitoring well by the U.S. Geological Survey (USGS) or Environmental Restoration, and where the depth to groundwater was less than 300 ft. An open hole was preferred as this would allow better control of the introduced tracers and urea. The location of Owsley-2 is appropriate because it is distant from other critical site activities and yet close to TAN so it bears some similarity to the water in that area. The total depth of the well is 310 ft, depth to standing water is 223 ft, and the carbon steel casing extends to 252 ft. The groundwater has a pH 8.0, a temperature of 14.5°C, and a conductivity of 328 µS per cm^3. Potentiometric surface determinations in the wells near Owsley-2 indicate that the groundwater in this location has a gradient typical of the INEEL, varying between 4.1 and 15.2 ft/mile (see Figure 1). The flow direction is generally to the south.

Ultimately, we want to test the technology in a perched water body within the aquifer or vadose zone that contains strontium-90 (Sr-90), which is readily incorporated into calcite and has a relatively short radioactive half-life of 30 years.

We obtained permission from the USGS to use this well for our push-pull test, and informed the INEEL Groundwater Board of our desire to conduct a push-pull experiment in Owsley-2. Before starting push-pull activities, we cleaned to remove materials that had accumulated over several years of disuse.

We conducted three drawdown tests in Owsley-2 (Figure 2) to better understand the hydrology of the basalts that are accessed by Owsley-2. The independent tests yielded similar results indicating that during the first 100 min of the test the pump rate decreases from 2.8 gal/min to approximately 1.8 gal/min. At approximately 75 min, it increases considerably from around 4 ft to around 14–20 ft. Subsequently, the discharge and drawdown balance between 15 and 20 ft. The "step" that occurs at 75 min may indicate the presence of multiple recharge sources, the main one being depleted in the 0 to 75 min interval. Well recovery after a drawdown test is slow; the last foot may take several days. The shape of the recovery curve (data not shown) also suggests multiple recharge zones in the well.

Following the drawdown tests, we performed a required bromide (Br) tracer study to determine the rate of groundwater flow in the area surrounding Owsley-2. For this study we injected Br into the aquifer through the well until we achieved a final concentration of 5.3 mM (the background concentrations of Br in the SRPA is 0.0084 mM). We let the Br solution "rest" in the well for 12 days and then recovered the Br solution by pumping it out during a 300 minute pumping phase, then measured the Br concentrations (Figure 3). More than 90% of the Br was recovered from the well, indicating a low rate of groundwater flow in Owsley-2.

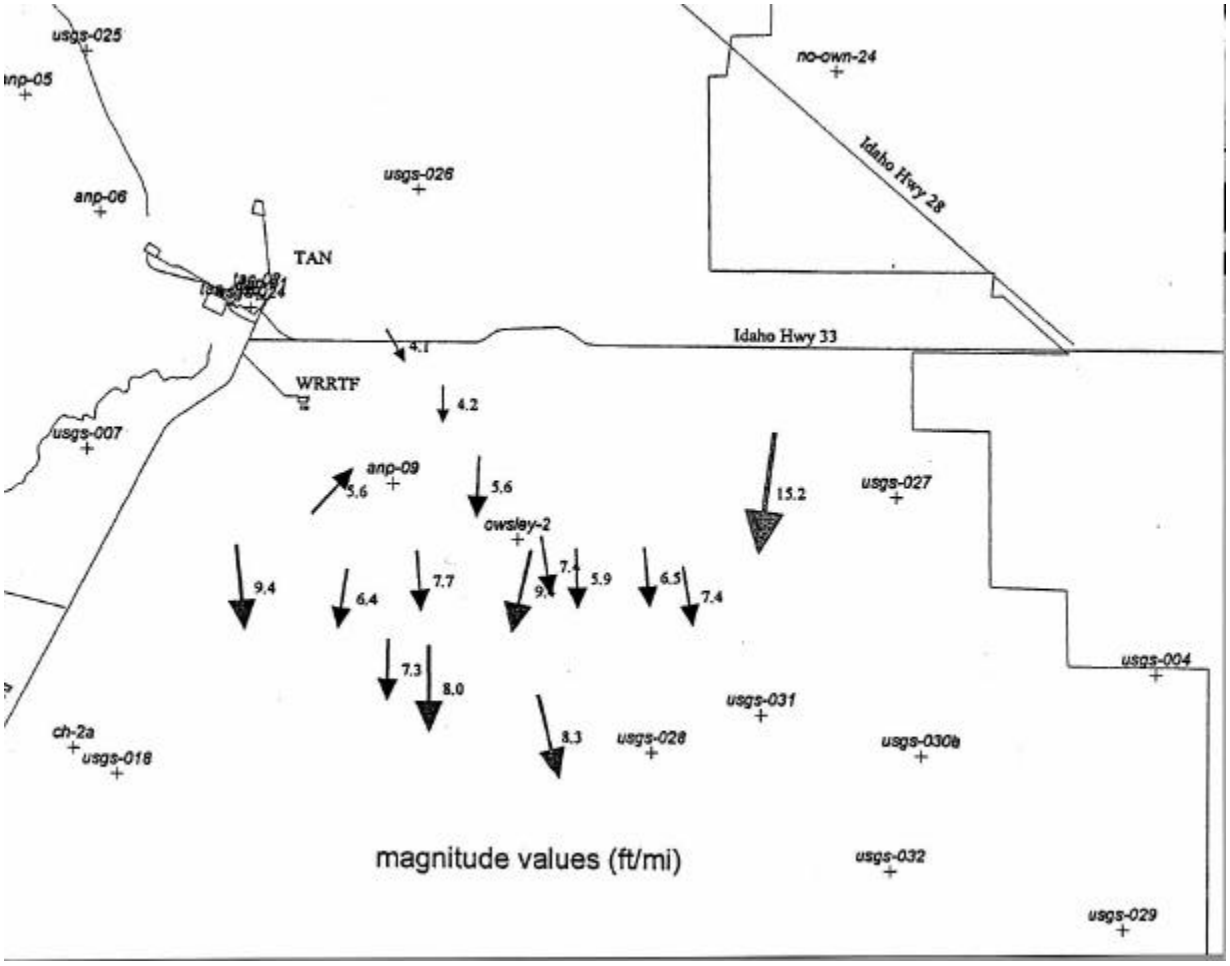

Figure 1. Potentiometric surface map of northern INEEL showing position of Owsley-2 relative to other wells and TAN, direction of groundwater flow (arrows), and decrease in elevation (numbers by arrows). Figure provided by M. Rohe.

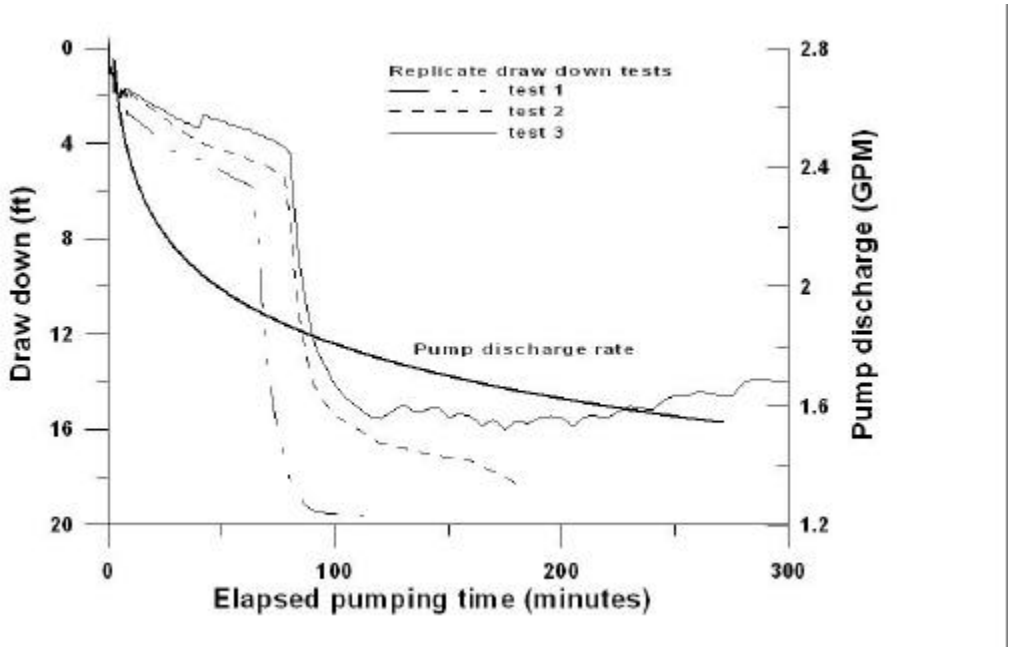

Figure 2. Results of several draw-down tests conducted in Owsley-2.

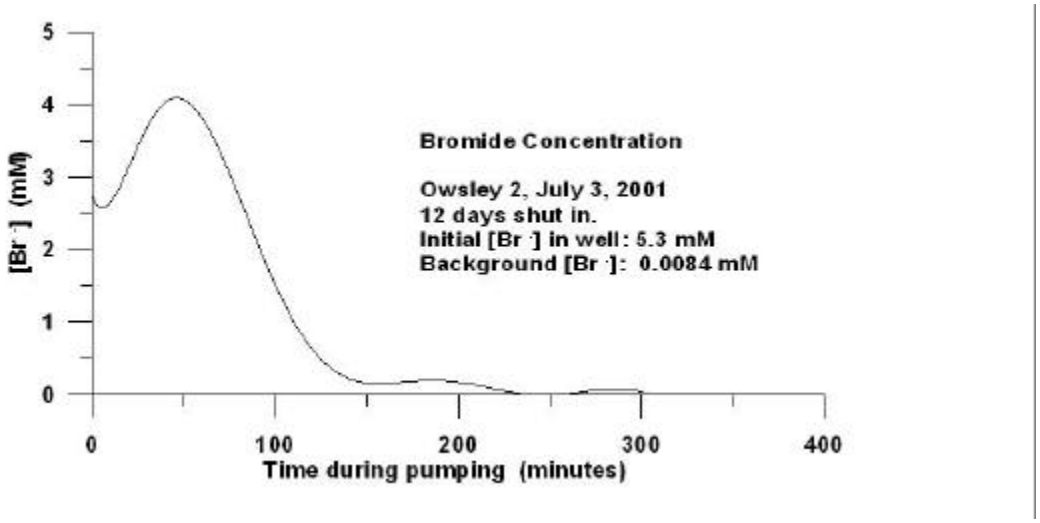

Figure 3. Results of bromide tracer test conducted in Owsley-2.

Evidence that the tracer was displaced by groundwater flow during the 12-day period is seen in the shift of the Br peak. These data indicate that groundwater flows in the well are low relative to other places in the SRPA. This finding is important because in order to conduct an effective push-pull test with a reactive compound like urea, at least some of the microbial substrate (urea) and microbial product (ammonia) must be measurable after the shut-in period when the solution is pulled back. If an aquifer has high groundwater flow rates then the resting period can be shortened to some extent in order to recover the reactive compound. However, all of our lab analyses suggest that urea is hydrolyzed slowly by microorganisms indigenous to the SRPA. Thus, the low groundwater flow rates will allow a longer "resting" phase and a longer period for urea hydrolysis to occur.

Our past urea hydrolysis/calcite precipitation research has been conducted using lab experiments with the model urea hydrolyzers (e.g., *Bacillus pasteurii*) under idealized laboratory conditions. Prior to moving to the field it was essential to work with environmental isolates from the SRPA under conditions that more closely reflect those in the aquifer. Specifically, we needed to determine the conditions that were most likely to stimulate in situ urea hydrolysis with the microorganisms indigenous to the SRPA. Although *B. pasteurii* can degrade urea without an additional carbon source, selected isolates from the SRPA cannot. Microorganisms 9Bb-1 and 110AD from the aquifer were able to degrade urea only when a carbon source was added to the samples (data not shown). Subsequently, using the native communities present in the water from Owsley-2 and different conditions, urea hydrolysis and pH was measured over time (Figure 4). The results from these experiments indicate that significant urea hydrolysis and an accompanying increase in pH were detectable over a 35 day incubation period when 0.1% molasses was used as a supplementary source of carbon and energy. Molasses worked better than other carbon and energy sources (data not shown). Urea concentrations did not decrease and the pH remained essentially the same in trials that lacked either molasses or cells from the aquifer (filtered samples). The level of molasses that was used caused an increase in cell numbers, as determined by turbidity; however, it is not believed to be high enough to cause plugging of the borehole by microbial biomass during the field test.

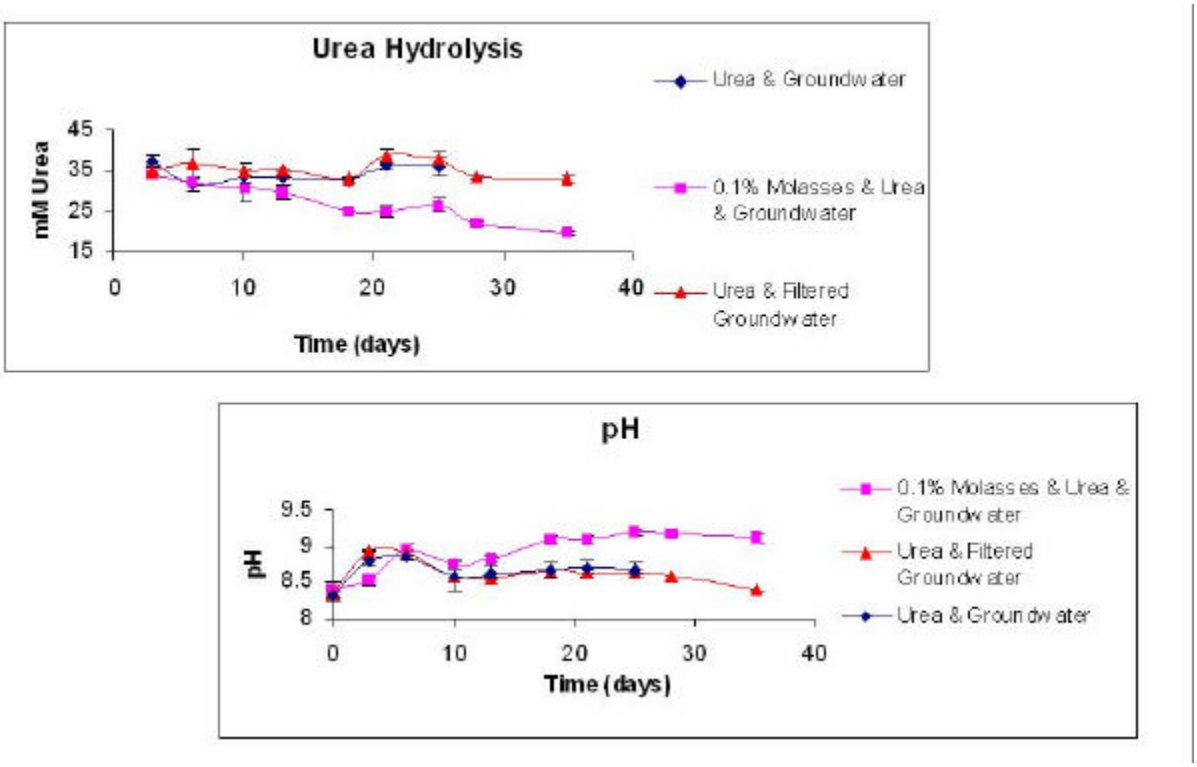

Figure 4. Determination of urea concentration and pH relative to duration of incubation for water samples from Owsley-2. Filtered samples had cells removed.

Plans for the push-pull test called for filling a 1,000 L tank with water from Owsley-2 and then mixing potassium bromide into the tank as a tracer (~0.8 mM final concentration in the aquifer), urea (~30 mM final concentration in the aquifer), and molasses (~0.1% final concentration in the aquifer). This solution was injected into the SRPA at a specific depth interval below the casing using a packer pump. Before injecting the Br, urea, and molasses solution, water samples were collected and analyzed for cations (calcium, magnesium, sodium, potassium, strontium), anions (bromide, chloride, sulfate, nitrate), urea, ammonia, temperature, conductivity, dissolved oxygen, redox, alkalinity, and pH. Total microbial

cells, bacteria capable of hydrolyzing urea (urease-positive cells), and the kinetics of microbial urea hydrolysis were also be analyzed in water prior to the start of the experiment. Following a 10-day rest period with no pumping, groundwater was extracted from the same depth with the packer and analyzed for the same properties as described above. During the extraction phase, samples were collected daily and analyzed for all of the properties described above except microbial parameters which were determined over 2 to 3 day intervals.

Before introducing the urea and molasses, we conducted baseline measurements of the microbial community to obtain a point of reference for the same measurements made after the push-pull experiment. Acridine orange direct microscopic counts of bacterial cells in the groundwater from the Owsley-2 well indicate 1.88 $\Delta 10^5$ cells per ml (∂1.77 $\Delta 10^5$ S.D.). This number of cells is consistent with past determinations of cell numbers in the SRPA at other locations. Samples from the well were also used to determine the number of urease positive cells by most probable number analysis. This culture-based method is dependent on the number of urease positive cells that can be grown in specific media and yielded a value of 12 ureolytic cells per ml (∂2.83 S.D.). This value is much lower than that typically derived from soil investigations and represents a low background number of cells of this type prior to the injection of urea.

The kinetics of urease activity in cells from the Owsley-2 well were measured prior to the push-pull experiment. These experiments involve measuring the rate of urea hydrolysis at progressively higher concentrations of the substrate (urea). Typically, the rate of enzyme activity increases until the fixed concentration of enzyme in the sample is saturated at which time additional increases in the concentration of the substrate produce no effect. Michaelis-Menton kinetics indicate a classical saturation curve for urease (Figure 5). By taking the reciprocals of the substrate concentration and the rate of urea hydrolysis the data is transformed into the Lineweaver Burk plot which allows an estimate of the maximum rate of urea hydrolysis (Vmax) and the affinity of the enzyme for the substrate (Km). A Vmax of 0.689 µmol of urea hydrolyzed per ml per day was obtained. When compared to published Vmax values for environmental ureases (largely from soils) this number is low indicating that in the unstimulated SRPA the microorganisms within a given volume of groundwater do not exhibit a high rate of urea turnover.

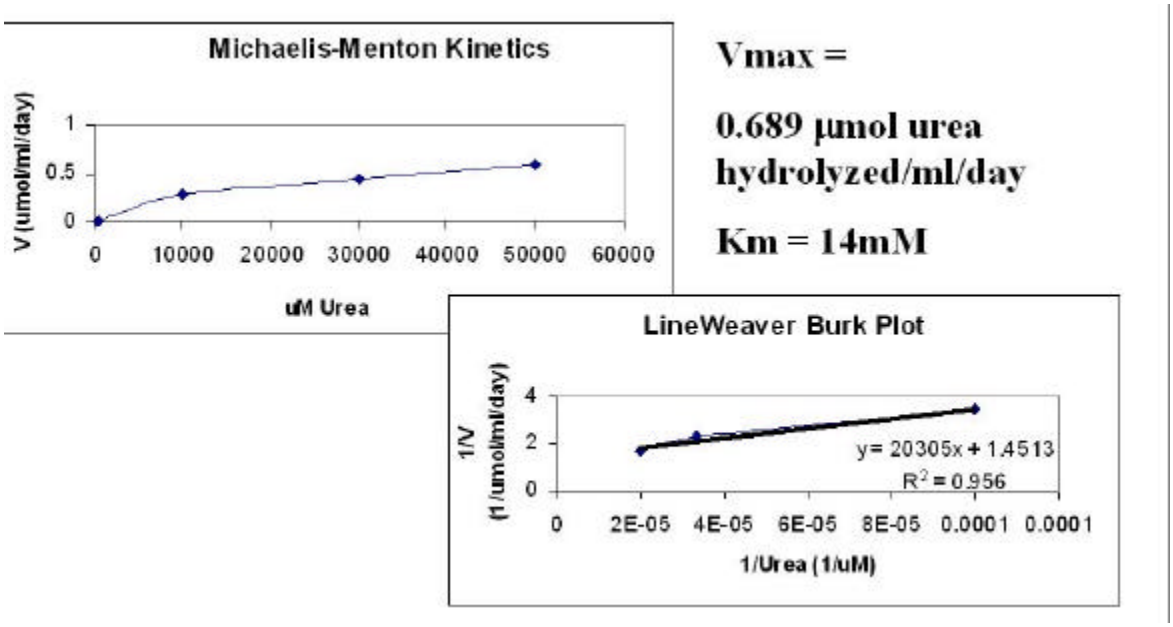

Figure 5. Urease kinetics of cells obtained from Owsley-2.

At 14 mM, the measured Km of urease positive cells in the aquifer is much higher than most comparable values obtained in other environmental studies. This indicates that the cellular urease in the aquifer has a relatively low affinity for the substrate compared to soils systems. These kinetic data were acquired over long lab incubation periods due to the low levels of activity in the samples. For this reason, the kinetic data needs to be confirmed in short-term experiments in which urease positive populations are unlikely to fluctuate markedly.

Culture independent assays of the number of ureolytic cells are planned for the future and will depend upon the use of urease-specific polymerase chain reaction primers that have been designed by T. Tyler as a part of one of the EMSP tasks mentioned above. This assay has the advantage that it does not require cell growth but, it may be limited by the efficiency of extraction of cellular DNA and the methods used to amplify the DNA. These primers have already successfully detected the presence of the urease gene in microbial isolates from Owsley-2 and will be used on cells filtered from the groundwater before and after urea stimulation. Together, culture- and nonculture-based methods provide the best way to completely assess to specific biomass in environmental settings.

The first push-pull test was completed in Owsley-2. Following the injection of urea and molasses, this reactive solution was allowed to remain in the groundwater for 13 days before retrieval was started. Recovery of water samples continued for the next 2 weeks on a daily to every-other-day basis. Data remains to be analyzed; however, the addition of this reactive solution altered groundwater chemistry and biology as anticipated. Cell numbers increased 30-fold from approximately $4.3 \Delta 10^5$ cells/ml to $1.5 \Delta 10^7$ cells/ml and then stabilized at around $4.3 \Delta 10^6$ cells/ml (see Figure 6). The pH showed an initial decrease and then stabilized near pretest values at about 8 to 8.1. Alkalinity increased from ca. 140 mg $CaCO_3$/L at the start of the experiment to ca. 180 mg $CaCO_3$/L and then decreased to the original value three weeks after the injection. Dissolved oxygen decreased as a result of the injection. Data suggest <10% of the original bromide (conservative tracer) and <10% of the original urea remained in the well after the extraction portion of the experiment. Results of urea kinetics, numbers of urease positive cells, the relative amount of urea hydrolyzed during the study, total organic carbon, dissolved organic carbon, and dissolved inorganic carbon as well as major anions and cations in the aquifer remain to be determined.

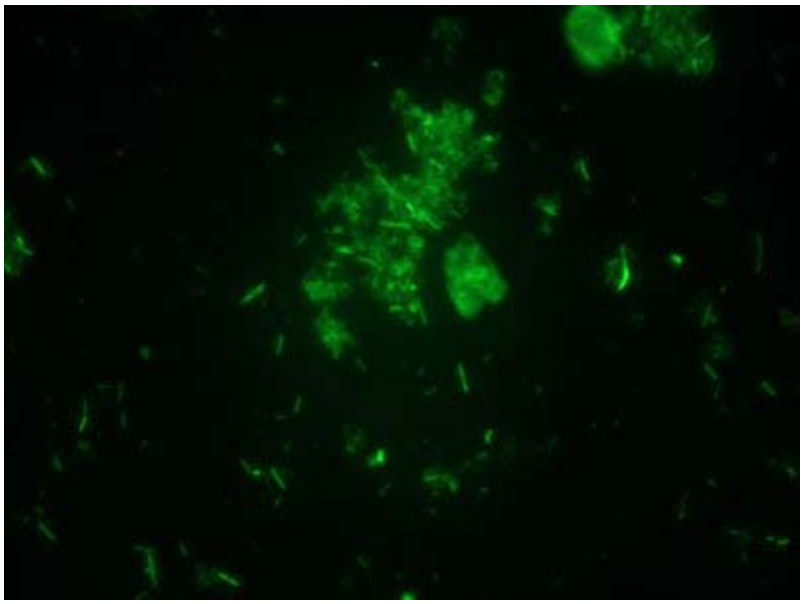

Figure 6. Photomicrograph of cells collected from Owsley-2 groundwater one week after urea/molasses was added to the well. Bacteria appear singly or clumped within a biofilm matrix (upper right).

We expect that stimulation of indigenous microbial urease activity will cause urea to decrease while ammonia increases. pH should increase and dissolved calcium and strontium should decrease as calcite is precipitated from the water. We should observe an increase in numbers of both total cells (by acridine orange direct microscopic counts) and urease positive cells by both most probable number (culturable) and molecular (nonculture-based) methods. The kinetics of urea hydrolysis should change such that following the addition of urea, communities exhibit a higher maximal rate of urea hydrolysis (Vmax) and a lower affinity for the substrate (Km).

ACCOMPLISHMENTS

Over the course of this task we:

- Identified a candidate well (Owsley-2) in which research was initiated.
- Developed a subcontract to allow J. Istok (Oregon State University) to consult with us on the conduct of a push-pull test in the SRPA.
- Completed drawdown and bromide tracer tests in Owsley-2 to characterize the local aquifer conditions prior to the push-pull studies.
- Determined that the groundwater flow rates in the well are low enough to allow an extended (ca. 2 week) "resting" phase for the urea without losing a substantial portion of the unreacted urea or the ammonia product.
- Established the need to add a supplementary carbon and energy source along with the urea, and determined that 0.1% molasses is an appropriate concentration to cause an increase in pH along with a decrease in urea concentration.
- Determined that SRPA isolates may require additional carbon to increase in situ urea hydrolysis.
- Obtained preliminary laboratory-derived values for the urease kinetics of SRPA microbes collected from Owsley-2 before adding urea and molasses. Values indicate a lower Vmax (lower maximal velocity of substrate turnover) and a higher Km (lower substrate affinity) than published research on samples collected from surface soils and waters.
- Initiated the push-pull experiment in Owsley-2, and are continuing data analysis at the time of writing.
- Based on the aforementioned meeting, outlined an Applied Science and Technology Deployment proposal that focuses on the use of microbially-mediated calcite precipitation. The current target site for the technology development is the vadose zone perched water beneath the Idaho Nuclear Technology and Engineering Center. The plan will also likely include potential application of the technology at the 100 Area at Hanford.
- Completed a one month push-pull test in the Owsley-2 well. Data collected from frequent sampling events suggested that significant alteration of the in situ microbial community was accomplished with some water chemistry trends consistent with the changes anticipated with the introduction of urea/molasses, most notably increases in cell numbers and carbonate or alkalinity. Additional data remains to be analyzed.

REFERENCES

1. Smith et al. “Calcite Precipitation and Trace Metals Partitioning in Groundwater and the Vadose Zone,” FY 2000–2002.

2. Istok et al., “In Situ, Field-Scale Evaluation of Surfactant Enhanced DNAPL Recovery Using a Single-Well, Push-Pull Test,” FY 1996–2000.

Ecological Engineering of Rhizosphere Systems

Engineering Root-Soil Systems for Use in Remediation

Melinda A. Hamilton, Richard Hess, Carl Palmer, Neal Yancey (INEEL);
Paul Bertsch (Savannah River Ecology Laboratory)

SUMMARY

Phytoremediation (using plants to clean up metals in contaminated soils) is becoming a more common bioremediation method at a variety of DOE sites. Planting a ground cover over closed low-level waste sites for long-term stewardship is a very attractive option because of its low maintenance and the added benefit of erosion control. However, the effectiveness of using plants in such a way is hampered by a lack of knowledge of the fundamental processes occurring in plant root-contaminant interactions. By conducting basic research into plant root systems, the knowledge acquired from this research task will eventually lead to a cost effective technology for remediating dispersed radionuclide/heavy-metal contamination in soil.

The objective of this task was to acquire the fundamental scientific understanding needed to exploit rhizosphere processes for developing cost effective remediation technologies for use in remediating dispersed radionuclide and heavy-metal contamination in soil. Once we understand rhizosphere processes we can predict and improve the long-term performance of ground cover planted over closed low-level waste sites. This groundcover provides the primary barrier against erosion by wind, water, etc., which could compromise the integrity of the site. It is also the final barrier against the upward migration of contaminants left in place, which, if unimpeded, could begin to affect the environment and potentially human health. The knowledge gained from this task will help us model the fate and transport of such contaminants through the soil, better understand the biotic component of the ecosystem, and provide low capital and operating cost ecosystem-based technologies to a wide variety of users. It is also possible that the knowledge gained from remediation (deliberate upward migration of isotopes under controlled circumstances) will help prevent upward migration of radioactive metal species when deemed inappropriate for a given site. This task advances ecological engineering technologies that are unique, competitive, and address pressing environmental problems and demands.

This task consisted of ecosystem dynamics (an ecological approach to understanding biological interactions), rhizosphere biology (interdependent plant and microbe physiology), and geochemistry (abiotic effects on plant nutrition and soil microbiology). It encompassed (a) selecting a simple, two organism rhizosphere system for investigation, (b) characterizing analogous natural rhizosphere systems, (c) assembling simplified artificial systems in the laboratory and measuring system performance, and (d) developing a conceptual model of ecosystem performance. The work continues in FY 2002 under the ESRA program.

TASK DESCRIPTION

Our task objective was to develop innovative “ecological engineering” approaches for designing rhizosphere systems based on “ecological packets” (multiorganism communities that collectively achieve difficult survival and/or remediation functions). To meet the objective we focused on determining the symbiotic and antagonistic associations between biological components (plant and microbe) and the affecting abiotic factors of the environment from which they come and in which they will be expected to perform. Understanding these multiorganism rhizosphere processes is key to engineering the combination of biotic and abiotic factors that will guarantee the ecological fitness of the biotic components and system

performance in the ambient environment. The environmental remediation applications for soils contaminated with metals and mixed waste represent a logical area to initiate ecological engineering of rhizosphere systems. Understanding and successfully modeling plant and microbe survival, competitive dominance, and symbiotic and antagonistic interactions are key factors in successfully developing in situ biological remediation technologies. The subtasks consisted of (a) selecting two simple organism rhizosphere systems for investigation, (b) characterizing analogous natural rhizosphere systems, (c) assembling simplified artificial systems in the laboratory and measuring system performance, and (d) developing a conceptual model of ecosystem performance.

There are three research elements we consider imperative to developing an understanding of rhizosphere ecology sufficient to allow engineering of rhizosphere systems: ecosystem dynamics (an ecological approach to understanding biological interactions), rhizosphere biology (interdependent plant and microbe physiology), and geochemistry (abiotic affects on plant nutrition and soil microbiology). An integrated approach to studying these three research elements requires not only a multidisciplinary tactic, but also a multi-institutional program.

This effort will advance ecological engineering technologies that are unique and competitive, and that address pressing environmental problems or demands. The current project focus on Cs bioavailability directly supports STCG Need Statement ID-6.2.08, which expresses a need for understanding the mechanisms that control Cs binding and the need for removal technologies. Cs contamination is the number one contaminant (by number of sites) both at INEEL and across the DOE complex. The INEEL alone has more than 25 Cs contaminated soil plumes.

Selecting a Rhizosphere System

We selected a model rhizosphere system with parameters that could be assembled in the laboratory and investigated with sufficient control to reduce factors that may confound experimental results.

Field Characterization of the Selected Natural INEEL Rhizosphere Ecosystem

Results from the detailed characterization of the natural rhizosphere system support the selection of those ecological and physicochemical components that must be incorporated into a growth chamber or greenhouse-based physical model rhizosphere system. First, we used modeling and simulating ecological population dynamics and physicochemical response curves of key plant and microbe nutrients and growth factors that affect symbiotic or antagonistic associations to mimic the natural system in the laboratory. From that laboratory baseline, we used the computer model developed in the following task as a basis for generating hypotheses to be investigated in the laboratory rhizosphere system. These laboratory manipulation studies defined the desired biological and abiotic factors and their associated temporal profiles to facilitate survival, competitive dominance, and symbiotic functions that extract Cs from soil under a wide range of potential "real-world" conditions.

Mineralogy of the Site

There have been several mineralogical analyses of surficial materials, sedimentary interbeds, and basalt at the INEEL site. Bartholomay et al. summarized these analyses and used the results with additional analyses to determine the correlation of different geological units with potential source areas.[1] The mineralogy of the sedimentary interbeds at Test Area North correlate with the Birch Creek drainage, while those at the Radioactive Waste Management Complex (RWMC), Test Reactor Area, and Idaho Chemical Processing Plant (now the Idaho Nuclear Technology and Engineering Center) correlate with

the Big Lost River drainage.[2] Bartholomay suggests that the sedimentary interbeds at the INEEL site were deposited in a depositional basin similar to the present day basin.

The sediments near the SL-1 site are mapped as loess.[3] These windblown materials were likely derived from the sediments of the Big Lost River, Little Lost River, and Birch Creek. The analyses from a pit and cores near RWMC are likely to be the most useful for determining the potential mineralogy at the rhizosphere study site.[4]

Based on these previous studies, we expect that the surficial sediments at the rhizosphere study site will be comprised of quartz, feldspars, pyroxenes, and clays; the clays will be predominantly illite and mixed I/S with some smectite and kaolinite; some micas may also be present in the soil; and paleosols containing increased amounts of iron hydroxides but relatively low amounts of calcite may exist within a few meters of the surface.

Soil and Plant Sample Collection and Analysis Methods

We conducted sampling on two plots in the uncontaminated zone surrounding the SL-1 burial ground—one disturbed and one undisturbed. The disturbed plot contains considerable gravel, and is bound by gravel roads on three sides and an exclusion fence on the fourth. The area has been scraped and planted with crested wheatgrass that now constitutes the dominant plant species within the plot. The undisturbed site is about 200 m north of the disturbed site, and is characterized by a native sagebrush and/or steppe plant community common to the INEEL. Both plots were located using geodetic survey point (GSP), and mapped using geographical information system (GIS). The purpose of including both a disturbed and an undisturbed site in the study is to determine the effects of disturbance on the various processes that influence Cs uptake. A site within the SL-1 CERCLA area known to be contaminated was added during FY 2001.

Eleven sampling points within the disturbed site were identified and marked with flags, and three 25 ft vegetation transects were established. These transects were used to determine plant cover on a monthly basis. The sampling points and transects were selected to provide a reasonable representation of the plot, and spaced so as to lend to spatial interpolation or kriging. One of the 11 sampling points was subsequently eliminated because sampling at that location was found to influence the transect data. The boundaries of the undisturbed site were selected to approximate the size of the disturbed site. Because the undisturbed site appeared much more homogeneous than the disturbed site, nine sampling points were selected systematically within the plot. Three transects were also established within the undisturbed site.

Samples were collected monthly at both uncontaminated sites (disturbed and undisturbed) starting in July 2000. These samples included bulk soil for nutrient analysis, bulk soil for microbial analysis, wheatgrass rhizosphere soil for nutrient analysis, wheatgrass rhizosphere soil for microbial analysis, and above-ground wheatgrass tissue for nutrient analysis. During the initial sampling, all 20 points (11 disturbed and 9 undisturbed) were sampled. In subsequent sampling, samples were collected at only six sample points in each of the two sites because of the time required to process the microbial samples. Plant community structure was determined monthly for all six transects using the line-intercept method. Soil and vegetation analyses were conducted under contract by Western Laboratories of Parma, ID using established analytical methods.[5]

Soil Microbial Analysis Methods

For bulk soil samples, approximately 1 g of soil (weighed) was suspended in 100 mL of sterile distilled water and shaken for approximately 20 minutes. From this suspension, serial 10-fold dilutions were made by transferring 0.5 mL into 4.5 mL sterile distilled water in a fresh tube. Triplicate 0.1 mL

aliquots from appropriate dilutions were then inoculated onto plates using a spreader, and the plates incubated at room temperature for 2 to 3 days. For the rhizosphere soil samples, approximately 8 to 12 g of roots, with their associated monolayer of soil, were cut from the root mass, weighed, and put into sterile flasks along with 100 mL of sterile distilled water. The flasks were shaken for approximately 20 minutes to wash off and suspend the microorganisms; the 100-mL sample was then treated the same as for the bulk soil. After all inoculations onto the plates, the roots were thoroughly rinsed over a screen, blotted, allowed to air dry, and weighed. The weight of soil sample (that dislodged from the roots) was calculated by difference. Selected dilutions from each sample were inoculated onto plates containing four different types of media: one-tenth-strength tryptic soy agar, to enumerate total heterotrophs; one-tenth tryptic soy agar containing neutral red, to look for acid producers; minimal medium containing 1 g/L phenol as a sole carbon and energy source, to enumerate phenol degraders; and minimal medium containing a mixture of three organic acids (citric, succinic, and lactic) as sole sources of carbon and energy, to enumerate organic acid metabolizers.

Development and Assembly of Simplified Laboratory Artifical Rhizosphere

Creating and maintaining sterile conditions in the plant root zone is a challenging but necessary task if compounding biological and ecological parameters are to be included in experiments in a logical, stepwise progression. The root-zone environment is ideal for the rapid growth of a wide range of microorganisms.[6] Creating sterile conditions requires that all parts of the project apparatus and the germinating seedlings be sterile. The project apparatus was constructed using inert, autoclavable materials, which are autoclaved prior to each study. Obtaining sterile seedlings was more challenging. After exposure to the sterilizing environment, the seeds were thoroughly rinsed in sterile deionized water and germinated on nonselective agar to confirm sterility. The safest, most effective seed treatment procedures were identified and used in subsequent studies. After germination, seedlings were transferred in a sterile hood to sterile plant growth containers custom designed for these studies.

Our sterile plant culture container was modified from similar designs used by other workers.[7,8,9] A dilute nutrient refill solution is added daily to replenish the solution removed in transpiration. We have done extensive work to develop the composition of this solution so that it replaces both the nutrients and the water without the need to drain and replace the entire contents of the container.[10,11,12]

The same apparatus will be used for studies in solid porous media. These studies will be conducted by filling the root zone volume with either small diameter glass beads or silica sand. The water status in the root zone will be maintained by daily addition of nutrient solution to replace transpiration. Water loss in transpiration will be determined by periodically weighing the vessels. Using a relatively inert substrate, such as glass beads, is important to the recovery of exudates, which quickly bind to organic matter and clays in soils. Exudates will be recovered by drawing a solution sample from the porous media.

Modeling Cesium Bioavailability as Affected by the Rhizosphere Ecosystem

The goal of this effort was to model the geochemical, biological, and physical factors affecting Cs solubilization in the rhizosphere. To accomplish the goal we needed to (a) develop a comprehensive conceptual model that integrates the various effects on Cs solubilization, (b) develop a quantitative mathematical model relating root exudates and Cs solubilization, and (c) incorporate the exudate model into the comprehensive model. The conceptual and quantitative models were to be implemented iteratively for validation and refinement.

To achieve these objectives, we first identified the factors and relationships affecting Cs solubilization and then selected those assumed to warrant inclusion in the comprehensive conceptual model. A model rhizosphere system was also chosen such that the parameters of the model plant/soil system to be studied could be investigated with sufficient control. A preliminary conceptual model established basic associations using software that allowed these relationships to be set up in sectors, with each sector representing a submodel. Available data was used to determine functional relationships within and among submodels. Parametric values were evaluated only for functional relationships that were well understood and properly presented in the literature or experimental data. The conceptual model code was validated and the performance evaluated and refined as needed. We developed the exudate model using field and experimental data to characterize exudate production and fate in the rhizosphere system. The rate of binding and release of Cs^+ from phyllosilicates, commonly found at INEEL and DOE sites and known to bind Cs, were quantified. A mathematical model relating the aqueous concentration and release rate of root exudates to Cs solubilization was developed based on field and experimental data. Using additional experimental data, the equation(s) were solved and the results used to evaluate and update the specific model. Finally, the exudate model was incorporated into the comprehensive conceptual model, which was then evaluated and refined as needed.

ACCOMPLISHMENTS

Selecting a Rhizosphere System

For the model we selected a crested wheatgrass (*Agropyron cristatum*) ecosystem growing in and around Cs contaminated soil; the model system was also practical and relevant to cesium (Cs) contamination within INEEL soils. Crested wheatgrass is a perennial bunch grass native to the steppes of Asia and very tolerant of high temperatures and low moisture, typical of the arid environment of the INEEL and Intermountain West (see Figure 1). The model rhizosphere system is of interest to DOE, but even more so, the INEEL. We chose INEEL field sites at Waste Area Group (WAG) 5 (SL-1) and the Central Facilities Area (CFA) drainfield (CFA-08; WAG 4) to represent a natural crested wheatgrass ecosystem for evaluation of the biological and ecological parameters.

Figure 1. A planted crested wheatgrass stand on a disturbed site outside the radiologically contaminated area at SL-1 (INEEL WAG 5).

Field Characterization of Selected Natural INEEL Rhizosphere Ecosystem

We established two study plots near SL-1 and located and mapped their boundaries, sampling locations, and transects (see Figures 2, 3, and 4). An accident in January 1960 resulted in approximately 100-acres being contaminated with radiocesium. Previous radiological surveys of area soils have identified the highly contaminated area, which is controlled (fenced with locked gate and the fenced area designated as a radiological controlled area) to limit personnel access.

We started field characterization of the two plots outside this highly contaminated area during the summer of 2000. One plot was disturbed during the movement of materials from the SL-1 accident, as evidenced by the planted crested wheatgrass. The second plot is undisturbed as evidenced by the prevalence of native sagebrush (*Artemisia* spp.) and fescue (*Festuca* spp.). A third plot was located within the highly contaminated area.

We sampled and characterized both the Cs contaminated site and the uncontaminated control site at SL1. Both were similar to the undisturbed ecosystem previously characterized. Access to and sample analysis from the contaminated site was considered a major accomplishment. Sampling was initiated in April 2001, and conducted on three dates that captured crested wheatgrass development from emergence to boot stage—a complete growth cycle.

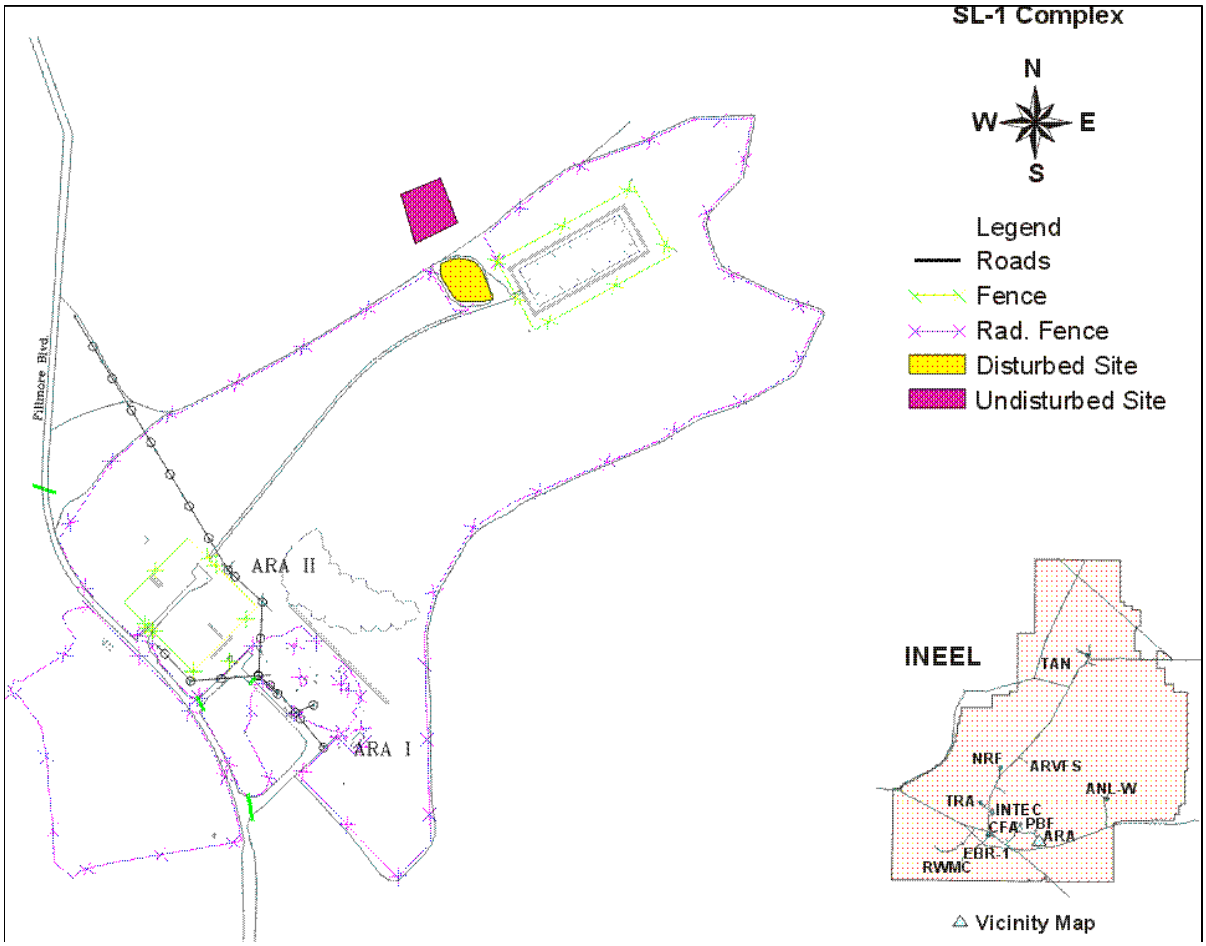

Figure 2. Study plot locations near SL-1.

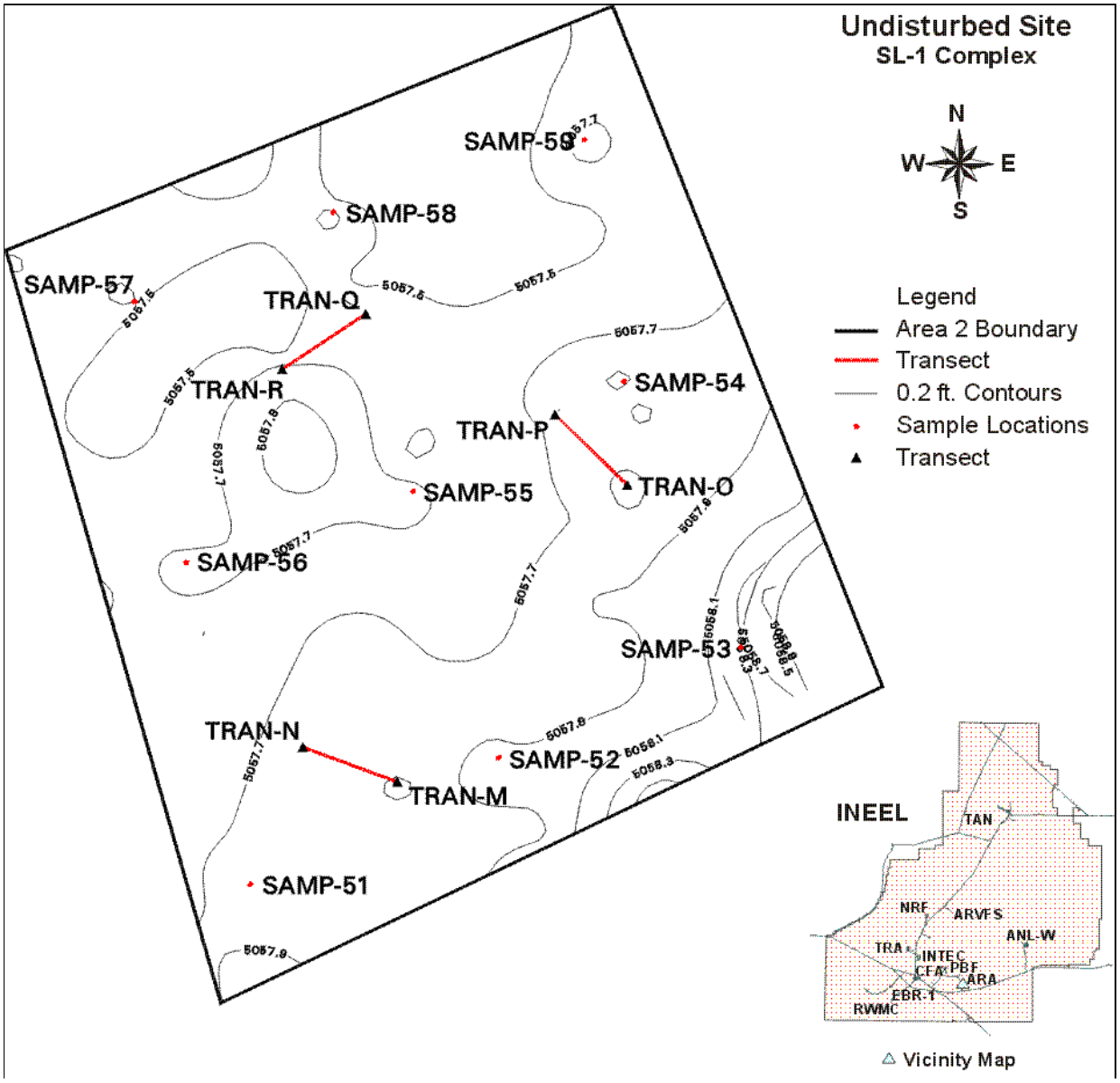

Figure 3. Undisturbed study plot showing sampling locations and vegetation transect.

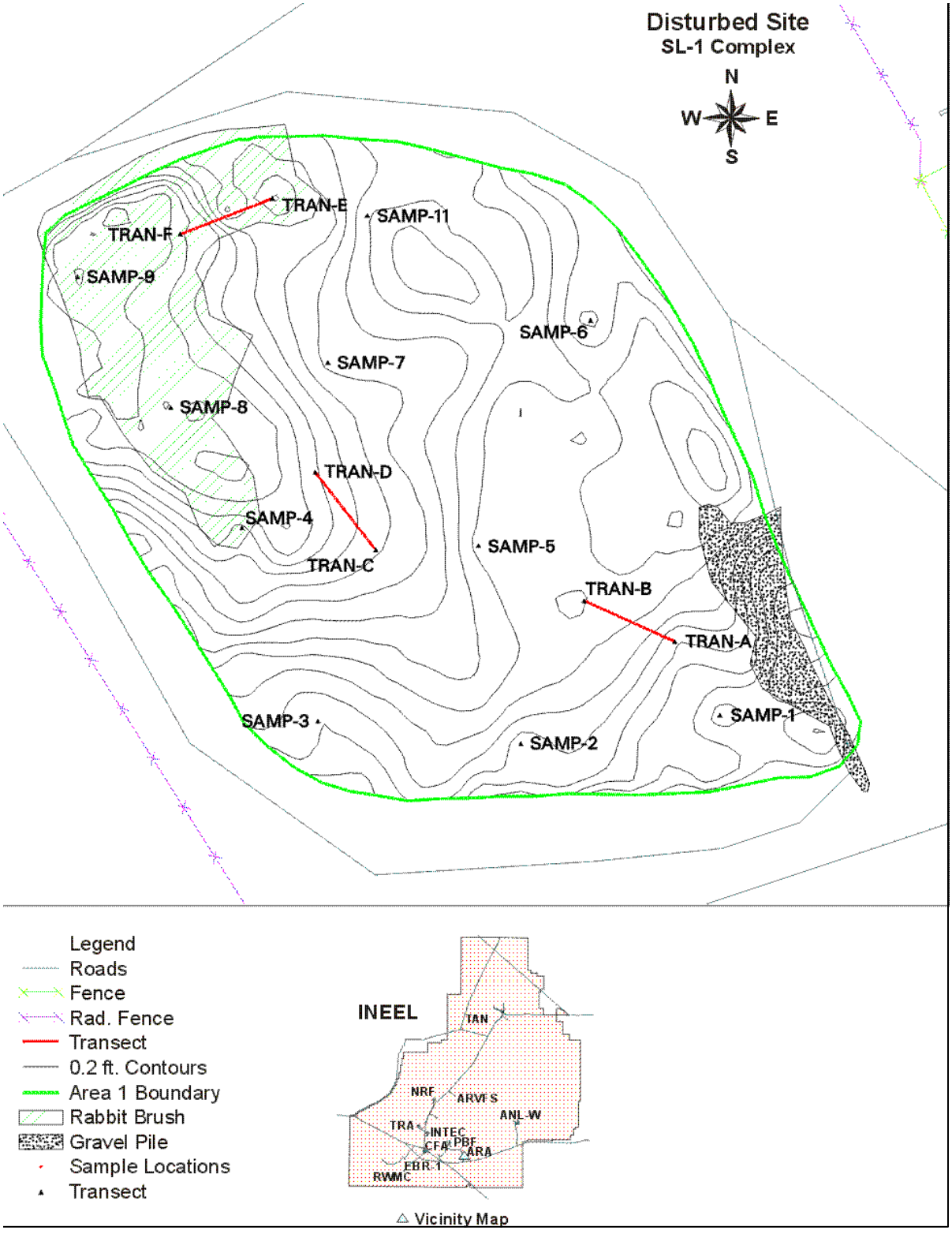

Figure 4. Disturbed study plot showing sampling locations and vegetation transect.

At the uncontaminated site, we obtained bulk soil, root zone soil, crested wheatgrass shoots, and crested wheatgrass roots for analysis. We sampled eight locations within the uncontaminated area were on all three sampling dates (April, May, and June 2001). Plant development was assessed in the field through visual assessment of growth stage and measurement of plant height. Eight locations were sampled within the contaminated site in April, but only three locations were sampled in May and June. These sample locations were strategically selected so that information from the physiological assessment of the cold site and the April sampling could be used to extrapolate the data from limited sampling in the latter dates. This was done to minimize costs associated with sample analysis. Bulk soil, root zone soil, crested wheatgrass shoots, and crested wheatgrass roots were obtained for analysis. As in the uncontaminated site, plant development was assessed in the field through visual assessment of growth stage and measurement of plant height.

Soil Sampling and Analysis Accomplishments

From July through October 2000, 100 soil samples were collected and analyzed by Western Laboratories. As expected, the analyses showed a much greater variability in most parameters among the samples from the disturbed site compared to the undisturbed site.

Lessons learned on soil sampling from the 2000 field season are as follows:

- To better understand the spatial variation we must take frequent soil samples from all sample locations and have them analyzed, rather than restricting the sampling to the same number of samples that can be accommodated for microbial analyses.

- To better understand the temporal changes we must begin sampling as early in the season as possible and continue as late into the fall as possible.

The characterization of soil samples collected from the SL1 disturbed and undisturbed sites in 2000 was completed in 2001. All samples were from uncontaminated areas. A suite of agronomic parameters was measured. A statistical analysis of the data was completed that allowed us to compare soil characteristics between disturbed versus undisturbed sites and between root versus bulk soil.

We have hypothesized that Cs is bound primarily to phyllosilicate minerals, particularly mica and illite, and that soil bound Cs, much like K, exists in both a more easily exchangeable pool and a tightly bound fixed pool. The easily exchangeable pool is expected to be associated with the surfaces of oxide minerals and organic matter and more readily available for plant uptake. The recalcitrant pool is associated with the interlayers of phyllosilicates (See Figure 5).

Quantification of K concentration, organic matter, and cation exchange capacity may serve as an indication of the available sites for exchangeable Cs to bind to in these soils. Further, we have hypothesized that the plant root systems facilitate the movement of Cs from the fixed pool to the exchangeable pool through a weathering mechanism that increases the exchangeable site concentrations in the soil. We would therefore expect that the vegetation present at a field site would influence the weathering process and rate of Cs transfer between fixed and exchangeable pools (see Figure 6).

Soil samples (both bulk soil and root soil) collected in 2001 from all locations and all sampling dates for the uncontaminated site were analyzed for total Cs concentration, easily extractable Cs concentration, moisture content, bulk density, buffer capacity by acid-base titration, and a suite of agronomic chemical analyses. Total and radiocesium concentrations were measured for soil samples from the contaminated area. Analysis results of the field soil samples suggest that the concentration of exchangable sites is greater in both the root zone and the undisturbed site, which has a more mature plant community.

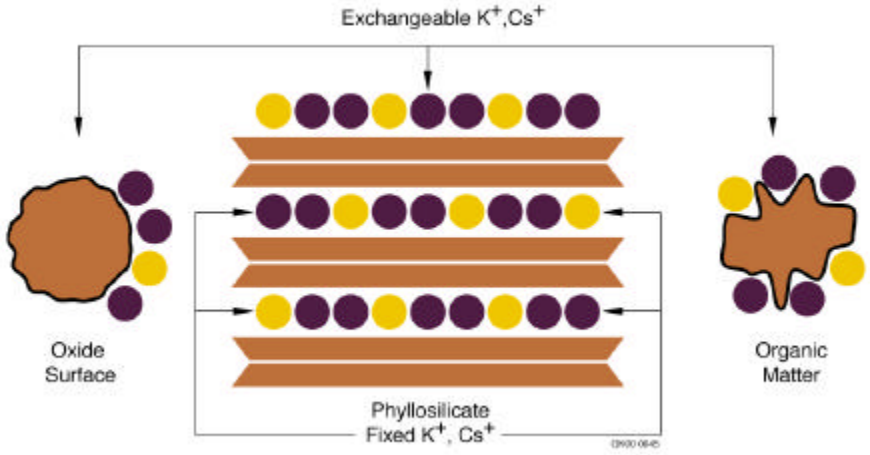

Figure 5. Expected pools of soil bound cesium.

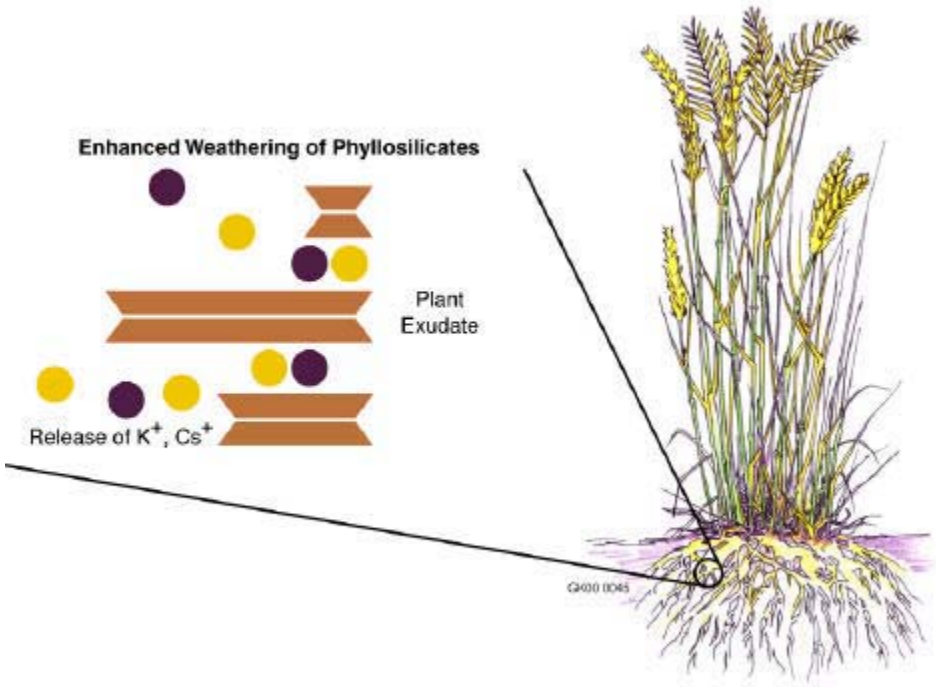

Figure 6. Hypothesized mechanism of plant facilitated release of Cs and K from phyllosilicate minerals.

The results of the acid-base titration indicate a reasonably large buffer intensity for the INEEL soils. The results will be used in the modeling effort to account for changes in pH due to the addition of organic acids excreted from plant roots. This information is needed to predict the weathering rates and hence the rate of Cs release from soils.

Vegetation Sampling and Analysis Accomplishments

Three vegetation transects were established in each of the two plots. Transect data collected in the summer showed that we were introducing too much variability, which we remedied in September 2000.

Lessons learned from the 2000 field season on vegetation transect sampling are as follows:

- The transect line must be inflexible
- Methods must be established to measure the early season small ephemeral plants that will grow next spring for a short time period
- Other methods must be examined to better measure the plant community's composition, size, canopy, and root volume.

The method and capability to quantify root and shoot morphology and physiology from field samples was developed in 2001. The WinRHIZO system was acquired, set up, and adapted for analysis of 2001 field collected crested wheatgrass root and shoot samples (from the uncontaminated site only). WinRHIZO is an automatic and interactive image analysis system specifically designed for root measurement including morphology, topology, architecture, color, and disease analysis.

A sample collection, preparation, and analysis method was designed such that root characteristics measured for subsamples of field-collected roots using the WinRHIZO system could be expressed in terms of volume of soil. Entire grass plant root systems were extracted from the field and subsamples prepared and root area, length, and mass measured. In addition, the plant shoots from entire crested wheatgrass plants were collected and sampled. A photosynthetic area was determined using the WinRHIZO system. Mass and plant size and total Cs concentration in the root and shoot biomass were measured (presented below in Cs partitioning section).

Statistical analyses on the field plant physiological data for the plant samples from the uncontaminated site were conducted using Statgraphics Plus 5.0. The first objective of these analyses was to compare the data collected from the two sampling dates and the data from each sample location; the second was to determine correlations between the various parameters.

Plant sampling and analysis from the contaminated site was minimal due to cost. However, based on the data obtained from analysis of plant shoot and root biomass samples taken during the growing period at the uncontaminated site, we were able to obtain enough detailed physiological characterization of the plants to determine the shoot/root ratios of Cs as a function of physiological status. This will now allow us to use plant growth and development parameters collected on the contaminated site to extrapolate transfer of Cs from roots to shoots in with a minimal number of samples.

Environmental factors were also measured continuously throughout the field season for FY 2001. Data was acquired from the nearby NOAA station. This data will allow us to estimate growth-controlling parameters such as heat units and evapotranspiration rates. These parameters can then be correlated with the detailed plant growth and development data collected and used to determine the relationship between environmental growth conditions and Cs transfer.

Cesium Partitioning

Statistical analyses on the Cs partitioning data for the soil samples collected during April, May, and June 2001 were conducted using Statgraphics Plus 5.0. The first objective was to summarize the mean,

standard deviation and median of Cs concentrations in each pool (bulk soil, rhizosphere soil, roots, and shoots) according to Cs type (radiocesium and stable Cs). The second objective of these analyses was to compare the uptake of Cs by the various pools. We also made comparisons between sampling dates.

The plant analysis data, combined with the Cs characterization of the soils collected with the plant samples, provides the data necessary to calculate Cs transfer factors between bulk soil, root zone soil, roots, and shoots as a function of stage of plant development. In addition, the data obtained from the contaminated site will now allow us to understand the relationship between the movement of total Cs and radiocesium, and determine if stable Cs can be used to predict the fate of radiocesium in the rhizosphere.

Microbial Analyses Accomplishments

Preliminary data from the microbial analyses of the bulk soil and rhizosphere soil indicate the following trends:

≠# For the bulk soil samples:

- The heterotroph numbers are generally between 10^5 and 10^6 per gram.
- Acid degraders and phenol degraders are uniformly very low, either below detection limits or between 10^3 and 10^4 per gram.

≠# For the rhizosphere soil samples (these numbers have not yet been corrected for the amount of soil sampled and will probably fall):

- Heterotrophs are generally between 10^7 and 10^8 per gram, i.e., roughly 10 to 100Δ as many as in the bulk soil.
- Phenol degraders are below detection limits in most samples.
- Numbers for the acid degraders varied more than for the heterotrophs. A majority of samples fell in the range of high 10^6 to low 10^7, but a few were in the high 10^5 to low 10^6. Generally acid degraders were in the range of 10 to 30% of the heterotroph counts, whereas in the bulk soil they were generally closer to 1% of the heterotrophs.

Several of the analyses cannot yet be interpreted because the numbers for the plates at the various dilutions do not follow the 10-fold dilutions used to generate the inocula.

Development and Assembly of a Simplified Laboratory Artifical Rhizosphere

The Utah State University (USU) Crop Physiology Laboratory was contracted to develop an artificial rhizosphere environment with liquid and solid-phase hydroponic technologies to be used in examining crested wheatgrass exudate production. A graduate student was hired to help. As a result, genotypes of crested wheatgrass were selected, hydroponic systems for culturing those plants were constructed, extensive literature was reviewed, and detailed experimental plans were completed.

We discovered that creating and maintaining sterile conditions in the root zone is a challenging task. The root zone environment is ideal for the rapid growth of a wide range of micro-organisms and efforts to reduce microbial activity with antibiotics have been largely unsuccessful.[13] All components of

the plant growth system and the seeds must be sterilized and this sterility must be maintained throughout the duration of the study.

Seed Selection and Sterilization

Seed sterilization requires an aggressive treatment that typically decreases seed vigor. We rigorously selected the highest quality seed for sterilization. Seed sterilization techniques must eliminate all microorganisms with minimal effects on seed vigor. After several preliminary tests, we were surprised to find that the highest Clorox concentration and the longest time interval were necessary to obtain a high fraction of sterile seeds. Fortunately, this aggressive treatment did not significantly reduce seedling vigor.

Development of the Plant Growth Container

Several designs for plant growth in inert, sterile media have been published, but all have limitations. We combined ideas from previous designs and developed a unique plant growth container that supports rapid plant growth with a sterile root-zone (Figure 7). After conducting several preliminary studies using different growth media, Ottawa sand was selected as the growth medium because it is relatively inert, autoclavable, and has relatively good water holding capacity. We conducted a plant growth test of crested wheatgrass in three sizes of Ottawa sand grains to determine the tradeoff between water-holding capacity and air filled porosity; as a result, we used a 5-layer gradient of sand.

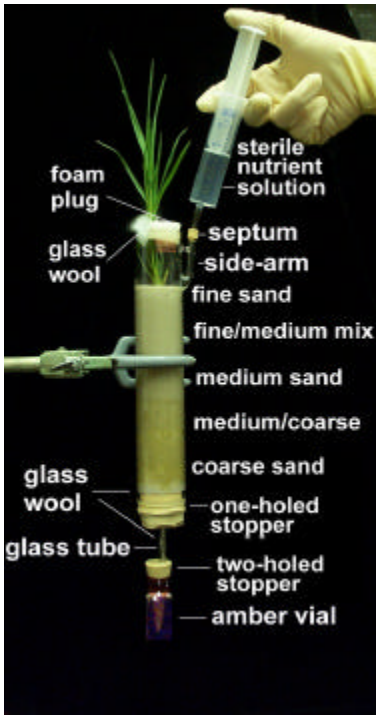

Figure 7. Plant growth container.

Procedures for Assembling System Components

We discovered significant organic contamination of the Ottawa sand that could not be removed by washing with a 0.1 molar NaOH solution (followed by a thorough deionized water rinse). After discussing several potential treatments to remove it we determined that heating the sand in a muffle

furnace at 550∀C for at least 10 hours is the most effective method of minimizing organic contamination from the sand. After muffling, the sand is packed into the five layers of the column.

We were surprised to find that the glass wool was also contaminated with organic matter. This contamination can be removed by thoroughly washing the glass wool with deionized water. We have switched to using silanized glass wool, which is deactivated by treatment with silane. Silanized glass wool contains less organic contaminants than standard reagent grade glass wool, and it has a lower affinity for binding organic matter. We are now using silanized glass wool in all studies, and silicone stoppers instead of rubber stoppers to minimize the carbon contamination from the stopper.

Sterilizing System Components Prior to Planting

After assembly, columns are autoclaved twice, 24 hours apart, placed in boxes to shield the root zone from light, and placed in the growth chamber.

Plant Growth Conditions

Sterile plants are grown in a reach-in plant growth chamber where the columns are housed in boxes that shield the root zones and leachate collection vials from light (see Figure 8). The photo-period and daytime and nighttime temperatures are set. The plants are watered every other day with a complete nutrient solution, at which time the leachate is also collected.

Figure 8. Planted columns inside of the growth chamber (left). Removal of the black front panel allows easy access to the leachate collection vials (right).

Verification of Sterility

Once a week, samples of both leachate and the sand from the top surface of the column are plated on one-tenth-strength nutrient agar to check for microbial contamination. Our contamination tests indicate differences between contamination detected in the surface sand and contamination in the leachate. We expected that most contamination originates at the top of the column, from watering or changing the foam plug, and that contamination would be detected first in the surface sand.

Modeling Cesium Bioavailability as Affected by the Rhizosphere Ecosystem

After first identifying the key variables affecting Cs solubilization in the rhizosphere, we categorized the factors. We then selected the relationships within and between these categories assumed to warrant inclusion in the comprehensive conceptual model. This selection was based on hypotheses developed from the initial literature review.

The modeling effort is being implemented using Systems Thinking, which integrates the relationships between the many factors affecting Cs solubilization. To date, we have established the basic associations using software (Stella/iThink) based on this approach. The software (developed by High Performance Systems, Inc., Hanover, New Hampshire) allows for these relationships to be set up in sectors, with each sector representing a submodel. The submodels are defined as geochemistry, physical factors, root system density, microorganisms, nutrients, and root exudates. A seventh submodel relates the three specific forms of Cs (bound, aqueous, and phytoextracted), and is the most critical element of the comprehensive model being developed. The basic relationships within each submodel, as well as the interactions between submodels have been established. This approach allows for expertise in defining each sector while simultaneously promoting the ecological packet.

Conceptual Comprehensive Model

The conceptual comprehensive model has been implemented using the Stella 6.0 software. User interface files have been created in Microsoft Excel, facilitating the model's practicality in modifying parametric values. Figure 9 presents an overview of the model. Functional relationships within and between the submodels drive the comprehensive model and define its required inputs.

Currently, hypothetical data consistent with those presented in the literature are used to define the relationships. However, statistical analyses have been performed on available field characterization data, which have been used to replace hypothetical data and guide future field characterization tasks. The Cs fate submodel includes the most critical functional relationships (for the flows between the bound phase and the aqueous phase and between the aqueous phase and the phytoextracted phase ($Flow_{sol}$ and $Flow_{phy}$, respectively). The codes for these relationships have been derived and incorporated into the model.

The power of Stella lies in its ability to integrate the variables within and between submodels. Each submodel may also be analyzed individually or with selected other submodels. Running the model for a selected sector isolates the efficacy of that sector by holding elements outside the sector constant at their initial values. Sensitivity analyses isolate the effects of individual factors on the model output.

Numerical Root Exudates Submodel

The modeling effort currently focuses on the effects that the root exudates have on Cs solubilization. Literature has been used to formulate the functional relationships and estimate parametric values within the root exudate submodel and between the root exudate submodel and the geochemistry and Cs fate submodels. Sensitivity analyses have been performed to assess the effects that the exudates have on Cs partitioning, as well as the effects that certain parameters outside these submodels have on the root exudates and accordingly Cs partitioning.

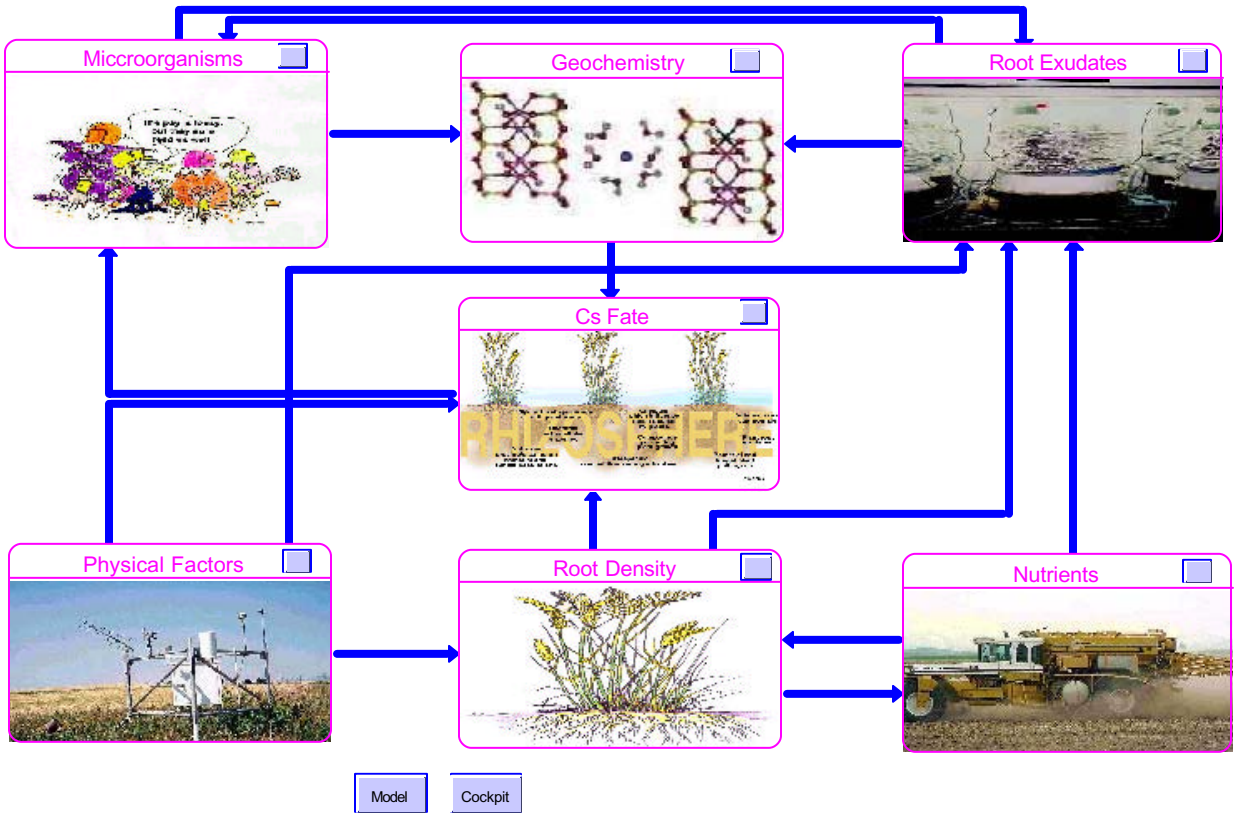

Figure 9. Interface level of Stella software indicating the Cs Fate sector and the six sectors affecting it.

Other Accomplishments

WAG 4 requested the assistance of the rhizosphere engineering team in determining vegetation uptake and Cs movement at the CFA-08 sewage treatment plant drainfield located at the Central Facilities Area (CFA). The milestones for this work were as follows:

1. Sample vegetation from three plant species found on the drainfield and on a control site, and sample the soil adjacent to the plants at each sample location. Analyze the samples for Cs-137, total elemental Cs, and extractable nitrates in the soil.

2. Compile the results of the sample collection and analysis and the literature review and present the information at a Decision Analysis Forum for WAG 4 where the current Record of Decision (ROD) for the site was being reconsidered.

3. Participate as a voting member in the Decision Analysis Forum for WAG 4, where we determined that there was sufficient data to merit a reconsideration of the current ROD for CFA-08.

4. Prepare a final report of the characterization results and literature review.

Results

We met the milestone for sample collection and analysis as follows:

- All of the plants (crested wheatgrass, sagebrush, and rabbit brush) accumulated detectable levels of Cs-137.
- Cs-137 was found to be accumulating at significant levels in the roots of crested wheatgrass on the CFA-08 drainfield.
- Elemental Cs was found at about 3 ppm on both the control site and the CFA-08 drainfield.
- Cs-137 did not contribute to the overall elemental Cs concentration.
- Cs is migrating upward in the soil. This upward mobility is assumed to be a result of vegetation creating an upward hydraulic gradient.
- A major issue and concern that developed within the rhizosphere project was the amount of training required to conduct the field research. This training consumed a significant amount of the budget and time, causing fieldwork to be delayed. However, being able to leverage our scientific knowledge in support of Operations problems within the WAGs gives us additional field experience and opportunities to learn more about the rhizosphere, and shows the significance and potential benefit of our rhizosphere project in support of environmental management problems and issues at INEEL and elsewhere.

The report for the WAG manager was completed and follow-on work with INEEL Operations is being pursued. We presented the results from this work in March 2001 at the 2001 11th Annual West Coast Conference on Contaminated Soils, Sediments, and Water held in San Diego, CA. The presentation was titled, "Cesium Concentrations in Idaho National Engineering and Environmental Laboratory Soil and Vegetation." A manuscript is being prepared for journal submittal.

One member of the research team (Lawrence Cook) enrolled in the Ph.D. program at Idaho State University through the Department of Biological Sciences. This summer he completed the first of two planned field seasons for sampling the soils and vegetation of the Eastern Snake River Plain as part of a survey to determine the distribution of stable cesium and strontium across the region. This survey constitutes the first of two phases of his thesis research. Information from this survey will be used in planning field phytoremediation trials for removing cesium and strontium from soils at the INEEL using an assemblage of native plant species. Eventually this approach could be used to remediate radionuclide-contaminated soils at the INEEL. Also, knowledge of cesium and strontium uptake is helpful to radioactive waste facility operators, since native vegetation may absorb and transfer radioactive isotopes of cesium and strontium from breached waste containers to the ground surface.

REFERENCES

1. R. C. Bartholomay, L. L. Knowbel, and L. C. Davis, "Mineralogy and Grain Size of Surficial Sediment from the Big Lost River Drainage and Vicinity, with Chemical and Physical Characteristics of Geologic Materials from Selected Sites at the Idaho National Engineering Laboratory, Idaho," *U.S. Geological Survey*, 1989, p. 74.

2. R. C. Bartholomay, "Mineralogical Correlation of Surficial Sediment From area Drainages with Selected Sedimentary Interbeds at the Idaho National Engineering Laboratory, Idaho," *U.S. Geological Survey*, 1990, p. 18.

3. G. L. Olson and D. J. Jeppson, "Idaho National Engineering Laboratory Soils Map," 1995.

4. C. T. Rightmire and B. D. Lewis, "Hydrogeology and Geochemistry of the Unsaturated Zone, Radioactive Waste Management Complex, Idaho National Engineering Laboratory, Idaho," *U.S. Geological Survey*, 1987, p. 89.

5. R. O. Miller, J. Kotuby-Amacher, and J. B. Rodriguez, "Western States Laboratory Proficiency Testing Program Soil and Plant Analytical Methods," Ver 4.10, 1998; from R. G. Gavlak, D. A. Horneck, R. O. Miller, *Plant, Soil and Water Reference Methods for the Western Region*, WREP 125, 1994.

6. D. Smart, A. Ferro, K. Ritchie, and B. Bugbee, "On the Use of Antibiotics to Reduce Rhizoplane Microbial Populations in Root Physiology and Ecology Investigations." *Physiol. Plantarum,* Vol. 95*,* 1995, pp. 533–540.

7. A. J. M. Smucker, and A. E. Erickson, "An Aseptic Mist Chamber System: A Method for Measuring Root Processes of Peas," *Agron. J.,* Vol. 68. 1976, pp. 59–62.

8. E. Benizri, A. Courtade, and A. Guckert, "Fate of Two Microoorganisms In Maize Simulated Rhizosphere Under Hydroponic Sterile Conditions," *Soil Biol. Biochem.,* Vol. 27(1.), 1995, pp.71–77.

9. V. Groleau-Renaud, S. Plantureux, and A.Guckert, "Influence of Plant Morphology on Root Exudation of Maize Subjected to Mechanical Impedance In Hydroponic Conditions," *Plant Soil,* Vol. 201, 1998, pp. 231–329.

10. B. Bugbee and F. B. Salisbury, "An Evaluation of MES (2(N-Mor-pholino)Ethanesulfonic Acid) and Amberlite IRC-50 as pH Buffers for Nutrient Solution Studies," *J. Plant Nutr*., Vol. 8, 1988, pp. 567–583.

11. T. Grotenhuis and B. Bugbee, "Super-Optimal CO_2 Reduces Seed Yield but Not Vegetative Growth in Wheat." *Crop Sci.,* Vol. 37, 1997, pp. 1215–1222.

12. O. Monje and B. Bugbee, "Adaptation to High CO_2 Concentration In an Optimal Environment: Radiation Capture, Canopy Quantum Yield, and Carbon Use Effic iency, *Plant, Cell, and Environment,* Vol. 21, 1998, pp. 315–324.

13. D. Smart, K. Ritchie, J. Stark, and B. Bugbee, "Evidence that Elevated CO_2 Levels Can Indirectly Increase Rhizosphere Denitrifier Activity," *Applied & Environmental Microbiology*, Vol. 63, 1997, pp. 4621–4624.

Investigation of Factors Influencing Cesium Mobility and Uptake in Plant/soil Systems

Melinda A. Hamilton and Carl D. Palmer

SUMMARY

This research task focused on biogeochemical processes that affect the mobility and bioavailability of metals in the rhizosphere. We combined the information obtained from this task with the ecological and biological understanding of rhizosphere gained from its sister task, "Ecological Engineering of Rhizosphere Systems," to develop a comprehensive understanding of fate of Cs in the rhizosphere. Many of the activities in this task are leveraging activities from that task, such as site selection, field characterization, and model development.

The objective of this research was to investigate specific biogeochemical processes occurring in plant soil systems that are necessary to engineer remediation technologies, which includes work at the molecu-lar and atomic scales. Environmental remediation applications for metal and mixed-waste contaminated soils that depend on the fundamental understanding of these processes will be the driver for this research. Metal bioavailability is a key factor in successfully developing biological remediation technologies; therefore, the important research objective for this project is to develop the capability to understand and predict the fate and transport of metals in plant/soil systems. Initial focus of this research is investigation of the binding, solubilization, mobility, and plant uptake of Cs in rhizosphere systems. The interaction of biomolecules (microbial or plant produced) with Cs will be investigated. This effort advances ecological engineering technologies that are unique and competitive, and that address pressing environmental problems or demands. The work continues in FY 2002 under the ESRA program.

PROJECT DESCRIPTION

The goal of this project was to develop a sufficient understanding of rhizosphere processes to allow for prediction, modeling, and ultimately the control of contaminants in the rhizosphere. The rhizosphere can be viewed as the window to the vadose zone. The knowledge gained will lead to the development of cost effective technologies for remediation of dispersed radionuclide/heavy metal and mixed waste contaminated soil in both vegetated surface soil and subsurface soil. The current focus of this project on Cs bioavailability directly supports STCG Need Statement ID-6.2.08, which expresses a need for understanding the mechanisms that control Cs binding and the need for removal technologies. Cs contamination is the number one contaminant (by number of sites) both at INEEL and across the DOE complex. The INEEL alone has more than 25 soil Cs contaminated soil plumes.

The objective of this research was to investigate, at molecular and atomic scales, specific biogeochemical processes occurring in plant/soil systems that are necessary to engineer remediation technologies. Environmental remediation applications for metal and mixed-waste contaminated soils that depend on the fundamental understanding of these processes will be the driver for this research. Metal bioavailability is a key factor in successfully developing biological remediation technologies. Therefore, the initial research objective for this project will be to develop the capability to understand and predict fate and transport of metals in plant/soil systems. Two research elements are considered imperative to developing an understanding of plant/soil ecology sufficient to allow engineering of plant/soil remediation technologies: rhizosphere biology (a molecular approach to plant and microbial genetics, biochemistry, and physiology), and geochemistry (an atomic approach to rhizosphere soil chemistry and physics). These rhizosphere biology and geochemistry studies focus on the biological and geochemical

phenomenon that greatly affects cesium (Cs) bioavailabilty in the rhizosphere of the crested wheatgrass ecosystem at the INEEL. These laboratory investigations focused on:

- Characterizing the quantity of plant root exudates and the quality of these exudates with respect to metal bioavailability

- Characterizing the quantity and quality of rhizosphere bacterial secreted Cs chelators

- Determining how Cs is bound to reactive mineral phases in soils at the INEEL and elsewhere

- Combining the biological and geochemical phenomenon to determine the rate of Cs and potassium (which is chemically similar to Cs) release from reference clays in the absences and presence of key components of plant exudates and microbial chelators.

This approach combined scientific investigations on biogeochemical rhizosphere mechanism affecting metal bioavailability with the ecological and biological understanding of rhizosphere gained from the task, "Ecological Engineering of Rhizosphere Systems," to develop a more comprehensive understanding of fate of Cs in the rhizosphere.

Characterization of Crested Wheatgrass Root Exudates

The objective of this work is to identify root exudates from crested wheatgrass by quantifying the effect of environmental factors on the production of exudates. Root exudates are typically comprised of low-molecular-weight compounds including organic acids, sugars, phenols, and amino acids. The quantity and quality of these compounds have a significant effect on microbial activity in the rhizosphere and are important in the function of the plant/soil system. Some of these compounds can increase the mobility and bioavailability of metals such as Cs from contaminated soils.

Under a subcontract with the INEEL, the Utah State University (USU) Crop Physiology Laboratory performed experiments on crested wheatgrass using sterile root-zone environments. Solutions collected from these model systems are being analyzed to characterize root exudates. The amount and composition of these exudates were expected to vary with the type and amount of plant stress; therefore, USU examined the effects of nutrient, water, and oxygen stresses by manipulating these conditions in hydroponic and sterile media model systems (develop under the task, "Ecological Engineering of Rhizosphere Systems") to determine conditions that promote exudates production. The information obtained in this study is crucial to INEEL operations and DOE for their estimation of contaminant migration from the shallow soil system, the quantification of the bioavailability of metal contaminants, and their evaluation of potential remedial strategies of metals-contaminated soil. These specific studies involved:

- Experiments to recover and measure the quantity and quality of root exudates of select genotypes of crested wheatgrass in sterile hydroponic systems

- Experiments to measure the quantity and quality of root exudates as a function of plant stress, including nutrient availability (particularly K^+), nitrogen form, root-zone water potential, root-zone oxygen availability, and plant age

- Experiments to quantify the effect of microorganisms on the net rhizosphere production of organic compounds by comparing inoculated and sterile plant cultures.

Crested Wheatgrass Root Exudates Sterile Hydroponic Systems

"Hycrest" crested wheatgrass has been used by researchers at USU in phytoremediation studies,[1] but a new cultivar of crested wheatgrass (CD-II) is more vigorous and stress resistant than Hycrest. Using these cultivars, the root exudate quantity and quality of healthy (nonstressed) hydroponically grown crested wheatgrass plants is being studied at different stages of plant development. These studies are designed to determine the effect of physiological and morphological stages of plant growth and development during which exudate production occurs. To determine which factors have the greatest effect on exudate production, exudate production is being determined on the basis of total plant biomass, root biomass, and root density.

Exudates accumulate in the sterile hydroponic solution, but many exudates are too dilute for direct measurement. To address this challenge, aliquots of hydroponic solution will be concentrated on selective ion exchange columns. These columns will then be desorbed and analyzed.[2,3]

Initially, the exudate analysis focuses on the identification and quantification of acids because of their importance in metal complexation (oxalic and citric acid). The secretion of low molecular weight organic acids contributes to the acidification of the rhizosphere and possibly the formation of soluble metal complexes.

Root Exudates as A Function of Plant Stress

Root-zone stress damages membranes and it is generally thought that stress increases the rate of exudation from roots. These studies are examining the effect of three types of stress on exudate quantity and composition. Potassium stress is of particular interest because of its chemical similarity to Cs. Potassium stress is imposed in hydroponic culture by adding potassium at 10 and 50% of the concentration of the control. USU's previous experience indicates that these levels are sufficient to impose mild and severe potassium stress. Nutrient imbalances caused by excess potassium are rare and thus high levels of potassium are not being studied in these initial tests. A Cs toxicity/stress treatment is also being examined using nonradioactive $CsCl_2$ (available from Sigma Chemical Co.). The Cs concentration in hydroponic solution will be determined based on the naturally occurring Cs levels in the contaminated soils at sites of interest to the INEEL, which we have determined to be about 3 mg/kg.

The form of nitrogen available at the root surface determines rhizosphere pH and may significantly influence the efflux and type of exudates. Nitrogen represents over 80% of the ions absorbed by plant roots. All plant cells must maintain charge balance with the external solution; when nitrate is absorbed an OH^- ion is excreted, when ammonium is absorbed a H^+ ion is excreted. The rhizosphere pH can be up to 2 pH units above or below the bulk soil pH because of the effect of differential forms of nitrogen absorption. Nitrogen form can be manipulated in the field and readily manipulated in hydroponics.

Root zone oxygen availability can vary considerably in the field. Anaerobic conditions have a significant effect on the integrity of root membranes.[4] The effect of oxygen availability in the root zone will be studied by turning off the flow of air to the root zone in hydroponic culture. The oxygen in solution is depleted within a few hours and the resulting change in exudate efflux can be determined.

Root zone water potential will be studied using solid porous media. Polyethylene glycol (PEG) has been used to impose water stress in hydroponic culture, but plants can take up even high molecular weight PEG compounds and cause reduced, abnormal growth. Additionally, the PEG in solution may interfere with the analysis of exudates in the solution. Given that a hydroponic system can be developed that will allow the effective manipulation of root zone water potential for the purpose of studying exudate

production, exudates resulting from mild and severe water stress will be measured by eluting the organic compounds from the media

Effect of Microorganisms On the Net Efflux of Organic Compounds

To determine the net efflux of organic compounds as affected by microorganism, the hydroponic culture vessels will be inoculated with the prominent bacteria found in INEEL crested wheatgrass community soils. We anticipate using pseudomonas- and pseuomonad-like bacteria as of this writing, but the final selection will be determined by the characterization studies in the Ecological Engineering of Rhizosphere Systems task. Our experience with inoculation of hydroponic cultures suggests that the inoculation is much more effective if the microorganisms are cultured on a solid substrate, such as a diatomaceous earth, and the solid substrate is then added to the liquid hydroponic vessel.

Characterization of Cs Chelators Secreted by Bacteria

The purpose of this research is to determine whether bacteria present in the rhizosphere secrete compounds that affect the solubility and mobility of Cs and potentially other metals by chelating/binding those metals. To search for such compounds, bacteria will be grown in a minimal salts medium (medium B which we have been using for plating rhizosphere samples) with a neutral (nonmetal-binding) carbon and energy source, such as glucose or glycerol. After growth, all the bacteria will be removed by a combination of centrifugation (10 min. at 5,000 rpm) followed by filtration of the supernatant through a 0.2 σm filter. The cell-free supernatant will be analyzed by high performance liquid chromatography (HPLC) on a column (Brownlee Polypore H, 10 σm particle size) designed to separate small organic acids. Any nonmedium-derived peaks present in the chromatogram will be identified, by elution time if possible, and then subjected to mass spectrometry for either confirmation or initial identification. This supernatant will then be analyzed for binding to Cs as described below.

The bacteria to be evaluated in these experiments will be several individual isolates from INEEL rhizosphere samples collected in the Ecological Engineering of Rhizosphere Systems task, as well as consortia derived from those rhizosphere samples. Use of mixed populations allows one to test many individual bacteria in the same experiment, but requires isolation of the responsible individual strain if a positive result is observed for the mixed culture. In addition, consortia have a greater probability of degrading organic molecules that are secreted, thus leading to false negative results.

The above experiments will then be repeated, with the modification of growing the bacteria in the presence of Cs, using only bacterial strains previously found to be producing potentially chelating compounds. For these experiments the potassium concentration in the minimal medium will be reduced. The organic molecules in the cell free supernatant will again be analyzed by HPLC, and the chromatographic pattern will be compared to that produced in the absence of Cs. Peaks showing significant changes (newly appearing, significantly increased or decreased) will be identified. The compounds in this supernatant will then be analyzed for Cs binding activity as for the non-Cs-treated supernatant using the various assays described below. The difference for these analyses will be that the Cs will have to be removed from the supernatant, probably an ion exchange chromatography method, before analysis of chelator activity. For both potential chelator preparations ($^{+}$Cs) the activity of the total supernatant will be assayed first. If activity is observed, the various peaks separated by HPLC will be individually analyzed to identify the components possessing Cs binding activity.

Several types of assays will be initially investigated to determine which is best for analyzing Cs binding capability. One type is a spectrophotometric assay in which a complex possessing a well defined spectrum is formed between Cs and a known chelator. An aliquot of the sample containing potential chelator(s) is added, and if the Cs is removed from its complex with the known chelator by any

components of the sample, the spectrum of the complex will change. A second type of experiment is a chromatographic or electrophoretic shift experiment, in which the mobility of Cs is analyzed in the presence and absence of the potential chelator. Binding of Cs by a chelating molecule in the sample will alter the mobility of the Cs ions under such analytical conditions. A third type of experiment makes use of NMR. When potential chelators have been identified (see above), the NMR spectra of these organic molecules can be analyzed in the absence and presence of Cs. If there is a significant interaction of the organic molecule with the Cs ion, the NMR spectrum of the organic molecule will change.

Characterization of Cs Binding to Soils

The purpose of this work is to examine how Cs is bound to reactive mineral phases in soils at the INEEL and elsewhere. In some INEEL soils, Cs is very tightly bound and has proven almost impossible to remove from soil particles except by complete particle dissolution. There is some belief that Cs, as well as other contaminant metals, can become incorporated into the structure of reactive mineral phases; however, it is more probable that contaminants are strongly bound to minerals in some very tight manner. The latter concept has not been proven or demonstrated on INEEL soils. The strong association with certain mineral types, primarily highly charged 2:1 phyllosilicates, is thought to be by intercalation and fixation. The latter process may be due to replacement of potassium in the crystalline matrix of the mineral. For these studies, the Savannah River Ecology Laboratory, operated by the University of Georgia, is:

- Characterizing mineral and organic constituents of soils from the INEEL and elsewhere, and determining their associated physicochemical properties
- Determining the association of Cs with reactive mineral phases in soils
- Determining the primary mineral phases controlling Cs sorption in soils
- Investigating Cs short-term sorption/desorption mechanisms in soils.

The characterization phase of the study will involve complete chemical and mineralogical analyses of the selected soils. The physical, chemical, and mineralogical characterization of the sediments will be conducted following well established methods[5,6] and will include particle size analysis, organic carbon, exchangeable cations, cation exchange capacity, pH, X-ray diffraction, and thermal analysis of the clay fraction. Relationships between mineralogical characterization, ion exchange selectivity, Cs bonding environments, and Cs distributions between planar, selective, and fixed sorption sites will be developed.

Cs Uptake and Release by Phyllosilicates

The purpose of this work is to quantify the rate of binding and release of Cs^+ from phyllosilicates commonly found at INEEL and DOE sites. This work plan is based on the hypothesis that the release of Cs^+ in the rhizosphere is controlled by diffusion from the interlayers of phyllosilicates. Cs^+ occurs in a readily exchangeable form that is bioavailable (planar surfaces of phyllosilicates, Fe- and Al-hydroxides, organic matter) and a more recalcitrant form bound in the interlayers of phyllosilicate minerals common in soils (mica, illite, vermiculite, smectite). The rate of exchange of Cs^+ from the interlayers of the phyllosilicates by other ions with low hydration energies (e.g. K^+) is controlled by diffusion of ions in the interlayers. In a closed system, we expect the amount of Cs^+ bound to the exchangeable sites to decrease over time, and the concentration of Cs^+ in the "fixed" interlayer sites to increase. When plants are K^+ limited, exudate production increases. Root exudates are typically comprised of low-molecular-weight compounds including organic acids, sugars, phenols, and amino acids. The organic acids, attack (weather)

the phyllosilicates, by breaking down the octahedral layers and releasing K^+ and consequently Cs^+ from the interlayers. The rate of release of "fixed" K^+ and Cs^+ from phyllosilicates by weathering reactions driven by plant exudates is expected to be greater than the rate of release by diffusion. At the INEEL site, those phyllosilicates are most likely, mica, illite, and interlayered illite/smectite clay. This work includes:

- Reviewing the literature on Cs^+ binding and release from soils and specific soil components including minerals, amorphous oxides, and organic matter
- Developing mathematical models for the long-term uptake and release of Cs^+ by ideal clay structures
- Performing long-term uptake and release studies of Cs^+ by reference clays
- Measuring the rate of release of Cs^+ and K^+ by reference clays in the presence of model compounds representative of key components of plant exudates (e.g., specific organic acids).

Task 1 is essential to the project and will be the initiated immediately. Tasks 2 and 3 complement one another. Although Task 2 will be initiated before Task 3, results from experimental work in Task 3 will feed back into the modeling effort in Task 2. These tasks will rely on input from Dr. Bertsch's work to insure that the clay materials are good choices and that the conceptual model is consistent with field observations. The mathematical model will be used to quantify the migration of the Cs^+ from the recalcitrant pool to the more bioavailable pools in the Stella model. The experimental work in Task 3, does not involve the use of any plant or microbial exudates, and it will serve as the control experiments for the plant exudate-clay interaction work in Task 4. This task will require input from the plant exudate work to insure that the organic acids and other exudates used in these experiments are reasonable choices.

Literature Review On Cs^+ Binding and Release from Soils

There is extensive literature on Cs^+ binding to different soil materials. It is essential that we review these papers and summarize this literature in a general review. This review will help to insure that we do not overlook important processes affecting Cs^+ binding in the rhizosphere.

Mathematical Models for the Long-Term Uptake and Release of Cs^+

The release of the "fixed" K^+ from soils and minerals has been considered a diffusion-controlled process.[7,8] Since both K^+ and Cs^+ have low hydration energies, we suspect that the behavior of theses two ions will be similar. Several mathematical models of K^+ release from soils have been proposed[9–13] and may be applicable to Cs^+ uptake and release. Simple analytical solutions for diffusion in rectangular regions and parallelepipeds can be adapted.[14,15] However, there are several potential limitations to these solutions. For example, collapse of the interlayer thickness can occur when monovalent ions with low hydration energies substitute in the interlayer. The interlayer thickness depends on the concentration of the substituting ion, consequently, the interlayer diffusion coefficient may also be concentration dependent. The boundary conditions for many applications may be more complex than constant concentration (dirichlet type boundary condition), constant flux (Neuman type boundary condition), or a linear mass transfer boundary ("radiation" type boundary condition). The jumps in the concentration versus time data observed by Comans and Hockley[16] clearly suggests that more than one process is involved in the binding of Cs^+ even in mono-mineral systems. Indeed, they propose a four-box model that includes an instantaneous equilibrium process, a kinetically reversible process, and an irreversible kinetic process. Based on our literature review, we will propose several mathematical models for Cs^+ binding in monomineral systems. These solutions may be either analytical or numerical. The actual equations we use will depend on the appropriate boundary conditions and other processes that are operating in the experim-

ents we will be conducting and in the field situations that are likely to be encountered. It is important for us to link the aqueous concentration to the concentration at the boundary of the particle. If the diffusion coefficients are concentration dependent or there are too many complexities it may be simpler to use a numerical solution. We will adjust our approach following the literature review and modify our models as experimental data become available.

Long-Term Uptake and Release Studies of Cs^+ by Reference Clays

Reference phyllosilicates (illite, smectite, interlayered illite/smectite) will be obtained through various sources including the Clay Minerals Society. The samples will be pretreated to remove carbonates, organic matter, and iron oxides.[17] The clays will then be sieved to remove any coarse materials and then dispersed using ultrasonics. A relatively narrow range of grain size will be obtained by sedimentation of this dispersed suspension. The samples will then be washed three times with a 1 M solution of NaCl, washed with ultrapure (>14 MT cm) water until the $AgNO_3$ test for Cl^- is negative, and stored in a refrigerator as a suspension until needed.

An aliquot of the suspension will be filtered and dried in a desiccator over a saturated $CaCl_2$ solution (relative humidity ~30%) and characterized by powder x-ray diffraction, simultaneous thermal analysis, and Fourier infrared spectroscopy. Brunauer, Emmett, Teller surface areas will be obtained for each size fraction and reference clay. Samples of the clay will be viewed using electron microscopy (SEM and TEM) to measure the relative dimensions of the clay particles. Chemical composition will be obtained by x-ray fluorescence. The ammonium acetate method[18,19] will be used to obtain exchangeable cations and cation exchange capacities. Grain-size distribution will be obtained by photon correlation spectroscopy.

Batch adsorption experiments will be conducted by spiking suspensions of the mineral material with CsCl and KCl. At least three concentrations will be used for each salt. The aqueous concentrations of the salts and the solid-to-solution ratios to be used in the experiment will be estimated from literature review and from the modeling. The experiments will be conducted at near-neutral pH. Although we suspect that the nonspecific binding will be pH dependent, the specific binding occurring in the interlayers is less likely to be pH dependent. For Cs sorption on illite, only minor variations in K_d with pH have been observed.[20] Cs^+ and K^+ concentrations will be measured using ICP-MS.

Samples for the release experiments will be prepared by placing the clay in a 1 M solution of CsCl and KCl at 85ºC for at least three months. The time scale will be better estimated based on the modeling and literature review. The samples will then be washed with ultrapure water until the $AgNO_3$ test is negative. The suspension will then be filtered and the filter cake air-dried until needed.

The release experiments will be conducted as flow-through experiments to keep the aqueous concentrations low, thereby increasing the gradient near the boundary and decreasing the time for completion of the experiment.

Samples of the clay at different times during the release experiment will be analyzed by powder x-ray diffraction and x-ray absorption spectroscopy (XAS). This aspect of the task should be done in cooperation with Paul M. Bertsch at the University of Georgia.

Rate of Release of Cs^+ and K^+ by Reference Clays in the Presence of Key Components of Plant Exudates

Plants can affect the weathering rates of minerals through both physical and chemical processes.[21] Physical processes include physical disintegration of bedrock material, changes in soil permeability,

evapotranspiration, and binding and retention of soil particles. We will focus on the more direct chemical effects, which include lowering of pH by CO_2 generated by root and microbial respiration, lowering of pH by the addition of organic acids, and introduction of organic chelates from plant roots and microbes. To understand how these chemical processes can increase the bioavailability of Cs in the rhizosphere, we must understand weathering of silicate minerals, primarily, the phyllosilicates that are known to bind Cs^+.

In general, rates of oxide and silicate mineral dissolution are known to be fairly constant at circumneutral pH and to increase in both acidic and alkaline solutions. In addition, the rate of dissolution can also be increased by the presence of organic ligands. The dissolution of minerals is believed to involve two key steps.[22] In the first step, surface species are formed. This process has been shown to be relatively fast and reversible, hence it can be described as an equilibrium reaction. The second key process is the detachment of the metal ion from the surface into solution.

This detachment process is the rate-limiting step and the surface complex is the precursor of the activated complex (Reference 21). Thus, the rate of ligand-promoted dissolution, r_L, is proportional to the activity of the surface species:

$$r_L \mid k'_L [L]_S \tag{3}$$

where $[L]_S$ denotes the concentration of the surface complex.

Proton- and hydroxyl-promoted dissolution requires coordination of several ions around the metal ion. The rates of proton- and hydroxyl-promoted dissolution, r_H and r_{OH}, are given as

$$r_H \mid k'_H [H^2]_S^j \tag{4}$$

and

$$r_{OH} \mid k'_{OH} [OH^4]_S^i \tag{5}$$

where the exponents j and i correspond to the valance of the coordinated metal ion, $[H^+]_S^j$ is the concentration of protonated surface hydoxy groups in excess of the zero point charge (ZPC) and $[OH^-]_S^i$ is the concentration of deprotonated surface groups in excess of the ZPC. The overall rate of dissolution of the mineral, is therefore given by

$$r \mid k'_H [H^2]_S^j \; 2 \; k'_{H_2O} 2 k'[OH^4]_S^i \; 2 \; k'_L [L]_S \tag{6}$$

where the term k'_{H_2O} refers to a zero-order process to describe the circumneutral pH region where the rate of dissolution is independent of pH (Reference 21).

The rate equation given in Eq. (6) was developed for simple oxides. Nonetheless, the general concepts presented should also apply to more complex silicates. A key difference when considering the dissolution of phyllosilicates such as kaolinite and muscovite is that the tetrahedral layers are relatively nonreactive. Dissolution is controlled by the detachment of Al, which is primarily in the octahedral layer of the phyllosilicates. Therefore, reactions are going to occur at the edges of the crystallites where the octahedral layers are exposed to the solution.

We will conduct experiments to measure the ligand-promoted release of K^+ and Cs^+ from reference clays. The reference clays saturated with CsCl and KCl solutions in Task 3 will also be used in

experiments to measure the release of Cs^+ and K^+ in the presence of key components of plant exudates. We will focus on organic acids and most likely aliphatic and aromatic dicarboxylic acids that have been demonstrated to strongly bind metal ions. The specific acids that will be used will be based on the plant exudate work being done at USU. Experiments will be conducted in the presence of a 0.1 M NaCl solution. A control experiment containing no organic acids will also be conducted. $HClO_4$ will be used to adjust the pH of the control experiment to be the identical to that of the experiments with organic acid. All solutions will be prepared using ultrapure water (>14 MT-cm). Water will be purged for at least 10 minutes with N_2 bubbled through 0.1 m NaOH to remove CO_2. All solutions will be prepared in a glove box equipped with a CO_2 scrubber. Experiments will be conducted in high-density polyethylene bottles. These bottles will be sealed in glass canning jars before they are removed from the glove box. All materials will be sterilized prior to use to eliminate potential biological activity in the reaction vessels.

Because the rate of weathering of the phyllosilicates is proportional to the adsorbed ligand concentration, it is necessary to determine the amount of adsorbed ligand in the experiments. The adsorbed ligand concentration is a function of the total ligand concentration, pH, the acid/base properties of the absorbent, and total surface area of the absorbent. The acid/base properties of the clays will be measured by potentiometric titration at at least three different ionic strengths using an autotitrator. Specific surface areas will be obtained in Task 3.

Experiments will be conducted using clay suspensions in 0.1 M NaCl solutions. Time-series of concentrations will be obtained to test proposed kinetic models for the release of K^+ and Cs^+ in the presence of organic chelating agents. Experiments be conducted at various pH and ligand concentrations. The pH will be kept constant by periodically adjusting the pH with $HClO_4$ and NaOH. The suspensions will be prepared in HDPE bottles in the glove box, sealed in canning jars, removed from the chamber, and placed in a shaking constant temperature bath set at 25∀C. The jars will be returned to the glove box for periodic sampling. Aliquots of sample will be filtered through a 0.4-σm filter. A portion of this sample will be used to measure pH. A second portion will acidified with nitric acid for subsequent analysis by AAS and ICP-MS. A third portion of the sample will be saved as a nonacidified sample for Si and organic ligand analysis. Na, K, Cs, and Al concentrations will be measured on the acidified samples by a combination of atomic absorption spectrophotometry and ICP-MS. Si concentrations will be measured colorimetrically using an ammonium molybdate method (ASTM D 859-94). Ligand concentration will be measured by ion chromatography.

In a second series of experiments, the model clays will be subjected to dissolution at a fixed ligand concentration and pH, but with the particle concentration (clay concentration) at 5 different values. A third set of experiments will be conducted with a fixed particle concentration, a fixed ligand concentration, and a fixed pH, but on three different size fractions of the clay.

Samples of the reacted clay material will be characterized by powder x-ray diffraction, thermogravimetry, and XAS. These studies will provide a rate equation for the release of Cs^+ and K^+ in the presence of pertinent organic ligands.

ACCOMPLISHMENTS

Parameter Identification

The parameters to be considered initially in the field characterization and conceptual modeling tasks were selected. A database of literature was compiled. Based on findings from the literature review, data from previous studies conducted here at the INEEL, and vegetation/soil Cs concentration data available from INEEL sites, we have identified biogeochemical parameters to be measured in the crested

wheatgrass system. The sampling and analysis to be conducted in the field characterization studies are included in the Ecological Engineering of Rhizosphere Systems task report. As stated in that report: "Field site selection has been completed and field characterization (including geochemical parameter characterization) has been initiated."

The parameters being evaluated are included in the preliminary conceptual model. The modeling effort is being implemented using Systems Thinking, which integrates the relationships between the many factors affecting Cs solubilization. To date, we have established the basic associations using software (Stella/iThink) based on this approach. The software allows us to set up these relationships in sectors, with each sector representing a submodel. We have established many of the basic relationships within each submodel, as well as the interactions between submodels. This approach allows for expertise in defining each sector, while simultaneously promoting the ecological packet. The model setup still requires refinement, with a few elements and the interactions between elements still need to be incorporated. As data is obtained, it will be incorporated into the model that will iteratively be updated. Refinement of the geochemical submodel (Cs binding to soil) and integration of the Cs binding submodel with the ecological and biological submodels is being conducted as part of this task (see Figure 1).

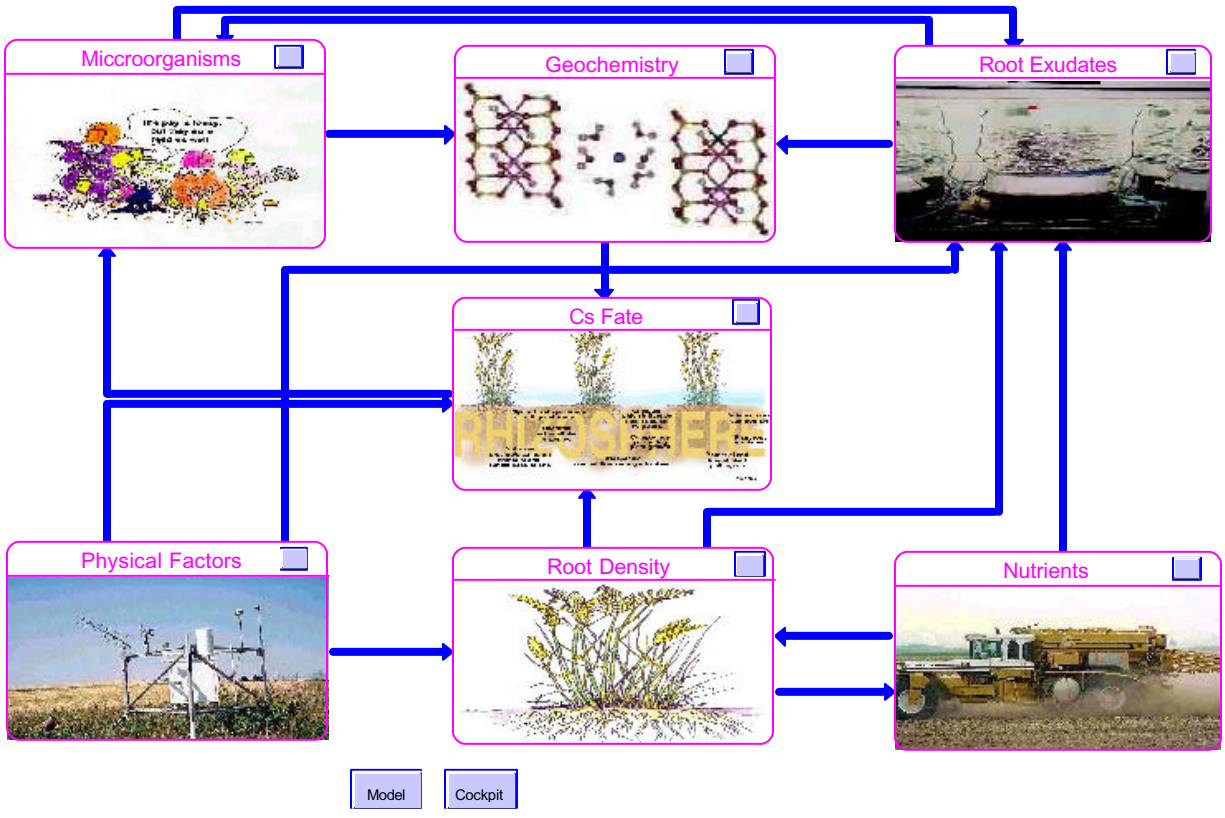

Figure 1. Stella/iThink modeling software interface level showing the Cs Fate sector (center box) and the six sectors (or submodels) affecting it.

Characterization of Root Exudates and Microbial Chelators

The USU Crop Physiology Laboratory was contracted in 2000 to to examine how crested wheatgrass exudate production is affected by environmental/nutrient induced plant stress, microbes, and plant growth and development. Genotypes of crested wheatgrass were selected, hydroponic systems for culturing those plants are under construction, extensive literature was reviewed, and detailed experimental plans for these studies were completed.

Plant Exudates and System Components

We made significant progress on identifying plant exudates. We discovered significant organic contamination of the Ottawa sand that could not be removed by washing with a 0.1 molar NaOH solution (followed by a thorough deionized water rinse). After discussing several potential treatments to remove the organic contamination we determined that heating the sand in a muffle furnace at 550ºC for at least 10 hours is the most effective method of minimizing the organic contamination from the sand. After muffling, the sand is packed into the five layers in the column.

We were surprised to find that the glass wool was also contaminated with organic matter. This contamination can be removed by thoroughly washing the glass wool with deionized water. We have switched to using silanized glass wool, which is deactivated by treatment with silane. Silanized glass wool contains less organic contaminants than standard reagent grade glass wool, and it has a lower affinity for binding organic matter. We are now using silanized glass wool in all studies. We are also now using silicone stoppers instead of rubber stoppers to minimize the carbon contamination from the stopper.

Analysis of Organic Carbon in Leachate

The leachate is analyzed for total organic carbon (TOC) using a TOC analyzer. Leachate is also analyzed to identify individual organic constituents using gas chromatography with flame-ionization detection (GC/FID). Data acquisition and analysis are performed using Agilent Chem-station System Version G2072AA

TOC Analysis

It was necessary to make several modifications to our TOC analyzer to accurately measure the relatively low levels of organic carbon in our leachate solutions. After these modifications were complete we discovered that the unplanted columns had considerable contamination with organic carbon. These results were measured before any of the changes listed above were made to reduce carbon contamination from the setup components.

Identification of Organic Compounds in Exudates

Leachate samples have been analyzed for organic acids based on GC retention time. Compounds will also be identified by GC/FID. Organic compounds that were detected in unplanted samples were measured before reduced-carbon column components were used.

Effects of Selected Root-Zone Stresses

It is necessary to carefully determine the effect of moderate stress on plant growth so that the results can be extrapolated to the field and reproduced in other laboratories. We conducted preliminary studies to determine the appropriate level of stress on plant growth. It is much easier to grow nonsterile than sterile plants, so these studies were conducted with nonsterile plants. Four types of root-zone stress

were induced: low potassium (K^+), high ammonium (NH_4^+), low water (drought) and high water (hypoxia). The stresses are applied by

- Reducing potassium in the nutrient solution
- Increasing ammonium in the nutrient solution
- Watering with lower amounts of nutrient solution
- Replacing the stopper in the bottom of the column with a solid stopper and filling the column with water to induce water logging.

Plants exposed to the K^+ and NH_4^+ stresses appeared to grow as well as the controls. Plants exposed to both types of water stress grew less vigorously and the drought-stressed plants used lower amounts of water (water use in the hypoxic treatments was not determined). These stresses will be applied to sterile plants and the effects of each stress on exudate production will be determined. Concentrations of NH_4^+ and K^+ in the nutrient solutions for these respective stresses will be changed to increase the stress for the next study.

Characterization of Cs Binding to Soil

The Savannah River Ecology Laboratory (SREL) is examining how Cs is bound to reactive mineral phases in soils at the INEEL and elsewhere.

Particle Size Analysis

The soil materials received from the INEEL were crushed and sieved to pass a 2 mm sieve. A size distribution was analyzed for both the disturbed and undisturbed samples.

Chemical and Mineralogical Characteristics of the Soil

Soil pH was measured according to the procedures of McLean[23] with a standard Calomel electrode calibrated using standard buffer solutions of pH-7 and pH-10. Results of four replicates were averaged. Free iron oxide removal from duplicate samples was carried out by reduction with Sodium dithionite in suspension buffered with Sodium citrate/Sodium bicarbonate solution. The iron concentration in the resulting solutions was analyzed using atomic absorption spectroscopy.

Carbon and nitrogen were estimated using a Leco CNS analyzer. Once total and organic portions were measured, inorganic carbon content was obtained by a calculation of difference. The undisturbed soils have more organic carbon and total nitrogen, but less inorganic carbon then do the undisturbed soils.

Triplicate samples from each of the two soil types were taken and sent to SREL for total digestion and elemental analysis. Triplicate subsamples from each sample were HF digested and analyzed via ICP-MS for 18 different elements. These data are thus averaged over nine analytic data points.

Exchangeable Cations and Effective Cation Exchange Capacity

Triplicate 3–5g samples were taken from both soil types for total elemental analysis. Triplicate sub-samples were taken from each sample. These sub-samples were HF digested, and analyzed via ICP-MS for a suite of 18 elements.

Indigenous levels of water soluble and exchangeable Cs were estimated by extraction with water and 1M ammonium chloride (NH_4Cl). The resulting filtrates were analyzed for Cs^+ using ICP-MS.

Effective cation exchange capacity (ECEC) and exchangeable cations were determined by similar extractions with ammonium chloride. Triplicate samples were subjected to the same extraction sequence as above using 1M NH_4Cl as the extractant. A second identical extraction was conducted on these same samples immediately following the first. The filtrates were analyzed independently for Ca, Mg, K, Na, Al, Cs, Sr, and Rb using ICP-MS . The sum of the two concentrations measured for each element was taken to be the exchangeable value for that element. The summation of the exchangeable cation concentrations served as a measure of ECEC.

There is little or no water-extractable Cs and the undisturbed soil has greater amount of easily extractable Cs. The effective cation exchange capacity (ECEC) of the undisturbed soil is about 1.5 times the ECEC of the disturbed soil.

Frayed Edge Sites and Cs-K Selectivity Coefficients

Experiments were conducted to estimate FES concentrations, solid/liquid distribution coefficients for Cs (Kc), and calculate the radiocesium interception potential (RIP). Three variations on Wauters et al.[24] were undertaken on "disturbed" and "undisturbed" whole soils as a basis on which to judge the usefulness of the different methods. The experiments were called FES Measurement, Method 1, and Method 2. Methods 1 and 2 each contain steps to estimate both FES concentration and Kc, while the FES Measurement method only measured the FES concentration.

FES Abundance Calculations. Extracted Cs^+ and K^+ were used as a direct measure of FES abundance. The calculation was made for each sample. Averages and standard deviations were calculated over the triplicate samples. Percent calculations comparing FES concentration with ECEC (measured previously) were also carried out. The three methods show remarkable similarity in results.

K_c^{FES} (Cs^+/K^+) Calculations. Selectivity coefficients were calculated using the solid phase Cs^+ concentration, liquid phase K^+ concentration, solid phase K^+ concentration, and liquid phase Cs^+ concentration in this manner for each replicate. Average K_c values were calculated along with their corresponding standard deviation values and 95% confidence intervals.

Accelerated Aging of the Cs-illites

Accelerated aging techniques focused on the removal of interlayer K^+ from micaceous minerals and their weathering products. The method used was based on the work of Maes et al.[25] who also drew from Dreher and Diederbudde.[26] An incremental weathering sequence was attempted on four groups of "undisturbed" soil. Each group consisted of triplicate samples of sand, silt, clay and one blank. The four groups received different degrees of artificial weathering according to the number of weathering episodes to which they were subjected. This technique is very useful because it allows us to prepare clays in a relatively short period of time that are more like real materials that have been exposed to Cs^+ for decades. Clays prepared in this manner can be used in laboratory experiments to provide better insight into the time scales for the removal of Cs^+ from soils by plant uptake as well as by other processes.

Cs Uptake and Release by Phyllosilicates

We recruited a geochemist to work with the rhizosphere group and hired Carl D. Palmer, Ph.D., who began work on this project. Dr. Palmer is taking the lead in directing the work on Cs binding to phyllosilicates and the coordinating work at SREL being done under subcontract.

A Work Plan for determining the rates of uptake and release of Cs by phyllosilicates has been written. A literature review of Cs binding in soils has been initiated. Based on this literature review we have developed a hypothesis concerning the uptake and release of Cs by phyllosilicates in rhizosphere. Based on a review of studies of the mineralogy at the INEEL site, we have tentatively identified illite, Ca-smectite, interlayered illite/smectite, and mica, these being the most likely phyllosilicates at the our field site. We have acquired reference illite and smectite clays for our experimental work.

We acquired illite clays from the Clay Minerals Society (Imt-1 and Imt-2). The clays were handled and prepared accordingly and diffraction patterns confirmed that the clays are illite. Particle size analysis was performed on an aliquot of the suspension using a Coulter N4 Plus particle-size analyzer. The acid/base properties of the illite were investigated by titrating a suspension of illite in three ionic solutions of KCl. The differences may be accentuated by increasing the concentrations of the clay in the suspension. Additional tests are required to verify the zero point of charge of illite suggested by the titration curves. The curves provide a measure of the buffer intensity of clay. Calculation of the acidity constants for the illite surface requires greater separation in the curves.

Weathering Experiment

Experiments were conducted to determine the rate of weathering of illite. Two experiments were conducted, one in a deionized water suspension, the other in an oxolate suspension. Changes in K^+ concentrations were used as a measure of the amount of weathering. K^+ concentrations were measured using ion chromatography. The measured concentrations (see Figure 2) show that the concentrations in the oxalate solution are greater than those in the deionized water suspension. This result is primarily the result of cation exchange as a consequence of the higher Na^+ concentrations in the oxalate solution.

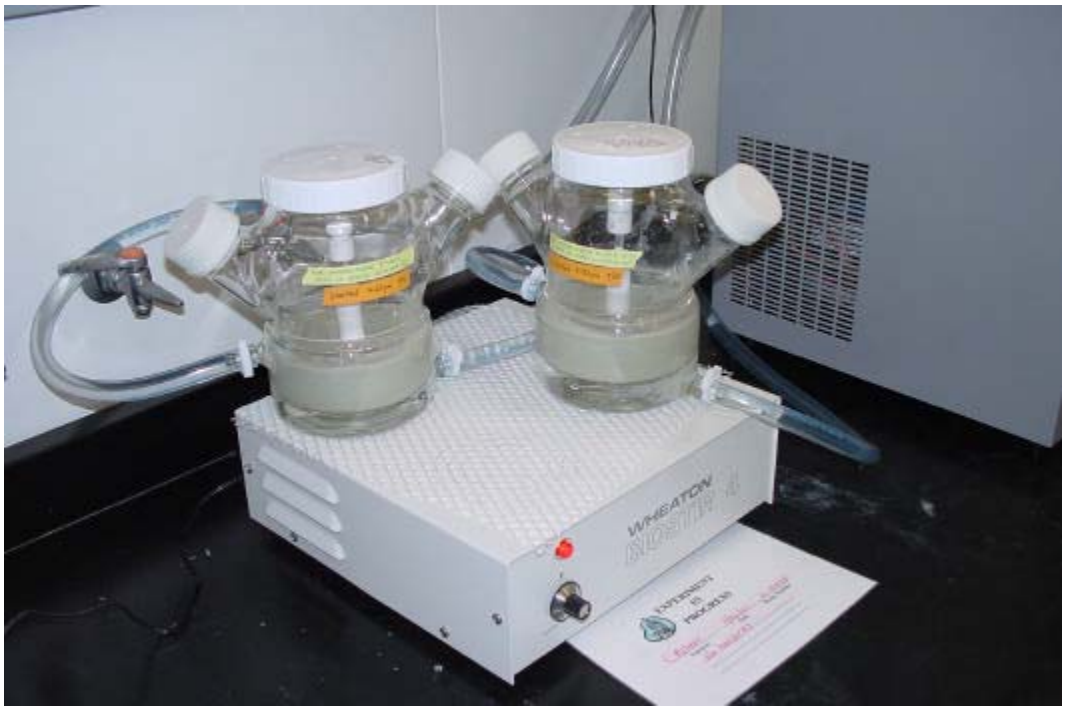

Figure 2. Setup for the illite weathering experiments. The 250 mL jacketed bioreactors contain a 24.1 g/L^{-1} suspension of illite. Temperature is maintained at 25∀C by a recirculating bath.

Rate of Cs^+ Sorption on Illite

A stirred suspension of K^+-saturated illite was spiked with a CsCl solution. Cs concentrations were measured using ion chromatography. The aqueous Cs^+ concentrations rapidly decreased to approximately half of the total Cs concentration in less than 20 minutes. The concentrations continued to slowly decrease over the next 1,440 minutes. Similarly, the sorbed Cs^+ concentrations determined by difference between the measured aqueous concentrations and the total Cs^+ concentrations rapidly increased in the first 20 minutes and showed a slow increase. K_d values were computed.

Sorption

Batch adsorption tests on illite were conducted. A solution of 0.005 M $CaCl_2$ was mixed with a suspension of illite. Three series of experiments conducted. The pH is these three sets were adjusted to 8.5, 7.5, and 6.5. The pH values drifted during the experiment so the final pH values are closer together. Ten mL aliquots of the pH-adjusted suspension were placed in culture tubes, then spiked with CsCl to yield 10 various total concentrations of Cs^+, and placed on a reactor (Figure 3). After reacting for 24 hours, the sample was filtered and pH of the remaining suspension was measured (Figure 4). Cs^+ as well as Ca^{2+}, Mg^{2+}, Na^+, and K^+ were measured by ion chromatography.

Figure 3. Batch sorption samples on rotator. Samples were reacted for 24 hours.

Figure 4. General setup for measuring Cs^+ sorption. Samples collected with a syringe are filtered through a 0.22 σm syringe filter while the pH is measured.

Sorbed Cs^+ concentrations were fit to a Langmuir isotherm:

$$S = S_{\max}\left(\frac{K_L C}{1 + K_L C}\right) \tag{7}$$

where S is the concentration on the solid, S_{max} is the maximum sorption density, K_L is the Langmuir sorption coefficient, and C is the aqueous Cs^+ concentration. In fitting the data, the lowest total Cs^+ concentration data was not used because the aqueous concentrations were close to the detection limits; the highest total Cs^+ data was not used because it consistently plotted well above the rest of the data. Because the measured aqueous concentrations range over approximately two orders of magnitude the regression were weighted by the inverse of the aqueous concentrations. The fits to the data are good with correlation coefficients, r^2, 0.92 in all three of the series. The S_{max} are similar with the values being with one standard error of each other. Similarly, the K_L are not significantly different from each other.

These results can be used directly in the general model that we are developing for Cs^+ in the rhizosphere. The sorption constants can be used to model the more labile sorption of Cs^+ to the illite fraction of the soil. Further, since the values did not vary greatly with pH, they will likely apply over the range of pH values encountered in the INEEL soils.

Additional Collaborations

In addition to the collaborations that we have developed with Dr. Bruce Bugbee at the Crop Physiology Laboratory at USU and Dr. Paul Bertsch at SREL, we have been developing a collaboration with Dr. James Harsh in the Department of Crop and Soil Science at the Washington State University

(Pullman). This collaboration is through the Inland Northwest Research Alliance program that is supporting Dr. Harsh's work on sorption of Cs to natural sediments. This summer Dr. Harsh met with us at the INEEL to discuss our current research, the status of his project, and the potential for future funding. In July 2001, Laura Hanson, a graduate student under Dr. Harsh's supervision, worked at the INEEL for two weeks and we are currently discussing the possibility of her returning in January 2002 for a longer period of interaction. Ms. Hanson will be supported through an INRA grant and a National Science Foundation IGERT grant to the Washington State University.

REFERENCES

1. A. Ferro, R. Simms, and B. Bugbee, "Hycrest Crested Wheatgrass Accelerates the Degradation of Pentachlorophenol in Soil," Journal, *Environmental Quality*, Vol. 23, 1994, pp. 272–279.

2. B. J. Orchard, W. J. Doucette, J. K. Chard, and B. Bugbee, "Uptake of Trichloroethylene by Hybrid Poplar Trees Grown Hydroponically in High Rate, Flow-Through Plant Growth Chambers," *Environmental Toxicology and Chemistry,* Vol. 19, 2000, pp. 895–903.

3. B. J. Orchard, , W. J. Doucette, J. K. Chard, and B. Bugbee. "A Novel Laboratory System For Determining the Fate of Trichloroethylene In Plants." *Environmental Toxicology and Chemistry,* Vol. 19, 2000, pp. 888–894.

4. H. Marschner, *Mineral Nutrition of Higher Plants*, 2nd Edition, 1995, Academic Press, NY, p. 889.

5. M. L. Jackson, *Soil Chemical Analysis-Advanced Course*, 2nd ed. Pub. by author, Dept. of Soils, University of WI, Madison, WI. M. L. Jackson, Madison, WI, 1979.

6. F. W. Kunze and J. B. Dixon, "Pretreatment for Mineralogical Analysis," *In A. Klute (ed.) Methods of soil analysis, Part 1, 2nd ed. Agron. Monogr.,* Vol. 9, ASA and SSSA, Madison, WI, 1986.

7. S. Feigenbaum, R. Edelstein, and I. Shainberg, "Release Rate of K and Structural Cations From Mica to Ion Exchangers in Dilute Solutions," *Soil Science Society of America Proceedings*, Vol. 45, 1981, pp. 501–506.

8. H. W. Martin and D. L. Sparks, "Kinetics of Nonexchangeable Potassium Release From Two Coastal Plain Soils," *Soil Science Society of America Journal*, Vol. 47, 1983, pp. 883–887.

9. M. G. Reed and A. D. Scott, "Kinetics of Potassium Release From Biotite and Muscovite in Sodium Tetraphenylboron Solution," *Soil Science Society of America Proceedings*, Vol. 26, 1962, pp. 437–440.

10. M. M. Mortland and B. Ellis, "Kinetics of Potassium Release From Biotite," *Soil Science Society of America Proceedings*, Vol. 22, 1959a, pp. 503–508.

11. M. M. Mortland and B. Ellis, "Release of Fixed Potassium as a Diffusion Controlled Process," *Soil Science Society of America Proceedings*, Vol. 23, 1959b, pp. 363–364.

12. Quirk J. P. and J. H. Chute, "Potassium Release From Mica-Like Clay Minerals," *Transactions of the 9th International Congress of Soil Science*, 1968, pp. 671–681.

13. J. A. Rausell-Colom, T. R. Sweatman, C. B. Wells, and K. Norrish, "Studies in the Artificial Weathering of Mica," *In Experimental Pedology* (ed. E. G. Hallsworth and D. V. Crawford), Butterworths, 1965, pp. 40–72.

14. H. S. Carslaw and J. C. Jaegar, *Conduction of Heat in Solids*, Oxford University Press, 1959.

15. J. Crank, *The Mathematics of Diffusion*, Oxford University Press, 1975.

16. R. N. J. Comans and D. E. Hockley, "Kinetics of Cesium Sorption on Illite," *Geochimica et Cosmochimica Acta*, Vol. 56, 1992, pp. 1157–1164.

17. G. W. Gee and J. W. Bauder, "Particle-Size Analysis," *Methods of Soil Analysis, Part 1, Physical and Mineralogical Methods*, Vol. 9 (ed. A. Klute), 1986, pp. 383–411, American Society of Agronomy, Inc. and Soil Science Society of America, Inc.

18. J. D. Rhoades, "Cation Exchange Capacity," *Methods of Soil Analysis, Part 2: Chemical and Microbiological Properties*, Vol. 9 (ed. A. L. Page, R. H. Miller, and D. R. Keeney), 1982, pp. 149–157. American Society of Agronomy, Inc. and Soil Science Society of America, Inc.

19. G. W. Thomas, "Exchangeable Cations," *Methods of Soil Analysis, Part 2: Chemical and Microbiological Properties*, Vol. 9 (ed. A. L. Page, R. H. Miller, and D. R. Keeney), 1982, pp. 159–165. American Society of Agronomy, Inc., and Soil Science Society of America, Inc.

20. C. Poinssot, B. Bayens, and M. H. Bradbury, "Experimental and Modeling Studies of Cesium Sorption on Illite," *Geochimica et Cosmochimica Acta*, Vol. 63(19/20), 1999, pp. 3217–3227.

21. J. I. Drever, The Effect of Land Plants On Weathering Rates of Silicate Minerals," *Geochimica et Cosmochimica Acta*, Vol. 58(10), 1994, pp. 2325–2332.

22. W. Stumm and E. Wieland, "Dissolution of Oxide and Silicate Minerals: Rates Depend on Surface Speciation" *Aquatic Chemical Kinetics* (ed. W. Stumm), John Wiley & Sons, Inc., 1990, pp. 367–400.

23. E. O. McLean, "Soil pH and Live Requirement," 1982, pp. 199–223, *in* A. L. Page et al. (ed.) "Methods of Soil Analysis, Part 2" 2nd ed., *Agron*. Monogr, ASA and SSSA, Madison, Wisconsin.

24. J. Wauters, A. Elsen, A. Cremers, A. V. Konoplev, A. A. Bulgakov, and R. N. J. Comans, "Prediction of Solid/Liquid Distribution Coefficients of Radiocaesium in Soils and Sediments. Part One: A Simplified Procedure for the Solid Phase Characterization," *Applied Geochemistry*, Vol. 11, 1996, pp. 589–594.

25. E. Maes, L. Vielvoye, W. Stone, and B. Delvaux, "Fixation of Radiocaesium Traces in a Weathering Sequence Mica-Vermiculite-Hydroxy Interlayered Vermiculite." *European Journal of Soil Science*, 1999, 50: 107–115.

26. P. Dreher and E. A. Niederbudde, "Potassium Release from Micas and Characterization of the Alteration Products, *Clay Minerals*, 1994, 29:77–85.

Innovative Approaches to Characterize Vadose Zone Hydraulic Properties

New Methods for Measuring Water Flow Through INEEL Subsurface Samples

David N. Thompson, Kristine E. Baker, and Adam P. Poloski (INEEL); Clark Lindenmeier and Antoinette Owen (PNNL)

SUMMARY

This research explored the application of a relatively new commercially available instrument, the unsaturated flow apparatus (UFA™), which promises to reduce the time and cost required to measure hydraulic properties in subsurface samples. The UFA can also be used to adjust water contents for determination of microbial activities in vadose zone soil cores for in situ bioremediation, which is a major thrust of Environmental Management's (EM's) research and development. This research supports EM's mission and contributes to understanding the relationship between compact subsurface soils and water retention. Being able to predict hydraulic characteristics of the subsurface will support long-term stewardship with engineering solutions to predict and manage contaminants.

This novel application of UFA technology to compactible soils (used in microbial activity studies) requires that we first characterize the effects of centrifugal force on compaction of vadose zone soils. In collaboration with researchers at the Pacific Northwest National Laboratory (PNNL), we then used x-ray microtomography (XMT) to develop a predictive model to quantify the relationship between changes in soil porosity and centrifugal force.

TASK DESCRIPTION

Typical laboratory methods for characterizing hydraulic properties of soil cores are extremely time consuming, which limits the number of samples often used in site characterization of vadose zone environments. However, the recent development of the UFA is expected to significantly reduce the time required to analyze hydraulic properties of vadose zone materials. The UFA is a flow-through centrifuge device used to measure fluid transport properties of porous media. Analysis is accomplished typically in a matter of days, compared to weeks or months using traditional methods, by subjecting the sample to fluid driving forces up to 10,000 Δ g. However, these high driving forces result in a high degree of sample compaction in poorly consolidated soils. The relationship between compaction and moisture retention of a compactible soil is expected to be unique for individual soil types. Our intent, however, is to develop a stress-strain-compaction model that can be used to address the effects of compaction on various soil types and pressures. Such a relationship would offer a new tool for characterizing compressible soils in the UFA, and would answer specific questions for an interfacing ESRA microbial activity task. A significant aspect of this task is our interaction with PNNL. The PNNL x-ray microtomography laboratory offers a unique way to study the effects of structure on hydraulic properties, which will be a valuable asset to subsurface research at the INEEL.

The overall scope of this task includes a learning period for a new UFA instrument (using undeformable materials), assessments of compaction in the UFA and in hanging columns, and evaluations of how UFA and hanging column data and observations are incorporated into model parameterization.

Our research involved five subtasks:

- Hanging column/pressure cell measurment of the moisture characteristic drainage curve of the compactible soil, and establishing a collaboration with PNNL to do baseline XMT analyses of the cores.

- Purchasing a J-6 UFA instrument from UFA Ventures, Inc., installing it at the INEEL, and completing instrument-specific training given by a technitian of UFA Ventures, Inc. Complete 2 weeks of general UFA training at PNNL, receiving direct hands-on instruction in the measurement of moisture characteristic curves and unsaturated hydraulic conductivity from experts in the use of the UFA.

- Complete hanging column/pressure cell measurement of the moisture characteristic drainage curve of the compactible soil in early FY 2001.

- Further develop expertise in the operation of the UFA at the INEEL while studying the effect of anisotropy on the moisture characteristic drainage curves of sandstone and basalt cores.

- Use the UFA to measure the moisture characteristic drainage curve of the compactible sandy loam from the interfacing ESR microbial activity task. Develop a stress/strain model for correcting moisture characteristic curves that have been altered due to compaction in the UFA.

Results

Hanging Column/Pressure Cell Experiments

We developed a method for coring undisturbed intact samples, shipping them to PNNL, scanning them by XMT, and shipping them back to the INEEL for analysis. Developing these methods is extremely important in obtaining reproducible hydraulic measurements from intact cores (as opposed to repacked samples) using both traditional methods and the UFA. The collaboration with PNNL to do XMT analyses offered us a rare look into the structure of the soil cores and alerted us to certain practices and materials that could cause preferential flow in the core.

Development of In-House Expertise with the UFA Instrument

We collaborated with PNNL, purchasing a J-6 UFA from UFA Ventures, Inc. (Richland, Washington), and installing it at the INEEL. Once the instrument was installed, a UFA Ventures, Inc. technician spent 3 days at the INEEL training two INEEL staff hydrologists and one lab technician in instrument-specific operation and maintenance. In addition, one INEEL hydrologist completed 2 weeks of hands-on training at PNNL.

Hanging Column/Pressure Cell Experiments

Standard laboratory techniques for measuring moisture characteristic curves of vadose zone materials include hanging column and pressure cell experiments.[1] The soil samples examined in this study were initially scanned by PNNL and then returned to the INEEL. The INEEL then measured moisture characteristic curves of the samples and returned them to PNNL for final XMT imaging. Neither XMT imaging nor visual observations of the samples indicated that the sample structure had been altered as a result of the analysis. Figure 1 shows the moisture characteristic curves obtained using the hanging column/pressure cell techniques.

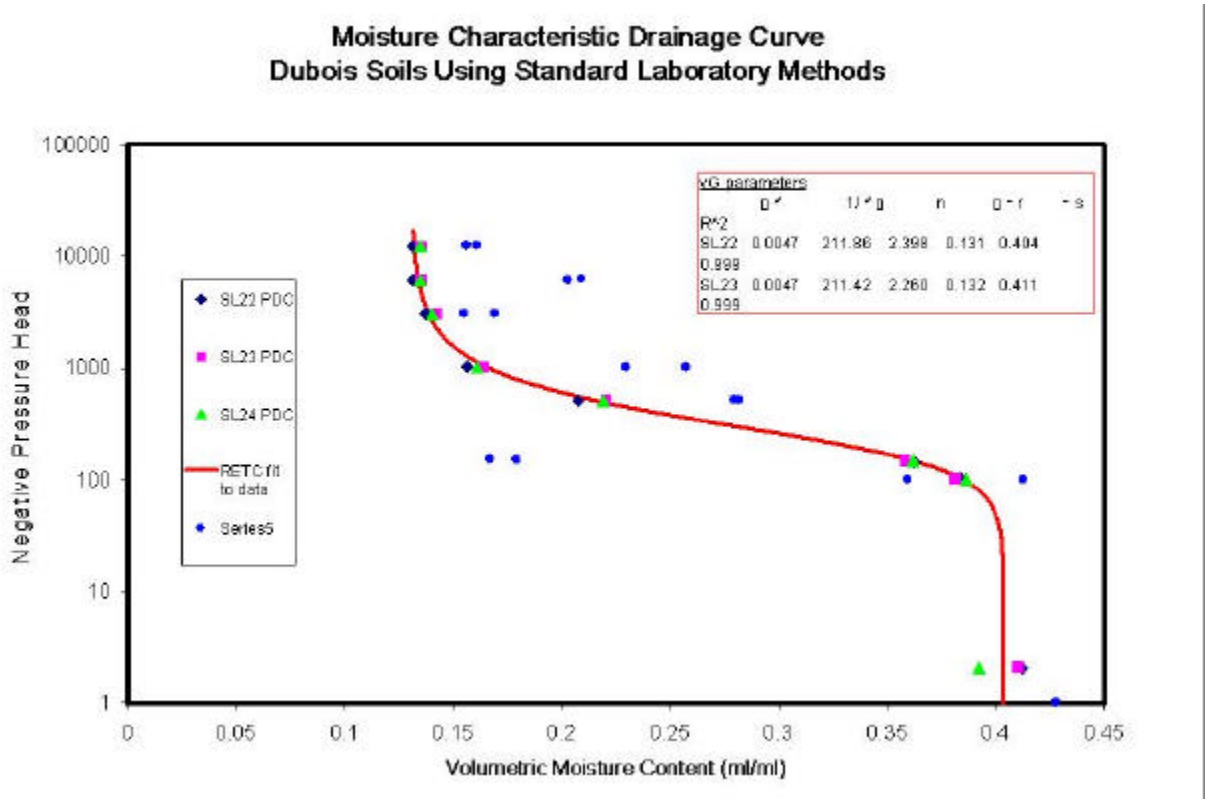

Figure 1. Moisture characteristic curves for soil samples measured using traditional laboratory methods such as the hanging column and pressure cells.

In-House Expertise with the UFA Instrument

We developed expertise on the UFA instrument with anisotropy studies conducted on undeformable, intact materials, including two types of basalt (Snake river plain dense and vesicular basalts), a layered sandstone (Massillon), and a poorly lithified sandstone (Berea). Once expertise on the UFA was acquired, studies on deformable soils were initiated to examine equilibrium times and to determine moisture characteristic curves.

Anisotropy Studies. The rock cores were subcored in three orthogonal directions, saturated under vacuum, and then drained in the UFA at various pressures. Once the samples had reached steady state, moisture content was determined at each pressure head. The curve fitting program RETC[2] was used to obtain the van Genuchten curve fitting parameters (ζ, n, and χ_r) shown in Equation 1, which describe the shape of the moisture characteristic curves for each sample:

$$\chi = \chi_r + \frac{\chi_s - \chi_r}{[1 + (\zeta h)^n]^m} \qquad (1)$$

where χ is the volumetric moisture content (mL/mL), χ_s is the saturated moisture content (mL/mL), χ_r is the residual moisture content (mL/mL), ζ is a fitting parameter (cm^{-1}), h is the pressure head (cm), n is a fitting parameter (describing slope of the curve), and m is defined as *1-1/n*.

The pressure head in Equation 1 is estimated from the UFA data as depicted in Equation 2:

$$h = \left(\frac{\omega^2}{2g}\right)\left(r_1^2 - r_2^2\right) \quad (2)$$

where h is the pressure head (cm), ω is the rotational speed (radians/s), g is the gravitational constant, r_1 is the horizontal distance from center of rotation to the top of the sample (cm), and r_2 is the horizontal distance from center of rotation to the bottom of the sample (cm).

Moisture characteristic curves for the cores are shown in Figure 2. Anisotropy was observed in the vesicular basalt, while the other materials appeared to be isotropic at the scale observed. These results suggest that rock formation processes, such as cooling rates and cementation, may have a greater effect on moisture retention than sedimentary structure. This is of great potential interest to the INEEL because the vesicular basalts that underlie the site may be a conduit for contaminant transport to the aquifer below, and accurately predicting directional flow is important for predicting contaminant mobility. Further work is needed to fully understand the underlying causes of anisotropy and its effect on directional transport.

Soil UFA Studies. The soil used in this study was characterized as a fine sandy loam, moderately calcareous, with a porosity of approximately 43%, mean particle density of approximately 2.6 g/cm^3, and a saturated hydraulic conductivity on the order of $1 \Delta 10^{-5}$ cm/s. The soil has a fairly high clay content of approximately 8% by weight, causing the soils to compact during desorption by centrifugation by as much as 14% by volume.

UFA Measurements. Two replicate samples were separately subcored for each of seven pressures measured in the UFA. The samples were saturated using vacuum saturation techniques (Reference 1), scanned at PNNL, then drained in the UFA. No compaction was observed in the soil cores at low rotational speeds (<500 rpm), however the samples analyzed at higher rpm did show a high degree of compaction. Comparison of the UFA-normalized moisture characteristic curve (Se(h) defined by Equation 3) to the traditional normalized curve (Figure 3) shows that the UFA curve resulted in a lower air entry pressure, a lower n value (less uniform pore size distribution), and higher pressures required to reach residual moisture content.

$$Se = \frac{\theta - \theta_r}{\theta_s - \theta_r} = \left[1 + (\alpha h)^n\right]^{-m} \quad (3)$$

where Se is the effective saturation.

X-ray Microtomography. Comparison of the digital radiograph images taken before (initial) and after (final) draining of the soils in the UFA show the amount of compaction resulting from centrifugal forces exerted on the samples (Figure 4). In order to quantify the degree of compaction, the height of the samples shown in the images were measured using XMT software. Figure 4 also shows initial and final XMT images of 0.10 mm thick cross sections along the length of the core.

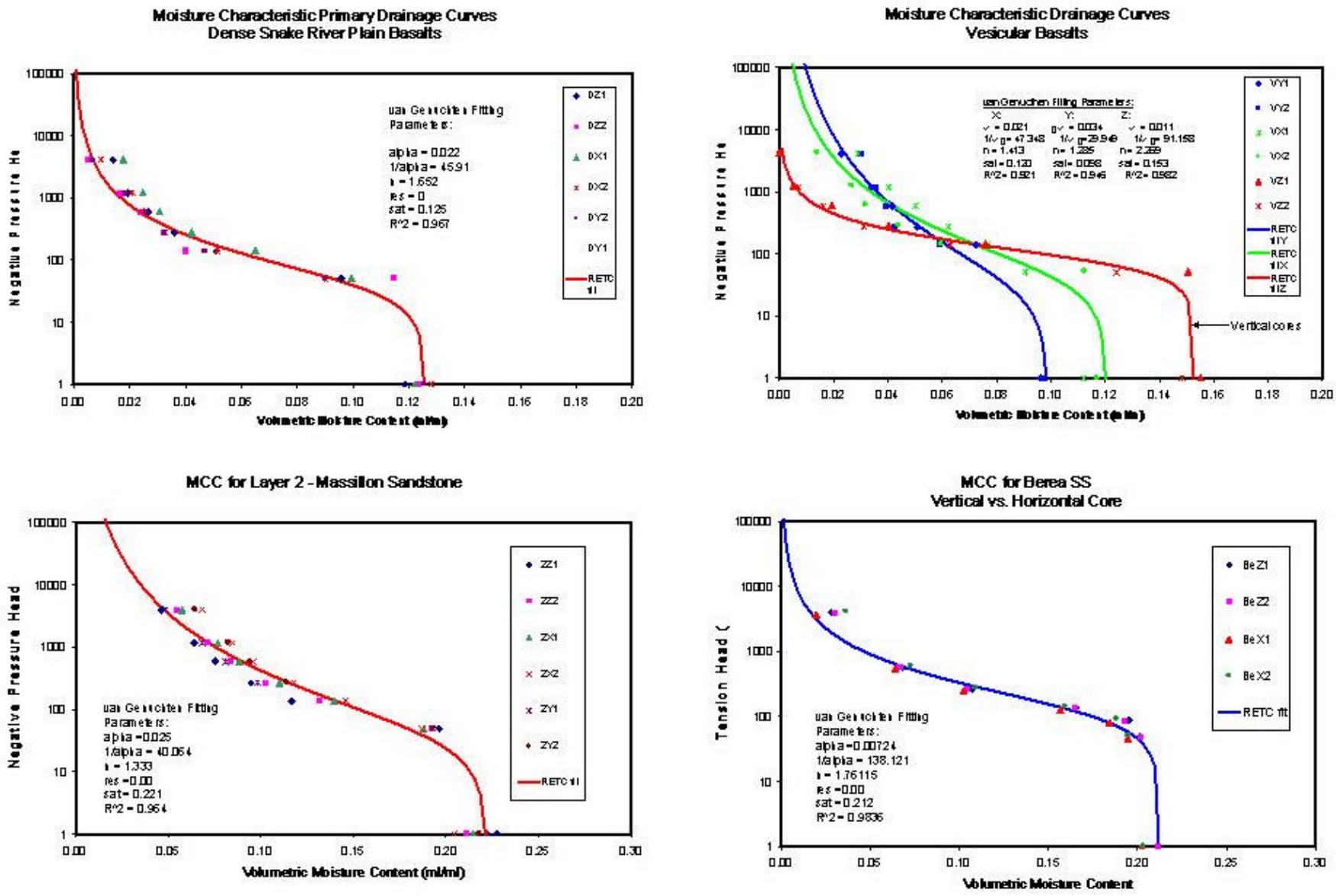

Figure 2. Moisture characteristic curve measured for basalts and sandstones examined in three orthogonal directions.

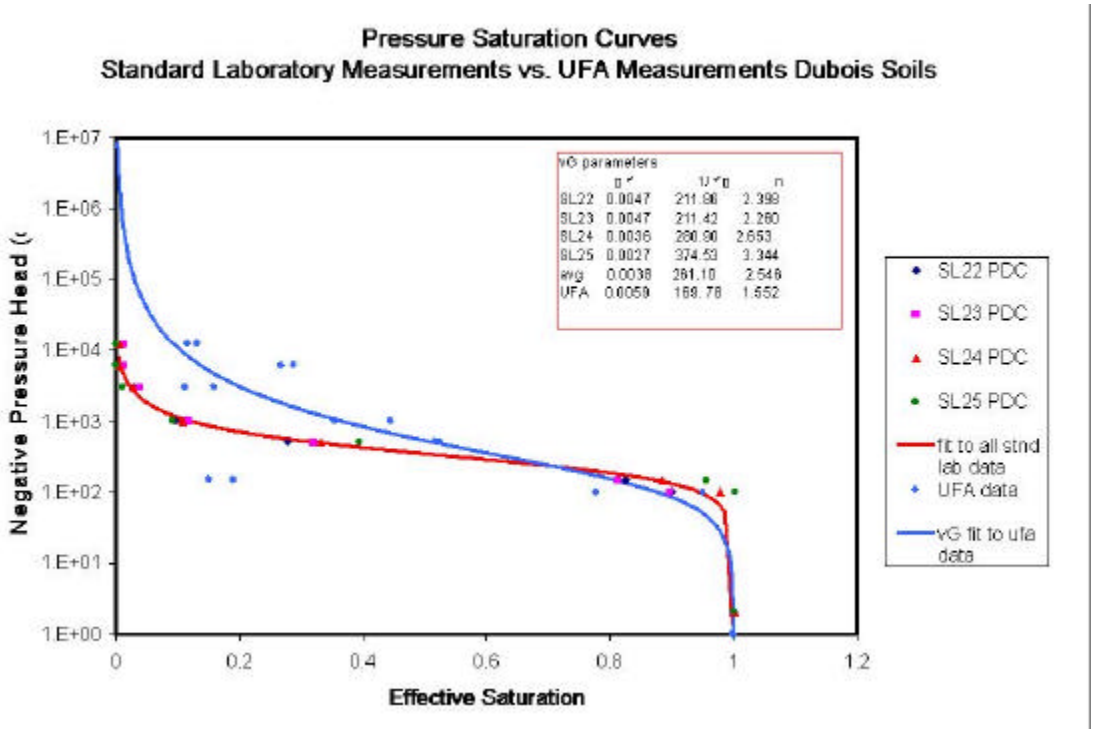

Figure 3. Comparison of moisture characteristic curves measured using traditional methods to curves measured using the UFA.

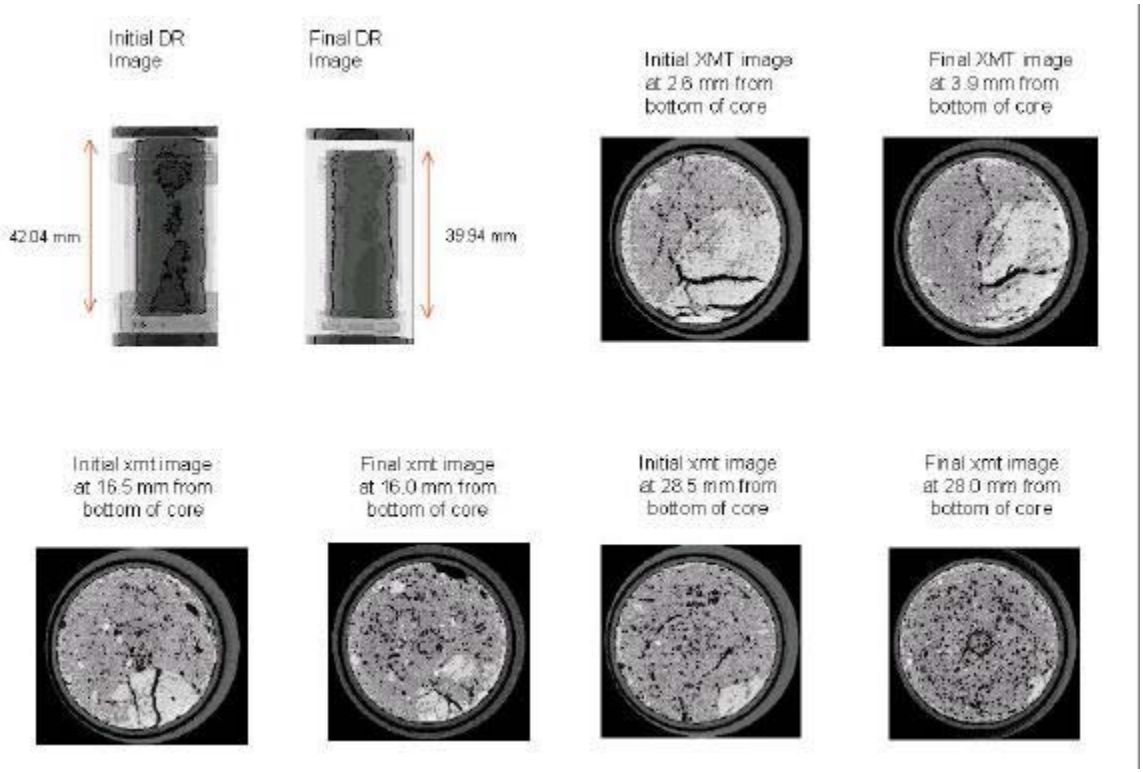

Figure 4. Digital radiograph and XMT images of core number 41 drained at 1,560 rpm (1,020 cm negative pressure head) in the UFA. The soil core compacted 2.1 mm during desorption.

Determining Relationships Between Moisture Characteristic Curves of Compactible Soil Measured in Hanging Columns and in the UFA

Centrifuge Modeling. The first step in this modeling effort was to account for the effects of the centrifugal field in the geocentrifuge. Water is forced through the soil by the generation of a matric potential, characterized by Equation 2 and compaction of the soil behaves as follows:

$$\kappa_2 \mid C_c \log\left(\frac{p_2}{p_1}\right) \mid 2\ \kappa_1 \tag{4}$$

Using iterative techniques, average porosity, density, and matric potential can be computed at various rotational speeds. However, the mass of the soil element varies with the porosity of the element and the mass of water in the soil element, therefore the volumetric water content of the soil as a function of pressure is calculated using the van Genuchten equation (Equation 1).

Compaction Modeling. As the soil compacts, the void fraction of small pores increases and the void fraction of large pores decreases.[3] These areas of increase and decrease are distinct and pore sizes in certain ranges are assumed to behave similarly. The similarly-behaving pore sizes were assigned a pore type. In general terms, pores of a certain type were said to increase or decrease their void fraction by a specified amount.

Modeling Results. The first step in obtaining model results was to define constants in the compression ratio equation (Equation 4). This was accomplished by conducting consolidometer experiments with the undisturbed soil samples.[4] Additional input parameters for the model inlcude estimates of the "true" van Genchten fitting parameters (Equation 1) describing the shape of the "uncompacted" moisture characteristic curve and the parameters obtained from UFA measurements of compacted soils.

The uncompacted "true" parameters required in the prediction were obtained using two separate methods. The first method used parameters obtained from direct measurements of the uncompacted soils using traditional techniques. Since direct measurements are time consuming, the objective of this study was to avoid these type of measurements. Therefore, the second method estimated the "true" parameters from "general" parameters listed in a soil hydraulic database (Unsatured Soil Hydraulic Database or UNSODA) complied by the U.S. Soil Salinity Laboratory (Referece 2). Results from fitting the van Genuchten equation to the predicted data using both methods are shown in Figure 5.

The predicted moisture characteristic curve using directly measured uncompacted parameters is in good agreement with the "true"curve, which validates the model. Using data from UNSODA to estimate the initial (uncompacted) van Genuchten parameters provided a poor prediction of the actual moisture charactersitic curve, which indicates that "general" parameters for various soil types are not adequate. Thus, the model can be used to predict the moisture characteristic curves for a large number of similar samples, provided that a small subset is initially measured using traditional methods. Other sources and methods than the UNSODA database are available for estimating these initial parameters as well (Reference 1). Future work should include alternative methods for estimating initial parameters that do not require direct time-intensive measurements. For example, one might use vacuum saturation techniques to measure the saturation, use the UFA to obtain the air entry pressure (since there was no compaction at low rpm), and traditional methods to measure the residual moisture. With these basic estimates, the inflection points in the moisture characteristic curve can be predicted, which provides soil-specific initial parameters for the model. The basic concepts of this model can be used in future studies to estimate hydraulic conductivity measurements of compacted soils using the UFA rather than traditional methods.

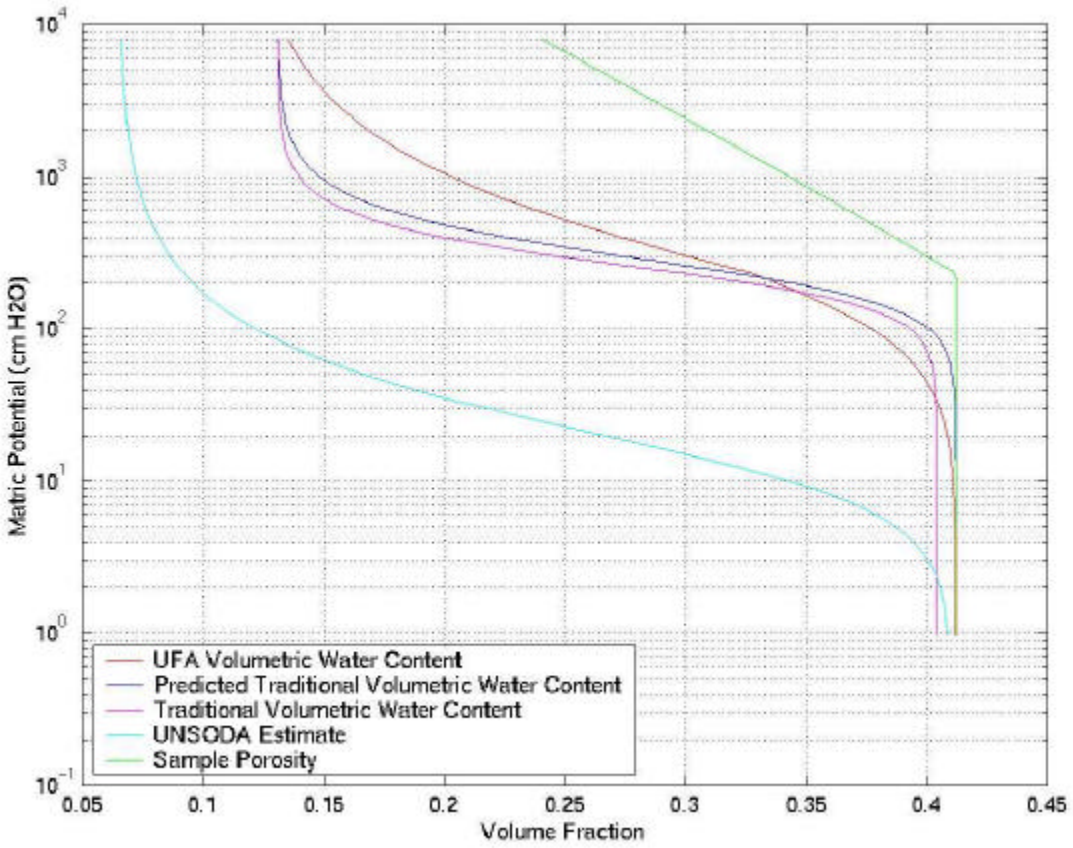

Figure 5. Predicted moisture characteristic curves obtained using UNSODA model parameters and model parameters obtained from traditional methods. Residual moisture content used in both predictions was assumed to be equal to measured residual moisture content from traditional methods.

ACCOMPLISHMENTS

We established collaboration with Clark Lindenmeier at PNNL, who has significant experience in both operation and interpretation of results from UFA instruments and with XMT.

We devised a coring and shipping method that should allow reproducible data from replicate cores.

We purchased and installed a J-6 UFA instrument at the INEEL.

We ran preliminary XMT tests with samples cored at the INEEL and shipped to PNNL, identifying preferred methods for coring, packing, and shipping the samples to and from each site.

We measured traditional moisture characteristic curves and examined soil structure using XMT technology.

We examined anisotropy of four different rock types, and identified anisotropy in vesicular basalts collected from the INEEL.

We developed methodologies for measuring moisture characteristic curves using the UFA, and determined UFA soil moisture equilibrium times for pressures examined in this study.

We measured moisture characteristic curves in the UFA and quantified changes in porosity due to compaction.

We developed a model to convert UFA measurements to moisture characteristic curves measured for noncompacted soils.

REFERENCES

1. K. E. Baker, *Investigation of Direct and Indirect Hydraulic Property Laboratory Characterization Methods for Heterogeneous Alluvial Deposits: Application to the Sandia-Tech Vadose Zone Infiltration Test Site*, U.S. Department of Energy, Office of Environmental Management, DOE Operations Office, Contract DE-AC07-99ID13727, INEEL/EXT-01-00471, 2001.

2. M. Th. van Genuchten, F. J. Leij, and S. R. Yates, *The RETC Code for Quantifying the Hydraulic Functions of Unsaturated Soils*, U. S. Salinity Laboratories, USDA, EPA/600/2-91/065, 1991.

3. G. Richard, I. Cousin, J. F. Sillon, A. Bruand and J. Guerif, "Effect of Compaction on the Porosity of a Silty Soil: Influence on Unsaturated Hydraulic Properties," *European Journal of Soil Science*, Vol. 52, 2001, pp. 49–58.

4. J. E. Bowles, *Engineering Properties of Soils and their Measurement*, 4th Ed., 1992, McGraw Hill.

Geological, Geophysical, and Hydrological Environs of the INEEL Site

Refining our Understanding of INEEL Groundwater Flow

Richard P. Smith (INEEL); Paul Link, Glenn Thackray, Joe Kruger, Rick Allison, and Andy Smith (ISU); Glen Embree and Kathleen Price (BYU Idaho); Bill Bonnichsen, Martha Godchaux, and John Welhan (Idaho Geological Survey/University of Idaho)

SUMMARY

Scientifically defendable decisions about disposal, cleanup, and stewardship alternatives require that INEEL-specific sites be understood in the context of regional geologic and hydrologic processes and subsurface environments. Existing data shows that groundwater flow directions in the aquifer are strongly influenced by the regional stress field in the earth's crust, variations in aquifer thickness, input of geothermal waters from depth, preferred orientations of sediment interbeds and lava flows, and fractures and dikes in volcanic rift zones. All of these factors produce an anisotropy (bias) in hydraulic conductivity that makes groundwater flow in directions quite different from that indicated by the hydraulic gradient.

The purpose of this task is to facilitate better understanding of the subsurface regional context of the INEEL by (a) synthesizing existing unpublished information and compiling it into a common format so that all information is available and useful for decision making, and (b) performing several short-term field investigations that will complete the aerial coverage and provide a comprehensive understanding of regional geologic and hydrologic processes. The area selected for these activities includes a large portion of the Eastern Snake River Plain and adjacent mountains (Figure 1). This provides INEEL-specific geologic and hydrologic data in its proper regional context. Such regional understanding is necessary because up-gradient processes in the Snake River Plain aquifer affect the INEEL, INEEL activities and past practices affect down-gradient regions of the aquifer, and regional seismic and volcanic processes affect the current operation of facilities and long-term stewardship of waste disposal facilities at the INEEL.

This research focuses on developing a better understanding of all the factors that influence aquifer dynamics and geometry. The results will improve our assessments of contaminant transport in the aquifer and furnish boundary conditions for detailed modeling of INEEL-specific sites.

The large body of unpublished geoscience information that exists for the region (geologic mapping, geophysical surveys, and investigations of volcanic processes) is being compiled digitally in the geographical information system (GIS) format on 1:100,000-scale maps so that it adjoins seamlessly with the current geologic map of the INEEL (see Figure 1).[1] GIS personnel were hired at Idaho State University (ISU) and trained at the Idaho Geological Survey (IGS) electronic map publication office, and three of the 7.5 minute quadrangles of the Rexburg 1:100,000-scale sheet were completed and sent to IGS for publication.

Several field investigations were started (see Figure 1). Field mapping of the Snake River corridor north of Idaho Falls, the rhyolitic volcanic rocks along the north margin of the Eastern Snake River Plain, and several quadrangles northwest of Rexburg will fill the biggest areas where very little geologic data exists. Detailed geophysical data for an area in the southern Great Rift were collected to test the ability of magnetic and gravity surveys to detect dikes in the subsurface.

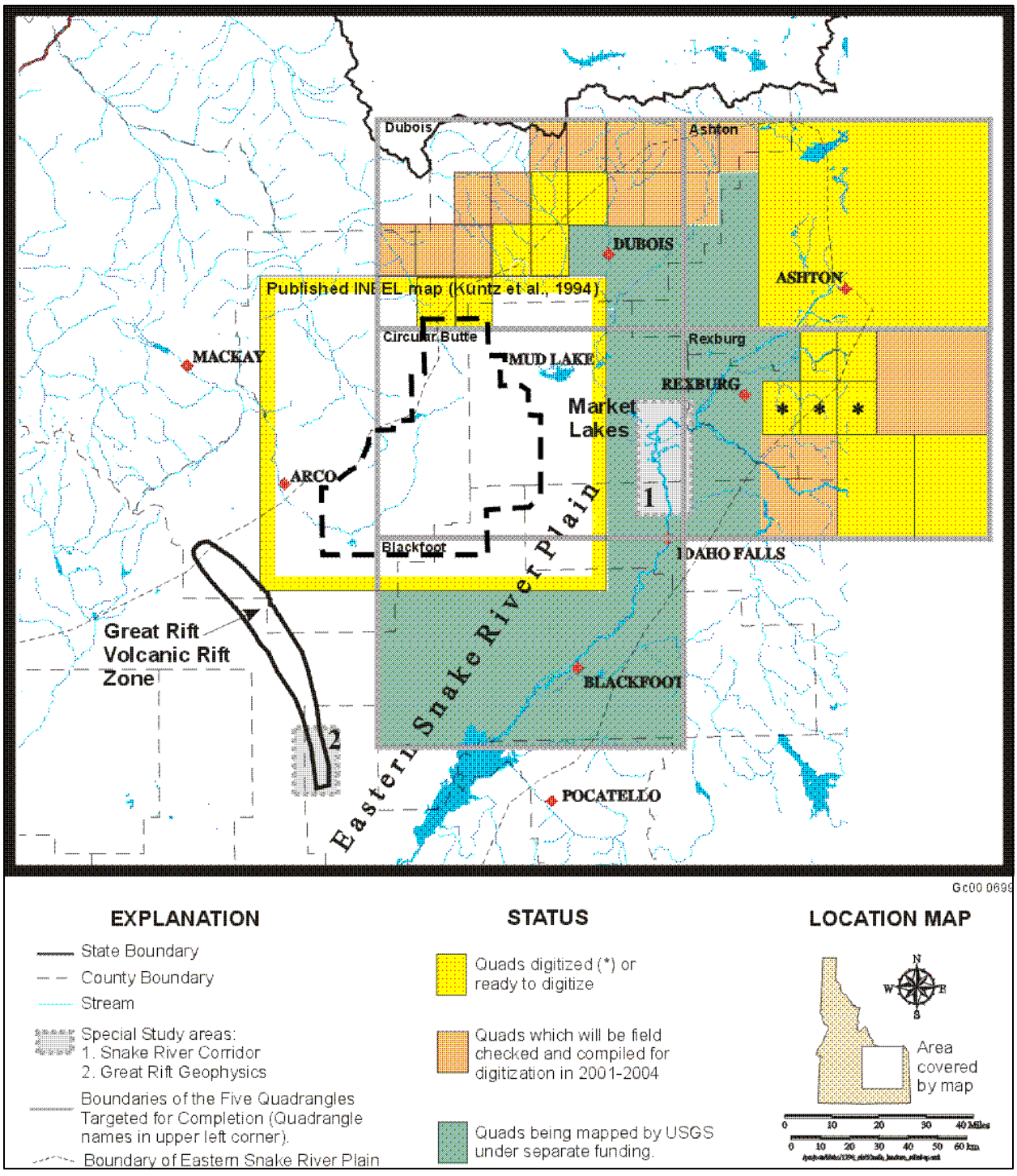

Figure 1. Regional map showing stream drainages, major towns, locations of the five 1;100,000-scale quadrangles to be completed during this task, locations of special study areas, and status of geologic mapping.

TASK DESCRIPTION

This is a broad integration and synthesis task. It employs the expertise of geoscientists with specific knowledge of various aspects of Eastern Snake River Plain geology, and takes advantage of the following unpublished geologic mapping activites relevant to regional aquifer problems in the INEEL area.:

- Mapping by the United States Geological Survey (USGS)
- Mapping by geologists at ISU and BYU Idaho
- Geophysical surveys performed by INEEL programs
- Geophysical surveys performed by other institutions
- State-of-the-art knowledge of volcanic processes operating during the origin of the Eastern Snake River Plain by IGS personnel
- Several short-comings of the existing database, in terms of both unstudied areas near the INEEL and gaps in geologic understanding, are being addressed by relatively inexpensive short-term field investigations. The purpose of this task is to synthesize the existing informa-tion and to compile it into a common format so that all information is available and useful for decision making, and perform several short-term field investigations that will complete the aerial coverage and provide a comprehensive understanding of regional geologic and hydrologic processes.

This task is divided into the following subtasks, each with a focused objective and overarching synthesis, that incorporate the results from each activity into the development of improved conceptual models of INEEL-area geology and hydrology:

1. *Define the geomorphology and geology of the Snake River corridor north of Idaho Falls (Figure 1, Special Study Area 1).* We are focusing on this because very little information exists for the area, and the Snake River in this region exhibits agradation features (suggesting crustal subsidence) and a lack of terraces typical of down-cutting rivers. This task fills in an area of unknown geology on the map and addresses a lack of conceptual understanding of riverine processes in the area.

2. *Perform microgravity and magnetic surveys of known dike systems in the Great Rift volcanic rift zone (see Figure 1, Special Study Area 2).* This is the field acquisition part of the assessment of geophysical techniques to identify subsurface dikes that affect aquifer flow. The field acquisition phase includes the collection of raw microgravity and magnetic data across known dikes. Complete data reduction and processing to interpret the relationships of gravity and magnetic anomalies to dike positions and depth beneath the surface will occur in the following years.

3. *Compile and field verify existing geologic mapping in the Rexburg quadrangle (see Figure 1, status blocks for Rexburg quadrangle).* This task takes advantage of several decades of geologic mapping by Glenn Embree and Roger Hoggan and their students at BYU Idaho. Much of the work was supported by the USGS in their Snake River Plain research project in the 1970s, some was supported by the INEEL for seismic hazards assessment in the 1990s, and some was supported by field activities at BYU Idaho. Several 7.5 minute quadrangles are completed or nearly completed. This task comprises field verification and compilation of existing maps and development of plans for additional study of unmapped areas in follow-on years. As the maps are compiled and field checked, they will be sent to the GIS laboratory at ISU for digitization.

4. *Evaluate rhyolites and calderas beneath the INEEL area.* Rhyolitic volcanic rocks that erupted from calderas beneath the INEEL area are exposed along the north margin of the Snake River Plain in the Dubois and western part of the Ashton quadrangles (see Figure 1, status blocks for the Dubois and Ashton quads). These rocks contain information about the eruption mechanisms, caldera locations, and magmatic processes in the early evolution of the Eastern Snake River Plain, but they have not been studied in the detail necessary to yield that information. Geologists from the IGS, who are recognized experts on similar rock sequences in the Western Snake River Plain, are applying their expertise to evaluate the rocks in this area.

5. *Produce digital geologic maps so the spatial geologic information acquired in this task will be of maximum value for modeling of the subsurface physical environment.* The information will be digitized by the GIS laboratory at the ISU Geology Department. This will allow analysis of the information with hydrologic and contaminant data already existing in GIS format. The task involves training an ISU GIS technician to the state-of-the-art in digital map preparation at the Idaho Geological Survey GIS laboratory and digitization of compiled maps as they are completed. Digitized maps will be published by the IGS, which has developed and maintains a national leadership role in digital geologic map publication.

6. *Conduct geoscience workshops.* A field workshop held towards the end of the fiscal year will allow the participants to actively interact and learn from each other's discoveries. The participants will present the results of the first year's work and develop plans for the following year. After this first year, workshops will be held twice each year, once in the spring to discuss data analysis completed during the previous winter and to plan the summer's activities, and once in the fall, to summarize the year's work, discuss field results, and plan work for the following year.

7. *Synthesize task results*. The results of the specific tasks are likely to provide maximum benefit to the INEEL conceptual models only if they are interpreted in relationship to each other and to existing conceptual models. The synthesis task is designed to assure that we reap maximum benefit by examining all the implications of specific task results to regional processes that affect the aquifer and subsurface environment beneath the INEEL area.

ACCOMPLISHMENTS

The major accomplishments summarized below are keyed by number to the tasks introduced in the Task Summary section above.

1. We completed aerial photograph and topographic map interpretation of flood plain and sediment landform features along the Snake River between Idaho Falls and Menan (see Figure 1, Special Study Area 1), field investigations (descriptions, sampling, relative age assessments, stratigraphic sequence determinations), and a preliminary map of surficial deposits along the river. In addition, we drilled four boreholes into the area to examine stratigraphic relationships and obtain samples for age determinations. This work shows that the area had been the site of a lake during much of recent geologic time (Market Lake is a remnant), that the river's course has been affected by basaltic volcanism, and that river terraces characteristic of down-cutting rivers are absent north of Idaho Falls but present between Idaho Falls and Blackfoot. Instead of characteristic terraces, the South Fork has built a large alluvial fan that forces the river westward against basalt lava flows. The absence of terraces appears to be partly due to intensive farming activities in the area, but the fact that farming practices can destroy geomorphic evidence of terraces indicates that any original terraces were very small. This corroborates first-order leveling data[2,3] that reveal rapid crustal subsidence in the Snake River Plain north of Idaho Falls, and suggests a long duration for the subsidence, extending back into Pleistocene time. This is independent evidence for differential

crustal subsidence in the Eastern Snake River Plain, a process suspected based on variations in basalt accumulation rates and stratigraphic correlation in INEEL area wells.[4]

2. We collected detailed geophysical data along three lines across a known dike in the southern Great Rift, south of the Craters of the Moon volcanic field (see Figure 1, Special Study Area 2). The goal of these surveys is to test the ability of detailed magnetic and gravity data to detect dikes or dike swarms in the subsurface. There is both a theoretical and observational basis for believing that magnetic and gravity data are sensitive to dikes of basalt cutting basalt lava flows[5,6] and this is the first test in the Snake River Plain. Only the data collection step was completed during FY 2000, and the data processing and interpretation necessary to complete the test will be done in follow-on years. This is an important test because we know that many dikes exist in the subsurface of the INEEL area and their NW trending orientation is almost perpendicular to the regional direction of groundwater flow. They are likely to affect the direction and velocity of groundwater flow because of their much lower permeability than interlayered basalt lava flows, but we lack ways to detect their presence and geometry. This activity is the first step in assessing the viability of using geophysical techniques to detect locations and geometries of dikes that may influence aquifer flow.

3. We completed field verification and compiled three 7.5-minute quadrangles in the Rexburg 30 Δ 60 ft sheet, the compilation sheets were digitized at the ISU GIS laboratory, and the digital files are in review and preparation for publication at the IGS (see Figure 1, yellow status blocks with asterisks). We completed field verification of several more of the 7.5-minute quadrangles; compilation during the winter months will provide more maps to be digitized at ISU (see Figure 1, orange status blocks in the Rexburg quad).

4. We completed reconnaissance examination of rhyolitic rocks along the northern margin of the Snake River Plain. This included field checks of previous mapping in six 7.5-minute quadrangles and confirmation that all six are adequate and ready for digitization and publication (see Figure 1, yellow status blocks in Dubois and Ashton quads, and Figure 2). Mapping was incomplete in 14 quadrangles, but field activities will focus in those areas over the next 3 years (see Figure 1, orange status blocks in Dubois and Ashton quads). We recognized five different domains of faulting in the area, each represents a different time period and style of tectonism. Investigations of the relationships among these domains over the next 3 years will clarify tectonic and volcanic relationships and improve seismic hazards assessments for the INEEL. We recognized many flow-direction indicators in the rhyolitic rocks; they suggest that some of the rhyolitic units had multiple sources beneath the basalts of the Snake River Plain, and that the calderas that fed them had a complex eruptive history. Additional work on these features will provide a better conceptual understanding of the probable volcanic structures and geothermal systems to be found beneath the basalts in the INEEL region. The interaction of geothermal systems with the Snake River Plain aquifer can potentially influence aquifer flow directions and velocities. Reconnaissance investigations completed this summer helped develop a work plan for detailed investigations to be carried out in follow-on years.

5. A GIS laboratory was developed at ISU and staffed with trained personnel. This lab can produce digital geologic map files in formats compatible with Idaho Geological Survey map publication standards. Three 7.5 minute digital quadrangle maps were produced and sent to IGS for peer review and publication (see Figure 2). The ultimate publication of digital geologic maps of the entire region affecting the INEEL will provide the regional context of aquifer processes and valid boundary conditions for the INEEL aquifer flow and contaminant transport models. Early in September 2000, the participants gathered in Idaho Falls for the first of several scheduled workshops. The 2-day workshop consisted of a field-based examination of the areas where work was done during FY 2000. It allowed participants to present the results of the first year's work,

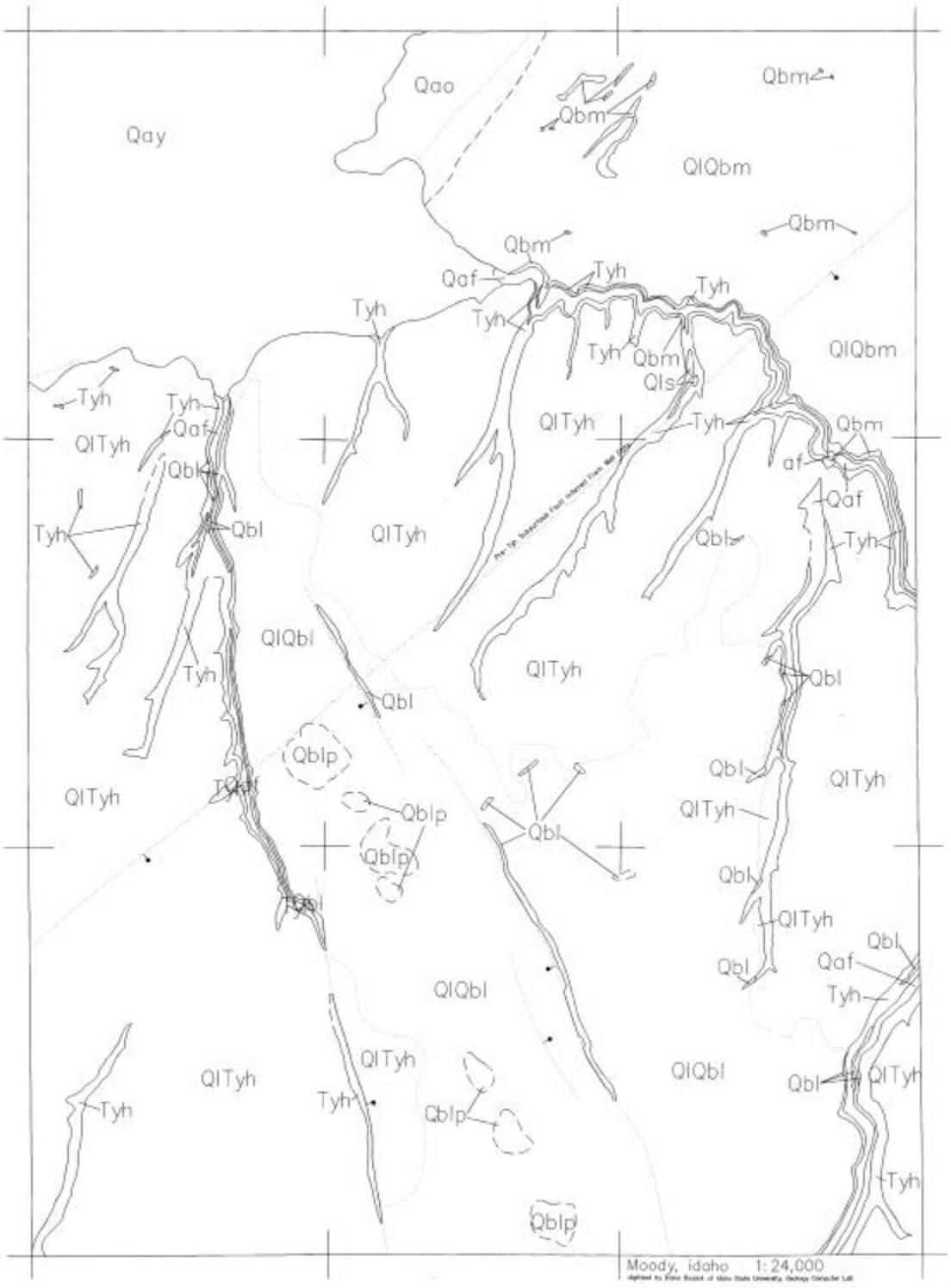

Figure 2. One of the completed digital geologic map files sent to IGS for publication. The outlined areas represent the outcrop areas of a different rock units and the letter designations are abbreviated identifiers for each rock type. The geologic information in the digital files will be presented in the final published maps as areas of different color overlain on topographic maps whic h show landforms, drainages, and political boundaries.

receive feedback from the other researchers, and develop plans for the following year. The synergy developed in this workshop was especially productive in the area along the Snake River north of Idaho Falls (see Figure 1, Special Study Area 1), where the lava flow eruption history and theaccumulation history of river sediments were brought together for the first time. This provided ideas for testable hypotheses about crustal subsidence, river agradation, the potential role of lava dams in developing lake sediments and river course migration, and the isolation of the Mud Lake basin (and INEEL area) from the Snake River drainage system. All of these processes have important implications for INEEL-area hydrology, and seem to converge in the a single area of the Snake River drainage.

6. The synthesis of the results of the work on this task confirmed our expectations that advances in regional understanding would appear, and that unforeseen relationships would come to light. We made the following important advances:

   - Turned up independent evidence of differential crustal subsidence along the Snake River north of Idaho Falls, which provides more confidence in interpretations that differential subsidence occurs in the crust beneath the INEEL. This is important to aquifer understanding because differential subsidence rates can help to explain variations in aquifer thickness across the INEEL and help us to better predict the areas where the aquifer is unusually thick or thin. It is also important from a seismic and volcanic hazards point of view because it provides a better picture of regions where faulting and volcanism are concentrated.

   - The discovery of spatially and temporally different faulting domains along the northern margin of the Snake River Plain will improve seismic hazards assessments at the INEEL by giving us a better picture of the mechanisms and rates of crustal subsidence of the Snake River Plain, and of the interaction of the subsidence process with faulting related to regional basin-and-range extension in the mountains adjoining the Snake River Plain.

   - Our best hope for improved understanding of rhyolitic volcanic processes that operated in the Snake River Plain before the accumulation of the basaltic lava flows is by detailed investigations of the erupted rhyolites that are still preserved in the valleys north of the Snake River Plain. The discovery that there were multiple source areas for one of these rhyolite units provides a clearer picture of the geometry of calderas underlying the basalts on the Snake River Plain. This is important because caldera geometry is one of the major controls of the locations of deep-seated geothermal systems that impinge on the base of the aquifer and affect its chemistry, temperature, and flow dynamics.

   - We collected an extensive geophysical data set, consisting of gravity and magnetic data at thousands of stations across known dike systems. This will allow assessment of the viability of geophysical detection of unknown dikes. Knowledge of the locations and geometries of dikes in the subsurface will help to understand aquifer flow and provide better seismic and volcanic hazards assessments.

REFERENCES

1. M. A. Kuntz, et. al., “Geologic Map of the Idaho National Engineering Laboratory and Adjoining Areas, Eastern Idaho,” *U.S. Geological Survey Miscellaneous Investigation Map*, I-2330, 1:100,000 scale, 1994.

2. J. R. Pelton, *Analysis of Geodetic Leveling Data in the Vicinity of the INEL*, EG&G, Informal Report EGG-NPR-10691, 1991.

3. R. E. Reilinger, G. P. Citron, and L. D. Brown, "Recent Vertical Crustal Movements from Precise Leveling Data in Southwest Montana, Western Yellowstone National Park, and the Snake River Plain," *Journal of Geophysical Research*, Vol. 82, No. 33, 1977, pp. 5349–5359.

4. S. R. Anderson, M. J Liszewski, and L. D. Cecil, "Geologic Ages and Accumulation Rates of Basalt-flow Groups and Sedimentary Interbeds in Selected Wells at the Idaho National Engineering Laboratory, Idaho," DOE/ID-22134, *U.S. Geological Survey Water Resources Investigations Report*, 97-4010, 1997.

5. V. J. Flanigan and C. L. Long, 1987, "Aeromagnetic and Near-surface Electrical Expression of Kilauea and Mauna Loa Volcanic Rift Systems," *Volcanism in Hawaii*, *U.S. Geological Survey Professional Paper 1350*, R. W. Decker, T. L. Wright, and P. H Stauffer, editors,1987, pp. 935–946.

6. G. Schoenharting and G. Palmason , "A Gravity Survey of the Reydarfjordur Area, Eastern Iceland, with Interpretation," *Journal of Geophysical Research*, Vol. 87, 1982, pp. 6419–6422.

Advanced Geophysical Characterization to Enhance Earth Science Capabilities at the INEEL to Support Remediation and Stewardship

Enhanced Geophysical Characterization of Subsurface Contaminants

Russ Hertzog and Gail Heath

SUMMARY

The advanced geophysical characterization research task consisted of acquiring and using enhanced systems to characterize the vadose zone and groundwater, which will allow definitive evaluation of contaminant migration and has the ability to evaluate the performance of engineered subsurface barriers. The key to successful advanced geophysical characterization is a strongly integrated collaboration among the other major scientific disciplines to determine the appropriate physical, geological, biological, and chemical measurements needed to fully understand and characterize the relevant geoscience processes and properties in the vadose zone affecting contamination movement.

TASK DESCRIPTION

This research consisted of two subtasks. The first supported an ongoing acoustic tomography research effort to develop measurements and analyses for characterizing Pit 9. The second contributed to the purchase of state-of-the-art electrical magnetic (EM) survey equipment for use in evaluating and developing enhanced numerical simulation and visualization capabilities for integrating the borehole measurements with the geophysical characterization into better representations of the vadose zone. A specific goal of this task being to better relate the commonly measured geophysical (e.g., electrical resisitivity tomography (ERT), resistivity, velocity, etc.) characteristics of the subsurface to the corresponding characteristics important for fluid transport such as permeability or porosity.

Acoustic Tomography in Pit-9

Gail Heath provided geophysics support to the Center for the Subsurface Sensing and Imaging Systems (CenSSIS) team during the acoustic diffraction tomography, data-acquisition experiments at Pit-9. This support included training the CenSSIS team and preparing all environmental and safety work for data acquisition. Data acquisition support was also provided during the experiment. The CenSSIS team consisted of Dr. Sean Lehman from Lawrence Livermore National Laboratory, California; Dr. Anthony Devaney from the Department of Electrical and Computer Engineering, Northeastern University, Boston, MA; Dr. Alan Witten from the School of Geology and Geophysics, University of Oklahoma, Norman, OK; and Michael MacNeil, also from the Department of Electrical and Computer Engineering, Northeastern University, Boston, MA.

Equipment to Evaluate and Geophysical Characterization in the Vadose Zone

This subtask helped commit and realign laboratory resources through geophysical characterization support of the Vadose Zone Research Park, enhanced ERT imaging, and ongoing fracture flow experiments at the INEEL (Figure 1). The Vadose Zone Research Park (see Figure 2), which consists of 28 new wells, was built by other funding. These experiments will help researchers understand and

Figure 1. ERT measurements are used to study fracture flow properties in laboratory experiments (*top left*). A two-dimensional (2-D) experimental tank helps understand the limitations on ERT imaging resolution and inversion processing (*top right*). The Vadose Zone Research Park (*bottom*).

characterize flow paths in the vadose zone at the INEEL. ERT wells were placed around the percolation ponds and adjacent to the Big Lost River to examine the influence of water migration from two new percolation ponds and the nearby Big Lost River.

ACCOMPLISHMENTS

Acoustic Tomography in Pit-9

Two reports describing the experiments and preliminary results on acoustic tomography in the Cold Test Pit and Pit-9 were submitted by the CenSSIS team during the year.[1,2]

The data acquisition supported by this project was deemed of good quality even though the nature of the unconsolidated Pit-9 soils—poor soil compaction leads to very slow acoustic velocities and large attenuation—made data acquisition difficult. Multiple-offset, vertical-profile, acoustic measurements were made in four boreholes. A sledgehammer hitting a square aluminum plate was used as the acoustic source at 1-ft intervals on radial lines laid out from each borehole.

All data from Pit-9 was processed using the Born and Rytov-based diffraction tomography methods. The Born diffraction tomography method, which is wave based, is good for small to medium sized objects; the Rytov-based diffraction tomography method, which is complex-phase based, is good for large extended objects. A third method (Time-Reversal Imaging), which is good for locating small objects in inhomogeneous backgrounds, was not used because it hadn't been fully developed for this application.

The processing results produced 2-D, pseudo-3-D (made from multiple 2-D slices stacked together without interpolation), and true full 3-D images. Overall, the data quality was good and the images show the presence of underground objects as well as layering in Pit-9. Correlations within each imaging modality (2-D and 3-D Born-based and Rytov-based processing) were good to excellent. Subjectively, the 3-D images from the Rytov-based tomography provided the most realistic images of the buried waste materials in Pit-9 (Figure 2), which also compares favorably with photos taken in the 1950s of waste dumping at one of the other INEEL sites.

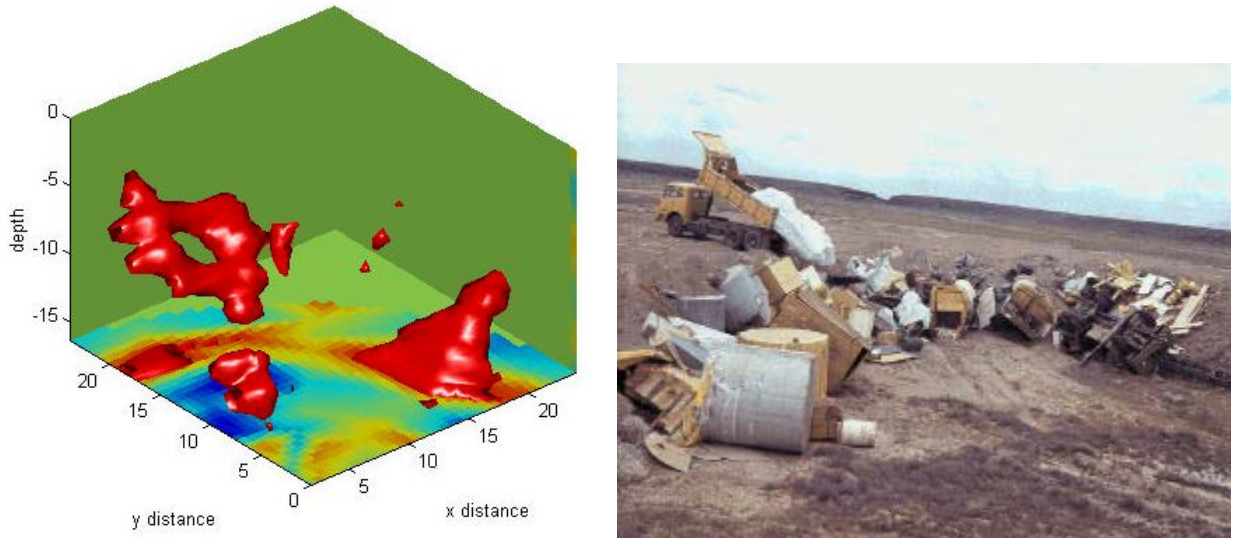

Figure 2. The 3-D-anomaly image from the Rytov-based acoustic diffraction tomography inversions (*left*) compared with a photo taken in the 1950s of waste dumping at one of the other INEEL sites *(right).*

Future data processing plans include optimizing wave speed and frequency selection for increased imaging capability away from the boreholes. In addition, 3-D-image interpolation could be weighted by the distance from the borehole for improved resolution. Restricting view angles and using distorted-wave Born approximations could improve resolution of horizontal layers. Comparisons with "ground truth" would help to evaluate the inversion algorithms; tank experiments with well-characterized targets would also be helpful. Fortunately, such experiments are planned at the INEEL to develop imaging catalogs for geophysical techniques. Finally, using a background layered model and completing the Time-Reversal Imaging theory for this application should improve the ability to see buried materials in the layered and inhomogeneous Pit-9 environment.[3]

Capital Equipment to Evaluate Geophysical Characterization in the Vadose Zone

This project contributed to the purchase of state-of-the-art Zonge Engineering electrical magnetic (EM) survey equipment. The equipment included a mutifunction receiver (model GDP-32), an EM/Resistivity transmitter (model ZT-30), a power supply (model ZPB-600) and a multiplex switch (model MX-30), which provides computer-controlled switching between the transmitter, receiver, and an array of up to 30 electrodes. This equipment will be used for both field and laboratory measurements. Figure 3 shows the new EM survey equipment connected to an electrical resistivity tomography array in a well at the Vadose Zone Science Park near the Idaho Nuclear Technology and Engineering Center. The measurements are used to monitor water infiltration from the new percolation ponds nearby.

Figure 3. The new EM survey equipment connected to an electrical resistivity tomography array. The transmitter is the grey box shown in foreground, the receiver is the white box on the left, and the multiplexer is the yellow box in the background.

REFERENCES

1. A. J. Devaney and A. Witten, "Acoustic Diffraction Tomography Studies at Pit-9," Cooperative Agreement DE-FC07-00ID13968, Interim Report (7/15/00 through 2/01/01), February 2, 2001.

2. A. J. Devaney and Alan Witten, "Acoustic Diffraction Tomography Studies at Pit-9, Data Processing Summary Report," Cooperative Agreement DE-FC07-00ID13968, Interim Report (2/01/00 through 6/01/01), July 15, 2001.

Environmental Computational Modeling

The objective of this area is to develop improved computational resources at INEEL to met current and future EM needs. To this end, computational hardware, interfaces, methods, and models must all be upgraded. Our computing infrastructure must be enhanced to support subsurface science, vadose zone roadmapping, environmental cleanup, restoration, and long-term stewardship responsibilities.

A few examples of present and future activities for which these capabilities are essential include: (a) Modeling the behavior of chemical contaminants in the subsurface; (b) Modeling of contaminated facilities before decommissioning and decontamination; (c) Producing accurate roadmaps of the vadose zone; and (d) Archiving, computing, and external interfacing.

The following task is reported in this section:

⊄# Computing Framework for Environmental Cleanup, Restoration, and Long-Term Stewardship

Computing Framework for Environmental Cleanup, Restoration, and Long-term Stewardship

Advancing INEEL Computing in Support of the DOE-EM Mission

William R. Nelson, L. Eric Greenwade, Donald D. Dudenhoeffer, and May R. Chaffin

SUMMARY

The objective of this task was to develop a computing framework comprised of advanced computing infrastructure, improved computation models and methods, interface methods and tools, and application methods and tools to support EM programs at the INEEL. This computing framework is required to accelerate the development and application of scientific and engineering knowledge to address significant issues in support of subsurface science, vadose zone roadmapping, environmental cleanup, restoration, and long-term stewardship activities at the INEEL and DOE complex. There were two major thrusts for this task: enhancing the advanced computing infrastructure for EM computing at the INEEL, and implementing a collaborative visualization system that demonstrates how new computing capabilities at the INEEL can be applied to environmental management research and operations.

This task has enabled the INEEL to achieve a step-function increase in computing capability through the implementation of two new high-speed lines with the associated computing and storage equipment. As a result of this task, the INEEL purchased and installed a new Silicon Graphics Incorporated (SGI) 64 processor Origen 3800 computer with associated disk and tape storage systems, and implemented a DS-3 line (45 MB/s) to Idaho State University (ISU) and from there to the Internet2 Abilene network. (Internet2 is a collaboration of educational institutions dedicated to developing and using advanced internet capabilities.) Through this task the INEEL became a Sponsored Participant in Internet2 under the sponsorship of ISU.

In cooperation with INEEL Information Resource Management, this task also coordinated the installation of a new 45 MB/s DS-3 line to DOE's energy sciences network (ESNet) at Lawrence Livermore National Laboratory, through which INEEL researchers are now able to transmit large data files, access high-end computing resources, and collaborate with researchers at other DOE laboratories.

All together, these new capabilities allow INEEL researchers to perform complex calculations and simulations, store the results, transfer the resulting data files between the INEEL and other computing centers, analyze and visualize the data, and collaboratively share data visualizations with researchers elsewhere. By combining new processing and storage equipment with the new high-speed data connections, INEEL researchers now have the capability to collaborate with environmental management researchers at other DOE facilities, universities, and federal agencies.

These activities have led to significant improvements of the EM-focused computing infrastructure at the INEEL. Installation of the dual DS-3 lines increased the total data transfer rate into and out of the INEEL by a factor of 30 times. The installation of the new archival and processing equipment improved the maximum processing rate by a factor of approximately 10 times. The base of regular users of high-performance computing at the INEEL has increased by a factor of three as a result of these developments, allowing for user support and development of a significant user base for the new 64-processor machine.

By working with EM researchers and program management we established requirements for environmental management computing at the INEEL and implemented a prototype collaborative

visualization system, which we demonstrated to key EM and subsurface modeling and program management personnel.

The implementation of this computing architecture and framework has increased the overall effectiveness of EM computing capabilities at the INEEL. Taken together, the improvements initiated in this task lay the foundation to enable the INEEL to apply advanced computing technologies to the solution of the major scientific and technical issues facing EM programs.

TASK DESCRIPTION

Many environmental management challenges benefit from the effective use of scientific computing and simulation capabilities. This task focused on developing a computing framework at the INEEL to support subsurface science, vadose zone roadmapping, environmental cleanup and restoration, and long-term stewardship. The resulting computing framework is comprised of the computing infrastructure, computation models and methods, interface methods and tools, and applications methods and tools that are integrated to address the EM needs identified above. Figure 1 shows the structure of the EM computing framework, the initial phases of which have been put in place by this task. In terms of hardware, the computing infrastructure consists of onsite computing resources and storage devices for performing EM calculations, and high-speed links to other computing centers for transmitting large data files and collaborating with research programs at other DOE facilities and universities.

As Figure 1 illustrates, the EM computing framework enables INEEL researchers to address all the major categories of environmental management issues. For example, in the category of above-ground issues, (a) advanced simulation and modeling of a facility to be decommissioned allows further cost reduction, waste volume reduction, and radiation exposure reduction as decontamination and decommissioning (D&D) engineers explore options and "what-if" scenarios; (b) operations personnel can simulate actual D&D operations; and (c) stakeholders can examine the ramifications of different choices. Regarding the below-ground issues. The computing framework can be used to collect and analyze data from field studies and experiments to explore the fate and transport of contaminants in the vadose zone, and to develop new modeling tools and computer codes for prediction of the chemical, physical, and biological properties of subsurface environments.

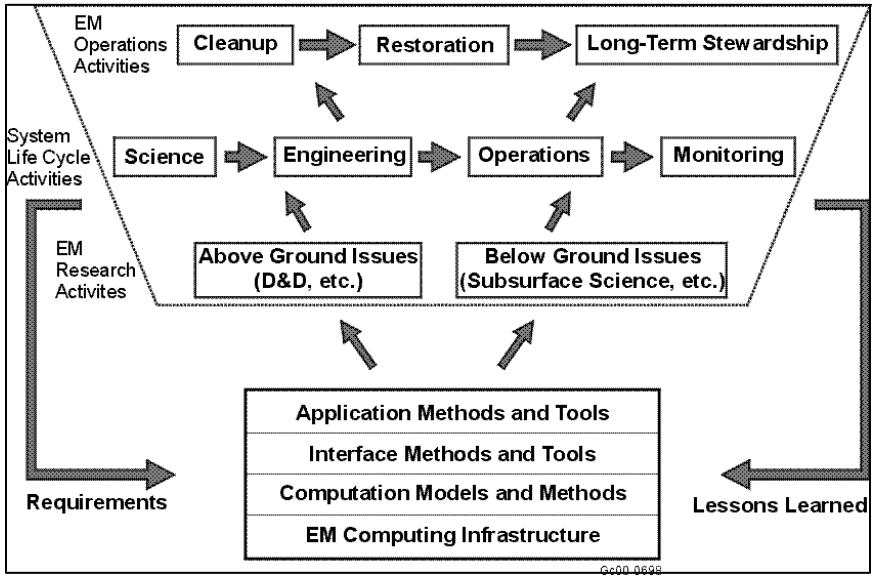

Figure 1. Illustration of conceptual structure of the EM computing framework developed by this task.

ACCOMPLISHMENTS

Computing Infrastructure Development

Needs Analysis

Based on systematic analysis of the issues facing environmental management computing at the INEEL, the following key issues were identified that needed to be addressed when considering upgrades of the INEEL computing infrastructure:

- Previous computer analyses for full scale field problems of 10,000 to 15,000 nodes required anywhere from 4 days to months using then-available INEEL computing capabilities.
- Current and future subsurface science modeling efforts require greater nodalization (e.g., 10^6 to 10^8 nodes to explore transport phenomena in greater detail over larger areas).
- Long-term stewardship models require calculations for periods up to 10,000 years.
- There is a need to run coupled (physical/chemical/biological) models.
- There is a need for visualization of large data sets.
- There is a need to run 4-D (space and time) D&D models to allow exploration of "what-if" scenarios to consider how best to D&D a facility.
- There is a need for collaboration with other environmental management research programs at other DOE laboratories and universities.
- There is a need to transfer large data files (e.g., 10^{11} to 10^{13} data points) between the INEEL and other computing centers in a reasonable time.
- The planned Subsurface Geosciences Laboratory (SGL) will include high-end visualization and virtual environments requiring the processing and transfer of large data sets.
- There is a need to perform teleconferencing, file transfer, group analyses, and virtual collaboration for subsurface science and long-term stewardship programs.

Recognizing that it requires a long-term strategy to upgrade and maintain environmental management computing capabilities at the INEEL, we developed a balanced acquisition strategy so that funding resources available for this task could provide an initial platform upon which future investments could be added to ensure that computing resources keep pace with programmatic needs. The plan developed for this task included acquisition of high-speed offsite connectivity, onsite data archival, and onsite processing capacity.

Installation and Testing of New Computing and Storage Equipment

The new 64-processor SGI Origin 3800 machine was installed in February 2001. Installation of this equipment provided a 5.5 to 11 times increase over previous INEEL processor/memory capacity. The new memory is substantially different from the old memory; not only is it 11 times larger, but it can also be accessed approximately 4 times faster than the old memory. In addition, there is twice as much cache

memory between the processor and this new memory. Hence the overall increase in per processor performance is approximately 10 times compared to the old system—this is highly problem dependent.

At the same time, we installed data archival and storage capabilities including a 5 TB RAID (Redundant Array of Inexpensive Disks) high performance disk array and a 30 TB digital tape archival system. This equipment will be used to store both simulation and experimental results, including those produced at the INEEL and those produced offsite and transferred to the INEEL via the new high-speed communication links.

The 5TB RAID disk array system provides for a sustainable 200 MB/s transfer rate of data from the host to the disk subsystem. We run RAID Level 1 on the system disks. This provides for disk mirroring, that is, a constant backup is done to a second device. There is also automatic failover between these disks. Along with the RAID disk subsystem, we acquired a 30 TB digital tape archival system. This system appears to users as a "normal" disk partition. However, it is actually a tape robot controlling 200 high-capacity digital tapes, front-ended by a large disk cache. When a user writes a file to this partition, it only temporarily resides on the disk. Then it is moved to the tape system. However, all directory information continues to live on the disk. Hence it appears to the users to still be on disk. If a read operation is initiated, the robot loads the correct tape and streams the data back to disk, so that the user may interact with it in a normal fashion. The data are streamed to the user, that is, they can begin interacting with the first parts of the file before the file has been completely transferred back to disk.

The acquired systems were received and installed in the Spring and Summer months of 2001. After an initial period necessary to stabilize the equipment, performance, robustness and usability testing was initiated. These activities continued through the end of the fiscal year. Many problems issues regarding the integration with INEEL hardware and users were identified, the major ones were resolved or workarounds identified.

The potential computational capacity of the INEEL (as mentioned) above has increased by at least an order-of-magnitude. The actual computing load is very problem and time dependent. Within 3 months of the installation of the new equipment, usage had increase by a factor of three. Presently, the new resource is completely utilized and there is a backlog for requests for cycles.

New User Base and Specifics of Applications

The three biggest codes that are currently being used on the new 64-processor machine are TETRAD, MCNP and ABAQUS. Priority for use of the machine is being given to environmental management users, but other users are allowed on the machine when processors are available to help test and integrate the overall system. The programs supported include a large number of environmental management research activities. In addition, several waste area groups including RWMC, INTEC, and TAN use the equipment for subsurface fate and transport calculations as well as atmospheric modeling for air quality permitting.

The TETRAD code, presently the primary subsurface fate and transport code, consumes about 62% of the machine cycles. The MCNP (a nuclear physics code) and ABAQUS (a structural dynamics code used for spent nuclear fuel calculations) take about 20% and 18%, respectively.

Taken together, these codes represent a cross section of the kinds of high end applications that can be implemented on our new computing machinery, and highlight many of the issues that must be addressed to optimize performance to address environmental management computing needs at the INEEL. TETRAD is not a parallel code, and would be very difficult to adapt for parallel operation. TETRAD users are currently using multiple processors simultaneously to carry out the numerous

TETRAD runs that are necessary to perform the required regulatory analyses for Waste Area Groups at the INEEL. To support the future needs of the INEEL subsurface science research program, it will be necessary to obtain, adapt, or develop subsurface fate and transport codes that can adequately model subsurface phenomena and efficiently analyze and compare experimental data and code predictions. It will also be necessary to develop and integrate codes that can effectively assess the behavior of coupled physical, chemical, and biological phenomena in the subsurface. Thus a significant code development program will be required to support the Subsurface Science Initiative and the experimental programs of the Subsurface Geosciences Laboratory at the INEEL. In addition, the INEEL will need to maintain its momentum in upgrading our high performance computing capabilities and infrastructure so that we can attract the modeling and simulation talent that will be required for success of the subsurface science research program.

The MCNP and ABAQUS codes are parallel codes, and are being operated on the new machine in parallel mode. MCNP has been run using as many as 35 processors simultaneously. ABAQUS has been run using as many as 16 processors, but seems to function most efficiently on about four processors.

The experience using advanced codes on our new 64-processor machine has highlighted the need for users to adequately support optimizing and developing a high-performance computing framework at the INEEL. Our future efforts will need to focus on building up capabilities in the computational sciences, geoscience modeling, code parallelization, and performance optimization to ensure that our computing resources are effectively and efficiently utilized.

There are now over twice as many total users as there were prior to the installation of the new equipment, and approximately 3–4 times as many active users (those who make daily, rather than occasional, use of the machines).

User Support

We have implemented a basic level of user support as part of this task. This level of support enables us to keep the equipment running most of the time, but is insufficient for full-time coverage and complete user support. Depending on the demands of the particular situation, there is not always sufficient staff available to help users better utilize the equipment. In the future, INEEL users could benefit from the availability of full-time domain expertise to effectively utilize the new computing capabilities; a core group with the requisite education, training and experience will be essential to serve as the interface between end users and the complexities of modern high-performance computing environments. This will require a staff of approximately 8–10 people. Approximately half of this resource should be broad based, working on INEEL-wide environmental management issues. The other half could be focused on specific programs to provide the most increase in efficiency to those programs. Hence when a critical or short-term need arose, those resources assigned to the sitewide issues could be temporarily redirected to provide the necessary relief.

Connectivity Upgrades

We developed a dual approach to provide near-term and longer-term connectivity from the INEEL to other computing centers as our needs grow. The first step implemented a DS-3 (45 MB/s) connection to Idaho State University (ISU) in Pocatello, 50 miles south of Idaho Falls. This connection allows the INEEL to use another DS-3 connection from ISU to the University of Utah (Salt Lake City, UT, 200 miles south of Idaho Falls) and Internet2. This connection was installed and tested during September 2000. At the same time, the INEEL was approved for Internet2 Secondary Participant status under the sponsorship of ISU.

In cooperation with the INEEL Information Resources Management organization, a DS-3 connection (45 MB/s) was installed to the ESnet at Lawrence Livermore National Laboratory. When this connection was installed during FY 2001 we increased our total data transfer rate by a factor of 30 compared to the situation prior to this task. In addition, we now have direct access for collaboration with other DOE laboratories through ESnet and university researchers through Internet2. This dual pathway architecture maximizes INEEL's opportunities to conduct collaborative environmental management research. We are currently evaluating the need to upgrade the DS-3 connection to ESNet to OC-3 (155 MB/s).

Computing Framework Application Development

This portion of the report documents the research accomplishments in developing and implementing a collaborative visualization framework at the INEEL. The purpose of this framework is to allow subsurface researchers who are at different physical locations to simultaneously interact with subsurface model data.

Background

The INEEL has a research charter for studying fate and transport of elements within the subsurface. This is not an easy task. This task is characterized by complex data models, large input data sets, large simulation output data sets, and multiple interpretations of the results. Given the nature of subsurface research, collaboration among scientists on these models and the potential implications of the research results is a significant challenge.

To address this challenge, discussions with subsurface scientists identified the following specific needs:

- Data visualization to promote understanding among lay people and fellow scientists.
- Collaboration tools to facilitate the discussion and interpretation of field data, the selection of model parameters, the interpretation of simulation results, and assessment of the validity of forecast models.
- Graphical user interface tools to facilitate the interpretation of subsurface data models, including the ability to interact with large data subsets.

Figure 2 illustrates the type of advanced visualization that is needed to analyze subsurface models. This project has sought to address the above stated needs for advances in subsurface research tools and also advances in scientific collaboration and visualization technologies.

The specific goals of this task have been to:

- Develop and implement at the INEEL a distributed environment to promote collaboration among scientists and researchers.
- Provide a tool to support INEEL subsurface research.
- Develop and integrate large-scale, complex simulation models into a collaborative analysis environment. More precisely utilizing newly acquired supercomputing resources to integrate into a shared environment visualization data sets too large and complex to be visualized or analyzed using previous INEEL computational resources.

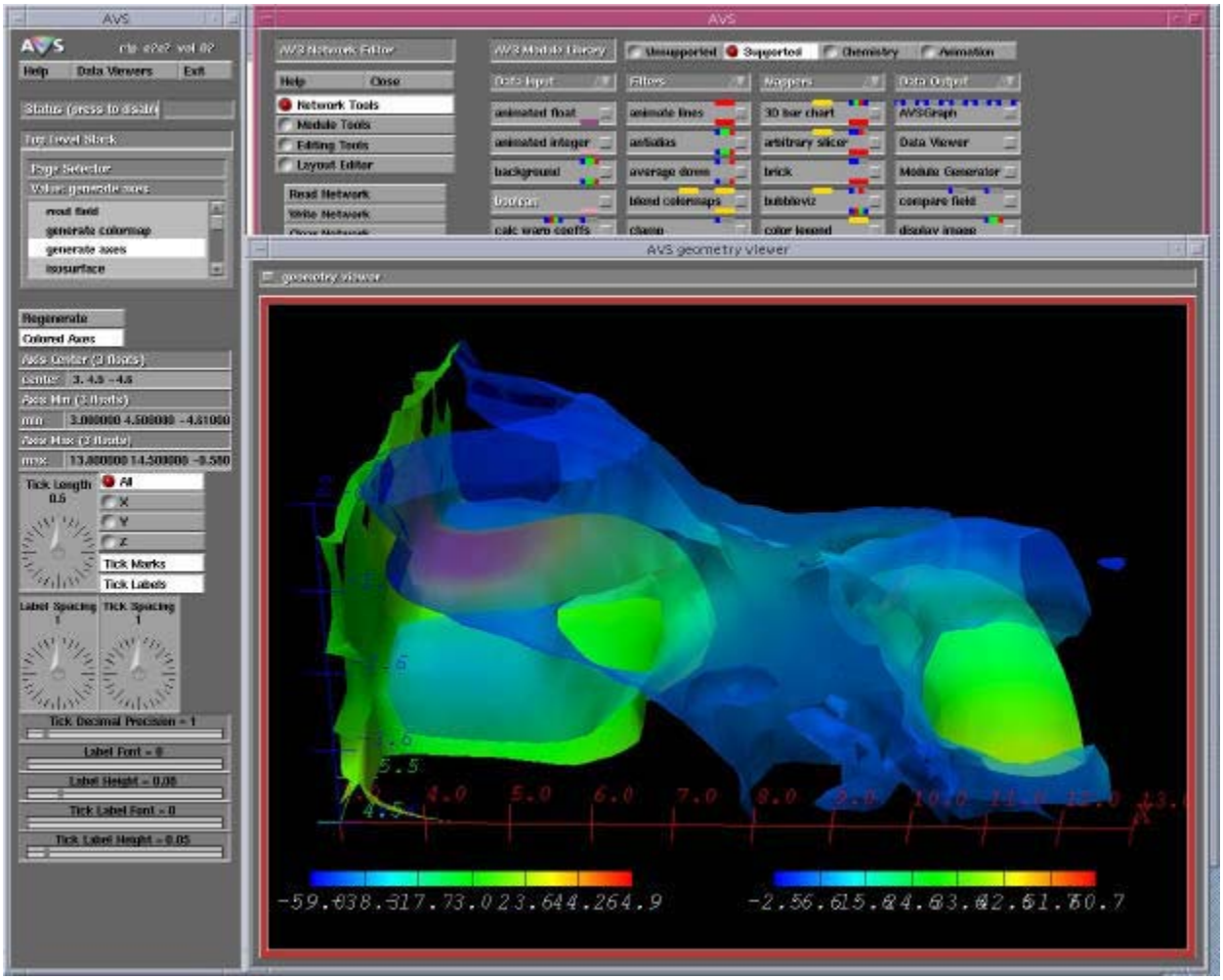

Figure 2. Collaborative tool for scientific visualization of 3-D subsurface data.

⁄# Advance INEEL scientific computing capability.

⁄# Develop a framework for collaboration between the INEEL and other national laboratories and research facilities (via standard networking, including new INEEL networking capabilities).

Implementation of the Collaborative Visualization Framework

The scientific visualization package that was chosen to implement the collaborative framework is a software package called Advanced Visualization System (AVS). AVS is a well known and widely used commercial scientific visualization package. In order to implement a collaborative framework, a collaborative module add-on AVS (cAVS), developed by Greg Johnson at the San Diego Supercomputing Institute, was used.

In this approach each member in the collaboration has his/her own copy of the data and is running an independent application of AVS. The cAVS module allows collaboration between session participants by sharing common module parameter and data ports between the various instances of AVS. In the initial setup, users select a set of common ports aligned to specific modules within cAVS. During the session, participant machines monitor these ports for commands and data to update their current view. Updates

occur when a change is noted in one of these ports. In this way, the cAVS modules coordinate by synchronizing data and parameters on each instance of AVS; thus, synchronizing all participants' views (see Figure 3). One requirement for this approach is that all machines must be aligned with the same initial view and parameter set (all views must be aligned in the same position). This is required since the current implementation of cAVS does not coordinate all parameters associated with the current collaboration modules.

The implementation of this system at the INEEL requires that participants have an account and access to one of the INEEL supercomputers. Currently the system allows only collaboration among internal participants, those within INEEL's firewall.

Another implementation that has been evaluated is Collaborative AVS Java Extension (CAJE). CAJE is a useful and addition to the library of collaborative modules provided by Greg Johnson at the San Diego Supercomputing Institute. CAJE is a java client that can connect to and share parameters with a preexisting collaborative AVS session. CAJE presents the view in a web browser-like application. It does not require the user to have a copy of AVS, but must connect to a participant who does have AVS with the cAVS modules. It only provides shared controls for rotating, translating, and resizing the view. Updates made by other participants using AVS directly will be reflected in the CAJE view.

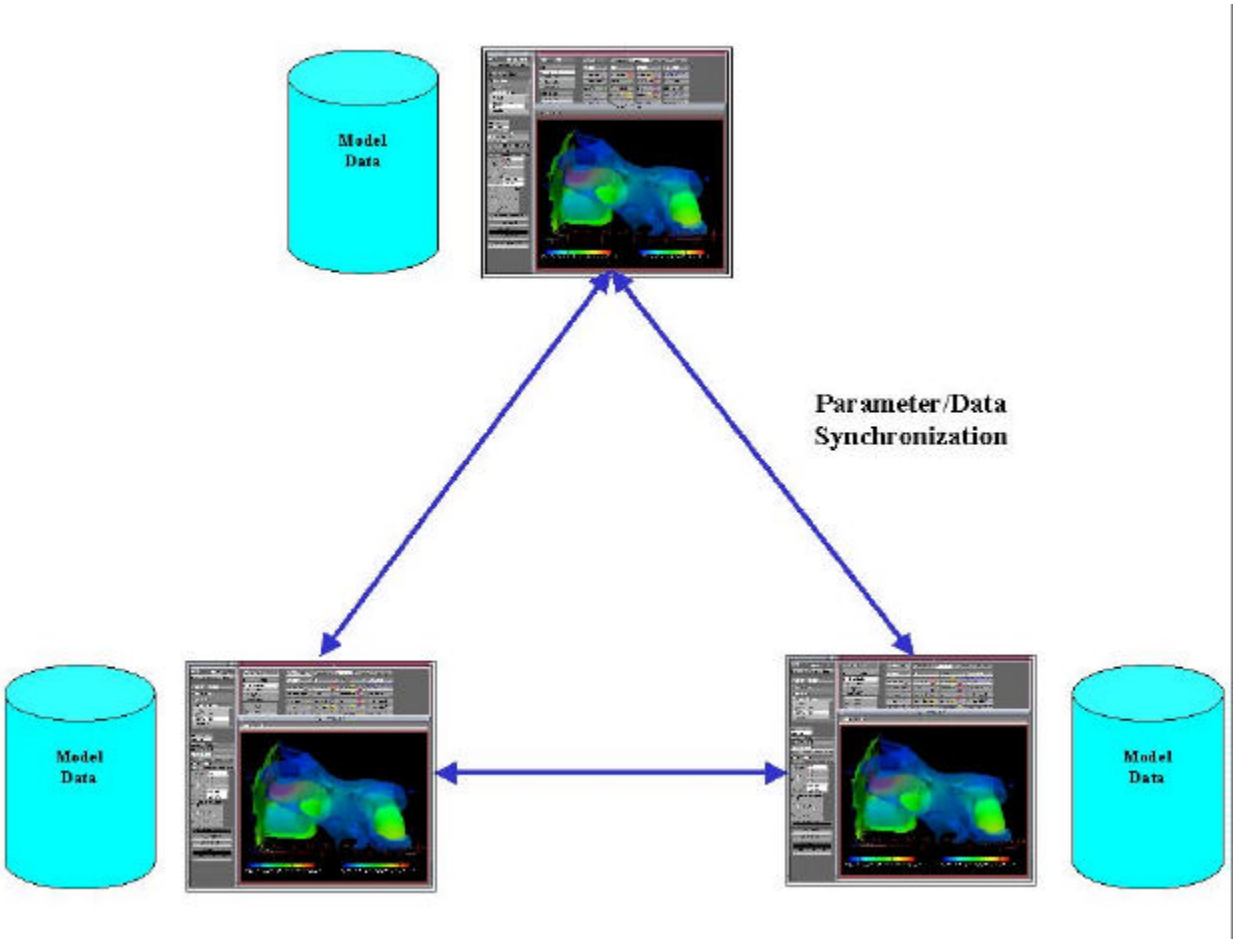

Figure 3. Collaboration implementation.

Development of Collaborative Tools

This project did not implement a full scope integrated framework for collaboration among subsurface scientists. Rather, it addressed one of the first major steps necessary for its development. Within the time and resources allotted for this project, the goal was to develop and integrate a framework which supports distributed collaboration among the scientists at the INEEL. The framework will support both a shared view of a subsurface model and shared control over that view. Within the scope of this effort, the shared view consisted of a 4D (X, Y, Z and time) model of a TETRAD data model as the subject of discussion. The collaborative (shared) controls include:

- rotation of the model in the XYZ plane
- modification of the color scheme
- time series analysis (i.e. viewing the model over time—specifically the fate and transport of contaminants through the subsurface)
- changing data view parameters—extracting specific data sets from the TETRAD model for viewing.

These tools provide a starting point for distributed collaboration.

Demonstrations of Collaborative Visualization

Two collaborative demonstrations have been conducted as of this writing. In June 2001, an initial implementation of the AVS collaborative framework was distributed to a subsurface scientist at the INEEL. To fit his operational needs, this researcher needed to visualize TETRAD models of INEEL data. Part of this effort involved improving a converter to translate TETRAD model output data into an AVS readable format. Now TETRAD model data from the INEEL can easily be imported into AVS for single user analysis or collaborative analysis. The ability to view this data in an advanced visualization software package has been a valuable contribution of this project.

On July 30, 2001 a collaborative session was demonstrated between the researcher at the INEEL ROB building and one of the system developers at the Visualization Lab at the EROB building. During this session one of the managers in the subsurface research program sat at the terminal in EROB and discussed the model visualization with the researcher at the ROB. It was an interesting exchange in that the majority of the discussion was not focused on the implementation of the collaborative framework, but involved a discussion of the visualization itself. Through the use of color, rotation, and time series analysis, the researcher explained the model to the manager. In many ways this served as a validation to the utility of the collaborative framework.

Project Contributions

The collaborative visualization portion of this research task has made the following contributions:

- Implemented a collaborative framework to allow INEEL scientists to simultaneously view and analyze complex data models from distributed locations.
- Enhanced an existing data converter to allow INEEL model data generated in TETRAD to be viewed in an advanced visualization software package.

- Promoted used of advanced visualization methods to the subsurface scientist at the INEEL.
- Expanded the utilization of the supercomputing framework at the INEEL.
- Created a potential usage for high speed, high band width external data connections between the INEEL and other research facilities (INRA and other national labs).
- Increased INEEL experience in collaboration technologies and methods.

Future Research in Collaborative Visualization

This project uses one specific visualization program, AVS. Additional scientific visualization programs exists that may be better suited for the INEEL's needs. OpenDX is an example of one such package. While these other packages may not exist with collaborative capabilities, it may be possible to leverage the knowledge gained in this project to create a collaborative form of these programs.

The current method of collaboration uses a shared data approach, which requires all participants to have a copy of AVS and their own copy of the data. This is not so much of an issue within the INEEL in that the computational complexities are easily handled by the supercomputers. However, there may be applications where either the data is not readily available to all participants or the AVS software is not licensed to all participants. Another approach is a "shared view" method. This approach has one instance of the application with the data set of interest serving as the session host. The data set is manipulated only on this machine with a view of the data broadcasts to the participants. The view itself could be presented in a "browser" type application on the participants' machine. Unlike many "whiteboard" type applications, however, the participants have a subset of commands that allow them to actually manipulate the data view on the host's machine. The view is manipulated on the host's machine and rebroadcast to the other participants. Advantages with this method include the ability to maintain the data in one location without the worry of ensuring all participants have the same data set. Additionally, each participant would only require a view browser, and not the original scientific visualization program. One major disadvantage is that this approach may require significant bandwidth to transmit near real time views from the host machine to other participants.

REFERENCES

None

Environmental Systems Science and Technology

This area of research explores novel processes or materials to treat, decontaminate, and store hazardous and radioactive waste, which includes several tasks that will assist decommissioning activities.

The following tasks are reported in this section:

- Decontamination, Decommissioning, and Remediation of Optimal Planning System for the Advanced Decontamination and Decommissioning System
- Robotic Waste Packaging System for the Advanced Decontamination and Decommissioning System
- Waste Characterization and Sorting Station for the Advanced Decontamination and Decommissioning System
- Environmental Separations and Barriers
- Proton Conducting Ceramic Membrane Applied to Spent Nuclear Fuel Stewardship
- Spectroscopic Investigations at Solid Supercritical Fluid Interfaces in Support of Advanced Supercritical Separation Techniques

Decontamination, Decommissioning, and Remediation Optimal Planning System for the Advanced Decontamination and Decommissioning System

Automated Planning for Decontamination and Decommissioning of Contaminated DOE Facilities

Julia L. Tripp, Michael G. McKellar, and Mark Landon

SUMMARY

The current baseline decommissioning techniques being used are labor intensive and extremely costly. Decontamination and decommissioning (D&D) liability-holders require new and improved technologies that significantly reduce costs and improve safety. The Decontamination, Decommissioning, and Remediation Optimal Planning System (DDROPS) is a computer-based planning system previously developed at the INEEL that allows an operator to model a facility for remediation preplanning and waste minimization purposes. DDROPS incorporates solid geometric modeling and optimization techniques to help identify locations for segmenting contaminated materials (pipes, tanks, etc.) to improve packaging densities within waste boxes and minimize radiation exposure to D&D workers.

The work completed during this task included (a) optimal tank cutting, (b) radiation exposure calculations and visualization of exposure to individuals working on the 3-D model, (c) a 3-D model of a contaminated facility, and (d) initiation of integration of various portions of DDROPS (radiation visualization, optimization, 3-D modeling, radiation calculations, etc.) into one coherent package.

The potential benefits from this task will be a reduced personnel radiation exposure and a minimized number of waste containers required for a given volume of waste.

TASK DESCRIPTION

Background

The DDROPS was developed by the INEEL as a computer-based planning system for use in simulating a facility for remediation preplanning and waste minimization purposes. To improve packaging densities within waste boxes, DDROPS incorporates solid geometric modeling via Parametric Inc.'s Pro/Engineer software and INEEL proprietary algorithm/optimization techniques to help identify locations for segmenting contaminated materials (pipes, tanks, etc.). It also includes visualization of radiation fields and can calculate the radiation dose to an individual working or walking through the model, and can thus be used to minimize radiation exposure to D&D workers. The system includes smart data-bases, proprietary code/algorithms, geometry model preprocessors, and robotic path planners.

DDROPS is valuable for operator training, operation planning, and historic preservation. Through the use of DDROPS, an operator can create a simulated model of the facility to be dismantled and then move throughout the model to familiarize themselves with the surroundings without becoming exposed to the hazards of the actual facility. By accessing a series of proprietary code/algorithms an operator can preplan the entire D&D operation.

D&D operations involve equipment removal and object segmentation. Through DDROPS, an operator can determine the optimal location for making all required object cuts and facility dismantlements. This optimization is calculated as a result of operator-controlled constraints, such as waste dimensions, radiation levels, mass properties, schedule, etc. Following the virtual segmentation, an operator can continue to model the operation through the packaging stage until all segmented objects are placed into their various waste containers. A manifest/object inventory generation procedure is also maintained to provide the operator with a complete record of waste packages.

Many of the nuclear facilities now undergoing D&D are one-of-a-kind, state-of-the-art facilities. Some of these facilities are being remediated for additional use while others are being completely dismantled. In either case, a detailed record of their condition is required. DDROPS provides a means of capturing and maintaining an improved historic and visual record of the facility. This record is vital to updating as-built drawings, and provides a complete record of dismantled facilities.

The INEEL has implemented DDROPS during D&D operations at the INEEL's Central Facility Area (CFA) Sewage Treatment Plant (CFA-691) (Figure 1) through the EM-50 funded Accelerated Site Technology Deployment Idaho D&D Project. The facility demolition, completed according to normal practices, resulted in six filled waste boxes. The DDROPS estimate, using optimal cutting, was two boxes. The results of this implementation have shown the system provides several significant benefits. For example, the use of DDROPS results in waste containers with a greater packaging density as compared to conventional techniques. This in turn reduces the volume of waste—three times less in this implementation—transported for disposal, resulting in a direct decrease in D&D disposal costs. Second, a reduction in worker exposure can be realized by familiarizing workers with the hazardous environments without exposing them to actual hazards.

A patent (No. 5936863) was awarded on this Optimal Segmentation and Packaging Process. This system is in the process of potentially being licensed to a commercial company who will incorporate the DDROPS system into the new D&D preplanning software they are creating. This company is obtaining additional funding to allow the INEEL personnel to complete software development in several areas.

Subtasks

This project started with the basic DDROPS algorithms and allowed the addition of the ability to optimally cut nonpipe parts, incorporate radiation visualization and calculation of worker exposure into the models, and initiate integration into a coherent software package. The subtasks for this task included:

- Completion of optimal tank cutting
- Completion of radiation exposure calculations, visualization on the 3-D model, and calculation of worker exposure
- Completion of a 3-D model on a contaminated facility
- Initiation of integration of the various portions of DDROPS into one coherent package.

The optimal tank cutting procedure was completed in FY 2000 (see Figure 2). Radiation exposure calculations were completed on a Test Area North facility, TAN-616 (a liquid waste treatment facility shut down in 1970), but were never verified. The characterization of TAN-616 for decommissioning is currently being completed. Existing data shows that some areas of this facility, in particular the evaporator pit, have very limited access and fairly high radiation levels, which adds credence to performing detailed planning to better protect worker health and safety. A new 3-D model of the evaporator pit was completed. Investigation into the best approach to integrate the various portions of DDROPS into one coherent package was also completed.

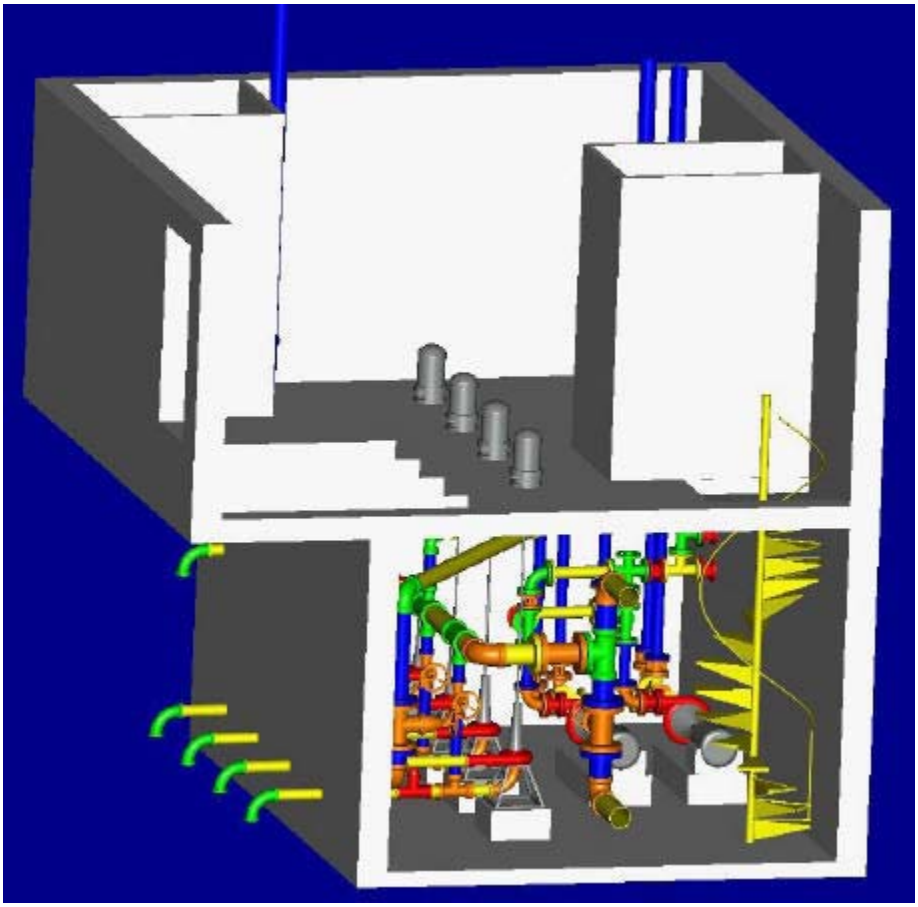

Figure 1. A DDROPS model of a facility undergoing D&D.

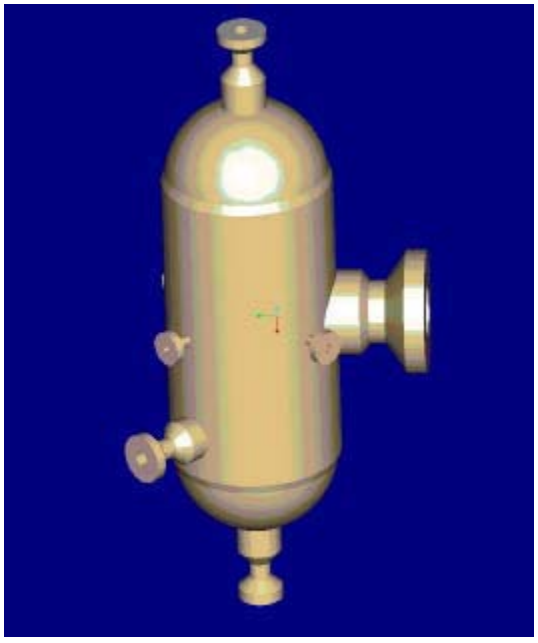

Figure 2. DDROPS algorithms used to optimally cut simulated tanks for disposal.

Need for DDROPS

Although industry can successfully perform D&D operations by using a variety of baseline techniques, these techniques are labor intensive, extremely costly, and result in considerable volumes of waste. It is expected that the amount of radioactive waste to be generated during decontamination, decommissioning, and remediation of DOE's nuclear and associated facilities is significant. This waste, and its subsequent disposal, will have a direct impact on the operational costs associated with the D&D operations of these facilities. As such, the cost of remediating these facilities with baseline technologies has been estimated to be in excess of $36 billion. For this reason, DOE and other commercial D&D liability-holders require new and improved technologies that provide significant cost and safety improvements over conventional technologies.

The INEEL recognizes the need for advanced technological solutions that can significantly reduce the cost of performing D&D operations, and has taken an aggressive role in integrating its D&D operations with its applied engineering expertise. This integration allows INEEL facilities to be used as test beds for evaluating, demonstrating, and deploying innovative D&D technologies that generate less secondary waste, cost less, require less labor, reduce exposure of personnel to radioactive and hazardous materials, and improve safety for workers and the environment.

This subtask deals specifically with several needs identified by the Idaho Site Technology Coordination Group (STCG), including removal of two reactors as single units, remote demolition of machinery, remote demolition of metal structures, and remote demolition of piping.

It also offers opportunities for lowering the need for long-term monitoring by allowing more cost-effective cleanup and removal of contaminated sites, thus reducing the number of facilities requiring long-term stewardship. There are also possible applications to EM problems beyond this work package and funding, such as waste management and planning for D&D of subsurface burial sites.

R&D/Operations Integration

The INEEL Facilities Deactivation Department conducts D&D activities at the INEEL. Representatives from this group have been involved in reviewing this technology and giving ideas on needed improvements. They have already implemented portions of DDROPS to obtain planning information to aid in safe removal of an underwater reactor (see Figure 3) and estimate waste packaging, as previously mentioned. D&D operations personnel have continued to express an interest in using the system and a willingness to demonstrate it, once it is completed.

Requests for information and possible deployment have been received from the Savannah River Site, Mound, and Rocky Flats. As stated previously, a commercial vendor is in the process of licensing this technology and is obtaining funding to allow the INEEL to complete integration of the software.

Possible Future Activities

The following bullets describe some of the future activities being pursued:

- Ongoing discussions are being held with the Atomic Energy Authority of the United Kingdom, London, to determine the applicability of DDROPS to their D&D operations. An umbrella work-for-others contract is already in place.

- DDROPS was a technology included in a contractor's bid for an SRS project.

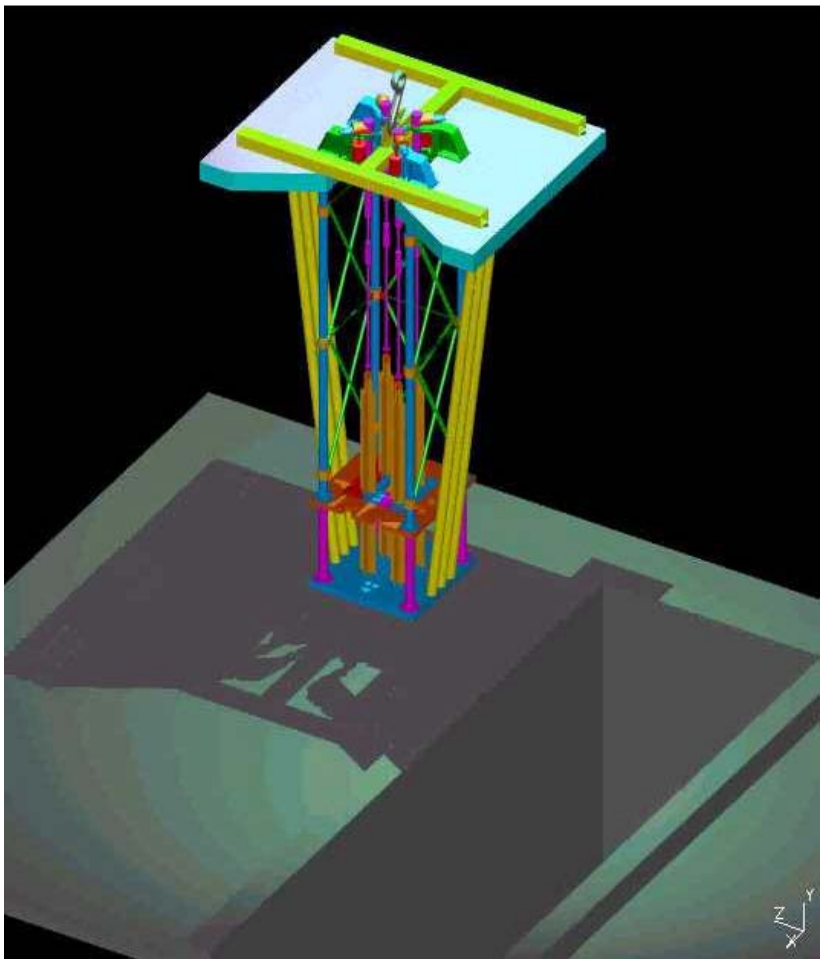

Figure 3. Reactor simulation done with DDROPS.

- The DDROPS technology received funding from a proposal for the EM-50 funded, Large Scale Demonstration and Deployment projects, and will be evaluated as a potential technology for deployment at other DOE locations.

- Ongoing discussions are being held at Rancho Seco with the Electric Power Research Institute to deploy new D&D technologies, such as DDROPS. An unsolicited proposal was submitted to the National Energy Technology Laboratory in October 2000.

- A commercial licensee is obtaining a patent on DDROPS and is obtaining funding to complete the integration of this software.

ACCOMPLISHMENTS

Our accomplishments during this task were as follows:

- The optimal tank-cutting subtask was completed.

- The evaporator pit at the TAN-616 facility, which is slated for D&D soon, was modeled and radiation calculations were completed, but not verified.

- An initial overview of the requirements of software integration was completed, and software integration initiated.

- Radiation fields were visualized on a 3-D facility model, and a method to calculate and visualize worker exposure for completing work in the facility was completed. The ability to vary the work paths is included in the worker exposure calculation (Figure 4).

REFERENCES

None

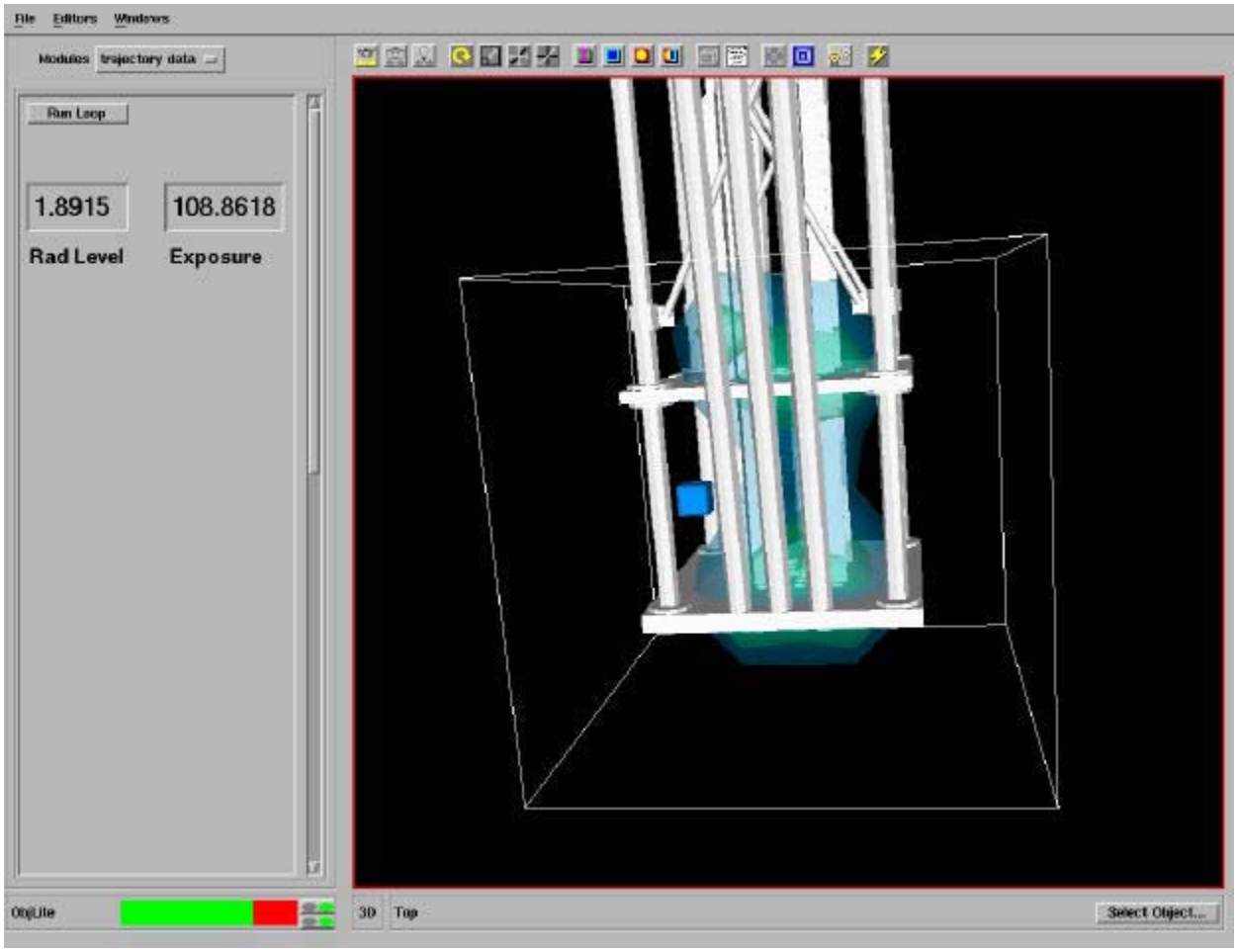

Figure 4. Radiation mapping and exposure calculation software.

Robotic Waste Packaging System for the Advanced Decontamination and Decommissioning Systems

Automated Waste Packaging for Decontamination and Decommissioning of Contaminated DOE Facilities

Julia L. Tripp and Cal D. Christensen

SUMMARY

The DOE weapons complex has been transitioning from production to environmental restoration. As a result, a decontamination and decommissioning (D&D) effort is underway to eliminate a large number of obsolete facilities. The nuclear utility industry faces similar challenges with university reactors, nuclear laboratories, research reactors, and other laboratory test facilities. Although industry can successfully perform D&D operations with a variety of baseline techniques, they are potentially hazardous and too expensive. Therefore, DOE and other commercial D&D liability holders require new and improved technologies that are safer and more affordable.

This task focused on developing a Robotic Waste Packing System (RWPS) to perform the material handling, optimal waste packaging, and sorting/recycling step of the D&D process. We consequently designed a RWPS material sorting station and constructed a prototype of essential components.

TASK DESCRIPTION

The INEEL has been aggressive in applying its engineering expertise to D&D operations. Doing so allows INEEL facilities to be used as test beds for evaluating, demonstrating, and deploying innovative D&D technologies. Our objective was to develop technologies that require less labor, generate less secondary waste, reduce personnel exposures to radioactive and hazardous materials, protect the environment, and improve worker safety; thus, making D&D less expensive and diminishing the need for long-term monitoring by reducing the number of facilities requiring long-term stewardship. A fully developed and deployable RWPS would achieve all of these goals through packaging waste robotically, integrating with the waste characterization system to accurately manifest waste containers, and minimizing the number of waste containers required for a given volume of waste.

This task focused on developing a RWPS to perform the material handling, optimal waste packaging, and sorting/recycling step of the D&D process. To accomplish this we designed a RWPS material sorting station to (a) receive waste materials, geometrically identify each piece using a state-of-the-art vision system, physically move the piece to a waste container, orient it, and place it inside (see Figures 1 and 2); and (b) work in conjunction with the Waste characterization and sorting system and to fit into the envelope of a mobile trailer. This task also included research into real-time optimal packaging of the waste.

Environmental Management (EM) end users include the INEEL Facilities Deactivation Department that conducts the D&D activities at the INEEL. Representatives from this group and the department manager have been involved in reviewing this technology and giving ideas on needed improvements. They have continued to express an interest in using the system (and a willingness to demonstrate it) once it is completed.

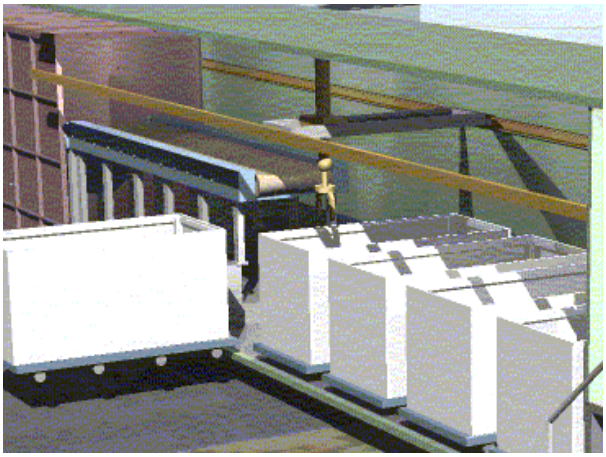

Figure 1. Conceptual robotic waste packaging system.

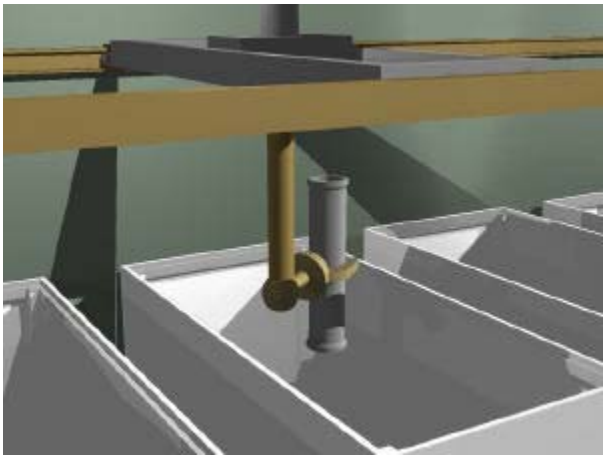

Figure 2. Conceptual low profile z-mast (to be designed) for operation in a trailer.

ACCOMPLISHMENTS

Our accomplishments during FY 2001 are as follows:

- Optimal packaging worked with the University of Utah (USU) to establish basic 3-D packing algorithms, and created a simulation of the "on-the-fly" packaging process for 2-D. The 3-D packing algorithm could pack a 3-D bin at 85–95% efficiency, depending on the size of the boxes being packed.

- We designed, built, and tested a low-profile z-mast that would be appropriate for deployment in a semitrailer (see Figures 3 and 4). This is the only z-mast that would allow deployment of an xyz robotic arm system in a trailer while leaving enough room for the waste containers. This low-profile z-mast design is also being used by the HANDS-55 project.

Figure 3. Low-profile z-mast extended to show total length (A).

Figure 4. Low-profile z-mast retracted to show maximum clearance allowed.

- The RWPS coordinated its research with the INEEL Robotics HANDS-55 project, and initially used their base material handling design to prove-out that aspect of the RWPS. The design of the material handling station and a vision system for the RWPS was completed. The vision system software uses depth, color, and edge detection to distinguish overlapping/adjacent objects specified by an operator. A real-time packaging algorithm for optimal packing of 2-D items was completed in FY 2000.

REFERENCES

None

Waste Characterization and Sorting Station for the Advanced Decontamination and Decommissioning System

Automated Waste Characterization for Decontamination and Decommissioning of Contaminated DOE Facilities

Julia L. Tripp and Douglas W. Akers

SUMMARY

Current baseline decommissionin g techniques are labor intensive and costly. Decontamination and decommissioning (D&D) liability holders require new and improved technologies that will significantly reduce costs and improve safety. One of these new technologies is the Waste Characterization and Sorting System (WCSS). The WCSS supports material identification and characterization, sorting and recycling during the disassembly process, and accurate manifestation of waste containers. The WCSS determines physical measurements, including weight, volume, and density, and isotopic radiological characteristics of each waste item. This information can then be sent to a central database. The system requires limited operator interaction as it has a number of self-test functions, including calibration, that notify the operator if the system is not operating correctly or if the item being processed is outside the waste characteristics appropriate for characterization or disposal.

The work for this task was separated into four subtasks: (a) building the scanning/conveyor system, (b) completing the graphical user interface and software modifications required to run the system as an integrated unit, (c) completing the gamma spectrometry algorithms and calibration system, and (d) completing integrated system testing. The scanning/conveyor system assembly was completed in FY 2000, all other subtasks were started in FY 2000 and completed in FY 2001.

The WCSS system uses algorithms to determine detector efficiencies for each waste item as it is processed and performs quantitative gamma-ray spectrometry on D&D waste without a trained operator. This capability allows the system to be replicated and used to produce systematic and reproducible quantitative analysis results for wastes from numerous sites. This has a number of benefits to help meet proposed DOE and Nuclear Regulatory Commission (NRC) regulations concerning the “free-release” of scrap metal and other wastes for reprocessing and disposal at locations other than low-level radioactive waste disposal sites. Other potential benefits from this task will be improved waste characterization through automation, reduced personnel hazards exposure, and a more accurate manifest of waste containers.

TASK DESCRIPTION

Background

A basic waste characterization system was previously developed as part of the ROVER decommissioning project. This ROVER system will be used as the basic platform for the WCSS. The ROVER Waste Assay System (RWAS) is a nondestructive assay system designed for the rapid assay of U-235 contaminated items. A scanning system translates a NaI(Tl) detector/collimator system over the structural components where both relative and calibrated measurements for Cs-137 are made. Concentrations of U-235 are determined from CS-137:U-235 ratios measured by radiochemical methods.

The system currently in operation is sufficiently automated that the computer system does the system calibration, problem identification, collimator control, data analysis, and reporting.

Subtasks

The following upgrades were completed as part of this project.

- An automated component recognition system was added to the basic system to define the item volume and shape based on a laser scanning technique.
- An automated calibration technique that uses the volume and weight data (density) to determine the quantities of radioactive or hazardous materials associated with a particular component was added.
- A computerized self-testing system that allows the characterization system to determine whether it is working correctly was added.
- A camera system with digital interface for data storage was included.
- A conveyor system is used to automatically transport the waste item under the laser scanner and radiation detector.
- A germanium gamma-ray detector with appropriate detector efficiencies for standard waste types expected at D&D waste sites is included in the system.

Need for WCSS

Although industry can successfully perform D&D operations by using a variety of baseline techniques, these techniques are labor intensive, extremely costly, and result in considerable volumes of waste. The amount of radioactive waste expected to be generated during the decontamination, decommissioning, and remediation of DOE's nuclear and associated facilities is significant. This waste, and its subsequent disposal, will have a direct impact on the operational costs associated with the D&D operations of these facilities. As such, the cost of remediating these facilities with baseline technologies has been estimated to exceed $36 billion. The DOE and other commercial D&D liability holders require new and improved technologies that will significantly reduce cost and improve safety over conventional technologies.

The INEEL has recognized the need to advance technical solutions that can significantly reduce the cost of performing D&D operations, and has taken an aggressive role in integrating its D&D operations with its applied engineering expertise. This integration allows INEEL facilities to be used as test beds for evaluating, demonstrating, and deploying innovative D&D technologies that generate less secondary waste, cost less, require less labor, reduce exposure of personnel to radioactive and hazardous materials, and improve safety for workers and the environment.

This task also offers opportunities to decrease the need for long-term monitoring by allowing more cost-effective cleanup and removal of contaminated sites, thus reducing the number of facilities requiring long-term stewardship.

Possible Future Activities

The following future activities are being pursued:

- Ongoing discussions are being held with the Electric Power Research Institute (EPRI) to deploy new D&D technologies, such as WCSS, at Rancho Seco. An unsolicited proposal was prepared and submitted to the National Energy Technology Laboratory in October 2000.

- An outside commercial vendor is in the process of licensing this system. This interaction is being addressed through the INEEL Technical Transfer Department. Funding is being obtained through this company to complete a system operability test and a field demonstration at Rocky Flats.

- Both the NRC and DOE have been interested in the completed system as it provides an implementing technology that can be licensed for characterization of wastes for disposal without operator induced uncertainties.

ACCOMPLISHMENTS

The hardware assembly for the WCSS was completed. The gamma spectroscopy unit was mounted in a box on the scanning bed and integrated into one cable from the various instruments (Figures 1 and 2). A laser scanner was included at the start of the conveyer belt and a camera attached to take pictures of the waste item as it is transported on the belt.

In addition, to the hardware, the software development was completed to allow automated calibration, computerized self-testing, and data storage for producing accurate waste manifests.

Initial system tests were completed, and the system is ready for system operability testing for a particular application.

Figure 1. View of assembled WCSS hardware.

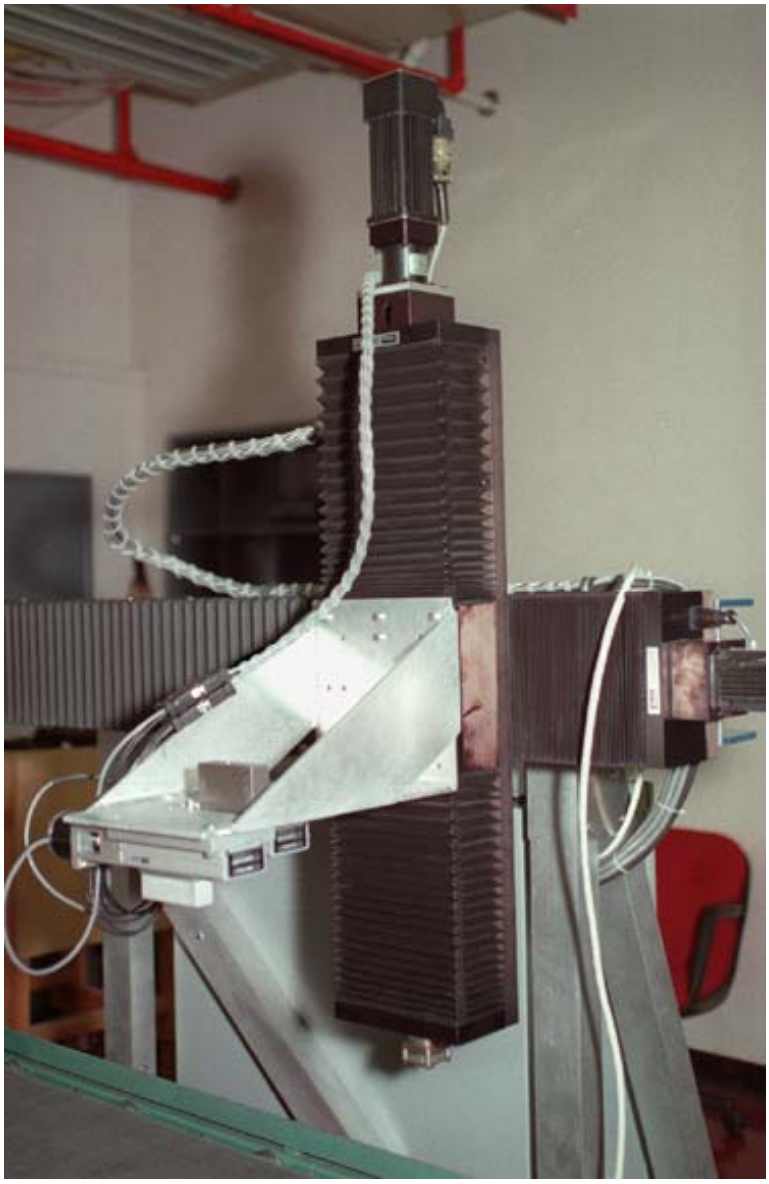

Figure 2. Closer view of the assembled WCSS collimator.

REFERENCES

None

Environmental Separations and Barriers

Controlling Hazardous Environmental Chemicals by Developing Membranes for Chemical Separations and Barriers

Eric S. Peterson, Fred F. Stewart, Mason K. Harrup, Mark L. Stone, and Thomas A. Luther

SUMMARY

A major aspect of environmental management (EM) is being able to control chemical movement; this includes being able to (a) separate chemicals from one another, such as in removing contaminants from water, and (b) prevent the movement of chemical contaminants out of storage areas. For this reason, polymer membranes are important for long-term stewardship of such waste because they can be developed to either separate contaminants from liquids, thus reducing the volume of waste to be handled, or form impermeable barriers to prevent chemical movements.

The use of polymer membranes in chemical separations is a promising technical area experiencing rapid advancements. Even so, a detailed understanding of chemical separations processes and what drives and controls them is fragmented at best. Historically, membrane separations research was focused on gas transport and separations, giving the areas of condensable gases, vapors, and liquids lower priority. However, liquid separations technology capable of functioning in harsh environments is urgently needed by both DOE and industry. Early polymer membranes did not have the chemical and thermal stability to meet this need, but the development of newer materials is rapidly overcoming this problem. And even with the newer materials, only a few programs are focusing on polymer-based liquid separations membranes for harsh DOE- and industry-type environments. Previously, the INEEL has completed a variety of successful programs on various separations schemes under the sponsorship of both government and commercial sectors, but they have had very little sponsorship directed toward developing critical polymer membranes capable of functioning in harsh liquid chemical and ionic environments. The goal of this task was to focus on the separations technologies needed for these DOE applications.

The work for this task was divided into three subtasks; each is critical, and all are mutually complementary in meeting DOE's waste separations needs:

- *Materials development for solid-phase selective-metal ion removal.* Both DOE and industry need efficient methods for removing specific metal ions from solutions that possess high background concentrations of interfering ions without using mobile organic phases (solvent extraction). Our current research specifically addresses this need by using novel solid-phase selective extractants, thereby eliminating the need for organic solvents that are typically toxic, expensive, create numerous disposal issues, and may also reduce chelate/ion specificity. To date, the INEEL has developed a set of proprietary materials that provide selective copper concentration in the presence of high concentrations of iron. The most critical intellectual property involved has been the subject of two invention disclosure records, already elected to patent title (DOE Case No. S-91,266; LIT-PI-470, and DOE Case No. S-93,273; LIT-PI-573), two invited presentations, and one peer reviewed paper describing the materials.

- *Membrane development for high flux-efficient separations*. Both DOE and industry need to control and remove organic contaminants from groundwater and aqueous waste streams. This subtask focuses on developing highly durable and chemically resistant membranes for reverse osmosis applications. Current reverse osmosis (RO) technology offers good throughput with little chemoselectivity. The challenges for this subtask are to combine the chemoselective nature of

pervaporation membranes with the throughput efficiency of RO, and to significantly reduce the cost of phosphazene polymers by evaluating the use of a unique synthetic method developed at the University of Vermont. The work on this subtask has resulted in an invited paper presentation at a national society meeting, a patent, and a nomination for a Presidential Green Chemistry Award for the environmentally friendly synthetic pathway that has been discovered.

¢# *Barrier charactrization*. Barriers will be used as one of the prime technologies to stop present problem sites from growing larger and to prevent future contamination. Because polymer layers will be used in many barrier systems, there is an urgent need to characterize the candiate materials. Membrane introduction mass spectrometry (MIMS) is a sensitive analytical method that will be used to test the abilities of present membrane films to prevent permeations of typical waste plume chemicals. In addition to currently used materials, other films will also be tested to determine if improved formulations can be developed. This task has resulted in four presentations and three peer reviewed juornal articles.

TASK DESCRIPTION

The goal of this task was to further EM's mission by developing cost effective methods for long-term monitoring and surveillance, developing methods to support the integration of land management with long-term stewardship, and find engineering solutions for permanent control of residual contamination and waste left in place. This task focused on separations technologies needed for DOE applications. The work for this task was divided into three subtasks; each one critical, each relying on the other's data and synthetic know how to be completed, and all three mutually complementary in meeting DOE's waste separations needs, even though they appear to be discrete subtasks.

Materials Development for Solid-Phase Selective Metal Ion Removal

Both DOE and industry need efficient methods for removing specific metal ions from solutions that possess high background concentrations of interfering ions without using mobile organic phases (solvent extraction). Our research specifically addressed this need by using novel solid-phase selective extractants, thereby eliminating the need for organic solvents that are typically toxic, expensive, create numerous disposal issues, and may also reduce chelate/ion specificity. These solid-phase extractants solve another major problem with current technology by obviating unavoidable losses from the volatile organic solvent, which is both expensive and environmentally unacceptable. Initial results from our efforts to synthesize a commercially viable solid-phase extractant are very promising. To date, the INEEL has developed a set of proprietary materials that provide selective copper concentration in the presence of high concentrations of iron. The fundamental synthetic routes to these materials have already been established, and attachment to solid supports achieved in an efficient manner. The most critical intellectual property involved has been the subject of two invention disclosure records, already elected to patent title (DOE Case No. S-91,266; LIT-PI-470, and DOE Case No. S-93,273; LIT-PI-573). However, additional development of these materials is needed to optimize efficiency and to resolve some problematic issues.

Novel solid-phase extractants will be synthesized that possess a high degree of specificity for copper in the presence of iron and other interfering ions. Our synthetic strategy employs the third-generation route, based upon the Mitsunobu coupling, combined with the cyclization self-protection strategy for the isoxazazole already developed. Both possible coupling approaches will be explored to determine which is the most effective. These new "head and tether" species will be fully characterized by nuclear magnetic resonance spectroscopy and other appropriate techniques. They will then be covalently attached to silica gel to render the final solid-phase product. If resources permit, these solid materials will

be evaluated in column tests against a challenge solution to obtain selectivity and capacity data. Three tasks are being worked to develop this technology:

- *Head and tether synthesis*. A benzisoxazole "head" group will be synthesized and purified. This will then be coupled to an aliphatic "tether" via the Mitsunobu route. This product will be purified and fully characterized.

- *Solid-phase material synthesis*. The "head and tether" species generated in Task 1 will be attached to the surface of silica particles to form the novel solid-phase material. This product will be isolated and fully characterized.

- *Preliminary testing.* As resources permit, data will be collected from batch and column experiments using the solid materials from Task 2 versus the appropriate challenge solutions.

Membrane Development for High Flux-Efficient Separations

Both DOE and industry need to control and remove organic contaminants from groundwater and aqueous waste streams. To meet this challenge, new materials need to be developed and characterized. This work will concentrate on the development of highly durable and chemically resistant membranes for RO applications. Phosphazene polymers, which have a higher level of chemical and thermal resistance than commonly employed organic polymers, are significant to developing new membranes. The INEEL has a well established polymer and membrane research group that is ideally positioned to take advantage of this technology in creating new separations systems. Current technology in the field of RO offer good throughput with little chemoselectivity. The driving force behind this process is size exclusion—using "molecular sieving" to allow the smallest molecule to pass through the membrane while retaining larger molecules. Routes for separations based on chemical affinity reside largely in the technique of pervaporation. In pervaporation, chemicals are separated based on their ability to diffuse through and evaporate from the membrane. The efficacy of these two processes are dictated by the solubility of the selected permeate and its vapor pressure. Pervaporation, however, has two disadvantages; flux rates and energy requirements. Pervaporation, in general, is characterized by lower fluxes than RO, that often reduce the economic benefits of membrane processes. Additionally, the energy requirements for pervaporation are higher than for RO. The challenge of this work is to combine the chemoselective nature of pervaporation membranes with the throughput efficiency of RO, and to significantly reduce the cost of phosphazene polymers by evaluating the use of a unique synthetic method developed at the University of Vermont.

To develop this technology we performed an economic evaluation and pilot synthetic studies for the new phosphazene polymer synthesis developed in collaboration with the University of Vermont.

Barrier Characterization

Barriers will be used as one of the prime technologies to stop present problem sites from growing larger and to prevent future contamination. Because polymer layers will be used in many barrier systems, there is an urgent need to characterize the candiate materials. MIMS is a sensitive analytical method that will be used to test the abilities of present membrane films to prevent permeations of typical waste plume chemicals. In addition to currently used materials, other films will also be tested to determine if improved formulations can be developed. To develop this technology we performed six tasks:

- Identify the types of materials now being used and those being considered as barrier materials. This will involve personal communications, books, and other literature search methods.

- Collect specimen amounts of the materials for testing.
- Manipulate the materials to produce thin films that are suitable for MIMS testing.
- Test the materials in a MIMS configuration against the four contaminants listed above.
- Perform a limited number of gas barrier film tests.
- Report the results.

ACCOMPLISHMENTS

Materials Development for Solid-Phase Selective Metal Ion Removal

New syntheses have been performed to accomplish the initial goal of obtaining a purified "head and tether" specie with which to functionalize the surface of silica particles. To this end, a new tether was synthesized, one that improves upon the previous generation by possessing a more hydrophilic character which allow for better solvent (water) surface interactions; thus, speeding the kinetics of ion capture. The synthesis is shown below in Figure 1.

The primary coupling reaction for attaching the "head" to the "tether" is the Mitsunobu ether reaction.[1] This reaction was run in a homogeneous fashion, and while successful, the purification was problematic leading to lower than desired yields. To overcome this problem, a new reagent was employed that contained the triphenylphosphine as a surface functionalized polymeric material, allowing the reaction to proceed in a heterogeneous fashion. The subsequently produced by-product, triphenylphosphine oxide, is then easily removed by bulk filtration through a fritted glass funnel, greatly simplifying subsequent purification steps and thereby improving product yields, see Figure 2.

We originally thought that the final step in producing the deliverable product was the silylation of the olefinic tail for condensation onto the surface of the ceramic. Another possible synthetic route, silylation of the alkene first followed by Mitsunobu coupling and oxime formation, was rejected. It was believed that the inherent instability of the carbon-oxygen bonds would make the Mitsunobu coupling problematic. Further, the inclusion of moisture during any later reaction would drive the hydrolysis of the silicon ethoxide, forming an intractable solid phase material before such a product was desired.

In conclusion, the first synthetic pathway—Mitsunobu coupling followed by benzisoxaole formation—worked the best and gave the highest yields. For the allyldi(ethylglycol) alkylated series the overall yield was 41% with the product distribution being split 10:31 for the alkylated isoxazole and aldoxime respectively. For the undecylenyl alkylated series the overall yield was 52%, split 39:13 for the alkylated isoxazole and alkylated aldoxime respectively. Subsequent hydrosilylation of both the benzisoxazole and benzaldoxime species with triethoxysilane and a platinum catalyst, platinum divinyltetramethyldisiloxane, gave 85% yields of silylated products as shown by NMR. Future work could focus on further optimizating yields from our preferred route and testing of the final solid phase extractant.

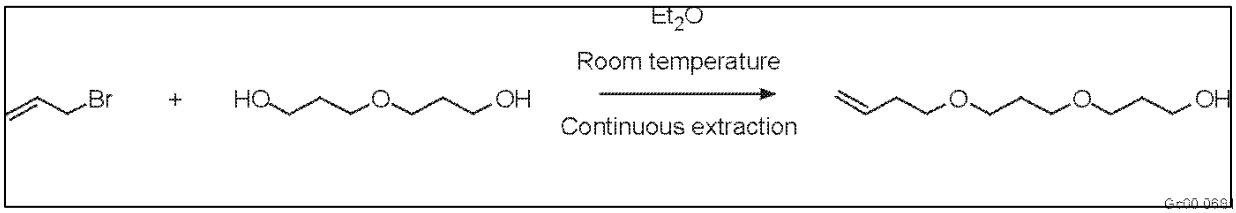

Figure 1. Synthetic scheme for the production of the hydrophilic tether.

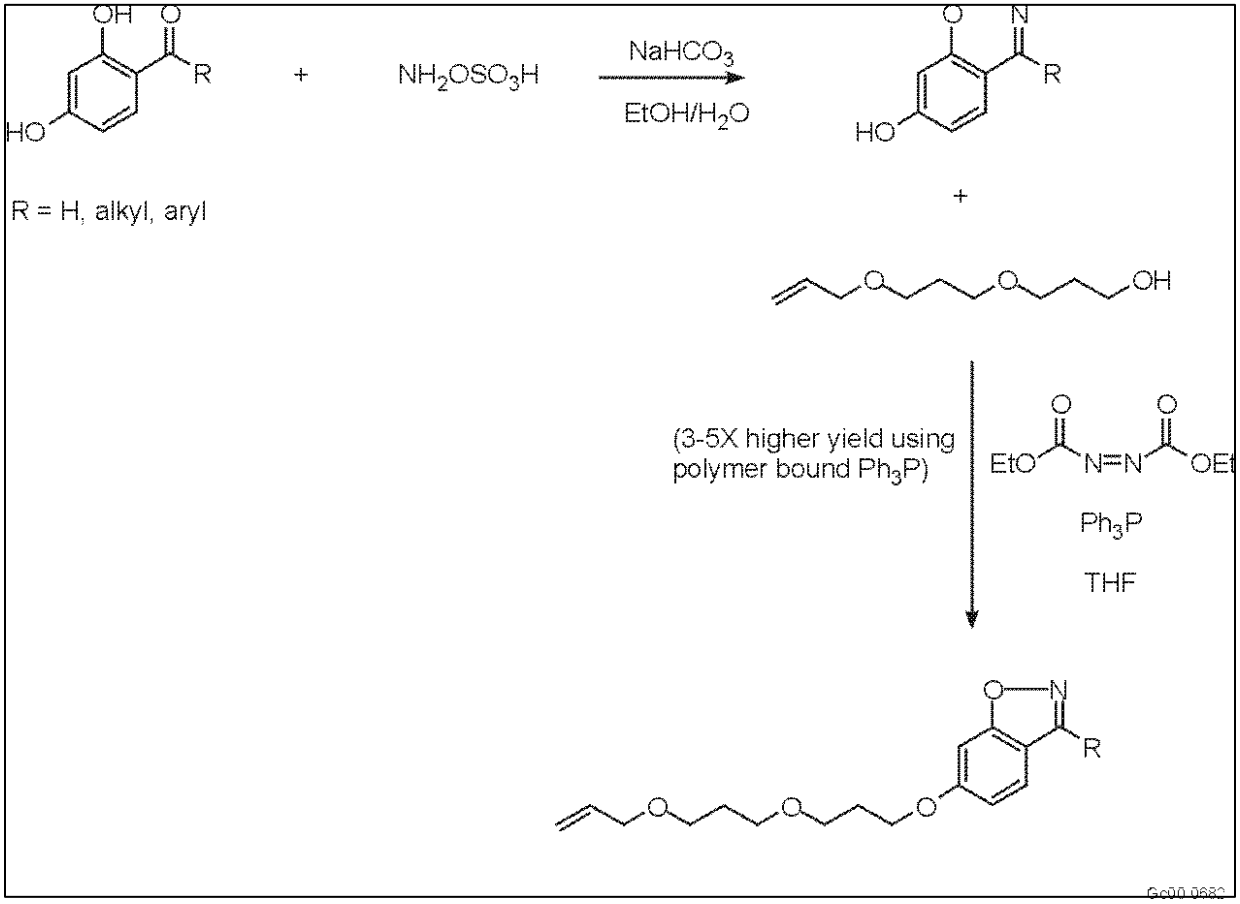

Figure 2. Synthetic scheme for attaching the tether to the head group.

Magnetically Enhanced Filtration

For a theoretical focus, we significantly modified an existing theoretical treatment[2] of the influence of a magnetic field upon particle capture in a magnetically active column. In this activity the practical advancement that we sought to provide was the addition of a flow vector component to the previous model. This important expansion allows for prediction of column optimal performance in a "true to life" situation where a feed stream is being treated in a flowing column instead of a still batch-mode process.[3] The limiting assumption necessary to make this model tractable was that only one contaminant particle interacting with one column particle could be considered as a function of time and position.

This model (Figure 3) describes the magnetically enhanced separation system, a natural clash of forces: drag on the contaminant particle from the moving liquid feed stream resisting capture against magnetic attractive forces between the contaminant particle and the column bed material inducing capture. From this fundamental clash, three differing potential interactions are predicted (see Figure 3). In path one, extreme distance between the contaminant and the bed pack lead to no interaction and hence no capture. Conversely, in path three, direct collision ensures capture. The dominant and defining path, path two, considers the balance of forces when a contaminant particle comes within the "sphere" of influence of the bed particle. The net result is that, although the magnetic force is theoretically spherically distributed about the bed particle, factoring in Brownian motion and a flow component vector signify-cantly alter this shape as shown in Figure 4. In Figure 4, the bed particle is shown as an ideal sphere and the line drawn around this particle is where the balance of forces, defined very simply as $F_{capture}/F_{escape}$, = 1.0. Within this boundary, capture should occur, while outside the boundary, escape will occur.

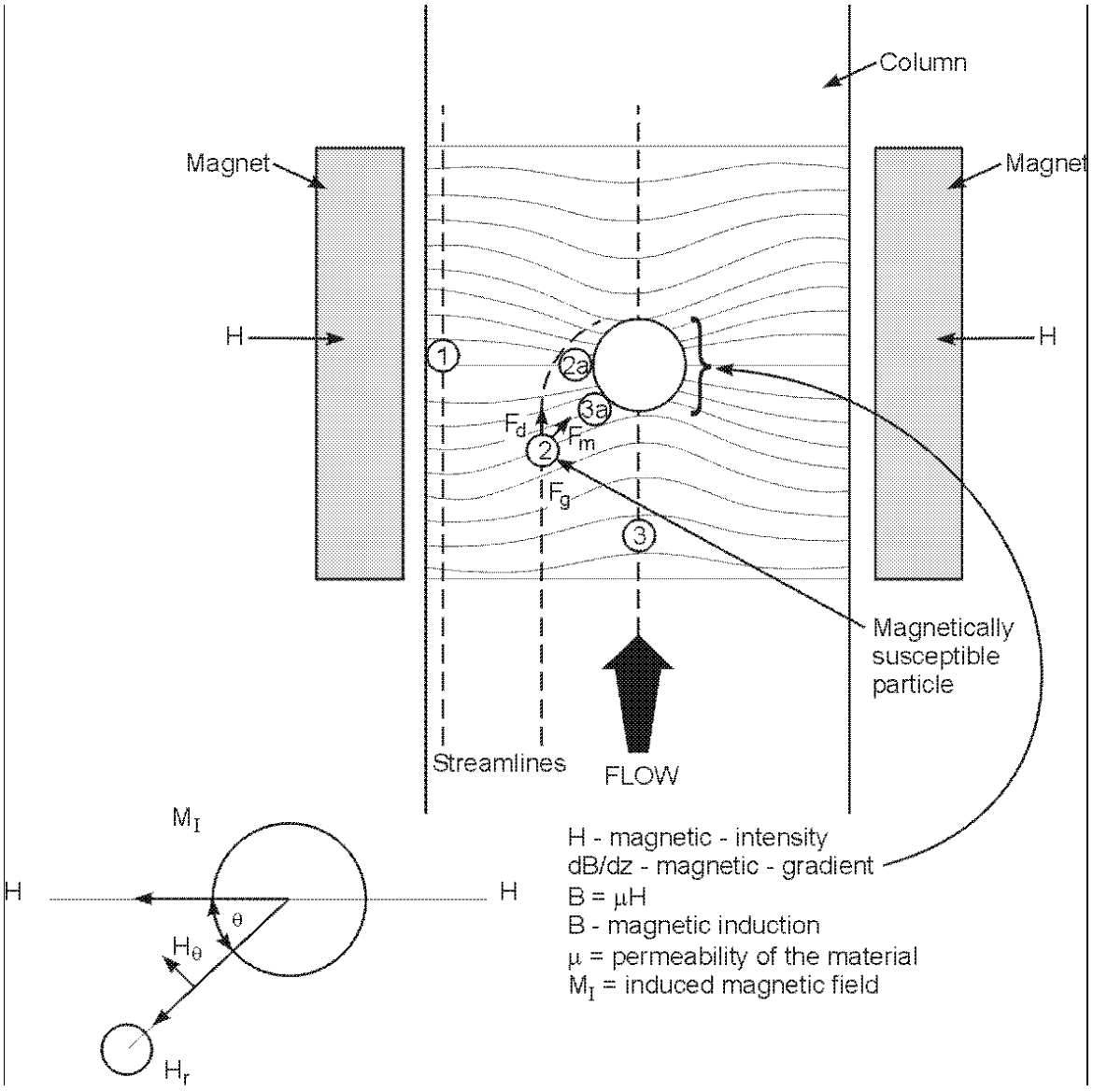

Figure 3. Representation of the three potential particle paths through a magnetic separator.

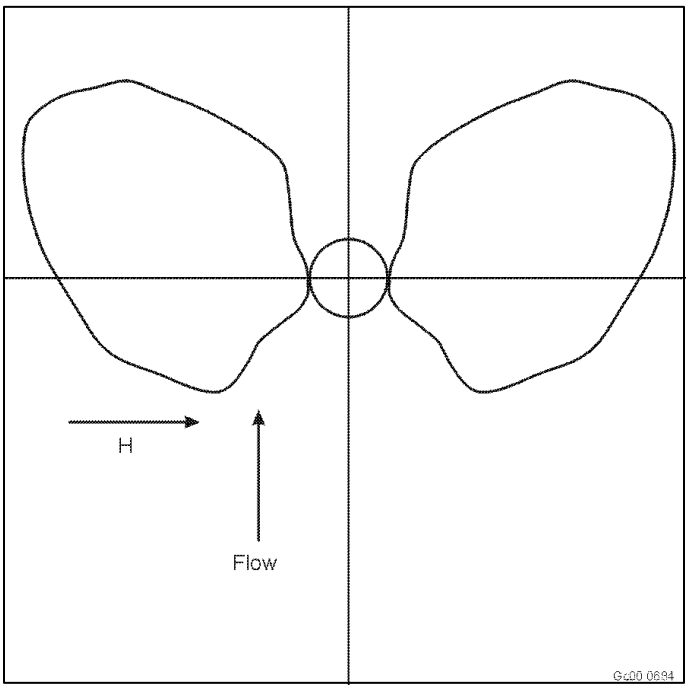

Figure 4. Graphical representation of the limiting radius of capture in a theoretical system. The line represents the boundary where Fcapture/Fescape ? 1.0.

Magnetically Enhanced Filtration Experimental Work

Physical experiments were performed on both diamagnetic (silica) nanoparticles and ferromagnetic, nonflocculating (magnetite encapsulated within polyacrylic acid) nanoparticles to determine the effects of flow velocity, the strength of the externally applied magnetic field, and complement existing data that was previously collected for paramagnetic nanoparticles. Column flow experiments were conducted on particles of various discreet size ranges to determine when the threshold of capture was achieved. These data were then correlated and compared to the results expected based on the above theoretical work from which we determined that the correlation between theory and experiment is surprisingly good (see Figure 5). These experimental results add credibility to the validity of this theoretical model. It must be noted, however, that experimental data exhibits consistently poorer performance than is predicted by the model. This reduction in performance is due primarily to two factors: first, multiple particle systems have particle/particle physical impacts that would reduce capture efficiencies; and second, as the magnetite column particles are packed in a random orientation, the fields that they exhibit will have some regions of destructive overlap, reducing the effective magnetic field below the theoretical threshold in some areas of the column.

Membrane Development for High Flux-efficient Separations

We developed economic evaluation and pilot synthetic studies for the new phosphazene polymer synthesis developed in collaboration with the University of Vermont. The synthetic process (see Figure 6) is designated as the “New Process.” This task resulted in signature of a nondisclosure agreement with Technically, Inc. of Woburn, Massachussets. A contract for performance of the pilot-scale synthesis studies coupled with execution of an economic evaluation of the process was issued. Technically, Inc. signed the contract and work was executed from October 2000 until August 15, 2001.

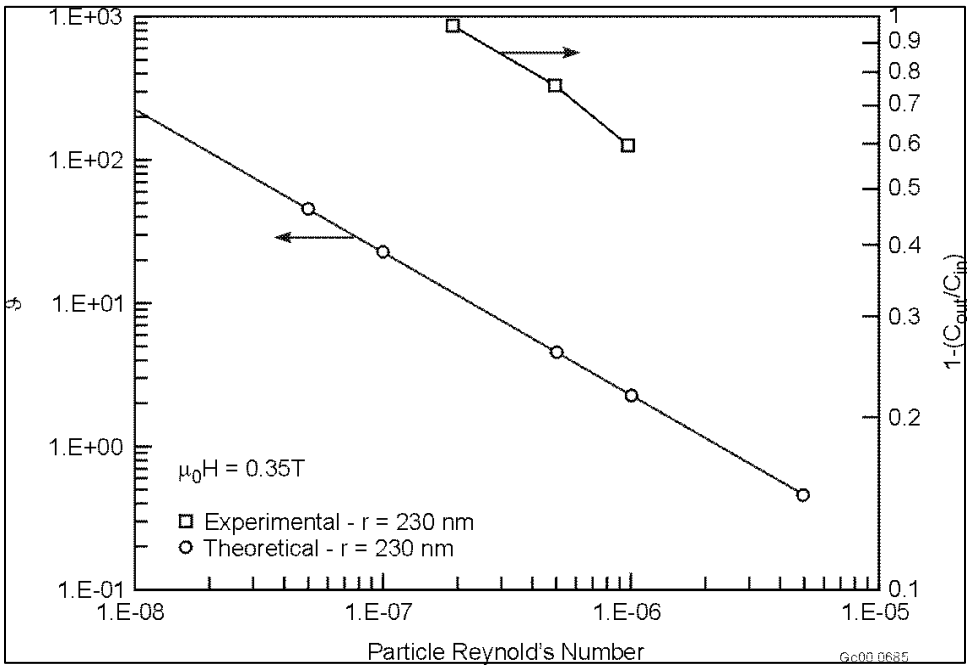

Figure 5. Graph of the correlation between experimental results and theoretical expectations in a magnetic separator (230 nm paramagnetic particles at a magnetic strength of 0.35 T).

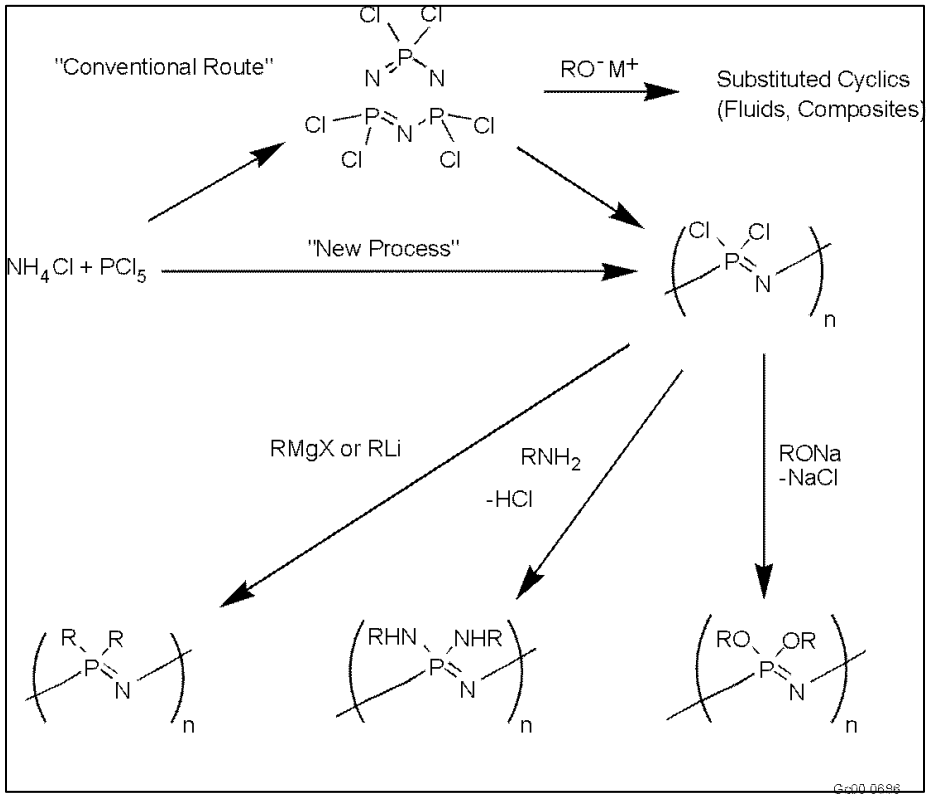

Figure 6. Synthetic Scheme for the new phosphazene polymer synthesis.

Six experimental runs were performed by the contractor, Technically, Inc. Four of these batch runs were performed in smaler scale (200 gram scale) to obtain experience with the process, Table 1. In Table 1, the initial batch (No. 1) was lost, and therefore not reported by the contractor. Each of the batches provided about 45% theoretical yeild. Two larger batches (1-kg scale) were then made with appproximately 60% theoretical yeild, Table 2. These polymers proved to be very high molecular weight materials of 5–6 million daltons. The contractor confirmed the previous work at University of Vermont, that demonstrated the process could be brought to the single kilogram batch scale without any significant problems. However increasing the size of the batches beyond the single kilo level produced varied results probably due to thermal transfer difficulties. Additional problems with polymer molecular weight control at larger scale became evident, but no data were reported. The project was therefore terminated with the hope that future funding could be obtained to address the critical issues of obtaining appropriate corrosion resistant reaction systems for the larger scale syntheses, molecular weight control, thermal transfer issues, mixing issues, and viscosity measurement.

Table 1. Results of small scale process testing.

Run	Batch Temperature, Oligomer	Yield Oligomer Distillate	Batch Temperature, Polymerization	Yield Polymer	Yield Bis-Phenoxy Derivative	Appearance
2	152∀C	49.7 g	245.8∀C	13.85 g	43% theor.	Gummy white solid
3	156∀C	51.3 g	247.6∀C	15.32 g	41% theor.	Rubbery white solid
4	155∀C	51.8 g	246.2∀C	13.01 g	44% theor.	Fluffy white solid

Table 2. Results of 1 kiogram batch process testing.

Scale-Up Run	Batch Temperature Oligomer	Yield Oligomer Distillate	Batch Temperature Polymer	Yield Polymer	Derivative	Yield
1	166.3∀C	202.7 g	255.8∀C	65.9 g	Bis[4-carboethoxyphenoxy]	55.1% theor.
2	165.8∀C	213.8 g	255.4∀C	69.9 g	Bis[3-methylphenoxy]	62.0% theor.

Barrier Characterization

The purpose of this subtask was to evaluate the use of MIMS as a tool to determine if different materials could be effective barriers for DOE waste containment applications. The approach was to obtain a partial list of the types of materials used as barriers and pond liners, obtain representative samples of these classes of materials, and to use MIMS to determine the permeability's of analytes that might be present in subsurface contamination plumes.

There are many types of barriers that are needed in different applications. Very general categories of barriers include air sparging walls of water, cement walls, grouted barriers, clay fillers, reactive permeable barriers (amorphous ferric oxyhydroxides and other zero valent iron systems), and a wide variety of polymer sheets or films. The list of polymers includes urethanes, polyethylene, linear low density polyethylene, polypropylene, polystyrene, polyvinylchloride, vinylesters, and many other elastomers such as ethylene propylene diene monomer (EPDM) rubber. Only the materials that can be formed into thin films are suitable for MIMS analysis. This includes all of the polymeric materials.

Our primary objective was to evaluate MIMS as an analytical technique for determination of permeabilities for potential barrier materials. A Varian Saturn II gas chromatograph (GC)/mass spectrometer was modified by removing the GC and replacing it with a special valve, port, and probe assembly, (see Figure 7). The probe is a commercial unit that has an integrated pump and heater system specifically designed for MIMS. The system flows a pure solvent (water) stream across the membrane at a constant rate (e.g., 1 mL/min). There is an injection port, into which a 1 ml slug of the test solution is inserted into the feed system. The slug of material passes across the membrane and exits to a collection unit. Figure 8 shows how the membrane is attached to the tip of the probe inserted into the spectrometer.

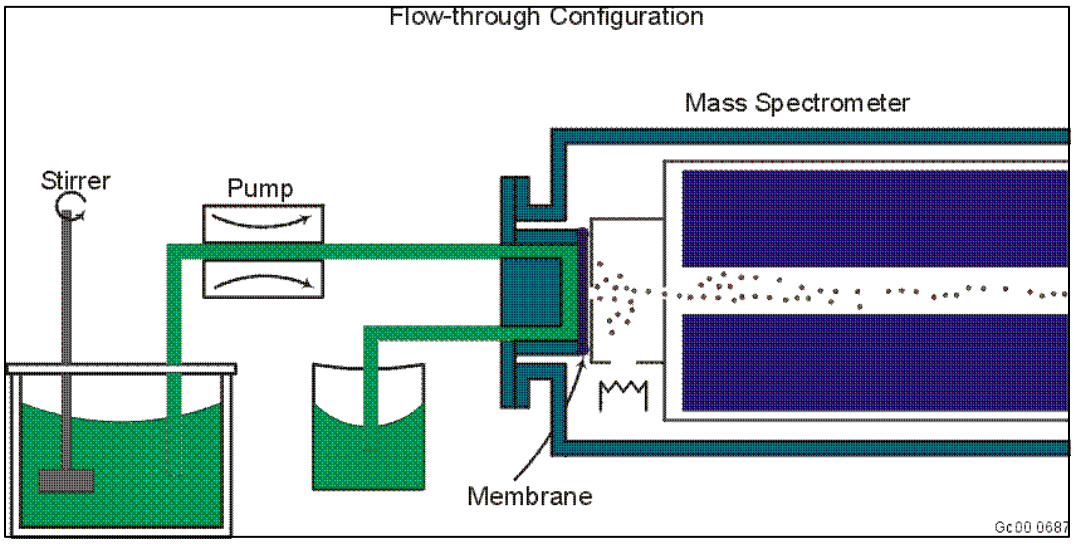

Figure 7. Sheet membrane MIMS probe.

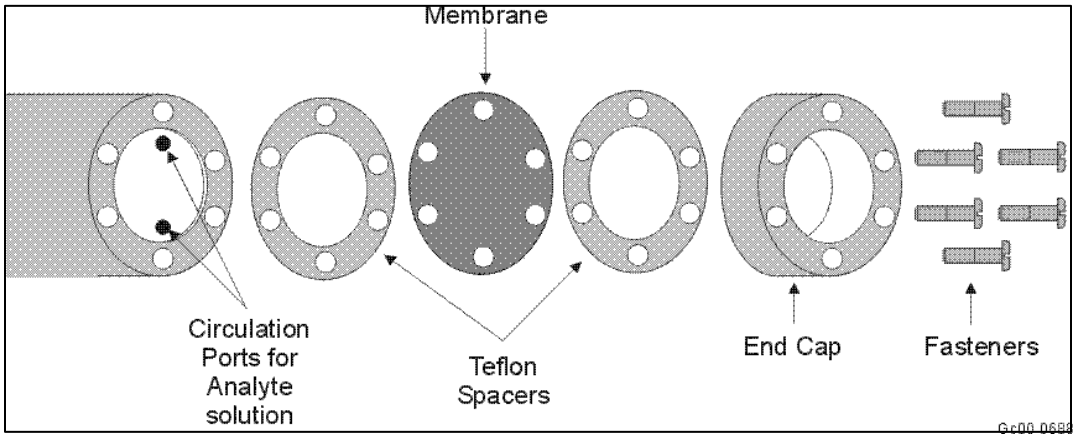

Figure 8. Illustration showing how the membrane is attached to the probe.

MIMS can be an extremely sensitive analytic technique. Several authors have reported parts per billion detection limits; there are some that have reported parts per quadrillion detection of organics in water. The membrane does the separation so the only sample preparation is filtering enough so that one has a nonclogging fluid that can be pumped across the membrane. In addition to the ultimate sensitivity of the technique another benefit is the detection range. It is not uncommon to be able to make measurements over five or six orders of magnitude without making any system changes.

The primary driver in the development of the MIMS technique is to develop improved analytical detection methodologies and detection limits of the desired analytes. The strength of MIMS resides in its ability to allow the transfer of volatile and semivolatile compounds from aqueous solution or other matrices to the gas phase with good efficiency. The transfer involves the adsorption of the analyte onto the membrane followed by diffusion across the membrane and into the vacuum, thus providing some degree of enrichment. As researchers develop new materials that are designed for use as subsurface barriers, MIMS can be used to determine how permeable they are to the target chemicals.

The long range goals of the task were divided into two logical components: test existing barrier films, and correlate structure and function (build a database). This program will benefit greatly by leveraging past programs in which many new polymers have been produced.

Table 3 summarizes the data obtained from the MIMS experiments in which four chlorinated hydrocarbons (trichloroethylene TCE, methylene chloride $MeCl_2$, chloroform, and carbon tetrachloride) were used against five different polymers.

MIMS appears to be well-suited for the kind of testing needed to characterize film/sheet materials as potential barriers. The mass spectrometer (the detector for the system) is extremely sensitive. The main drawbacks to using the MIMS technology for this kind of evaluation is that it is not very portable and the ion trap type of spectrometer that we are using is not well suited to films that have high water permeation rates. Literature reports suggest that one can manage water better using quadrapole mass spectrometers.

Table 3. Comparison of MIMS experiments and polymers.

Polymer	TCE	Methylene Chloride	Carbontetra chloride	Chloroform
EPDM (thick)[a]	20 ppm	200	>200 ppm[c]	>200 ppm
Neoprene (thick)[a]	>200 ppm	>200 ppm	>200 ppm	>200 ppm
EPDM (thin)[b]	200 ppb	20 ppm	Too noisy	20 ppm
Neoprene (thin)[b]	>200 ppm	>200 ppm	>200 ppm	>200 ppm
Polyvinylidene chloride	20 ppm	>200 ppm	>200 ppm	200 ppm

a. The thick films are membranes cast in thicknesses such that they were self supporting, on the order of 100 to 200 µm thick.

b. The thin films were made by painting a thin coating of a solvent containing the polymer onto the surface of a microporous support layer.

c. The concentration of the analytes used in this test started at 200 ppm and then if peaks were observed the concentrations were reduced by a factor of ten until no peaks were observed. If no peak was observed at the 200 ppm level then that is designated in the table as >200 ppm.

REFERENCES

1. J. March, "Advanced Organic Chemistry—Reactions, Mechanisms, and Structure," *Wiley Interscience*, 4th ed, New York, 1992.

2. A. D. Ebner, J. A. Ritter, and H. J. Ploehn, "Feasibility and Limitations of Nanolevel High Gradient Magnetic Separation," *Separation and Purification Technology*, Vol. 11, 1997, pp. 199–210.

3. G. B. Cotton and H. B. Eldridge, “Nanolevel Magnetic Separation Model Considering Flow Limitations,” *Chemical Engineering Science*, Submitted.

Proton Conducting Ceramic Membrane Applied to Spent Nuclear Fuel Stewardship

Removing Water and Hydrogen from Spent Nuclear Fuel

Paul A. Lessing (INEEL); Yang-Ki Hong (University of Idaho); Shekar Balagopal (Ceramatec, Inc.)

SUMMARY

Part of EM's mission is to reduce high-level waste and place it in one long-term dry storage facility at Yucca Mountain, Nevada. Proposed regulations for Yucca Mountain, however, allow for only a very small amount of total water to be present in any large canisters placed there. High-level waste such as spent nuclear fuel normally contains more water than Yucca Mountain will allow; some of that water is chemically bound to the waste, making it difficult to remove. High temperature calcination is the current process used to remove water from high-level waste, but requires the installation of large, expensive equipment.

Our objective with this research has been to develop a unique ceramic membrane that will transport water and hydrogen at relatively low temperatures (e.g., 100–300°C) in response to chemical and electrical potential differences. If successful, this research will offer an alternative method for packaging damaged or corroded spent nuclear fuel and high-level waste containing excessive levels of water (especially chemically bound water).[1] Hydrogen in canisters is the result of water radiolysis or the reaction of water with uranium or other internal canister materials. When developed, the membrane will permit gaseous water and hydrogen to escape from the package while completely retaining back-filled helium, radioactive decay gases, radioactive particulate, and oxygen. This will enable compliance with shipping regulations and proposed storage regulations (e.g., draft Waste Acceptance System Requirements Document, DOE/RW-0351) that allow for only very small amounts of total water (e.g., 200 g) to be present in large canisters.[2]

We conducted research in cooperation with the University of Idaho and Ceramatec, Inc. (a small high-technology ceramics company). Our research has brought the project to the point where direct current (dc) performance testing of the resulting cells can be performed in a facility built at the INEEL. Ceramatec developed a new type of NASICON ceramic called ProNas, which can be proton-exchanged while remaining gas-tight. ProNas ceramic exhibits relatively high conductivity at low temperatures when measured using complex impedance techniques, even in liquid solutions. The University of Idaho developed sputtering technology to apply well-adhered palladium/silver electrodes to the ProNas electrolytes.

We built and tested equipment that could measure proton conductivity (related to hydrogen flux) in practical dc cells using gaseous atmospheres. The testing will differentiate the type of hydrogen bonding and transport mechanisms within the crystal structure of the ProNas ceramic. The dc testing requires well-adhering electrodes (from the University of Idaho) that exhibit high-hydrogen solubility.

TASK DESCRIPTION

Figure 1 shows a schematic of two different hydrogen-conducting membranes that we have proposed to relieve hydrogen pressure in DOE canisters. The *passive* design at the left is a Pd/Cu metal alloy membrane that is starting to become available (for high temperature hydrogen separation) from commercial sources. It is strictly a temperature-activated, pressure-driven process; high-hydrogen fluxes

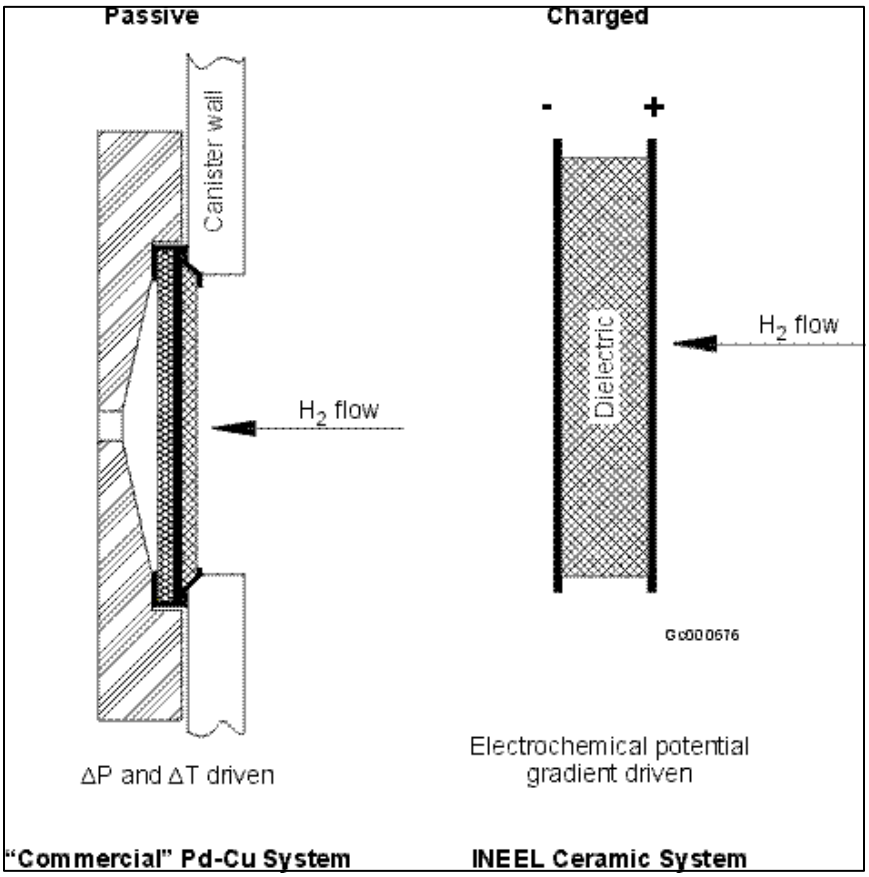

Figure 1. Schematics of hydrogen-conducting membrane concepts.

are measured at elevated pressures and temperatures. The charged INEEL design at the right is the subject of this task. The ceramic membrane also conducts via activated pressure-driven processes. However, since the ceramic is a dielectric (does not conduct electrons), the flux can also be increased by applying a dc voltage (electrical gradient) across the electrolyte that drives the charged protons. Consequently, the ceramic membrane (with appropriate electrodes) conducts hydrogen in response to both pressure and applied dc voltage (e.g., a battery).

Without an applied dc voltage, the ceramic membrane (with electrodes) will still transport hydrogen in response to a pressure differential. However, for the transport to continue under pressure-only conditions, the anode must be electrically connected (shorted) to the cathode. Otherwise, electrode polarization (build up of electrons) will occur and stop the process.

The INEEL ceramic design has the advantage of allowing the device to be operated at lower temperatures (depending on specific composition of the membrane), and it can remove the hydrogen down to extremely low equilibrium levels, as determined by the Nernst[3] equation applied at equilibrium. The appropriate Nernst relationship is given in Equation 1:

$$V = RT/nF\ [\ ln\ (PH^{II}_2 / PH^{I}_2)] \qquad (1)$$

Where:

V = a applied voltage

n = number of electrons transferred (2) per hydrogen molecule during the reduction reaction

R = universal gas constant

T = absolute temperature

F = Faraday's constant

PH^{II}_2 = partial pressure of hydrogen on canister side of cell

PH^{I}_2 = partial pressure of hydrogen on the atmospheric side of the cell.

Water vapor might also be removed, depending on the type of hydrogen bonding and conduction mechanisms occurring within the ceramic.[4] For instance, one type of bonding can be H_2O molecules associated with protons as hydronium ions with hydrogen bonds. This bonding is known for beta-alumina type ceramics.[5] Another type of bonding could consist of a proton bound to an oxygen ion of the ceramic lattice; conduction arises from the proton hopping along adjacent oxygen ions (also can be present in beta-alumina).[6] Different fluxes of hydrogen gas or water vapor will result from varying the water vapor content (partial pressure) of the pressurized (up stream/canister) gas atmosphere. Heating to excessively high temperatures dehydrates the ceramic (if it is primarily a hydronium conductor) and can also drive out bound protons. This destroys the ionic conductivity and may also fracture the ceramic membrane. Rehydration or protonation may occur reversibly at lower temperatures (in water vapor or hydrogen containing atmospheres) but would be pointless if the membrane has been cracked or is irreversible because the basic crystal structure has changed (collapsed).

Performance measures for the proton-conducting ceramic membranes are that the cell must be hermetic (leak-tight), and the hydrogen flux must be a function of temperature, hydrogen pressure (from a canister), and applied voltage. The total available hydrogen flux of a cell must be sufficiently high to relieve gas pressure within a canister before it reaches an unacceptable level. Of course, the total flux of a cell increases with total cell surface area, operation temperature, gas pressure, and applied voltage. A reasonable (e.g., 100- to 500-cm^2) maximum cell area will have to be specified. A worst-case estimate for a hydrogen generation rate in a spent fuel canister would be from water's reaction (oxidation) with uranium metal. A worst-case generation rate (maximum) of hydrogen gas can be estimated as 200.17 scc/min.[7] Therefore, a successful cell must transport approximately 200 scc/min through an area of approximately 500 cm^2, using an applied voltage that does not decompose the ceramic (e.g., less than 2 volts). This translates to a minimum goal for hydrogen transport across a ceramic membrane (in a cell) to be about $4.0 \Delta 10^{-1}$ scc/min-cm^2 at temperatures and internal pressures that are reasonable for a given canister (e.g., 100∀C and 100 psig). The hydrogen generation rate, temperature, and pressure will vary, depending on the internal physical and chemical situation of the canister being addressed.

ACCOMPLISHMENTS

Since electrolytes provided from the University of Stuttgart were not gas tight, we worked exclusively with Ceramatec, Inc., as a company that could provide a type of ceramic that could be successfully proton-exchanged. This material is proton-exchanged NASICON (ProNas). ProNas is an emerging material that was originally developed for ionic conduction in liquid solutions (rather than gases). It is chemically stable in both acidic and caustic conditions. Ceramatec has measured its proton conductivity to be $9.8 \Delta 10^{-3}$ S/cm at 55∀C in a liquid. Three shipments of ProNas were received from Ceramatec, including both proton exchanged and nonexchanged samples of two slightly different chemical compositions (PRONAS Z and PRONAS 3). The proton exchange process is electrochemically driven in the apparatus as illustrated in Figure 1.

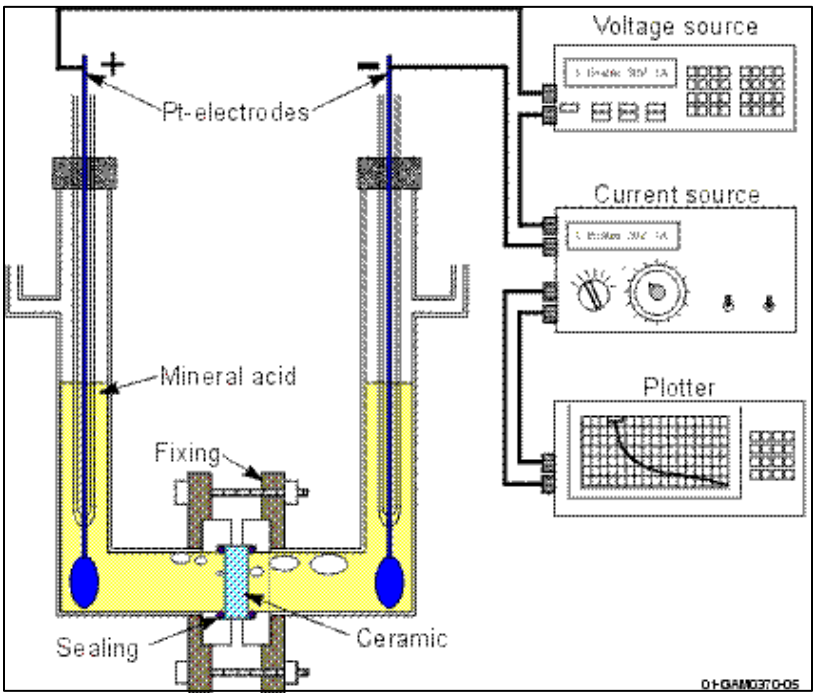

Figure 1. Proton Exchange Apparatus.

Driving an ion current through the sample carries out the electric field-assisted ion-exchange process. The ceramic sample separates two compartments filled with dilute mineral acid. Applied voltage varies from 10 to 30 V; current density correlates with extent of ion exchange.

Very little compositional or conductivity data is available for the proprietary ProNas material. However, an independent party reportedly measured ProNas conductivity at $4 \Delta 10^{-3}$ S/cm at 80∀C in a H_2/O_2 cell (H_2 gas stream containing 3% H_2O). This indicates that ProNas will conduct protons in a gaseous atmosphere (at temperatures lower than the H-η"-alumina).[8]

Prof. Yang-Ki Hong (University of Idaho [U of I]) submitted six progress reports and a final report on electrode development. His undergraduate laboratory assistant, Matthew L. Mottern, won a 2nd Place Award in a research paper contest sponsored by the Inland Empire Chapter of ASM International for his original research performed within the U of I's Magnetic and Electronic Materials Research Laboratory. The title of the research paper was, "Thickness Dependence of Metallic Thin Film Adhesion." Mottern's technical work covered five major activities: (1) design of dark shield and substrate holder for sputtering systems, (2) optimization of sputter deposition parameters, (3) characterization of morphology for the substrate (electrolyte) and Pd-25%Ag films, (4) adhesion testing, and (5) delivery of Pd-25%Ag electrodes on ceramic membranes to the INEEL. The deposition of Pd/Ag films was conducted under controlled conditions using various ceramic substrates (including ProNas). Figure 2 shows a scanning electron micrograph of thin, dense Pd/Ag film produced at the U of I. The films could also be made crystalline as illustrated in Figure 3. Crystallinity promotes rapid and reversible gaseous hydrogen conversion to protons and the subsequent conduction of the protons to and from the ceramic electrolyte. It was observed that (a) the as-deposited film crystallized without substrate heating, (b) a sputtering rate of about 200 nm/min could be achieved, (c) the (111) peak height decreased with increasing substrate temperature in the range of 25 to 450∀C, and (d) the (111) peak shifted toward lower angle with substrate temperature. Some optimization studies were conducted using ProNas as the substrate, including adhesion experiments (Figure 4) that show thin coatings adhere better than thick ones. This behavior was modeled.

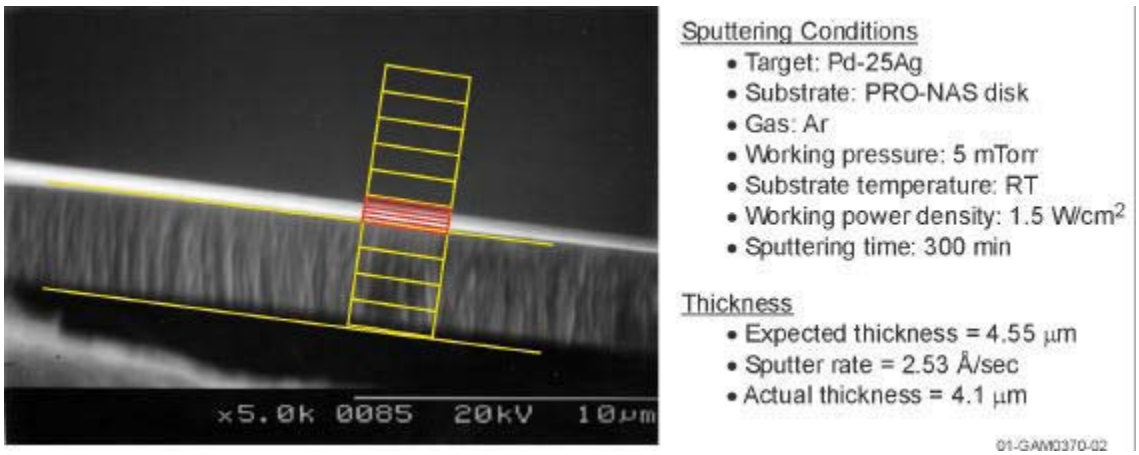

Figure 2. SEM micrograph of the cross section of Pd-25%Ag films deposited on a ProNas substrate.

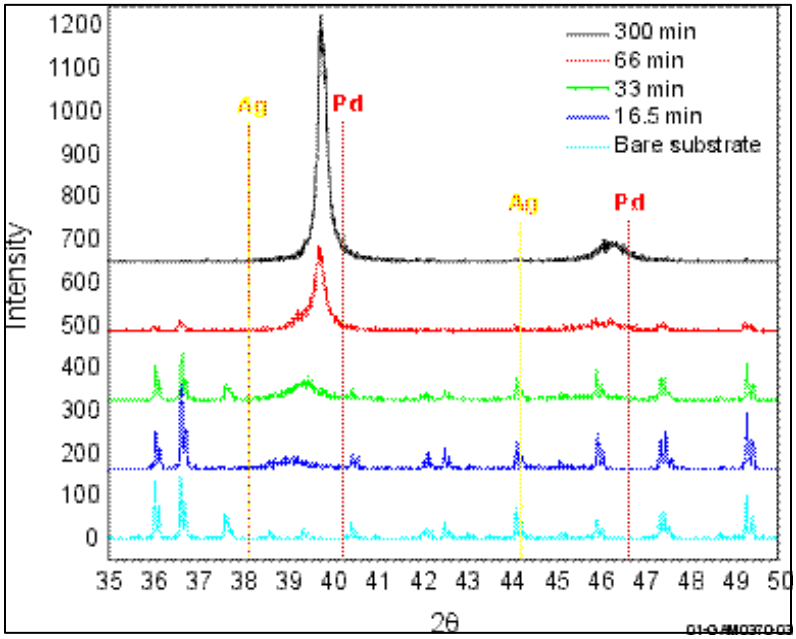

Figure 3. XRD patterns of Pd-25%Ag films deposited on ProNas.

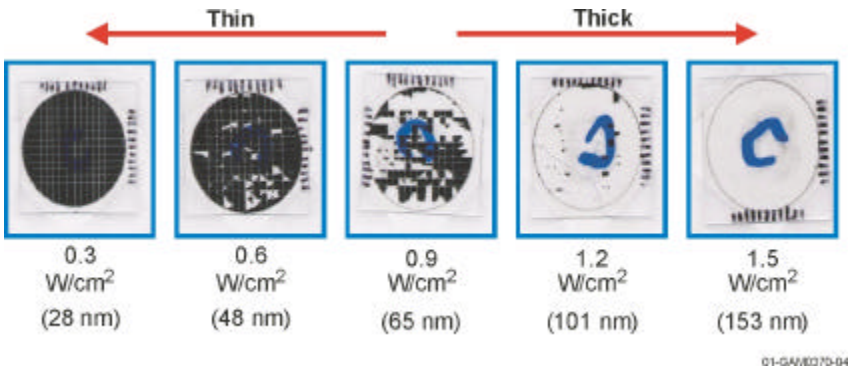

Figure 4. Photographs of some results from adhesion tests of Pd/Ag on ProNas electrolytes.

The INEEL designed and fabricated a dc cell, hydrogen flux testing system (Figure 5). The dc cells are driven by a Gamry Model PC4/750 Potentiostat/Galvanostat/Zero Resistance Ammeter. Additional software was purchased to enable the instrument to perform complex ac impedance tests. The hydrogen flux will be measured on the "permeate" side using an evacuated chamber and the "robust hydrogen sensor" developed by Sandia National Laboratory and marketed by DCH Technology (blue-colored box at lower left of Figure 5). This sensor is based on a unique palladium nickel alloy used to create a series of resistors and transistors on a microchip. It has a range of 10 ppm to 100% hydrogen with a sensitivity of +/- 10 ppm and can work in vacuum. Back-up measurements will be made using a more conventional (but complicated) mass spectrometer and gas chromatograph system.

We successfully completed validation testing of the flux testing apparatus which covered design and fabrication of the cell holder, testing of DCH hydrogen sensor, high-pressure testing of the system, evaluation of various high-temperature conducting and nonconducting epoxies to cement the electrolyte into the cell holder, firing and testing of commercial palladium-based pastes on NASICON for use as electrodes, and proton exchange of the NASICON into ProNas after firing of the electrodes.

Figure 6 shows a fired paste electrode on a ProNas electrolyte with the current collector and electrical connection wire, and Figure 7 shows an electrolyte being cemented into the sample holder assembly using a special high-temperature epoxy. The system is ready to make hydrogen flux measurements using existing ProNas electrolytes with Pd/Ag electrodes already attached using either the U of I sputtering technology or fired commercial paste electrodes.

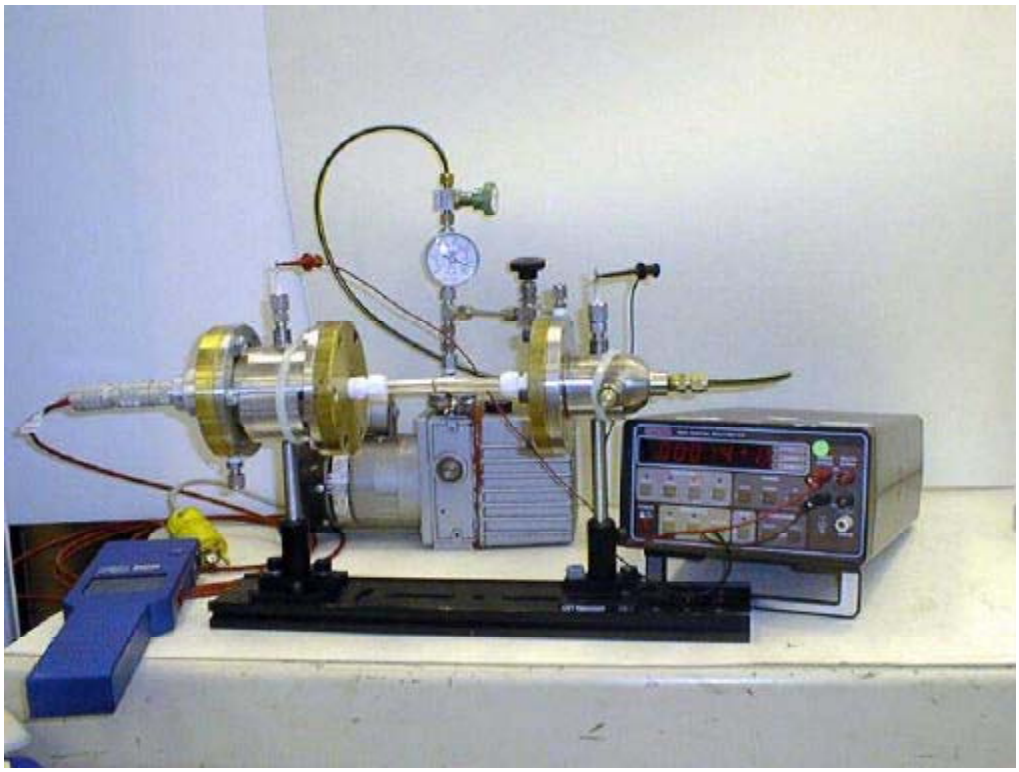

Figure 5. New hydrogen flux cell testing apparatus fabricated at the INEEL.

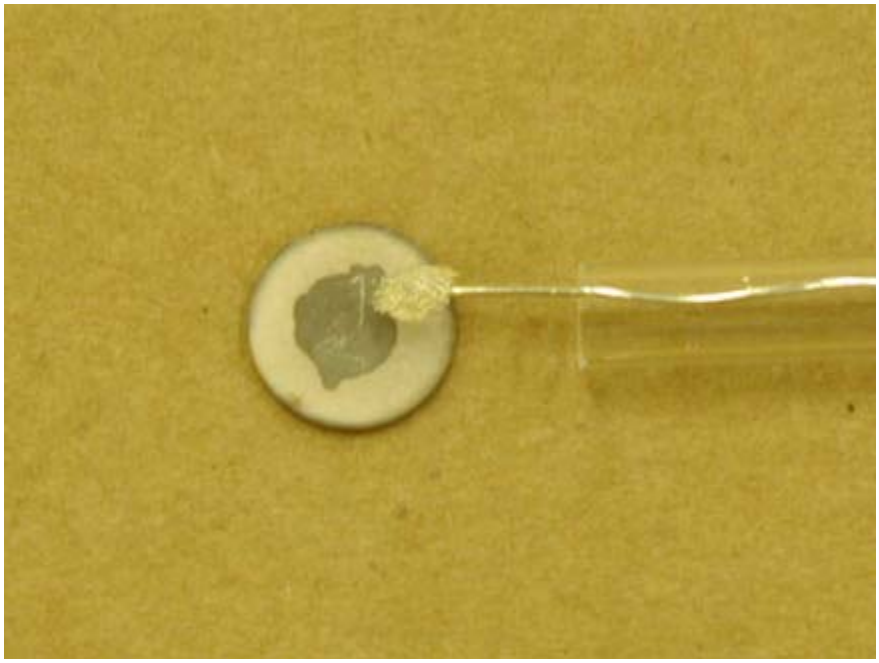

Figure 6. ProNas electrolyte with electrode, current collector, and connection wire.

Figure 7. ProNas electrolyte inserted into cell holder assembly.

REFERENCES

1. P. A. Lessing, "Effects of Water in Canisters Containing DOE Spent Nuclear Fuel," DOE/SNF/REP-017, Rev 0, United States Department of Energy, National Spent Nuclear Fuel Program, peer reviewed, October 1998.

2. P. A. Lessing, "Standard Guide for Dryness in Canisters Containing DOE Spent Nuclear Fuels," DOE/SNF/G-003, United States Department of Energy, National Spent Nuclear Fuel Program, Rev 0, peer reviewed, May 1999.

3. A. J. Bard and L. R. Faulkner, *Electrochemical Methods—Fundamentals and Applications*, John Wiley and Sons, 1980, pp. 51 and 100.

4. C. K. Kuo, A. Tan, P. Sarkar, and P. S. Nicolson, "Water Partial Pressure-dependent Conductance and Humidity Effects on Hydronium-η"-Al_2O_3 Ceramics," *Solid State Ionics,* Vol. 58, 1992, pp. 311–314.

5. N. J. Dudney, J. B. Bates, and J. C. Wang, "Hydration of Lithium η-alumina," *J. Chem. Phys,* 77, 1982, pp. 4857–4869.

6. G. C. Farrington, "H_2 and H_2O Oxidation at a Pt/Na^+-Beta Alumina Interface," *J. Electrochem Soc: Electrochemical Science and Technology,* 1976, pp. 833–834.

7. Paul A. Lessing, *Scientific Investigation Plan for Qualification of Palladium/Copper Membrane*, Rev 0, Report DOE/SNF/PP-021, United Sates Department of Energy, National Spent Nuclear Fuel Program, peer reviewed, April 2000.

8. G. W. Schafer and R. Gadow, *Fabrication of H-η-alumina Polycrystals*, special report prepared for the INEEL, University of Stuttgart, Institute for Fabrication of Ceramics (IFKB), Allmandring 5b, D-70569 Stuttgart, Germany.

Spectroscopic Investigations at Solid-Supercritical Fluid Interfaces in Support of Advanced Supercritical Separation Techniques

Advanced Environmental Separations Science for Remediation

Daniel M. Ginosar, Harry W. Rollins, and Robert V. Fox

SUMMARY

To meet its mission, EM must develop the techniology to separate chemical species from one another. This technology (advanced separations science) must also encompass remediating contaminated materials in tanks and the ground. Supercritical fluid separation is one of the possible approaches, but our knowledge of the interface between solids (e.g., porous solids such as soil) and supercritical fluid is inadequate, which limits the potential uses of supercritical fluid separation in solving EM problems. Supercritical fluids, which are held at high pressures and low temperatures, exhibit both liquid and gas characteristics that can influence chemical reactions, extractions, and other processes in unusual ways. The objective of this task was to gain a better understanding of those unique properties, and improve supercritical fluid-based environmental remediation technologies.

This task involved the fundamental investigation of supercritical fluid properties at the solid-supercritical interface. It employed spectroscopic probe molecules with known photophysical mechanisms sensitive to local solvent environmental effects. We impregnated selected polymer thin films that had either hydrophilic or hydrophobic properties with well characterized spectroscopic probe molecules. We then determined the spectral characteristics of the probe molecules as we exposed the doped polymers to normal liquid solvents and supercritical fluids. From the collected data, we are developing a fundamental understanding of the structure and nature of the supercritical fluid at the solid-supercritical fluid interface. The information gained from this study will improve supercritical fluid-based environmental remediation technologies. The work does not duplicate previous EM-funded work involving water as the supercritical fluid.

TASK DESCRIPTION

The existence of supercritical fluid as matter has been known since the early 1800s. Scientific investigation of the properties of supercritical fluids occurred in the mid-1800s. By the late 1800s, the solvent properties of supercritical fluid carbon dioxide had been reported, and by 1936, supercritical fluid had been used in a large-scale commercial industrial application.[1] Today, fluids in the supercritical and near-critical region, hereafter referred to collectively as critical fluids, are exploited in the food and beverage, petroleum, pharmaceutical, microelectronics, and chemical industries, to name just a few. A renewed interest in critical fluids resulted during the 1970s when the U.S. faced an energy crisis and needed to become more energy efficient, and when enforcement of Federal environmental regulations brought such phrases as *pollution prevention* and *environmentally benign solvent* into the public arena. Recent advances in critical fluid technology have brought about new applications in the areas of supercritical fluid chromatography; synthesis of aerogel and nanoparticle materials; heterogeneous catalysis; extractions of organics, metals, and radionuclides; advanced energy efficient separations; and ultra-high-purity cleaning applications. The number of critical fluid applications has increased, owing to the unique fluid properties that can influence chemical reactions, solubility, and material structure properties in unusual ways. The most important properties of critical fluids are liquid-like solvent powers

with gas-like transport properties, and the microscopically inhomogeneous nature of the fluid (clustering), which is much more pronounced than in liquids or gases.[2–6]

A significant number of fundamental investigations have been conducted over the past 20 years in an effort to understand the physical and chemical properties occurring in homogeneous, bulk critical fluids. More recently, a small number of studies focused on the properties of critical fluid molecules adsorbed to heterogeneous solid surfaces have been conducted in the field of chromatography and to study the physisorption of hydrogen, methane, and carbon dioxide on heterogeneous surfaces in connection with secondary energy storage technologies and carbon dioxide sequestration technologies.[7–13] Those studies have successfully extended existing theory describing adsorption processes of critical fluid hydrogen and methane onto heterogeneous solids. Classical adsorption isotherms have been successfully modified to fit the empirical data. Complimenting studies have been conducted by Afrane and Chimowitz for calculating and predicting thermodynamic properties of adsorbed critical fluid carbon dioxide and ethane onto solid heterogeneous surfaces.[14] They caution that future investigators could arrive at erroneous conclusions if they rely too heavily on existing methods for predicting thermodynamic properties of other systems that are based on a limited number of select data available for solid/critical fluid carbon dioxide-ethane systems. Despite some initial successes focused on macroscopic solvent adsorption/desorption phenomena, a number of contradictions have arisen from experimental evidence, computer simulations, and theoretical calculations focused on macroscopic interactions at the solid/fluid interface.[15–18] For example, Yang and Saunders speculate that, for a combination of reasons, surface clustering and multilayer formation under supercritical fluid conditions is unlikely.[19] Takeba et al. have shown by way of molecular dynamics computer simulation that solvent clusters may indeed form and arrange themselves around adsorbate molecules on a MgO(001) surface.[20] Other investigations show evidence that adsorbate molecules are desorbed from the surface under critical fluid conditions at a bulk fluid density well below the critical point, suggesting either an extension of bulk phase properties onto the surface, or direct surface clustering behavior that leads to enhanced desorption of adsorbate into the bulk fluid phase (References 9 and 15). The same phenomenon does not occur for adsorbate molecules under liquid or gas conditions.

These preliminary investigations point to phenomena occurring at the solid/fluid interface that, at this point, are not clearly discernable from an intrinsic property of the bulk fluid phase itself or from the surface adsorbed species. Apart from those macroscopic studies, no published experimental study to date seeks to describe phenomena occurring at the solid/fluid interface at a molecular level under critical fluid conditions. Until accurate experimental data are obtained, a molecular level description of the adsorbed phase and the adjacent fluid phase will remain unknown, the controversy will continue, predictive tools will be imprecise, and our understanding will not be advanced. We will fail to exploit the fluid properties of critical fluids and lag behind in design and development of new critical fluid techniques useful for solving EM-50 problems.

This research directly addresses EM-50 problems by promoting a better understanding of the chemical reaction and mass transport phenomena occurring at the solid/fluid interface. Liquid solvent and critical fluid solvent extraction techniques have a very high potential for selectively extracting hazardous and recalcitrant compounds from liquid and solid environmental media. The research focused on the molecular level chemical and physical phenomena occurring at the solid/fluid interface. Research involved initiation of an innovative exploration of the fundamental properties of fluids at the solid/fluid interface. The goal was to obtain quantitative information regarding the structure of a super-critical fluid at the solid/supercritical fluid interface as a function of fluid density using well known and well understood spectroscopic probe molecules. The research was broken into three subtasks: spectroscopic probe molecule selection and characterization, polymer selection and characterization, and characterization of probe-doped-polymers in carbon dioxide. Each subtask, with its associated milestone, is described below.

Spectroscopic Probe Molecule Selection and Characterization

We selected and screened fluorescent probe molecules with known photophysical mechanisms for spectral responsiveness in solvents having different polarity. The desired trait is for either the shape of the spectral band to change as a function of solvent polarity or the wavelength of maximum absorbance to shift as a result of changes in solvent polarity, or both. Two dye molecules were selected and investigated.

Polymer Selection and Characterization

We selected and further characterized polymers having either hydrophobic or hydrophilic properties and capable of being cast into thin films. Characterization included a study of solubility, swelling, and chemical compatibility with carbon dioxide. Characterization also included a study of the probes' spectral response in the presence of the polymer. We entrained probe molecules into a polymer and cast the mixture into a thin film on a quartz slide. Two polymers were investigated.

Characterization of Probe-doped-Polymers In Carbon Dioxide

We made probe-doped-polymers, cast them into thin films, then subjected them to liquid, gas, and supercritical fluid carbon dioxide conditions. We determined the spectral response of the probes in carbon dioxide and other solvents as a function of solvent condition, and we determined the spectral response of probes in the polymer thin films. The results of this characterization are the basis of a comparative study.

ACCOMPLISHMENTS

Optical cells were designed for use at pressures up to 5,000 psi and temperatures up to 100∀C. Additional high-pressure optical cells for fluorescence and absorption measurements were designed and manufactured based on the Clemson design.

The absorption spectral properties of the probe molecule (Nile red) were evaluated in a series of liquid organic solvents (Figure 1). As the solvent polarity changed from hexane to methanol, we observed both a change in the shape of the peak and a shift toward the red. Nile red exhibits excellent properties as a probe of solvent polarity in this regard. A plot of the absorption peak width as a function of solvent polarity (E_t^N) demonstrates a relatively linear response for this probe molecule (see Figure 2).

We also completed a more extensive investigation of the fluorescence spectral properties of Nile red in organic solvents (see Figure 3). The fluorescence response exhibits a spectral shift, a change in the shape of the emission band, and a change in relative fluorescence quantum yield. This type of spectral response exhibited by Nile red is an excellent example of an ideal probe. A plot of the fluorescence peak maximum versus solvent polarity also yields a relatively linear probe response (see Figure 4).

The solubility and spectral properties (absorbance and fluorescence) of Nile red in supercritical carbon dioxide at 35∀C were determined as a function of pressure (Figures 5, 6, and 7). Figure 5 demonstrates the solubility of Nile red in carbon dioxide as a function of pressure and provides the characteristics of the absorption band in carbon dioxide solvent. A plot of absorbance versus pressure shows the pressure dependence of solubility for Nile red (Figure 6). The fluorescence spectra of Nile red in carbon dioxide exhibits a change in the shape of the emission peak and a spectral shift toward shorter wave-lengths (blue) as the pressure of the carbon dioxide solvent is increased (Figure 7). The probe's response in carbon dioxide is to be compared and contrasted with the response of the probe toward liquid solvents.

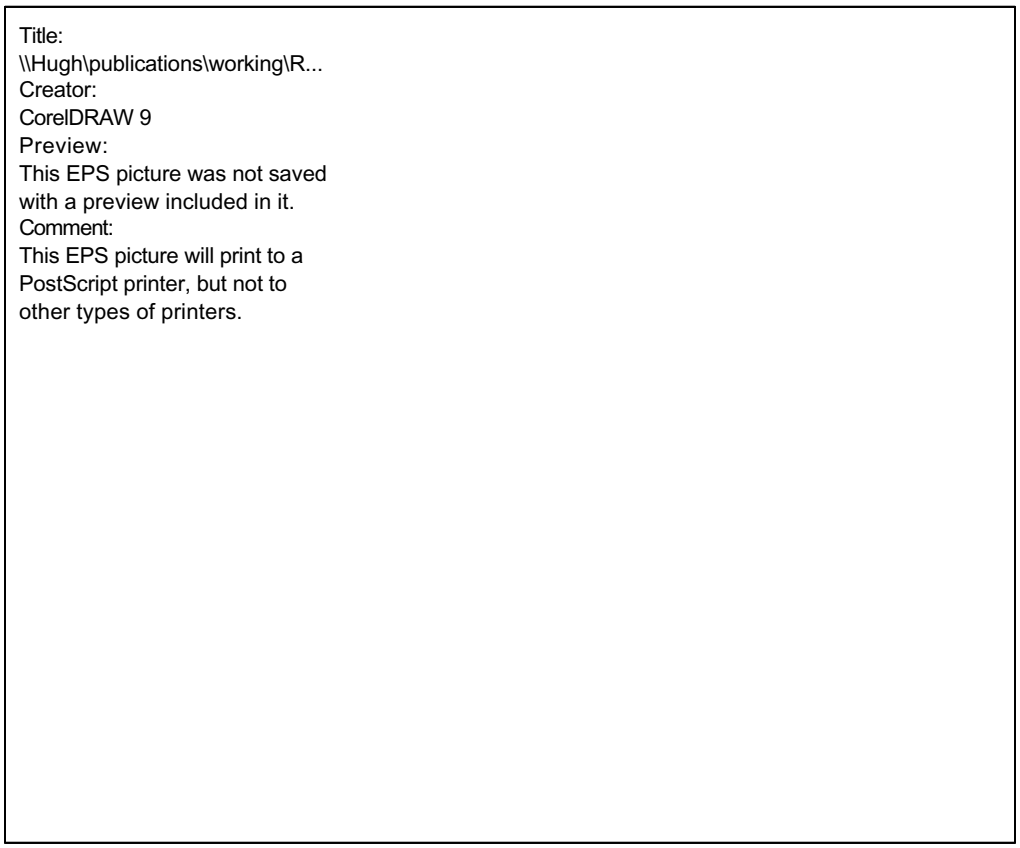

Figure 1. Absorbance spectra of Nile red in various solvents.

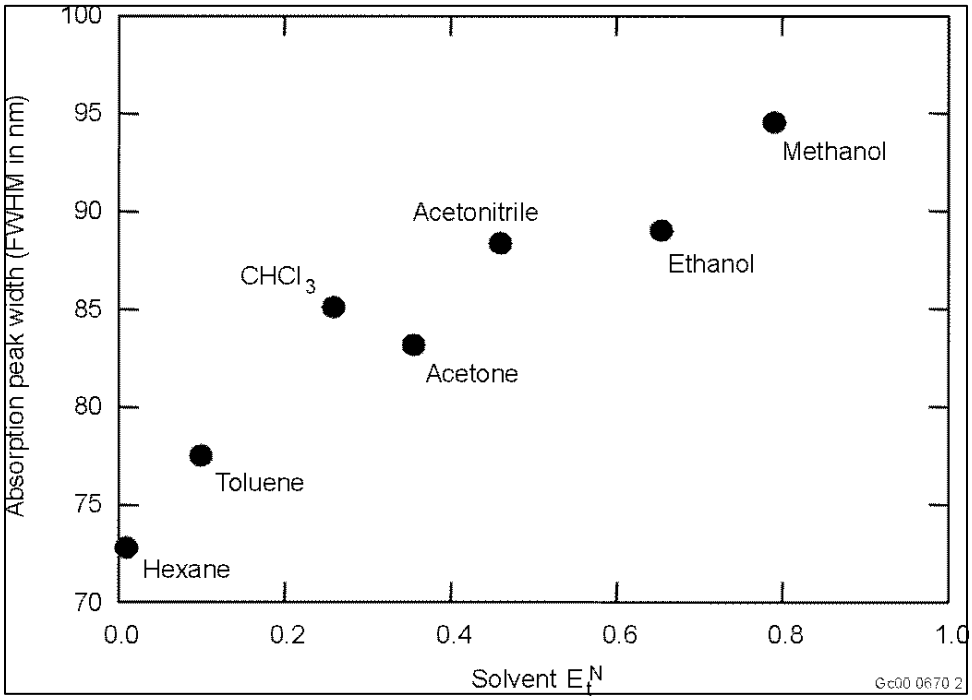

Figure 2. Plot of Nile red absorbance peak FWHM in various liquid solvents.

Title:
\\Hugh\publications\working\R...
Creator:
CorelDRAW 9
Preview:
This EPS picture was not saved
with a preview included in it.
Comment:
This EPS picture will print to a
PostScript printer, but not to
other types of printers.

Figure 3. Florescent spectra of Nile red in various liquid solvents.

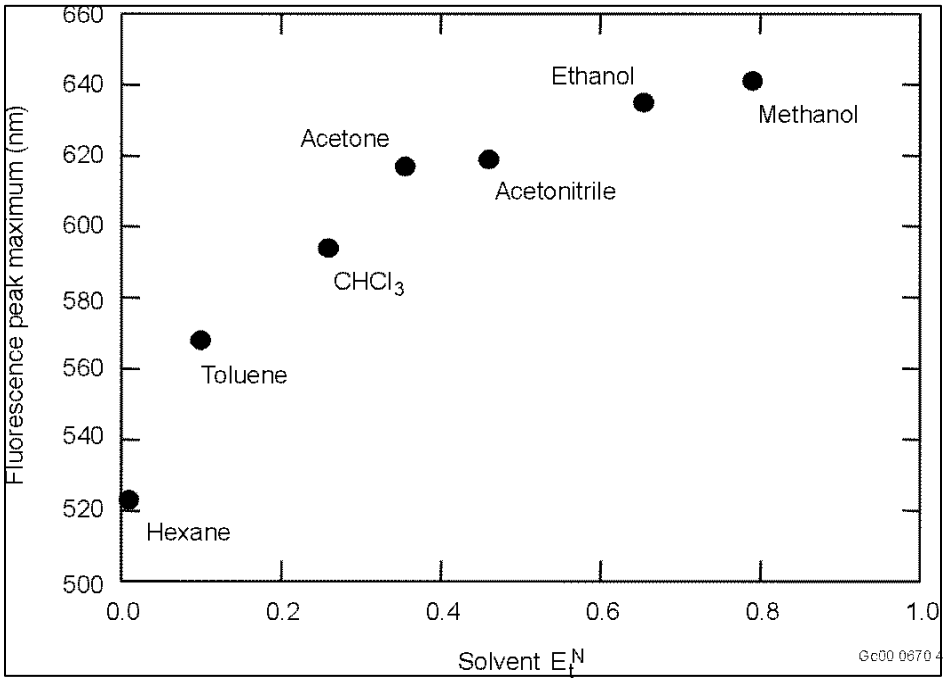

Figure 4. Plot of florescent peak max of Nile red in various liquid solvents.

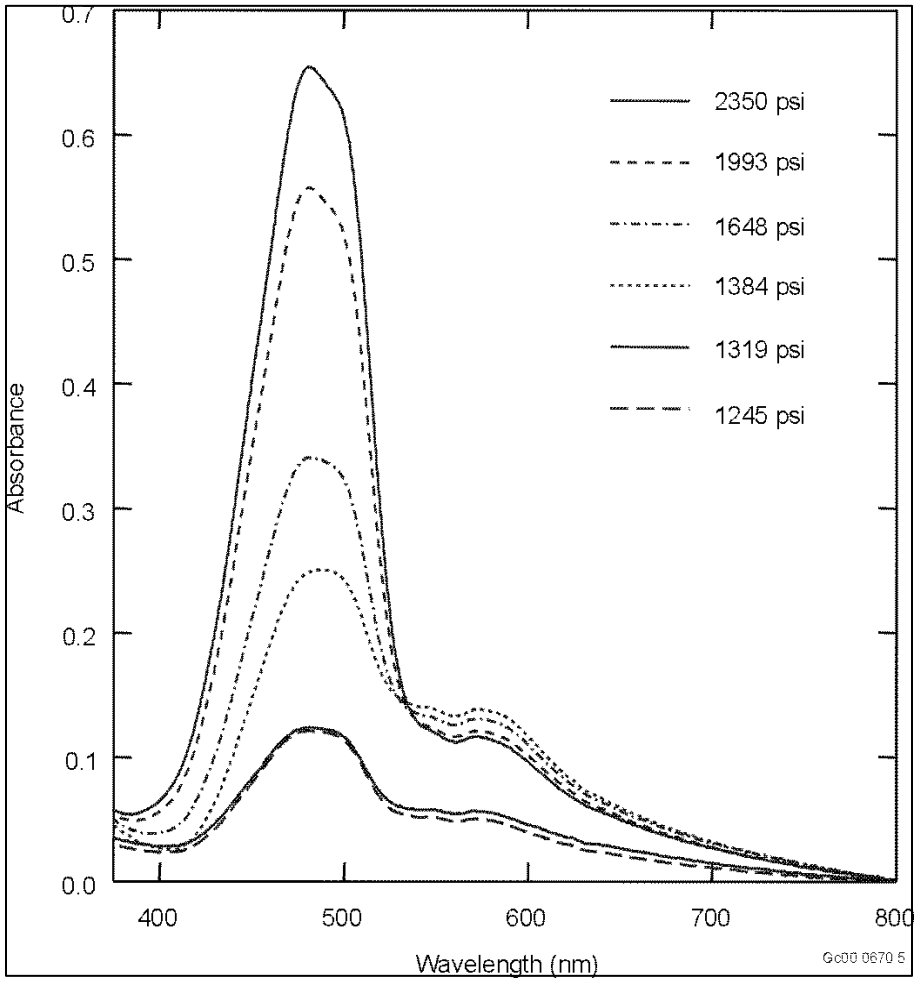

Figure 5. Nile red in CO_2 at 35∀C.

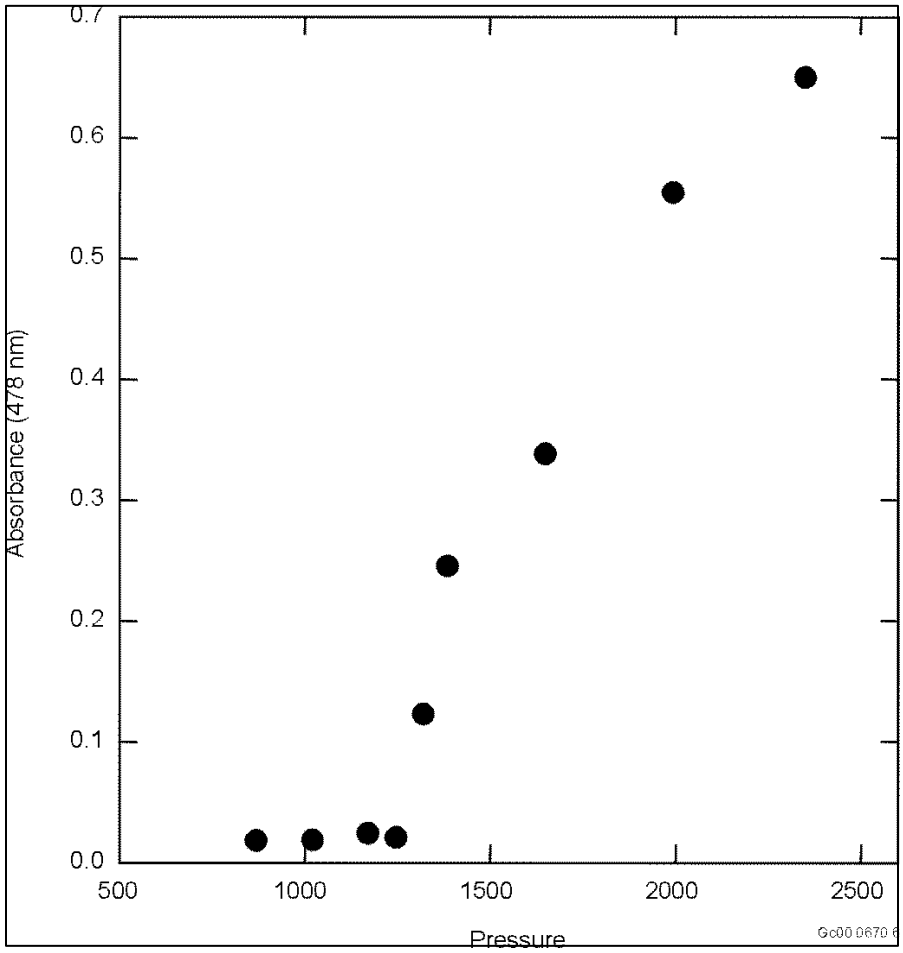

Figure 6. Nile red in CO2 at 35∀C.

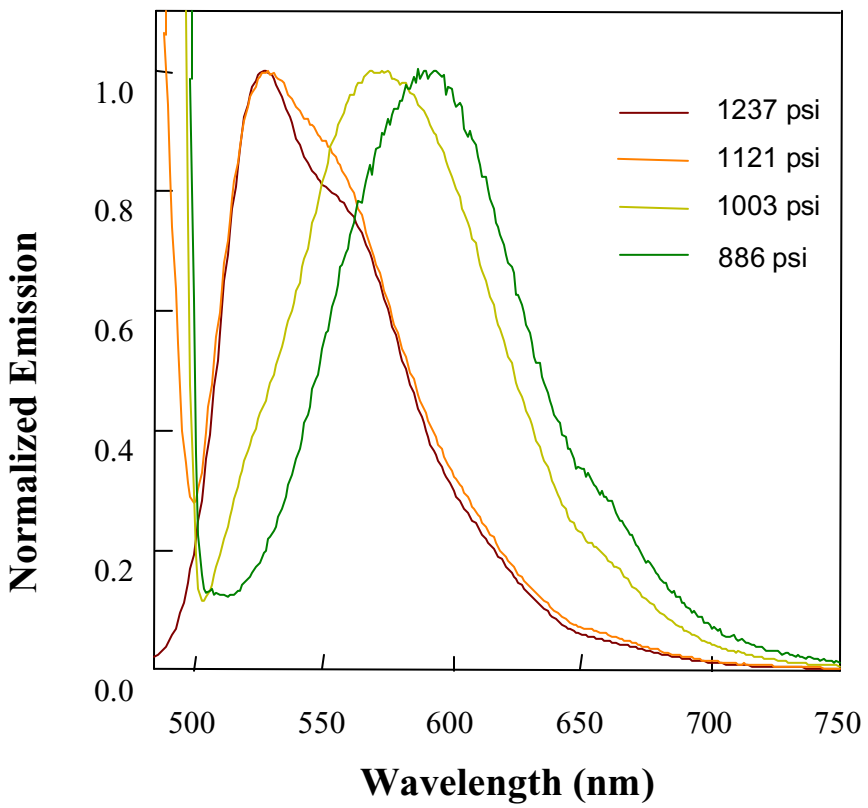

Figure 7. Florescence spectra of Nile red in CO2 at 35∀C.

We prepared and doped thin films of the polymer poly(methyl methacrylate) (PMMA) with Nile red. Thin PMMA films containing Nile red were soaked in hexane, toluene, and methanol, and the fluorescence spectra were monitored as a function of time. The PMMA/Nile red film soaked in hexane showed very little change, even after soaking for four days due to poor swelling of the PMMA film by hexane. The PMMA/Nile red soaked in toluene showed a systematic shift with time; however, the shift was relatively minor due to the similarity of the Nile red fluorescence spectra in toluene and in PMMA films. The fluorescence peak maximum for PMMA/Nile red films soaked in methanol shift from 575 nm in PMMA to 612 nm after soaking in methanol for 95 minutes and is the most notable example of spectral shift of the probe in the polymer (see Figure 8). The large spectral shift is due to both the high degree of swelling of the polymer by methanol and the large difference in the Nile red spectra in methanol and in PMMA films. Figure 9 shows the fluorescence spectra of PMMA/Nile red films in the presence of supercritical CO_2. The same figure shows that in the presence of CO_2, the observed spectra shows a large shift and a decrease in intensity. The decrease in intensity is due to the extraction of the Nile red from the PMMA film. Current investigations are focusing on the dynamics of PMMA swelling in CO_2 and quantitating the degree of extraction of Nile red. It is likely that if significant amounts of Nile red leach from the polymer, then the polymer/Nile red spectra will be indistinguishable from the carbon dioxide phase Nile red, thus rendering the probe useless for evaluation.

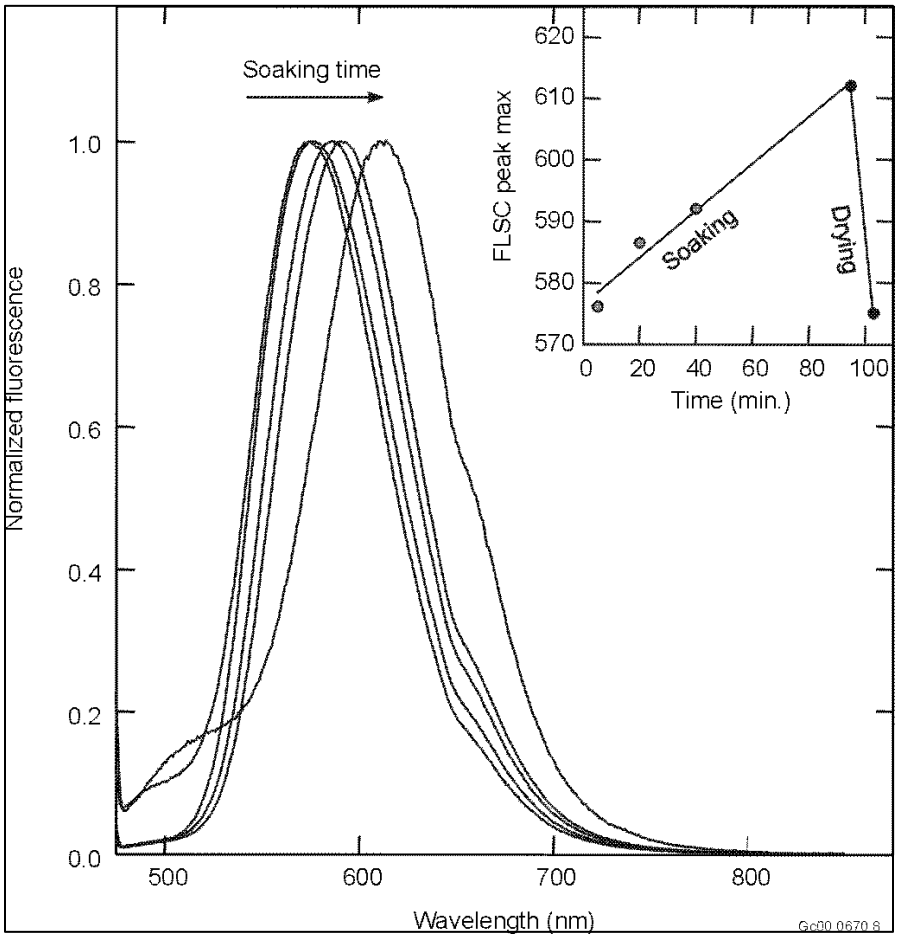

Figure 8. Nile red in methanol-swollen PMMA films.

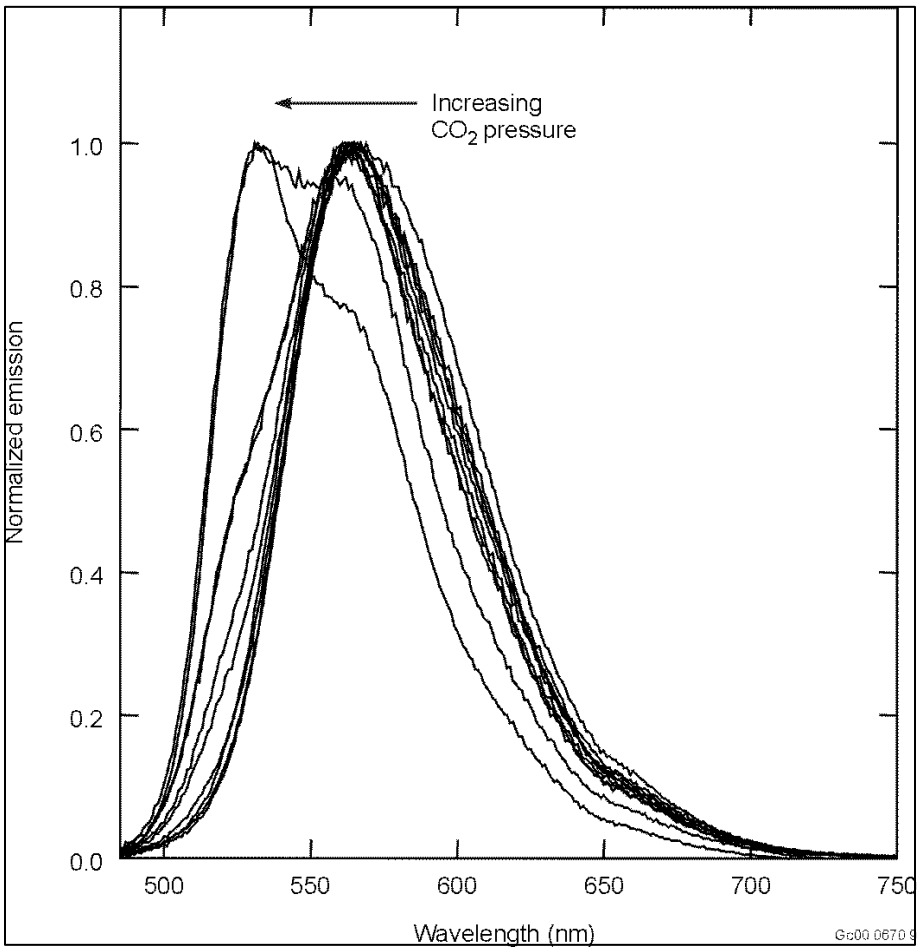

Figure 9. Nile red in CO2-swollen PMMA at 35∀C.

REFERENCES

1. M. McHugh and V. Krukonis, *Supercritical Fluid Extraction,* 2nd Edition, Butterworth–Heinemann Publishers, Boston, MA., 1994.

2. S. Kim and K. P. Johnston, *AIChE J.*, 1987, 33, 1603.

3. S. Kim and K. P. Johnston, *Ind. Eng. Chem. Res.,* 1987, 26, 1206.

4. P. G. Debenedetti, *Chem. Eng. Sci.,* 1987, 42, 2203.

5. Y. P. Sun et al., *Chem. Phys. Lett.,* 1993, 210, 111.

6. Y. P. Sun, et al., *Ber. Bunsenges. Phys. Chem.*, 1995, 99, 976.

7. C. R. Clarkson, et al., *Carbon*, 1997, 35(12), 1689–1705.

8. P. Braeuer, et al., *Separation and Purification Technology*, 1997, 12, 255–263.

9. T. Nitta and T. Shigeta, *Fluid Phase Equilibria*, 1998, 144, 245–256.

10. A. Shapiro and S. Erling, *Fluid Phase Equilibria*, 1999, 158–160, 565–573.

11. L. Zhou, and Y. Zhou, *Chemical Engineering Science*, 1998, 53(14), 2531–2536.

12. G. L. Aranovich, and M. D. Donohue, *Carbon*, 1995, 33(10), 1369–1375.

13. K. Kaczmarski and D. Antos, *Journal of Chromatography A*, 1999, 862, 1–16.

14. G. Afrane and E. H. Chimowitz, *Fluid Phase Equilibria* ,1995, 111, 213–238.

15. K. Murata and K. Kaneka, *Chemical Physics Letters*, 2000, 321, 342–348.

16. L. L. Lee and H. D. Cochran, *Journal of Supercritical Fluids*, 1998, 13, 77–81.

17. C. Tapia–Corzo, et al., *Journal of Supercritical Fluids*, 2000, 17, 25–33.

18. G. M. Martinez and D. Basmadjian, *Chemical Engineering Science*, 1996, 51(7), 1043–1054.

19. R. T. Yang and J. T. Saunders, *Fuel*, 1985, 64, 616.

20. H. Takeba, et al, *Surface Science*, 1996, 357–358, 703–707.

Appendix A

Publications and Presentations

Publications and Presentations

Publications

Nondestructive Assay Science and Technology Proof-of-Concept Testing for Environmental Characterization and Stewardship

Cordes, G. A., "Patterns and Intelligent Systems," *Nuclear Technologies Journal of the American Nuclear Society*, June 2000.

Cordes, G. A., "Patterns and Intelligent Systems," *Proceedings of the Third American Nuclear Society International Topical Meeting on Nuclear Plant Instrumentation, Control and Human–Machine Interface Technologies,* Washington, D.C., November 13–17, 2000.

Cordes, G. A., L. Van Ausdeln, J. L. Jones, and K. J. Haskell, "Intelligent Pattern-based Techniques to Monitor the Operation of Nondestructive Analysis Equipment and Contribute to Multivariate Feedback Control," *Proceedings of the ANNIE 2001 Conference 'Smart Engineering System Design'*, ASME, St. Louis Missouri, November 4–7, 2001.

Cordes, G. A., M. E. Velasquez, L. A. Van Ausdeln, M. J. Connolly, "Current INEEL Research in Pattern-Based Information Processing for NDA," *Proceedings of the 8th Environmental Management Nondestructive Assay Characterization,* Denver, CO, December 11–13, 2001.

Determan, J. D., and G. K. Becker, "An Expert System for Nondestructive Waste Assay Data Review," *Proceedings of the 2001 International High-Level Radioactive Waste Management Conference*, Las Vegas NV, April 20–May 3, 2001.

Tonchev, A. P., D.P. Wells, F. Harmon, J. L. Jones, "Application of Unconventional X-ray Resonance Fluorescence for Subsurface Science," *Pacifichem 2000 Conference*, Honolulu, Hawaii, December 14–19, 2000.

Van Ausdeln, L. A., G. A. Cordes, J. L. Jones, and K. J. Haskell, "Research on Utilizing a Multivariate Feedback Algorithm to Maintain Stable Operation of Variable Energy Electron Accelerators," *Proceedings of the American Nuclear Society Topical Meeting 'Nuclear Applications in the New in the New Millenium',* Reno, Nevada, November 11–15, 2001.

Van Ausdeln, L. A., K. J. Haskell, and J. L. Jones, "A Personal Computer-Based Monitoring and Control System for Electron Accelerators," *Proceedings of the American Nuclear Society Topical Meeting 'Nuclear Applications in the New in the New Millenium,'* Reno, Nevada, November 11–15, 2001.

Velasquez, M. E., and K. W. Bosworth, "Detection of Single Isotopes in Composite Gamma-ray Spectrum:An Application of Wavelet Theory to Gamma-ray Spectra Analysis," *Proceedings of the 2001 American Nuclear Society International Topical Meeting on Mathematical Methods for Nuclear Applications*, Salt Lake City, Utah, September 9–13, 2001.

Wells, D. P., F. Harmon, J. L. Jones, and W. Y. Yoon, "Development of Cabinet-Safe Accelerator Technology for Environmental Applications," *Proceedings of the Pacifichem 2000 Conference,* December 14–19, 2000.

Isobaric Ground Water Well for Precise Water Level Measurement For Long-Term Surveillance and Stewardship

Hubbell, J. M., and J. B. Sisson, "Isobaric Groundwater Well," U.S. Patent and Trademark Number 5,969,242, October 19, 1999.

Hubbell, J. M., J. B. Sisson, and R. G. Taylor, "Well Design to Reduce Barometric Pressure Effects On Water Level Data in Unconfined Aquifers," submitted to *Water Resources Research*, June 2001.

Assessment of Mercury Environmental Fate and Transport from INEEL Waste Processing Facilities for Long-Term Stewardship Concerns and Development of Improved Modeling Methods

Abbott, M. L., D. D. Susong, and D. P. Krabbenhoft, "Comparison of Mercury Measurements in Snow with ISCST3 Model-Predicted Deposition Near an Industrial Emission Source in Southeastern Idaho," *Proceedings of the International Symposium on the Measurment of Toxic and Related Air Pollutants, Research Triangle Park, NC, September 12–14, 2000*.

Abbott, M. L., D. D. Susong, D. P. Krabbenhoft, "Mercury Deposition in Snow Near an Industrial Emission Source in Southeastern Idaho and the Teton Range, Wyoming," Kluwer Academic Publishers, *Water, Air, and Soil Pollution*, July 24, 2001.

Abbott, M. L., D. D. Susong, D. P. Olson, and D. P. Krabbenhoft, "Mercury in Soil Near a Long-Term Emission Source in Southeastern Idaho," *Environmental Geology*, Sp.Ed.

Susong, D. D., M. L. Abbott, K. P. Krabbenhoft, "Reconnaissance of Mercury Concentrations in Snow from the Teton and Wasatch Ranges to Assess the Atmospheric Deposition of Mercury from an Urban Area: Abstract H12b-06, Eos," *Transactions of the American Geophysical Union, 80,* No. 46, 1999.

Using Environmental Records in Midlatitude Glacier Ice to Better Define EM Contaminant Inputs to the Subsurface

Cecil, L. D. and J. R. Green, "Radon-222 as a Tracer in the Hydrogeologic Environment," *Environmental Tracers in Subsurface Hydrology*, eds., P. G. Cook, and A. L. Herczeg, Kluwer Academic Publishers, pp. 175–194, 2000.

Cecil, L. D., J. A. Welhan, E. R. Sudicky, and J. R. Green, "Use of Chlorine-36 to Determine Regional-Scale Aquifer Dispersivity, Snake River Plain Aquifer, Idaho/USA," *Nuclear Instruments and Methods in Physics Research,* B 172, pp. 679–687, 2000.

Cecil, L. D., J. R. Green, and D. L. Naftz, "Global Ice-Core Research: Understanding and Applying Environmental Records of the Past," *U.S. Geological Survey Fact Sheet*, FS-003-00, 2000.

Cecil, L. D., L. L. Knobel, J. R. Green, and S. K. Frape, "In Situ Production of Chlorine-36 in the Eastern Snake River Plain Aquifer, Idaho: Implication for Describing Ground-Water Contamination Near a Nuclear Facility," *U.S. Geological Survey Water Resources Investigations Report*, 00-4114, 2000.

Davis, S. N., L. D. Cecil, M. Zareda, and S. Moysey, "Chorine-36, Bromide, and the Origin of Spring Water," in press for a special issue, *Journal Chemical Geology.*

Green, J. R., L. D. Cecil, D. L. Naftz, H. A. Synal, K. J. Kreutz, V. B. Aizen, C. P. Wake, and S. K. Frape, "Cosmogenic Isotopes in Mid-latitude Glacial Environments in the Northern Hemisphere, Indicators of Global Fallout," *Nuclear Instruments and Methods in Physics Research*, B 172, pp. 812–816, 2000.

Johnson, T. M., R. C. Roback, T. L. McLing, T. D. Bullen, D. J. DePaolo, C. Doughter, R. J. Hunt, R. W. Smith, L. D. Cecil, and M. T. Murrell, "Groundwater 'Fast Paths' in the Snake River Plain Aquifer: Radiogenic Isotope Ratios as Natural Groundwater Tracers," *Geology,* 2000.

Morin, R. H., G. E. Descamps, and L. D. Cecil, "Acoustic Televiewer Logging in Glacier Boreholes, in press, *Journal of Glaciology*, Vol. 46, No. 15.

Morin, R. H., G. E. Descamps, and L. D. Cecil, "Characterizing Englacial Structure from Analysis of Acoustic Televiewer Logs, Upper Fremont Glacier, Wyoming," *Proceedings of the Seventh International Symposium on Geophysics for Minerals, Geotechnical, and Groundwater Applications,* October 24–26, pp. 235–243, 2000,

Complex Systems Theory Applied to Subsurface Transport

Faybishenko, B. A., C. Doughty, M. Steiger, J. C. S. Long, T. R. Wood, J. Jacobsen, J. Lore and P. Zawislanski, "Conceptual Model of the Geometry and Physics of Fluid Flow and Chemical Transport in Unsaturated Fractured Basalt: Box Canyon Site, Idaho," *Water Resources Research*, 37(12), pp. 3499–3522, 2000.

Faybishenko, B. A., P. A. Witherspoon, C. Doughty, T. R. Wood, R. K. Podgorney, and J. T. Geller, "Multiscale Investigations of Liquid Flow in the Vadose Zone of Fractured Basalt," *Geophysical Monograph, "Flow and Transport in Fractured Rocks*," *American Geophysical Union*, T. Nicholson ed., In Review.

Glass, R. J., M. J. Nicholl, and S. E. Pringle, Unsaturated flow through a fracture-matrix-network: A first experiment. "Bridging the Gap between Measurement and Modeling in Heterogeneous Media" International Association of Hydrology, Groundwater Symposium, Berkeley, March 25–2, 2002 Conference proceedings, in review

Glass, R. J., S. E. Pringle, M. J. Nicholl, and T. R. Wood. "Unsaturated Flow Through a Fracture-Matrix-Network: Dynamic Pathways in Meso-scale Laboratory Experiments" Water Resources Research, in review.

LaViolette, R. A., C. R. Tolle, T. R. McJunkin and D. L. Stoner, "Combining the ApEn Statistic With Surrogate Data Analysis for the Detection of Nonlinear Dynamics In Time Series" Submitted to *Physica D.,* 2001.

LaViolette, R. A., Ph.D., "Exposing Nonlinear Dynamics In Time Series via Surrogate-Data Analysis with a Regularity Statistic," *General Colloquium of the Physics Dept.*, University of Oklahoma, March 29, 2001.

Podgorney, R. K., T. R. Wood, B. A. Faybishenko, and T. M. Stoops, "Unstable Infiltration Into Variably Saturated Fractured Basalt On a 1-Meter Field Scale," in *Geophysical Monograph "Dynamics of Fluids in Fractured Rocks: Concepts and Recent Advances," American Geophysical Union*, 2000.

Wood, T. R., R. K. Podgorney, and B. Faybishenko, "Small-Scale Field Tests of Water Flow In a Fractured Rock Vadose Zone," Case Study to Chapter 3 of the book: *Vadose Zone Science and Technology Solutions*, B. Looney and R. Falta, eds., Battelle Press, OH, 2000.

Unified Hydrogeophysical Parameter Estimation Approach Subsurface Contaminant Transport—Subsurface Imaging Collaboration With the Center for Subsurface Sensing and Imaging Systems

Mattson, E. D., E. R. Lindgren, and R. S. Bowman, "Electrically Induced Movement of Ions in Unsaturated Soil: 1. Model Development Assuming Constant Electrical Conductivity," *Journal of Contaminant Hydrology.*

Mattson, E. D., E. R. Lindgren, and R. S. Bowman, "Electrically Induced Movement of Ions in Unsaturated Soil: 2. Field and Modeling Results," *Journal of Contaminant Hydrology.*

Mattson, E. D., R. S. Bowman, and E. R. Lindgren, "Electrokinetic Remediation in Unsaturated Soils Using Surfactant-Coated Ceramic Casings," *Journal of Environmental Engineering*, Vol 126, No. 6, pp. 534–540, 2000.

Ecological Engineering of Rhizosphere Systems

Siegel, L. S., A. N. Alshawabkeh, and M. A. Hamilton, "Conceptual Model of Cs Partitioning in the Rhizosphere," 17th Annual International Conference on Contaminated Soils, Sediments & Water. Amherst, MA, October 22-25, 2001. Submitted to Journal.

Siegel, L. S., A. N. Alshawabkeh, and M. A. Hamilton, "Modeling Cs Partitioning in the Rhizosphere." Wetland & Remediation: The Second International Conference Burlington, Vermont, September 5–6, 2001, Conference Proceedings, in press.

Siegel, L. S., A. N. Alshawabkeh, and M. A. Hamilton, "Modeling Cs Fate in the Rhizosphere. Poster presented at the International Containment and Remediation Technology Conference and Exhibition," Orlando, Florida, June 10-13, 2001, Conference Proceedings, in press.

Innovative Approaches to Characterize Vadose Zone Hydraulic Properties

Baker, K. E. and D. N. Thompson, "Improved Methods for Estimating Microbial Activity and Moisture Characteristic Curves in Intact Unsaturated Soil Cores," submitted to the 2001 *Fall Meeting of the American Geophysical Union*, San Francisco, CA, December 10–14, 2001.

Baker, K. E. and D. N. Thompson, "Utilization of a Geocentrifuge for Evaluating Anisotropy in Basalt and Sandstone Cores," Poster, INRA Subsurface Science Symposium. Idaho Falls, ID, September 6–7, 2001.

Baker, K. E. and D. N. Thompson. "Evaluation of Moisture Dependent Anisotropy in Lithified Vadose Zone Porous Media," Poster, Eighth Biannual Unsaturated Zone Interest Group (UZIG) Meeting, United States Geological Survey. Idaho Falls, ID, July 30–August 2, 2001.

Baker, K. E. and D. N. Thompson. "Evaluation of Moisture Dependent Anisotropy in Lithified Vadose Zone Porous Media," being prepared for submission in 2001.

Baker, K. E., A. P. Poloski, A. Owen, C. Lindenmeier, and D. N. Thompson, "The Effect of Compaction on Moisture Characteristic Curves of Compactable Soils Measured in a UFA," Submitted to the 2001 *Fall Meeting of the American Geophysical Union*, San Francisco, CA, December 10–14, 2001.

Lindenmeier, C. W., A. T. Owen, K. E. Baker, and D. N. Thompson, "X-ray Microfocus Tomography as a Tool for Examination of Compaction in Intact Soil Cores Drained in a Geocentrifuge," in preparation.

Poloski, A. P., K. E. Baker, and D. N. Thompson, "Prediction of Moisture Characteristic Curves for Compactable Soils in a UFA," being prepared for submission in 2001.

Poloski, A. P., K. E. Baker, and D. N. Thompson. "Rapid characterization of moisture retention of compactible soils in a geocentrifuge: Semi-empirical correction method for compaction during measurement," to be submitted to Soil Science Society of America Journal, January 2002.

Geological, Geophysical, and Hydrological Environs of the INEEL Site

Embree, G. F., "Geologic Map of the Moody 7.5 Minute Quadrangle, Eastern Idaho; Idaho Geological Survey Map," in review, 2000.

Embree, G. F., "Geologic Map of the White Owl Butte 7.5 Minute Quadrangle, Eastern Idaho; Idaho Geological Survey Map," in review, 2000.

Embree, G. F., "Geologic Map of the Wright Creek 7.5 Minute Quadrangle, Eastern Idaho; Idaho Geological Survey Map," in review, 2000.

Environmental Separations and Barriers

Cotton, G. B., "Magnetic Separations With Magnetite: Theory, Operation and Limitations," *Ph. D. Dissertation*, University of Idaho, 2000.

Cotton, G. B., and H. B. Eldridge, "Nanolevel Magnetic Separation Model Considering Flow Limitations," *Chemical Engineering Science*, June 2000.

Stone, M. L. and L. A. Polson, "Chlorocarbon Permeablilities of Several Polymeric Membranes Determined by Membrane Introduction Mass Spectrometry (MIMS)," Invited for submission to Separation Science and Technology, November 2001.

Orme, C. J., M. L. Stone, M. T. Benson, and E. S. Peterson, "Testing of Polymer Membranes for Selective Permeability of Hydrogen," Invited for submission to Separation Science and Technology, November 2001.

Peterson, E. S., J. Trudeau, and W. Cleary, "Die Casting Waste Water Treatment Using A Membrane Process," Invited for submission to Separation Science and Technology, October 2001.

Presentations

Nondestructive Assay Science and Technology Proof-of-Concept Testing for Environmental Characterization and Stewardship

Connolly, M. J., "Waste Technology Management Research Linking Accelerator XRF NDA, Patterns, and Subsurface Science," *INEEL Technical Seminar, Idaho Falls, Idaho, January 16, 2001*.

Cordes, G. A., "Patterns and Intelligent Systems for Idaho," *2001 Annual Conference of the Idaho Society of Professional Engineers, Idaho Falls, Idaho, April 27, 2001*.

Cordes, G. A., M. E. Velasquez, and L. A. Van Ausdeln (INEEL), "Using Wavelets and Pattern Recognition to Unfold Gamma-Ray Spectra," *Transactions of the 2001 Winter Meeting of the American Nuclear Society, Reno, NV, November 11–15, 2001.*

Harker, Y. D., J. D. Cole, M. W. Drigert, R. J. Gehrke, J. K. Hartwell, J. L. Jones, J. W. Mandler, C. A. Mcgrath, C. V. McIsaac, G. K. Becker, J. C. Determan, G. A. Cordes, and M. J. Connolly (INEEL), "INEEL Environmental Management Nondestructive Assay Activities," *27th Waste Management Conference, Tucson, Arizona, February 25–March 1, 2001*.

Van Ausdeln, L. A., K. J. Haskell, and J. L. Jones (INEEL), "A Personal Computer-Based Monitoring and Control System for Electron Accelerators," poster session paper presented to the *2001 Particle Accelerator Conference (PAC2001), Chicago, Illinois, June 17-22, 2001*.

Isobaric Ground Water Well for Precise Water Level Measurement For Long Term Surveillance and Stewardship

Hubbell, J. M., "Isobaric Groundwater Well for Precise Water Level Measurement Relevant to Long Term Surveillance and Stewardship," *ESRCP Seminar, Idaho Falls, ID, September 6, 2001*.

Hubbell, J. M., "Precise Water Level Measurements Using the Isobaric Technique at the INEEL," *INEEL Groundwater Committee Meeting, Idaho Falls, Idaho, August 28, 2001*.

Hubbell, J. M., and J. B. Sisson, "Isobaric Well Design and Removal of Barometric Pressure Response on Water Level Data," *Unsaturated Zone Interest Group Meeting, July 30- August 2, Idaho Falls, ID*.

Hubbell, J. M., and J. B. Sisson, "Removal of Barometric Pressure Response from Water Level Data in Unconfined Aquifers," Poster and Abstract, *Fall 2000 AGU Meeting, San Francisco, CA, Hydrology H07-Natural Fluctuations of Groundwater Systems Session, December 18–21, 2000*.

Hubbell, J. M., and J. B. Sisson, "Removal of Barometric Response from Water Level Data in Unconfined Aquifers," Poster and Abstract, American Geophysical Union (AGU) *Fall 2000 Meeting, Hydrology H07-Natural Fluctuations of Ground Water Systems Session, San Franscisco, CA., December 19, 2000*.

Assessment of Mercury Environmental Fate and Transport from INEEL Waste Processing Facilities for Long-term Stewardship Concerns and Development of Improved Modeling Methods

Abbott, M. L., D. D. Susong, D. P. Krabbenhoft, "Comparison of Mercury Measurements in Snow with ISCST3 Model-Predicted Deposition Near an Industrial Emission Source in Southeastern Idaho,"

International Symposium on the Measurment of Toxic and Related Air Pollutants, Research Triangle Park, NC, September 12–14, 2000.

Abbott, M. L., D. D. Susong, D. P. Krabbenhoft, M. L. Olson, "Mercury Distribution in Soil Near a Major Atmospheric Emission Source at the Idaho National Engineering and Environmental Laboratory in Southeastern Idaho," http://www.geosociety.org/pubs/abstracts/2000/50248.htm. *Geological Society of America (Summit 2000) Annual Meeting, Reno, NV, November 9–18, 2000.*

Susong, D. D., M. L. Abbott, D. P. Krabbenhoft, "Mercury Accumulation in Snow on the Idaho National Engineering and Environmental Laboratory and Surrounding Region, Southeastern Idaho," http://www.geosociety.org/pubs/abstracts/2000/50087.htm, *Geological Society of America (Summit 2000) Annual Meeting, Reno, NV, November 9–18, 2000*.

Secondary Ion Mass Spectrometry Characterization of Environmental Microbial Processes

Ingram, J. C., F. S. Colwell, R. M. Lehman, W. F. Bauer, A. Shaw, "Interrogation of Intact Microorganisms by Static Secondary Ion Mass Spectrometry," *47th American Society for Mass Spectrometry Meeting in Long Beach, CA, June 2000*.

Ingram, J. C., F. S. Colwell, R. M. Lehman, W. F. Bauer, A. Shaw, "Secondary Ion Mass Spectrometry Investigation of Interfacial Chemistry of Intact Microorganisms," *American Geophysical Union, San Francisco, CA, December 2000*.

Ingram, J. C., F. S. Colwell, R. M. Lehman, W. F. Bauer, A. Shaw, "Static Secondary Ion Mass Spectrometry Analysis of Intact Microorganisms," *Joint 55th NORM/16th Rocky Mountain Regional ACS Meeting, Idaho Falls, ID, June 2000*.

Molecular Engineering and Genomics for Development of Environmental Biosensors using Robust Biocatalysts

Miller, A. M., "Microbial Genome Sequencing at the INEEL," Intermountain Branch, American Society for Microbiology, Pocatello, ID, April 28, 2001.

Roberto, F. F., "Extremophile Research at the INEEL," NASA Life in Extreme Environments Workshop, Big Sky, MT, March 6–7, 2000.

Roberto, F. F., "Genomics Activities at the INEEL," Thermal Biology Institute, Montana State Univ., Bozeman, MT, July 16, 2001.

Using Environmental Records in Mid-Latitude Glacier Ice to Better Define EM Contaminant Inputs to the Subsurface

Cecil, L. D. and J. R. Green, "Global Environmental Change Research: Evidence in Mid-Latitude Glaciers," *Idaho State University Lecture Series.*

Cecil, L. D., J. R. Green, D. L. Naftz, P. F. Schuster, D. D. Susong, "The U.S. Geological Survey's Global Ice Core Research Program," *Lanzhou Institute of Glaciology, Chinese Academy of Sciences, April 2000*.

Cecil, L. D., J. R. Green, D. L. Naftz, P. F. Schuster, D. D. Susong, "The U.S. Geological Survey's Global Ice Core Research Program," *National Polar Research Institute, University of Tokyo, Japan, April 2000.*

Green, J. R., L. D. Cecil, and D. L. Naftz, "USGS Research on Three Mid-Latitude Glaciers," *Western Snow Conference, Port Angeles Washington, April 2000*.

Complex Systems Theory Applied to Subsurface Transport

Fairley, J. A., T. R. Wood and T. R. McJunkin, "Comparison of Numerical Modeling Results with Laboratory Experiments of Flow in Unsaturated, Fractured Rock," *2001 Fall meeting of the American Geophysical Union, San Francisco, CA, December 10–14, 2001*

Fairley, J. P., "Analysis of a fracture/matrix interaction test in low-permeability, welded tuff," *Spring meeting of the American Geophysical Union, Boston, MA, June 2001*.

Fairley, J. P., "Numerical simulation for the design of in-situ injection tests," *2001 International High-Level Radioactive Waste Management Conference, Las Vegas, NV, April 2001*.

Fairley, J. P., "Numerical simulation for the design of in-situ injection tests," *Proceedings of the International Conference on High-Level Radioactive Waste Management, American Nuclear Society, 2001*.

Fairley, J. P., "Wetting front instability in unsaturated, fractured rock," Unsaturated Zone Interest Group meeting, Idaho Falls, ID, August, 2001.

Fairley, J. P., "Wetting front instability in unsaturated, fractured rock," *Annual meeting of the American Geophysical Union, San Francisco, CA, December 2000*.

Glass, R. J., and T. R. Wood, "Transport Within the Earth's Vadose Zone: Process Based Issues for Scaling," *Fall 2001 meeting of the American Geophysical Union, San Francisco, CA, December 10–14, 2001*.

Glass, R. J., S. E. Pringle, and M. J. Nicholl, "Unsaturated flow through a fracture-matrix-network: Laboratory experiments at the meter scale," *Fall 2001 Annual Meeting of the Geological Society of America, Boston, MA, November 1–10, 2001.*

LaViolette, R. A., "Obstacles to Realistic Models of Contaminant Fate in the Subsurface," *Joint Northwest/Rocky Mountain Regional Meeting of the American Chemical Society, Seattle WA June 14–17, 2001*.

LaViolette, R. A., "Exposing nonlinear dynamics in time series via surrogate-data analysis with a regularity statistic," *Invited Seminar, General Colloquium of the Physics Dept., University of Oklahoma, March 29, 2001*.

LaViolette, R. A., "Obstacles to Realistic Models of Contaminant Fate in the Subsurface, " *2001 Fall meeting of the American Geophysical Union, San Francisco, CA, December 10–14, 2001*.

Peak, D., R. Datwyler, N. Rasmussen, P. Simonson, T. R. Wood, T. Stoops, "Giant Fluctuations in Flow Through Fractured Media: A Stochastic, Self-Organized Dynamics Model," *International Conference on Chaos and Non-linear Dynamics: Dynamics Days University of Maryland, Baltimore, MD, 2002*.

Pringle, S. E., R. J. Glass, and M. J. Nicholl, Unsaturated Flow Through a Fracture-Matrix-Network: Dynamic Behavior of Flow Pathways," *2001 Fall meeting of the American Geophysical Union, San Francisco, CA, December 10–14, 2001*.

Reardon, C. L., T. R. Wood, J. M. Barnes, J. Fairley, K. S. Noah and D. L. Stoner, "Impact of Microbial Activity on Fluid Flow through Fractured Rock Systems," *Subsurface Science Symposium, Idaho Falls, ID September 6–7, 2001*.

Stoner, D. L., T. R. Wood, D. Peak, R.J.Glass, and R.A. LaViolette, "The Role of Complexity in the Prediction of Contaminant Transport in a Fractured Rock Vadose Zone Abstract," *2001 Fall meeting of the American Geophysical Union, San Francisco, CA, December 10–14, 2001*.

Wood, T. R., "Implications of Conceptualizing a Basalt Vadose Zone as a Complex System," *Fractured Rock 2001, Toronto, Ontario, Canada, sponsored by the US EPA, US DOE and Ontario Government (Ministry of the Environment), March 26-28, 2001.*

Wood, T. R., D. L. Stoner, R. LaViolette, R. Glass, T. R. McJunkin, R. Podgorney, K. Noah, R. Starr, G. Heath, C. Reardon, M. Kerschbaum and D. LeBrecque, "Integrated Experimental and Computational Analysis of Fluid Flow in Unsaturated Fractured Systems," *Eighth Biannual Unsaturated Zone Interest Group Meeting, Idaho Falls, Idaho, July 30 –August 2, 2001.*

Wood, T. R., D. L. Stoner and C. R. Tolle, "Communicating the Results of Modeled Predictions of Contaminant Transport in Fractured Rock Vadose Zones," *Earth System Processes, Global Meeting, Scotland, Geological Society of America and Geological Society of England, Edinburgh, Scotland, June 24-28, 2001*.Wood, T. R., D. L. Stoner, C. Tolle, R. A. Laviolette, B. Faybishenko and R. K. Podgorney, "Alternative Analyses of Non-ideal Water Movement in a Variably Saturated Fractured Basalt," *38th U.S. Rock Mechanics Symposium, Washington, DC, July 7-10, 2001*.

Wood, T. R., D. L. Stoner, R. LaViolette, R. Glass, T. R. McJunkin, R. Podgorney, K. Noah, R. Starr, G. Heath, C. Reardon, M. Kerschbaum and D. LeBrecque, "Wood, T. R., D. Stoner, C. Tolle, J. James, D. Peak, B. Faybishenko, and J. Crepeau, "Can a Fractured Basalt Vadose Zone be Characterized as a Complex System?," *Summit 2000, Abstracts with Programs, Volume 32, Number 7, Geological Society of America, Annual Meeting and Exposition, November 9–18, 2000, Reno, Nevada, 2000*.

Wood, T. R., T. R. McJunkin, R. K. Podgorney, R. J. Glass, R. C. Starr, D. L. Stoner, K. S. Noah, R.A. Laviolette and J. P. Fairley, "Assessment of Surrogate Fractured Rock Networks for Evidence of Complex Behavior," *2001 Fall meeting of the American Geophysical Union, San Francisco, CA, December 10-14, 2001.*

Unified Hydrogeophysical Parameter Estimation Approach Subsurface Contaminant Transport—Subsurface Imaging Collaboration With the Center for Subsurface Sensing and Imaging Systems

Mattson, E. D., "Underground Pollution Assessment," CenSSIS Retreat, Center for Subsurface Sensing and Imaging Systems, Woods Hole Oceanographic Institution, Quisset Campus, June 4–6, 2000.

Long-term Biogeochemical Destruction and Control of Aquifer Contaminants Using Single-Well Push-Pull Tests

Delwiche, M. E., "Plans for a Push-Pull Test in the Snake River Plain Aquifer to Enhance Precipitation of Divalent Cations," *INEEL Groundwater Committee Meeting, Idaho Falls, Idaho, March, 30, 2001.*

Taylor, J., Y. Fujita, M.E. Delwiche, F. Colwell, and M. Watwood, "Urease Activity in Organisms Collected from the Snake River Plain Aquifer," *INRA/INEEL Subsurface Science Symposium , Idaho Falls, Idaho, September 7, 2001.*

Ecological Engineering of Rhizosphere Systems

Chard, J., A. Henry, B. Doucette, J. Norton, S. Jones, C. Palmer, R. Hess, and B. Bugbee, "Sterile Culture Techniques for Characterization of Root Exudates," *2001 American Society of Agromony Annual Meeting, Charlotte, NC, October 2001*.

Hamilton, M. A., J. R. Hess, L. L. Cook, G. J. White, C. D. Palmer, and N. A. Yancey, "The Effect of Environmental and Ecological Factors on Cesium Bioavailability," *2001 American Society of Agromony Annual Meeting, Charlotte, NC, October, 2001.*

Henry, A., J. Chard, B. Doucette, B. Bugbee, J. Norton, J. R. Hess, and C. Palmer, "Characterization of Root Exudates from Crested Wheatgrass," *2001 American Society of Agromony Annual Meeting, Charlotte, NC, October, 2001*.

Siegel, L. S., A. N. Alshawabkeh, and M. A. Hamilton, "Systems Thinking for Predicting Cs Fate in the Rhizosphere," *Canadian Society of Civil Engineering 7th Specialty Conference on Environmental Engineering, Victoria, British Columbia, May 30 –June 2, 2001*.

Yancey, N., G. White, L. Cook, M. Hamilton, J. R. Hess, "Cesium Concentrations in Idaho National Engineering and Environmental Laboratory Soil and Vegetation," *2001 11th Annual West Coast Conference on Contaminated Soils, Sediments, and Water held in San Diego, CA, March 2001.*

Innovative Approaches to Characterize Vadose Zone Hydraulic Properties

Baker, K. E., A. P. Poloski, A. Owen, C. Lindenmeier, and D. N. Thompson, "The Effect of Compaction on Moisture Characteristic Curves of Compactible Soils Measured in a UFA," *Fall Meeting of the American Geophysical Union (AGU), San Francisco, CA, December 10–14, 2001*.

Baker, K. E., and D. N. Thompson, "Improved Methods for Estimating Microbial Activity and Moisture Characteristic Curves in Intact Unsaturated Soil Cores," submitted to the 2001 *Fall Meeting of the American Geophysical Union, San Francisco, CA, December 10–14, 2001.*

Baker, K. E., and D. N. Thompson, "Utilization of a Geocentrifuge for Evaluating Anisotropy in Basalt and Sandstone Cores," Poster, *INRA Subsurface Science Symposium. Idaho Falls, ID, September 6–7, 2001.*

Baker, K. E., and D. N. Thompson. "Evaluation of Moisture Dependent Anisotropy in Lithified Vadose Zone Porous Media," Poster, *Eighth Biannual Unsaturated Zone Interest Group (UZIG) Meeting, United States Geological Survey. Idaho Falls, ID, July 30–August 2, 2001.*

Computing Framework for Environmental Cleanup, Restoration, and Long-Term Stewardship

Arnett, R. C., and L. E. Greenwade, "Parallel Processing of a Groundwater Contaminant Code," *Summit 2000 Proceedings, Noodwijk, Netherlands, May, 2000*.

Chaffin, M., "Collaborative Visualization of Subsurface Data," *DOE Computer Graphics Forum, Orcas Island, WA, May 8, 2001*.

Greenwade, L. E., "Communication to a Remote non-Technical User," *DOE Computer Graphics Forum, Orcas Island, WA, May 8, 2001*.

Greenwade, L. E., "INEEL Visualization Status," *DOE Computer Graphics Forum, Orcas Island, WA, May 7, 2001.*

Greenwade, L. E., "Necessary Improvements in Parallel Programming Environments," *Parallel Tools Consortium, San Diego, CA, May 17, 2001.*

Greenwade, L. E., "Strategies for High Performance Computing Solutions," *Summit 2000, Indian Wells, CA, May 22, 2001*.

Greenwade, L. E., and A. G. Shewmaker, "Beowulf-class Sun Supercomputing Clusters," *SUPerG Amsterdam Proceedings, Amsterdam, Netherlands, October 9, 2001*.

Greenwade, L. E., and M. R. Chaffin, "Geographically Distributed Collaborative Environments," *SUPerG Tokyo Proceedings, Tokyo, Japan, April 12, 2001.*

Greenwade, L. E., et al, "Effective Multi-resolution Visualization for Subsurface Science," *Invited Lecture, SUPerG 2000 Proceedings, Paris, France, April, 2000*.

Greenwade, L. E., et al., "Subsurface Bioremediation Code Porting and Optimization," *SUPerG Vancouver Proceedings, Vancouver, BC, Canada, October 11, 2000.*

Decontamination and Decommissioning Optimal Planning System (DDROPS) for the Advanced Decontamination and Decommissioning System (ADDS)

Kostelnik, K., et al., "Optimal Planning of Decontamination, Decommissioning and Remediation," *American Nuclear Society 8th International Topical on Robotics and Remote Systems, April 1999*.

Smith, A. M., R. Meservey, J. L. Tripp, C. Hubbard, H. Shoemaker, "Achieving Efficiencies in D&D Work Through Technology Deployments," *International Decommissioning Symposium (IDS 2000), June 2000*.

Tripp, J. L. "Optimal Planning of Decontamination, Decommissioning, and Remediation," *ANS 8th International Topical on Robotics and Remote Systems, November 2001*.

Tripp, J. L., "Optimal Waste Packaging During D&D," *American Nuclear Society 2001 Winter Meeting, November 2001*.

Tripp, J. L., "Advanced Decontamination and Decommissioning System," *Waste Management 2001 Conference, February 2001*.

Tripp, J. L., and A. M. Smith, "D&D Technology Cost Benefit Analyses," *Waste Management 200 Conference, March 2000*.

Environmental Separations and Barriers

Polson, L. A., M. L. Stone, and G. L. Gresham, "Characterization of Phosphazene Materials as Membranes in Membrane Introduction Mass Spectrometry (MIMS)," Poster (070), *2000 Northwest and Rocky Mountain Joint Regional Meeting, Idaho Falls, ID, June 15–17, 2000*.

Polson, L. A., M. L. Stone, and G. L. Gresham, "Membrane Introduction Mass Spectroscopy (MIMS): An Overview of System Components and Variables," *National American Chemical Society Meeting, Washington, D.C., August 22, 2000.*

Stone, M. L., L. A. Polson, and G. L. Gresham, "Analysis of Chlorocarbon Transport Through Polymeric Membranes Using Membrane Introduction Mass Spectrometry," Oral Presentation (096), *2000 Northwest and Rocky Mountain Joint Regional Meeting, Idaho Falls, ID, June 15–17, 2000*.

Stone, M. L. and L. A. Polson, "Chlorocarbon Permeablilities of Several Polymeric Membranes Determined by Membrane Introduction Mass Spectrometry (MIMS)," *Poster for the 12th Symposium on Separation Science and Technology for Energy Applications, Gatlinburg, TN, October 14–18, 2001.*

Orme, C. J., M. L. Stone, M. T. Benson, and E. S. Peterson, "Testing of Polymer Membranes for Selective Permeability of Hydrogen," *Poster for the Twelvth Symposium on Separation Science and Technology for Energy Applications, Gatlinburg, TN, October 14–18, 2001*

Peterson, E. S., J. Trudeau, and W. Cleary, "Die Casting Waste Water Treatment Using A Membrane Process," *Invited presentation at the 13th Conference on Separation Science and Technology for Energy Applications, Gatlinburg, TN, October 2001.*

Appendix B

Comparison of ESRC Tasks with EM Site Technology Coordination Group Needs

Comparison of ESRC Tasks with EM Site Technology Coordination Group Needs

This appendix summaries how ESRC tasks link with EM needs as captured in the Site Technology Coordination Group (STCG) database. This summary was created for two reasons:

- To help ensure that ESRC funds were being used to address EM needs.
- To formulate a methodology for integrating research and development efforts at the INEEL with Site Operations, thereby facilitating moving science and technology toward ultimate demonstration and deployment.

ESRC and the INEEL Integration and Roadmapping (II&R) Department linked ESRC tasks to EM Site Operational Needs. Those needs, which are tabulated in the STCG, were mapped to the research in each of the funded tasks. II&R maintains the STCG database.

The ESRC tasks are tabulated and mapped to STCG needs (see Table B-1). All research activities had a link to one or more identified site needs.

The planned application of this approach in FY 2001 to other R&D programs will improve the process of moving science and technology toward real EM needs.

This mapping is facilitating improving communication between R&D and Operational Users, e.g., arranging selected meetings between PIs and STCG end users. Finally, a series of ESRC seminars were established to disseminate information on the progress of the research effort and to provide focus and feed back from operational personnel.

Table B-1. ESRC tasks tabulated and mapped to STCG needs.

Task Title	STCG ID No.	STCG Description
Ion Mobility Spectrometry for Environmental Monitoring and In Situ Measurements of Hazardous Organics	2.1.18	Continuous Emissions Monitor for Offgas Analysis
	2.1.19	EPA Methods Sample Collection and Analysis Verification/Development
	6.1.02	Real-time Field Instrumentation for Characterization and Monitoring Soils and Groundwater
	6.1.27	Integrated Suite of In Situ Instruments to Determine Flux in the Vadose Zone
	6.1.30	Instrumentation to Reliably Measure Soil Gas Flux Accounting for Barometric and Temporal Variations
	7.2.17	Field Screening of Samples and Equipment Surfaces to Identify PCB Contamination
Nondestructive Assay (NDA) Science and Technology Proof-of-Concept Testing for Environmental Characterization and Stewardship	1.1.09	Nondestructive Radiological Assay Methods for SNF
	3.1.06	Advanced Nuclear Assay for CH-TRU Waste Drums
	3.1.32	Develop Nondestructive Assay (NDA) Capability for Remote-Handled TRU Waste and Contact-Handled TRU Waste with Shielded RH Components
	3.1.42	Non Destructive Assay for RCRA metals and chlorine in WERF incinerator feed
	3.1.46	Develop Nondestructive Examination (NDE) Capability for Remote-Handled TRU Waste and Contact-Handled TRU Waste with Shielded RH Components
	S.1.05	Nondestructive Assay (NDA) Capability for Remote-Handled Transuranic Waste
Isobaric Groundwater Well for Precise Water Level Measurement Relevant to Long Term Surveillance and Stewardship	6.1.02	Real-time Field Instrumentation for Characterization and Monitoring Soils and Groundwater
	6.1.04	In-situ Treatment of VOC Contaminated Groundwater in Saturated and Unsaturated Deep Fractured Rock
	S.1.04	Real-time Field Instrumentation for Character-ization and Monitoring Soils and Groundwater
	S.1.11	Modeling of Flow and Transport in the Vadose Zone
	S.1.17	Development of Sensors for Large Scale Measurements in the Vadose Zone to Define Spatial Variability
Assessment of Mercury Environmental Fate and Transport from INEEL Waste Processing Facilities for Long-term Stewardship Concerns and Development of Improved Modeling Methods	2.1.36	Mercury Removal from Liquid Wastes

Table B-1. Continued.

Task Title	STCG ID No.	STCG Description
	2.1.56	Mercury Treatment for Aluminum Calcine
	3.1.49	Mercury Emissions Control for Mixed Waste Thermal Treatment
Advanced Robotic Technologies for Remote Environmental Surveillance and Stewardship	2.1.26	Direct Tank Sampler for Tank Solution Characterization
	3.1.46	Develop Nondestructive Examination (NDE) Capability for Remote-Handled TRU Waste and Contact-Handled TRU Waste with Shielded RH Components
	7.2.06	Remote Characterization for Building Release, Large Area Surface Soil Characterization, and Characterization of Sumps, Debris, Underwater Areas, and Buried Pipes and Utilities
	7.2.08	Robotics for D&D
	7.2.19	Remote/Robotic Technologies for Access and Deployment of Characterization and Sampling Tools
Secondary Ion Mass Spectrometry Characterization of Environmental Microbial Processes	6.1.25	Pretreatment of Explosives Contaminated Soil for Biological Remediation
	S.1.01	Microbial Alteration of Heavy Metal and Radionuclide Partitioning at Mineral Surfaces
Biologically Based Catalysts as Sensors to Detect Contaminants in Harsh Service Environment	6.1.02	Real-time Field Instrumentation for Characterization Monitoring Soils and Groundwater
	S.1.04	Real-time Field Instrumentation for Characterization and Monitoring Soils and Groundwater
	S.1.19	In Situ Biologic Activity Sensor for Vadose Zone and Groundwater Monitoring, Characterization and Remediation
Molecular Engineering and Genomics For Development of Environmental Biosensors Using Robust Biocatalysts	S.1.01	Microbial Alteration of Heavy Metal and Radionuclide Partitioning at Mineral Surfaces
	S.1.06	Detect and Mitigate Microbiologically Induced Corrosion in Spent Nuclear Fuel Dry Storage Containers
	S.1.19	In Situ Biologic Activity Sensor for Vadose Zone and Groundwater Monitoring, Characterization and Remediation
Determining Soil Moisture Over Wide Areas for DOE Site Stewardship Hydrology	6.1.02	Real-time Field Instrumentation for Characterization and Monitoring Soils and Groundwater
Using Environmental Records in Mid-Latitude Glacier Ice to Better Define EM Contaminant Inputs to the Subsurface	S.1.16	Quantifying Uncertainty in Risk Calculations
Complex Systems Theory Applied To Subsurface Transport	S.1.09	Characterization of Scale and Spatial Heterogeneity and Preferential Flow

Table B-1. Continued.

Task Title	STCG ID No.	STCG Description
	S.1.10	Geochemistry of Contaminants in the Vadose Zone
	S.1.11	Modeling of Flow and Transport in the Vadose Zone
	S.1.12	Understanding the Behavior of Waste Forms and their Near-Field Transport
	S.1.15	Physics of Flow in the Vadose Zone
	S.1.17	Development of Sensors for Large Scale Measurements in the Vadose Zone to Define Spatial Variability
	6.1.24	Understanding the Migration of VOCs Around an ISV Melt
	6.1.32	In Situ Stabilization Techniques to Isolate Metals and Radionuclides from the Biosphere, including both Surface an Deep Fractured Rock
Unified Hydrogeophysical Parameter Estimation Approach to Subsurface Contaminant Transport—Subsurface Imaging Collaboration With the Center for Subsurface Sensing and Imaging Systems	S.1.09	Characterization of Scale and Spatial Heterogeneity and Preferential Flow
	S.1.17	Development of Sensors for Large Scale Measurements in the Vadose Zone to Define Spatial Variability
	S.1.18	Development of Indirect Sensing Instrumentation for Spatial Variability Analyses of State Variables
Long-term Biogeochemical Destruction and Control of Aquifer Contaminants Using Single-Well Push-Pull Tests	6.1.32	In Situ Stabilization Techniques to Isolate Metals and Radionuclides from the Biosphere, including both Surface and Deep Fractured Rock
Ecological Engineering of Rhizosphere Systems	2.1.17	Develop New Filter Leach Process
	3.1.33	Develop In-Situ Hydrogen and Volatile Organic Compound (VOC) Reduction
	7.2.09	Develop a Rapid Wood Radiological Contamination Monitor
	S.1.12	Understanding the Behavior of Waste Forms and their Near-Field Transport
Investigation of Factors Influencing Cesium Mobility and Uptake in Plant/Soil Systems	2.1.28	Cs and Sr Removal from Newly Generated Liquid Waste
Innovative Approaches to Characterize Vadose Zone Hydraulics Properties	S.1.09	Characterization of Scale and Spatial Heterogeneity and Preferential Flow
	S.1.10	Geochemistry of Contaminants in the Vadose Zone
	S.1.11	Modeling of Flow and Transport in the Vadose Zone
	S.1.17	Development of Sensors for Large Scale Measurements in the Vadose Zone to Define Spatial Variability

Table B-1. Continued.

Task Title	STCG ID No.	STCG Description
	S.1.19	In Situ Biologic Activity Sensor for Vadose Zone and Groundwater Monitoring, Characterization and Remediation
	6.1.02	Real-time Field Instrumentation for Characterization and Monitoring Soils and Groundwater
	6.1.04	In-situ Treatment of VOC Contaminated Groundwater in Saturated and Unsaturated Deep Fractured Rock
	6.1.27	Integrated Suite of In Situ Instruments to Determine Flux in the Vadose Zone
Geological, Geophysical and Hydrological Environs of the INEEL Site	S.1.10	Geochemistry of Contaminants in the Vadose Zone
	S.1.11	Modeling of Flow and Transport in the Vadose Zone
	S.1.19	In Situ Biologic Activity Sensor for Vadose Zone and Groundwater Monitoring, Characterization and Remediation
Advanced Geophysical Characterization to Enhance Earth Science Capabilities at the INEEL to Support Remediation and Stewardship	S.1.09	Characterization of Scale and Spactial Heterogeneity and Preferred Flow
	S.1.17	Development of Sensors for Large-Scale Measurements in the Vadose Zone to Refine Spatial Variability.
	6.1.27	Integrated Suite of In Situ Instruments to Determine Flux in the Vadose Zone
Computing Framework for Environmental Cleanup, Restoration, and Long-term Stewardship	S.1.11	Modeling of Flow and Transport in the Vadose Zone
	S.1.12	Understanding the Behavior of Waste Forms and their Near-Field Transport
	S.1.13	Longevity of Engineered Barriers
	S.1.14	Transport of Contaminants in the Vapor Phase
	S.1.16	Quantifying Uncertainty in Risk Calculations
Decontamination, Decommissioning, and Remediation Optimal Planning System for the Advanced Decontamination and Decommissioning System	7.2.21	Removal of Two Reactors as Single Units
	7.2.29	Remote Demolition of Machinery
	7.2.30	Remote Demolition of Metal Structures
	7.2.31	Remote Demolition of Piping
Robotic Waste Packaging System for the Advanced Decontamination and Decommissioning System	7.2.08	Robotics for D&D
	7.2.23	Copper Wire Recycle
	7.2.27	Reuse of Metal Pipes, Lumber, Lead, and Other Metals

Table B-1. Continued.

Task Title	STCG ID No.	STCG Description
Waste Characterization and Sorting Station for the Advanced Decontamination and Decommissioning System	7.2.08	Robotics for D&D
	7.2.23	Copper Wire Recycle
	7.2.27	Reuse of Metal Pipes, Lumber, Lead, and Other Metals
Environmental Separation and Barriers	S.1.01	Microbial Alteration of Heavy Metal and Radionuclide Partitioning at Mineral Surfaces
Proton Conducting Ceramic Membrane Applied to Spent Nuclear Fuel Stewardship	2.1.64	Solid-Liquid Separation Equipment Development and Application
	3.1.33	Develop In-Situ Hydrogen and Volatile Organic Compound (VOC) Reduction
Spectroscopic Investigations at Solid Supercritical Fluid Interfaces in Support of Advanced Supercritical Separation Techniques	2.1.06a	TRU and Sr Removal from High Activity Waste
	2.1.06b	Cs Removal from High Activity Waste
	2.1.25	Ion-Exchange System for Water Runoff
	2.1.28	Cs and Sr Removal from Newly Generated Liquid Waste
	2.1.56	Mercury Treatment for Aluminum Calcine
	2.1.66	Treatment/Disposition of Spent Ion Exchange Resins
	2.1.68	Technetium Removal from INEEL High Level Waste
	7.2.14	Technology for Decontaminating Radionuclide Contaminated Lead Shot, Brick (including lead plate), and Sheeting Allowing Free-Release
	S.2.06	Understanding the Physics and Chemistry of Metal Decontamination
	S.1.10	Geochemistry of Contaminants in the Vadose Zone
	S.2.05	Understanding the Physics and Chemistry of Concrete Decontamination

Appendix C

ESRC Portfolio Characterization

ESRC Portfolio Characterization

This appendix characterizes the ESRC portfolio from the perspectives of technology maturity and building INEEL R&D capabilities relevant to the DOE-EM mission. ESRC objectives include providing science and technology for meeting the DOE-EM mission and enhancing the INEEL's science and technology capabilities for longer-term challenges like environmental stewardship.

Technology Maturity

DOE-EM categorizes technology maturity in seven stages or "gates":

1. Basic Research
2. Applied Research
3. Exploratory Development
4. Advanced Development
5. Engineering Development
6. Demonstration
7. Deployment

We categorized the tasks according to this scheme. Figure C-1 illustrates the portfolio. Two-thirds of the work is applied research; this is fully appropriate given ESRC objectives. Also consistent with the objectives and nature of ESRC, none of the tasks were categorized at stages 5 through 7 (see Table C-1).

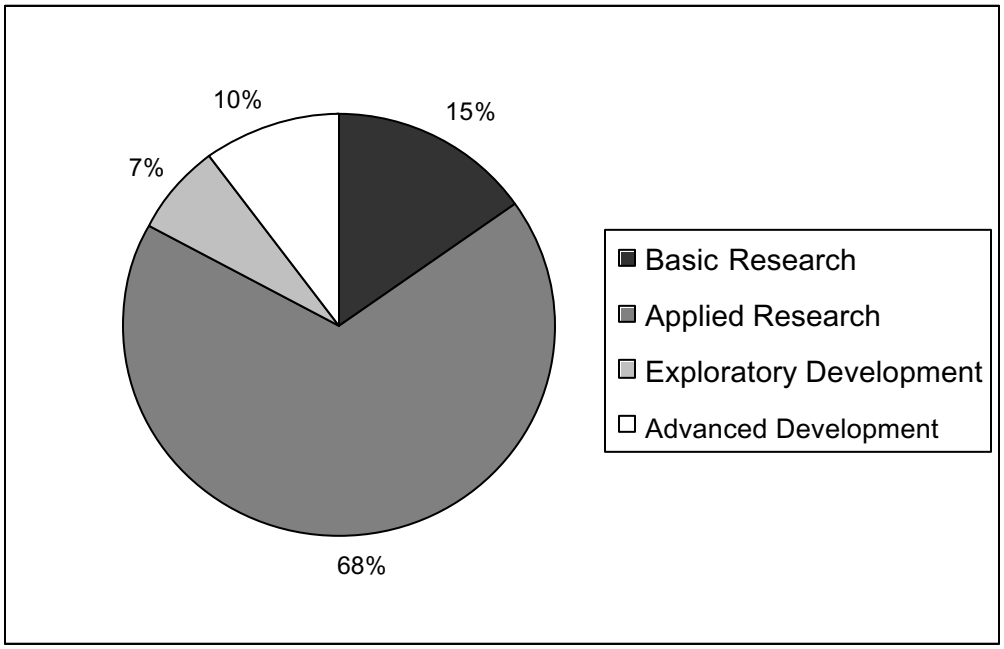

Figure C-1. ESRC portfolio funding by technology maturity.

Table C-1. Technology maturity of ESRC tasks.

	Technology Maturity P = Primary type; S = secondary type						
Title	Basic Research	Applied Research	Exploratory Development	Advanced Development	Engineering Development	Demonstration	Deployment
Ion Mobility Spectrometry for Environmental Monitoring and In Situ Measurement of Hazardous Organics		P	S				
Nondestructive Assay Science and Technology Proof-of-Concept Testing for Environmental Characterization and Stewardship		S	P	S			
Isobaric Groundwater Well for Precise Water Level Measurement Relevant to Long Term Surveillance and Stewardship		S		P			
Assessment of Mercury Environmental Fate and Transport from INEEL Waste Processing Facilities for Long-term Stewardship Concerns and Development of Improved Modeling Methods		P	S				
Advanced Robotic Technologies for Remote Environmental Surveillance and Stewardship	S	S	P				
Secondary Ion Mass Spectrometry Characterization of Environmental Microbial Processes		P					
Biologically Based Catalysts as Sensors to Detect Contaminants in Harsh Service Environments	S	P					
Molecular Engineering and Genomics for Development of Environmental Biosensors Using Robust Biocatalysts	S	P					
Determining Soil Moisture Over Wide Areas for DOE Site Stewardship Hydrology			P				
Using Environmental Records in Mid-Latitude Glacier Ice to Better Define EM Contaminant Inputs to the Subsurface	P	S					
Complex Systems Theory Applied to Subsurface Transport	S	P					
Unified Hydrogeophysical Parameter Estimation Approach to Subsurface Contaminant Transport—Subsurface Imaging Collaboration with the Center for Subsurface Sensing and Imaging Systems		P					

Table C-1. Continued.

Title	Technology Maturity P = Primary type; S = secondary type						
	Basic Research	Applied Research	Exploratory Development	Advanced Development	Engineering Development	Demonstration	Deployment
Long-Term Biogeochemical Destruction and Control of Aquifer Contaminants Using Single-Well Push-Pull Tests		P					
Ecological Engineering of Rhizosphere Systems	P	S					
Investigation of Factors Influencing Cesium Mobility and Uptake in Plant/Soil Systems	P	S					
Innovative Approaches to Characterize Vadose Zone Hydraulic Properties		P					
Geological, Geophysical and Hydrological Environs of the INEEL Site		P	S				
Advanced Geophysical Characterization to Enhance Earth Science Capabilities at the INEEL to Support Remediation and Stewardship	S	P	S				
Computing Framework for Environmental Cleanup, Restoration, and Long-term Stewardship		P	S				
Decontamination, Decommissioning , and Remediation of Optimal Planning System for the Advanced Decontamination and Decommissioning System				P			
Robotic Waste Packaging System for the Advanced Decontamination and Decommissioning Systems				P			
Waste Characterization and Sorting Station for the Advanced Decontamination and Decommissioning System				P			
Environmental Separations and Barriers	S	P	S				
Proton Conducting Ceramic Membrane Applied to Spent Nuclear Fuel Stewardship		P	S				
Spectroscopic Investigations at Solid Supercritical Fluid Interfaces in Support of Advanced Supercritical Separation Techniques	P						